# PRIMATE BONE MICROSTRUCTURAL VARIABILITY: RELATIONSHIPS TO LIFE HISTORY, MECHANICAL ADAPTATION AND PHYLOGENY

by

JOHANNA WARSHAW

A dissertation submitted to the Graduate Faculty in Anthropology in partial fulfillment of the requirements for the degree of Doctor of Philosophy,
The City University of New York

2007

UMI Number: 3287140

Copyright 2007 by
Warshaw, Johanna

All rights reserved.

UMI®

UMI Microform 3287140
Copyright 2008 by ProQuest Information and Learning Company.
All rights reserved. This microform edition is protected against unauthorized copying under Title 17, United States Code.

ProQuest Information and Learning Company
300 North Zeeb Road
P.O. Box 1346
Ann Arbor, MI 48106-1346

© 2007

JOHANNA WARSHAW

All Rights Reserved

This manuscript has been read and accepted for the Graduate Faculty in Anthropology in satisfaction of the dissertation requirement for the degree of Doctor of Philosophy.

Timothy G. Bromage

_____ _____

Date Chair of Examining Committee

Louise Lennihan

_____ _____

Date Executive Officer

Frederick S. Szalay

Carl J. Terranova

Donald H. Enlow

THE CITY UNIVERSITY OF NEW YORK

Abstract

PRIMATE BONE MICROSTRUCTURAL VARIABILITY:
RELATIONSHIPS TO LIFE HISTORY, MECHANICAL ADAPTATION
AND PHYLOGENY

by

Johanna Warshaw

Advisor: Professor Timothy G. Bromage

At the microstructural level, bone is hypothesized to record aspects of the mechanical adaptation and life history of vertebrates. It follows that information with bearing upon the biology and behavior of fossil taxa is potentially encoded therein. However, before interpretations of microstructure in extinct species are possible, the extent of variability that exists in living groups, and the relationship of this variability to biological and behavioral features, must be understood.

Here I report on variation in three bone microstructural features: primary bone tissue types, intracortical remodeling, and collagen fiber orientation. These were examined in midshaft cortices from the femur, humerus, tibia, radius and ulna in a sample of extant strepsirhine, tarsiid and platyrrhine primates. Employing conventional and polarized light microscopy techniques, the aims were to qualitatively and quantitatively describe the relationship of these microstructural features to several mechanical adaptation and life history characteristics of species: developmental patterns, body size, growth rate, positional behavior, and phylogenetic status.

This study has shown that variation in the three microstructural variables exists among primates, that this variation is often non-randomly distributed, and that it is partly

explicable via a consideration of development, growth rate, body size, positional behavior and phylogeny. Primary tissue types vary with body size, growth rate and, concurrently, phylogenetic status as well as, potentially, positional behavior. Percent intracortical remodeling varies principally as a function of body size, with a subsidiary relationship to positional behavior. Finally, contrary to predictions based on previous descriptions in the literature, collagen fiber orientation shows little relationship with positional behavior and inferred diversity in mechanical loads. Rather, the limited variation that does exist correlates best with primary tissue type.

The study also clearly demonstrates that much of the diversity in the sample is not explained by the factors examined here. This suggests that more work must to be done to illuminate the variables impacting upon bones as they grow. It also serves as a warning that, at present, micro-morphological features must be employed only with a full understanding of their current limitations – in addition to their exciting potential – as tools in the study of fossil taxa.

**Acknowledgements**

It would not have been possible for me to develop, undertake, and complete this doctoral dissertation without the help and support of many people and institutions. First, I thank Tim Bromage, my advisor, for encouraging me to become a doctoral student, for helping me to believe that I had it in me to do so, and for many years of patient and unfailing belief in my abilities. Tim's enthusiasm, creativity, unique vision and intellectual and technical skills have been, and continue to be, inspirational. This project could never have been conceived or completed without him and his one-of-a-kind lab. I thank Fred Szalay, as well, for sharing his huge and voracious intellect and interest in the natural world. He also encouraged me to embark on this education and helped me conceive of this project. His sparkling delight in, and profound knowledge of, all things biological have always served to remind me how rewarding the fields of vertebrate morphology and evolutionary biology can be. He too, has shown unfailing patience and care. Both Tim and Fred have always been there to help, both professionally and on a personal level, and I am very fortunate to have had classroom, lab, and field time with them, and fortunate as well to consider them my friends.

I also thank my other committee members. Carl Terranova's perspective and support has been invaluable, as has been his expertise. I would not have been able to organize and analyze my data without his critical input. My conversations with him have always served to realign my thinking, and have allowed me to get past a number of conceptual roadblocks. In addition, I am grateful to him for providing access to a great skeletal collection, both material of his own, and from the Duke University Primate Center. Donald Enlow proved to be a wonderful outside reader. He brought his

unmatched experience in the world of bone biology to the discussion; this I expected. But he also offered kindness, respect and welcoming encouragement. My exchanges with him have been illuminating and exciting. Finally, John Wahlert, a committee member during the development stages of this project, has been considerate throughout, both of my work and my well-being. His somewhat different background and perspective has also helped me put together this work.

Others in the field have been of assistance to me. Jim McMahon provided me with an incredibly patient, thorough and useful tutorial in various aspects of statistical analysis, without which I would have been utterly lost. Mitchell Schaffler advised me early on, allowing me to pinpoint some weaknesses and address them. Likewise, I thank anonymous grant application reviewers for both their favorable and critical comments.

Several museums were open-minded enough to provide me with skeletal material, despite the somewhat destructive nature of the preparation methods undertaken in this project. I am therefore very grateful to the following people and institutions: the Field Museum of Natural History and Lawrence R. Heaney & William Stanley, the Museum of Comparative Zoology at Harvard University and Maria Rutzmoser, the Museum für Naturkunde of Humboldt University and Manfred Ade, the National Museum of Natural History and Richard Thorington & Helen Kafka. It goes without saying that this project could not have happened without them.

It would have been exceedingly difficult to pursue this research without the financial support of the following: Eric Delson and the New York Consortium in Evolutionary Biology (NYCEP) for a graduate fellowship and for access to the unparalleled resources of New York City, The Leakey Foundation for a Research Grant,

and the National Science Foundation for a Dissertation Improvement Award (DDI-0205185). I have also been happy for the opportunity to teach at Hunter College, Baruch College, and Lehman College, all of the City University of New York, both for the financial rewards, and also for the professional experience.

My use of the Hard Tissue Research Unit (HTRU) and Analytical Microscopy and Imaging Center in Anthropology (AMICA) facilities was made possible in part by laboratory funding to Tim Bromage from the National Science Foundation and the National Aeronautical and Space Administration. The use of the Syncroscopy system (Synoptics Ltd.) for image acquisition was feasible thanks to the attention of Stephen McJonathan. David Thomas (from the School of Dental Science, University of Melbourne, Australia) developed the Optimas Image Analysis software macro that I used, and both he and Stuart Marquis contributed to its modification for use with non-human primate material. Jan Hinsch at Leica Microsystems, Inc. provided expertise regarding polarized light microscopy, and help with acquiring CPL filters.

My educational and research experience would have been much impoverished in the absence of a number of people. Shannon McFarlin and Haviva Goldman – labmates first and friends foremost – have always been there to knock around new ideas, work out problems, develop methods, share presentations, experiences, successes and frustrations, and laugh about it all. I cherish the many, MANY hours we spent together in the lab, in particular a certain summer of black T-shirts and flip-flops. Shannon has been a great colleague and traveling companion, and I think happily of our collection trip to Berlin. Thanks to Haviva, too, for pioneering the way and handing down her specimen preparation methods, as well as the Optimas macro she acquired from David Thomas.

Justine Salton was yet another fellow student who became a beloved friend. We shared specimen collection and conference trips, a memorable field summer in Bolivia, and many hours talking of both professional and personal matters. I miss her intellect, creativity, energy and, mostly, her friendship. Other people at Hunter College made my tenure as a graduate student more enjoyable: John Oates, Kieran McNulty, Eric Sargis, Josh Linder and other NYCEP students, Warren Pardi, Jennifer Jonak, and undergraduate and graduate students in the lab, some of whom also helped with the specimen preparation for this project.

Several friends, unconnected to the academic part of my life, have been great supporters and I am lucky to have been able to have them around throughout: Diana Ayton-Shenker, Naomi Azrieli, Yuval Brisker, Anne Donovan, Wendy Friedman, Julie Hermos, Sharon Kay, Julie Lenner, Johanne Miucci, and Karen Rutberg.

I could not have asked for a more wonderful family. My parents, Len and Mary Warshaw, have never questioned my path, have always been there to support me in any way they can, and are in large measure responsible for the part of me that is curious, confident and dogged enough to do this work. I know they have never doubted me, and this is the best that a daughter can ask for. My two brothers, Kell and Gabby, and their families, have always allowed me to feel that I have somewhere to go where I can be myself, a great antidote to the sometimes angst of graduate school. A day does not go by that I don't miss Gabby.

Finally I thank my husband Joseph Luders, and my daughter Ivy. Joseph has been my best friend, the one who has had to be most patient, most willing to hear me complain and encourage me to keep going, and most loving. He has done it all like nobody else

could have, and I wouldn't have made it through without him. The dream of Ivy, and then her reality, provided the last push to get it all done.

## Table of Contents

**Abstract** ..... iv

**Acknowledgements** ..... vi

**Table of Contents** ..... xi

**List of Tables** ..... xviii

**List of Figures** ..... xx

**Chapter 1. Introduction** ..... 1
1.1 Introduction ..... 1
1.2 Background: previous comparative bone histology studies ..... 4
1.3 Relevance of this study ..... 8
1.4 Background on bone as structure and tissue ..... 10
*1.4.1 Bone as structure ..... 10*
*1.4.2 Bone as tissue ..... 14*
1.5 Summary ..... 16

**Chapter 2. Materials and Methods** ..... 18
2.1 Materials ..... 18
*2.1.1 Sample composition and provenience ..... 18*
*2.1.1.1 Sample selection ..... 18*
*2.1.1.2 Element selection and section sampling location ..... 23*
2.2 Methods ..... 24
*2.2.1 Specimen collection and labeling ..... 24*
*2.2.2 Specimen processing ..... 27*
*2.2.3 Section preparation ..... 28*
*2.2.4 Specimen imaging ..... 30*
*2.2.5 Image processing and data analysis ..... 31*

**Chapter 3. Sample Primate Natural Histories** ..... 32
3.1 Introduction ..... 32
3.2 Background ..... 32
*3.2.1 General background on life history ..... 32*
*3.2.2 General background on positional behavior ..... 33*
*3.2.3 General Background on phylogeny ..... 35*
3.3 Individual taxon natural histories ..... 37
*3.3.1 Strepsirhini ..... 40*
*3.3.1.1 Galagidae: lesser galagos ..... 40*
*3.3.1.2 Galagidae: greater galagos ..... 43*
*3.3.1.3 Lorisidae ..... 45*
*3.3.1.4 Lemuridae ..... 49*
*3.3.1.5 Indriidae ..... 52*
*3.3.1.6 Cheirogaleidae ..... 55*

*3.3.2 Haplorhini*……..58
*3.3.2.1 Tarsiidae*……*58*
*3.3.2.2 Callitrichidae*…… *60*
*3.3.2.3 Cebidae*……..*62*
*3.3.2.4 Atelidae*……..*64*
3.4 Conclusion…….. 66

**Chapter 4. Primary Tissue Type Distributions** ……67
4.1 Introduction ……67
4.2 Background on bone tissue typology ……68
*4.2.1 Fibrillar structure*…….. *69*
*4.2.2 Primary tissue patterns*……..… *71*
*4.2.2.1 Vascular canals*…… *71*
*4.2.2.2 Lamellar-zonal bone*…… *71*
*4.2.2.3 Fibro-lamellar bone*…….. *72*
*4.2.2.4 Compacted coarse cancellous bone*…….. *73*
*4.2.2.5 Cancellous bone*…… *73*
*4.2.2.6 Other patterns*……... *73*
4.3 Existing hypotheses regarding the factors determining primary tissue type variability……74
*4.3.1 Tissue types and development*…… *75*
*4.3.2 Tissue types and growth rate*…… *75*
*4.3.3 Tissue types and mechanical properties of bone*……... *77*
4.4 Objectives of the current study……... 78
4.5 Methods …… 79
*4.5.1 Tissue typing scheme used here*…… *79*
*4.5.2 Tissue type identification*……... *82*
*4.5.2.1 Woven-fibered born (WOV)*…….. *83*
*4.5.2.2 Parallel-fibered bone (PF)*……*83*
*4.5.2.3 Lamellar bone (LAM)*……*83*
*4.5.2.4 Hybrid bone (HYB)*……*84*
*4.5.2.5 Slow fibrolamellar bone (SFBL)*……... *84*
*4.5.2.6 Fast fibrolamellar bone (FFBL)*……... *85*
*4.5.2.7 Compacted coarse cancellous bone (CCC)*…….. *85*
*4.5.2.8 Sharpey's fibers (SF)*……*85*
*4.5.2.9 Intracortically remodeled bone (HAV)*…… *86*
*4.5.2.10 A note on collapsing tissue type categories*…… *86*
*4.5.3 Image processing and quantification of tissue types*……. *87*
*4.5.4 Subjectivity in tissue identification*…… *89*
*4.5.5 Statistical and descriptive analyses*……... *90*
*4.5.6 Independent variables included in the multiple regression analyses*……*92*
*4.5.6.1 Total cortical area*……*92*
*4.5.6.2 Phylogenetic status*……*93*
*4.5.6.3 Positional behavior*……... *94*
*4.5.6.4 A note on growth rate*……*95*

*4.5.7 Key to abbreviations used in the following sections……. 96*
4.6 Results……97
*4.6.1 Periosteal/endosteal comparisons……97*
*4.6.2 Sample-wide patterns of tissue types in endosteal bone……99*
*4.6.3 Sample-wide patterns of tissue types in periosteal bone…... 100*
*4.6.3.1 Femur…… 101*
*4.6.3.2 Humerus…… 102*
*4.6.3.3 Radius, ulna and tibia……... 102*
*4.6.4 Factors accounting for variation in primary tissue types across the entire sample……107*
*4.6.4.1 FAST bone……108*
*4.6.4.2 PF bone……111*
*4.6.4.3 LAM+HYB bone……114*
*4.6.5 Comparison between elements: individual specimens……...119*
*4.6.6 Characterization of individual taxa and targeted comparison amongst taxa……..……122*
*4.6.6.1 Intra- and intertaxonomic diversity……...122*
*4.6.6.2 Consistency within taxa: intrataxonomic variation for individual elements…….. 123*
*4.6.6.3 Consistency within taxa: comparing means for skeletal elements within taxa……..… 126*
*4.6.6.4 Consistency between taxa: means for skeletal elements across taxa……..126*
*4.6.6.5 Characterization of femoral patterns of primary tissue type distributions for individual taxa…….. 127*
*4.6.6.5.1 Lesser galagos 127*
*4.6.6.5.2 Greater galagos……... 128*
*4.6.6.5.3 Lorisidae…….. 129*
*4.6.6.5.4 Cheirogaleidae…… 131*
*4.6.6.5.5 Indriidae……...132*
*4.6.6.5.6 Lemuridae…… 133*
*4.6.6.5.7 Tarsiidae…….. 134*
*4.6.6.5.8 Callitrichidae……... 135*
*4.6.6.5.9 Cebidae…… 136*
*4.6.6.5.10 Atelidae…… 137*
*4.6.7 Comparisons of femoral means between select pair of taxa……137*
*4.6.7.1 Lesser galagos vs. greater galagos……..…138*
*4.6.7.2 Greater galagos vs. Lorisidae…… 139*
*4.6.7.3 Tarsiidae vs. Lesser galagos……...140*
*4.6.7.4 Lesser galagos vs. Cheirogaleidae……141*
*4.6.7.5 Lesser galagos vs. Indriidae……...143*
*4.6.7.6 Indriidae vs. Lemuridae……..143*
*4.6.7.7 Indriidae vs. Atelidae……..144*
*4.6.7.8 Cheirogaleidae vs. Callitrichidae……...145*
*4.6.7.9 Cebidae vs. greater galagos……... 146*

*4.6.7.10 Cebidae vs. Lorisidae…… 147*
*4.6.7.11 Callitrichidae vs. Cebidae…….. 148*
*4.6.7.12 Cebidae vs. Atelidae……149*
*4.6.7.13 Summary of paired comparisons of means…….150*
4.7 Discussion……...151
*4.7.1 Primary tissue types and element specific ontogenies……...151*
*4.7.2 Primary tissue types and body size……157*
*4.7.3 Primary tissue types and growth rate……159*
*4.7.4 Primary tissue types and positional behavior……163*
*4.7.5 Primary tissue types and phylogeny…….. 166*
4.8 Summary and conclusions……..…… 168

**Chapter 5. Intracortical Remodeling**……...170
5.1 Introduction……170
5.2 Background on intracortical remodeling…… 171
5.3 Existing hypotheses regarding the factors determining variation in intracortical remodeling……...175
*5.3.1 Mechanical factors…… 175*
*5.3.2 Life history factors……179*
*5.3.3 Mineral metabolism……... 181*
*5.3.4 Growth processes……...182*
*5.3.5 A combination of factors……183*
5.4 Objectives of the current study……... 183
5.5 Methods…….…. 184
*5.5.1 Identification of intracortical remodeling……. 184*
*5.5.2 Image processing and quantification of tissue types……. 185*
*5.5.3 Statistical and descriptive analyses……... 186*
5.6 Results……188
*5.6.1 Sample wide patterns of remodeling: whole cortices…… 188*
*5.6.2 Sample wide patterns of remodeling: quadrant patterns 190*
*5.6.3 Factors accounting for variation in primary tissue types across the entire sample…...……..……192*
*5.6.4 Variation in quadrant patterns of remodeling: comparison within and among positional behavior groups…….…… 196*
*5.6.5 Comparison between elements: PB or PHYLO patterns…... 199*
*5.6.6 Characterization of individual taxa ……..…200*
*5.6.6.1 Intra- and intertaxonomic diversity…….. 200*
*5.6.6.2 Consistency within taxa: intrataxonomic variation for individual elements……...200*
*5.6.6.3 Characterization of patterns of primary tissue type distributions for individual taxa…… 203*
*5.6.6.3.1 Lesser galagos……. 204*
*5.6.6.3.2 Greater galagos……..…. 205*
*5.6.6.3.3 Lorisidae…….. 207*
*5.6.6.3.4 Cheirogaleidae…… 209*
*5.6.6.3.5 Indriidae…….. 211*

*5.6.6.3.6 Lemuridae…… 213*
*5.6.6.3.7 Tarsiidae…….. 215*
*5.6.6.3.8 Callitrichidae……... 216*
*5.6.6.3.9 Cebidae…… 217*
*5.6.6.3.10 Atelidae…… 219*
5.7 Discussion……...220
*5.7.1 Intracortical remodeling and developmental patterns…….. 220*
*5.7.2 Intracortical remodeling and body size……224*
*5.7.3 Intracortical remodeling and mechanical adaptation……...226*
*5.7.4 Intracortical remodeling, phylogeny, growth rate and metabolism…… 241*
5.8 Summary and conclusions……..242

**Chapter 6. Collagen Fiber Orientation**……...244
6.1 Introduction…….244
6.2 Background on collagen fiber orientation……...…….…….. 245
6.3 Hypotheses regarding the factors determining variation in collagen fiber orientation……..…….249
6.4 Objectives of the current study……...251
6.5 Methods…….…. 252
*6.5.1 Polarized light and circularly polarized light imaging …… 252*
*6.5.2 Standardization of light parameters for quantitative cpl imaging……. 254*
*6.5.3 Image processing……... 257*
*6.5.4 Quantification of collagen fiber orientation……..258*
*6.5.5 Statistical and descriptive analyses……... 260*
6.6 Results…….262
*6.6.1 Collagen fiber orientation in endosteal tissues……. 262*
*6.6.2 Sample-wide patterns of collagen fiber orientation in periosteal primary tissues: whole cortices…….……... 263*
*6.6.3 Sample-wide patterns of collagen fiber orientation in periosteal primary tissues: sectoral patterns……..... 267*
*6.6.4 Sample-wide patterns of collagen fiber orientation in intracortically remodeled tissue: whole cortices……...270*
*6.6.5 Sample-wide patterns of collagen fiber orientation in intracortically remodeled tissue: sectoral patterns……...273*
*6.6.6 Comparing periosteal primary and intracortically remodeled tissue: whole cortices……...274*
*6.6.7 Comparing periosteal primary and intracortically remodeled tissue: sectoral patterns……..…….276*
*6.6.8 Factors accounting for variation in collagen fiber orientation across the entire sample……..278*
*6.6.9 Collagen fiber orientation and tissue type……286*
*6.6.10 Comparison between elements: PB patterns in periosteal primary tissue…… 290*
*6.6.11 Comparison between elements: PB patterns in*

*secondary osteonal tissue*…….. *293*
*6.6.12 Comparison between sectors: PB patterns in periosteal primary tissue*……....*294*
*6.6.13 Comparison between sectors: PB patterns in secondary osteonal tissue*……..… 295
*6.6.14 Characterization of individual taxa*……*295*
*6.6.14.1 Intra- and intertaxonomic diversity*…… *295*
*6.6.14.2 Consistency within taxa: intrataxonomic variation for individual elements*……...*297*
*6.6.14.3 Characterization of patterns of collagen fiber orientation for individual taxa*……...*300*
*6.6.14.3.1 Lesser galagos*…….……*300*
*6.6.14.3.2 Greater galagos*……... *300*
*6.6.14.3.3 Lorisidae*……...*301*
*6.6.14.3.4 Cheirogaleidae*…… *302*
*6.6.14.3.5 Indriidae*……... *303*
*6.6.14.3.6 Lemuridae*…….……*303*
*6.6.14.3.7 Tarsiidae*…….……..*304*
*6.6.14.3.8 Callitrichidae*…….…... *305*
*6.6.14.3.9 Cebidae*…….…*305*
*6.6.14.3.10 Atelidae*…….…...*306*
*6.6.14.4 Summary of patterns of collagen fiber orientation for individual taxa*…….. *307*
6.7 Discussion……...307
*6.7.1 Range of variation in collagen fiber orientation in the study sample*…….…....*307*
*6.7.2 Collagen fiber orientation and primary tissue type*……...*311*
*6.7.3 Collagen fiber orientation and intracortical remodeling*…..*316*
*6.7.4 Collagen fiber orientation and body size*……...*322*
*6.7.5 Collagen fiber orientation and positional behavior*…….. *323*
*6.7.6 Collagen fiber orientation and phylogeny*……*338*
6.8 Summary and conclusions……... 338

**Chapter 7. Summary, Conclusions and Future Research**…….340
7.1 Introduction…….340
7.2 Summary of findings…….. 341
*7.2.1 Primary tissue types*……...*341*
*7.2.2 Intracortical remodeling*……*342*
*7.2.3 Collagen fiber orientation*……. *343*
7.3 Conclusions…….344
7.4 Contributions…….. 345
*7.4.1 To anthropology*……*345*
*7.4.2 Beyond anthropology*……*347*
7.5 Future research……349

**Appendix A. Cross Sectional Geometry**…….…… 352

A.1 Introduction……352
A.2 Background on cross-sectional geometry……..352
A.3 Some preliminary data……...356
A.4 Conclusions……358

**Appendix B. Color Mapped Specimen Images**…….. 359
B.1 Introduction……359
B.2 Lesser galagos……360
B.3 Greater galagos…….. 362
B.4 Lorisidae…….364
B.5 Lemuridae…….. 366
B.6 Indriidae……. 368
B.7 Cheirogaleidae……... 370
B.8 Tarsiidae……372
B.9 Callitrichidae……..374
B.10 Cebidae…….376
B.11 Atelidae…… 378

**Appendix C. Data Tables**……. 379

**Appendix D. Imaging and Image Processing Functions**……... 404
D.1 Introduction……404
D.2 LM imaging……... 404
D.3 Quantitative CPL imaging……. 405
D.4 LM image processing……406
D.5 CPL image processing……... 406
D.6 Quantitative CPL look-up-table……407

**References Cited**……... 408

## List of Tables


1.1 Relevant existing research, and proposed work ……...……..……... 9
2.1 Specimen list and provenience ……...……... 22
3.1 Taxon life history and positional behavior information ……...……..… 39
4.1 Correlation between skeletal element length and midshaft (TCA) ……... 93
4.2 Multiple regression results for primary tissue types for the entire sample ……107
4.3 Multiple regression results for FAST bone for the entire sample…….. 109
4.4 Multiple regression results for PF bone for the entire sample……112
4.5 Multiple regression results for LAM+HYB bone for the entire sample…….115
4.6 Femoral relative proportions of primary tissue types by taxon……..…. 124
5.1 Multiple regression results for LAM+HYB bone for the entire sample…….192
5.2 Multiple regression betas…… 194
5.3 Summary of percent intracortically remodeled bone for individual elements and taxa…….. 200
6.1 Multiple regression results for collagen fiber orientation in primary periosteal and intracortically remodeled bone for the entire sample……..279
6.2 Multiple regression betas for collagen fiber orientation in primary periosteal bone for the entire sample……..279
6.3 Multiple regression betas for collagen fiber orientation in intracortically remodeled bone for the entire sample…….280
6.4 Sign test results for comparison among primary periosteal tissue type mean gray values for all skeletal elements……. 287
6.5 Element ranges for mean gray values for all sample individuals……... 292
6.6 Summary of whole cortex mean grays for individual elements and taxa, for both periosteal primary and secondary osteonal tissue…….296
C.1 Femur primary tissue type and intracortical remodeling data Part I…….. 379
C.2 Femur primary tissue type and intracortical remodeling data Part II……. 380
C.3 Femur primary tissue type and intracortical remodeling data Part III……381
C.4 Femur collagen fiber orientation data Part I……...382
C.5 Femur collagen fiber orientation data Part II……. 383
C.6 Humerus primary tissue type and intracortical remodeling data Part I……... 384
C.7 Humerus primary tissue type and intracortical remodeling data Part II…….385
C.8 Humerus primary tissue type and intracortical remodeling data Part III……386
C.9 Humerus collagen fiber orientation data Part I……...387
C.10 Humerus collagen fiber orientation data Part II……. 388
C.11 Radius primary tissue type and intracortical remodeling data Part I ……389
C.12 Radius primary tissue type and intracortical remodeling data Part II…… 390
C.13 Radius primary tissue type and intracortical remodeling data Part III……... 391
C.14 Radius collagen fiber orientation data Part I…….. 392
C.15 Radius collagen fiber orientation data Part II……393
C.16 Ulna primary tissue type and intracortical remodeling data Part I……394
C.17 Ulna primary tissue type and intracortical remodeling data Part II……395
C.18 Ulna primary tissue type and intracortical remodeling data Part III…….. 396
C.19 Ulna collagen fiber orientation data Part I……..397
C.20 Ulna collagen fiber orientation data Part II…… 398

C.21 Tibia primary tissue type and intracortical remodeling data Part I…… 399
C.22 Tibia primary tissue type and intracortical remodeling data Part II……... 400
C.23 Tibia primary tissue type and intracortical remodeling data Part III……..401
C.24 Tibia collagen fiber orientation data Part I……402
C.25 Tibia collagen fiber orientation data Part II……403
D.1 Look-up-table (LUT) set-up……... 407

## List of Figures


2.1 Landmark standards for identifying maximum diaphyseal length ……..…. 24
2.2 Reconstructed bone ……...…… 26
2.3 Diagram of bone block notch orientation ……...……..…. 27
3.1 Sample primate taxonomy and systematics ……...……..……. 36
3.2 Lesser galagos ……...……...…43
3.3 Greater galagos ……...…….. 45
3.4 Lorisidae …… 49
3.5 Lemuridae ……...52
3.6 Indriidae ……55
3.7 Cheirogaleidae ……... 58
3.8 Tarsiidae ……..... 60
3.9 Callitrichidae……...62
3.10 Cebidae …….. 64
3.11 Atelidae……...65
4.1 Tissue type examples……...82
4.2 Tissue map color code…… 88
4.3 Sample cortex…… 88
4.4 Tissue mapping repeated measures…… 89
4.5 Proportions (relative to TCA) of periosteal, endosteal and CCC bone in each element for all individuals combined…… 98
4.6 Midshaft sections from a single *Otolemur crassicaudatus* individual …….. 99
4.7 Proportions (relative to endosteal cortex) of FAST, PF and LAM+HYB bone in the femur for all individual combined……... 100
4.8 Proportions (relative to periosteal cortex) of FAST, PF and LAM+HYB bone in the femur for all individuals combined……...101
4.9 Proportions (relative to periosteal cortex) of FAST, PF and LAM+HYB bone in the humerus for all individuals combined……...102
4.10 Proportions (relative to periosteal cortex) of FAST, PF and LAM+HYB bone in the radius for all individuals combined……...103
4.11 Proportions (relative to periosteal cortex) of FAST, PF and LAM+HYB bone in the ulna for all individuals combined…… 104
4.12 Proportions (relative to periosteal cortex) of FAST, PF and LAM+HYB bone in the tibia for all individuals combined…… 104
4.13 Comparison of mean periosteal tissue type values for all five skeletal elements for all individuals……105
4.14 Comparison of individual values for LAM+HYB bone in the femur and tibia..106
4.15 Comparison of individual values for PF bone in the femur and tibia……106
4.16 Comparison of individual values for LAM+HYB bone in the humerus and radius……106
4.17 Proportions of periosteal FAST bone relative to the periosteal cortex, as a function of TCA……...109
4.18 Femoral proportions of periosteal FAST bone, categorized by PB……111
4.19 Femoral proportions of periosteal PF bone relative to the periosteal cortex, as a function of TCA……...112

4.20 Femoral proportions of periosteal PF bone, categorized by PHYLO……113
4.21 Femoral proportions of periosteal PF bone, categorized by PB……114
4.22 Proportions of periosteal LAM+HYB bone relative to the periosteal cortex, as a function of TCA……...117
4.23 Femoral proportions of periosteal LAM+HYB bone, categorized by PHYLO..117
4.24 Tibial proportions of periosteal LAM+HYB bone, categorized by PB……..118
4.25 Proportions of LAM+HYB and LAM bone in the humerus and femur of all sample individuals, categorized by taxon……... 121
4.26 Mean proportions of LAM+HYB and LAM bone in the humerus and femur of all sample individuals, categorized by taxon……... 121
4.27 Absolute values of LAM+HYB in the humerus and femur of all sample individuals, categorized by taxon……... 122
4.28 Individual values for the proportions of FAST, PF and LAM+HYB bone in the femur of Cebidae, greater galagos and Lorisidae……. 125
4.29 *Galago senegalensis* midshaft femur……..…128
4.30 *Otolemur crassicaudatus* midshaft femur…….. 129
4.31 *Nycticebus coucang* midshaft femur……...130
4.32 *Mirza coquereli* midshaft femur……. 131
4.33 *Propithecus* sp. midshaft femur……..…… 132
4.34 *Varecia variegata* midshaft femur……..…133
4.35 *Tarsius spectrum* midshaft femur……134
4.36 *Callithrix geoffroyi* midshaft femur…… 135
4.37 *Saimiri* sp. midshaft femur……. 136
4.38 *Ateles* sp. midshaft femur……137
4.39 Relative mean proportions of primary tissue types in the greater and lesser galagos……... 139
4.40 Relative mean proportions of primary tissue types in the greater galagos and lorisids……..…… 140
4.41 Relative mean proportions of primary tissue types in the lesser galagos and tarsiids…….……. 141
4.42 Relative mean proportions of primary tissue types in the lesser galagos and cheirogaleids……..….. 142
4.43 Relative mean proportions of primary tissue types in the lesser galagos and indriids……..…... 143
4.44 Relative mean proportions of primary tissue types in the indriids and. the lemurids……...…… 144
4.45 Relative mean proportions of primary tissue types in the indriids and atelids……..… 145
4.46 Relative mean proportions of primary tissue types in the cheirogaleids and challitrichids…….....146
4.47 Relative mean proportions of primary tissue types in the greater galagos and cebids……..…. 147
4.48 Relative mean proportions of primary tissue types in the lorisids and the cebids…… 148
4.49 Relative mean proportions of primary tissue types in the callitrichids and cebids……... 148

4.50 Relative mean proportions of primary tissue types in cebids and atelids……...149
5.1 Secondary osteon formation……... 174
5.2 Cortical sectors……... 186
5.3 Proportions (relative to TCA) of intracortically remodeled bone in each element for all individuals combined……. 189
5.4 Proportions (relative to TCA) of intracortically remodeled bone in the femur vs. humerus and ulna……189
5.5 Proportions (relative to TCA) of intracortically remodeled bone in the femur vs. tibia and humerus vs. ulna…….. 190
5.6 Proportions (relative to TCA) of intracortically remodeled bone in the ulna vs. radius……. 190
5.7 Femoral and tibial proportions (relative to TCA) of intracortically remodeled bone for individual quadrants……... 191
5.8 Humeral proportions of remodeled bone relative to TCA, as a function of TCA…… 194
5.9 Humeral and femoral proportions of remodeled bone, categorized by PB…… 195
5.10 Humeral proportions of remodeled bone, categorized by PHYLO…… 196
5.11 Quadrant patterns of remodeling within PB categories……...197
5.12 Quadrant patterns of remodeling within PB categories……...198
5.13 Proportions of remodeled bone in all sample individuals, categorized by PB... 200
5.14 Individual values for proportions of intracortical remodeling……202
5.15 Muscular origins and insertions at the midshaft……203
5.16 Lesser galago femora……..205
5.17 Greater galago femora…… 207
5.18 Lorisid femora…… 209
5.19 Cheirogaleid femora……... 210
5.20 Indriid femora……213
5.21 Lemurid femora…….. 215
5.22 Tarsiid femora…….216
5.23 Callitrichid femora……..217
5.24 Cebid femora…….. 219
5.25 Atelid femora……...220
5.26 Cheirogaleid radii……... 227
5.27 Cebid tibiae……228
5.28 Cebid humeri…….. 235
6.1 CPL filter configuration…… 254
6.2 Image of turkey tendon standard, with high-band green filter……... 257
6.3 Stretching of turkey tendon standard……...258
6.4 LUT color coding scheme…….. 259
6.5 *Galago senegalensis* humerus with masking and application of LUT……... 259
6.6 *Galago senegalensis* humerus with conversion of LUT to Optimas-appropriate format……260
6.7 LUT bin values for all sample femora……263
6.8 LUT bin values for all sample humeri……264
6.9 LUT bin values for all sample tibiae……... 264
6.10 LUT bin values for all sample radii……264

6.11 LUT bin values for all sample ulnae…….. 265
6.12 LUT bin1 means for all sample elements……...265
6.13 LUT bin2 means for all sample elements……...266
6.14 Mean gray values for all elements……..267
6.15 Mean gray value of humeri relative to femora……... 267
6.16 Mean gray value of medial vs. lateral quadrants in the femur……268
6.17 Mean gray value of medial vs. lateral and medial vs. posterior quadrants in the humerus……269
6.18 Mean gray value of medial vs. posterior quadrants in the radius……... 270
6.19 Mean gray value of anterior vs. posterior quadrants in the ulna…… 270
6.20 Mean gray value for intracortically remodeled bone comparing skeletal elements……. 272
6.21 Mean gray value for intracortically remodeled bone in the femur vs. the ulna……. 272
6.22 Mean gray value for intracortically remodeled bone in the humerus vs. the tibia……. 273
6.23 Mean gray value for intracortically remodeled bone in the anterior vs. posterior quadrants of the humerus…….274
6.24 Mean gray value for periosteal primary vs. intracortically remodeled bone for all skeletal elements……... 275
6.25 Mean gray value for periosteal primary vs. intracortically remodeled bone in the femur……275
6.26 Mean gray value for periosteal primary vs. intracortically remodeled bone for the tibia…….276
6.27 Mean gray value for periosteal primary vs. intracortically remodeled bone for the humerus……... 276
6.28 Periosteal primary vs. intracortically remodeled bone for the medial quadrant in the femur……...277
6.29 Periosteal primary vs. intracortically remodeled bone for the medial quadrant in the tibia…… 277
6.30 Tibial mean gray values for periosteal primary tissue, as a function of TCA… 281
6.31 Femoral mean gray values for periosteal primary tissue, categorized by PB….283
6.32 Femoral mean gray values for periosteal primary tissue, as a function of TCA, categorized by PB…….……... 283
6.33 Femoral mean gray values for intracortically remodeled bone, categorized by PB…….……...285
6.34 Femoral mean gray values for individual periosteal primary tissue types……. 287
6.35 Mean gray values for LAM vs. PF bone in the femur…… 288
6.36 Femoral mean gray values for individual periosteal primary tissue types and intracortically remodeled bone……... 289
6.37 Mean gray values for LAM vs. intracortically remodeled bone in the femur… 289
6.38 Mean gray values for all sample individuals in the femur vs. the tibia, categorized by PB…….……...291
6.39 Mean gray values for all sample individuals in the humerus vs. the tibia, categorized by PB……...292

6.40 Mean gray values for all sample individuals in the femur vs. the radius, categorized by PB……...293
6.41 Humeral periosteal primary bone mean gray values for individual quadrants, categorized by PB…….. 294
6.42 Radial periosteal primary bone mean gray values for individual quadrants, categorized by PB……...295
6.43 Example of similar magnitude and pattern of brightness……... 298
6.44 Example of similar magnitude and pattern of brightness with a single outlier.. 298
6.45 Example of similar magnitude of brightness, but variable pattern…….298
6.46 Example of similar pattern of brightness, but variable magnitude…….299
6.47 Example of variable magnitude and brightness……..299
6.48 Examples of bright bone areas imaged with the turkey tendon standard…….. 310
6.49 Example of an area with both bright and dark lamellar bone…….....312
6.50 Example of fibrolamellar bone with bright primary osteons……...313
6.51 Examples of bright secondary osteons……..……. 321
6.52 Example of a grouping of bright secondary osteons…….. 321
6.53 Example of ringed secondary osteons…… 322
6.54 Example of dark secondary osteons replacing bright primary tissue……. 322
6.55 Examples of three classically categorized secondary osteon types…… 326
A.1 Relative strength of the femur and humerus in axial compression or tension…357
B.1 Lesser galago femora……...360
B.2 Lesser galago humeri……...360
B.3 Lesser galago tibiae…… 361
B.4 Lesser galago radii……. 361
B.5 Lesser galago ulnae…….361
B.6 Greater galago femora…… 362
B.7 Greater galago humeri…… 362
B.8 Greater galago tibiae……...362
B.9 Greater galago radii…… 363
B.10 Greater galago ulnae……...363
B.11 Lorisid femora…… 364
B.12 Lorisid humeri…… 364
B.13 Lorisid tibiae……...365
B.14 Lorisid radii…… 365
B.15 Lorisid ulnae……... 365
B.16 Lemurid femora……... 366
B.17 Lemurid humeri……... 366
B.18 Lemurid tibiae…….367
B.19 Lemurid radii……... 367
B.20 Lemurid ulnae…….367
B.21 Indriid femora…….368
B.22 Indriid humeri…….368
B.23 Indriid tibiae…….369
B.24 Indriid radius……...369
B.25 Indriid ulna……..369
B.26 Cheirogaleid femora……... 370

B.27 Cheirogaleid humeri……... 370
B.28 Cheirogaleid tibiae……..370
B.29 Cheirogaleid radii……... 371
B.30 Cheirogaleid ulna……371
B.31 Tarsiid femora……372
B.32 Tarsiid humeri……372
B.33 Tarsiid tibiae……... 372
B.34 Tarsiid radii……373
B.35 Tarsiid ulnae……... 373
B.36 Callitrichid femora……..374
B.37 Callitrichid humeri……..374
B.38 Callitrichid radius……... 375
B.39 Callitrichid ulna…….. 375
B.40 Cebid femora…….. 376
B.41 Cebid humeri…….. 376
B.42 Cebid tibiae……376
B.43 Cebid radii…….. 377
B.44 Cebid ulnae……377
B.45 Atelid femora……...378
B.46 Atelid humeri……...378

# Chapter 1

# Introduction and Background

## 1.1 Introduction

The study of comparative osteology has yielded an abundant literature regarding the form, function and biological roles of bones and whole skeletons. These data have been variably applied to the fossil record, contributing to the reconstruction of locomotion, life history features and the evolutionary histories of the better-known extinct animals, yet many questions regarding the paleobiology of fossil taxa remain. The vast majority of work to date has examined whole bones and their macroscopically defined parts, rather than their microstructure. However, such inquiry often suffers from superficial analogies with living taxa, as well as from the frequent incompleteness of fossil material (e.g., Szalay, 2000; Szalay & Sargis, 2001). These shortcomings in turn limit phylogenetic interpretations. The additional insights to be offered from an exploration of bone microstructure have been relatively neglected. As de Ricqlès notes, "thin section techniques…have been used more rarely and somehow reluctantly by vertebrate palaeontologists…even up to the present day" (de Ricqlès, 1992, p. 40). The situation has somewhat ameliorated in the years since de Ricqlès made this statement, in particular with respect to the study of dinosaur paleohistology. For example, the histological studies of researchers such as Chinsamy, Erikson, Horner, de Ricqlès, and their colleagues have provided dramatic support for the reevaluation of the physiology and life history in a number of fossil reptilian and mammal-like reptile species (Curry, 1998; Botha & Chinsamy, 2000; Erickson & Tumanova, 2000; Erickson et al., 2001; Horner et al., 2000;

Horner & Padian, 2004; de Ricqlès et al, 2000; Padian et al., 2001). However, with a few notable exceptions, there remains a dearth of data regarding both extant and extinct mammalian taxa (de Ricqlès et al., 1991).

At the microstructural level, bone is hypothesized to record aspects of the biomechanics and life history of vertebrates. It follows that significant information with bearing upon the biology and behavior of fossil taxa is potentially encoded therein (Enlow, 1966). The potential for recovery of this information is particularly exciting in light of recent methodological advances (e.g., automated capturing of high resolution images of entire bone cross-sections). However, before interpretations of microstructure in extinct species are possible, the extent of variability that exists in living groups, and the relationship of this variability to biological and behavioral features, must be understood.

I report here on variation in primary bone tissues, intracortical remodeling, and collagen fiber orientation in midshaft cortices from the long bone postcrania of a range of extant primates. Employing conventional and polarized light microscopy techniques, as well as original methods of comparison between histological variables, the goal has been to qualitatively and quantitatively describe the relationship of these microstructural features to the kinematic, adaptive and life history features of species. The study is the first to quantitatively examine these three features within a single sample. This study also represents a departure from most earlier comparative mammalian bone microstructural studies in that the sample is focused, yet broad enough to provide a phylogenetic context and to explore a wide range of variability.

The objectives are twofold. First, employing a carefully selected comparative sample, I assess hypotheses regarding the principal factors affecting the intertaxonomic variability in each of the microstructural features, within the context of their macrostructure. Many hypotheses, at times conflicting, exist regarding the causal factors behind the variability that has been observed. Second, I explore the possibilities for use of these variables to test specific ideas about organismal mammalian biology: given a cross section of bone, what can we learn of the positional behavior and life history of an individual? In conclusion, I consider the potential application of the results of living models to the fossil taxa.

The remainder of this chapter is devoted to a review of previous bone microstructural studies relevant to the current research, a discussion of the macrostructural context for bone histological research, and a review of the fundamentals of bone microanatomy. Chapter 2 describes the materials and methods used in this work, including sample selection and composition, specimen collection and processing, and microscopic imaging techniques. In Chapter 3 I provide life history and positional behavior background for all taxa included in the sample. Chapters 4, 5 and 6 are devoted to an account of diversity in primary tissue types, intracortical remodeling (Haversian bone) and collagen fiber orientation patterns respectively. Variation across cortices, within individuals, and between taxa is qualitatively and quantitatively described, and the relationship between observed patterns and the life history and positional behavior features of the sample taxa is discussed. Image processing methods and data analysis approaches, specific to the variables discussed in each of Chapters 4 through 6, are included in each chapter. In addition, each of these three chapters includes a review of

relevant research. Chapter 7 offers a summary and synthesis of findings, a discussion of contributions to anthropology and beyond, and future research directions.

### 1.2 Background: previous comparative bone histology studies

Since the invention of the microscope there have been many investigations into the structure and composition of the bony tissue of vertebrates. The 17th to 19th centuries witnessed the description of its microscopic constituent parts and varied organization by such workers as Leeuwenhoek, the renowned Havers (employing a magnifying glass), and others (see Enlow, 1962a, 1962b, 1963; Bromage, 1986; Martin & Burr, 1989; for reviews). By the mid-19th C., scholars had produced broadly comparative works in bone histology (e.g., Quekett 1849, 1855; Foote, 1913, 1916; Crawford, 1940). In these publications, the objective was primarily taxonomic: it was believed that bone histology could be employed by paleontologists to identify otherwise intractable specimens.

> "*In each of the four great classes of animals [fish, reptiles, birds, mammals], the bone-cells present certain peculiarities in their form, which, when once an observer is conversant with, he would be enabled to satisfy himself as to the true affinities of doubtful specimens of organic remains*" (Quekett, 1849, p. 47).

This work, whether pre- or post *The Origin of Species*, tends to be *scala naturae*-like in approach, emphasizing the coincidence of more "primitive" and less functionally "perfect" bony tissues with more "primitive" groups of vertebrates. Although there is some consideration of life history and functional factors as important determinants of bone microstructure (e.g., Foote, 1916), the studies are of limited interest largely because of the lack of knowledge regarding bone biology at the time. However, in later works such as de Ricqlès (1968-1978), Amprino & Godina (1947), and Enlow & Brown (1956,

1957, 1958), a modern understanding of bone was applied to broad comparative samples. These seminal publications emphasized the diversity of tissue types that can be found among vertebrates and, while recognizing that group patterns do exist, did not place primary importance on taxonomy. There was an appreciation that convergences, either kinematic or with respect to life history, can lead to near identity in bone histology among disparate groups of vertebrates (de Ricqlès, 1992). Therefore, today the emphasis is on function, and the possibility that bone microstructure may offer a record of such adaptive aspects of organismal biology as patterns of growth, size, age, physiological adaptations, mineral homeostasis, and biomechanics (de Ricqlès, 1992).

> *"…distinction [between species] is not always easy and often not even possible…Evidently structure…particular to the order and single species is masked by changes dependent on similar factors in all the species, for which the bones of all mammals are resembling one another a certain amount"* (Amprino & Godina, 1947, p. 346-347, translated from the original Italian by the author).

> *"The impression that the bone of all lower vertebrates is simple and primitive in structure, and that the developing bone of mammals recapitulates such phylogeny, is not justified. Neither can the bone tissues of mammals be regarded as a culmination of skeletal tissue evolution"* (Enlow & Brown, 1958, p. 227).

It follows that comparative bone histology should take into account a variety of interdependent factors, and that comprehensive accounts of comparative bone microstructure – reaching beyond description to attempt functional analysis – are thus limited in number and scope. Nevertheless, despite the inherent difficulties, a number of important studies pertinent to the proposed research (i.e., including comparative mammalian samples) have been produced within the context of this more modern understanding of bone (e.g., Amprino & Godina, 1947; Burr, 1979, 1992; Enlow & Brown, 1958; Jowsey 1966, 1968; Singh et al., 1974). Following is a brief review of these. With regard to each, the

questions that I address are as follows: 1) What microstructural variables have been examined? 2) What are the explanations that have been put forth to account for differences between taxa? (See Table 1.1).

Studies which include comparative descriptions of mammalian bone histology span works of the 19th Century through those undertaken in recent years. The earliest of these, produced when the understanding of bone tissue was less comprehensive than today – as discussed above – can be used principally for their descriptions and illustrations of bone cross-sections (e.g., Quekett, 1855; Foote, 1916). Additional early non-English publications exist (e.g., Demeter & Mátyás, 1928), but I am aware of no other recent papers, beyond those reviewed below, which address the intertaxonal variability in histological features among primates or other groups of mammals.

Within a contemporary framework, Amprino & Godina (1947) described the microstructure observed in random postcranial elements from a range of mammals, including Old World monkeys, New World monkeys and apes, as part of a larger study of vertebrate bone microstructure. These authors discuss variation in tissue type distribution, among other features (Haversian system patterning around the cortex and, to a limited degree, variation in collagen fiber patterns). Their data are wholly qualitative, and they consider variation to be largely determined by age, body size and ontogenetic processes. Similarly, the descriptions in Enlow & Brown (1958) are qualitative and refer to differences in tissue type distributions. For these authors, it is the processes of growth and development that are considered to be largely responsible for the variable patterns observed in all vertebrates (see also Enlow, 1963, 1982; Enlow & Hans, 1996). Enlow & Brown do not differentiate among species of living primates, but rather describe extant

representatives of the order as a whole, as well as the somewhat different tissue type pattern observed in the dentary of a single Paleocene plesiadapiform primate, *Plesiolestes*.

Other comparative mammalian studies include those of Jowsey (1966, 1968), and Singh et al. (1974). The first author has undertaken an investigation of Haversian systems and the degree of mineralization in a limited number of mammalian species from diverse orders (including rhesus macaques), and has identified some taxonomic differences attributed to variability in longevity and body size. Singh et al. (1974) published the first in what was to be a series of papers documenting the variability in mammalian bone histology, including in his study strepsirhine and haplorhine primates. Variables that Singh et al. examine include tissue type variation, degree of vascularity of the cortical bone, extent of intracortical remodeling, and density of osteocyte lacunae, both within and between taxa. The effects of mechanics, diet, age and specimen preparation are mentioned. While fairly comprehensive in its coverage of mammals, the work ultimately fails to plumb the potential of the comparative approach, and as such does not contribute much to the still nascent field beyond what had been done in the past, despite the quantification of some variables.

Burr (1979; 1992) and Schaffler & Burr (1984) have explored variation in mineral density and the degree of intracortical remodeling among primates. Results point primarily to a relationship between mechanics and variation in these features. In particular the 1984 paper is significant in that it is the first study to purposefully examine selected primate postcranial bone microstructure with the intent to explain the diversity found therein. For this reason, and as the authors suggest, this paper serves as “a baseline

for other studies" (p. 196). An equally important paper by Paine & Godfrey (1997), addresses the same variable in seven primate species, but obtains contrasting results. In this case the principal factor thought to affect intracortical remodeling is body size, with a subsidiary locomotor effect.

### 1.3 Relevance of this study

> *"No similar intensive surveys [focusing on a few closely related species with documentation of ontogenetic and bone-specific changes]…seem to available for extant species, even man. Such documents, if available, would nevertheless be of great value in providing histological comparative standards for further comparisons and such a research program is encouraged"* (de Ricqlès, 1992, p. 60).

The research reviewed above, individually and collectively, examines microstructural features in a wide range of vertebrates. However, it is only with some measure of phylogenetic control that the causal factors accounting for variability can begin to be identified. Therefore, research that focuses on a smaller number of closely related taxa, while still maintaining a broad taxonomic and adaptive context, is a necessary follow-up to the more extensive studies of the past (de Ricqlès, 1992). With three notable exceptions in the primate literature (Burr, 1979; Schaffler & Burr, 1984; Paine & Godfrey, 1997), such studies are veritably non-existent. These papers, while pioneering in their approach and significant in their findings, address only a limited range of microstructural features (mineral density and intracortical remodeling), and only in the femur and humerus. Therefore, Ruff & Runestad's 1992 statement that "microstructural analysis is a potentially informative but currently under-explored method of studying

primate limb bone adaptations" (p. 427) holds true today, for both primate and non-primate mammals.

The goal of the current study is to build upon this earlier research by examining a larger number of variables, in sections from five postcranial elements belonging to 10 primate taxa, including wild-caught specimens (unlike most of the primates in previous studies). In addition, the current sample will be used for examination of additional microstructural variables (osteocyte lacunar form and density, canalicular patterns, and mineral density) in the future.

| | **Variables examined** | | | | | | **Primary causal factors explored** | | | | | |
|---|---|---|---|---|---|---|---|---|---|---|---|---|
| **Authors** | 1 | 2 | 3 | 4 | 5 | 6 | A | B | C | D | E | F |
| Quekett, 1849, 1855 | ■ | ■ | | | ■ | | ■ | | | | | |
| Foote, 1913, 1916 | ■ | ■ | | | ■ | | ■ | | | | | |
| Amprino & Godina, 1947 | ■ | ■ | | ■ | | | ■ | | ■ | ■ | | ■ |
| Enlow & Brown, 1958 | ■ | ■ | | | ■ | ■ | ■ | | ■ | ■ | ■ | ■ |
| Jowsey, 1966, 1968 | | ■ | ■ | | | | | | ■ | ■ | | |
| Singh et al., 1974 | ■ | ■ | | | | ? | | | | | | |
| Burr, 1979 | | | ■ | | | | | | | | | |
| Schaffler & Burr, 1984 | | ■ | | | | | | ■ | | | | |
| Burr, 1992 | | ■ | | | | | | ■ | | | | |
| Paine & Godfrey, 1997 | | ■ | | | | | | ■ | ■ | | | |
| **Current Research** | ■ | ■ | Future Work | ■ | Future Work | | ■ | ■ | ■ | | ■ | ■ |

**Table 1.1: Relevant existing research, and proposed work.**
Variables examined: 1) Tissue type, 2) Intracortical remodeling, 3) Mineral density, 4) Collagen fiber orientation, 5) Osteocyte lacunar form and canalicular patterns, 6) Osteocyte lacunar density. Causal factors explored: A) Phylogeny, B) Mechanical environment, C) Size, D) Age/longevity, E) Physiology, F) Growth processes.

## 1.4 Background on bone as structure and tissue

### *1.4.1 Bone as structure*

The bones of vertebrates serve as stores of calcium and phosphate required for the regulation of cellular function, and are active in the maintenance of mineral homeostasis in the body (e.g., Rizzoli & Bonjour, 1999). In addition they house the hematopoietic marrow that is the source of a constantly renewed supply of blood cells. Consequently, bone shapes accommodate these demands. However, by far the most important selective determinant of whole bone shapes is their function as inseparable components of the musculoskeletal system. Bone and skeletal morphologies reflect mechanical and ecological environments – the pull of muscle attachments, the gravitational load of body weight – and therefore vary according to the size, postures and movements of organisms in their niche. The form of cartilage precursors in endochondral bones is at least partly genetically determined (Enlow, 1968; Lanyon, 1984; Thomason, 1995; Hamrick, 1999a; Hamrick et al., 2000; Lovejoy et al., 1999), but because bone is a plastic tissue that facilitates change in response to load (although the degree to which this occurs is debated, e.g., see Lovejoy et al., 1999), the achievement of the adult morphology beyond the underlying phylogenetic component is likely largely mediated by loads incurred during development of the mineralizing bone matrix, both pre- and post-natally (Lanyon, 1984; Carter et al., 1991, 1996; Hamrick, 1999b). It follows that, through genetic programs mediated by epigenetic factors, postcranial whole bone morphology largely depends on habitual positional behavior. Positional repertoires are, for the most part, constant within species; therefore, whole bone morphology remains relatively invariant.

This is not to suggest that small differences between individuals do not exist, but rather that genetically determined species-specific patterns are identifiable.

Because the varying loading regimes included in the complex positional behaviors of vertebrates may impose conflicting demands on bones, morphology by necessity reflects a compromise. A given form may be associated with a number of functions, and therefore form-function complexes may have more than one biological role in nature, and may interact with more than one selective force (Bock, 1977). In addition, the bone morphology of any given species is in part constrained by physical-chemical laws, and the species' ontogenetic and evolutionary histories (Bock, 1991). Therefore, while macrostructure largely reflects mechanical adaptation, selection proceeds within the parameters of physical-chemical attributes, development, multiple functions, and historical constraint.

Some fundamental principles of mechanical engineering can be applied to the analysis of bone morphology. Although the complexity of biological systems makes a one-to-one analogy with inanimate models impossible, there is a general conformation to expectations. First and foremost, bones must achieve adequate strength to withstand the range of loads they are subjected to during life history up to reproduction, that is, they must resist breaking (Biewener, 1990). However, strength is optimized to be achieved with a minimum of mass, as more bone mass requires more energy to transport, and perhaps to construct (Currey, 1984). This requirement accounts at least in part for the hollow structure of long bones (Currey, 1984; Lanyon & Rubin, 1985). The swelling at the ends of long bones is another macrostructural feature that is reasonably explained given an appreciation of biomechanical principles. The shape of epiphyses is, of course,

determined in large part by the modes and the degrees of freedom of movement that occur at the articulations located there, and by the need for the congruence between articular elements (e.g., Ruff & Runestad, 1992). But the widening can partly be accounted for by the fact that the articular cartilage in joints is less strong than bone material, and therefore larger surface areas are required to withstand equivalent loads (Currey, 1984). Similarly, the presence of a thin cortex combined with trabecular fill at the epiphyses is related to the need for some degree of elastic deformation beneath the articular cartilage in order to prevent its destruction during loading, combined with a mechanism for resisting substantial deformation of the joints and a transferring of loads from the joint area to the diaphyseal cortices. Finally, epiphyses and articular regions may be swollen relative to the shaft of the bone in order to increase the mechanical advantage of the stabilizing ligaments located around joints.

Other aspects of bone macro-morphology are less easily explained. For example, a general, well tested, theory to explain the presence of curvature in many long bones has not been proposed. Because bones are stronger in axial compression than in bending, the expectation is that they will be curved such that bending moments are minimized. However, the curvature of the bone is often oriented in a manner that would appear to accentuate the bending strains (Currey, 1984; Lanyon, 1987; Biewener, 1991). It has been hypothesized that this may function to allow space for muscles, to equalize strains within the cortex, to generate strains for some unknown physiological gain, or to resist large, abnormal loads. Perhaps the most compelling hypothesis is that bone curvature, developing in response to mechanical stimulus, may be related to the maintenance of load predictability (Lanyon & Rubin, 1985; Lanyon, 1987; Biewener, 1991; Biewener &

Bertram, 1994). The maintenance of strain patterns, rather than local strain magnitudes, appears to be an important factor in the regulation of growth remodeling during ontogeny, as well as adult intracortical (secondary osteonal) remodeling in response to changes in loading patterns (Biewener et al., 1986; Biewener, 1991). If dynamic strains are always distributed in a similar fashion, then the bone tissue can be distributed to accommodate that pattern, and to resist fracture.

The need for bones to resist fracture also means that they may be "over-designed" to a degree, meaning that the optimal structure may take into consideration safety factors: increases in the mechanical strength of bones beyond that required during habitual movement. The size of safety factors may vary according to the degree of load predictability, the potential load magnitude beyond that experienced during habitual locomotion, and the cost of structural failure (Lanyon, 1987; Biewener, 1990, 1992). In theory, the costs of increasing the safety factor must be weighed against the costs of increasing bone mass (Currey, 1984; Biewener, 1990), which can vary according to the locomotory mode of the animal. However, safety factors have been observed to be fairly uniform among mammals (Biewener, 1989a, 1990, 1991). Between species, even given large differences in body size or locomotion, peak stresses are also broadly equivalent (Currey, 1984; Biewener, 1989a, 1989b, 1990). This is achieved at least in part by changes in posture with size (Biewener, 1989a, 1990, 1991). Alternatively, differences in ground reaction forces during locomotion (e.g., due to speed) in animals of similar size are accompanied by differences in the thickness of bone cortices (and aspect of bone cross-sectional geometry) to maintain similar peak stresses and/or strains (Biewener, 1990; Lanyon & Rubin, 1985). However, as explained below, stress and strain patterns

are likely affected by microstructural variables as well. It follows that the integration of macro- and microstructural levels of investigation offers a means to more fully understand the way in which skeletons achieve and maintain the appropriate mechanical properties, within the context of species-specific growth patterns and life histories.

### *1.4.2 Bone as tissue*

The following is a brief description of the microstructural composition of bone, aspects of which will be described in greater detail in subsequent chapters.

Bone is a composite of organic and non-organic components, comprising a protein (primarily collagen) and mineral matrix, cells that are associated with this matrix, and a system of surrounding and penetrating blood vessels and nerves. Bone tissue cells include osteoblasts, osteoclasts, osteocytes, and bone lining cells.

Osteoblasts, developing from mesenchymal stem cells (passing first through several preosteoblastic phases; Aubin 1998; Martin 2000a), are found on the surfaces of growing bone, and are responsible for the synthesis of the bone matrix (both collagen and non-collagenous proteins) (Francillon-Vieillot et al., 1990; Aubin, 1998). Select osteoblasts differentiate into osteocytes, which become embedded within the matrix of bone that they or their neighbors have extruded. They are housed in small spaces termed osteocyte lacunae, and surrounded by extracellular fluid (Martin & Burr, 1989; Martin, 2000b; Marotti et al, 1992; Aubin, 1998). The majority of osteoblasts do not become incorporated into the bone matrix in this way, and it has been suggested that they undergo apoptosis following their secretory life (become fragmented and are phagocytosed, in a programmed fashion) (Aubin, 1998). Both osteoblasts and osteocytes (as well as bone

lining cells and preosteoblasts) are connected to their nearest neighbors in a syncytium (connected cellular network) via an intricate web of cytoplasmic processes terminating in gap and adherens junctions (Doty, 1981; Palumbo et al., 1990; Marotti et al., 1992). When extending from the mature osteocyte, these processes travel through canaliculi, tiny channels formed in the bone matrix during the osteoblastic secretory phase.

Bone lining cells are found on the surfaces of bone. These are thought to be another non-matrix synthesizing form in the osteoblast lineage (Aubin, 1998), but one that, upon receiving signals from osteocytes or hormones, may function to regulate the basic multicellular units (BMU) responsible for bone remodeling (Martin, 2000a and see Chapter 5).

Osteoclasts, the cells responsible for bone resorption, are not part of the osteoblast lineage. Rather, these large multinucleate cells are derived from the fusion of precursors of a monocyte-macrophage blood cell origin (e.g., Owen, 1978). They secrete enzymes with an acid pH capable of solublizing the hydroxyapatite mineral. This results in characteristic Howship's lacunae, or resorption bays, as bone is removed.

Type I collagen comprises the majority of the organic phase of bone matrix (c. 90%, Cowles et al. 1998) synthesized and extruded by osteoblasts. This fibrous structural protein will be discussed at greater length in Chapter 6. The variable organization of collagen fibers within bone is one of the features used to identify tissue types, as described in Chapter 4. Other organic compounds present in small quantities in the interfibrillary ground substance of bone tissue include a range of non-collagenous proteins (such as glycoproteins) and lipids. These likely have varied functions in the mineralization and remodeling of bone (Bonucci, 1984; Francillon-Vieillot et al. 1990;

Cowles et al. 1998; Martin et al, 1998). Water, serving both structural and metabolic functions, constitutes 5-10% of the weight of bone (Boyde & Jones, 1998; Martin et al., 1998).

Bones are fed by an extensive network of blood vessels that surround and penetrate the bone, with the blood supply coming from nutrient, epiphyseal, metaphyseal, and periosteal arteries. Nutrient arteries (of which there are one or two for any given long bone) pass through the diaphysis of a bone via a perforation, entering the medullar cavity where they then branch into ascending and descending components. Each of these branches gives off numerous branches of its own which progress helically around the medullary space. Yet more branches off of these penetrate the cortex. Peripheral capillaries of the nutrient arteries join and anastomose with capillaries of the epiphyseal (leading from local systemic arteries), metaphyseal (leading from vascular arcades near, but not at, the articular surfaces), and periosteal (networks of vessels in the fibrous periosteum) arteries (Singh et al., 1991). Canaliculi facilitate the transmission of substances from the vascular canals to osteocytes embedded in the mineralized matrix. The patterning of vascular canals within the cortex is another feature that has been used to identify bone tissue type (see Chapter 4).

**1.5 Summary**

In this chapter I have introduced the work to be described in the following chapters: an investigation of primary bone tissue type variability, intracortical remodeling, and preferred collagen fiber orientation at the midshaft femur, humerus, tibia, radius and ulna in a selection of primate taxa. I have also presented a brief background to understanding

this work, both in terms of previous research of a similar nature, and related materials that inform the interpretation and understanding of the data. More specific background information related to each variable of interest is provided in the relevant chapters to follow.

The study of bone is intriguing; bone is complex in its composition, structure, development, and function. In part because of this complexity, bone encodes a wealth of information regarding the lives of vertebrates. Additionally, because of its resistance to complete degradation during many taphonomic processes, fossilized bone offers a means to reconstruct the life-ways of extinct taxa. Therefore, for the student of living and past species alike, a deeper understanding of bone – as both structure and tissue – is invaluable.

# Chapter 2

# Materials and Methods

## 2.1 Materials

### *2.1.1 Sample composition and provenience*

#### 2.1.1.1 Sample selection

In selecting a sample range for a study of variation in bone microstructure, there are two useful, complementary levels of investigation, both of which focus on a subset of closely related mammals. One approach examines one or a few species in great depth, with large sample sizes for each taxon (e.g., Burr, 1979; Paine & Godfrey, 1997; McFarlin, 2006). This offers the opportunity to assess intra-specific variability and determine species patterns, including during ontogeny when juveniles are included. The other approach – one that serves as a bridge between intra-taxon studies and extensive mammalian reviews (e.g., Enlow & Brown, 1956, 1957, 1958) – is broad-based, but nevertheless restricts the bulk of the effort to taxa which are more phylogenetically constrained, such as the members of a single order (e.g., Schaffler & Burr, 1984). This is the method adopted here, with the intent to identify broad, biologically meaningful, patterns.

Using a carefully constructed comparative sample allows for correlation and assessment of similarities and differences, and thus elucidation of the possible causal relationships between forms, functions and adaptive significance. Primates are of interest for this work in part because of their anthropological relevance. However, the order is one that is suited to this research for three additional reasons. First, primates are well studied, and there exists a vast literature on their phylogeny, behavior, ecology, physiology, and functional skeletal morphology. Second, it is a group that includes

species varying greatly in size, other aspects of life history, and positional behavior. Finally, while many primates likely share similar growth and behavioral life histories due to common ancestry, there are also many instances of convergence in adaptations. These afford an opportunity to differentiate between features that may be functionally determined, and those that may reflect evolutionary heritage.

Due to the labor-intensive nature of specimen preparation (as well as the difficulty in obtaining specimens for destructive work), including a large number of taxa necessitates small sample sizes for each taxon. In the construction of this sample there was reason to believe that consistent patterns would nevertheless be identifiable. For example, in a pilot study on an ontogenetic series of *Didelphis virginiana* (Warshaw et al., 2000), it was found that patterns of collagen fiber orientations are comparable throughout growth. Similarly, Biewener et al. (1986) have determined that the magnitude and strain patterns in chick tibiotarsi during growth is "markedly similar among individuals" (p. 392).

The sample is composed of a selection of primates including members of five strepsirhine families (Galagidae, Lorisidae, Cheirogaleidae, Indriidae, Lemuridae), three platyrrhine families (Callitrichidae, Cebidae, Atelidae), and the family Tarsiidae. The sample encompasses representatives of several broad primate positional behavior categories, as well as a range of body sizes and life history strategies.

In some cases the taxonomic level of analysis is the genus (e.g., *Otolemur*, *Callithrix*), although more than one species may be represented. In other cases, several genera from a single family are included as a single taxon unit. Such generalization is only applied in cases where, in terms of positional behavior and broad life-history

features, the genera are very similar to one another. For example, *Nycticebus*, *Loris* and *Perodicticus* are referred to as a single unit for analysis: the Lorisidae. These three genera display very comparable (albeit not identical) ecological, kinematic and life history adaptations (Müller, 1982; Gebo, 1987; Rasmussen & Izard, 1988; Demes et al., 1990; Kappeler, 1996; Weisenseel et al., 1998). With the exception of the galagids, whenever the genus is the level of analysis the nominal taxon is the sole representative of its family. So, for example, *Saimiri* is the only genus from the family Cebidae included in the study. Effectively therefore, in all but one case, families are the units of analysis, with some containing one representative genus, and some more than one. The galagids have been divided into two subgroups (greater and lesser galagos) because of the distinctive variation in positional behavior between the two. This offers an opportunity to examine a smaller range of variation within a single family.

Sample composition was designed so that the following kinds of comparisons could be made: a) between closely related taxa with greatly differing positional behavior in terms of frequencies of locomotor modes (e.g., Lemuridae/Indriidae), b) between closely related taxa with moderately differing positional behavior (e.g., lesser galagos/greater galagos), c) between phylogenetically distant taxa with similar positional behavior (e.g., Tarsiidae/lesser galagos), d) between species of differing size and/or growth rates but similar positional behavior (e.g., lesser galagos/Indriidae), and e) between species with similar size and positional behavior but differing growth rate (e.g., Cheirogaleidae/Callithrichidae).

All individuals are adults, as determined by the fusion of all epiphyses and eruption of all adult dentition (when skulls were available). While adulthood – as defined

by the attainment of stable body mass – does not necessarily coincide with dental and skeletal maturity (e.g., Smith & Jungers, 1997), these are the only features that can be used to identify adulthood in the absence of body mass records. In addition, epiphyseal fusion is an appropriate measure given that the features of interest are related to skeletal growth and development. Geriatric individuals, identified from tooth wear and overall condition of the skeletal material, were avoided.

| Taxon | Genus | Species | Provenience | F | H | T | R | U |
|---|---|---|---|---|---|---|---|---|
| Lesser galagos | *Galago* | *senegalensis* | MNHU 60601 | | | | | |
| | *Galago* | *moholi* | DUPC 2062 | | | | | |
| | *Galago* | *moholi* | DUPC 3173 | | | | | |
| | *Galagoides* | *demidovii* | HC 25 | | | | | |
| Greater galagos | *Otolemur* | *crassicaudatus* | DUPC 725 | | | | | |
| | *Otolemur* | *crassicaudatus* | CT OA | | | | | |
| | *Otolemur* | *crassicaudatus* | HC 31 | | | | | |
| | *Otolemur* | *crassicaudatus* | USNM 365721 | | | | | |
| Lorisidae, *sensu stricto* | *Nycticebus* | *coucang* | MCZ 36116 | | | | | |
| | *Nycticebus* | *coucang* | MCZ 422 | | | | | |
| | *Nycticebus* | *coucang* | HC 27 | | | | | |
| | *Nycticebus* | *coucang** | USNM 317187 | | | | | |
| | *Nycticebus* | *coucang* | DUPC 1972 | | | | | |
| | *Loris* | *tardigradus* | DUPC 1964 | | | | | |
| | *Perodicticus* | *potto* | DUPC 930 | | | | | |
| Cheirogaleidae | *Cheirogaleus* | *major* | MCZ 44850 | | | | | |
| | *Cheirogaleus* | *major* | DUPC 2612 | | | | | |
| | *Mirza* | *coquereli* | DUPC 359 | | | | | |
| | *Microcebus* | *murinus* | DUPC 825 | | | | | |
| Lemuridae | *Varecia* | *variegata* | MCZ 18740 | | | | | |
| | *Lemur* | sp. | HC 30 | | | | | |
| Indriidae | *Propithecus* | sp. | MNHU 44684 | | | | | |
| | *Propithecus* | sp. | MNHU 44685 | | | | | |
| | *Indri* | *indri* | HC 19 | | | | | |
| Tarsiidae | *Tarsius* | *spectrum* | MNHU An11318 | | | | | |
| | *Tarsius* | *spectrum* | HC 16 | | | | | |
| | *Tarsius* | *syrichta* | DUPC 81 | | | | | |
| | *Tarsius* | sp. | HC 23 | | | | | |
| Callitrichidae | *Callithrix* | *geoffroyi* | MNHU 34381 | | | | | |
| | *Callithrix* | sp. | HC 28 | | | | | |
| Cebidae | *Saimiri* | *sciureus* | HC 12 | | | | | |
| | *Saimiri* | sp. | HC 13 | | | | | |
| | *Saimiri* | sp. | HC 14 | | | | | |
| | *Saimiri* | sp. | MNHU 85197 | | | | | |
| Atelidae | *Ateles* | *fusciceps* | FMNH 68811 | | | | | |
| | *Ateles* | sp. | MNHU 44079 | | | | | |

**TABLE 2.1: Specimen list and provenience.**
CT = Carl Terranova, DUPC = Duke University Primate Center, HC = Hunter College of the City University of New York, FMNH = Field Museum of Natural History, MCZ = Museum of Comparative Zoology at Harvard University, MNHU = Museum für Naturkunde of Humboldt University, USNM = National Museum of Natural History; F = midshaft femur section, H = midshaft humerus section, T = midshaft tibia section, R = midshaft radius section, U = midshaft ulna section. *This individual was removed from statistical and most qualitative analyses because of apparent pathology.

2.1.1.2 Element selection and section sampling location

Midshaft sections were taken from the femur, humerus, tibia, radius and ulna on one side of the body. Sections along the entire shaft of the bone would provide a continuum of information with regards to the mechanics of the bone, patterns of drift and linear growth (the latter determined from analysis of the stratigraphy of bone tissues in the section). The midshaft was selected, rather than more distal or proximal locations, as this has long been a standard in the literature and provides for comparability among studies (e.g., Schaffler & Burr, 1984; Paine & Godfrey, 1997; Goldman, 2001). In addition, beam theory has provided a superior understanding of the mechanical loads at the midshaft relative to the potentially more complicated mechanical environments closer to the joints (Lanyon & Rubin, 1985). This allows for the construction of testable hypotheses with respect to the midshaft loads.

While the majority of previous comparative bone microstructure studies have concentrated on the femur, all the elements of the skeleton will differentially reflect posture and locomotion, as well as growth (e.g., Erickson & Tumanova, 2000). Diaphyseal rather than maximum length was used in order to maintain consistency between juvenile specimens examined in the Hard Tissue Research Unit (HTRU, previously housed at Hunter College of the City University of New York, where all specimens were prepared, and currently relocated to the New York University College of Dentistry) – which may not have epiphyses – and adults. For each bone, landmark standards were established to determine the proximal and distal extent of the diaphysis. In total, 124 sections were made, of which two (USNM 317187, humerus and femur) were pathological, and therefore were not included in most analyses.

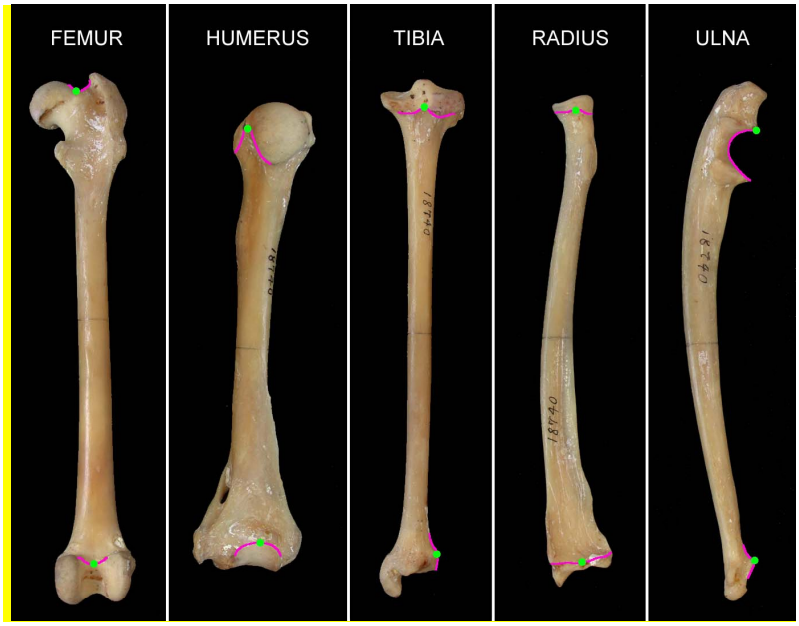


**Figure 2.1: Landmark standards for identification of maximum diaphyseal length.**
**Femur.** *Proximal landmark:* the inferior-most point in the notch between the femoral head and greater trochanter. *Distal landmark:* on the posterior aspect of the bone, the midpoint of the fusion scar delineating the superior boundary of the intercondylar fossa.
**Humerus.** *Proximal landmark:* on the posterior aspect of the bone, the superior inflection point of the ridge marking the fusion scar between the diaphysis and epiphysis. *Distal landmark:* on the posterior aspect of the bone, the midpoint of the superior margin of the distal articular surface.
**Tibia.** *Proximal landmark:* on the posterior aspect of the bone, the proximal-most point along the fusion scar (ridge) between the diaphysis and epiphysis. *Distal landmark:* the lateral-most point of the distal tibia.
**Radius.** *Proximal landmark:* on the anterior aspect of the bone, the midpoint of the distal margin of the radial head articular surface. *Distal landmark:* on the anterior aspect of the bone, the mid-point of the fusion scar between the diaphysis and epiphysis. If this is not visible, use the medial-most point of the projection forming the ulnar notch.
**Ulna.** *Proximal landmark:* the proximal-most tip of the semilunar notch. *Distal landmark:* the anterior-most projection of the distal ulna.

## 2.2 Methods

### *2.2.1 Specimen collection and labeling*

Prior to sectioning, standard whole bone measurements (maximum length, diaphyseal length) were recorded, and each bone was digitally photographed in four views (anterior, posterior, medial, lateral). Length measurements on large bones were acquired using a field osteometric board customized with a laser diode attachment (Paleo-Tech Instruments). The laser diode attachment, which slides along the edge of the board,

produces a thin red laser line across the bone and scale, and was used to mark the diaphyseal landmarks and determine diaphyseal midshaft (marked with pencil) while the bone was oriented on the board for maximum length. Length measurements for smaller bones were acquired, and mid-diaphysis was determined, using dental calipers. For all bones, maximum midshaft width was determined using dental calipers, and the anterior midline was marked with pencil with the bones lying flat on a surface, posterior aspect of the bone down. For the ulna the medial midline was marked while the bone lay on its lateral aspect.

For specimens collected from FMNH, MCZ, MNHU and USNM, high-resolution casts of the midshaft region of the bone were made in order to provide a record of the removed block. This was done as a means of mitigating the destructive nature of the sampling protocol, and to maximize the usefulness of these precious collections for future researchers.

First, Exaflex vinyl polysiloxane injection material (GC America Inc.) was applied around the midshaft of the bone at a thickness of approximately 1-2 mm. When dry, a base for the entire bone was made out of Exaflex vinyl polysiloxane putty. The intact bone, along with the midshaft sleeve of injection material, was pressed into the putty base while it was still malleable. This base was designed to hold the bone while resting flat, coming up around the shaft approximately halfway, so that the bone could easily be removed from this base when dry, and easily repositioned into it after the midshaft block was removed. After the base cured, the injection material sleeve was slit along the top and the bone was removed.

For MCZ, subsequent to midshaft block removal, the bone was reconstructed to its original dimensions by replacing the cut ends of the bone into the molded base and filling in the removed midshaft portion within the sleeve with epoxy resin (Figure 2.3).

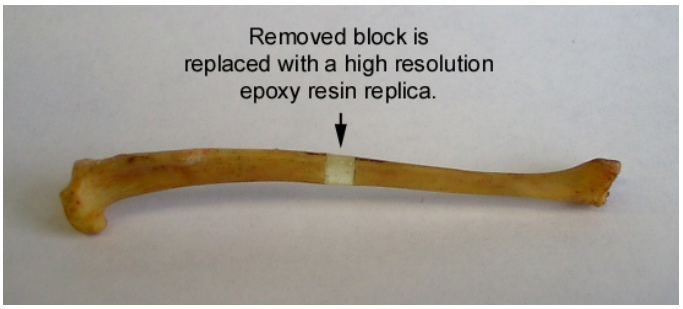


**Figure 2.2: Reconstructed bone.**

Midshaft blocks were extracted using a Buehler Isomet low-speed diamond saw, or portable gem saw modified for long bones. The length of the blocks ranged between 0.3-1 cm dependent upon animal and element size. One end of the block was located 0.5-1mm distal to midshaft, with the rest of the block proximal to that point. A small groove was sawed at the anterior midline of the block on the end away from the midshaft surface (Figure 2.3). To label the blocks, a piece of nylon string was attached to a small piece of 0.4 mm thick Zinnfolie tinfoil (Denerica) and tied through the medullary cavity of the bone block. The specimen number can easily be etched onto the aluminum sheeting with a pen tip or other pointed implement. The nylon thread and etched aluminum withstand all chemicals used in cleaning and embedding the specimens.

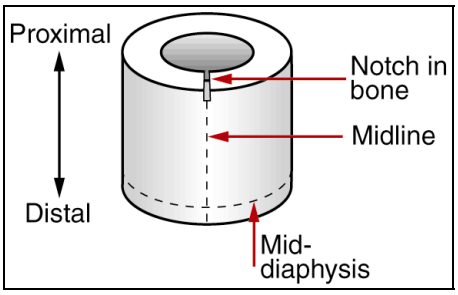


**Figure 2.3: Diagram of bone block notch orientation.**

*2.2.2 Specimen processing*

In the HTRU, the collected bone blocks were cleaned of organics in a 1% enzymatic solution (Terg-a-zyme, Alconox) over the course of a few days to two weeks in an oven set at 50º C, with daily changes of the solution and daily examination of the specimens. Cleaning was deemed complete when the blocks appeared free of soft tissue when examined with a dissecting microscope, and/or had not changed their appearance for two or three consecutive days. Attention was paid not to leave the specimens in the enzymatic detergent longer than necessary, as the removal of excessive non-mineralized matrix in some frail specimens leads to a breaking down of the block.

Blocks were next dehydrated in a series of graded ethanols. They were first immersed in a 50% solution of ethanol and left for 24 hours. After 24 hours the blocks were moved to a second, fresh, solution of 50% ethanol and left for 24 hours. This was repeated with two changes of 70% ethanol, and two changes of 95% ethanol. Next the blocks were defatted and further dehydrated in a soxhlet reflux unit with a 50:50 solution of heptane and isopropanol, for a period of one to two weeks, depending on the size of the specimens. Upon removal from the soxhlet, they were passed through one change each of 100% acetone, 75:25 acetone:polymethy-methacrylate (PMMA), 50:50

acetone:PMMA and 25:75 acetone:PMMA, resting at least 24 hours in each solution. Subsequently, the blocks were left at least 24 hours in three successive changes of 100% PMMA. At this point, the jars containing the specimens were kept refrigerated to inhibit curing of the PMMA. Finally, each block was placed, midshaft surface down, in a separate small labeled jar (large enough to contain the block with at least a few millimeters of space around the bone) filled with PMMA, after the aluminum labels had been clipped off, and individual jars had been labeled. Care was taken at all times not to allow the bone to rest outside of solution and to dehydrate. The bone was centered at the bottom of the jar and placed in a bright spot to cure. Direct sunlight was avoided, as excess heat can cause the PMMA to outgas and form bubbles while curing. Complete hardening of the PMMA took approximately one week to one month. Cured embedded bone blocks could be removed from their jars by breaking the glass. The clear, hard, PMMA embedded blocks were then ready for section preparation.

For all the solutions listed above, the jars holding the specimens were ultrasonicated for 1-5 minutes and vacuumed until all outgassing ceased (while covered with pierced lids) in a chamber attached to a vacuum pump configured with a refrigerated trap. This was done in order to enhance the infiltration of each solution into the bone spaces.

*2.2.3 Section preparation*

The midshaft end of the embedded block was ground on graded carbide papers (240 grit, 320 grit, 400 grit, 600 grit) on a Buehler Handimet II hand grinder to expose the midshaft surface of the bone. The block was ultrasonicated and rinsed between successive papers

to avoid contamination of large grit on smaller grit papers. Examination of the surface with a dissecting scope was performed to assure uniform topography before moving to a smaller grit paper. A final polish was achieved with a 1200 grit paper.

The ultrasonicated, rinsed and dried blocks were then ready for mounting on glass slides using dental adhesives according to the methods modified from those previously developed in the HTRU (Goldman et al., 1999; Goldman, 2001). The ground surface of each block was first submerged to a depth of approximately 1mm in acetonitrile for 1.5-4 minutes (depending on the size of the bone) – to yield PMMA surface topography in preparation for mounting – and gently air-dried (i.e., with compressed air). The exposed *bone area only* was then brushed with Dentin Activator (Parkell, Inc.), left for 10 seconds, rinsed and air-dried. A 1:1 ratio of Self Cure Activator and Prime and Bond 2.1 (Dentsply International) was mixed (a few drops of each) and this solution was then brushed over the prepared surface of the block and around its edges for a period of 30 seconds. The surface was next dried with a warm hairdryer for 20 seconds, and allowed to rest for five minutes.

A glass slide was etched with a 20% hydrofluoric acid solution for four minutes, rinsed and air-dried. The area to which the block was to be adhered was then brushed with a few drops of Silane Porcelain Primer (Bisco, Inc.) and dried for 20 seconds with a hair dryer. A few drops of ProBond Adhesive (Dentsply International) were then placed onto the slide, taking care to avoid the production of bubbles (the number of drops dependent upon the size of the block to be adhered). Working quickly to avoid the initiation of curing, the pool of adhesive was checked under a dissecting microscope for small bubbles and/or fibers and dirt specs, which were gently removed with a dental pick.

The prepared block was then placed onto the pool of adhesive, beginning at one edge, and pressed down with even and firm pressure. Without moving the slide or block, a light gun was used to cure the adhesive for 20 seconds. At this point, the slide could be picked up and light curing continued for an additional 1.5 minutes, aiming the light gun at both surfaces of the slide and around the block. The mounted blocks were allowed to rest overnight, but no longer than 24 hours for very large blocks (e.g., human femora) to prevent breaking of the slide due to adhesive shrinkage.

Mounted blocks were sectioned on the Isomet to produce 120μm ±4μm thick sections and ground to 100μm ± 5μm on a Buehler Handimet II hand grinder as described above, with the final polish achieved on 1200 grit paper. Final section thickness was determined using an Edge R400 real-time 3D microscope, providing a more accurate determination of thickness than is possible with a micrometer (Greenberg & Boyde, 1997; Goldman et al., 2000). Standardized section thickness – across and between sections – is necessary for the quantification of collagen fiber orientation (discussed in Chapter 6), as variation in thickness will affect the brightness in polarized light (Boyde & Riggs, 1990).

Using the remaining embedded block as a guide, completed sections were marked with a small indelible ink dot to indicate anterior midline.

*2.2.4 Specimen imaging*

The image acquisition process is entirely digital, with data transferred directly from CCD cameras to Pentium-based computers. Sections were imaged at low magnification (5X objective) in conventional transmitted light (LM) and circularly polarized transmitted

light (CPL) using a Leica-Leitz DMRX/E Universal Microscope, configured with a Marzhauser motorized stage and CPL filters. The benefits of CPL over linearly polarized light (LPL) are discussed in Chapter 6. LM and CPL images of entire sections were acquired with a JVC KY-F55B color video camera using Syncroscopy Montage Explorer software (Synoptics, Ltd.). The Syncroscopy software allows for real-time montaging during image acquisition, resulting in high-resolution images of entire sections. Lighting parameters for CPL imaging were standardized following a method developed in the HTRU (Bromage et al., 2003). This is necessary for the comparison of quantified gray level patterns among specimens (e.g., Goldman, 2001). (See Chapter 6 for a more in depth discussion of this issue). Care was taken to include the orientation dot in the image.

*2.2.5 Image processing and data analysis*

Details regarding image processing and data analysis are discussed in the ensuing chapters as relevant to each of the variables examined. See also Appendix D.

# Chapter 3

# Sample Primate Natural Histories

## 3.1 Introduction

The aspects of natural history that are of direct interest to the study of bone microstructure are those related to growth and development (i.e., life history), and those related to the mechanical adaptation of bones (i.e., positional behavior). Therefore, in the following review, I concentrate on these aspects of organismal biology in relation to my sample taxa, as well as on the proposed phylogenic relationships among the taxa.

## 3.2 Background

### *3.2.1 General background on life history*

Relative to other mammals of equivalent body size, primates display a uniquely extended life history. Development is delayed, and they live longer lives (Watts, 1990; Ross, 1998). Associated with this adaptation is a larger brain and a host of social, behavioral and ecological features (Watts, 1990; Joffe, 1997). Within primates, as with other mammals, there is a general correlation between body size and other morphological, physiological and life history features, such as metabolic rate, neonate weight, weaning age, eruption of the first adult molar, age at first female breeding, age at sexual maturity, lifespan, interbirth interval, and brain weight (e.g., Harvey & Clutton-Brock, 1985; Harvey et al., 1987; Smith, 1989; Ross, 1991; Hartwig, 1996; Kozlowski & Weiner, 1997). Simply put, life history strategy and size are intimately related, and there is often an allometric relationship between body size and/or brain size and/or metabolic rate and

other life history variables (Sacher & Staffeldt, 1974; Harvey et al., 1987; Smith, 1992; Parker, 1999), although it is not yet well understood why scaling laws apply to all aspects organismal life history in the way that they do (Harvey et al., 1987; Partridge & Harvey, 1988; Ross, 1998). Among primate subfamilies, there may be deviation from the overarching pattern of extended life-history, increasing with body size. Some primate taxa may "live fast and die young" for their size, others may "live slow and die old", and the relationship among specific variables in some taxa may deviate from the allometry (or allochrony, see Smith, 1992) found in the order as a whole (Rasmussen & Izard, 1988; Watts, 1990; Ross, 1998; Parker, 1999; Godfrey et al., 2001) (e.g. folivorous primates tend towards relatively smaller brains, Harvey at al., 1987). Thus, although a broad primate pattern exists, taxa can be characterized by specific life-history adaptations that may be related to phylogenetic, ecological, developmental, physiological, demographic (i.e., mortality schedules), social and other variables, including proximate factors (Harvey & Clutton-Brock, 1985; Partridge & Harvey, 1988; Ross, 1991, 1998; Hartwig, 1996; Kappeler, 1996; Garber & Leigh, 1997; Godfrey et al., 2001; Wickelski & Ricklefs, 2001). So, for example, growth rate relative to body mass has been observed to be fastest in strepsirhines, somewhat slower in platyrrhines, slower yet in catarrhines, and slowest in hominoids (Kirkwood, 1985).

*3.2.2 General background on positional behavior*

In a very basic way, size is related to ecology, which in turn is related to positional behavior (Fleagle & Mittermeier, 1980; Fleagle, 1985; Harvey et al. 1987; Godinot, 1990). As Szalay & Dagosto have stated, "in the simplest terms, the postural, locomotor,

and manipulative behavior of a species, given the canalizing constraints of its heritage, is probably closely linked to its feeding preferences" (1980, pp.2-3). For example, small primates are more likely to be insectivores, or to feed on exudates, and engage in leaping behavior, while large primates are more frequently suspensory and folivorous. In terms of positional behavior, these trends are reflected in gross skeletal morphology, including limb indices, element robusticity, cross-sectional geometry, joint structures, shaft curvatures, and muscle moment lengths (Jouffroy & Lessertisseur, 1979; Jungers, 1985; Ruff & Runestad, 1992; Runestad Connour et al., 2000). In general, for example, intermembral indices tend to increase with increasing body size within groups of closely related primates (i.e., lower limbs are shorter relative to the upper limbs as primates get bigger). Similar patterns exist for humerofemoral, brachial and crural indices (Jungers, 1985). Importantly, muscle force, which must decrease relative to size if muscles are not to become prohibitively large, results in slower movements, lower movement frequency, and relatively shorter and straighter hindlimbs in larger primates (Demes & Günther, 1989).

However, just as is the case with life history, there are taxon specific deviations from general primate patterns, and skeletal morphologies may deviate from size-related regressions of hypothesized functional equivalence, if functional equivalence is even possible to identify (Fleagle, 1985; Oxnard et al., 1981b). For instance, leaping primates may have shorter forelimbs and/or longer hindlimbs than is expected for their size (Jungers, 1985). Members of the genera *Loris* and *Galago* are roughly the same size, but have vastly different intermembral indices, due to divergent locomotor adaptations.[1] In

[1] Similarly, size does not always correlate with diet (Fleagle & Mittermeier, 1980; Fleagle, 1985; Rosenberger, 1992).

addition, the mechanism by which these allometric patterns are achieved can vary. In the example of relative limb lengths, the hindlimb may shorten relative to the forelimb, or the forelimb may lengthen relative to the hindlimb, with both situations yielding the same intermembral index. Positional behavior, body size, gravity and phylogeny all interact to produce limb proportions and other gross morphological features of the skeleton (Jungers, 1985; Jouffroy & Petter, 1990; Preuschoft, 1990; Terranova, 1995a). Regardless of how one understands the interaction between selection and phenotype (i.e., how genetic determination of development and form occurs, and what is the unit of genetic determination, see Lovejoy et al., 1999; Chiu & Hamrick, 2002) and the degree to which epigenetic factors play a role, it is clear that individual taxa have recognizable and consistent gross skeletal morphologies. These are in some way the manifestations of the interaction among phylogenetic and developmental constraints, and functional adaptation.

*3.2.3 General background on phylogeny*

Although debate remains within the anthropological community regarding the origins of, relationships among, and taxonomy of various primate groups (e.g., Shoshani et al., 1996; Poux & Douzery, 2004; Schmitz et al., 2005) – with morphological, behavioral and molecular data providing both complementary and conflicting evidence – there is sufficient consensus to allow for the categorization that I adopt here and in the following chapters. Specifically, it is agreed upon that all extant members of the order Primates can be allocated to one of two major suborders – Strepsirhini and Haplorhini (e.g., Szalay & Delson 1979; Martin, 1995; Fleagle, 1998) – regardless of whether or not these two groups are held to be valid monophylies. Within Strepsirhini are found all Malagasy primates (i.e., all lemurs *sensu lato*), as well as the African and Asian loris and galago

groups. Within Haplorhini are found all Old World monkeys and apes (the infraorder Catarrhini, not included in the current study), all monkeys of Central and South America (the infraorder Platyrrhini) and the Southeast Asian tarsiers.

For the purposes of the current study, I suggest that the allocation of sample species to families or subfamilies (e.g., Lorisidae vs. Lorisinae, or Cebinae vs. Cebidae) is less important than the monophyletic grouping of closely related genera. I am aware of no current research that would invalidate the 10 groups I use (with the possible exception of paraphyly among lorisids; see Yoder et al., 2001; Poux & Douzery, 2004), in terms of both the taxa I place within the groups, and the separation between them, despite the likelihood that some would quibble with the use of the family level (e.g., Rosenberger, 2002). Therefore, there is no further consideration here of competing taxonomies.

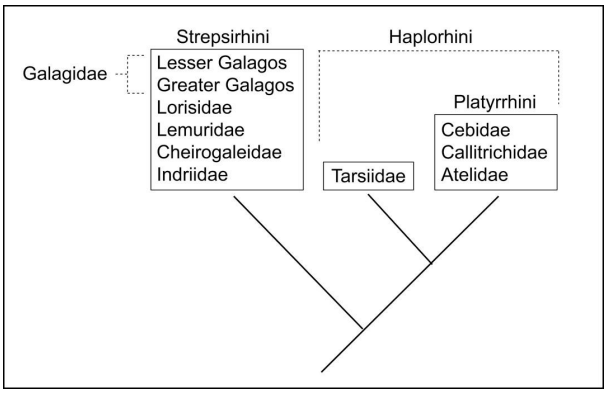


**Figure 3.1: Sample primate taxonomy and systematics.**

Within this generally accepted paradigm, however, interesting questions, some potentially relevant to this study, remain. First, there is a lack of consensus on the relationships between euprimate groups such as the Eocene Adapidae and Omomyidae on the one hand, and suborders of extant primates on the other (e.g., Krishtalka & Schwartz,

1978; Rosenberger & Szalay, 1980; Szalay et al., 1987; Szalay & Dagosto, 1988; Dagosto, 1988, 1993; Rasmussen, 1994; Simons et al., 1995; Simons, 1997; Shoshani et al., 1996). Second, the origins and affinities of the tarsiids, relative to strepsirhines and anthropoids, are unresolved, despite recent insights into the antiquity and uniqueness of this lineage (Krishtalka, 1978; Beard et al., 1991; Shoshani et al., 1996; Porter et al., 1997; Poux & Douzery, 2004; Schmitz et al., 2005). Third, the relationships among some strepsirhine groups, and the timing and frequency of primate colonizations of Madagascar, remain subjects under discussion (e.g., Szalay & Katz, 1973; Yoder et al., 1996; Rasmussen & Nekaris, 1998; Porter et al., 1997; Kappeler, 2000; Poux & Douzery, 2004; Roos et al., 2004; Masters et al., 2005). Fourth, the ancestry of, relationships among, and means by which the platyrrhines arrived in the New World are somewhat obscure (e.g., Delson & Rosenberger, 1980; Sussman & Kinzey, 1984; Hartwig, 1994; Fleagle et al., 1997; Porter et al., 1997; Rosenberger, 2002; Singer et al., 2003; Steiper & Ruvolo, 2003; Poux & Douzery, 2004; Schneider et al., 2004). Finally, and perhaps most fundamentally, there is debate regarding the origins, earliest membership, and affinities of the primate order as a whole (e.g., Szalay & Decker, 1974; Szalay & Lucas, 1993, 1996; Szalay et al., 1975, 1987; Kay et al., 1990, 1992; Krause, 1991; Beard, 1993; Simmons, 1993; Covert & Williams, 1994; Shoshani et al., 1996; Silcox, 2002; Poux & Douzery, 2004; Schmitz et al., 2005).

### 3.3 Individual taxon natural histories

The following descriptions are not meant to be exhaustive, but rather to provide a general overview of the ecological, life history and positional behavior adaptations of each sample taxon. In particular, there is variation in the literature with respect to descriptions

of positional behavior – due at least in part to methodological differences, but also habitat, season, locality, etc. (e.g., Dagosto & Gebo, 1998) – which are not fully accounted for here. Rather, my goal is to provide a description that represents a broad consensus view with regard to each taxon, as summarized in Table 3.1.

| Taxon group | Species | Adult Mass (g) | Scaled Growth Rate Score | Infant Scaled Growth Rate | Positional Behavior |
|---|---|---|---|---|---|
| Cheirogaleidae | *Cheirogaleus major* | 362-438 | 53[k] | 0.0364 | AQ |
| | *Mirza coquereli* | 304-326 | -- | 0.0309 | AQ |
| | *Microcebus murinus* | 59-63 | 48[k] | 0.0458 | AQ |
| Lesser galagos | *Galago moholi*<br>*Galago senegalensis* | 173-315 | 43[w] | 0.0248-0.0347 | VCL |
| | *Galagoides demidovii* | 60-63 | -- | -- | VCL |
| Greater galagos | *Otolemur crassicaudatus* | 1110-1190 | 36[w] | 0.0308-0.0350 | VCL/AQ/SC |
| Lorisidae, *sensu stricto* | *Nycticebus coucang* | 626-1100 | 55[w] | 0.0279 | SC |
| | *Perodicticus potto* | 830-1250 | -- | 0.0175 | SC |
| | *Loris tardigradus* | 192-269 | 77[w] | 0.0132 | SC |
| Lemuridae | *Varecia variegata* | 3520-3630 | 31[w]-68[k] | 0.0278 | AQ |
| | *Lemur* sp. | 1080-2510 | 112[w] | 0.0195 | AQ |
| Indriidae | *Propithecus* sp. | 2950-3250 | 244[w] | 0.0134 | VCL |
| | *Indri indri* | 5830-6840 | -- | -- | VCL |
| Tarsiidae | *Tarsius spectrum*<br>*Tarsius syrichta*<br>*Tarsius* sp. | 104-134 | -- | 0.0128 | VCL |
| Callitrichidae | *Callithrix geoffroyi*<br>*Callithrix* sp. | 330-360 | 165[w]-234[k] | 0.0171-0.0212 | AQ |
| Cebidae | *Saimiri sciureus*<br>*Saimiri* sp. | 662-1020 | 210[k]-262[w] | 0.0179 | AQ |
| Atelidae | *Ateles fusciceps*<br>*Ateles* sp. | 7290-9410 | 225[w] | 0.0053-0.0065 | SUS |

**TABLE 3.1: Taxon life history and positional behavior information.**

Adult mass ranges are from Smith & Jungers (1997). Where there are more than one species per genus, the range for all species combined is provided. For *Propithecus*, although the species is unknown for these specimens, the weights provided are for *P. verreauxi*.

Scaled growth rate scores coded with a *k* are from Kirkwood (1985). The values are derived from the number of days (D) between age at 25% of adult mass and attainment of 75% of adult mass (Wa), following the equation $DxWa^{1/4}$. A larger number indicates slower growth rate (i.e., greater number of days to increase mass by the same amount). Scaled growth rate scores coded with a *w* are those compiled by the author using the same equation. However, in these instances, D represents the number of days

between birth and attainment of adult mass, as data for age at 25% and 75% of adult mass were not available.

Scaled infant growth rate scores are derived from the daily mass increase (g/day) relative to adult mass (Wa) following the equation $(g/day)/Wa^{3/4}$, (adapted from Kirkwood, 1985). In this case, a lower number indicates a slower growth rate relative to body mass.

AQ=arboreal quadruped; VCL=vertical clinger leaper; SC=slow climber; SUS=suspensor. See Chapter 4 for a discussion of positional behavior categories.

Data compiled from the following sources, in addition to those cited in the descriptions below: Acharjyo & Misra, 1973; Gebo, 1987; Harvey et al., 1987; McNab & Wright, 1987; Rasmussen & Izard, 1988; Haring & Wright, 1989; Ross, 1991; Leigh, 1992; Dagosto, 1994; Roberts, 1994; Hartwig, 1996; Garber & Leigh, 1997; Smith & Jungers, 1997; Terranova & Coffman, 1997; Kappeler, 1998; Preuschoft et al., 1998; Warren & Crompton, 1998; Weisenseel et al., 1998; Richard et al, 2000; Godfrey et al., 2001, 2004; Leonard et al., 2003.

### *3.3.1 Strepsirhini*

#### 3.3.1.1 Galagidae: Lesser galagos

Specimens in the current sample: *Galago senegalensis* (1); *Galago moholi* (2); *Galagoides demidovii* (1)

The lesser galagos, found in Central and South-Central Africa, are small nocturnal insectivores with a varied consumption of insects relative to other components of the diet (e.g., gums) (Warren & Crompton, 1998). For example, 70% of the *G. demidovii* diet consists of insects (especially orthopterans, lepidopterans and coleopterans which they detect by sound with their mobile ears and can catch mid-flight with the forelimbs while standing on the hindlimbs), while 19% is fruit and 10% is gums (Charles-Dominique, 1971a, 1971b; Walker, 1979). Like many strepsirhines, the lesser galagos are hypometabolic (have low basal metabolic rates relative to other mammals of their size), but not to the same extent as the lorisids (see Table 3.1 and references therein). They develop rapidly and frequently give birth to more than one offspring in a single litter (Rasmussen & Izard, 1988).

The small galagos are among the primates most specialized for vertical clinging and leaping, but they also hop, and more rarely climb, walk quadrupedally, or engage in bridging behaviors (Walker, 1979; Gebo, 1987; Preuschoft et al., 1998). Within this general adaptive scheme, the predominance of leaping in the locomotory repertoire varies from one species to the next. In one study, leaping accounted for 63% of all observed locomotor bouts among lesser galagos (more than all other strepsirhines in the study), while climbing accounted for 26% of locomotor bouts. *G. senegalensis* was very rarely observed locomoting quadrupedally, and only when moving very slowly (5% of bouts) (Gebo, 1987). Otherwise, even on horizontal branches or the ground they will hop bipedally (Walker, 1979; Gebo, 1987). In contrast, *G. demidovii* leaps less than *G. senegalensis* or *G. moholi*; in this small species leaping accounts for only about 40% of observed locomotor bouts (only slightly more than *Microcebus* and some lemurids), followed by quadrupedalism and climbing at about 25% each. It is suspensory for 6% of observed bouts and, on the ground, will either hop or progress quadrupedally (Gebo, 1987).

As a good demonstration of the propulsive strength of the hindlimbs in galagos, *G. demidovii* has been observed leaping 1.5-2 m without losing height. When leaping onto a vertical support it can stop, or pivot around the support and leap again. The tail is used to modify the rotation of the body in flight. During quadrupedal movement, while the hindlimbs are propulsive, the forelimbs are used mainly for stabilization. Running is often punctuated by little jumps. The ricochetal leaping adaptation of galagos allows them to evade most kinds of predators (Charles-Dominique, 1971b).

In a species of *Galago* not included in this study (*G. alleni*) preparation for a leap was observed to involve, in sequence: 1) flexion at the hip and knee, 2) even more flexion at the knee, decreasing the tibio-tarsal angle, and 3) leaping force applied to the substrate at the tarso-metatarsal joint (Jouffroy et al., 1974). During a leap (except for immediately after takeoff), galagos maintain a curled body position, unlike the outstretched flight position in indriids (Oxnard et al., 1981b). *G. moholi* lands hindlimbs first on all support types. It is believed that *G. senegalensis* is also hindlimb dominated in landing, and that *G. demidovii* lands quadrupedally, or forelimbs first (Terranova, 1995a).

Within galagos as a whole, there is a gradation in morphology that matches the gradation in the degree of leaping as a proportion of all locomotor behaviors (McArdle as cited in Oxnard et al., 1981a). The lesser galagos are characterized, as are all vertical clingers and leapers, by long hindlimbs relative to the forelimbs. In the case of galagos, much of this hind-limb elongation is due to the proportions of the calcaneus and navicular, which vary somewhat among genera and species (Jouffroy & Lessertisseur, 1979). Features of the forelimb allow for effective maintenance of posture on vertical substrates (e.g., a large medial humeral epicondyle, for the attachment of strong flexor muscles). Hindlimb morphology facilitates both the flexed joint clinging posture, and leaping (e.g., a deep and narrow patellar groove, a cylindrical rather than spherical femoral head, a posterior extension of the femoral head articular surface onto the femoral neck, a short femoral neck, large knee extensor muscles, tibial plateaus that angle posteriorly relative to the tibial shaft, a ventrally raised patellar articular surface to increase the leverage of the quadriceps femoris) (Burr et al., 1982; Anemone, 1990, 1993; Demes et al., 1998; see Demes et al., 1996 for an alternate explanation of the cylindrical

femoral head). The femur is more robust proportionately than the femur of "walkers" such as macaques or humans, and has a "barreled" midshaft to resist the large peak forces that are generated by leaping (relative to walking at a constant velocity) and buckling from compressive loads (Napier & Walker, 1967; Stevens et al., 1971; Jolly & Gorton, 1974; Walker, 1974; Burr et al., 1982; Dagosto, 1988; Gebo & Dagosto, 1988; Ruff & Runestad, 1992).

**Figure 3.2: Lesser galagos.**
A) *G. moholi*, B) *G. senegalensis*, C) *G. demidovii*. Image from Rowe, 1996.

3.3.1.2 Galagidae: Greater galagos

Specimens in the current sample: *Otolemur crassicaudatus* (3); *Otolemur* sp. (1)

The greater galagos are nocturnal, arboreal primates (Warren & Crompton, 1998) found in South-Central Africa. These are insectivore/gummivores. For example, 62% of the diet of *O. crassicaudatus* has been observed to be plant gums (McNab & Wright, 1987). Like the lesser galagos, *Otolemur* is hypometabolic (see Table 3.1 and references therein).

The greater galagos share many locomotor and morphological features with lesser galagos. However, they engage in less leaping, and more hopping, slow quadrupedalism and climbing than their smaller counterparts. In addition, they show a preference for take-off and landing from oblique rather than vertical supports (Napier & Walker, 1967;

Walker, 1974, 1979; Ruff & Runestad, 1992; Terranova, 1995a, 1995b; Preuschoft et al., 1998). *O. crassicaudatus* (as described by Crompton and cited in Gebo, 1987) leaps 23% out of all locomotor bouts, is quadrupedal 40% of all bouts, and climbs for 34% of all bouts.

When leaping, landing styles in *Otolemur* vary depending upon the species and substrate orientation. *O. crassicaudatus* lands mostly on oblique supports, using quadrupedal or forelimb landings, and only lands hindlimbs first on horizontal supports, a rare occurrence altogether. *O. garnetti* lands quadrupedally most often on vertical supports, hindlimbs first or quadrupedally on oblique supports, and forelimbs first about one third of the time on vertical supports (for shorter leaps) (Terranova, 1995a, 1995b).

Overall galagos have a negative allometry of the hindlimb, while the forelimb scales isometrically or only with slight negative allometry. In other words, in the larger galagos, the forelimbs are relatively the same length as in the smaller galagos, but the hindlimbs are shorter (Jungers, 1985). This is expressed in the tarsus, which is relatively shorter than in lesser galagos, but still longer than in all other primates except *Tarsius* (Jungers, 1985). The femora too are shorter, and display less femoral rigidity, than what is seen in the specialized leapers (Runestad Connour et al., 2000). Other features, such as an increase in the distance between the lesser and greater trochanters of the femur, relative to the lesser galagos, also point to the reduced dependence on leaping in greater galagos (Anemone, 1993).

**Figure 3.3: Greater galagos.**
*O. crassicaudatus*. Image from Rowe, 1996.

3.3.1.3 Lorisidae

Specimens in the current sample: *Nycticebus coucang* (5)*; Loris tardigradus* (1); *Perodicticus potto* (1)

*P. potto* (pottos), *N. coucang* (slow lorises) and *L. tardigradus* (slender lorises) are nocturnal, arboreal primates found in India and Sri Lanka (*L. tardigradus*), Southeast Asia (*N. coucang*) and coastal west and central Africa (*P. potto*). They are insectivore/frugivore/gummivores (Walker, 1969). For example, for *P. potto*, 65% of the diet is composed of fruit, 21% of gums and 10% insects (McNab & Wright, 1987). In contrast *L. tardigradus* is mostly insectivorous (Petter & Hladik, 1970). For some or all of the lorisids, the insectivorous portion of the diet includes species (e.g., ants, termites) that other primates likely avoid because of their toxicity (Petter & Hladik, 1970; Charles-Dominique, 1971a; Rasmussen & Izard, 1988). Pottos appear to detect these odiforous prey, as well as fruiting trees, by smell (Charles-Dominique, 1971a). Lorisids may also include larvae, geckos, birds, eggs and small mammals in their diet (Walker, 1969). As is the case for many strepsirhines, the loris basal metabolic rate is low relative to other mammals (including primates) of the same size. Lorisids are more hypometabolic than

the galagos, with rates 40% or less than what is predicted by the Kleiber relationship (see Table 3.1 and references therein). Gestations are long, pre- and postnatal developmental rates are also relatively slow, and, unlike other strepsirhines of comparable size, lorisids generally have single births (Müller, 1982; Rasmussen & Izard, 1988; Kappeler, 1996; Weisenseel et al., 1998).

Lorises are typically described as slow climbers, specialized for steady and stealthy movement that emphasizes smoothness, consistency in speed, and acrobatic flexibility (Jouffroy & Petter, 1990). Although seeming to prefer above branch locomotion, they are equally adept at walking suspended below branch, and can move fluidly, and without interruption, from one to the other (Charles-Dominique, 1971b; Dykyj, 1980; Jouffroy et al., 1983; Jouffroy & Petter, 1990; Glassman & Wells, 1984; personal observation). Their locomotor repertoire includes bridging, cantilevering and suspension, but none have been observed to leap, hop or bound (Preuschoft et al., 1998). In all cases (except for a rare release of the hindlimbs slightly prior to grasping with forelimbs during bridging) lorisids keep at least one hand or foot on the substrate, and usually two or three (Walker, 1979; Dykyj, 1980; Jouffroy et al., 1983; Jouffroy & Petter, 1990). The bridging of gaps is accomplished carefully and precisely, facilitated by the flexibility of the joints (including the vertebral column) and the powerful grasp in the cheiridea (Dykyj, 1980; Jouffroy et al., 1983). In the absence of bridgeable connecting branches, pottos have been observed to backtrack on a route and find another more navigable one (Charles-Dominique, 1971b). When on large vertical trunks they wrap their limbs around it and move only one at time (Petter & Hladik, 1970; Charles-Dominique, 1971b). Feeding and resting postures are varied, and include suspension by

the hindlimbs (Walker, 1969, 1979; Glassman & Wells, 1984). Movement of the spine is serpentine, particularly on the ground, with a flexion of the posterior portion of the spine laterally with the movement of the hindlimb (Dykyj, 1980; Jouffroy et al., 1983; Gebo, 1987; Demes et al., 1990). When progressing quadrupedally, the hand and foot on each side meet each other on the substrate while the other hand and foot stretch anteriorly and posteriorly respectively, in a gait pattern that has variously been described as both diagonal and lateral sequence (Charles-Dominique, 1971b; Dykyj, 1980; Glassman & Wells, 1984; Demes et al., 1990; Ishida et al., 1992).

There are differences among the lorisids in frequencies of various positional behaviors and in their niches within the forest structure (Petter & Hladik, 1970; Charles-Dominique, 1971b). In addition, while all lorisids can move more quickly than descriptions often suggest (even running or trotting, although without a "floating phase"), *L. tardigradus* has peak speeds that are almost twice those of *N. coucang*, and *P. potto* has also been observed to move at faster speeds than the slow loris (Walker, 1969; Jouffroy et al., 1983; Demes et al., 1990; Jouffroy & Petter, 1990). Nevertheless, overall the lorisids are very similar in their modes of locomotion and posture (Gebo, 1987; Demes et al., 1990). A cryptic approach is used in both foraging and predator defense, although lorisids can display a range of surprisingly aggressive behaviors when necessary, and are armed (to a greater or lesser degree depending on the genus) with features in the nuchal region adapted to ramming a predator or conspecific (Charles-Dominique, 1971a, 1971b).

In lorisids, unlike other primates, locomotion is not strongly hindlimb dominated. Rather, there is a kinematic similarity in the way the hindlimbs and forelimbs are used in

locomotion and, depending upon the behavior, the forelimbs may have an active, equal, or perhaps even dominant role in pushing or pulling the body (Ishida et al., 1990; Jouffroy & Stern, 1990), although Jouffroy & Stern still suggest a "front steering/rear driving" mode (1990, p. 234). Ishida et al. (1990) have found that the hand supports more of the weight of the body than the foot and sustains greater vertical loads. Loads on both sets of limbs, and the muscles that are used to resist gravity, are different depending on whether the animal is above or below branch, climbing up, or climbing down (Jouffroy & Stern, 1990; Ishida et al., 1992).

Morphological and anatomical features associated with the unique lorisid adaptation are numerous. The intermembral index is high, with forelimbs that are close in length to the hindlimbs, facilitating the equivalent usage of both sets of limbs. Joint surfaces are large, for extreme mobility at the carpal, tarsal, knee, elbow, hip and shoulder joints (Charles-Dominique, 1971b). Four to five extra presacral vertebrae allow for added flexibility the spine (Walker, 1969). The hands and feet are large and powerful with a reduced or stump-like second ray to reduce bending stress in this digit, a large first digit, and a pincer-like grasping action (Walker, 1969; Charles-Dominique, 1971b).

**Figure 3.4: Lorisidae.**
*A) N. coucang*, B) *L. tardigradus*, C) *P. potto*. Images from Rowe, 1996.

3.3.1.4 Lemuridae

Specimens in the current sample: *Varecia variegata* (1); *Lemur/Eulemur* sp. (1)

Lemurids are endemic to the island nation of Madagascar. Depending upon the species, these arboreal primates can be diurnal, cathemeral or even nocturnal (*V. variegata* is a diurnal species). They may be highly folivorous (potentially supplementing with fruit and flowers), principally frugivorous (potentially supplementing with flowers, herbs, leaves and insects), and in some cases may specialize on flowers, or seasonally on nectar (McNab & Wright, 1987; King et al, 2001; Sussman, 2002; Godfrey et al., 2004). As an example, the diet of *E. fulvus* has been observed by some to comprise 71% leaves (McNab & Wright, 1987), although others have suggested their diet is primarily frugivorous (King et al, 2001; Godfrey et al., 2004). *V. variegata* specializes principally on ripe fruits (73-90% of the diet) with some leaves (4-21%) and supplementation of nectar and flowers (King et al, 2001; Godfrey et al., 2004). *L. catta* is has an

approximately equivalent proportion of fruit and leaves in the diet, with some flowers (Godfrey et al., 2004).

Members of Lemuridae can have twin births (Godfrey et al. 2004), and achieve adult body mass by about two-three years of age with the exception of *V. variegata*, which grows for about four years, with a very gradual deceleration in growth (although differences in size between taxa are overall likely due more to differences in growth rate than differences in duration of growth) (Terranova & Coffman, 1997; Leigh & Terranova, 1998; Godfrey et al., 2004). For all species, growth is fastest in the first six months. The overall lemurid growth pattern is likely faster, for a shorter duration, than what is seen, for example, in anthropoids (with some exceptions, particularly when they are compared to folivorous anthropoids) (Leigh & Terranova, 1998).

All lemurid species are principally arboreal, although with dependence on terrestrial travel in some cases, with walking, running or galloping, and some bipedal running when on the ground (Walker 1979). For example, *L. catta* is arboreal one third of the time, (70% of its travel is on the ground), and otherwise utilizes all levels of the forest, while *E. fulvus* rarely comes to the ground and generally stays in the canopy (85% of all its travel) (Sussman, 2002).

Lemurids overall have a varied, mostly quadrupedal locomotor repertoire, displaying a combination of climbing, leaping, walking, running, and bounding in varied proportions (Walker 1979; Preuschoft et al., 1998). In *V. variegata* the majority of movements are quadrupedal walking and running above large horizontal branches, and leaping is more rare than in other lemurid species (21% of bouts compared to 25-37% of bouts in other lemurs) (Gebo, 1987). *V. varecia* individuals have been observed to be

more cautious in their locomotion than other lemurids, perhaps not surprising given their larger body size (Walker, 1974, 1979; Gebo & Dagosto, 1988; Preuschoft et al., 1998). *V. variegata* also suspends more frequently than other lemurids, as well as indriids (21% of all observed locomotor bouts), usually by the hindlimbs (Gebo, 1987; Meldrum et al, 1997).[2] There is variation in the leap landing styles among lemurs, both within and between species, including forelimb first, hindlimb first, and quadrupedal modes, depending in part on the orientation of the landing substrate (Dunbar, 1988; Terranova, 1996). All leaps begin with a crouch, and forelimbs are outstretched at the onset of the leap. However, the body and limb position during flight depend upon the orientation of the landing support, and the landing style (Terranova, 1996). Dunbar (1988) describes vertical clinging and leaping in *L. catta*, where the tail assists in rotating the body appropriately during the leap.

All lemurs have longer hindlimbs than forelimbs (in accord with some incidence of leaping), with relatively longer forelimbs in larger species (Terranova, 1996). Despite features indicative of leaping, however, the lemurids as a whole have been considered to be the "least specialized" of all the prosimians (Jouffroy & Lessertisseur, 1979). Features of quadrupedalism that lemurids generally display (in contrast to more specialized leapers) include an olecranon process that is angled posteriorly to increase the mechanical advantage of the elbow during walking and running, a wrist configured to resist extension and weight bearing, a patellar groove that is wider and shallower than in habitual leapers,

[2] It should be noted that different researchers have observed dramatically divergent frequencies of leaping in the same lemurid species. So, for example, in contrast to the description above, Dagosto (1994), in a field study, finds that *V. variegata* leaps in 53.5% of all observations (still less than other lemurs). Dagosto (1994) also finds more suspension in *V. variegata* than does Gebo (1987): 33% of observations, in a captive study. Terranova (1996, in a captive study) and Dagosto (1994) both find that lemurs in general leap for about 50% or more of their translocations, in contrast to the 37% maximum found by Gebo (1987).

and longer relative forelimb lengths than leapers (Walker, 1974; Godfrey, 1988). Lemurs are intermediate between the specialized leaping indriids (see below) and the more scansorial cheirogaleids (see below) in the relative lengths of the tarsals and metatarsals (Jouffroy, 1975).

Coincident with decreased dependence on leaping, *V. variegata* is distinguished from other lemurs by its shorter limbs – especially the hindlimb – relative to precaudal vertebral column length (Jouffroy & Lessertisseur, 1979). Nor does is display the large knee extensors seen in leaping prosimians, including the indriids (Demes et al., 1998). *V. variegata* is otherwise also morphologically distinct relative to other lemurids, for example not having their low humeral cortical area (Runestad Connour et al., 2000), and displaying features coincident with foot reversal during hindlimb suspension (Meldrum et al., 1997).

**Figure 3.5: Lemuridae.**
*V. varecia*. Image from Wolfe & Sleeper, 1997.

3.3.1.5 Indriidae

Specimens in the current sample: *Propithecus* sp. (2); *Indri indri* (1)

Both *Propithecus* and *I. indri* are endemic to Madagascar, the former found in the dry forests of the west and extending into the north and the desert-like conditions of the

southwest, and the latter in the wetter evergreen forests of the east. Both include substantial proportions of leaves and fruits in their diet with *I. indri* more folivorous (up to 82% of the diet) than at least some *Propithecus* species (up to 46% of the diet for *P. verrauxi*). They eat flowers as well, and *I. indri* may also specialize on seeds, for which they are equipped with a particularly large cecum and colon (Ravosa et al., 1993; Sussman, 2002, Godfrey et al., 2004).

Relative to lemurids of equivalent body mass, indriids grow slowly, both pre- and post-weaning, despite far more rapid dental development than in lemurids (Schwartz et al., 2002; Godfrey et al., 2004). For example, long bone growth completion is achieved at approximately five years of age in *P. verreauxi* (Richard et al., 2000). Neither genus typically has twin offspring (Godfrey et al., 2004).

Like the lesser galagos, indriids are considered to be vertical clingers and leapers, but have evolved this leaping adaptation in parallel to that of galagos, and therefore there are both behavioral and morphological differences between the two families (Szalay & Dagosto, 1980; Godfrey, 1988). For example, leaps often are preceded by a preparatory movement in the opposite direction of take off; either a crouch, or a crouch and hop (Demes et al., 1996). They engage in a greater range of postural behaviors than galagos, as well as tarsiers, and may position the limbs in a variety of ways when clinging vertically, most notably abducting and laterally rotating the thighs (Oxnard et al., 1981b; Demes et al., 1996). Both *P. verreauxi* and *I. indri* engage in frequent, powerful ricochetal leaping, with one leap followed immediately by the next (Walker, 1979; Gebo, 1987; Runestad Connour et al., 2000). In *P. verreauxi*, leaping has been observed to comprise 46% of all locomotor bouts (Gebo, 1987), with horizontal leaps easily covering

10 m (Demes et al., 1991). Landing is always hindlimb first, and the arms, as well as the tail in *Propithecus*, are used to achieve appropriate rotation of the body during flight. During a leap, the body is extended and horizontal, with splayed upper limbs (Walker, 1979; Oxnard et al., 1981b; Demes et al., 1996).

Indriids can be quite versatile in their locomotor behavior. So, while they often vertically cling and leap, they also may engage in slow quadrupedalism, quadrupedal suspensory behaviors (when feeding), and distinctive, powerful, bipedal hopping on the ground (Walker, 1974; Runestad Connour et al., 2000).

As with other specialized leapers, the hindlimbs in indriids are significantly longer than the forelimbs, and other typical features are present (e.g., a deep and narrow patellar groove, a ventrally raised patellar articular surface on the distal femur). In fact, even *I. indri*, with shorter hindlimbs and longer forelimbs relative to the smaller *P. verreauxi,* has among the longest hindlimbs relative to body size of all primates (Jungers, 1985; Anemone, 1993). In the forelimb of indriids, another likely correlate of vertical clinging and leaping is the high and narrow trochlea, logically associated with extremely flexed elbow joints during clinging (Runestad Connour et al., 2000). However, unlike in galagos and *Tarsius* (see below) the tarsus in indriids is not elongated, the foot morphology emphasizes grasping, and leaping propulsion is primarily achieved at the hip and knee ("thigh-powered" jumping), with longer relative femora (Walker, 1974; Jouffroy, 1975; Gebo & Dagosto, 1988; Godfrey, 1988; Demes & Gunther, 1989: Demes et al., 1996). The metatarsals are long, although the foot overall is relatively short compared to the hindlimb (but with an elongated big toe). The digits in the hand are also elongated (Jouffroy, 1975; Jouffroy & Lessertisseur, 1979).

Because of dependence of the hip and knee for leaping propulsion, the indriids display a peculiarity of the sartorius muscle origination, such that it does not interfere with the mobility of both these joints. This is compared to other lemurs, where the sartorius holds together the hip and knee joint, propulsion being focused on the ankle joint (Jouffroy, 1975). In addition, the extensors of the hip have a large mass relative to other specialized leapers, while the muscles of the ankle plantarflexors are relatively small (Demes et al., 1998).

**Figure 3.6: Indriidae.**
A) *P. verreuaxi.* Image from Wolfe & Sleeper, 1997. B) *I. indri.* Image from Rowe, 1996.

3.3.1.6 Cheirogaleidae

Specimens in the current sample: *Cheirogaleus major* (2); *Mirza coquereli* (1); *Microcebus murinus* (1)

The cheirogaleids are a group of small lemurs endemic to various coastal regions of Madagascar. *C. major* (greater dwarf lemur), *M. coquereli* (dwarf lemur) and *M. murinus* (mouse lemur) are all nocturnal and arboreal, and have varied diets including fruit, leaves, flowers, gums, nectars, exudates, insects and other small animals. For example, *M. murinus* is primarily frugivorous, supplementing the diet with leaves, insects and

insect secretions, while *M. coquereli* has been described as obtaining a full 50% of its diet from the secretions of homopteran insects (Ortmann et al., 1997; Schmid, 2001; Sussman, 2002).

All cheirogaleids, with the exception of *M. coquereli*, are characterized by a metabolic adaptation unique among primates, in which they undergo periods of reduced activity, metabolic rate and body temperature.[3] These can be long, seasonally-determined periods of hibernation, as has been observed in *C. major* and occasionally *M. murinus*, or seasonally-determined daily torpor (which can last several days) as is more typically described for *M. murinus* (Ortmann et al., 1997; Schmid & Kappeler, 1998; Schmid, 2001; Wright, 1999; Sussman, 2002). In both these species, reduced activity is during the dry season when food availability is diminished and predation is on the rise. *M. murinus* will accumulate fat stores in the body and tail prior to the onset of this period (Ortmann et al., 1997; Schmid & Kappeler, 1998; Schmid, 2001; Sussman, 2002). The seasonal behavior appears to be variable among *M. murinus* individuals, with some (particularly males) not reducing activity at all during the dry season (Schmid, 2001; Sussman, 2002). Cheirogaleids may have multiple births (2-3 offspring in a litter) (Schmid, 2001). Gestation is short, and pre- and post-natal growth rates are relatively rapid (Kappeler, 1996).

Cheirogaleids display quadrupedal locomotion over a range of speeds, commonly with short bouts of branch running, or scurrying. Leaping, hopping, bounding, climbing, suspending and cantilevering are also included in their positional behavior repertoire

[3] During the daily torpor in *M. murinus*, for example, the metabolism is depressed by 80-90% (relative to resting metabolic rate) and the body temperature descends to near ambient temperature. These both return to nomothermia during active periods of the day, with body temperature rising passively as the ambient temprature rises. This behavior achieves a 30%-60% savings in energy relative to a day spent in a nomothermic state (Ortmann et al., 1997; Schmid & Speakman, 2000)

(Walker, 1974; Gebo, 1987; Preuschoft et al., 1995, 1998). For example, *C. major* moves quadrupedally with the body held close to the branch, only infrequently jumping from one branch to another, and not often engaging in suspension (Walker, 1979; Gebo, 1987). *M. murinus* move rapidly in short bouts, more frequently jumps than other cheirogaleids (38% of all observed locomotor bouts, with quadrupedal landing) and may grasp branches to swing across a gap. While they have been observed to cantilever, and hang by the hindlimbs while feeding, suspension comprises the smallest proportion of their positional behavior among cheirogaleids (Walker, 1979; Gebo, 1987). *M. coquereli* employs a very diverse positional behavior repertoire, with equal amounts of above branch quadrupedalism, leaping, climbing and suspension, the latter more than all other cheirogaleids. It may also cantilever to bridge gaps (Gebo, 1987).

All cheirogaleids have been observed to vertically cling and leap (Gebo, 1987). However, the leaping style is typically different from what is seen in committed vertical clingers and leapers such as the lesser galagos, indriids and tarsiids. For example, cheirogaleids are more likely to have pronograde (rather than vertically clinging) postures, to be locomoting quadrupedally before a leap, and are more likely to leap horizontally or downward (Oxnard et al., 1981b).

The predominant quadrupedalism among cheirogaleids is reflected in features of the fore- and hindlimb described above for *Lemur*, as well as a greater trochanter that extends more proximally than the femoral head (Walker, 1974; Ford, 1988). Cheirogaleid limbs are short relative to body size; both forelimbs and hindlimbs are the shortest among primates, although the relative lengths increase with body size, particularly for the hindlimb (Jungers, 1985). The tarsus is somewhat elongated,

intermediate in length between the condition seen in galagids and that found among lemurids, while metatarsals are short (Jouffroy, 1975; Jouffroy & Lessertisseur, 1979; Jungers, 1985).

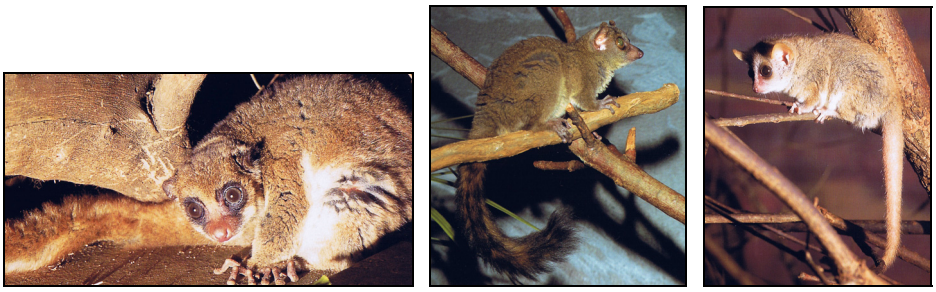

**Figure 3.7: Cheirogaleidae.**
A) *C. major,* B) *M. coquereli,* C) *M. murinus.* Images from Rowe, 1996.

### *3.3.2 Haplorhini*

#### 3.3.2.1 Tarsiidae

Specimens in the current sample: *Tarsius spectrum* (2); *Tarsius syrichta* (1); *Tarsius* sp. (1)

Tarsiids are nocturnal, arboreal primates found principally in the forests of Borneo, Sumatra, Sulawesi and the southern Philippines (McNab & Wright, 1987; Warren & Crompton, 1998). They are faunivores (eating mostly insects, but other small animals as well), unique among primates in that they include no plant matter in their diet (McNab & Wright, 1987; Roberts, 1994; Warren & Crompton, 1998).

It is thought that the life history of tarsiids is very "slow", more closely resembling what is seen in anthropoids than in strepsirhines (Ross 1991; Roberts, 1994). Prenatal development is extended[4], gestations and life span are long, postnatal development is also suggested to be slow (relative to all other prosimians), sexual

[4] Roberts (1994) states that fetal growth rate is "among the lowest recorded for any mammal" (p.21).

maturity comes late, and only a single (very large) offspring is produced at a time (Roberts, 1994; Runestad Connour et al., 2000).

Tarsiids are committed vertical clingers and leapers – resting on and moving rapidly between vertical supports – although they will also walk and climb quadrupedally, as well as climb and hop bipedally, the latter including on the ground (Walker, 1974, 1979; Niemitz, 1983; Runestad Connour et al., 2000). The positional behavior adaptation in this taxon is thought to represent yet another independent evolution of vertical clinging and leaping (Szalay & Dagosto, 1980; Jouffroy et al., 1984). The remarkable leap of tarsiids can reach 50 times the body length (Runestad Connour et al., 2000), with very fast acceleration during the leap (Niemitz, 1983). Before take-off, the hip, knee and ankle joints are greatly flexed, and the leaps are launched at a 45-degree angle. During flight, the legs rotate forwards while the tail rises behind the torso, and the body remains curled like a ball, as in galagos, and unlike the more splayed-limb posture in indriids. Tarsiids land feet first (Oxnard et al., 1981b; Niemitz, 1983).

The morphology of the tarsiids is in many ways similar to that of galagids, yet with even more extreme specialization for clinging and leaping, as the tarsiers apparently particularly avoid quadrupedal travel (Walker, 1974; Dagosto, 1988; Gebo & Dagosto, 1988). So, for example, the hindlimbs are relatively longer than those of a galago, the femoral head is larger, and the distal tibia and fibula are fused (for about 60% of their length), a feature unique among primates (Jouffroy & Lessertisseur, 1979; Jouffroy et al., 1984; Jungers, 1985; Ford, 1988; Rasmussen et al., 1998; Runestad Connour et al., 2000). The hands and feet are long, and the tarsus is also elongated, although slightly less so than in galagids, relative to the precaudal vertebral column (Jouffroy & Lessertisseur,

1979). Other features related to leaping include a high anterior attachment for the patellar tendon on the tibia to maximize the leg-extending leverage of the quadriceps femoris tendon, a ventrally raised patellar articular surface to further increase the leverage, tibial condylar surfaces structured to restrict action to the sagittal plane, a posterior expansion of the articular surface of the femoral head onto the femoral neck, and large knee extensor muscles (Anemone, 1993; Demes et al., 1998; Rasmussen et al., 1998).

**Figure 3.8: Tarsiidae.**
A) *T. spectrum.* Image from Rowe, 1996. B) *T. syrichta.* Image from Wolfe & Sleeper, 1997.

3.3.2.2 Callitrichidae

Specimens in the current sample: *Callithrix geoffroyi* (1); *Callithrix argentata* (1)

Callitrichids (marmosets) are small-bodied, diurnal, arboreal South American monkeys, living in a diverse range of treed habitats. They subsist on a varied diet of fruits, flowers, insects and other invertebrates, small vertebrates, and eggs. They also specialize on tree exudates – which they extract by gouging the bark with modified long, narrow, mandibular incisors (Sussman & Kinsey, 1984) – comprising a high proportion of their diet (e.g., 31-34% of the diet in *C. kuhli* is exudates, and 29% of the daily activity of *C.*

*jacchus* has been observed to be accounted for by feeding on exudates) (Sussman & Kinzey, 1984; Rosenberger, 1992).

It has been suggested that small body size in challitrichids is a case of dwarfing from a larger bodied ancestor (Martin, 1992; Rosenberger, 1992). Given their size, they have the lowest metabolic rates known for anthropoids, and it is thought that this may be related to their gum eating (Genoud et al., 1997). *Callithrix* species have smaller neonates that would be expected, and appear to limit their adult size by growing slowly relative to other larger callitrichids, rather than shortening the growth period (Ross, 1991; Garber & Leigh, 1997). Adult size and postcranial maturity is achieved at approximately 1.5-1.9 years of age (Kohn et al., 1997; Tardif & Bales, 2004). However, the growth rate of all callitrichids is elevated relative to that of most other platyrrhines, as well as catarrhines, approximating that found in many strepsirhines (Ross, 1991). Birth rates are also high relative to other primates, twinning is common, and monogamy and allocare are typical (Ross, 1991; Garber & Leigh, 1997).

*Callithrix* individuals engage in quadrupedal bounding, walking and running, moving in short bouts, as well as vertical claw-clinging – particularly when feeding on gums – and some vertical leaping. They will move scansorially up and down vertical supports (Falsetti & Cole, 1992; Preuschoft et al., 1995). Because they have secondarily evolved claw-like tegulae from a nailed primate ancestor on all digits except the hallux, they can locomote and cling on large vertical trunks without the reliance on grasping found in other primates (Szalay, 1981; Sussman & Kinzey, 1984; Martin, 1992). Other postcranial features are in accordance with both quadrupedalism (e.g., a more proximal greater trochanter than femoral head, a long olecranon process to withstand high

moments at the elbow during flexed limb scurrying) and clinging/leaping (e.g., a deep patellar groove) (Ford, 1988; Rose, 1993).

**Figure 3.9: Callitrichidae.**
A) *C. geoffroyi.* Image from Rowe, 1996. B) *C. jacchus.* Image from Wolfe & Sleeper, 1997. *C. jacchus* is not included in the sample, but the picture is provided to demonstrate the typical *Callithrix* morphology.

3.3.2.3 Cebidae

Specimens in the current sample: *Saimiri sciureus* (1); *Saimiri* sp. (3)

Among cebids, the members of the genus *Saimiri* (squirrel monkeys) are arboreal, diurnal species found in northern and western South America, in a range of arboreal habitats (Ross, 1991). They are omnivores that include a large proportion of fruits and insects in their diet, as well as other foods such as nectar (with seasonal changes in the dietary composition) (Fleagle & Mittermeier, 1980; Boinski, 1989). For example, *S. boliviensis* has been observed to subsist on a diet that is 93% fruit (Rosenberger, 1992). In contrast, *S. oerstedii* is mostly insectivorous, but also includes other animals as well as plants in its diet (Boinski, 1989).

Relative to other platyrrhines of their size, members of the genus *Saimiri* exhibit an extended growth period with slow growth rates (growth cessation occurs at an age comparable to substantially larger platyrrhines; 3-4 years or more), and give birth to single babies that are larger relative to maternal size than in any other anthropoids (Long

& Cooper, 1968; Manocha, 1979; Galliari, 1988; Garber & Leigh, 1997; Pucciarelli et al., 2000). Prenatal growth rates are surprisingly high, and both adults and neonates have large brains relative to body size (Hartwig, 1996).

Squirrel monkeys are walking and running quadrupeds that also leap (no more than 2-3 meters), climb, and may occasionally travel on the ground or vertically cling. They typically grasp small branches with their hands and feet, rather than traveling plantigrade on wider branches (Boinski, 1989). Depending on whether they are traveling, feeding or foraging, one study has indicated that quadrupedal locomotion accounts for 55% to 87% of bouts, and leaping accounts for 11-42% of bouts. In this study, individuals are more frequently found in the understory than in higher levels of the canopy (Fleagle & Mittermeier, 1980). Similar proportions were found by Fontaine (1990) with quadrupedal locomotion during 74% of focal observation, leaping during 20%, and climbing during 4%, while Boinski (1989) found 87.5% of focal samples during locomotion bouts involved quadrupedalism, 8.3% involved leaping, and 4.2% involved climbing. In summary, it is fair to conclude that *Saimiri* is primarily an arboreal quadruped. Unlike other platyrrhines, *Saimiri*'s long tail is not particularly prehensile, is principally used as a counterweight, to brace the body, or to wrap around the body for warmth, and only rarely as a grasping "fifth limb" (Boinski, 1989; Johnson & Shapiro, 1998).

The emphasis on rapid parasagittal quadrupedalism is supported by such features as a stable humeroulnar joint (wide anteroposteriorly, with a ventral extension of the trochlea medially), a shallow bicipital groove relative to suspensory primates, a shallow femoral head articulation (without the posterior expansion onto the femoral neck seen in

committed leapers), an absence of the anterior expansion of the patellar articular surface on the distal femur seen in specialized leapers, and femoral condyles of even size (Szalay & Dagosto, 1980; Anemone, 1993; Rose, 1993; Nakatsukasa et al., 1997).

**Figure 3.10: Cebidae.**
*S. sciureus.* Image from Wolfe & Sleeper, 1997.

3.3.2.4 Atelidae

Specimens in the current sample: *Ateles fusciceps* (1); *Ateles* sp. (1)

Members of the genus *Ateles* (spider monkeys) are large, diurnal, arboreal monkeys found in northern and western South America, as well as in Central America. Depending upon the species, spider monkeys may inhabit different parts of the canopy. For example, *A. paniscus* is mainly an upper forest level inhabitant, while *A. geoffroyi* favors the lower forest (Mittermeier, 1978). They are primarily frugivores (80-83% of the diet in one study), but will supplement with leaves, flowers and buds (Fleagle & Mittermeier, 1980; Rosenberger, 1992). It is believed that spider monkeys grow slowly, as do other platyrrhines, relative to strepsirhines (Ross, 1991; and see Table 3.1).

Spider monkeys engage in a wide range of positional behaviors – including quadrupedal running and walking, climbing and bipedalism – but they are best known for their acrobatic suspensory locomotion, including rapid ricochetal bimanual brachiation

(Jenkins et al., 1978; Mittermeier, 1978; Fleagle & Mittermeier, 1980; Turnquist et al., 1999). One study finds that suspension is used in 25-39% of bouts, quadrupedalism in 22-25%, and climbing in 31-47%, with much lower frequencies of both leaping and bipedalism (Mittermeier, 1978; Fleagle & Mittermeier, 1980). Similarly, Fontaine (1990) finds that 51% of focal observations involve, quadrupedalism (generally slow walking), 24% involved suspension, 11% involved leaping, and 9% involve climbing. Again, comparable frequencies of suspension are described by Cant et al., (2001). In contrast to *Saimiri*, members of the genus *Ateles* have a fully prehensile tail, from which they can suspend (Mittermeier, 1978; Cant et al., 2001).

The reliance on suspension is expressed in such features as a dorsally positioned scapula, an elongated clavicle, atrophied thumbs, forelimbs that are slightly longer than hindlimbs, a narrow bicipital groove to keep the tendon of the long head of the biceps brachii in place through a large range of forearm movement, and a straight humerus, perhaps reflecting the predominance of torsional loads (Jenkins et al., 1978; Ford, 1988; Mittermeier, 1978; Swartz et al., 1989; Turnquist et al., 1999).

**Figure 3.11: Atelidae.**
*A. belzebuth.* Image from Wolfe & Sleeper, 1997. This species is not included in the sample, but the picture is provided to demonstrate the typical *Ateles* morphology and suspensory abilities.

### 3.4 Conclusion

In this chapter I have presented a brief background on primate life history, positional behavior and phylogeny, as well as overviews of the natural history of each of the 10 primate taxon groups included in the study sample. The descriptions make clear that, although each taxon can be characterized by a unique assemblage of morphologies, developmental patterns, ecologies and behaviors, there is much overlap between them. This is particularly evident with respect to positional behavior. However, for the purpose of the comparative investigation undertaken in this study, a broad (albeit partly artificial) differentiation between groups is necessary, and has a precedent in previous studies of bone microstructure (e.g., Schaffler & Burr, 1984; Paine & Godfrey, 1997; Runestad, 1997). In addition I contend that, while observations of behavior alone may illuminate the variety in postural and locomotor modes, behavior and morphology together provide a clearer picture of the adaptive scheme for a given group. So, for example, while lemurids, cheirogaleids and challitrichids are all observed to vertically cling and leap, their postcranial morphologies underscore the essentially generalist quadrupedal nature of their positional behaviors relative to the specialized vertically clinging and leaping groups.

# Chapter 4

# Primary Tissue Type Distributions

## 4.1 Introduction

Bone primary tissue types have been observed to vary considerably within cross-sections, along the shafts of bones, between elements, and among individuals and taxa (Enlow, 1966). Explanations for this diversity in form and pattern have ranged from the typological (e.g., in early comparative studies such as those of Quekett, 1849; Foote, 1913) to the functional, associating different tissue types with variation in life history parameters, physiological features, and mechanical adaptations. In particular, the relationship between growth rate and primary tissue type has been a subject of intense study since first described by Amprino in 1946.

In this study, variation in distributions of primary tissue types at the midshaft cortex of primate long bones are examined with the objective of: 1) describing the diversity among a phylogenetically and adaptively wide-ranging selection of primates, and 2) investigating the relationship with potential causal factors, as described in the existing literature. Although broad comparative studies of primary tissue types exist (e.g., Aprino & Godina, 1947; Enlow & Brown 1956, 1957, 1958; Jowsey, 1968; de Ricqlès, 1968-78; Singh et al., 1974), the variation present within a single mammalian order, including the order Primates, has not been systematically, and quantitatively, explored. The following questions, not posed or addressed so far, need to be considered before some causal understanding of variation in primary tissue types can be achieved. Do primates vary in their primary tissue type distributions at the midshaft cortex of long

bones? Does variation in growth rate among primate taxa express itself in bone histology? Does body size influence the observed patterns? Is there any indication that mechanical adaptations may in part determine the presence of one tissue type or another? Finally, are there phylogenetic signals to be found in the microstructure of bones at any particular taxonomic level?

### 4.2 Background on bone tissue typology

> *"The laws of Nature are undeviating in the construction of the skeleton of vertebrate animals: the same regularity in structure, the same method of arrangement of the bone-cells, has existed from the time when the surface of our planet was first inhabited by a vertebrate animal up to the present period…The bones of the Mastadon and the huge Megatherium, the giants of the land, are no more remarkable for the coarseness of their structure than are those of the smallest mammiferous quadrupeds, the mouse, and such has been the prevailing law from the commencement of the earth's existence, and such, no doubt, will continue to the end of time"* (Quekett, 1849, p. 57-78).

It appears that bone tissues of living vertebrates have been composed of the same basic units of construction, with presumably similar function, since the appearance of earliest vertebrate skeletal fossils (Enlow & Brown, 1958; Moss, 1964; de Ricqlès, 1978). Bone is made up of a mixture of organic and non-organic components, comprising a collagen and mineral matrix, cells that are associated with this matrix, a system of surrounding and penetrating blood vessels, and nerves. These components of bone tissue come together in a range of relatively stereotyped patterns. The differentiation between, and naming of, tissue types is inherently problematic given that there exist, at least within some categories, seemingly many variations. In addition, one tissue type may grade imperceptibly into another, so that at times it becomes impossible to decide where one ends and the other starts, or whether to apply yet another term to the intervening area.

Nevertheless, because the features of bone tissue that are used to differentiate between types have biological (in terms of life history, physiology and mechanics) as well as descriptive value, it is essential to arrive at a satisfactory means by which to discuss them. In addition, such categorizations are necessary for the quantification of tissue type areas.

Ultimately, the most successful descriptive categorizations will consider several, if not all, of the meaningful features that differ between bone tissues, and there have been many attempts to construct workable systems of tissue typology. The most commonly applied classification that exists in the literature is one proposed by de Ricqlès in the 1970's, expanding upon earlier typologies (e.g., Enlow & Brown, 1956; Enlow, 1966), and modified by him, together with colleagues, in the intervening years. The terminology I employ, except where noted otherwise, is in accordance with this scheme (de Ricqlès, 1975; de Ricqlès et al., 1991; Francillon Vieillot et al., 1990).

### *4.2.1 Fibrillar structure*

The typology of bone using this system requires two levels of description. First, the fibrillar (i.e., collagen fiber) structure of the bone is identified. This is classically organized into one of three major patterns: 1) woven-fibered (= woven), 2) parallel-fibered, or 3) lamellar, depending on the degree of regularity in the organization of the collagen fibers and the shape and orientation of the osteocyte lacunae. Fibrillar structure types are effectively identified in polarized light microscopy with additional observation of osteocyte lacunar distribution and shape by conventional transmitted light (LM). Woven-fibered bone is characterized by the presence of loosely-packed collagen fibers

that vary in size and which are randomly oriented, leading to a "woven" appearance in circularly polarized light (CPL). In contrast, in parallel-fibered bone, collagen fibers are closely-packed and aligned parallel to each other in large swathes, appearing smooth in CPL (Francillon-Vieillot et al., 1990; Boyde & Jones, 1998). A classic interpretation of the lamellar type posits that within each sheet (or lamella) the fibers are all similarly aligned while adjacent sheets have fibers that differ in their orientation by 90° (e.g., Boyde 1972). This leads to a characteristic striped alternation of light and dark lamellae in polarized light. However, not all lamellar bone displays this regular alternation, and the structure of this matrix type has been, and continues to be, the subject of intense research, particularly with respect to the lamellae of secondary osteons (e.g., Smith, 1960a; Cooper et al., 1966; Frasca et al, 1978; Ascenzi et al, 1983; Giraud-Guille, 1988; Marotti, 1993; Pannarale et al., 1994; Weiner & Arad, 1997; Ascenzi et al., 2003; see Chapter 6).

These fibrillar structure types are found in both compact and cancellous bone, and may be primary or secondary in origin. While secondary bone is often used to refer solely to the tissue deposited intracortically around Haversian canals subsequent to resorption of existing bone, de Ricqlès and colleagues refer to secondary bone as all those tissues that have replaced previously deposited bone, identified by the presence of a cement line. However, as this group of workers has pointed out, the concept of primary versus secondary bone has a limited meaning, and can only be used as record of relative osteogenesis time at the very local level (de Ricqlès et al. 1991, Castanet & de Ricqlès, 1986-87).

*4.2.2 Primary tissue patterns*

Subsequent to the classification of fibrillar structure, the identification of vascular patterns and the spatial distribution of fibrillar types, as well as the ontogenetic origin of the tissue, assist in the second level of differentiation between types, as outlined below. A description of the practical identification of tissue types used in the current study follows in the Methods section.

4.2.2.1 Vascular canals

Compacta may comprise bone tissues of all fibrillar matrix types, and may be vascular or avascular. When vascular canals are present, these may be simple – no lamellae circumferentially surround the canal – or they may be in the form of primary osteons. The latter are surrounded by lamellae that have been circumferentially deposited around the blood vessels in the canals. Such canals may course longitudinally through a bone, or may follow perpendicular, oblique or radial directions. In addition, a single canal may change directions within the cortex, and may anastomose with other canals (Robling & Stout, 1999).

4.2.2.2 Lamellar-zonal bone

Whether vascular or not, areas of lamellar and/or parallel-fibered bone that extend circumferentially around a cortex are termed lamellar-zonal. Depending upon growth remodeling and drift patterns, swaths of lamellar-zonal bone may or may not completely encircle the bone. This type may display a depositional periodicity, where there is a differentiation between zones, annuli, and lines of arrested growth (e.g. Peabody, 1961;

Francillon-Vieillot et al., 1990). The periodic nature of lamellar-zonal bone is not considered further here. Rather, I separate between regions of lamellar-zonal bone that are lamellar and parallel-fibered (see Methods below).

4.2.2.3 Fibro-lamellar bone

This common type comprises woven areas punctuated by vascular canals that have become surrounded by lamellar tissue. Generally, the vascularization here will be denser than what is seen in lamellar-zonal bone. The fibro-lamellar arrangement is formed when spaces in rapidly forming woven bone are filled in around the vascular canals with lamellar matrix, establishing a more compact tissue (Currey, 1960; Francillon-Vieillot et al, 1990). As is the case with lamellar-zonal bone, the vascular canals in this type may vary in density, may course in all directions, may be randomly distributed, or may display a regular patterning. Some patterns are distinct enough to have been assigned names, such as reticular and radiating. When the canals are distributed such that the alternation between woven and lamellar bone progresses circumferentially, this common subset of the fibro-lamellar complex is termed laminar bone. At its most intricate, laminar bone becomes plexiform, wherein webs of vascular canals are arranged in circumferential sheets, connected by short radial canals. Recently it has been recognized that fibro-lamellar bone may also be zonal, forming with the kind of periodicity previously associated solely with lamellar-zonal bone (Castanet et al. 2001). Because distinct fibrolamellar patterns such as laminar and plexiform are not typically found in the current primate sample, I do not use these terms to distinguish among types (see Methods below).

4.2.2.4 Compacted coarse cancellous bone

Compacted coarse cancellous bone (*sensu* Enlow, 1962a, 1962b, 1963, 1982; Enlow & Hans, 1996), is a uniquely endosteal, and complex, tissue that forms when lamellar or parallel-fibered tissue fills in the spaces between trabeculae of cancellous bone, leaving only the vascular canals patent.

4.2.2.5 Cancellous bone

Cancellous (=trabecular) bone tissues include those of periosteal and endosteal origin, and may be woven, parallel-fibered or lamellar. Periosteal spongiosa is generally associated with embryonic or fetal stages of development. Endosteal trabeculae can be of three types with respect to their osteogenesis: primary or secondary endosteal, and endochrondral. While de Ricqlès (e.g., de Ricqlès et al., 1991) and others differentiate between these types, I suggest that these distinctions are, as noted above, only useful at the local level, as a way to discriminate between relatively younger and older tissues. A final cancellous tissue type – secondary cancellous deep cortex – is one that forms from via the resorption of compact bone. In this, trabeculae will display remnants of the patterns of bone tissue that were present in the cortex previous to the development of resorption spaces. The midshafts of bone typically do not display cancellous tissue; therefore, this type is not discussed or quantified in the analysis below.

4.2.2.6 Other patterns

Other bone tissue morphologies are recognized which cannot be included in the classification outlined thus far (e.g., the chondroid bone that resembles cartilage; Enlow,

1962b; Enlow & Hans, 1996; Francillon-Vieillot et al., 1990). Of relevance to this study are Sharpey fibers, or extrinsic fibers (*sensu* Boyde & Jones, 1998), marking the attachment of muscle, tendon, and ligament to the bone surface (Francillon-Vieilliot et al., 1990). These consist of closely packed bundles of collagen fibers that usually run at an angle to the surface of the bone. They can be found deep within the cortex, marking soft tissue attachments at earlier stages of growth remodeling, as well as at the surface, marking current attachment sites.

### 4.3 Existing hypotheses regarding the factors determining primary tissue type variability

Differences in primary tissue type patterns can be found among taxa, individuals, bones and parts of bones. The extent to which, and manner in which, these differences are mediated by genetically determined and environmental factors remains largely unknown. As de Ricqlès aptly comments, "histodiversity has…a complex, multifactorial causality which is mainly of an ontogenetic, functional origin, but which cannot generally be subsumed to any unique, single efficient cause" (1992, p. 47). Similarly, Enlow earlier noted that "the individual combinations of bone tissue types are a direct result of the particular circumstances of skeletal growth in any given group. Rate of body growth, body size, special skeletal adaptations, and seasonal or environmental factors all influence the nature of skeletal deposits" (1966, p. 102). Inroads have been made in this area, so that it has become possible to gain some understanding of the relationship between tissue types and a number of other biological variables. Following is a brief overview of three principal, and potentially interrelated, factors suggested to impact upon the distribution of primary tissue types: developmental processes, organismal growth rate

and mechanical adaptations. Each will be treated in more detail in the discussion section of this chapter. The phylogenetic status of a species is another factor that must be considered in conjunction with all of these. Tissue types and distributions may be group specific inasmuch as growth patterns, life histories, and/or positional behaviors are constrained by heritage. While the current literature does not offer strong support for the prospect that some microstructural features may be reflective of subordinal phylogenetic relationships – independent of proximate, adaptive factors – the possibility that this may occur should not be rejected *a priori*.

> *"It is true that <u>some</u> bone histological characteristics may sometimes appear as taxa-specific and, if they are not caused by homoplasy, used, at least tentatively, as synapomorphies…Many more may be discovered in the future using finer quantitative histological surveys, as permitted by image analysis"* (de Ricqlès, 1992, p. 53).

*4.3.1 Tissue types and development*

It is the work of Enlow (1962a, 1962b, 1976, 1963, 1982; Enlow & Hans, 1996) that is most responsible for bringing the process of osteogenesis to the forefront and taking this into account when assessing variation in tissue type distribution within and between bones, and between taxa. As animals grow, bones must change in size while maintaining mechanically functional shapes and relationships with adjacent bones and soft tissues. However, because the osteocytes within calcified matrix are not capable of movement or mitotic division, this relocation of bone requires deposition (or apposition, cf. Enlow) of new matrix at some surfaces and resorption of existing matrix at others; in this way the bone organ accomplishes "drift" through anatomical space. This process of growth remodeling leaves behind a record of its progression in the stratified patterning of tissue

types. For example, a zone of compacted coarse cancellous tissue at the midshaft indicates that the bone in this region was once metaphyseal and trabecular. Even when at the periosteal surface of a cortex, this tissue type indicates original endosteal deposition. Particularly with the assistance of lines of discontinuity marking pauses in growth or reversals between resorption and deposition, differences in tissue types offer a means to reconstruct the growth remodeling process of the whole bone.

*4.3.2 Tissue types and growth rate*

Amprino (1946) was the first to suggest a relationship between the rate of growth of bone and the tissue type that results; this was later coined "Amprino's rule" (de Buffrénil & Pascal, 1984). His observations have been supported by subsequent research (e.g., Newell-Morris & Sirianni, 1982; Burr et al, 1989a; de Ricqlès et al., 1991; Castanet et al., 1996, 2000; de Margerie et al., 2002, 2004) and have been applied to the palaeobiological reconstruction of fossil dinosaur growth patterns (e.g., Horner et al., 2000; de Ricqlès et al., 2000; Sander, 2000; but see Starck & Chinsamy, 2002 for a discussion of potential pitfalls).

In this two-level scheme, the degree of organization of the fibrillar structure is rate-dependent. Woven bone is deposited most quickly (e.g., on average 9.8μm/day in early macaque fetuses), parallel-fibered tissues have an intermediate deposition rate (e.g., 4μm/day in early postnatal macaques), and lamellar bone is deposited most slowly (e.g., 1.5 μm/day in a juvenile macaque) (Newell-Morris & Sirianni, 1982). The second determinant of rate is the intensity (Castanet et al., 1996, 2001; de Margerie et al, 2002) and perhaps patterning (de Margerie et al., 2004), of vascularization. More

vascularization is associated with greater rate of deposition (e.g., Castanet et al., 1996). Such a scheme suggests that variation in deposition rates will account for many of the patterns observed between species, reflecting the interaction between body size and growth rates. It follows that tissue types and distributions are group specific inasmuch as growth patterns, or life histories, are group specific.

*4.3.3 Tissue types and mechanical properties of bone*

Because the supporting function of the skeleton is the primary naturally selected characteristic, tissue deposition must proceed within the context of mechanical imperatives. This can be seen in the maintenance of strain patterns throughout ontogeny (Biewener et al., 1986; Biewener, 1991). Not all tissue types possess the same mechanical properties, due to variation in such compositional and organizational features as degree of calcification, collagen fiber organization, porosity, or presence of cement lines (Evans & Bang, 1967; Simkin & Robin, 1974; Burr, 1980; Martin, 1991; Currey, 1999). For example, it has been shown that bone cortices with more secondary osteons have reduced tensile strength – and reduced fatigue life – relative to cortex with more interstitial primary lamellar bone (Amprino, 1948; Evans & Bang, 1967; Simkin & Robin, 1974; Vincentelli & Grigorov, 1985; Rho et al., 1999) or fibro-lamellar bone (Martin & Ishida, 1989; Schaffler et al., 1990); these results are not corroborated in all studies however (Martin & Ishida, 1989; Riggs et al., 1993b). Osteonal remodeling has been explored at length as a subject distinct from consideration of primary tissues. Independent questions have been posed, and hypotheses formulated, regarding this feature of bone.

The difference in the mechanical properties among most primary bone tissue types largely remains to be explored, although a small literature hints that differences do exist. It has been suggested, for example, that woven bone is weaker than lamellar bone (Martin, 1991). Furthermore, the increase in porosity found in fibrolamellar bone relative to less vascularized lamellar-zonal tissues is expected to reduce strength and stiffness (Martin, 1991; Schaffler & Burr, 1988; Lieberman & Pearson, 2001). Finally, de Margerie and colleagues have recently proposed that a laminar vascular organization of fibro-lamellar tissue is an adaptation to torsional loads (de Margerie, 2002; de Margerie et al., 2005). There exists no body of work, however, examining the relative mechanical properties of lamellar and parallel-fibered matrix types, both ubiquitous among primates and other vertebrates. Given the histocompositional differences between these two types, the potential for mechanical significance should not be overlooked.

**4.4 Objectives of the current study**

Taking into account the research outlined above, the objectives of the current study are to answer the following questions. It is important to note that these are not discrete and are not designed to furnish answers that are mutually exclusive.

1) Are there patterns of primary tissue type distribution that are characteristic of the primates in this sample as a whole?
2) Within the Primates, is there significant variation in the distribution of primary tissue types among long bone midshaft cortices?
3) If significant variation exists, is it non-randomly distributed?

4) If variation is non-random, are the patterns within the entire sample explained in part or in whole by the life history and/or mechanical factors, as outlined above?
    a. Do patterns of tissue type distribution vary among skeletal elements in accordance with element-specific ontogenies?
    b. Do primary tissue type distributions vary among taxa that are different in their adult body size and or/growth rates, in accordance with the hypothesis that types are determined by deposition rates?
    c. Do primary tissue type distributions vary among taxa that are different in positional behavior, in accordance with the hypothesis that types are variably mechanically adaptive?
5) Are there identifiable phylogenetic patterns that are independent of taxon-specific adaptation?

## 4.5 Methods

### *4.5.1 Tissue typing scheme used here*

Standards developed in the Hard Tissue Research Unit (HTRU, formerly at Hunter College, City University of New York, where this work was done, and currently housed at the New York University College of Dentistry) were employed for the identification of tissues and the demarcation of boundaries between tissues, following the typology of de Ricqlès and colleagues, and Enlow, as outlined above. Both LM and CPL images were used to identify primary tissue type patterns throughout the cortex; LM images provide information regarding vascular canal and osteocyte lacunar shape and distributions while CPL images allow for the identification of collagen fibrillar matrix patterns. In addition,

the sections were examined real-time in LM and CPL to clarify type identification when the captured images did not provide sufficient resolution.

Tissues were first categorized as either endosteal, periosteal or intracortically remodeled (i.e., composed of secondary osteons, or Haverisan systems). Within the endosteal and periosteal areas, tissues were further assigned to one of seven primary types: 1) woven (WOV), 2) fast fibrolamellar (FFBL), 3) slow fibrolamellar (SFBL), 4) parallel-fibered (PF), 5) hybrid (HYB; see below), 6) lamellar (LAM), and 7) compacted coarse cancellous (CCC). The last of these appears only in the endosteal cortex. The majority of these categorizations follow previous typologies. Deviations from, or modifications of, previously published typologies are noted below.

Because there is no means to automate the identification of tissue types, and no quantification of bone features used for identification was performed, differentiation between types necessitated the subjective evaluation of the distribution and shape of some features (e.g, the distance between primary osteons, or the shape of osteocyte lacunae). Within an area where the distributions and shapes were consistent (e.g., within that area all primary osteons appeared equidistant from each other, or all osteocyte lacunae were flattened), the relevant parameters were assessed by eye to arrive at a tissue type categorization. The criteria employed to differentiate between types are described in detail below.

PF and LAM are tissues included in the lamellar-zonal category of de Ricqlès and colleagues. These authors often do not differentiate between the two types. However, because many of the primate cortices in this sample are composed of bone in these categories, and because it has been suggested that there are differences in growth rates

between PF and LAM bone (e.g., Amprino, 1946; Newell-Morris & Sirianni, 1982), the two types are considered independently, rather than lumped in a single lamellar-zonal category. The additional identification of a HYB type between PF bone and LAM bone is an innovation introduced in the HTRU to describe variation that is observable in primate bones and that would not otherwise be accounted for, and which may be of biologically significance (i.e., may indicate rates of growth intermediate between LAM and PF tissues). The description of this tissue is provided below. The degree of vascularization within lamellar-zonal tissues is not quantified, as vascularization is generally sparse.

In addition, within the category 'fibro-lamellar' there is a differentiation between tissues that are more heavily vascularized (FFBL), and those that are less so (SFBL). This is another HTRU-introduced standard, but is consistent with previous studies suggesting that the proportion of the cortex composed of primary osteons is related to growth rate (e.g., Castanet et al., 1996).

When dense Sharpey fibers prevented the identification of one of the other tissue types, the bone was labeled as Sharpey fiber bone (SF). In addition, intracortically remodeled bone was labeled as such (HAV). This tissue type is discussed separately in a Chapter 5.

*4.5.2 Tissue type identification*

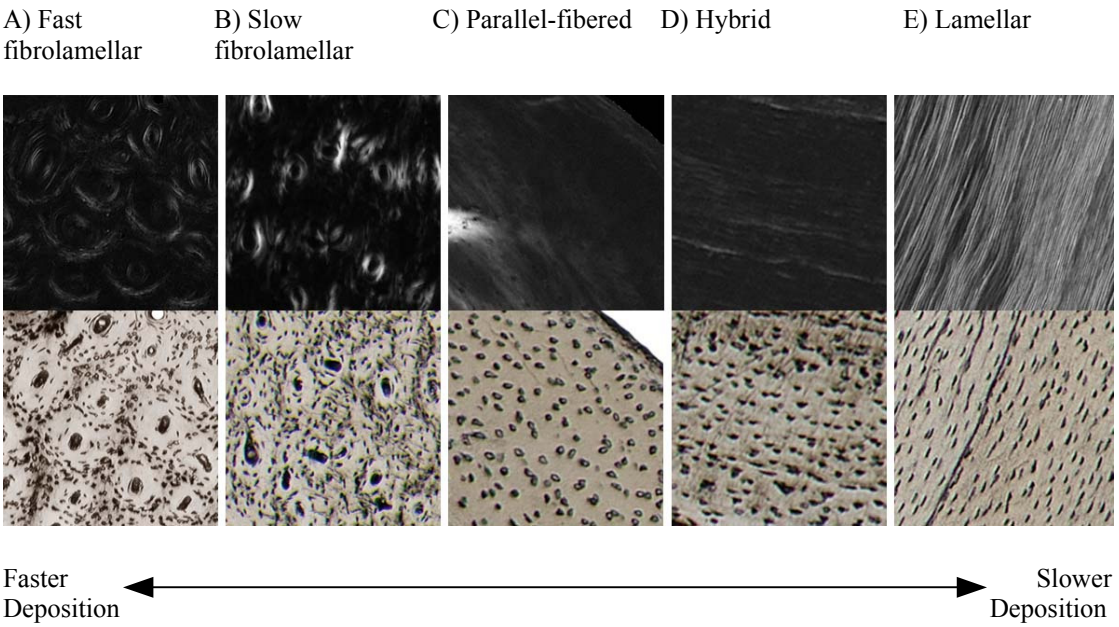


**Figure 4.1: Tissue type examples.**

For each pair, the upper was imaged in CPL and the lower in LM.

4.5.2.1 Woven-fibered bone (WOV): no image

WOV bone is identified on the basis of rounded or stellate-shaped, randomly distributed osteocyte lacunae (visible in LM images) and a multidirectional fibrillar texture (appearing "woven" in CPL images). This tissue, most often associated with infant and juvenile cortices, was absent in the majority of the sections in this study. When present, it was found in very small isolated areas, and in no cases does it comprise a significant proportion of the cortex.

4.5.2.2 Parallel-fibered bone (PF): Figure 4.1C

In PF bone, the osteocyte lacunae are typically more flattened and less randomly distributed than is the case for WOV bone. This is associated with regions within which collagen fibers are all similarly aligned, appearing smooth and featureless in CPL. In practice, tissue that appears to be parallel-fibered in terms of the collagen patterning may contain a range of osteocyte shapes (from rounded to more flattened) and distributions (from random to aligned in rows), in tissues of both periosteal and endosteal origin. In the current study, bone is considered to be PF based on the characteristic collagen patterning visible in CPL, that is, when 75% or more of the tissue in a given area (assessed by eye) is free of lamellar structure (see below).

4.5.2.3 Lamellar bone (LAM): Figure 4.1E

In this study, bone is recognized as lamellar when 75% or more of the tissue comprises visible lamellae, whether alternating in CPL birefringence or not. In some cases, lamellar structure is not visible in a CPL image, but can be seen in the LM image or when looking

at the section real-time via the microscope oculars. LAM bone is typically characterized by flattened osteocyte lacunae, aligned with their long axes coursing with the lamellae. Again, however, in practice the shape of the lacunae may vary, from very flattened to lozenge, or peach-pit shaped. In addition, the lamellae may be thick or thin, distinct and clear along their edges, or less evenly distributed and less clearly delineated.

4.5.2.4 Hybrid bone (HYB): Figure 4.1D

Bone is considered to be in the HYB category when more than 25% but less than 75% of the tissue displays lamellar patterning. The lamellae may appear in discrete circumferential rings or series of rings, interspersed with rings of PF bone, or may be fragmented and more randomly distributed within an area otherwise composed of PF bone. Osteocyte lacunar forms may be somewhat flattened, more rounded, or a combination of shapes.

4.5.2.5 Slow fibrolamellar bone (SFBL): Figure 4.1B

SFBL is distinguished from vascular LAM, HYB or PF bone (i.e., lamellar-zonal types) by the following criteria. First, 75% or more of the vascularization must consist of primary osteons rather than simple vascular canals, with at least two lamellae around the canal. Second, the distance between the primary osteons must be no more than twice the diameter of the osteons. Third, at least 25% of the extra-osteonal matrix must be composed of WOV tissue, as identified by rounded or stellate osteocyte lacunae that are distributed in a random clumping pattern. Fourth, no more than 75% of the osteocyte

lacunae are flattened and coursing in arched lines above and below the primary osteons (indicating LAM, HYB or PF tissue).

4.5.2.6 Fast fibrolamellar bone (FFBL): Figure 4.1A

FFBL is distinguished from SFBL by the following criteria. First, at least 75% of the primary osteons must contain more than two lamellae. Second, the distance between the primary osteons must be less than their diameter. Third, at least 50% of the extra-osteonal matrix must be composed of WOV tissue, as identified by rounded or stellate osteocyte lacunae that are distributed in a random clumping pattern. Fourth, no more than 25% of the osteocyte lacunae are flattened and coursing in arching lines above and below the primary osteons (indicating LAM, HYB or PF tissue).

4.5.2.7 Compacted coarse cancellous bone (CCC): Figure 4.1F

CCC bone, found only in the endosteal cortex, is characterized by odd-shaped convolutions of LAM, HYB or PF bone demarcated in some cases by resting or reversal lines. However, unlike the cement lines of secondary osteons, they do not form closed circles or ellipses.

4.5.2.8 Sharpey fibers (SF): Figure 4.1G

SF bone, whether abutting the periosteum or buried deeper in the cortex, is identified by the presence of collagen fiber bundles that run at an angle to the fiber patterns in the surrounding or underlying bone tissue, and at and angle, or even perpendicular to the periosteal edge of the bone. These are easily visible as parallel dark lines in LM imaging,

and parallel bright lines in CPL. Tissue is categorized as SF only when 50% or more of the area is composed of Sharpey fibers, masking the underlying histological structure.

4.5.2.9 Intracortically remodeled bone (HAV): Figure 4.1H

Secondary osteons are identified by the presence of a reversal line (cement line) at their perimeter, generally appearing dark in LM, and often (although not always) bright in CPL. The reversal line is often scalloped in appearance. Within this perimeter are found concentric lamellae. Secondary osteons are classically round or oval, but in practice can drift into elongated and convoluted shapes (Robling & Stout, 1999), although they will always, by definition, be completely encircled by a the reversal line, unlike the convolutions of CCC bone. Unlike primary osteons (which will have no reversal line) they will show a discontinuity with the primary interstitial bone around them.

4.5.2.10 A note on collapsing tissue type categories

Throughout the following analyses, the tissue type categories LAM and HYB have been collapsed into a single category: LAM+HYB. In addition, WOV, FFBL and SFBL have been collapsed into a single category: FAST.

During the mapping process, the HYB category was constructed because I, along with colleagues at the HTRU, found that this type fit comfortably neither in the lamellar category, as classically described, or in the parallel-fibered category. However, during the analysis stage of this work, it became evident that proportions of HYB bone did not vary in a patterned fashion, while PF and LAM proportions did. Resultant multiple regression adjusted $R^2$ values (see results section) were higher for the LAM+HYB

category than for either HYB or LAM alone. HYB was combined with LAM rather than PF bone because of the presence in HYB of lamellae, albeit as a reduced proportion of the tissue relative to LAM.

FFBL and SFBL categories were devised in the HTRU to account for the variation in the porosity of fibro-lamellar tissues, a feature that is hypothesized to correspond with differences in bone-formation rates. However, in the sample studied here, proportions of fibro-lamellar bone were generally very low, and in particular the incidence of FFBL bone was low. Therefore, the two categories were combined for the analyses, along with the fast depositing WOV bone (which occurs very infrequently).

Although both innovations were ultimately disregarded for this study, the tissue maps contain the necessary data for comparison with other studies where HYB, SFBL, and FFBL tissues are considered separately.

*4.5.3 Image processing and quantification of tissue types*

For each bone, CPL and LM images were overlain and aligned in Abode Photoshop (8.0), and non-bone areas were masked out (including vascular canals equal to or greater than a threshold diameter of nine pixels (for a 72 dpi image at 796 pixels/mm). To allow for quantification of the relative proportions of tissue types within a cortex, areas for each of the major bone tissue types were traced and assigned identifying colors (Figures 4.2, 4.3). Tissue type maps were imported into Optimas (Version 6.51; Media Cybernetics, L.P.) and the areas (in pixels) were calculated for each tissue type in each section using a macro developed for Optimas (Goldman, 2001). Absolute values were converted to proportions, relative to the total cortical area (TCA), or relative to the endosteal or

periosteal portion of the cortex (for the periosteal and endosteal tissues respectively), for use in the majority of analyses.

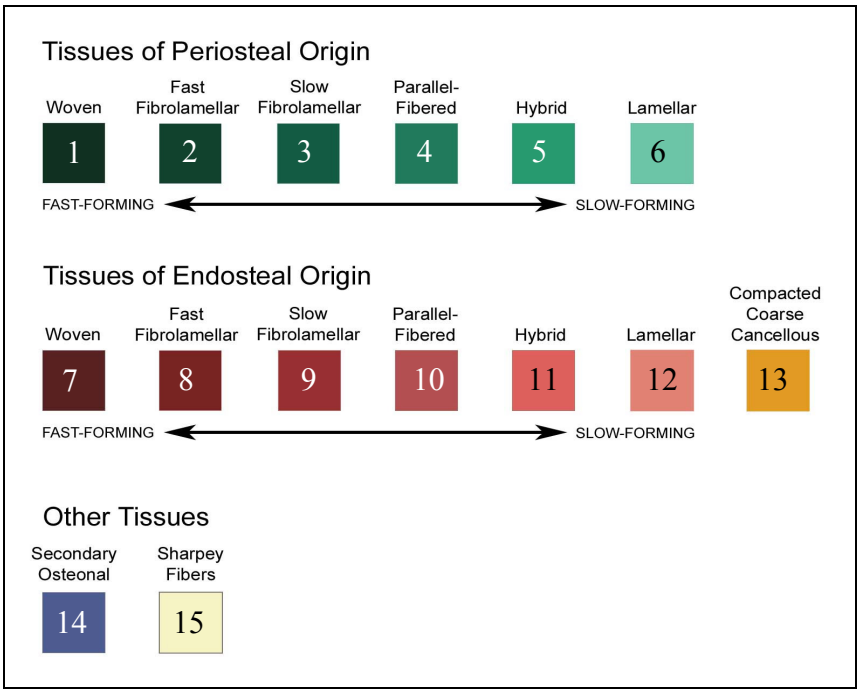


**Figure 4.2: Tissue map color code.**
See text for description. Numbers are present for decoding of grayscale reproductions of color images.

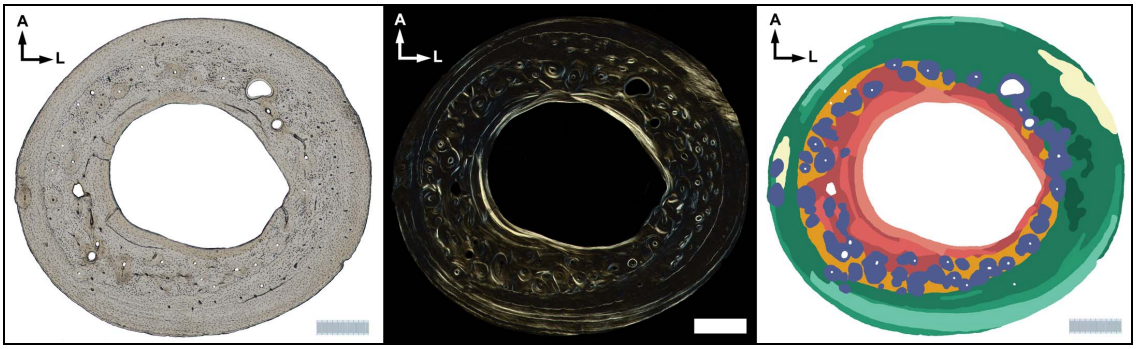


**Figure 4.3: Sample cortex.**
Midshaft *Nycticebus coucang* (HC 27) radius: a) imaged in LM, b) imaged in CPL, and c) translated into a tissue map.

*4.5.4 Subjectivity in tissue type identification*

Due to the continuous nature of tissue type variation, it is at times difficult to confidently assign boundary lines between types. There is therefore a measure of subjectivity, and resultant error, in the creation of these colorized tissue maps. To assess the degree of error that may exist in the identification of tissue types during mapping, a repeated measures test was performed. An area of cortex from a single section containing a range of tissues was mapped three times with an interval of several days in between each map to prevent the memory of the details of each mapping session to influence the next one. Results for relative proportions of tissue types are depicted in Figure 4.4. Variation in the proportion of tissue types, relative to the TCA, does not exceed 5% of the TCA. This error is reduced to a maximum of 3% when LAM and HYB tissues are combined.

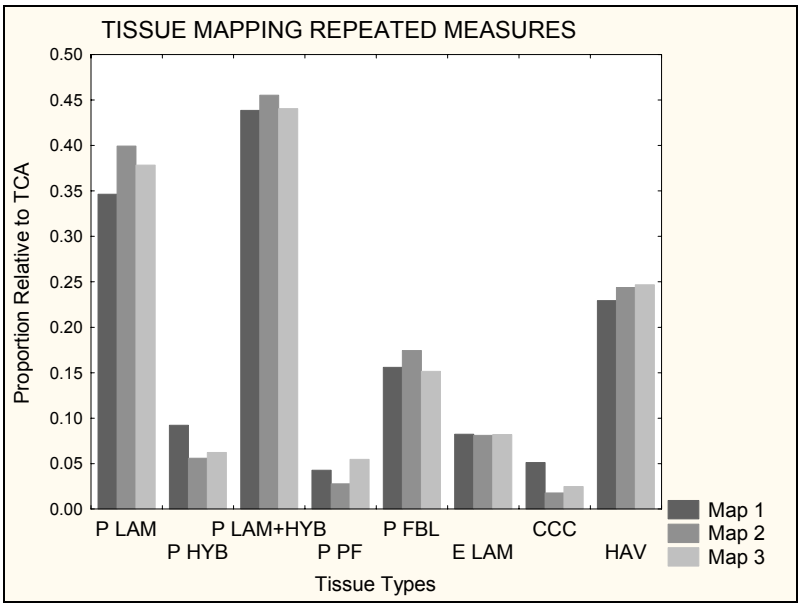


**Figure 4.4: Tissue mapping repeated measures.**

See text for description. P= periosteal; E=endosteal.

*4.5.5 Statistical and descriptive analyses*

Sample sizes are small, with a maximum of 34 (for all sample femora, and all sample humeri) and in some cases as few as a single specimen (for distal skeletal elements in some taxa). In many instances the data are not normally distributed and cannot be successfully normalized via transformation. This may be due to sample size and composition, or perhaps the nature of the variable itself. Because some sample distributions remained non-normal after transformation, non-parametric statistics are applied where possible. When p values are highly significant (e.g., $p<.01$), as is often the case, the reliability of results is more secure, despite the non-normal distributions. However, because of small sample sizes in many of the analyses, significances may be low or results may be insignificant despite visible differences in graphs or the sections themselves. In such cases, an observed pattern is also considered to be more reliable when it is repeated (for example among different skeletal elements, or among taxa). Even when results are statistically significant, identified patterns are checked for robusticity using graphical methods. In the absence of visible and consistent patterns, the results and conclusions must remain tentative. Finally, in many cases, sample sizes are so small as to preclude significance testing altogether. In those cases, only descriptive methods are used.

First, the relative proportions of periosteal tissue relative to endosteal and compacted coarse cancellous, and primary tissue type patterns within the endosteal portions of the cortex are described. All further analyses concentrate on the periosteal portion of the cortex. Periosteal and endosteal primary tissue type areas are calculated as the total of all primary periosteal and endosteal tissues respectively. Because secondary

osteons effectively replace primary tissue, the type that was initially deposited and present previous to intracortical remodeling is unknown. Although in some cases it might be possible to guess at the original tissue type, based on the interstitial bone (primary tissue surrounding secondary osteons), it cannot necessarily be assumed that the interstitial tissue is representative of the tissue replaced by intracortical remodeling. Therefore, no primary tissue type is assigned to areas that are occupied by intracortical remodeling. In order to maintain consistency, this is the case even for sections where the primary tissue can be deduced with some certainty. Nor has intracortical remodeling been assigned to either periosteal or endosteal regions, as it is not always possible to determine where the boundary between the two lies when obscured with secondary osteons. It follows that, depending on the taxon, the individual, and the skeletal element, some proportion of the periosteal and endosteal area may not be assigned a primary tissue type. In other words, in the analyses that follow, total periosteal area is equal to real total periosteal area minus periosteal intracortically remodeled area, and total endosteal area is equal to real total endosteal area minus endosteal intracortically remodeled area. Sharpey fiber bone is included with periosteal tissues as it is only found in periosteally deposited bone. Compacted coarse cancellous bone is of endosteal origin, but because of its distinct developmental trajectory it is examined in isolation, as it may provide information regarding taxon and element specific records of growth and drift.

Non-parametric Sign tests and Wilcoxon Matched Pairs tests were used to identify differences in the proportion of periosteal tissue types in the sample as a whole, examining each skeletal element independently. Subsequently, multiple regression analyses were employed to determine the importance of three independent variables in

accounting for the observed variation in primary tissue type proportions. The variables – total cortical area (TCA), phylogenetic status (PHYLO), and positional behavior (PB) – were chosen as best able address the questions raised by a review of the literature, and outlined in the objectives section. These variables are described below. Multivariate models were examined including all three variables, as well as combinations of two, and were compared to simple regressions for each variable. This was done in order to determine which model accounted for the greatest portion of variation exhibited in the sample. Given the frequent non-normality of the samples, the multiple regressions served as a rough guide to the link between dependent and independent variables, and suggested relationships were subsequently examined via descriptive graphical methods and basic statistics. Differences among PB or PHYLO categories were tested for significance using Kruskall-Wallis tests for multiple independent variables. If significance was identified with these tests ($p \leq 0.05$), pairwise comparisons (Mann-Whitney U tests) were utilized to pinpoint the source of significant variation.

Descriptive analysis is provided for intra-taxonomic variation in periosteal tissue-type proportions within and between skeletal elements. Subsequently, patterns characteristic of the femora of each taxon are described. Finally, femoral mean primary tissue type proportions in select pairs of taxa are compared in light of the multiple regression results.

### *4.5.6 Independent variables included in the multiple regression analyses*

#### 4.5.6.1 Total cortical area (TCA)

TCA, rather than body mass, is used as a proxy measure of body size, because only estimated body mass values, which were culled from the literature, are available for this sample. Long bone length could also be used as a body size indicator, but including this in addition to cortical area would introduce multicollinearity. The correlation between cortical area and bone length is significant and positive (depending on the element, r ranges between 0.9182 and .9536; Table 4.1). Of these two indirect measures of body size, cortical area is particularly appropriate to this study, given that the microstructural variables are examined as proportions relative to the midshaft cross-sectional area. In addition, it has been shown that the cross sectional properties of bones can function as reasonable predictors of body size (e.g., Paine & Godfrey, 1997; Delson et al., 2000; Ruff, 2003).

| logLENGTH x logTCA | | |
|---|---|---|
| | $r^2$ | r |
| Femur | 0.8430 | 0.9182 |
| Humerus | 0.9093 | 0.9536 |
| Radius | 0.8510 | 0.9225 |
| Ulna | 0.8592 | 0.9269 |
| Tibia | 0.8883 | 0.9425 |

**Table 4.1: Correlation between skeleton element length and midshaft section TCA.**

4.5.6.2 Phylogenetic status

For the multivariate analyses, the sample was split into three taxonomic groups: strepsirhines, *Tarsius,* and platyrrhines. Separation at this level, rather than at a lower one, was chosen because the multivariate analysis is designed to capture broad patterns of variation. Subsequent pairwise analyses are used to identify phylogenetic differences among more closely related taxa.

4.5.6.3 Positional behavior

Positional behaviors have been allocated to four broadly-defined categories: brachiation/suspension (SUS), grasp leaping/generalized arboreal quadrupedalism (AQ), grasp-clinging and creeping/slow climbing (SC), and vertical clinging and leaping (VCL). These follow the categories traditionally used to describe primate locomotion (e.g., Napier & Napier, 1967; Napier & Walker 1967; Szalay & Dagosto, 1980, Runestad Connour et al., 2000; Kimura, 2002). While the naming of these categories may vary, the association of individual taxa with each of them, and the descriptions of the *characteristic* behaviors with which they are associated, generally do not. As many researchers have pointed out, there is variation within these positional behavior groups, for example in the frequency and styles of locomotor modes associated with the category, in their morphological correlates, between sexes, with age, and with body size (e.g., Oxnard, 1973; Oxnard et al., 1981a, 1981b; Jouffroy & Lessertisseur, 1979; Walker, 1979; Fontaine, 1990; Terranova, 1995a, 1996). Variation in behavior may occur within species, and even individuals, dependent on factors such as habitat, time of day, or activity (Walker, 1979; Fleagle & Mittermeier, 1980). In addition, it is likely that certain positional behavior types evolved more than once among primates (e.g., vertical clinging and leaping, see Szalay & Dagosto, 1980) with convergent or different morphologies and kinematics. Nevertheless, because the sample is constructed to identify broad patterns of variation and, because ultimately it is designed for functional comparison with fossil specimens, such categorization is useful (see Godinot, 1990; Gebo 1987). And while primates of a given taxon may engage in a range of postures and locomotions, the frequencies with which they engage in certain behaviors makes it possible to generalize

about what is habitual for that taxon (Jouffroy & Lessertisseur, 1979). There is a precedent for this kind of broad categorization in past investigations of comparative bone microstructure, as well as other bone morphological features (e.g., Schaffler & Burr, 1984; Paine & Godfrey, 1997; Runestad, 1997).

#### 4.5.6.4 A note on growth rate

Despite the relevance of growth rate to primary tissue type variation, this variable was not included in the multivariate analysis. When PHYLO and the scaled growth rate data available for this analysis were compared, they were found to be significantly correlated with one another ($r = 0.9250$). This is not surprising given that prosimians display accelerated growth relative to platyrrhines (Kirkwood, 1985; Cubo et al., 2002), i.e., phylogeny and growth rate are not independent of each other. Therefore, these two variables are not included together in the multiple regressions to avoid the problem of multicollinearity and also to maximize the power of the regression analysis. Because data points exist for all individuals with regard to phylogenetic status, and given that these two variables are so highly correlated, PHYLO was selected over scaled growth rate to include in this portion of the analysis.

Following Kirkwood (1985), the equation $DxWa^{1/4}$ was used to arrive at a relative growth rate score, scaled to body weight (see Table 3.1 for a detailed explanation). This measure is a rough one due to error introduced by the paucity of detailed growth data for many of the taxa included in this study. In fact, age at attainment adult body weight was not available at all for some study taxa, and so these growth data are incomplete. In addition, as noted above, body mass was not available for

the majority of individuals and therefore previously published values were employed (the Smith & Jungers [1997] study was used, as the values in this publication were already compiled from the literature). An alternative measure of growth rate is grams/day for young individuals, scaled to body weight (daily weight increase in grams/$Wa^{0.75}$; see Table 3.1). There exist more data for pre-weaning growth patterns than those available for the later stages of growth (e.g., Ross, 1991; Garber & Leigh, 1997; Godfrey et al., 2004). However the adult cortices in the current study likely do not contain a record of early development. Given that growth curves generally display variation in rates throughout development, it is preferable when examining adult cortices to use an estimate of growth rate that is not restricted to patterns derived from studies of early development.

*4.5.7 Key to abbreviations used in the following sections*

LAM = Lamellar bone

HYB = Hybrid bone

LAM+HYB = Lamellar + hybrid bone

PF = Parallel-fibered bone

FAST = Woven + fast fibrolamellar + slow fibrolamellar bone

CCC = Compacted coarse cancellous bone

HAV = Intracortically remodeled bone

SF = Sharpey fiber bone

P = Bone of periosteal origin

E = Non-CCC bone of endosteal origin

TCA = Total cortical area

PHYLO=Phylogenetic status

STREP=Sterpsirhine

PLAT=Platyrrhine

TAR=Tarsiid

PB=Positional behavior

SUS=Suspension/brachiation

AQ=Arboreal quadrupedalism/grasp-leaping

SC=Slow climbing/grasp-clinging and creeping

VCL=Vertical clinging and leaping

## 4.6 Results

### *4.6.1 Periosteal/endosteal comparisons*

The taxon means for relative proportions of periosteal (P), endosteal (E) and coarse compacted cancellous (CCC) bone were examined for each skeletal element. Without exception, in all taxa and elements, there is a greater average proportion of P than CCC (Figure 4.5). Likewise, the proportion of periosteal tissue surpasses endosteal tissue, with the exception of the ulna and radius in the Cebidae and the humerus in the Cheirogaleidae, where there is almost as much or more endosteal bone (to the exclusion of compacted coarse cancellous) as periosteal bone. Indeed, this periosteal/endosteal disparity is so distinct that it is readily discernable with visual inspection of the cortices (Figure 4.6). There are patterned differences in the relationship among periosteal, endosteal and compacted coarse cancellous bone between elements (Figures 4.5 and 4.6). For example, there is a greater proportion of endosteal tissues in the elements of the

forelimb than in the hindlimb. In 31 out of 34 femora, periosteal areas are more than twice as large as either endosteal and compacted coarse cancellous tissue areas, the exceptions being one cheirogaleid, one lorisid and one cebid individual. The same is the case for all tibiae except one for that of a single lorisid (18 out of 19). In contrast, in 13 of 34 humeri, either endosteal or compacted coarse cancellous tissue areas are equal to one half or more of the periosteal area, in some cases surpassing it. The same is the case for 6 of 18 radii, and 7 of 15 ulnae. In addition, the tibia is characterized by an absence in all individuals, or near absence (with one exception), of compacted coarse cancellous bone.

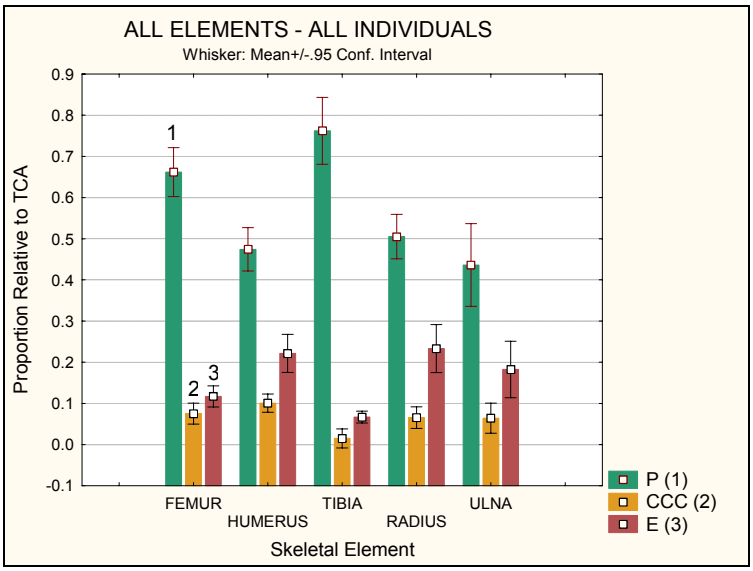


**Figure 4.5: Proportions (relative to TCA) of periosteal, endosteal and CCC bone in each element for all individuals combined.**

See text for description.

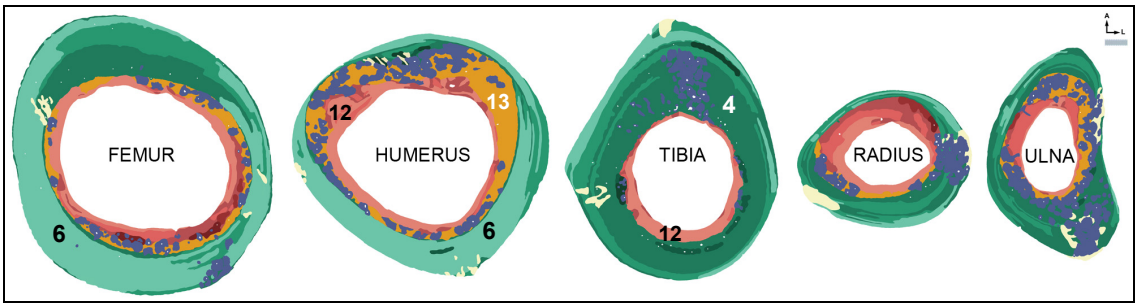


**Figure 4.6: Midshaft sections from a single *Otolemur crassicaudatus* individual (HC 31).** Proportions of slow-forming tissues (lighter green = 6) in the periosteal portion of the cortex are greater in the femur and humerus than in the other three elements. Also evident is the greater proportion of endosteal tissues (pinks = 12, and yellow = 13) in the elements of the forelimb. Patterns of element-specific growth, typical of most individuals in the sample, can be seen. For example, the humerus has a strong posterior-ward pattern of drift, whereas growth in the femur proceeds in a more evenly circumferential fashion. The tibia is characterized by the absence of compacted coarse cancellous bone (yellow). Scale indicates 0.5 mm. See Figure 4.2 for interpretation of numbers.

### *4.6.2 Sample-wide patterns of tissue types in endosteal bone*

In the sample as a whole, LAM+HYB bone is the most common tissue in the endosteal cortex, followed by PF and then FAST bone. Although there is variation among individuals in the relative proportions of these tissues (as evidenced by the outliers and extremes in Figure 4.7), in c. 75 percent of the cortices (90 out of 122) LAM+HYB bone is the most common. In particular, it is typical to find distinct circumferential lamellae lining the endosteal margin. This endosteal deposition of LAM bone apparently can begin very early in development, while the periosteal portions of the bone are still depositing faster tissues (Newell-Morris & Sirianni, 1982). The variation that does exist in endosteal tissues is restricted to the lesser and greater galagos, lorisids, lemurids, and tarsiids, where individuals may occasionally display more PF or FAST bone than LAM+HYB.

The distribution of primary tissue types is less variable endosteally than periosteally. This has also been found to be the case by de Margerie et al. (2002), in a sample of mallard long bones. As Enlow suggests, endosteal tissue may not reflect

growth rates in the same manner as periosteal tissues, given its primary function to adjust "shape and diameter as the various parts of the bone become successively relocated during growth" (1966, p. 105). Because of this, and because endosteal bone comprises less of the cortex than periosteal bone (and may be absent altogether in some sections), the remainder of the study focuses on the periosteal portion of the cortex.

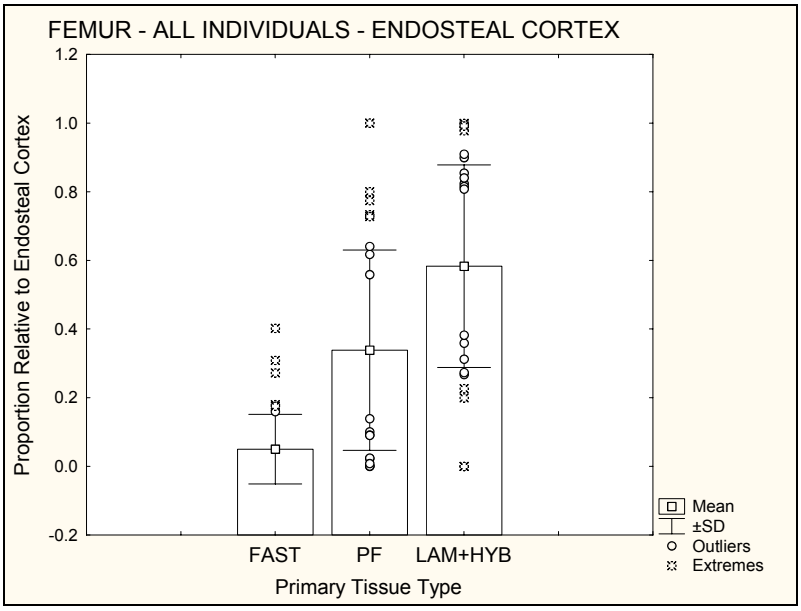


**Figure 4.7: Proportions (relative to endosteal cortex) of FAST, PF and LAM+HYB bone in the femur for all individuals combined.**

See text for description. Upper outliers > upper value of the box + outlier coefficient x (upper value of the box – lower value of the box). The inverse is true for the lower outliers. Upper extremes > upper value of the box + 2x outlier coefficient x (upper value of the box – lower value of the box). The inverse is true for the lower extremes. *Outlier coefficient = 1.5.

*4.6.3 Sample-wide patterns of tissue types in periosteal bone*

For each skeletal element, mean proportions of primary tissue types were examined for all individuals combined in order to identify sample-wide patterns.

4.6.3.1 Femur

In the femur, mean values for primary tissues types, as a proportion of the periosteal cortex, are lowest for FAST bone, higher for PF bone, and higher still for LAM+HYB bone (Figure 4.8). As a whole then, the primate femur is characterized by an emphasis on tissues at the slow deposition end of the spectrum. This is particularly evident in the contrast between LAM+HYB and FAST types. However, examination of the outliers and extremes of Figure 4.8 highlights the variability within tissue categories. Wilcoxen Matched Pairs tests indicate significant differences between all tissue type pairs (p ranges from <.01 to <.0001). The conclusion then is that the primates in this sample have, as a whole, more LAM+HYB bone than PF bone, and more PF bone than FAST bone at the midshaft cortical femur.

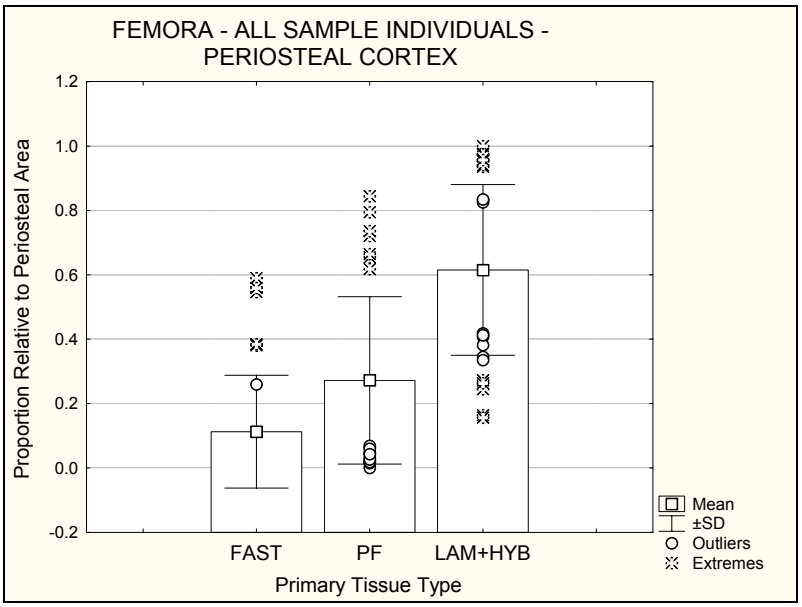


**Figure 4.8: Proportions (relative to periosteal cortex) of FAST, PF and LAM+HYB bone in the femur for all individuals combined.**

See text for description.

4.6.3.2 Humerus

In the humerus, the means for FAST and PF tissue types are low and near-equivalent, and the LAM+HYB category occupies the greatest relative area. In this case, the contrast between LAM+HYB and the tissue types on the slower end of the spectrum is pronounced (p-values of <.0001) (Figure 4.9). For the primates in this sample, therefore, as for the femur, there is a predominance of tissues that are relatively slow depositing. However, in the humerus this pattern is more pronounced than in the femur.

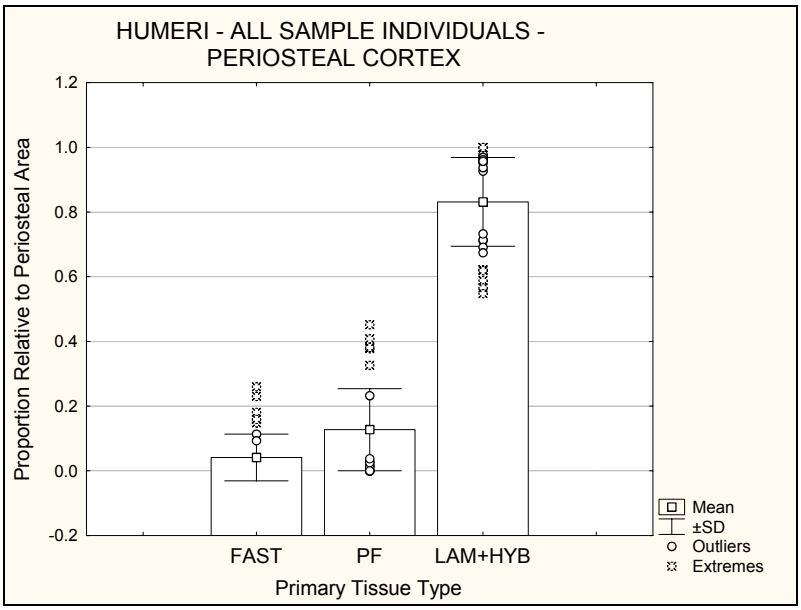


**Figure 4.9: Proportions (relative to periosteal cortex) of FAST, PF and LAM+HYB bone in the humerus for all individuals combined.**

See text for description.

4.6.3.3 Radius, ulna and tibia

In the radius, means for FAST bone are lowest, as is the case for the femur and humerus (Figure 4.10). However, in contrast with the latter two elements, the values for PF and the LAM+HYB category are nearly equivalent. The differences between FAST tissue proportions and PF and LAM+HYB proportions are highly significant (p<.001). The pattern of ulnar and tibial mean values are very similar to each other and to the radius

(Figures 4.11, 4.12). In both cases, the value for FAST bone is again lowest, and PF values are highest. Differences between PF and LAM+HYB bone are insignificant, but FAST bone values are significantly lower than PF and LAM+HYB values in both bones ($p<.001$).

As a whole, these three distal elements show relatively more PF bone, and relatively less LAM+HYB bone than the femur and humerus. In other words, there is a diminished emphasis on the slow-forming tissues. Figure 4.13 provides a visual summary of the contrast among elements.

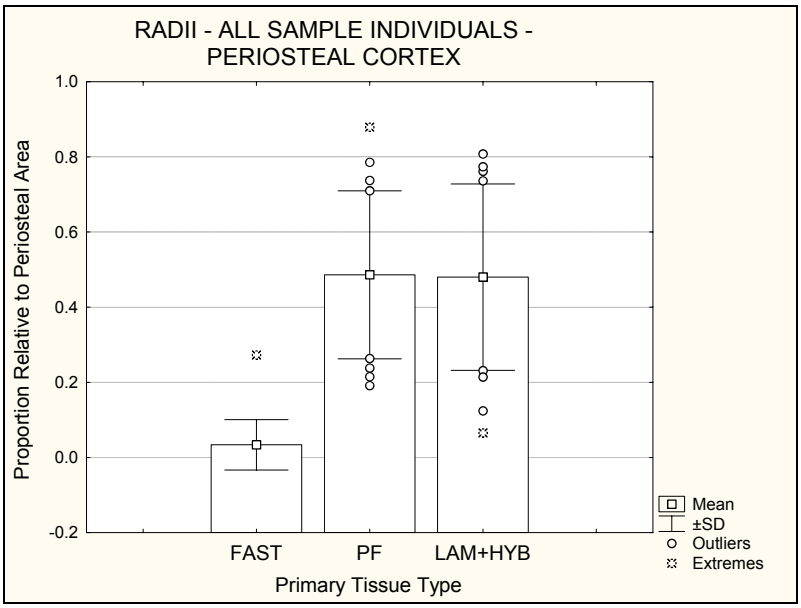


**Figure 4.10: Proportions (relative to periosteal cortex) of FAST, PF and LAM+HYB bone in the radius for all individuals combined.**

See text for description.

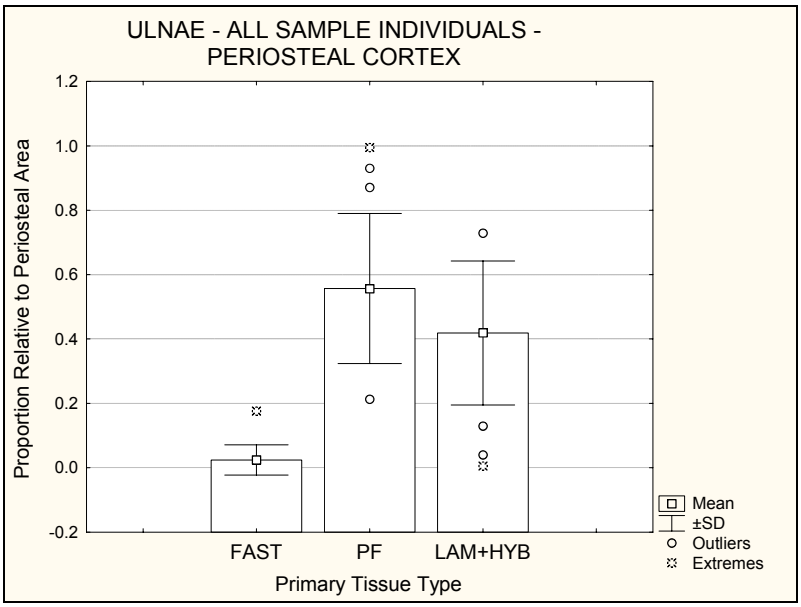


**Figure 4.11: Proportions (relative to periosteal cortex) of FAST, PF and LAM+HYB bone in the ulna for all individuals combined.**

See text for description.

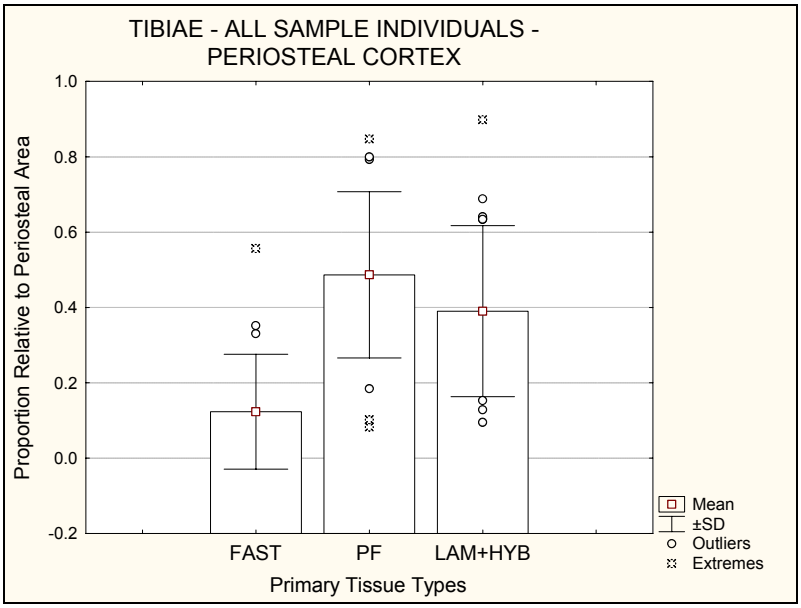


**Figure 4.12: Proportions (relative to periosteal cortex) of FAST, PF and LAM+HYB bone in the tibia for all individuals combined.**

See text for description.

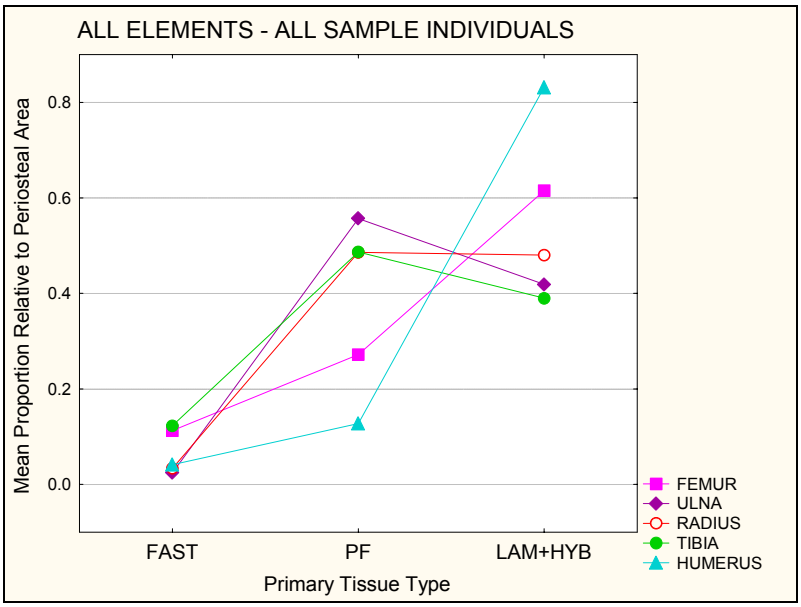


**Figure 4.13: Comparison of mean periosteal tissue type values for all five skeletal elements for all individuals.**

Proportions (relative to periosteal cortex) of FAST, PF and LAM+HYB bone. Femoral and humeral patterns of tissue type proportions in the periosteal cortex are similar, with highest values for the LAM+HYB category. In contrast, the distal bones for both forelimb and hindlimb contain as much, or more, PF tissue as LAM+HYB tissue.

A possible source of the discrepancy between proximal and distal elements is the difference among samples (see Table 1.1). There are 34 femora and 34 humeri with a nearly equivalent distribution among taxa, but only 18 radii, 17 ulnae, and 19 tibiae. In addition, there are fewer platyrrhines relative to strepsirhines in the sample of distal elements. If the distribution of tissue types is not equivalent between platyrrhines and the strepsirhines due to life-history and/or phylogenetic divergence (discussed in subsequent sections), this may bias the observed proximal/distal contrast. However, Figures 4.14-4.16 demonstrate that the pattern of tissue proportions described above is constant among all individuals, irrespective of taxonomic status, in that the proximal elements show higher proportions of LAM+HYB bone than distal elements.

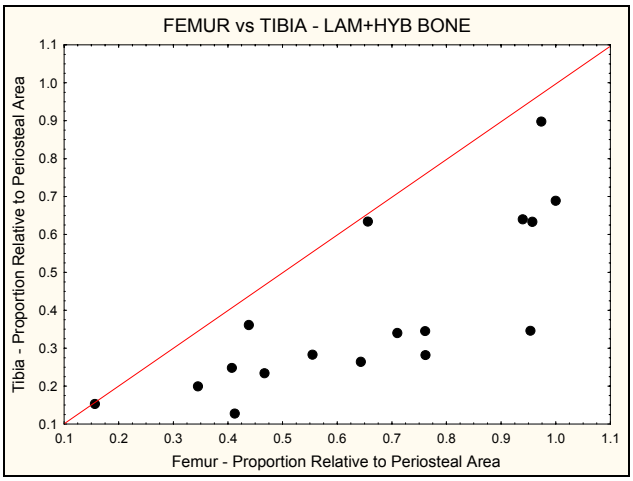


**Figure 4.14: Comparison of individual values for LAM+HYB bone in the femur and tibia.**

The value for each individual for the proportion of LAM+HYB bone in the femur and tibia were plotted. The diagonal red line indicates where data points would fall should the proportion of LAM+HYB bone be equivalent in both elements within an individual. For all individuals, the femur contains an equal, and usually greater proportion of LAM+HYB bone.

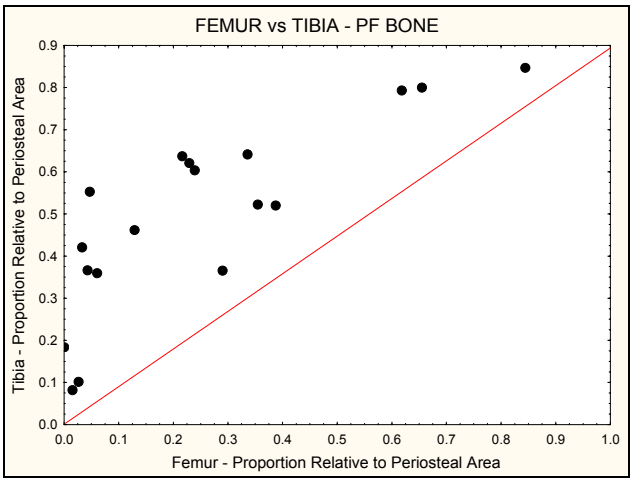


**Figure 4.15: Comparison of individual values for PF bone in the femur and tibia.**

The value for each individual for the proportion of PF bone in the femur and tibia were plotted. The diagonal red line indicates where data points would fall should the proportion of LAM+HYB bone be equivalent in both elements within an individual. In this case, and as expected, the opposite pattern to that for LAM+HYB bone is found. For all individuals, the tibia contains a greater proportion of PF bone than the femur.

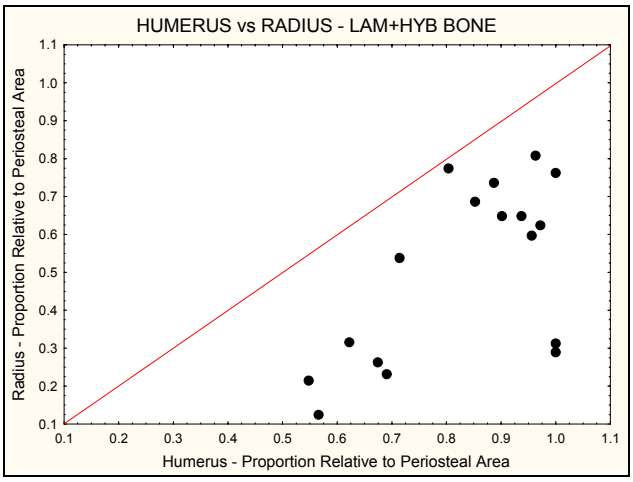


**Figure 4.16: Comparison of individual values for LAM+HYB bone in the humerus and radius.**

The value for each individual for the proportion of LAM+HYB bone in the humerus and radius were plotted. The diagonal red line indicates where data points would fall should the proportion of LAM+HYB bone be equivalent in both elements within an individual. For all individuals, the humerus contains a greater proportion of LAM+HYB bone than the radius.

*4.6.4 Factors accounting for variation in primary tissue types across the entire sample*

Multiple regression analyses confirm that the independent variables (TCA, PHYLO, PB), chosen based on their purported relationship with primary tissue type diversity, do account for a significant proportion of the variation observed in this sample, although some of it clearly remains unexplained. The models yielding the highest adjusted $R^2$ may include all three predictor variables, only two of the three, or in some cases just a single variable (Table 4.2). Depending on the tissue type, and to a lesser degree the element, the relationship between tissue type and the independent variables differs, both in the magnitude of the total variance explained, as well as in the independent variables accounting for the variation. Overall, significant $R^2$ values range between 0.22 and 0.77 with p-values of <.05 to <.0001.

| MULTIPLE REGRESSION RESULTS | | | |
|---|---|---|---|
| Tissue Type | Element | Adjusted $R^2$ | Model |
| FAST | Femur | 0.71*** | PHYLO, PB, TCA |
| | Humerus | 0.22* | PHYLO, TCA |
| | Tibia | 0.55** | PB, TCA |
| | Radius | 0.73** | PHYLO, PB, TCA |
| | Ulna | 0.74** | PHYLO, PB |
| PF | Femur | 0.77*** | PHYLO, PB, TCA |
| | Humerus | 0.41** | PHYLO, PB, TCA |
| | Tibia | 0.40* | PHYLO, PB |
| | Radius | 0.63** | PHYLO, PB, TCA |
| | Ulna | 0.64*** | PB |
| HYB+LAM | Femur | 0.67*** | PHYLO, PB, TCA |
| | Humerus | 0.55*** | PHYLO, PB, TCA |
| | Tibia | 0.60** | PHYLO, PB, TCA |
| | Radius | 0.75*** | PHYLO, PB |
| | Ulna | 0.69*** | PB |

**Table 4.2: Multiple regression results for primary tissue types for the entire sample.**
For each tissue type, the model with the highest adjusted $R^2$ was selected. The number of independent variables included in the model differs depending on the tissue type and element. * indicates p<.05; ** indicates p<.01; ***indicates p<.001.

4.6.4.1 FAST bone

In all elements except the ulna, TCA is the strongest predictor for the proportion of the cortex, relative to periosteal area, that is composed of FAST bone (Table 4.3). In the femur, humerus, tibia and radius, the relationship is positively allometric: the greater the cortical area, the greater the proportion of it that is composed of these fast-forming tissues (Figure 4.17). Given the consistency among these four elements, it is most likely that the absence of this pattern in the ulna is due to sample composition, rather than a difference in growth or functional adaptation in this bone relative to the others, although the latter is nevertheless a possibility.

For the femur and ulna, the multiple regression analyses indicate that taxonomic status is also a factor that accounts for variation in the proportion of FAST bone (Table 4.3). This is best appreciated in the femur, where a bivariate plot of FAST bone against TCA yields higher r and $r^2$ when it is categorized by PHYLO (Figure 4.17B). Figure 4.17 shows that small individuals (<500g) have very low values for FAST bone in the femur (<10% of the total periosteal area), and often have none of this tissue at all. While the amount of FAST bone increases with TCA in strepsirhines, this is not the case for platyrrhines; values for larger individuals remain close to zero. It should be noted however, that the large platyrrhines (atelid individuals) are also highly intracortically remodeled, and it is possible that the secondary osteons (Haversian systems) may have obscured areas previously occupied by FAST bone. This potential problem is mitigated by the fact that in the larger strepsirhines individuals (e.g., *Indri*), the cortex is also highly remodeled, yet the proportion of FAST bone that is still identifiable is high relative to what is seen in the atelids. The significance of PHYLO as a factor is corroborated by

non-parametric tests. For all elements, means for percentage of FAST bone in the periosteal cortex are higher in strepsirhines than in platyrrhines, significantly so in the femur, humerus and tibia ($p<.05$ to $<.01$). Strepsirhine means are also higher than tarsiid means for all elements, although only significantly so for the femur ($p<.01$). The consistency in this pattern suggests that PHYLO, along with TCA, is indeed an important predictor for the amount of FAST bone in the periosteal cortex.

| FAST - ALL INDIVIDUALS | | |
|---|---|---|
| Element | Predictor Variable | Beta |
| Femur | PHYLO | 0.60** |
| | PB | 0.34* |
| | TCA | 0.97*** |
| Humerus | TCA | 0.49* |
| Tibia | TCA | 0.56* |
| Radius | PB | 0.60** |
| | TCA | 0.70*** |
| Ulna | PHYLO | 1.22** |
| | PB | 1.52*** |

**Table 4.3: Multiple regression results for FAST bone for the entire sample.**

For each element, the independent variables for which there are significant betas are listed. Because the variables PHYLO and PB are dummy-coded, each includes more than one vector. Individual vectors may or may not have significant betas. Indicated significances are based on the highest p value for that variable. * indicates $p<.05$; ** indicates $p<.01$; *** indicates $p<.001$.

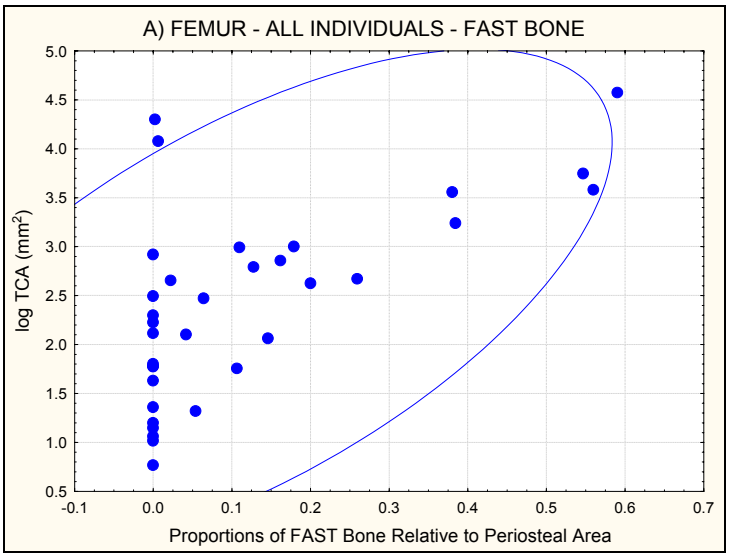


**Figure 4.17: Proportions of periosteal FAST bone relative to the periosteal cortex, as a function of TCA.**

A) There is a positively allometric relationship between the proportion of FAST bone, relative to periosteal area, and TCA ($r^2=.4$, $r=.64$, $p<.001$). B) This relationship is strengthened when the data are categorized by PHYLO (Strepsirhini $r^2=.67$, $r=.82$, $p<.001$; Platyrrhini $r^2=.69$, $r=.83$, $p<.05$).

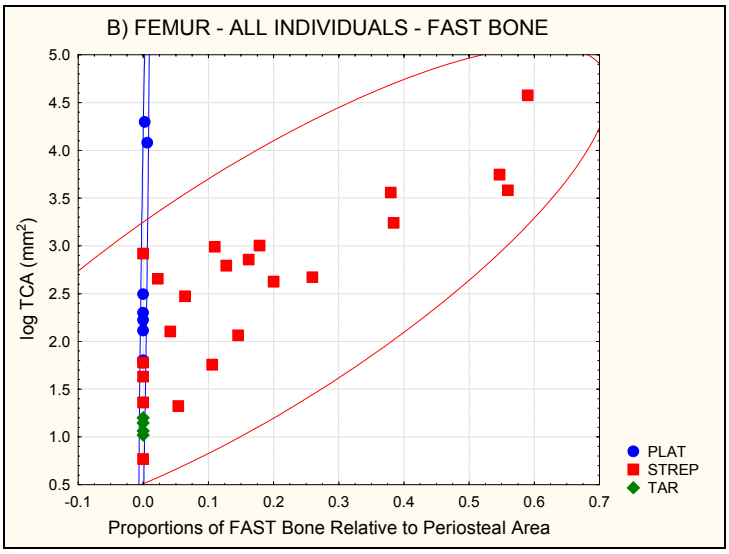


In the femur, radius and ulna, multiple regression analysis indicates that PB is also a factor accounting for a significant proportion of variation in FAST bone (Table 4.3). Significance is marginal for the femur however, and tests for differences among PB groups are non-significant except in one instance in the radius, where slow climbers (SC) have proportionately more fast bone than the VCL category. The femur boxplot (Figure 4.18) further points to the lack of a strong and consistent pattern of differentiation by positional behavior; in the femur, categories are poorly separated. And, while multiple regression results for the radius and ulna are stronger, the two elements show contradictory patterns. For the radius, slow climbers have the greatest mean proportion of FAST bone (although this could also be a taxon specific growth and/or phylogenetic pattern, which will be explored further in a following section). In the ulna, arboreal quadrupeds have the highest mean values. The lack of concordance between elements, combined with the generally marginal significance or lack of significance in Mann-Whitney U tests suggests that the relationship between PB and FAST bone as revealed in the multiple regression should be viewed with skepticism. Although the multiple

regression presumably highlights the significance of independent variables as they interact with each other, and the boxplots and bivariate tests for significance do not account for such interactions, it is nevertheless necessary to consider that the composition of the sample (i.e., small sample sizes and non-normal distributions) warrants caution when interpreting the results. Only in the case of robust and consistent results does it seem prudent to recognize the relationship between dependent and predictor variables. In the case of FAST bone, therefore, these data do not sufficiently make the case for positional behavior as a feature of importance.

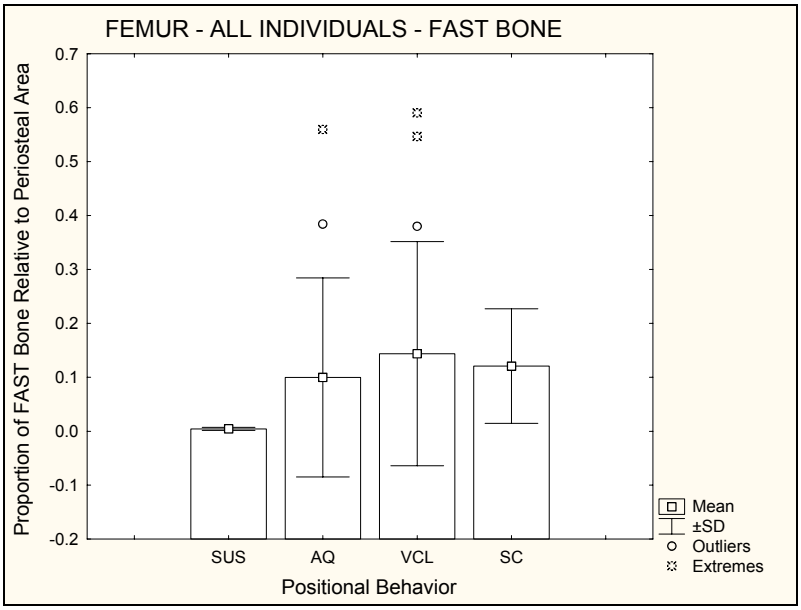


**Figure 4.18: Femoral proportions of periosteal FAST bone, categorized by PB.**

Positional behavior categories in the femur are poorly separated.

4.6.4.2 PF bone

Unlike the case for FAST bone, TCA does not appear to be an important predictor of the proportion of the periosteal cortex composed of PF bone (Table 4.4). Only in the femur and humerus does a multiple regression yield significant results for TCA. A bivariate plot of the femur (Figure 4.19) shows a weak negatively allometric relationship between

the proportion of PF bone and TCA. For all other elements, bivariate plots show no relationship between TCA and the proportion of PF bone relative to the periosteal cortex.

| PF - ALL INDIVIDUALS | | |
|---|---|---|
| Element | Predictor Variable | Beta |
| Femur | PHYLO | 0.51-0.56* |
| | PB | 0.68*** |
| | TCA | -0.36** |
| Humerus | PHYLO | 0.88** |
| | PB | 0.64** |
| | TCA | 0.43* |
| Tibia | PHYLO | 0.77-0.82* |
| Radius | PHYLO | 0.76-0.95** |
| | PB | 0.55-0.83* |
| Ulna | PB | 0.71-0.99** |

**Table 4.4: Multiple regression results for PF bone for the entire sample.**

For each element, the independent variables for which there are significant betas are listed. Because the variables PHYLO and PB are dummy-coded, each includes more than one vector. Individual vectors may or may not have significant betas. When a beta range is shown, this is because more than one beta was significant. Indicated significances are based on the highest p value for that variable. * indicates p<.05; ** indicates p<.01; *** indicates p<.001.

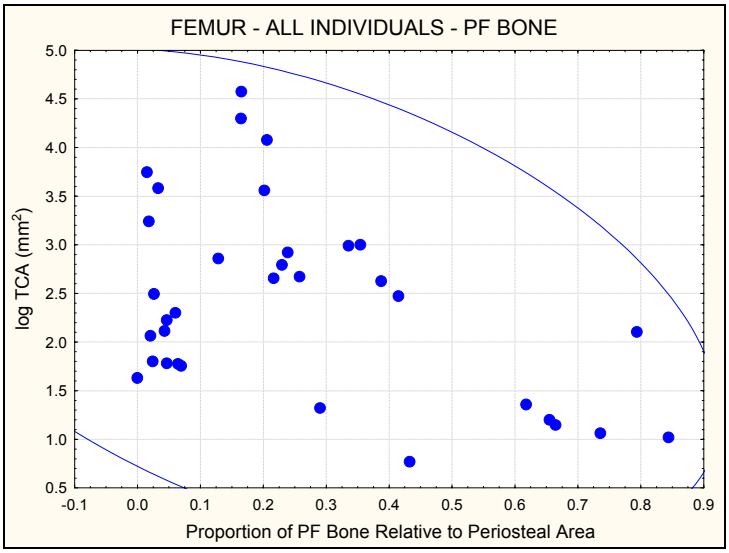


**Figure 4.19: Femoral proportions of periosteal PF bone relative to the periosteal cortex, as a function of TCA.**

There is a weak negatively allometric relationship between %PF bone and TCA ($r^2$=.19, r=.43, p=<.01).

More important are the predictor variables PHYLO and PB (Table 4.4). For all bones except the ulna, multiple regressions indicate that taxonomic status accounts for a significant proportion of the variation in the sample. The mean proportion of PF bone in the femur, humerus, tibia and radius is higher for tarsiids than strepsirhines and

platyrrhines as is evident in Figure 4.20. These differences are significant in the femur and humerus ($p<.05$ to $<.01$), as well as the tibia for the comparison between tarsiids and strepsirhines ($p<.05$). In all cases except the humerus, the mean value for the proportion of PF bone is higher in strepsirhines than platyrrhines, although the differences are not significant. The consistency of these patterns, with few exceptions, in conjunction with the multiple regression results, do indicate a significant taxonomic patterning in the proportion of the periosteal cortex composed of PF bone.

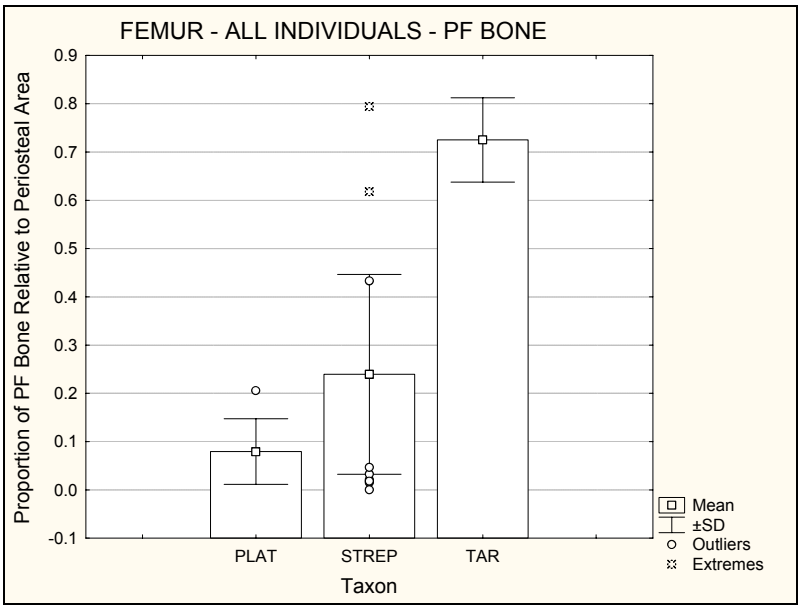


**Figure 4.20: Femoral proportions of periosteal PF bone, categorized by PHYLO.**

In the sample femora, the proportion of PF bone is significantly higher in tarsiids than in strepsirhines or platyrrhines. The proportion of PF bone is also higher in strepsirhines than in platyrrhines.

For all elements except the tibia, PB is also a significant predictor variable (Table 4.4). In all cases (including the tibia), arboreal quadrupeds display the smallest proportions of PF bone, while slow climbers include a greater mean proportion of PF bone than all other positional behaviors except in the femur, where vertical clingers and leapers and slow climbers display an equivalent amount of PF bone. Differences between arboreal quadruped and slow climber values are significant for all elements ($p<.05$ to

<.001). In all cases except the femur, vertical clingers and leapers display an intermediate amount of PF bone. Only the differences between VCL and AQ categories in the femur, and VCL and SC categories in the ulna are significant ($p<.01$). The values for the suspensory atelids, which are only available for the femur and humerus, are conflicting (the humerus value is almost as high as slow climbers, but the value for the femur is lower than both SC and VCL), likely due to the low sample size (n=2). In contrast to the FAST bone data, the consistency among elements in multiple regression results and comparison of mean values suggests that positional behavior is correlated with the proportion of the periosteal cortex composed of PF bone.

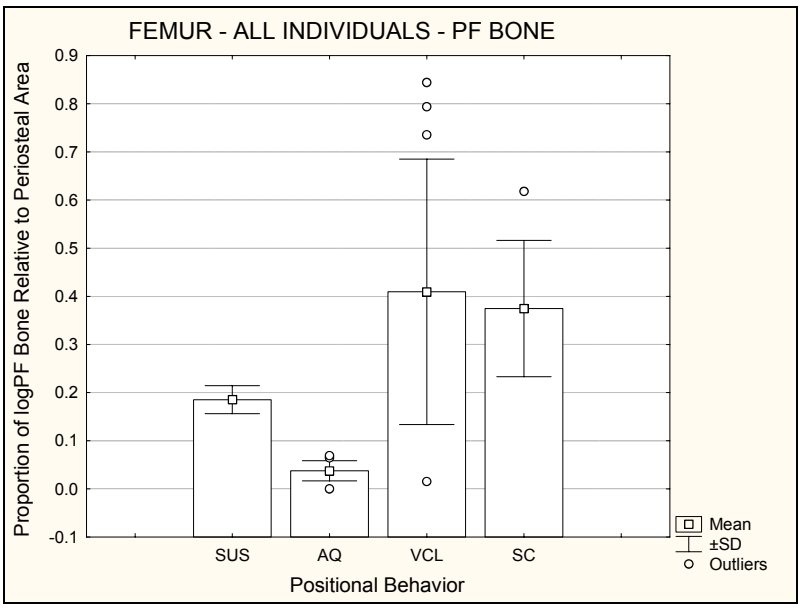


**Figure 4.21: Femoral proportions of periosteal PF bone, categorized by PB.**

See text for description.

4.6.4.3 LAM+HYB bone

Similar to PF bone, and unlike FAST bone, multiple regression analyses suggest that TCA is subsidiary to PHYLO and PB in its importance as a predictor of the proportion of LAM+HYB bone relative to periosteal cortex (Table 4.5). For both the femur and

humerus, TCA appears as a significant factor in the most robust multiple regression models. However, bivariate plots of LAM+HYB bone and TCA yield insignificant relationships (e.g., Figure 4.22A) for all elements. A categorization by PHYLO yields a significant regression for the platyrrhines in the femur (Figure 4.22B), humerus, and tibia, as well as for strepsirhines in the humerus and femur. This suggests a potential weak effect of TCA in the proportion of LAM+HYB bone in the periosteal cortex, where the larger the cortex, the less of this slow deposition tissue. The pattern is the inverse of that seen for FAST bone. In addition, as evident in Figure 4.22B, as the cortex in the femur and humerus gets larger, strepsirhines reduce the proportion of LAM+HYB bone more than the platyrrhines do, again the inverse of what is seen for FAST bone. However, this pattern is not repeated in the tibia or other bones, suggesting that the relationship between TCA and LAM+HYB bone should be viewed with caution.

| LAM+HYB - ALL INDIVIDUALS | | |
|---|---|---|
| Tissue Type | Predictor Variable | Beta |
| Femur | PHYLO | 0.69-0.89** |
| | PB | 0.47** |
| | TCA | -0.31* |
| Humerus | PHYLO | 0.82-0.89* |
| | PB | 0.37-0.69** |
| | TCA | -0.51** |
| Tibia | PHYLO | 0.71-0.99* |
| | PB | 0.62-0.72* |
| Radius | PHYLO | 0.81-0.96** |
| | PB | 0.63-0.94** |
| Ulna | PB | 0.88-0.95*** |

**Table 4.5: Multiple regression results for LAM+HYB bone for the entire sample.**

For each element, the independent variables for which there are significant betas are listed. Because the variables PHYLO and PB are dummy-coded, each includes more than one vector. Individual vectors may or may not have significant betas. When a beta range is shown, this is because more than one beta was significant. Indicated significances are based on the highest p value for that variable. * indicates $p<.05$; ** indicates $p<.01$; *** indicates $p<.001$.

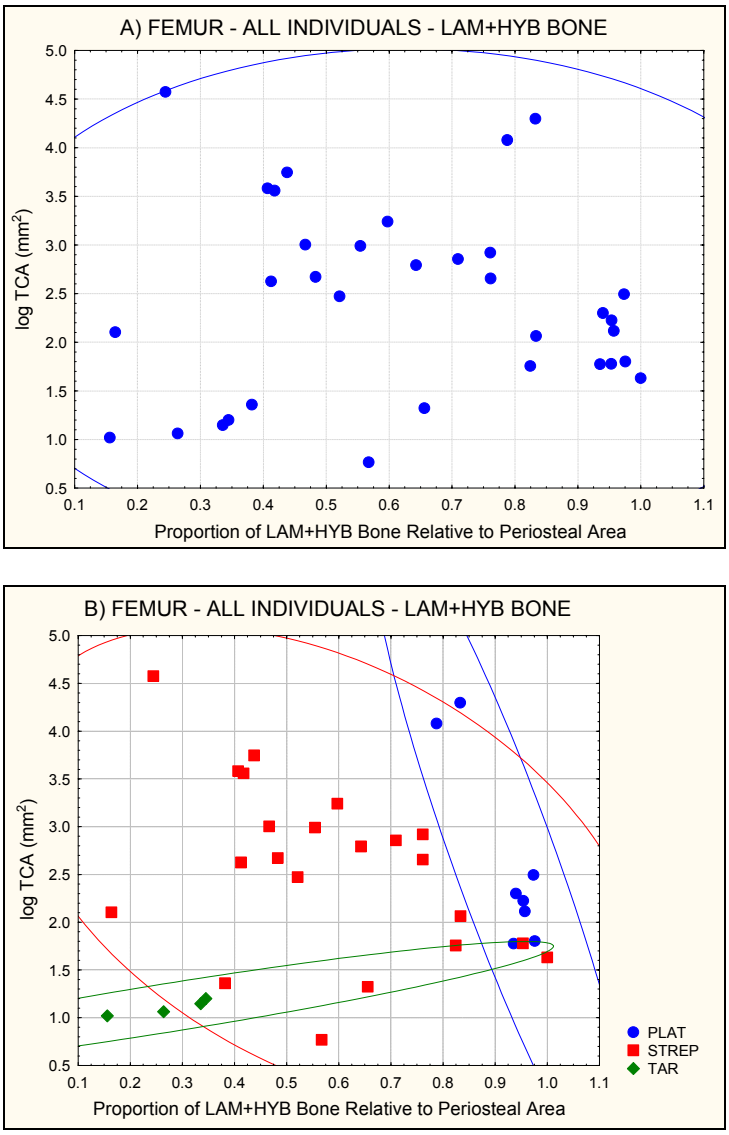


**Figure 4.22: Proportions of periosteal LAM+HYB bone relative to the periosteal cortex, as a function of TCA.**

A) There is no relationship between %LAM+HYB bone and TCA ($r^2$=.00, r=.00, p>.05). B) When the data are categorized by PHYLO the platyrrhine regression is significant ($r^2$=.83, r=-.91, p<.01), as is the strepsirhine regression ($r^2$=.18, r=-.42, p<.05).

For all elements except the ulna, multiple regression results point to PHYLO as a significant predictor variable for the proportion of LAM+HYB bone in the periosteal cortex (Table 4.5). In all elements (including the ulna) the mean value for LAM+HYB bone is higher in platyrrhines than in strepsirhines or tarsiids (e.g., Figure 4.23). The difference is significant for a comparison of platyrrhines and strepsirhines in the femur and tibia (p<.01), and significant when platyrrhines and tarsiids are compared for the femur and humerus (p<.05). In addition, in all cases except the ulna, mean values for

tarsiids are lower than for strepsirhines (significant only for the femur; p<.01). As with PF bone, the consistency among elements, and concordance between the multiple regression results and comparison of mean values suggests that PHYLO can indeed be considered an important factor for explaining variation in the proportion of LAM+HYB bone.

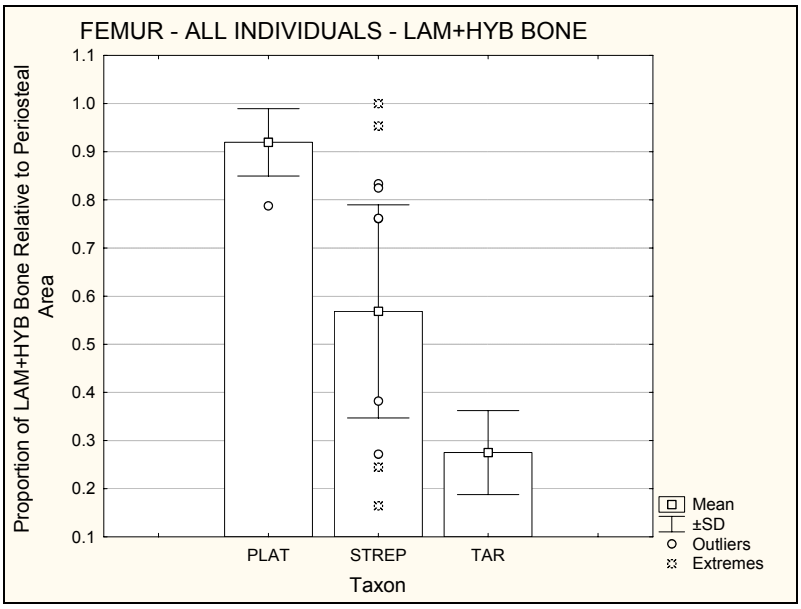


**Figure 4.23: Femoral proportions of periosteal LAM+HYB bone, categorized by PHYLO.**

See text for description.

Multiple regressions also show that PB is a significant predictor for proportion of LAM+HYB bone in the periosteal cortex. In all elements, arboreal quadrupeds have proportionately more of this tissue than vertical clingers and leapers, as well as slow climbers (e.g., Figure 4.24). As with the independent variable PHYLO, this is the inverse of what is seen in PF bone; not a surprising result given that most of the cortex in the majority of the specimens is composed of a combination of LAM+HYB and PF tissues. The differences are significant for the comparison between arboreal quadrupeds and vertical clingers and leapers in the femur and humerus (p<.001 and <.05 respectively), as

well as for arboreal quadrupeds and slow climbers in all five bones ($p<.05$ to $<.01$). In all cases except the femur, slow climbers have proportionately the least LAM+HYB bone, with vertical clingers and leapers intermediate between slow climbers and arboreal quadrupeds. In the femur however, vertical clingers and leapers have the least LAM+HYB bone, although the mean values for vertical clinging and slow climbing are close. The difference between vertical clingers and leapers and slow climbers is significant for the tibia, radius and ulna ($p<.05$ to $<.01$). Mean values for the suspensory category are lower than arboreal quadrupedalism in both the femur and humerus, higher than vertical clinging and leaping and slow climbing in the femur, and higher than slow climbing in the humerus. Only in the femur are these difference significant, for the comparisons between suspension and vertical clinging and leaping as well as suspension and slow climbing ($p<.05$). Overall, there are consistent PB patterns among skeletal elements for the proportion of the periosteal cortex composed of LAM+HYB bone, corroborated by both multiple regressions and comparisons between means.

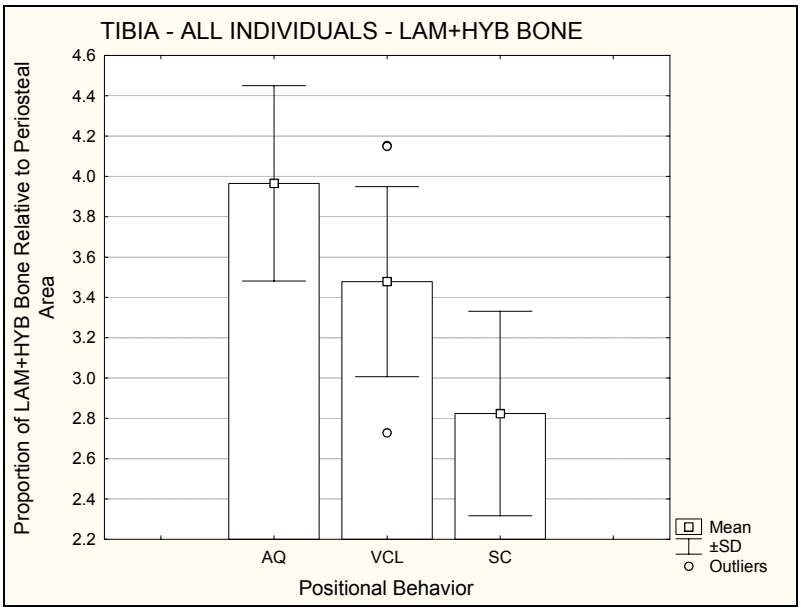


**Figure 4.24: Tibial proportions of periosteal LAM+HYB bone, categorized by PB.**

See text for description.

*4.6.5 Comparison between elements: individual specimens*

When the values for two different elements in individual specimens are compared for the entire sample, there appears to be no taxonomic or functional patterning to the resultant bivariate plots, with one exception. A femur/humerus comparison for LAM+HYB bone in the periosteal cortex suggests that the proportion of this tissue is generally greater in the humerus relative to the femur in vertical clingers and leapers as compared to the other primates in the sample (Figure 4.25A). This pattern is accentuated when LAM is examined to the exclusion of HYB bone (Figure 4.25B). As Figure 4.26 demonstrates, the most committed arboreal quadrupeds and suspensors have approximately the same proportion of LAM+HYB bone in the humerus as the femur. In contrast, the obligate vertical clingers and leapers have femora with less than half the proportion of LAM+HYB bone than their humeri. The greater galagos and lemurids – primates with varied positional behaviors that fit less well into the broad categories – as well as the lorisids, display intermediate patterns.

Figure 4.27 shows that, except for the suspensory spider monkeys, when absolute values rather than relative values are considered, this positional behavior pattern largely disappears. The majority of individuals lie closely along a single regression, indicating that the relationship between the amount of bone in the humerus and the femur is consistent for a given body size, regardless of positional behavior. The pattern seen in the bivariate plots of relative values likely reflects the fact that vertical clingers and leapers have a greater femur/humerus ratio for TCA. A vertical clinger and leaper may have relatively less LAM+HYB bone in its femoral cortex, relative to the humerus, than an arboreal quadruped of similar body size, but the absolute values will be the same.

Figures 4.25 and 4.26 are better understood in this context. The pattern in the lorisids, however, remains puzzling. It would be expected that these primates, with their comparable (although not identical) use of forelimb and hindlimb, as well as similarly sized midshaft femoral and humeral cortices, would have a pattern more similar to that found in the arboreal quadrupeds and suspensors. Alternatively, Figure 4.26 can be understood in terms of a prosimians/platyrrhine separation, in which case the lorisid pattern is consistent. In that scenario, however, the cheirogaleids become outliers, grouping with the platyrrhines. The persistent extremity of the pattern in suspensory atelids is interesting given their divergent positional behavior relative to all other primates in this sample. However, the small sample size means that interpretation of this pattern should be undertaken with caution.

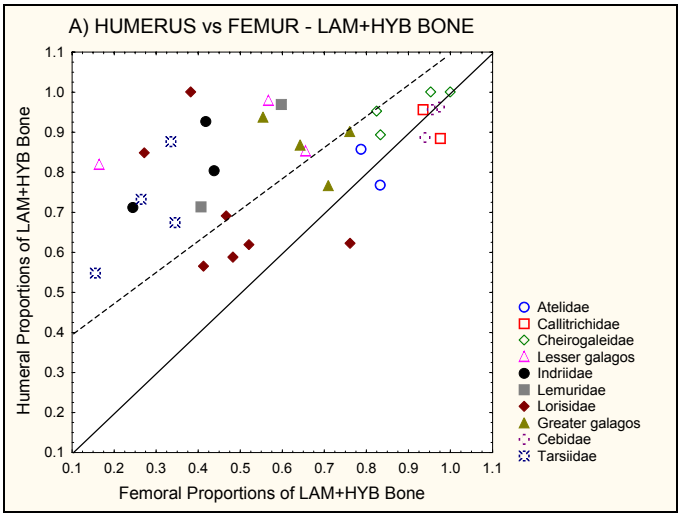

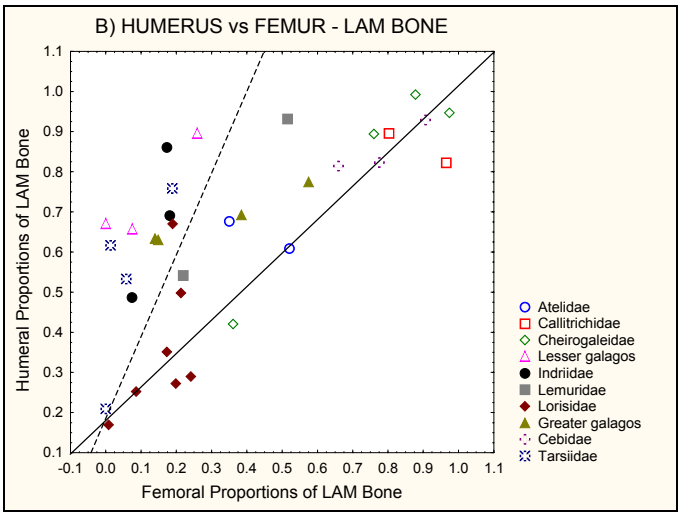


**Figure 4.25: Proportions of LAM+HYB and LAM bone in the humerus and femur of all sample individuals, categorized by taxon.**
A) In this bivariate plot of LAM+HYB bone, the solid diagonal line indicates where the values would fall should the proportion of LAM+HYB bone be equivalent in both elements within an individual. In almost all cases, the humerus contains a greater proportion of LAM+HYB bone than the femur. The dashed diagonal line is an arbitrarily drawn separation between vertical clingers and leapers (above the line) and taxa with all other positional behaviors (below the line). Greater galagos appear on both sides of the line, as do lorisids. The two lemurids, more arboreally quadrupedal than the indriids, group with the vertical clingers and leapers. B) A plot of LAM bone results in a clearer separation between vertical clingers and leapers, and other primates. Again, greater galagos do not group on one side or the other. In this case, however, all but one of the lorisids fall on the non-leaper side of the line, as do the two lemurids.

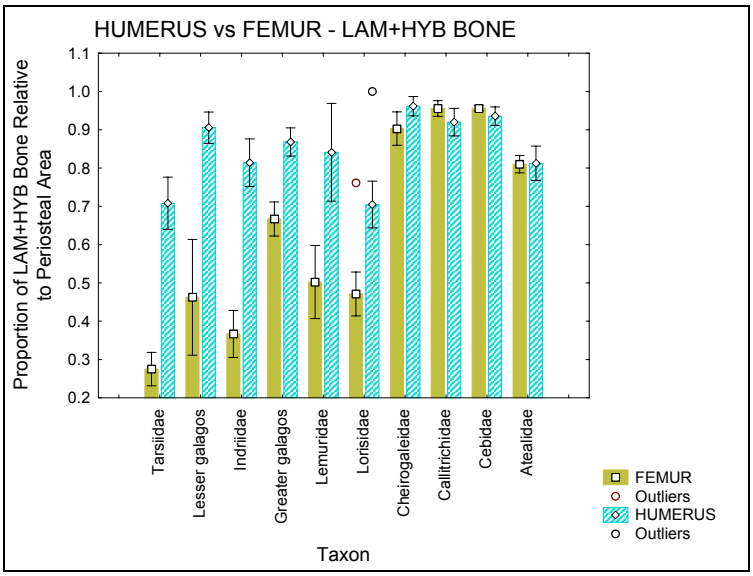


**Figure 4.26: Mean proportions of LAM+HYB and LAM bone in the humerus and femur of all sample individuals, categorized by taxon.**

Means for all arboreal quadrupeds show roughly the same proportion of lamellar bone in the femur as in the humerus. In the three most committed vertical clingers and leapers, the proportion of LAM+HYB bone in the humerus is more than twice what is found in the femur. The pattern is intermediate for the greater galagos, the lemurids and the lorisids.

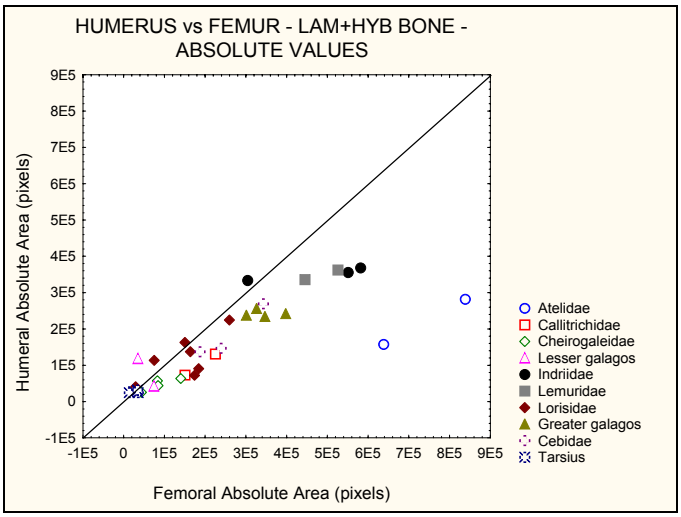


**Figure 4.27: Absolute values of LAM+HYB in the humerus and femur of all sample individuals, categorized by taxon.**

The diagonal line indicates where the plots would fall should the proportion of LAM+HYB bone be equivalent in both elements within an individual. Values for most individuals are near equivalent in the humerus and femur, with the femur most often displaying slightly more LAM+HYB bone. The one exception is the suspensory atelids, where the femur clearly displays far more LAM+HYB bone than the humerus.

*4.6.6 Characterization of individual taxa and targeted comparison amongst taxa*

4.6.6.1 Intra- and intertaxonomic diversity

Investigations of variation within the sample as a whole highlight patterned relationships between primary tissue types and body size, phylogeny and/or growth, and positional behavior. However, within the broad patterns described above, there is evidence of both intra- and intertaxonomic diversity (see for example the standard deviation of some of the means in Figure 4.21). Following is an exploration of this variability. Because within-taxon sample sizes are small, particularly for the tibia, radius and ulna, analyses remain descriptive.

4.6.6.2 Consistency[1] within taxa: intrataxonomic variation for individual elements

There is an overall pattern of intrataxonomic consistency in proportions of primary tissue types for individual elements. However, some skeletal elements appear to be more constrained in their distribution of tissues, both within and between taxa, than others.

For the femur, all taxa except the lorisids and the lesser galagos are remarkably uniform in their pattern of tissue type proportions (Table 4.6). The variation within the lorisids and the lesser galagos does not correspond to separation between individuals at the genus level (e.g., *Galago* vs. *Galagoides*, or *Nycticebus* vs. *Loris*), and concomitant body size differences.

[1] Patterns are considered to be consistent when all individuals within a taxon have approximately the same proportion of the three primary tissue types: FAST, PF and LAM. This is determined through graphical depictions of tissue type values.

| RELATIVE PROPORTIONS OF PRIMARY TISSUE TYPES | | | | | | | |
|---|---|---|---|---|---|---|---|
| **Taxon** | **Tissue Type** | **N** | **Mean** | **Min** | **Max** | **Variance** | **SD** |
| Cheirogaleidae | FAST | 4 | 0.06 | 0.00 | 0.15 | 0.0056 | 0.0746 |
| | PF | 4 | 0.03 | 0.00 | 0.07 | 0.0009 | 0.0302 |
| | LAM+HYB | 4 | 0.90 | 0.82 | 1.00 | 0.0076 | 0.0874 |
| Lesser galagos | FAST | 3 | 0.03 | 0.00 | 0.05 | 0.0008 | 0.0283 |
| | PF | 3 | 0.51 | 0.29 | 0.79 | 0.0675 | 0.2597 |
| | LAM+HYB | 3 | 0.46 | 0.16 | 0.66 | 0.0686 | 0.2620 |
| Greater galagos | FAST | 4 | 0.10 | 0.00 | 0.16 | 0.0049 | 0.0700 |
| | PF | 4 | 0.23 | 0.13 | 0.34 | 0.0072 | 0.0846 |
| | LAM+HYB | 4 | 0.67 | 0.55 | 0.76 | 0.0080 | 0.0892 |
| Lorisidae | FAST | 6 | 0.12 | 0.00 | 0.26 | 0.0113 | 0.1062 |
| | PF | 6 | 0.37 | 0.22 | 0.62 | 0.0200 | 0.1416 |
| | LAM+HYB | 6 | 0.50 | 0.38 | 0.76 | 0.0183 | 0.1354 |
| Lemuridae | FAST | 2 | 0.47 | 0.38 | 0.56 | 0.0154 | 0.1240 |
| | PF | 2 | 0.03 | 0.02 | 0.03 | 0.0001 | 0.0107 |
| | LAM+HYB | 2 | 0.50 | 0.41 | 0.60 | 0.0182 | 0.1347 |
| Indriidae | FAST | 4 | 0.38 | 0.00 | 0.59 | 0.0721 | 0.2686 |
| | PF | 4 | 0.26 | 0.02 | 0.66 | 0.0786 | 0.2804 |
| | LAM+HYB | 4 | 0.36 | 0.24 | 0.44 | 0.0078 | 0.0882 |
| Tarsiidae | FAST | 4 | 0.00 | 0.00 | 0.00 | 0.0000 | 0.0000 |
| | PF | 4 | 0.72 | 0.65 | 0.84 | 0.0076 | 0.0873 |
| | LAM+HYB | 4 | 0.28 | 0.16 | 0.35 | 0.0076 | 0.0873 |
| Callitrichidae | FAST | 2 | 0.00 | 0.00 | 0.00 | 0.0000 | 0.0000 |
| | PF | 2 | 0.04 | 0.02 | 0.06 | 0.0008 | 0.0286 |
| | LAM+HYB | 2 | 0.96 | 0.94 | 0.98 | 0.0008 | 0.0286 |
| Cebidae | FAST | 4 | 0.00 | 0.00 | 0.00 | 0.0000 | 0.0000 |
| | PF | 4 | 0.04 | 0.03 | 0.06 | 0.0002 | 0.0139 |
| | LAM+HYB | 4 | 0.96 | 0.94 | 0.97 | 0.0002 | 0.0139 |
| Atelidae | FAST | 2 | 0.00 | 0.00 | 0.01 | 0.0000 | 0.0028 |
| | PF | 2 | 0.19 | 0.16 | 0.21 | 0.0008 | 0.0291 |
| | LAM+HYB | 2 | 0.81 | 0.79 | 0.83 | 0.0010 | 0.0319 |

**Table 4.6: Femoral relative proportions of primary tissue types by taxon.**
See text for description.

The patterns among humeral sections within taxa are as regular as those in the femur, the exceptions in this case being lorisids and tarsiids. For the tibia, radius and ulna, reduced sample sizes make assessments of variability less reliable. In the tibiae and radii of the lesser and greater galagos, Cebidae, Lorisidae and Tarsiidae there are consistent patterns, while in Cheirogaleidae there are not. There are no atelid or

callitrichid tibia, no atelid radii, and only one specimen each of tibia and radius for Indriidae and Lemuridae examined. In the ulna, only lesser galagos and Lorisidae show a consistent pattern, while the tarsiids, cebids, and greater galagos do not. There are no atelid or cheirogaleid specimens, and only one each for Callitrichidae, Indriidae and Lemuridae. Figures 4.28A, B and C are examples of the uniform and non-uniform within-taxon patterning for the femur.

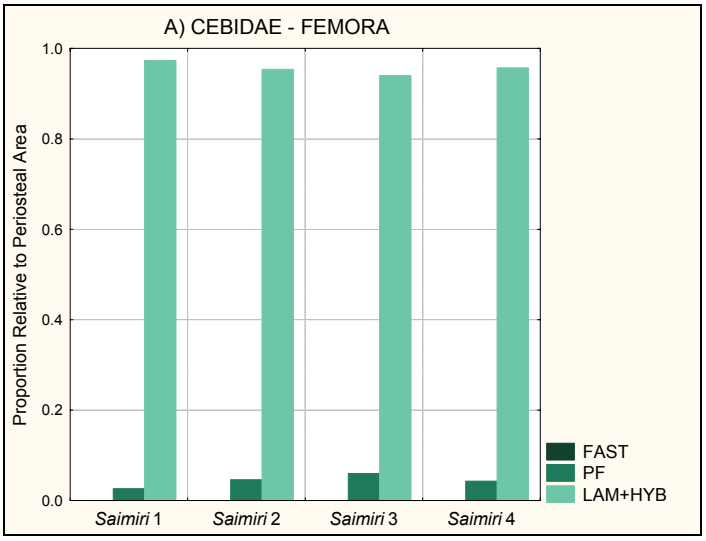


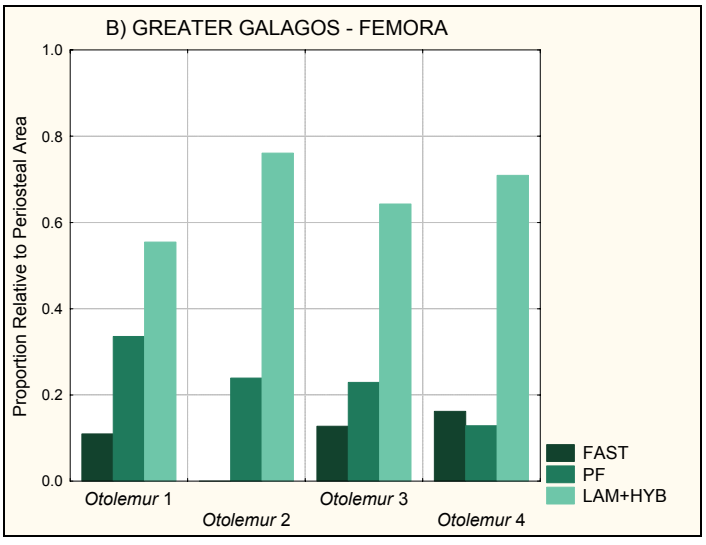


**Figure 4.28: Individual values for the proportions of FAST, PF and LAM+HYB bone in the femur of Cebidae, greater galagos and Lorisidae.**

A) Cebidae is an example of a taxon where femoral proportions of primary tissue types are highly uniform among individuals. B) Among greater galagos, proportions are still consistent, although somewhat less so than in cebids. C) Patterns of tissue type variation among the lorisid femora are inconsistent from one individual to the next, although several do show similar values.

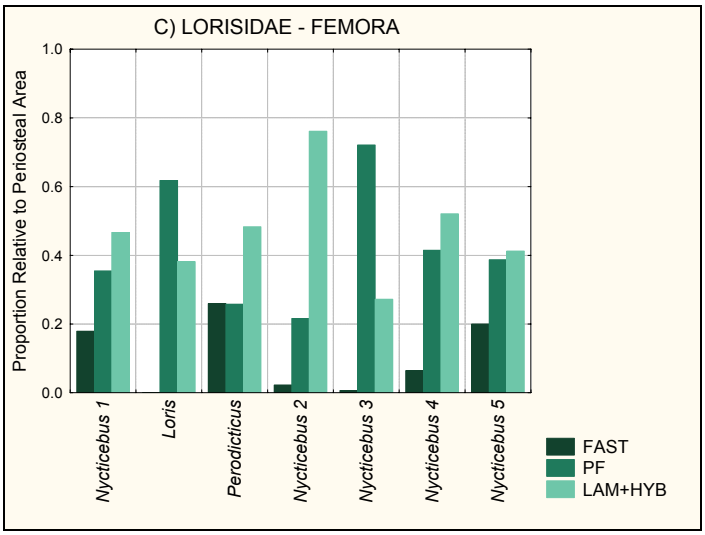


4.6.6.3 Consistency within taxa: comparing means for skeletal elements within taxa

Another question is the degree to which elements within a taxon show similar patterns of primary tissue type proportions. For the sample as a whole there is considerable variation among elements. When examining means within an individual taxon the disparities are again apparent. Only in the three platyrrhine taxa do all skeletal elements show a similar pattern of tissue type distribution, with LAM+HYB bone comprising the majority of the cortex, followed by PF bone and finally FAST bone (although all five skeletal elements are available only for the cebids). In all other taxa there is variation among elements in the tissue that predominates across the cortex, with the larger-bodied strepsirhine indriids and lemurids displaying the most diversity.

4.6.6.4 Consistency between taxa: means for skeletal elements across taxa

If differences in means among elements are compared across taxa it is clear that humeri are the least variable. In all taxa, LAM bone is the predominant tissue in the humerus, followed by PF and then FAST bone, or by similar values for PF and FAST. In all other

elements, the order of tissues in terms of their predominance in the cortex varies among taxa (but, as described above, not in a consistent fashion). The femur and tibia appear to be the most variable, with the radius and ulna intermediate between humeri and the hindlimb bones.

4.6.6.5 Characterization of femoral patterns of primary tissue type distributions for individual taxa

Because tissue types in the humerus appear to be more constrained, perhaps by developmental imperatives (see the discussion section), and because sample sizes for the tibia, humerus, and ulna are smaller than those for the femur – yielding less reliable means – the following description of taxon patterns and discussion of comparisons among individual taxa and correspondence with life history and function is restricted to the femur.

*4.6.6.5.1 Lesser galagos.* There is some heterogeneity in this group, with two of the three individuals (one *Galago*, and one *Galagoides*) displaying a predominance of LAM+HYB bone (>55%), and the third individual (a *Galago*) with more PF bone (c.80%) in the periosteal cortex. Small amounts (c. 5%) of FAST tissue are present in the two *Galago* individuals, in the anterior cortex (the thickest cortex), close to the boundary between endosteal and periosteal bone. This is consistent with faster deposition at earlier stages of growth, and in the thicker portions of the cortex. The LAM+HYB and PF tissues are

sparsely vascularized[2], with canals that are simple and course longitudinally. The bone may be avascular in the medial, lateral and posterior cortices.

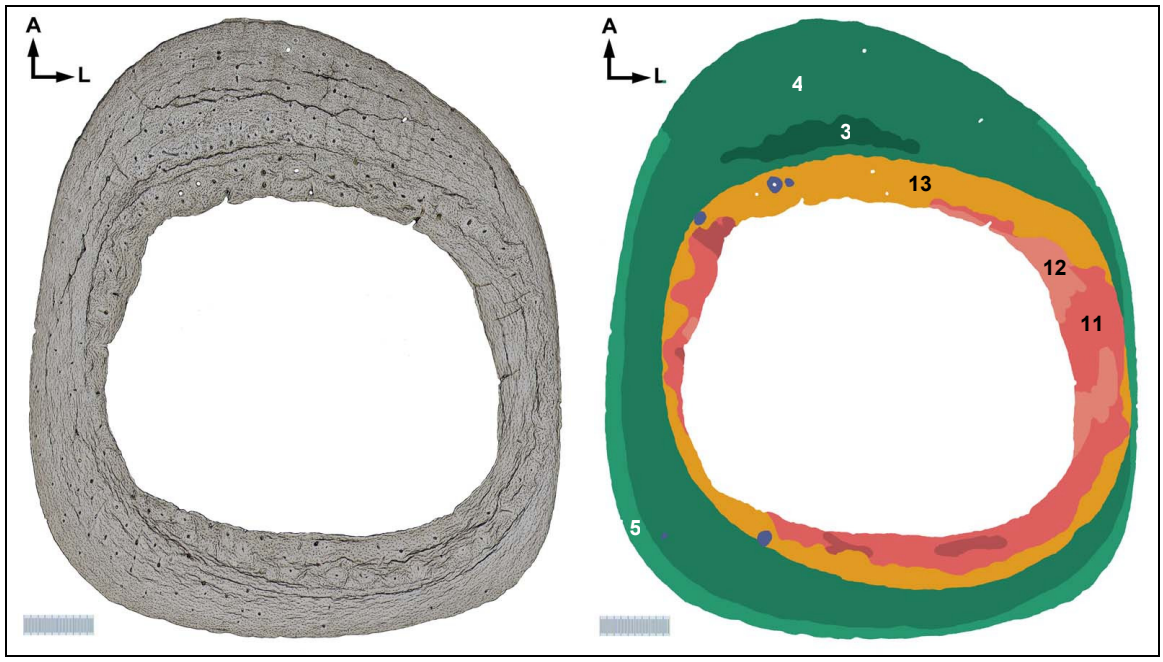


**Figure 4.29: *Galago senegalensis* midshaft femur (MNHU 60601).**
LM image on left. Color-coded tissue map on right. Scale bar = .5 mm. See text for description. See Figure 4.2 for interpretation of numbers.

*4.6.6.5.2 Greater galagos*. In all *Otolemurcrassidaudatus* individuals, LAM+HYB tissue makes up the largest proportion of the periosteal cortex (c.55-75%), with PF and FAST tissues generally (although not exclusively) concentrated in the anterior cortex. This cortex is the thickest in three of four individuals suggesting, as is the case with the lesser galagos, that deposition progressed more rapidly where the cortex is thickest. In addition, in three of four femora, faster tissues are more endosteally located, consistent with faster

[2] Vascularization in the sample has not been quantified. Therefore, the relative densities of vascular canals are assessed visually and described qualitatively. The following three terms are used: 1) sparse vascularization = vascular canals are irregularly distributed, with avascular stretches between them that generally exceed three times the diameter of the canals, 2) moderate vascularization = vascular canals are more regularly distributed, with the distance between canals frequently less than three times the diameter of the canals, 3) intense vascularization = vascular canals are separated from each other by less than the diameter of two canals.

bone formation earlier in development. There is a sparse to moderate amount of vascularization of the PF and LAM+HYB tissues with denser vascularization in the anterior cortex, and areas of avascular bone, particularly in the posterior cortex and close to the most periosteal boundaries of the bone. Vascular canals are generally of the simple type, coursing longitudinally, with one individual displaying short, radially oriented vascular canals.

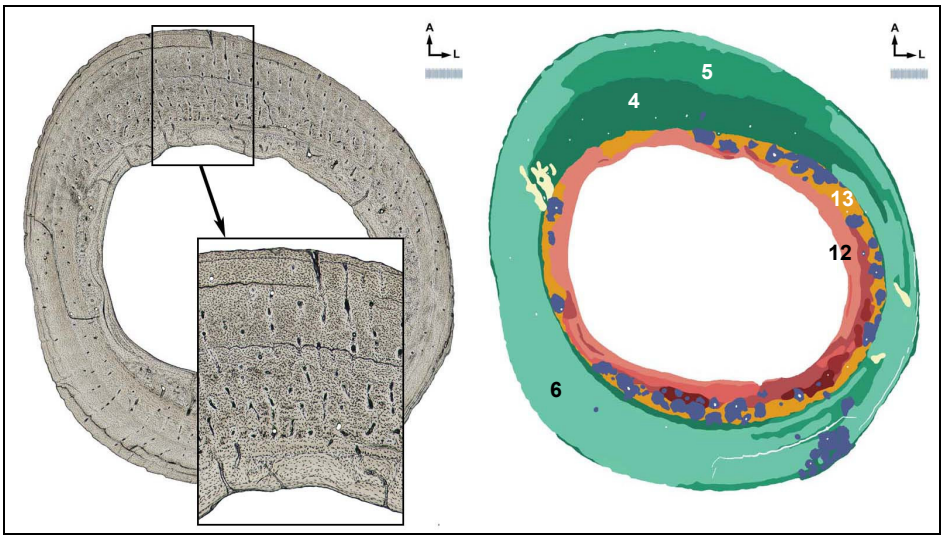


**Figure 4.30: *Otolemur crassicaudatus* midshaft femur (HC 31).**
LM image with magnified inset on left. Color-coded tissue map on right. Scale bar = .5 mm. See text for description. See Figure 4.2 for interpretation of numbers.

*4.6.6.5.3 Lorisidae sensu stricto.* Similar to the lesser galagos, there is some heterogeneity in this group. In four of the six individuals, LAM+HYB bone is the predominant tissue (c.47-77%). In one individual, proportions of LAM+HYB and PF are equivalent (c.40%). In the sole specimen of *Loris tardigradus*, PF is found in the majority of the periosteal cortex (c. 62%). In most instances, LAM+HYB tissue is found closer to the periosteal margin, while FAST bone is near the endosteum. FAST bone, present in all individuals except the noted specimen of *L. tardigradus*, is concentrated

posteriorly in the five individuals of *Nycticebus coucang*, and laterally in the sole specimen of *Perodicticus potto*. The majority of the LAM+HYB and PF bone is very sparsely vascularized, or avascular, with a single individual of *N. coucang* displaying denser, but still moderate vascularization. Where present, vascularization is not clustered in a single quadrant of the bone, but rather is evenly distributed around the section.

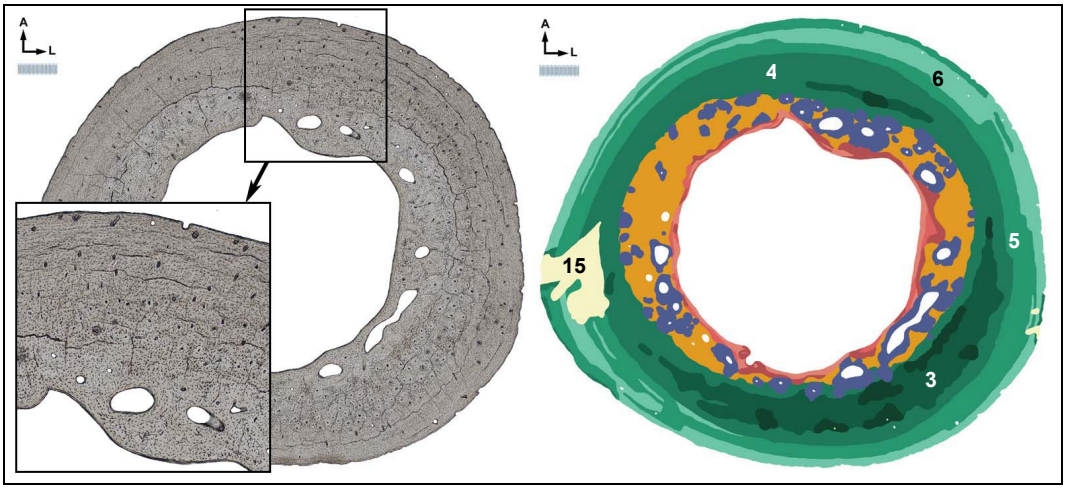


**Figure 4.31:** ***Nycticebus coucang*** **midshaft femur (DUPC 1972).**
LM image with magnified inset on left. Color-coded tissue map on right. Scale bar = .5 mm. See text for description. See Figure 4.2 for interpretation of numbers.

*4.6.6.5.4 Cheirogaleidae.* The cheirogaleids are characterized by a predominance of LAM+HYB bone in the periosteal cortex (>80%). Very little PF bone is present (<10%). The two *Cheirogaleus major* individuals display some FAST bone (c.10-15%) posteriorly in the thickest part of the cortex, close to the endosteal portion of the bone, as well as laterally in one individual. Neither the *Mirza coquereli* nor *Microcebus murinus* individuals have FAST bone in the periosteal cortex. The LAM+HYB bone is largely avascular, with few areas of sparse vascularization with simple longitudinal canals.

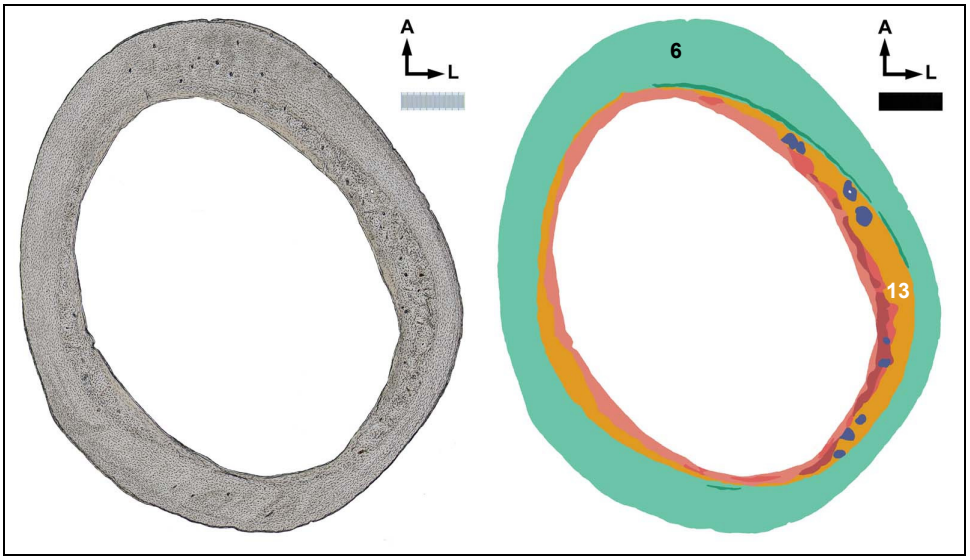


**Figure 4.32: *Mirza coquereli* midshaft femur (DUPC 359).**
LM image on left. Color-coded tissue map on right. Scale bar = .5 mm. See text for description. See Figure 4.2 for interpretation of numbers.

*4.6.6.5.5 Indriidae*. In the indriids, FAST bone makes up the greatest proportion of the periosteal cortex in one specimen of *Propithecus* sp. and *Indri indri* each (>50%), followed by LAM+HYB bone (<45%). In the second specimen *P.* sp., LAM+HYB and FAST values are close, with about 5% more LAM+HYB bone. In all individuals, PF is the least common tissue (≤20%). FAST bone is found in all quadrants of the section. The largest uninterrupted areas are close to the endosteum, but smaller strips, punctuated by circumferential swathes of LAM+HYB or PF bone are present closer to the periosteal margin. The cortex as a whole shows a periodic alternation of tissue types in the progression from endosteum to the periosteal margin. Vascularization in LAM+HYB and PF areas ranges from sparse to intense. Vascularization in these areas is by simple longitudinal canals.

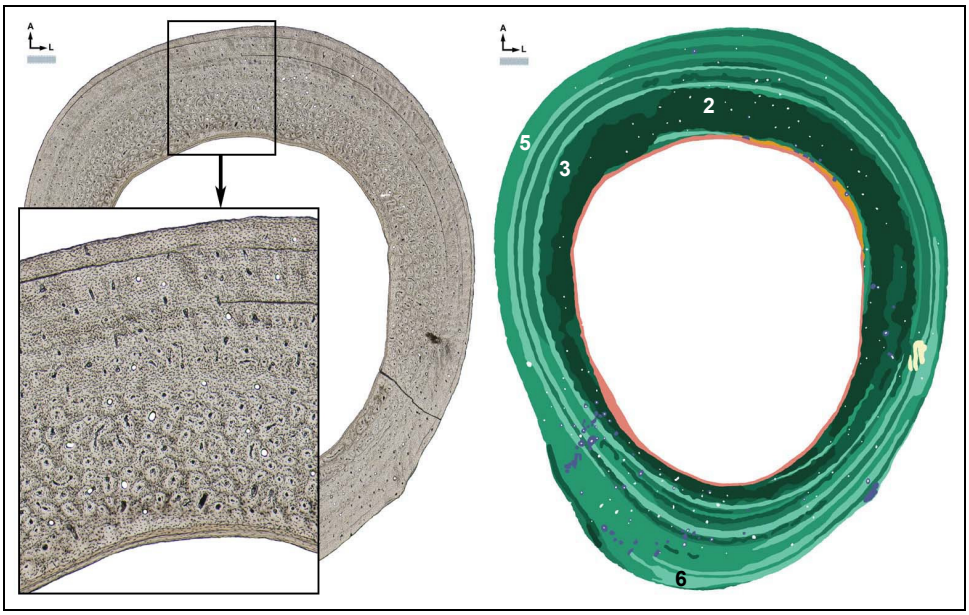


**Figure 4.33: *Propithecus* sp. midshaft femur (MNHU 44685).**
LM image with magnified inset on left. Color-coded tissue map on right. Scale bar = .5 mm. See text for description. See Figure 4.2 for interpretation of numbers.

*4.6.6.5.6 Lemuridae.* The lemurids on average display a near equivalent proportion of FAST and LAM+HYB tissues, with the single *Varecia variegata* individual having a greater proportion of FAST (c. 55% of the periosteal cortex), and the *Lemur* sp. more LAM+HYB (c. 60% of the periosteal cortex). The proportion of PF bone is low (<5% of the periosteal cortex) in both individuals. FAST bone is usually, although not always, concentrated close to the endosteal/periosteal boundary, particularly the larger uninterrupted areas of FAST bone, and is found in all quadrants of the cortex. Although FAST bone may not necessarily be the first tissue found abutting the endosteum, it is never present at the periosteal margins. As with the indriids, narrow circumferential strips of FAST bone, interspersed with strips of LAM+HYB, are also present, generally closer to the periosteal margin than the larger swathes of FAST bone. The LAM+HYB bone is sparsely to moderately vascularized. Vascular canals are of the simple longitudinal type, with some short radially coursing canals in the *V. variegata* individual.

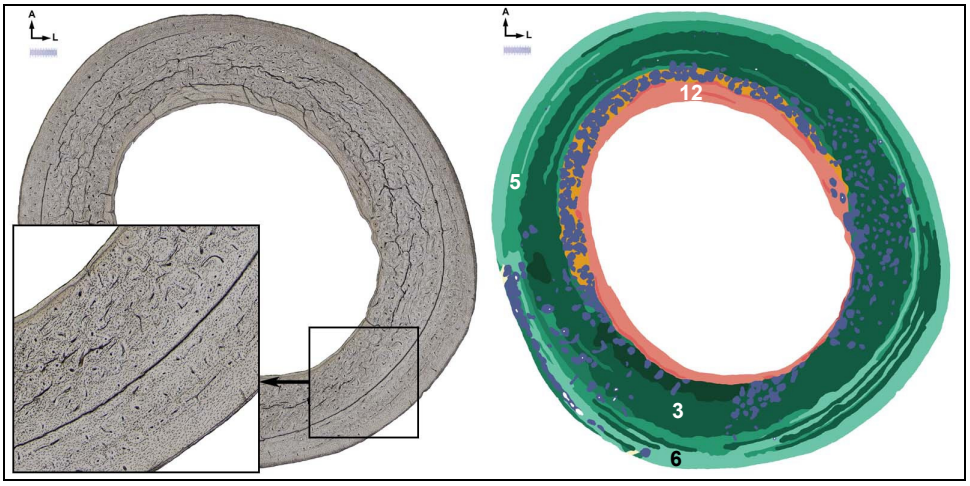


**Figure 4.34: *Varecia variegata* midshaft femur (MCZ 18740).**
LM image with magnified inset on left. Color-coded tissue map on right. Scale bar = .5 mm. See text for description. See Figure 4.2 for interpretation of numbers.

*4.6.6.5.7 Tarsiidae.* Tarsiids are characterized by a preponderance of PF bone in the periosteal cortex (c.65%-85%). The remainder of the tissue is of the LAM+HYB type. No FAST bone is present in the four individuals. When present, the LAM+HYB bone (and particularly the LAM bone) is often concentrated in the medial and lateral quadrants, where the cortex is thinnest. The periosteal cortex in the tarsiids is almost entirely avascular; in only one of the four individuals are a few simple vascular canals found (in the posterior cortex). These are of the simple longitudinal or short radial type.

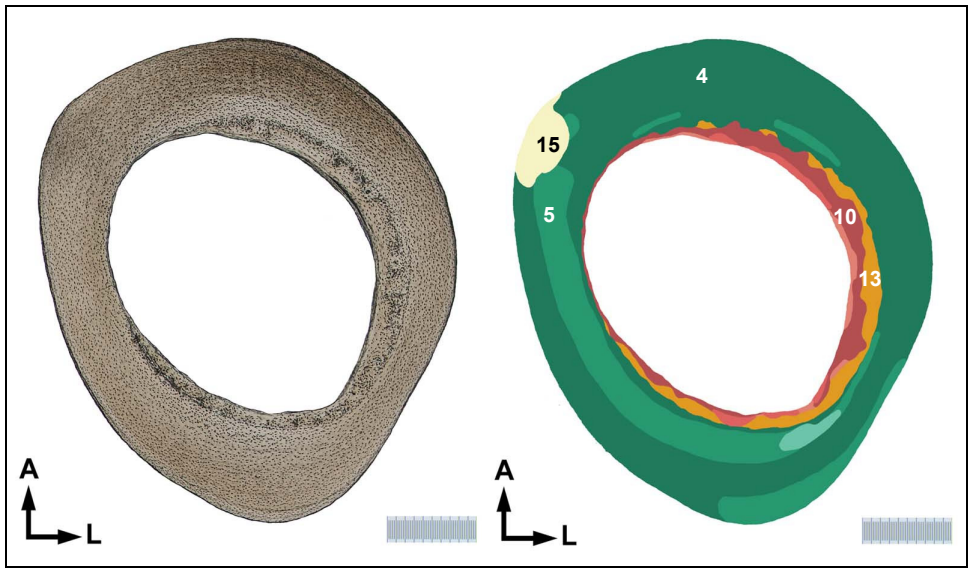


**Figure 4.35: *Tarsius spectrum* midshaft femur (MNHU An11318).**
LM image on left. Color-coded tissue map on right. Scale bar = .5 mm. See text for description. See Figure 4.2 for interpretation of numbers.

*4.6.6.5.8 Callitrichidae*. In the callitrichids, the vast majority of the cortex (>95% in both individuals) is composed of LAM+HYB bone, with the remainder of the PF type. PF bone is concentrated close to the endosteum. There is no FAST bone present in the two individuals examined here. The periosteal cortex is largely avascular, with each individual displaying only a few simple longitudinal canals. In one of the two specimens, these are concentrated in the femoral adductor and extensor muscle attachment region.

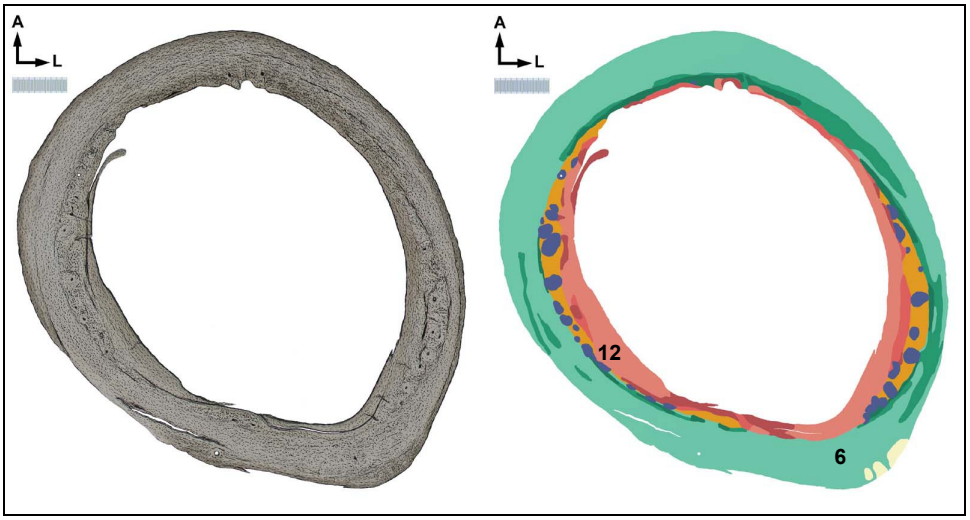


**Figure 4.36: *Callithrix geoffroyi* midshaft femur (MNHU 34381).**
LM image on left. Color-coded tissue map on right. Scale bar = .5 mm. See text for description. See Figure 4.2 for interpretation of numbers.

*4.6.6.5.9 Cebidae*. As is the case with the callitrichids, the periosteal cortex in cebid specimens is primarily composed of LAM+HYB bone (>95% in all four individuals). The remainder of the bone is PF with no FAST tissue in any of the four specimens. Almost all PF bone occurs close to the endosteum and may be in any of the cortical quadrants. In three of the four individuals, the periosteal cortex is entirely avascular, except for the occasional secondary osteon. The cortex of the fourth individual is also largely avascular, with a few short, simple, radial canals anteromedially.

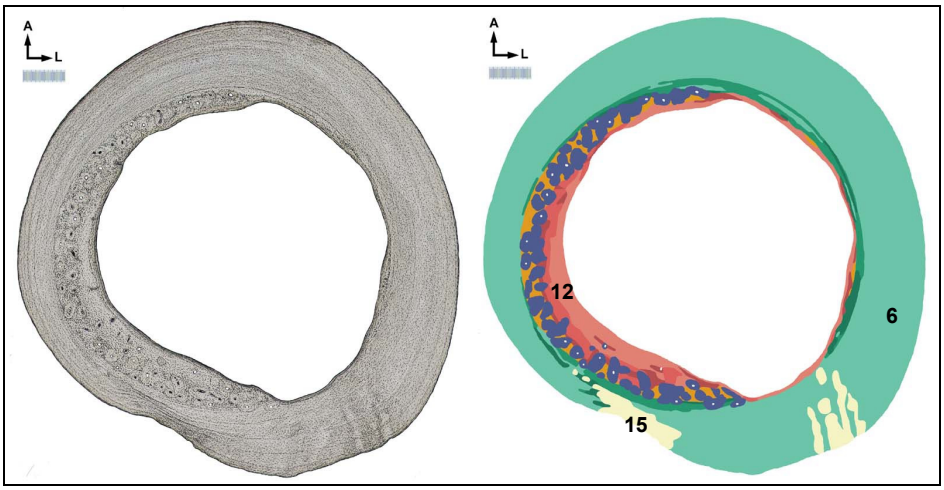


**Figure 4.37: *Saimiri* sp. midshaft femur (MNHU 85197).**
LM image on left. Color-coded tissue map on right. Scale bar = .5 mm. See text for description. See Figure 4.2 for interpretation of numbers.

*Atelidae*. The large atelid individuals also show a predominance of LAM+HYB primary tissue in the periosteal cortex (>75% in both specimens). The remainder of the tissue is mostly PF (distributed in patches throughout the periosteal cortex, with less frequency in the posterior quadrant). FAST bone takes up less than 2% of the periosteal primary bone cortical area. Excluding secondary osteons, the LAM+HYB and PF bone areas are avascular to moderately vascularized, with simple longitudinal canals and the occasional longitudinal primary osteon.

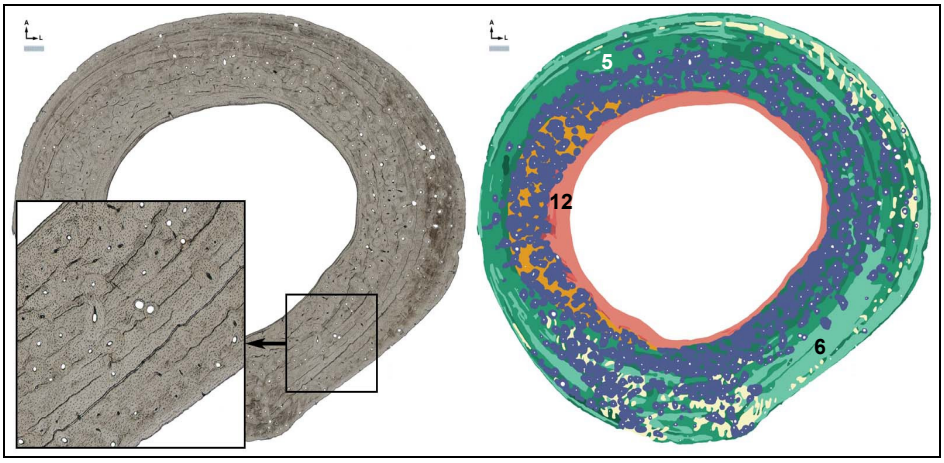


**Figure 5.38: *Ateles* sp. midshaft femur (MNHU 44079).**
LM image on left. Color-coded tissue map on right. Scale bar = .5 mm. See text for description. See Figure 4.2 for interpretation of numbers.

*4.6.7 Comparisons of femoral means in select pairs of taxa*

The multivariate analyses of patterns of variation were limited to broad taxonomic and positional behavior categories. In addition, growth rate was not included as an independent variable. The following targeted comparisons are therefore designed to determine whether: a) the patterns revealed in the multiple regression analyses with respect to both function and life history are repeated at a more detailed phylogenetic and functional level, and b) growth rate can be separated from phylogeny as a factor that can

predict variation in tissue type patterns. Within-strepsirhine or within-haplorhine patterns of phylogenetic difference (e.g., lemuroids vs. lorisoids) – independent of growth, size or positional behavior – are difficult to assess in this sample given the confluence of evolutionary heritage with positional behavior and/or body size and/or growth adaptation.

4.6.7.1 Lesser galagos vs. greater galagos.

A comparison of the mean FAST tissue values for these two taxon groups is consistent with prediction. Given that the lesser galagos have a smaller femoral TCA, it is expected that there will be a concomitant reduced proportion of the cortex composed of FAST bone, and this is indeed the case (maximum greater galago value>15%, maximum lesser galago value = c.5%). Because the two taxa are very closely related, it is suggested that any difference in the features the multiple regression showed to be correlated with PHYLO would be reflective of growth rather than phylogeny. Scaled growth rates in *Galago* (for both pre-weaning and later stages of growth; data unknown for *Galagoides*) are lower than those for *Otolemur*. Given this, the tissue type distribution in these two taxa does not conform to expectation. The slower-growing lesser galago should display a larger proportion of LAM+HYB bone and a smaller proportion of PF bone than the greater galagos, however the opposite is true. But, as Figure 4.39 shows, there is variation within the lesser galago sample, suggesting that the contrast between the two taxa may be an artifact of sample composition. In addition, the greater degree of vascularization may indicate faster growth for the same tissue type in the greater galagos relative to what is found in the lesser galagos. Finally, the patterns of LAM+HYB bone and PF bone may be related to PB. These two taxa differ from each other in the

frequency with which they leap; greater galagos are less saltatory and often locomote quadrupedally or even slow climb in a loris-like fashion. Arboreal quadrupeds are predicted to show the least PF bone and the most LAM+HYB bone, relative to vertical clingers and leapers, and slow climbers. Therefore, it is possible that the proportion of LAM+HYB and PF bone in the greater galagos, relative to the lesser galagos, has to do with the greater reliance on arboreal quadrupedalism. In summary, the comparison between lesser and greater galagos does not conform easily to prediction, except with respect to the proportion of FAST bone.

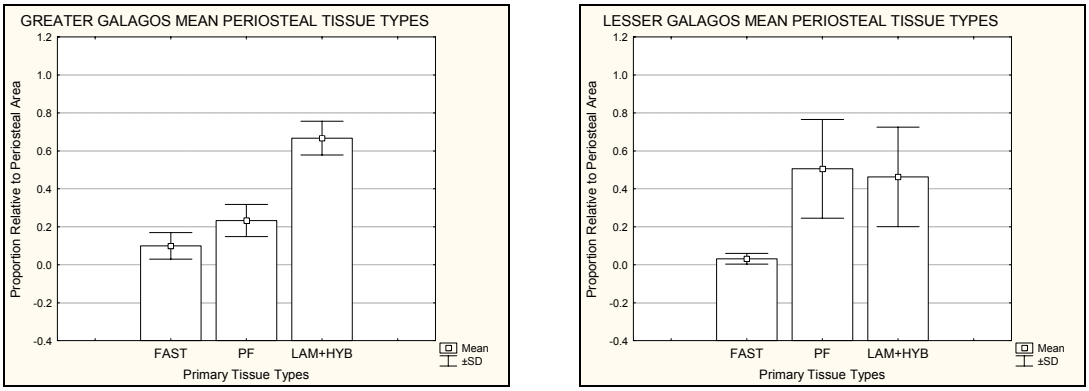


**Figure 4.39: Relative mean proportions of primary tissue types in the greater and lesser galagos.** See text for description.

4.6.7.2 Greater galagos vs. Lorisidae

In accord with expectation, these two similarly sized and closely related taxa show roughly the same proportion of FAST bone in the cortex (Figure 4.40). As with the comparison between the lesser and greater galagos, differences in primary tissue types correlated with phylogeny might in this case reflect differences in growth rates. However, again the observed patterns do not correspond. The scaled growth rate is slower for the lorisids than the greater galagos, as are scaled daily growth rates for lorisid

infants relative to greater galago infants, yet greater galagos show more of the slow-forming LAM+HYB bone and less of the faster-forming PF bone than do *Nycticebus* individuals. Again, however, greater galagos generally display denser vascularization than the lorisids, perhaps indicating increased growth rates for the same tissue types. Here, as above, a positional behavior comparison does match what is seen in the distribution of tissue types if the greater galagos are categorized as arboreal quadrupeds, or as intermediate in their locomotion between vertical clinging and leaping and arboreal quadrupedalism.

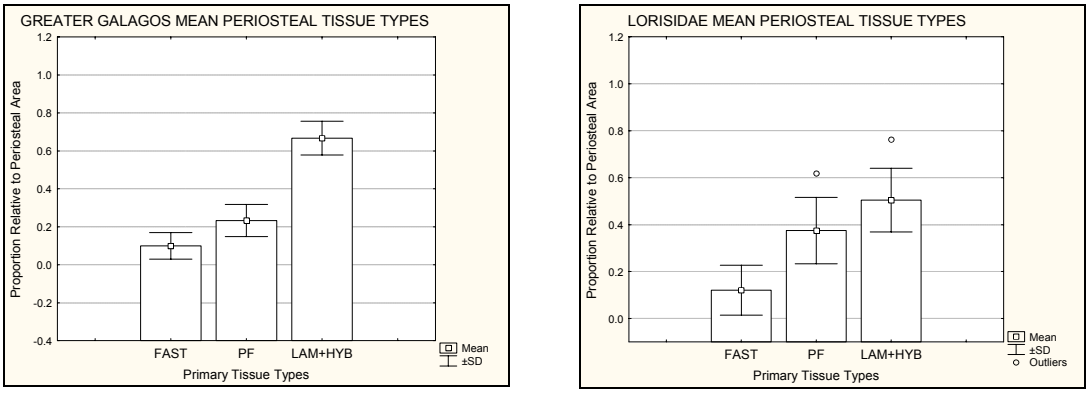


**Figure 4.40: Relative mean proportions of primary tissue types in the greater galagos and lorisids.** See text for description.

## 4.6.7.3 Tarsiidae vs. lesser galagos

These two taxa show a similar[3] proportional amount of FAST bone in the periosteal cortex (i.e., c. ≤5%), as would be expected given their similar small body size. The smallest individuals (tarsiids and *Galagoides demidovii*) have no FAST bone at all. Phylogenetic distance between the two taxa, as well as suggested differences in growth rates (based on infant growth) predict that divergence in the proportions of LAM+HYB

[3] Mean values are considered to be similar when the difference between them is <10% of the total periosteal area.

and PF tissues should be found, with tarsiids showing more slow-growth bone. No differences in these tissues are expected based on positional behavior, as the two taxa share very similar, if independently derived, locomotory adaptations. Again, the outcome for LAM+HYB bone does not support growth-related predictions, with the tarsiids showing larger proportions of PF, and concomitant lower proportions of LAM+HYB bone, than the galagos. However, as noted above, the lesser galago sample is variable, with one individual showing more PF bone than three out of the four tarsiid specimens. In addition, the lesser galagos, while displaying very sparse vascularization, are still more vascularized than the tarsiids, potentially an indication of faster deposition rates in the lesser galagos where primary tissue types are the same. The mean pattern seen in the tarsiids, with a predominance of PF bone, is unusual relative to all other primates in this sample.

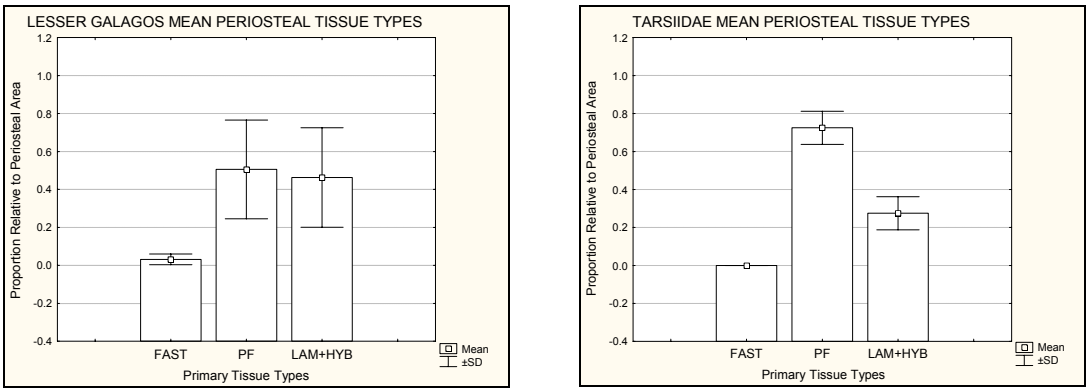


**Figure 4.41: Relative mean proportions of primary tissue types in the lesser galagos and tarsiids.** See text for description.

4.6.7.4 Lesser galagos vs. Cheirogaleidae

In this case, both groups are heterogeneous in terms of body size, with *Microcebus murinus* and *Galagoides demidovii* having roughly the same body mass, but with the larger cheirogaleids weighing more than the average *Galago*. In terms of sample

averages, the cheirogaleids are larger. Therefore the expectation is that the cheirogaleids would display more FAST bone than the lesser galagos. This is not borne out; values for this tissue type are very close for the two taxon groups. However, the highest values for the cheirogaleids (c.15%) are greater than the highest values for the lesser galago*s* (c.5%). The phylogenetic status of the cheirogaleids within Strepsirhini is the subject of interest, but phylogenetically determined patterns cannot be isolated from growth determined ones in this comparison, as the growth rates in the two groups are divergent. Adult growth scores are slightly higher for *C. major* than *Galago*, and even higher still for *M. murinus* (rates unavailable for *G. demidovii*). Scaled infant growth rates are also higher for the cheirogaleids. These data predict less LAM+HYB and/or more PF bone in the cheirogaleids. However, the opposite pattern is present. In addition, within groups, the variation in growth (e.g., *M. murinus* relative to the larger *C. major*) is not clearly reflected in the distributions of LAM+HYB or PF bone. Habitual positional behaviors are different between the two groups, with the cheirogaleids far more arboreally quadrupedal, and less saltatory than the galagos. In this case, as before, the proportions of LAM+HYB and PF are reflective of the separation in kinematic adaptation.

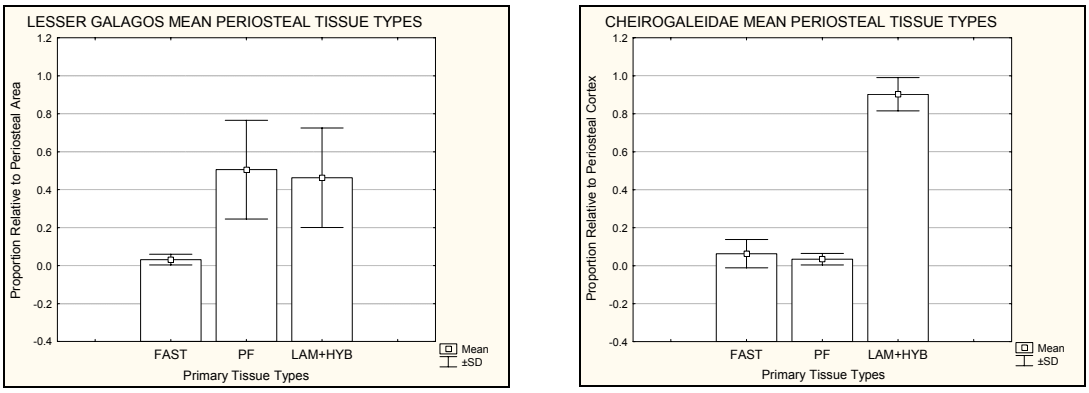


**Figure 4.42: Relative mean proportions of primary tissue types in the lesser galagos and cheirogaleids.**
See text for description.

4.6.7.5 Lesser galagos vs. Indriidae

Indriids have proportionately much more FAST bone than the lesser galagos, consistent with their vastly larger body sizes. Growth rates scaled to adult mass, as well as scaled infant growth rates, are higher for indriids than galagos; the prediction is therefore that a larger proportion of LAM bone will be found the galagos. Again, however, this is not reflected in the proportion of LAM+HYB bone; mean values for the two taxa are roughly equivalent. Given the similarity in positional behavior between the taxa, this parity conforms to expectation. However, in the galagos, the proportion of PF bone is higher (inconsistent with both growth data and positional behavior), perhaps reflecting the reduced amount of FAST bone relative to the indriids.

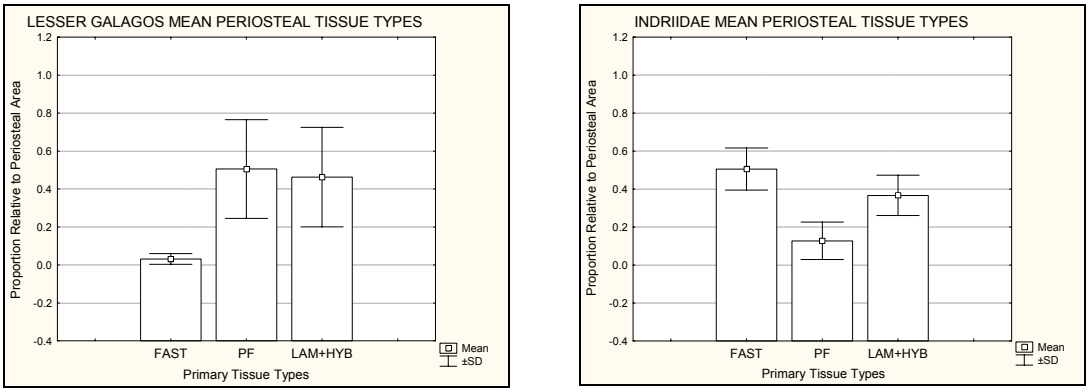


**Figure 4.43: Relative mean proportions of primary tissue types in the lesser galagos and indriids.** See text for description.

4.6.7.6 Indriidae vs. Lemuridae

A comparison of indriids and lemurids suggests that size is the primary predictor of tissue type patterns here. The similar body sizes for the members of these taxa (with the exception of *Indri indri*) are reflected in equivalent proportions of FAST bone. Relative proportions of LAM+HYB bone are not significantly different as would be predicted

given the slower growth (in infant scaled scores) for *Propithecus* relative to *Varecia* and to a lesser extent *Lemur*. Nor are the differences in positional behavior reflected between the two groups. Interestingly, however, within taxon variation conforms to expectation. The larger *I. indri* displays more FAST bone than the two *P.* sp. individuals. Within the lemurids, *V. variegata* has less LAM+HYB bone (and more FAST bone) than *Lemur* sp., consistent with its relatively high growth rates. Conclusions derived from samples of one, of course, should be viewed with much caution, and taken only as suggestive of future avenues for exploration.

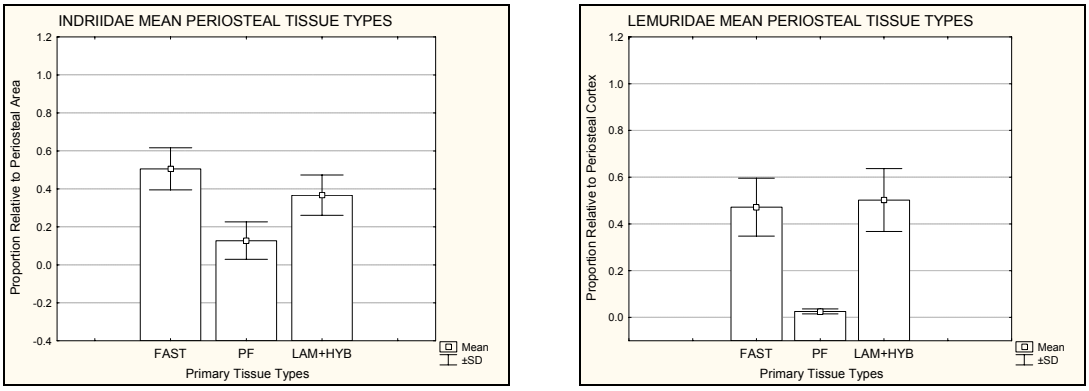


**Figure 4.44: Relative mean proportions of primary tissue types in the indriids and lemurids.** See text for description.

4.6.7.7 Indriidae vs. Atelidae

The larger size in atelids predicts for more FAST bone. However, in this case, phylogeny and/or associated differences in growth rate appear to relate to primary tissue proportions. The slower-growing platyrrhine (as described by scaled infant growth rates, since there are no post-weaning growth rates available for the indriids) displays more LAM+HYB bone, while more FAST bone is found in the indriids. The proportion of PF bone is similar between the two taxa. Results from the multiple regression suggest that the

vertical clinging and leaping indriids should display more PF and less LAM+HYB bone than the atelids, and this is borne out here for LAM+HYB bone, but not PF. The indriids have less PF bone than expected relative to the atelids, but this may be due to the large proportion of the cortex composed of FAST tissue.

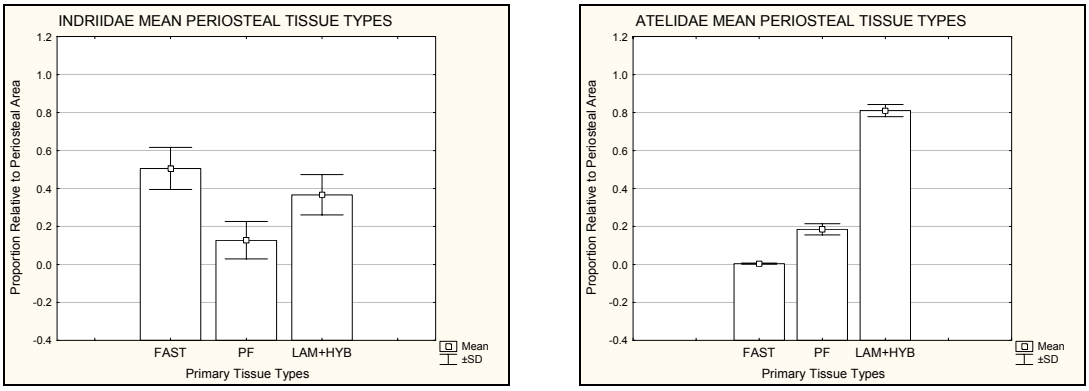


**Figure 4.45: Relative mean proportions of primary tissue types in the indriids and atelids.** See text for description.

4.6.7.8 Cheirogaleidae vs. Callitrichidae

Given that *Callithrix* and the larger cheirogaleids have roughly equivalent body sizes, the expectation is that they would display similar proportions of FAST bone. However, as is the case with the atelid/indriid comparison, the platyrrhines display less of this tissue. While cheirogaleids have very little FAST bone, there is none at all in any of the callitrichid femoral cortices. Here again, this may be due to the differences in growth rates between the two taxa, with *Callithrix* displaying the slower rates (both as infants and later in growth) associated with the haplorhine radiation. But, because of the presence of both growth and phylogenetic divergence between the taxa, it is not possible to separate between the effects of the two. Taxonomic affiliation also leads to the expectation that the cheirogaleids will display less LAM+HYB bone, relative to the

callitrichids. In this case, however, the values are nearly equivalent, with *Callithrix* displaying only slightly more LAM+HYB bone on average than the cheirogaleids, (perhaps because of the difference in FAST bone values). The values for PF are very similar. The equivalent proportions of LAM+HYB and PF bone in these two taxa are consistent with the general similarity in positional behavior (although clearly there are differences, such as the claw-clinging in *Callithrix*), but not with the phylogenetic separation between the two groups.

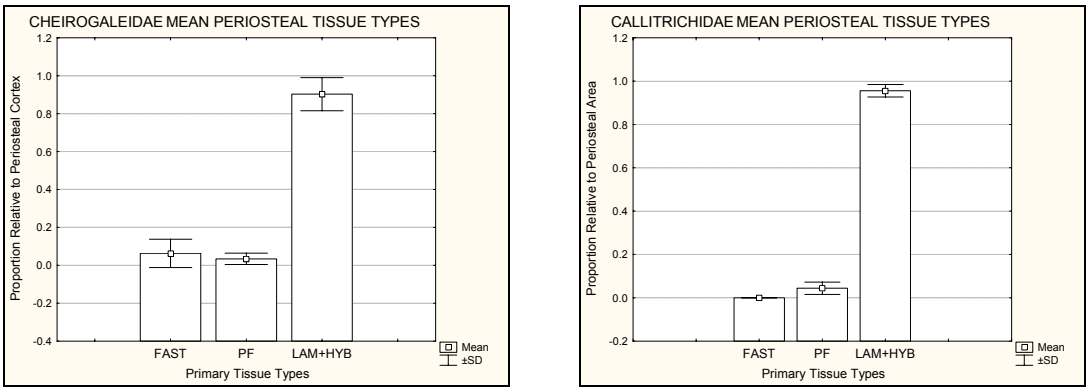


**Figure 4.46: Relative mean proportions of primary tissue types in the cheirogaleids and callitrichids.**
See text for description.

4.6.7.9 Cebidae vs. greater galagos

These two taxa share a similar body size. However, as with other platyrrhine/strepsirhine comparisons, *Otolemur crassicaudatus* displays more FAST bone than the cebids, in accordance with their phylogenetic distance, and associated faster growth rates in *O. crassicaudatus* (both in infancy and later in growth). Likewise, *O. crassicaudatus* shows less LAM+HYB bone, and more PF bone, also consistent with growth differences. These same patterns are also consistent with the positional behavior differences between the two taxa, with arboreal quadrupeds displaying more LAM+HYB bone and less PF bone than

vertical clingers and leapers. This is somewhat complicated by the variable positional behavior of *O. crassicaudatus*, as the greater galagos locomote frequently in non-leaping quadrupedal modes. Despite this, however, vertical clinging and leaping still comprises a greater proportion of the *O. crassicaudatus* locomotor repertoire than is the case for *Saimiri*.

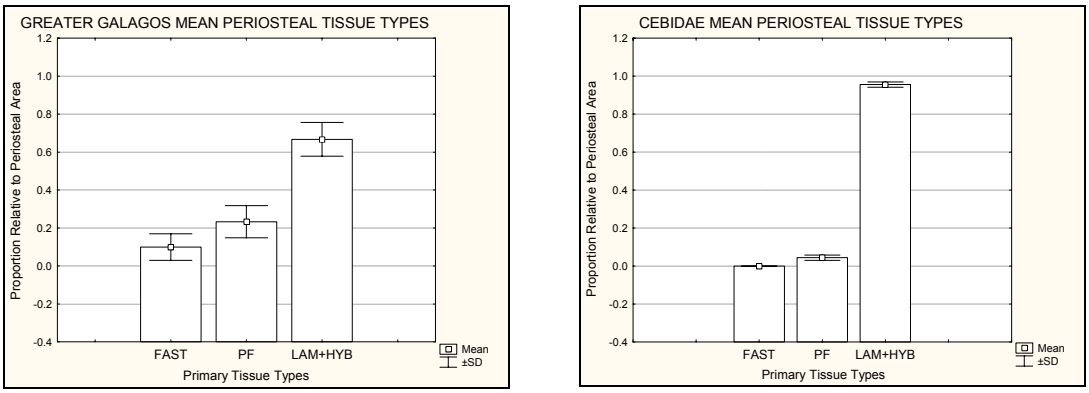


**Figure 4.47: Relative mean proportions of primary tissue types in the greater galagos and cebids.** See text for description.

## 4.6.7.10 Cebidae vs. Lorisidae

A comparison of the cebids and lorisids reveals a similar pattern as that seen when cebids are compared with greater galagos. This similarly sized but slower growing platyrrhine has less FAST and PF bone (no FAST bone at all) and more LAM+HYB bone than the strepsirhines. However, the difference in proportions of LAM+HYB and PF bone is more marked than what is seen in the previous comparison.

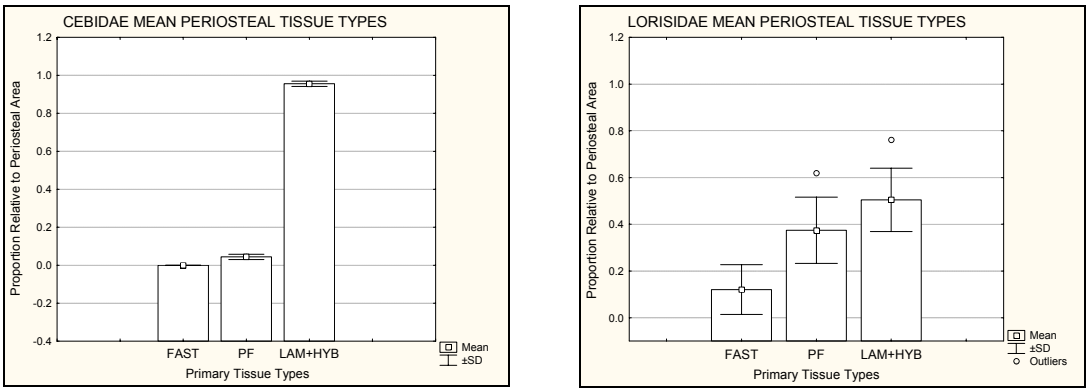


**Figure 4.48: Relative mean proportions of primary tissue types in the lorisids and cebids.**
See text for description.

## 4.6.7.11 Callitrichidae vs. Cebidae

The callitrichids and cebids are both platyrrhines, have similar positional behaviors (excepting the claw-clinging in the former), and overlapping scaled growth rates, but have different body sizes. It is expected, therefore, that they will display similar proportions of LAM+HYB as well as PF bone, and that any differences in tissue type patterns would be in the proportion of the cortex composed of FAST bone. In this case, neither has any FAST bone at all, perhaps indicating that a size threshold must be reached in platyrrhines before FAST bone is seen in the adult femoral cortex.

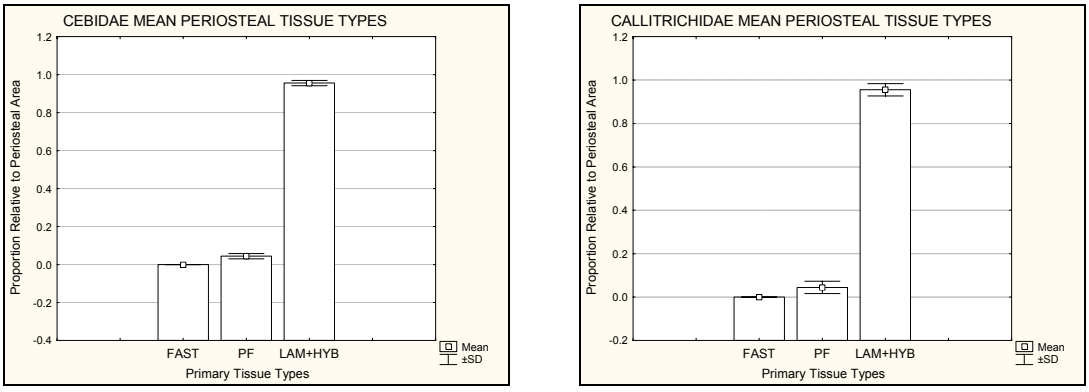


**Figure 4.49: Relative mean proportions of primary tissue types in the callitrichids and the cebids.**
See text for description.

4.6.7.12 Cebidae vs. Atelidae

The larger size of the atelids is reflected in the greater proportion of the cortex composed of FAST bone. Although values in the atelids are extremely low for this tissue, none of the cebid femora contain any FAST bone. The atelids also displays smaller proportions of LAM+HYB bone and larger proportions of PF bone relative to the cebids. This is not consistent with the relative growth rates of the two taxa, as values from infancy and later in growth both indicate slightly faster rates in *Saimiri*. It is possible that the pattern of LAM+HYB and PF may constitute a positional behavior pattern, but because *Ateles* is the only habitually suspensory primate in this sample (with an *n* of 2), the effect of positional behavior and taxonomy are difficult to distinguish.

Finally, although multiple regression analysis did not find TCA to be strongly associated with the proportion of LAM+HYB bone in the periosteal cortex, it nevertheless was included in the most robust models for some skeletal elements. Therefore, the higher proportion of LAM+HYB bone in the cebids could be related to smaller cortical area.

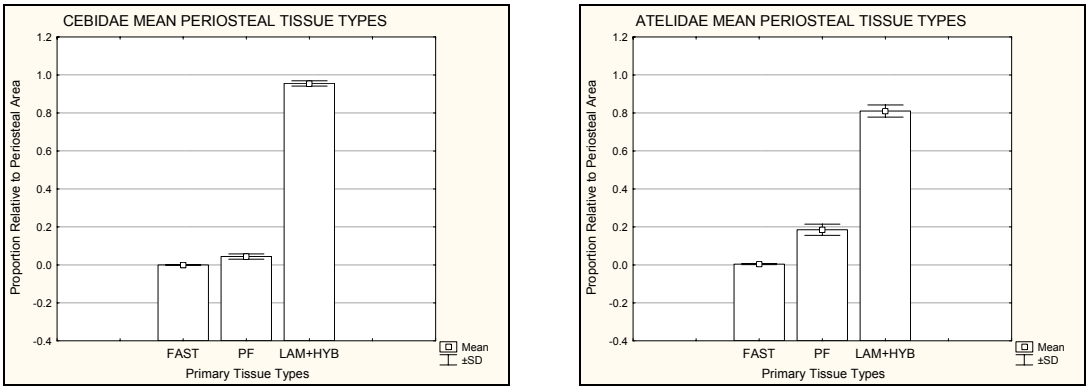


**Figure 4.50: Relative mean proportions of primary tissue types in cebids and atelids.**
See text for description.

4.6.7.13 Summary of paired comparisons of means

Overall, when looking at selected pairs of taxa, the proportion of FAST bone in the femoral cortex appears to coincide with predictions based on the results of the multiple regression analyses, where larger cortices (and larger animals) contain more FAST bone. This even extends to genus level comparisons within taxon groupings (e.g. *Galago* vs. *Galagoides*). The subsidiary relationship between FAST bone and phylogeny is also borne out, with strepsirhines showing more FAST bone than platyrrhines at a given body size.

The significance of proportions of LAM+HYB bone and PF bone is much harder to decipher at this more focused level of taxon comparison. With the exception of contrasts between distantly related groups (e.g., the platyrrhines vs. the tarsiers) differences in these two tissue types do no match the expectations based on relative growth rates. Within strepsirhines, for example, the faster growing taxa do not necessarily display less LAM+HYB bone than the slower-growing taxa. However, all platyrrhines display more LAM+HYB bone than strepsirhines of similar body size. The tarsiids are unusual in that they are the only taxon which displays more PF bone than the other tissues. Within-strepsirhine patterns of phylogenetic difference (e.g., lemuroids vs. lorisoids) – independent of growth, size or positional behavior – are not possible to assess in this sample.

When pairs of taxa are compared, there appears to be a positional behavior pattern in the relative proportions of LAM+HYB and PF bone, in particular among the strepsirhines in the sample. This pattern does not extend to the tarsiids, and is weaker among the platyrrhines. This pattern should be viewed with some skepticism; it is

difficult, in the case of suspension and slow climbing, to separate between the effects of positional behavior and taxonomy, since the species in this sample associated with the two forms of locomotion are restricted to single taxon groups (Atelidae and Lorisidae respectively). In addition, no slow climbers or vertical clingers and leapers are found among the platyrrhines. However, the consistency of this pattern among arboreal quadrupeds, spanning a range of body sizes and found among strepsirhines and platyrrhines alike suggests that the relationship between positional behavior and tissue type patterns should not be completely discounted.

The overall picture is one where large-scale phylogenetic differences (likely growth related, although growth rates cannot explain the unique tarsiid pattern, but see discussion on vascular density) are reflected in the proportions of all three tissue types, positional behavior within large groups corresponds with relative patterns of LAM+HYB and PF bone, and FAST bone tracks taxon differences in body size, particularly among larger taxa.

## 4.7 Discussion

### *4.7.1 Primary tissue types and element specific ontogenies*

As Enlow (e.g., 1962a, 1962b, 1963) has so clearly demonstrated, one of the most important factors determining the tissue types that will be found across a cortical cross-section is the developmental history of a bone. The shape that it must ultimately become in order to accommodate functional demands – given phylogenetic and constructional constraints – will leave a record throughout the hard tissue, varying from region to region dependent upon local growth remodeling. Every cross section, then, encodes part of the

story of element-specific development in length and diameter and it's interaction with surrounding soft tissue, in addition to the story that it may tell about the whole organism.

Comparison among skeletal elements in this study shows that not all long bone midshafts are built the same. In all sections (with two exceptions) there is a greater proportion of periosteally deposited bone than either CCC or endosteally deposited bone. This is in part a consequence of sampling at the midshaft, rather than in metaphyseal regions of the shaft. However, there is a distinctive separation between hindlimb bones (the femur and tibia) and forelimb bones (the humerus, radius and ulna). Mean values for the proportion of the cortex composed of endosteal tissues (not including CCC bone) are higher in the humerus, radius and ulna than in the femur and tibia. In other words, relative to the hindlimb bones, forelimb midshafts achieve adult cortical proportions either via more endosteal deposition, less periosteal deposition, or both. Studies of cortical expansion during development might differentiate between these options.

The humerus is almost always distinguished by a posteriorly directed pattern of drift, accounting in part for the increase in endosteal tissue relative to the femur and tibia. That is, the humeral midshaft moves posteriorly through anatomical space while growing. Lorisids are the exception to this rule, where humeri exhibit a more even circumferential deposition of tissue in all quadrants of the cortex, much like all femora in the sample.[4] The humeral drift observed in this study was also identified in a vital labeling study of macaque skeletal development by Newel-Morris & Sirianni (1982), as well as in descriptions of the macaque humerus provided by Enlow (1963). Greater deposition

[4] This finding is interesting in light of the unique positional behavior among the lorisids, where humeri and femora function in a more equivalent fashion than is seen in other primates (Ishida et al., 1990; Jouffroy & Stern, 1990), and where other features of humeral morphology also point to the distinctiveness of this group (Szalay & Dagosto, 1980).

rates in the posterior cortex relative to the anterior cortex for the prenatal period were found by Newell-Morris & Sirianni. Later in growth, they observed very slow anterior deposition relative to the posterior cortex, or none at all. Interestingly, in that study, tissue in both parts of the bone could be lamellar despite the disparity in deposition rates (see section on growth rate below).

Humeri are also distinguished by a relative paucity of variation in tissue types: diversity at the midshaft in this element is reduced relative to all others, with a predominance of LAM bone in all taxa. What might explain this unique pattern? On the one hand it is well established that primate humeral growth usually continues longer than other long bones (i.e., the proximal humerus is the last, or near last, epiphysis to fuse) (Galliari, 1998; Kohn et al., 1997; King 2003). However, it cannot be assumed that this necessitates a longer period of circumferential bone deposition at the midshaft. Might this highly organized tissue be indicative of some mechanical imperatives, universal among the humeri examined here? In the absence of studies to test these hypotheses, ideas regarding the constraints that might be acting to produce this pattern must remain speculative.

In almost all cases the tibia is characterized by a lack of, or reduced amount of, CCC bone. This suggests that the midshaft compacta of the tibia is not incorporating previously cancellous portions of bone, which would likely have been in the metaphyseal region in a previous growth phase. Rather, the tibia would have been lengthening at both ends to the same degree, as has been described by Enlow (1962b), and midshaft of the juvenile would remain midshaft in the adult.[5] In contrast, the midshafts of all other

[5] It is possible that cancellous, or CCC bone is present at the midshaft tibia at an earlier stage of growth, and that it is remodeled away as the bone reaches adult proportions. However, given the patterns observed

elements would have previously been parts of the bone that were either distal or proximal to the current midshaft, indicating that long bone linear growth likely proceeded more quickly on one end than the other. Serial sections would be required to determine growth directionality (but see the discussion of Bateman, 1954, below). In the femur, radius and ulna, unlike the humerus, this uneven linear growth would not have been accompanied by substantial drift; there is no consistent pattern of such evident in these bones.

Studies of primate epiphyseal closure sequences support these observation, although not unequivocally. For example, in *Saimiri boliviensis*, there is a significant lag time between distal and proximal humeral fusions (up to 37 months) (Galliari, 1988). This suggests considerable distal-ward relocation of the juvenile midshaft. In the tibia this lag is much reduced, but still present (up to 9 months). In the radius, ulna, and femur the lag is also reduced relative to the humerus, but reversed, with the proximal end fusing first (up to 22 months earlier). Kohn et al. (1997) find similar results for *Callithrix* and *Saguinas*, and these authors suggest that there is a "general pattern in Primate skeletal development" (p. 129). Indeed King's (2003) comparative study of epiphyseal fusion sequences shows that, despite some variation among taxa, there are consistent patterns. For example, among the long bones examined there, the distal humerus is always the first growth plate to fuse, while the proximal humerus fuses last or close to last. In contrast, the fusion times for the proximal and distal ends of the tibia are generally close to each other. In all cases the proximal radii and ulnae fuse before the distal ends. Fusion at the femoral head occurs before fusion at the distal femur in almost all cases except *Aotus*. While these data are mostly consistent with the distribution of primary bone tissues in the

---

in this sample, it is still likely that the tibial midshaft migrated less during growth, either proximally or distally, than the midshafts of other elements.

primate midshaft cortex, the observation of staggered epiphyseal unions in the tibia is not.

Relative epiphyseal union times, however, do not tell the whole story, as they cannot provide information regarding the rate at which the epiphyseal region serves to lengthen the bone. A given fusion may occur subsequent to extensive lengthening, moderate lengthening, or none at all. These would have different ramifications for the pattern found at the midshaft of the adult cortex. Although there exist no comparable data among primates, a study of the pattern of long bone lengthening in gray-lethal and microphthalmic mutant mice (Bateman, 1954) provides results that are entirely consistent with the pattern observed in the current study. Bateman found that during growth, 80% of femoral lengthening occurs at the distal end, with some proximal lengthening. In the radius and ulna, the pattern is similar, although with less growth at the proximal end. In the humerus, lengthening occurs proximally, with almost no distal growth. (The forelimb pattern is one where lengthening occurs minimally at the elbow joint, and extensively where the humerus joins the shoulder and the radius and ulna join the carpus). Finally tibiofibula growth is almost equivalent in both directions. These observations of mouse ontogeny match patterns of compacted coarse cancellous distribution at the midshaft in the sample primates. Either serial sectioning along the length of the shaft or observations of growth would serve to confirm the similarities.

In addition to differences in patterns of drift among skeletal elements, it is also evident that the tibia, ulna and radius generally display a smaller proportion of the slower-forming LAM tissues, relative to the humerus and femur. Given the smaller cortices of the distal elements (except for the tibia in many cases), the initial expectation

is that they would display larger proportions of LAM bone, having more time during growth to develop a smaller cortex. Several explanations can be put forth to account for this lack of concordance between total cortical area and tissue type within individuals.

First, growth of skeletal elements – including their circumferential expansion at midshaft – does not necessarily occur at the same rate, or for the same duration, in all cases. This can be seen at its extreme in the disparity between hindlimb and forelimb growth rates in marsupials (e.g., Hamrick, 1999). For primates, limb growth allometry studies also highlight differences in growth rates between skeletal elements (e.g., Falsetti & Cole, 1992).

Second, tissue deposition may not proceed at the same rate in all elements, even for the same type. For example, Castanet et al. (2000) note that the tissue formation in ratite bird hindlimbs is faster than in the forelimbs, and that bony "elements (i.e., femur, humerus) may provide different estimations of overall skeletal growth dynamics, even when similar bone tissue types are observed" (p. 549). Within the fibro-lamellar tissue category they identify a tremendous range of deposition rates, from 10 to 80 μ/day. de Margerie et al. (2004) confirm these observations in their fluorochrome study of king penguin chick long bones. While all skeletal elements in their study contain a range of fibrolamellar vascular organizations, rates in the radius were 38% lower than in the femur, humerus and tibiotarsus. Likewise, Starck & Chinsamy (2002) identify differences among skeletal elements: fibrolamellar bone deposition rates range between 10-50 μ/day, and cross-sections in the femur and humerus increase their thickness more rapidly than the cortices in more distal long bones. They suggest that "individual skeletal elements respond differently to environmental conditions, thus producing different

patterns in bone microstructure" (p. 244). It does not appear that rates are as variable in the PF and LAM categories, but ranges still may overlap. (See the section on growth rates below for more discussion of this issue.)

Lastly, there is the possibility that, within individuals, differences in growth rates between elements are not substantial enough to influence tissue type, and that variation in the organization of the tissue laid down is dependent upon other factors, such as difference between elements in mechanics at the midshaft (see section below on positional behavior).

*4.7.2 Primary tissue types and body size*

Results of this study indicate that total cortical area, as a proxy for body size, is a significant factor in determining the proportion of highly vascularized fast-forming bone (woven and fibrolamellar types= FAST bone) within a primate long bone cortex. This is not surprising; the larger the individual and the larger the cortical cross-section of its long bones, the more bone tissue it must deposit to achieve functional competence during growth and development. FAST bone is often found in the thickest quadrants of the cortex, further evidence of the relationship with cortical area. The data indicate that there may be a threshold to this size related pattern. Individuals with body masses below 500g display very little (i.e., less than 10% of the periosteal cortex) or no FAST bone tissue. This is consistent with findings of other researchers for disparate groups of vertebrates. For example, Bonis et al. (1972) found that small tetrapods have cortices composed of lamellar bone, while larger ones contain fibrolamellar tissues or remodeled bone. Castanet et al. (2001), in a study of bird long bones, find that small birds (<100g) do not

have densely vascularized cortices. In their review of Enlow & Brown (1956) and Klevezal (1996), they find this to hold true for all tetrapods, regardless of phylogenetic status and metabolic adaptation, where species up to 1 kg have poorly vascularized bones. They conclude that, in general, the larger the species, the more densely vascularized its bones will be, and the more likely they will be composed of fibrolamellar, rather than lamellar-zonal tissues. This is in accord with the results of the present study. Although the density of vascularization was not quantified, the presence of FBL bone indicates denser vascularization than LAM or PF bone.

This relationship between FAST bone and body size is not repeated to the same extent with the other, slower-forming, primary tissue types examined here: PF and LAM. A larger midshaft cortex does mean there will be more PF bone, hypothesized to be faster depositing than LAM tissue. Similarly, smaller cortices do not necessarily comprise more slow-forming LAM bone than PF bone. In addition, when values for FAST bone are high, this does not preferentially occur at the expense of either PF or LAM values. In some cortices, if the proportion of FAST bone is large, there is proportionately less PF tissue, while in others it is the proportion of LAM that is diminished. Finally, in some cases, both LAM and PF tissues are reduced relative to their proportions in bones that contain less FAST bone.

A potential explanation for the lack of a strong relationship between body size and PF or LAM bone is the subtle nature of the separation in the growth rates between these two, at least as described by Newell-Morris & Sirianni (1982) relative to the much faster rates of woven and heavily vascularized tissues (see discussion of growth rates below). Alternatively, or perhaps in addition to this, LAM and PF bone tissues may be

responding to other, non size related features, as I suggested may be the case for explaining the difference in tissue types among skeletal elements within an individual.

*4.7.3 Primary tissue types and growth rate*

As would be predicted from previous studies of primary bone formation rates, and in accordance with "Amprino's rule" (Amprino, 1946; de Buffrénil & Pascal, 1984), the results of this study suggest a broad relationship between growth rate and primary tissue types. However, this pattern breaks down when individual primate taxa are compared.

As a whole, the primates in this sample have a large proportion of the adult midshaft periosteal cortex (as well as endosteal) composed of slow-forming, sparsely vascularized tissues such as LAM bone. Comparative reviews (e.g., Enlow & Brown, 1958) show that many non-primate mammals (e.g., carnivores, rodents) are likely to display much higher proportions of faster tissues such as the highly vascularized fibrolamellar bone (see *Mustela*, *Bassariscus*, *Canis*, *Dasypus* and *Lepus* in Enlow & Brown, 1958). The preponderance of slower-forming bone tissue types in primates is consistent with the generally lengthened life histories (slow growth, delayed maturity) of members of the primate order (e.g., Watts, 1990; Ross, 1998; Cubo et al., 2002), but also with the small to medium body sizes of the species in this study (all species <10kg).

One indication of the relationship between growth rates and tissue types is that FAST tissue is often found close to the boundary between periosteal and endosteal bone, in older parts of the periosteal cortex of femora. These areas, having been deposited earlier in a developmental trajectory than more peripheral areas, are more likely to have formed when growth was more rapid. Another sign of the relationship between growth

rate and tissue type is the difference between platyrrhines and strepsirhines in proportions of all tissue types. The slower growing platyrrhines (reflected in scaled growth scores, and reported previously by Kirkwood, 1985; see also Cubo et al., 2002) exhibit more slow-forming LAM bone, less PF bone and less FAST bone than the strepsirhines. This is the case both for strepsirhine and platyrrhine means, and also when femoral values for pairs of comparably sized lower-level taxa are compared (with the exception of the comparison between the callitrichids and the cheirogaleids). Within suborders, however, the relationship between tissue type and growth rate is less evident (at least for the femur). So, for example, the lorisids, with lower growth rates relative to the comparably sized greater galagos, display less, rather than more LAM bone, and concomitantly more PF bone.

Even within infraorders there are two exceptions to the general concordance between growth rate and primary tissue type distributions. First, the cheirogaleids display a surprisingly high, plartyrrhine-like proportion of LAM bone at the midshaft femur. One could speculate that this may relate to the periods of lethargy, torpor or hibernation – a unique adaptation among primates – found in this family (Ortmann et al., 1997; Schmid, 1998, 2000, 2001). Growth curves are not know for cheirogaleids, but if periods of reduced activity, metabolic rate and body temperature occur during the later phases of growth when the adult cortex is forming, their rates of tissue deposition and primary tissue type proportions would be affected. *Microcebus murinus*, for example, has been observed to enter a period of dry season hibernation about four months after birth, remaining in hibernation for up to seven months (Schmid & Kappeler, 1998). In a study of lines of arrested growth in the tibia of captive *M. murinus*, Castanet et al. (2004)

found a diaphyseal cortical pattern suggestive of depressed rates of growth during the first seasonal hibernation (approximately .1 micron/day) after a more rapid phase of summer growth (with deposition rates of up to 8 microns/day). Thereafter, for a period of up to 6 years, bone was slowly deposited circumferentially. The transition from faster vascular tissue to slower avascular tissue concurrent with the first hibernation suggests that the unique life history adaptation of the cheirogaleids my indeed be reflected in its cortical bone microstructure. While *Mirza coquereli* is not known to have any daily or seasonal periods of reduced activity, it also displays a preponderance of slow-growth LAM bone at the midshaft femur. This would be explained if a pattern of growth similar to that found in *Cheirogaleus* and *Microcebus* were a family-specific trait.

A second surprising finding is that the tiny tarsiers, reported to have a slow life history relative to strepsirhines of their size (corroborated by infant growth rates), display a large proportion of the cortex composed of PF bone (a mean of about 70% of the periosteal portion of the cortex). Not only are mean values of PF bone for the femur higher than those found in the lesser galagos, the taxon with the best match in terms of size and positional behavior, but they are substantially higher (by at least 20% of the total periosteal area, and usually much more) than in any other taxon examined in this study.

There are several potential explanations for the cheirogaleid and tarsiid patterns, as well as the general lack of agreement with scaled growth rate scores when pairwise comparisons are made of closely related taxa. First, it may be that changes in primary tissue type are not necessary when the difference in growth rates needed to construct bones in an adequate span of time are small. So, for example, while the scaled growth rate data indicate that it will take a *Saimiri* individual approximately four times as long to

achieve the same increase in mass as a lorisid, the scaled growth rate values for lorisids are approximately two times, or less, the value for *O. crassicaudatus*. A related possibility is that the disparity in deposition rates between PF and LAM bone is too subtle to be reflected among species where somatic growth rate differences are not extreme, or that the deposition rates for these tissues vary and/or overlap with each other, as has been observed to be the case for fibrolamellar tissues. For example, Castanet et al. (2000), de Margerie et al. (2004), and Starck & Chinsamy (2002) have all identified a range of tissue deposition rates within the fibrolamellar pattern in vital labeling studies of ratite birds, king penguins, and Japanese quails respectively. Starck & Chinsamy in particular warn of the plastic and highly responsive nature of bone in its response to variation in environmental factors such as diet and mechanical stress. While data for rates among lamellar-zonal tissues are more limited, there are indications that in these types as well, variability and overlap are significant. Results of the vital labeling study of Newell-Morris & Sirianni (1982) suggest that there is only an average 2 μm/day difference in deposition rates between PF and LAM tissue (4 μm/day and 2 μm/day respectively), with overlaps in the ranges of rates between these two tissues.

Second, there are, in some cases, subtle differences in the density of vascularization of the LAM, HYB and PF tissues that are not quantified in this study, and which may reflect differences in growth rates. de Margerie et al. (2002), and Castanet et al. (1996) have shown that vascularized tissues deposit more rapidly than non-vascular tissues, that the inclusion of primary osteons indicates faster deposition than simple vascular canals, and that as the size of primary osteons increase, so does the growth rate.

Third, there is the possibility that the growth rate data available for the taxa included in this study are inappropriate for comparison to patterns of tissue types found in the adult midshaft cortex. As described in many studies (e.g., Leigh & Terranova, 1998) somatic growth rates are not constant throughout ontogeny. The scaled rates used here represent averages derived from the entire growth period from birth to attainment of adult mass, or averages of the rates of increase in mass between 25% of adult weight and 75% of adult weight. In both cases, these may not accurately reflect the latter periods of bone deposition found in an adult cortex, where much of the bone formed early in development has been resorbed away. In addition, age at attainment of adult mass was not available for all taxa, and in some cases was estimated from published growth curves (e.g., data for *Otolemur crassicaudatus* & *Loris tardigradus* estimated from Rasmussen & Izard, 1988), or based on rough estimates from the literature when the species was not known (e.g., data for *Lemur* sp. estimated from Leigh & Terranova, 1998).

*4.7.4 Primary tissue types and positional behavior*

There exists a voluminous literature on the mechanical properties of secondary osteons, both as individual units, and relative to primary bone tissue (Chamay & Tschantz, 1972; Bouvier & Hylander, 1981; Lanyon et al., 1982; Lanyon, 1984, 1993; Lanyon & Rubin, 1985; Portigliatti Barbos et al., 1983; Burr et al., 1985; Burr, 1993; Martin, 1993, 2000a; Schaffler et al., 1989, 1990; Lieberman & Crompton, 1998). A substantial and growing literature also considers the relationship between collagen fiber orientation and functional adaptation, although this is most frequently in reference to intracortically remodeled bone (Ascenzi & Bonucci, 1967, 1968, 1972; Ascenzi et al., 1973, 1987; Ascenzi & Benvenuti,

1986; Vincentelli & Evans, 1971; Portigliatti-Barbos et al., 1983; Carando et al., 1989, 1991; Boyde & Riggs, 1990; Riggs et al., 1993a, 1993b; McMahon et al., 1995; Goldman, 2001). The relative properties of various primary bone tissue types remain relatively unexplored. Interestingly, recent investigations of primary tissue types and whole bone mechanics have led to the suggestion that vascular patterning in primary bone may vary as a function of habitual loads on bone. de Margerie (2002) found that, in the mallard, the bones most likely to be subjected to torsional loads (e.g., most of the bones of the wing skeleton, as well as the femur) exhibited fibrolamellar bone complexes with a more laminar organization of primary osteons (primary vascular canals running in circumferential rings around the cortex) than found in other long bones. He hypothesized that this vascular scheme is adapted to resist the shearing that torsional loads impose, and that the "putative adaptation must have an ultrastructural basis, perhaps through particular collagen fibre orientation in the primary osteons of laminar bone" (p. 523).

In a subsequent study of turkey ulnae, Skedros & Hunt (2004), found "significant differences in [collagen fiber orientation] and/or other microstructural characteristics…between 'tension', 'compression' and 'shear' (neutral axis) regions of subadult bones" (p. 122) although these differences were less evident in adult bones. Portions of the cortex containing greater laminarity had more oblique to transverse collagen fibers, and these were most often found where compression was the predominant load. In addition, they determined that bones displaying more laminarity throughout the cortex are correlated with a more uniform distribution of preferred collagen around the cortex. In this case, the suggestion is that both the vascular and collagen fiber patterns may be adapting to torsion, although the authors caution that the

vascular patterns may be more directly a product of variation in growth rate than loading regime.

The data from those studies suggest that collagen fiber orientation is not the only microstructural feature of primary bone that may be related to mechanical adaptation. It follows that there may be functional significance to variable distributions of LAM and PF bone, as observed in this study. While in some cases (e.g., the lorisids) differences linked to positional behavior are impossible to separate from those due to other taxon-specific features (e.g., growth, phylogeny), members of other locomotor categories are more heterogeneous with respect to phylogeny and life history. In particular, the arboreal quadrupedalism category displays consistency in terms of the proportion of the femoral midshaft cortex composed of LAM bone, relative to other positional behavior types. This broadly defined group includes both strepsirhines and platyrrhines, and a range of taxa in terms of body size and life history.

The identification of the pattern, however, does not easily lead to an explanation of its significance. Given the histocompositional divergences between PF and LAM bone, it is likely that there are differences in mechanical properties between the two types. However, there are no data to support this proposition, or to suggest what specific mechanical variables might differ (e.g., strength, stiffness, fracture toughness). Second, no comparative strain gauge data exist for the non-human primate midshaft femur. And while in the past it has been assumed that the cross-sectional shape of a bone might reflect habitual patterns of strain, more recent studies have shown that this is often not the case (e.g., Demes et al., 2001). So, for example, while it has been reported that forces generated and absorbed at the midshaft femur of generalized arboreal quadrupeds are

greater than those in size-matched specialized vertical clingers and leapers performing equal locomotor tasks (Demes et al., 1999), the actual loading patterns at the level of the midshaft section are unknown.

Finally, it is important to keep in mind another potential explanation for the apparent mechanical patterns observed in this sample. Although the relative proportions of LAM and PF bone are not highly correlated with total cortical area (or periosteal cortical area), it is possible that cortical thickness (not measured here) may impact upon the distribution of tissue types. Two sections with a similar TCA may have difference diameters, with the smaller of the two displaying thicker cortices than the larger. This bears future investigation.

*4.7.5 Primary tissue types and phylogeny*

Related to all factors above, and difficult to separate from them, is the question of phylogenetic signals in bone microstructure, independent from more proximate, adaptive life history and kinematic features. Excluding the earliest comparative bone histology works (e.g, Foote, 1913; Quekett, 1849, 1955), previous studies have not often identified phylogenetically determined, taxon-specific bone microstructural features. For example, Castanet et al. (2001) find that only 1.3% of variation in the intensity of vascularization in the long bone cortices of birds is due to a phylogenetic effect, independent of adaptive features. Bonis et al. (1972) determine that most variation is explicable by differences in body size and growth rates. There are exceptions to this apparent rule cited in the contemporary literature; for example the presence of acellular bone and lepidosteoid tubules in some groups of fishes (Enlow and Brown, 1956; Castanet et al., 2001). Starck

& Chinsmay (2002) suggest that the absence of lines of arrested growth in extant birds, even when experimentally subjected to periods of food restriction, represents the loss of this adaptation in the stem lineage leading to ornithurine birds. Certainly group-specific patterns may be identifiable. For the most part, however, it is likely is that they can be explained via an understanding of growth, physiological and kinematic adaptations.

Here, taxon-specific patterns are clearly present. For example, platyrrhines exhibit less FAST and PF bone and more LAM bone than strepsirhines. The tarsiids have more PF bone at the midshaft femur than any other taxon in the sample. Cheirogaleids display high proportions of LAM bone relative to all other strepsirhines. The question remains: can these patterns be explained as reflections of other features that serve to segregate taxa along phylogenetic lines? In the case of the separation between platyrrhines and strepsirhines, it seems likely that this is related to the divergent growth rate adaptations in the two groups. The pattern seen in the tarsiids may reflect a phylogenetically determined peculiarity with no clearly adaptive explanation (at least with respect to extant members of the tarsiid lineage). Alternatively, the almost total lack of vascularization in the midshaft cortex – not the case even for the smallest galagid – may be compensated for by the slightly higher deposition rates of PF bone. With respect to the cheirogaleids, both life history (as outlined above) and phylogenetic explanations are speculative. Then again, there may be some as-yet unrecognized pattern related to cortical thickness that accounts for the seemingly uncharacteristic primary tissue type distributions in this taxon. The data presented here are insufficient to answer this question satisfactorily, and the prudent conclusion for the time being – given the

overwhelming evidence elsewhere in the sample – would be that a life history and/or mechanical explanation is likely.

### 4.8 Summary and conclusions

Returning to questions laid out in the Objectives section of this chapter, I offer the following conclusions. First, the primates in this study are characterized overall by a high proportion of slow-forming tissues (lamellar-zonal types). This emphasis on LAM+HYB and PF tissues is consistent with the observed "slow" life-history adaptation in the order as a whole. Second, within this generalized primate pattern there exists significant and non-random variation, both among skeletal elements, and among taxa. Such variation is partly explicable via consideration of ontogenetic processes at the level of the cross-section, reflecting whole bone development. Individual elements display typical patterns of periosteal and endosteal tissue distribution, with features that differentiate between the primate forelimb and hindlimb as well as between proximal and distal limb element ontogenies, and that highlight the distinctive growth trajectories of humeri and tibiae.

The range of patterns of tissue types is also partly accounted for by diversity in body size and growth rate – as has been previously suggested – as well as habitual positional behavior. Dependent upon the tissue type, different variables appear to play more or less of a significant role in accounting for the observed patterns (despite the obviously correlated nature of proportions among tissue types within a cortex[6]). Proportions of FAST bone relate primarily to body size (and therefore the need for more rapid bone formation), with a subsidiary phylogenetic effect likely related to subordinal

[6] When values for one tissue type increase, something else must decrease.

differences in somatic growth rates. In contrast, LAM+HYB and PF tissues exhibit little or no relationship with body size, but do appear to track broad phylogenetic and/or growth differences, as well as positional behaviors. Needless to say, the separation between factors such as body size, growth and habitual locomotion is somewhat artificial, as all are interrelated adaptive (and phylogenetically informed) features of a species. Nevertheless, it does appear that different primary tissue types may preferentially track different demands on the growing bone.

Both the multiple regression analyses and simpler qualitative and quantitative exploration of the data make clear that some of the observed variation remains to be explained. Given the apparent ability of bone to respond so efficiently to both organismal and environmental demands, it is possible that a range of factors not explored here may be relevant to a more full explanation of variation in primary tissue types at the midshaft. Diet, cyclical or catastrophic climate changes, physiological perturbations both normal and pathological; all have the potential to impact upon a growing bone, leaving records in the tissues of its cross-section. What I have shown, however, is that several factors commonly referred to in the literature – body size, growth rate, mechanical environment – do indeed leave signals in primate bone.

# Chapter 5

# Intracortical Remodeling

## 5.1 Introduction

Because adult human cortical bone is primarily composed of intracortically remodeled tissue (=secondary osteonal or Haversian bone), this tissue type is often considered to be 'what bone is', particularly in the realm of clinical bone biology inquiry. But a cursory examination of even a small number of non-human vertebrates or, for that matter, young human bone, reveals that this is far from the truth (Enlow, 1956, 1957, 1958, 1962a; de Ricqlès, 1992). Bones from individuals of all ages, from all species and from all time periods may be composed of any number of combinations of the primary tissue types described in Chapter 4. Many of these do accumulate large areas of Haversian tissue, others remodel selectively, and yet others never develop a single secondary osteon. Different parts of skeletons, bones and single cross-sections of bone will display different densities of secondary osteons (e.g, Enlow, 1962a, 1963; Burr, 1992; Pfeiffer et al., 1995; Horner et al., 2000), and individual secondary osteons will vary in their size, alignment (orientation) and in the orientation of their constituent collagen fibers (Ascenzi, 1967, 1968; Yeni et al., 1997; Robling & Stout, 1999; Ascenzi et al., 2003; Bromage et al., 2003).

What then accounts for this variation in intracortical remodeling patterns? While the question of factors impacting upon remodeling has yet to be satisfactorily answered in full, several potentially relevant areas have been fruitfully explored in the years since Todd & Bowman formally described and named the Haversian system in 1845 (named

after Clopton Havers, a 17th Century student of bone structure and physiology; see Enlow, 1962a, 1963; Martin & Burr, 1989). The objectives of this portion of the study are therefore: 1) to describe variation in patterns of intracortical remodeling in the long bones of adult primates of varied body sizes, positional behaviors and relatedness, and 2) to assess the relationship between intracortical remodeling and variables previously described in the literature as determinant of remodeling patterns.

**5.2 Background on intracortical remodeling**

I use the term *intracortical* remodeling to differentiate it from the *growth* remodeling that occurs at the endosteal and periosteal surfaces of bone and which may or may not involve coupled bone resorption and formation (as per Enlow, 1963, 1976, 1982; Enlow & Hans, 1996). In contrast, remodeling is held by many researchers to refer *only* to the process whereby bone is removed and replaced in a coupled fashion (in healthy bone), usually intracortically or on the surfaces of cancellous trabeculae (typically associated with maintenance). This is considered to be distinct from *modeling* (typically associated with growth), where the formative activity of osteoblasts and the resorptive activity of osteoclasts may occur independently of one another, primarily on the endosteal and periosteal surfaces of bone (Frost, 1986; Burr et al., 1989b; Martin, 1991, 2000b; Lieberman & Pearson, 2001; Skedros et al., 2001). The relative merits of the different conceptual approaches will not be further debated here, the salient point being that the term intracortical remodeling, as used here, involves the production of secondary osteons, also termed Haversian systems.

Secondary osteons mark the place where bone removing cells (osteoclasts) have resorbed bone around an invading capillary bud (or existing vascular canal) within the cortex, and bone building cells (osteoblasts) have then concentrically deposited bone within the generated intracortical space (Enlow, 1982; Enlow and Hans, 1996). A classic explanation of this process describes the activity of BMUs (basic multicellular units, as coined by Frost, 1963), composed of about ten osteoclasts and several hundred osteoblasts (Martin et al., 1998). These are found at the leading end of a capillary bud that likely supplies nutrients as well as the progenitor monocyte and mesenchymal cells necessary to produce the osteoclasts and osteoblasts (Owen, 1978; Aubin 1998; Martin 2000a). The osteoclasts (formed by the fusion of mononuclear cells of the monocyte/ macrophage family), along with mononuclear cells, line a cutting cone about 200μm in diameter (but varying within and between cortices, individuals, species, and with age; see Currey, 1964; Jowsey, 1966), which tunnels through the cortex (Martin & Burr, 1989; Robling & Stout, 1999; Teitelbaim, 2000). Preosteoblasts and osteoblasts, differentiated from multipotential mesenchymal tissue, line the walls of the closing cone that follows the cutting cone, with preosteoblasts deep to the osteoblasts on the formative surface (Aubin, 1998; Robling & Stout, 1999; Ducy et al., 2000). This cone is the site of centripetal deposition of bone lamellae, working inward until the only space that is left is the central vascular canal.

This BMU activity is said to involve three phases: activation, resorption and formation (ARF) (Martin et al., 1998). In the first phase a signal – biochemical and/or mechanical – results in the formation of osteoclasts from the fusion of monocyte cells. This is believed to be initiated proximately by the secretion of molecules by cells of the

osteoblast lineage (Ducy et al., 2000). In the second phase the osteoclasts resorb away the bone via the secretion of HCl (the low pH of which mobilizes mineral) and a lysosomal protease (which degrades the organic parts of the matrix). The products of resorption are transported into the osteoclast via endocytosis and released on the opposite, and non-resorptive, side of the cell (Teitelbaim, 2000). A ruffled membrane forms along the edge of the osteoclast that abuts and attaches to the bone matrix to be resorbed, likely shaped in this distinctive way because of the presence of acidifying vesicles along microtubules, inserted into the plasma membrane of the cell (Teitelbaim, 2000).

In phase three of ARF the new bone is formed via deposition, by osteoblasts, of collagenous osteoid that then becomes mineralized (Lanyon & Rubin, 1985; Martin et al., 1998). Osteoblasts are capable of synthesizing a number of molecules – primarily Type I collagen, which comprises approximately 90% of the organic component of bone – but also other organic molecules found in bone such as osteocalcin, bone sialoprotein and osteopontin among others. Osteoblasts also secrete alkaline phosphotase, thought to be involved in the mineralization process (Aubin, 1998). As the BMU tunnels, its leading end may be engaged in resorption at the same time that older parts of the tunnel are at various stages of the third, formation, phase.

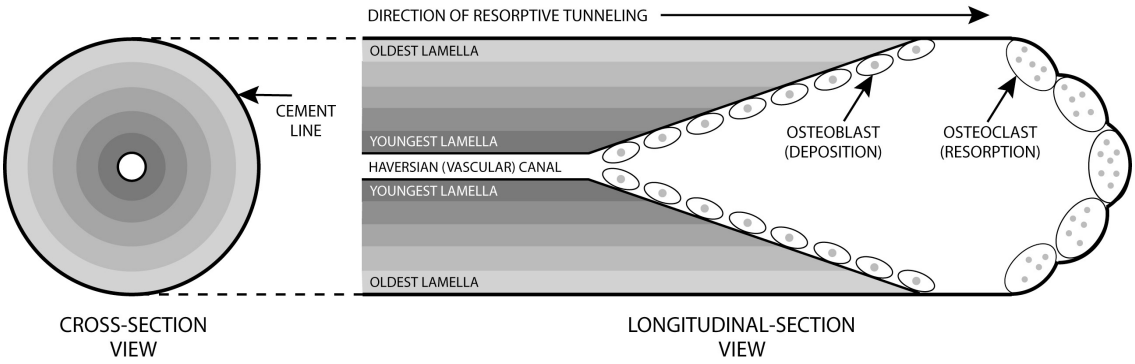


**Figure 5.1: Secondary osteon formation.**
Illustration adapted from Lanyon & Rubin, 1985

The resultant structure is a secondary osteon, marked in cross-section by a reversal line or cement line, delineating its boundary with previously deposited bone, whether primary or previously intracortically remodeled (Martin & Burr, 1989). Within the cement line are concentrically deposited lamellae surrounding a vascular canal. The vascular canal is maintained so that vascular supply to the osteonal bone and its constituent osteocytes continues. Each vascular canal contains vessels leading both to and from the vasculature in the medullary cavity or at the periosteal surface (Martin et al, 1998). Those lamellae closest to the canal were deposited later than those closer to the cement line. In highly remodeled bone, generations of secondary osteons are frequently found, with younger ones overlapped on top of earlier generations (Enlow, 1982). The canals of secondary osteons are typically described as running parallel to the long axis of a bone, thus appearing as round structures in cross-section. However, the remodeling tunnel may drift transversely within the cortex as it forms, and may also branch or anastomose with other canals (Cooper et al., 1966; Robling & Stout, 1999).

## 5.3 Existing hypotheses regarding the factors determining variation in intracortical remodeling

The degree to which bones remodel intracortically can vary widely between species, between skeletal elements, across sections, and with age (e.g., Enlow & Brown, 1956-58; Burr, 1992; Mason et al., 1995; Pfeiffer et al., 1995; Horner et al., 2000). While the factors that impact remodeling are not yet fully understood, several potentially relevant areas have been explored.

### *5.3.1 Mechanical factors*

Intracortically remodeled bone is not necessarily stronger than pristine primary tissue. For example, Vincentelli & Grigorov (1985) find that, in the human tibial diaphysis, primary circumferential lamellar bone tissue has higher tensile strength than secondarily remodeled tissue. Likewise, Evans and colleagues identify greater tensile strength in human hindlimb elements where secondary osteonal areas are lower, and find that the fatigue life of bone is reduced when osteonal area is greater (Evans & Bang, 1967; Evans & Riolo, 1970). Increased porosity – which may occur as a result of intracortical remodeling – can reduce tensile and shear fracture toughness, and reduced mineral density can result in more fatigue microdamage (Martin, 1991; Schaffler et al., 1990; Yeni et al., 1997). In addition, the interface between the secondary osteon unit and the surrounding bone is a possible source of weakness (Evans & Vincentelli, 1969; Martin, 1993). Nevertheless, intracortically remodeled bone is likely stronger than primary bone which has become damaged (Lanyon & Rubin, 1985). Thus, secondary osteons may appear where bone has accumulated fatigue microcracks, and may even be resistant to the propagation of microcracks when they are trapped within the concentric lamellae or at the

cement line (Burr et al., 1985; Lanyon & Rubin, 1985; Lanyon, 1993; Martin, 1993, 2000a). The observation that remodeling is often associated with osteocyte necrosis or apoptosis (e.g., Enlow, 1962a; Enlow & Hans, 1996) – in turn a possible result of microdamage – suggests that secondary osteocytes may ultimately be triggered to form as a means to replace essentially dead bone tissue.

The manner in which intracortical remodeling is activated by mechanical factors remains the subject of study and debate. Most researchers posit a mechanism for the monitoring of mechanical strain – mechanosensation – probably by osteocytes (Currey, 1968; Lanyon, 1987; Moss & Cowin, 1997; Wang et al., 1999). According to some researchers, in states where mechanical stimuli are either too low or too high, or in the presence of fatigue microdamage, the activation of osteoblasts and osteoclasts results. Others suggest that it is the removal of *inhibition* of the activity of osteoblasts and osteoclasts that results in remodeling (see Martin, 2000b for a review).

Support for the relationship between repair of fatigue microdamage and intracortical remodeling is found in studies that experimentally load bones in vivo and examine them histologically after death of the experimental animals (e.g., Chamay & Tschantz, 1972; Burr et al., 1985; Verborgt et al., 2000). For example, Verborgt et al. (2000) found that osteocytes in regions of fatigue damage preferentially underwent apoptosis (presumably resulting in a signal to initiate osteoblast and osteoclast activity), and that subsequently these regions began to remodel. Damage such as fatigue can and does occur at physiological loading levels and thus may accumulate regularly (Burr et al. 1985; Schaffler et al., 1989, 1990). In particular, it is intermittent, or cyclic, rather than continuous loads, that are thought to result in microfractures and consequent remodeling

(Chamay & Tschantz, 1972; Bouvier & Hylander, 1981; Lanyon et al., 1982; Lanyon, 1984; Burr et al. 1985, 1998), with time (i.e, the duration of loading), strain pattern, strain rate, strain frequency and the magnitude of loading cycles potentially critical factors (Schaffler et al., 1989, 1990; Zioupos et al., 2001; Biewener, 2005).

In this scheme, intracortical remodeling will be triggered in normal loading situations such as those imposed by habitual locomotory and masticatory modes (e.g., Bouvier & Hylander, 1981). This is important as it is hypothesized that, because fatigue microdamage reduces the elastic modulus of bone (Martin, 1991), accumulation of such damage may lead to fatigue fracture (as apposed to failure from monotonic loading) (Burr et al., 1985; Burr, 1993; Carter, 1987; Lanyon, 1987). While studies exist in which experimental loading at physiological levels leads to fatigue damage but not failure fracture, it is nevertheless possible that reduced stiffness and strength in microdamaged bone makes it more susceptible to fracture when subjected, even briefly, to higher strains (Schaffler et al., 1989, 1990). If secondary remodeling repairs fatigue microdamage, however, it is puzzling that this process does not regularly occur in all species, particularly since the peak stress levels are thought to be fairly uniform among mammals (Biewener, 1989a, 1989b, 1990, 1991, 2005). This question has not, to my knowledge, been addressed directly in the bone literature.

Studies that look at distributions of secondary osteons or increases in intracortical remodeling in response to elevated strain (particularly intermittent, or cyclic, loading) do not always examine fatigue damage, but nevertheless stress the relationship between specific loading regimes and patterns of Haversian remodeling within individual bones (e.g., Bouvier & Hylander, 1981; Lanyon et al., 1982; Lanyon, 1984; Skedros et al.,

1994; Lieberman & Crompton, 1998). For example, Portigliatti Barbos et al. (1983) find that remodeling in the human midshaft femur is particularly active in sites of tensile strain, as is microscopic crack accumulation, and related degradation of mechanical properties (Burr et al., 1998). Comparative primate studies (Schaffler & Burr, 1984; Paine & Godfrey, 1997) have shown that patterns of secondary osteonal remodeling roughly correlate with locomotor behavior category (where body size may be a confounding factor). Most of these authors infer that the BMUs are activated in response to damage incurred by loading. However there is the possibility that remodeling may occur before fatigue damage has accumulated, as a means to prevent it (by ameliorating mechanical properties), in the presence of an altered or heightened strain regime (Lanyon et al, 1982; Lanyon, 1993; Schaffler & Burr, 1984; Riggs et al., 1993a). In one compelling version of this scenario, secondary osteons may function to realign collagen fibers preferentially, that is to change the material properties of bone in a region where resistance to compressive or tensile loads is required (Lanyon et al., 1982; Riggs et al., 1993b; and see Chapter 6).

Finally – also related to mechanical competence – secondary osteons have been observed to cluster in zones of soft tissue attachment, functioning either to anchor that tissue, particularly during relocation due to growth remodeling (Enlow, 1962a, 1966), and/or to respond to tensile loading (Portigliatti-Barbos et al., 1983; Skedros et al., 1994; Goldman et al., 2003).

*5.3.2 Life history factors*

Among mammals, it is the smaller rather than the larger species that are less likely to display intracortical remodeling. So, for example, the bones of rats are generally composed entirely of primary tissue, while larger mammals such as humans and ungulates display extensive areas of secondary osteonal bone. In addition, according to Jowsey (1968), smaller mammals will have smaller Haversian systems although an increase in dimensions ceases in organisms with larger body sizes than a human. The reasons for these relationships are not evident, and results from past studies are not consistent. For example, Schaffler & Burr (1984) suggest that body size is not the primary determinant of percent intracortically remodeled bone, as animals with greatly differing body sizes may display similar values for this variable. In contrast, in another comparative primate study, Paine and Godfrey (1997) found that percent intracortically remodeled bone in a cortex does increase with body size, although these authors also find that additional variation in the relationship between relative areas of secondary osteonal bone in the humerus and femur correlates with differences in positional behavior.

A potential explanation for a scaling effect can be sought in the relationship between age and secondary remodeling (Enlow, 1962a, 1966, 1982). The bone biology literature is rife with accounts of changes in intracortical remodeling rates, porosity, osteon density, percent remodeled bone, and Haversian system morphology with age and during aging (e.g., Amprino, 1946; Enlow, 1962a, Currey, 1964; Epker & Frost, 1965; Kerley, 1965; Singh & Gunberg, 1970; Ericksen, 1991; Martin, 1993; Stout & Paine, 1994; although see Thomas et al., 2000 regarding the lack of relationship between porosity and age). This is particularly evident in research relating to women and

osteoporosis (e.g., Han et al., 1997). In recognition of these types of relationships, intracortical remodeling parameters (e.g., secondary osteon population density) in cortical sections has at times used to estimate age at death (e.g., Abbott et al., 1996). Because smaller bodied animals are often shorter-lived than larger ones, they may accumulate less microfracture and/or necrotic tissue, and therefore less secondary osteonal bone. In addition, animals of similar size but differing longevities may display differences in the amount of accumulated secondary bone (e.g., *Procyon* as compared to *Didelphis*, Warshaw et al., 2000). However, non-human primate studies suggest that, although percent secondary osteonal bone varies during growth, and bone mass and structure may change during lactation and with aging, percent secondary osteonal bone does not change in a predictable fashion in the adult (Schaffler & Burr, 1984; Burr, 1992; Paine & Godfrey, 1997; Jerome & Peterson, 2001). For example, Schaffler & Burr (1984) find only very small differences between subadult and adult *Pan troglodytes* and *Ateles paniscus* in percent secondary osteonal bone (but with only single individuals for each age group in each taxon). Similarly, Paine & Godfrey (1997) find no relationship between age and percent intracortically remodeled bone in an adult sample of a range of Old World monkeys for which ages are known. In addition, results from various studies, even regarding humans alone, are often at odds with each other. For instance, Jowsey (1968) finds that the size of secondary osteons in the human rib and femur remains the same throughout life, while Currey's research (1964) indicates a reduction in the size of femoral secondary osteons with age.

Additional life history features that may impact upon remodeling are growth rate and metabolic rate, also often correlated with body size (Schmidt-Nielsen, 1984; Harvey

& Clutton-Brock, 1985). It has been suggested that higher metabolic rates may lead to higher levels of secondary remodeling (e.g., de Ricqlès, 1980; Paine & Godfrey, 1997). In the past, different primary tissue types have been associated with particular physiologies (e.g., slow growing lamellar-zonal bone with low metabolic rate ectotherms), but upon examination of a range of vertebrates, this correlation has not held up. Rather, as described in Chapter 4, the association is most likely with growth rate, which may vary widely within endotherms and ectotherms (de Ricqlès, 1980). However, in a sample of Old World monkeys with varied growth rates, Paine & Godfrey (1997) have found no relationship between this variable and percent secondary remodeled bone.

*5.3.3 Mineral metabolism*

Another possibility is that secondary osteonal remodeling is initiated to satisfy the demands of mineral metabolism (e.g., Amprino, 1948; Enlow, 1962a, 1982; Jowsey, 1968; Lanyon, 1984). Adult individuals will remodel as a means to supplement dietary calcium (Lanyon, 1984). The demands for calcium in gestating and lactating individuals (or egg-laying birds) are particularly high, and such demands are thought to increase the intracortical remodeling activity in female mammals (Jowsey, 1968; Lanyon et al., 1982; Lanyon, 1986). A similar "raid[ing]" of the skeleton occurs during antler growth (Lanyon & Rubin, 1985, p. 7). Such extreme examples appear to provide reliable support for the relationship between mineral metabolism and Haversian remodeling. However, an argument for this as the sole factor is weakened by some research. For example, it has been shown that drifting osteons do not always move in the direction of older and more highly mineralized bone, as Robling & Stout (1999) suggest would be expected if

stimulated by the need for circulating mineral. In addition, Schaffler & Burr (1984) find that there are large differences in percent secondary remodeled bone among primates despite their essential similarity with respect to calcium metabolism. Finally, some mammals do not remodel intracortically at all (Enlow, 1962a), although these will often display high levels of trabecular remodeling (potentially satisfying the same metabolic demand). While it seems unlikely that the mineral metabolism factor alone can account for the presence and distribution of osteonal remodeling in mammals (Currey, 1984), an association between trabecular remodeling and mineral metabolism is more plausible (Swartz et al., 1998).

*5.3.4 Growth processes*

It has been suggested that Haversian systems most often (although not always, see Skedros et al., 1994) found concentrated in parts of the cortex that are vascular to begin with (but see Enlow 1962a for a contrasting view), in compacted coarse cancellous bone, and/or in those areas that are more endosteal (deeper in the cortex) (Smith, 1960b; Enlow, 1962a, 1962b, 1963, 1976; de Ricqlès, 1980). The argument explaining the latter statement is that peripheral regions of the periosteally deposited cortex are younger, and older parts of a cortex (which may in fact be close to, or at the periosteum in instances of drift) are in general more likely to be remodeled, as these are the parts of the bone that have been subjected to loads for more extended periods of time (Bouvier & Hylander, 1981; Curry, 1984; Burr, 1993; Pfeiffer et al, 1995; Skedros et al., 2001).

*5.3.5 A combination of factors*

Although there may be other factors that contribute to the regulation of intracortical remodeling (e.g., amount of hematopoietic marrow, see Martin, 2000a; storage of growth factors and cytokines), the most oft cited have been outlined here. Sex and ethnicity related differences have been described for humans, but these are not of primary relevance to the current discussion (but see Burr, 1992, and Seeman, 1997 for reviews). It is more than likely that intracortical remodeling is controlled by a number of interrelated factors, as many authors cited above have pointed out (e.g. Lanyon, 1984). However, the two existent comparative primate studies, while not entirely consistent in their findings, both suggest that kinematics (i.e., positional behavior) and body size are of primary importance (Schaffler & Burr, 1984; Paine & Godfrey, 1997). Therefore, in the following analysis, I concentrate on these two factors, with an additional consideration of cortical developmental patterns.

**5.4 Objectives of the current study**

The objectives of the current study are to explore the following questions. It is important to note, as was the case in Chapter 4, that the questions are not discrete and are not designed to furnish answers that are mutually exclusive.

1) Are there patterns of intracortical remodeling that are characteristic of the primates in the study sample as a whole?
2) Within the primate order, is there significant variation in the distribution of intracortical remodeling among long bone midshaft cortices?
3) If significant variation is present, is it non-randomly distributed?

4) If non-randomly distributed, are patterns explained in part or in whole by the life history and/or mechanical and/or developmental factors, as outlined above?
    a. Does percent intracortical remodeling vary among taxa that are different in their adult body size in accordance with the hypothesis that larger bodied individuals will display more remodeling?
    b. Do distributions of intracortical remodeling vary among taxa that are different in positional behavior, in accordance with the hypothesis that remodeling responds to mechanical load?
    c. Do distributions of intracortical remodeling vary with developmental patterns, in accordance with the hypothesis that more vascular and/or older tissue is more likely to display secondary osteons?
5) Are there identifiable phylogenetic patterns that are independent of taxon-specific adaptation?

## 5.5 Methods

### *5.5.1 Identification of intracortical remodeling*

A description and image of intracortically remodeled bone, and the criteria used to identify it, is provided in Chapter 4. To quantify the proportion of the cortex that is intracortically remodeled, I follow the methods of Paine & Godfrey (1997) where all remodeling events (including fragmentary osteons) are traced and the total area composed of remodeled bone is calculated. This is in contrast to studies that include only intact osteons (e.g., Abbot et al, 1996) and those that use point-counting methods to quantify secondary osteon density and area (e.g., Schaffler & Burr, 1984). The latter

method was deemed inappropriate for this sample because the number of remodeling events in the sample bones is often very low, obviating the necessity for, and usefulness of, point counting. In addition, I have chosen to quantify remodeling across the entire cortex, rather than sample in representative regions, both because remodeling is scant in many individuals and also since it has been shown that intracortical remodeling data can vary by sampling location (Pfeiffer et al., 1995).

### 5.5.2 *Image processing and quantification of tissue types*

Image processing and quantification of intracortical remodeling was accomplished concurrently with the acquisition of primary tissue type data, as described in Chapter 4. However, in the case of remodeling, proportions were calculated relative to the entire cortex, rather than the periosteal or endosteal portions of the cortex. In addition, each cortex was divided into quadrants and data were collected for the quadrants, as well as for the entire cortex, allowing for intracortical comparisons of the proportions of remodeled bone. The Optimas macro used to derive values for all tissue types, designed for use with the large midshaft human femur, divides the cortex into 16 sectors around the centroid, and three radial sectors, for a total of 48 sectors (Figure 5.2). For this study the 48 sectors were collapsed into a total of four quadrants (anterior, lateral, posterior, medial), as seen in Figure 5.2. This was done both because of the very small size of many of the sample specimens, and also because of the lack of mechanical hypotheses to suggest differences at a higher resolution.

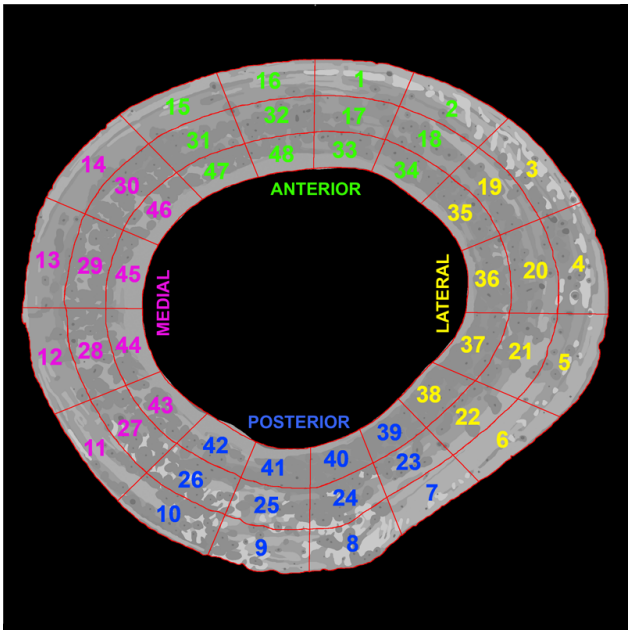


**Figure 5.2: Cortical sectors.**

48 sectors as output from Optimas, and partitioned into four quadrants for analysis. Anterior quadrant=sectors 15, 16, 1, 2, 31, 32, 17, 18, 47, 48, 33, 34. Lateral quadrant=sectors 3, 4, 5, 6, 19, 20, 21, 22, 35, 36, 37, 38. Posterior quadrant=sectors 7, 8, 9, 10, 23, 24, 25, 26, 39, 40, 41, 42. Medial quadrant=sectors 11, 12, 13, 14, 27, 28, 29, 30, 43, 44, 45, 46.

*5.5.3 Statistical and descriptive analyses*

Samples are the same as those described in Chapter 4, and the equivalent problems exist with respect to sample composition and distribution. Therefore, as before, I employ nonparametric statistical tests and seek a confluence of significant results as well as the examination of patterns identified via graphical methods to arrive at conclusions. Where sample sizes are too small to allow for meaningful statistical analysis, I utilize descriptive methods alone.

First, proportions of intracortically remodeled bone, relative to total cortical area, are described for the entire sample, and element means are compared. Subsequently, quadrant values are compared within elements for all individuals as a means to identify differences that may be determined by variation in strains across a cortex (e.g., tension vs. compression). Values for each quadrant are calculated as a proportion of the total cortical area. Non-parametric Sign tests and Wilcoxon Matched Pairs tests are used to

identify differences in the proportion of periosteal tissue types in the sample as a whole, examining each skeletal element independently.

Multiple regression analyses are employed to determine the importance of three independent variables in accounting for the observed variation in primary tissue type proportions. The variables, described in Chapter 4 – total cortical area (TCA), positional behavior (PB), and phylogenetic status (PHYLO) – were chosen as best able address the questions raised by a review of the literature, and outlined in the objectives section. TCA is included as a proxy for body size, and PB as a means to identify variation related to mechanical adaptation. While there are no studies to suggest that there is a phylogenetic effect on patterns of remodeling, independent of functional and life history adaptations, this variable is included to control for such an effect should it be present. In addition, as described in Chapter 4, PHYLO and growth rate are significantly positively correlated. Therefore, a relationship between the factor PHYLO and intracortical remodeling can be considered in light of growth differences among taxa. Multivariate models are examined including all three variables, as well as combinations of two, and are compared to simple regressions for each variable, as described in Chapter 4. Data are further explored via Kruskall-Wallis and Mann Whitney U tests. Descriptive analysis is provided for intra-taxonomic variation in intracortical remodeling proportions within and between skeletal elements. Subsequently, patterns characteristic of each skeletal element for each taxon are described.

## 5.6 Results

### *5.6.1 Sample-wide patterns of remodeling: whole cortices*

The taxon means for relative proportions of intracortically remodeled bone were examined for whole cortices for each element. Element means vary from between slightly over 10% of the bone to slightly under 30%, but ranges include values of zero up to approximately 70%. There are slight differences between elements in the proportions of intracortical remodeling, as seen in Figure 5.3, with the forelimb bones displaying higher mean proportions of remodeling. However, only differences between the femur and the three forelimb bones are significant, and these only marginally so (Mann-Whitney U Tests; $p<.05$).

Nevertheless, when values for the femur and the forelimb bones are compared for individual animals, it is clear that in most cases, the forelimb bones display more remodeling (Figure 5.4). In addition, for most individuals, the femur and humerus are less heavily remodeled, relative to total cortical area, than the tibia and ulna respectively (Figure 5.5). Finally, the ulna is, in most individuals, more remodeled than all other elements (Figure 5.6)

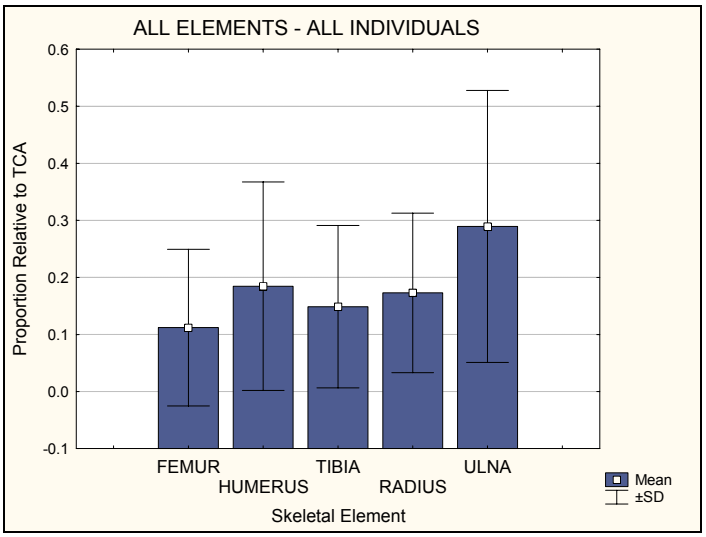


**Figure 5.3: Proportions (relative to TCA) of intracortically remodeled bone in each element for all individuals combined.**

See text for description.

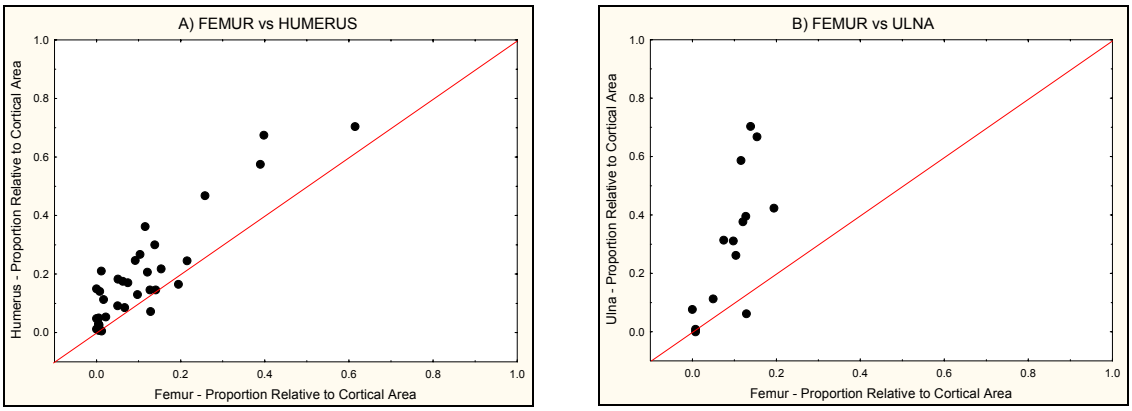


**Figure 5.4: Proportions (relative to TCA) of intracortically remodeled bone in the femur vs. humerus and ulna.**

The diagonal red line indicates where all data points would fall if percentages of remodeled bone were equivalent in both elements. Each data point indicates a single animal. In the majority of individual cases, the humerus (A) and ulna (B) display a greater proportion of remodeled bone than the femur. A similar pattern is observed when the radius is compared to the femur (not graphed here).

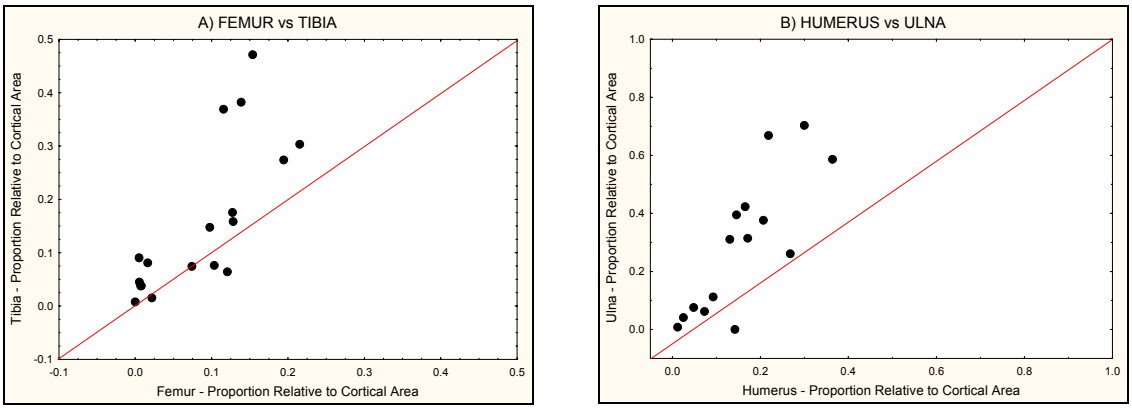


**Figure 5.5: Proportions (relative to TCA) of intracortically remodeled bone in femur vs. tibia and humerus vs. ulna.**
The diagonal red line indicates where all data points would fall if percentages of remodeled bone were equivalent in both elements. Each data point indicates a single animal. In the majority of individual cases, the tibia (A) and ulna (B) display a greater proportion of remodeled bone than the femur and humerus respectively.

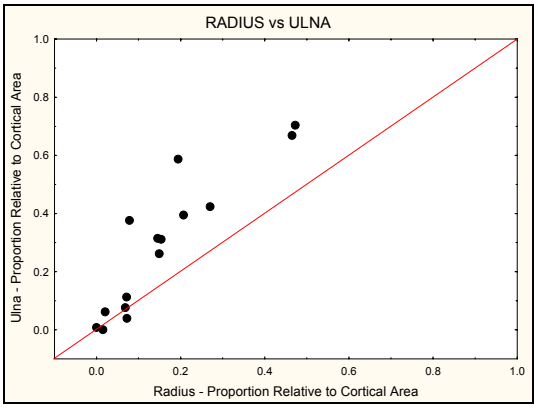


**Figure 5.6: Proportions (relative to TCA) of intracortically remodeled bone in the ulna vs. radius.**
The diagonal red line indicates where all data points would fall if percentages of remodeled bone were equivalent in both elements. Each data point indicates a single animal. In the majority of individual cases, the ulna displays a greater proportion of remodeled bone than the radius. A similar pattern is observed when the ulna is compared to the humerus, tibia and femur.

### *5.6.2 Sample-wide patterns of remodeling: quadrant patterns*

The quadrant means for relative proportions of intracortically remodeled bone were examined for each element. In the femur and ulna, there are no significant differences among quadrants in the proportion of the cortex composed of remodeling events (Figure

5.7A). In contrast, significant quadrant differences are present in the humerus, radius and tibia. In the humerus, anterior quadrants contain more intracortical remodeling than the posterior and lateral quadrants, and medial quadrants more than posterior quadrants ($p<.05-<.01$). In the radius the lateral quadrant is more highly remodeled than all other quadrants ($p<.05-<.001$), and in the tibia the anterior quadrant contains more remodeling than all other quadrants ($p<.05-<.0001$) (Figure 5.7B).

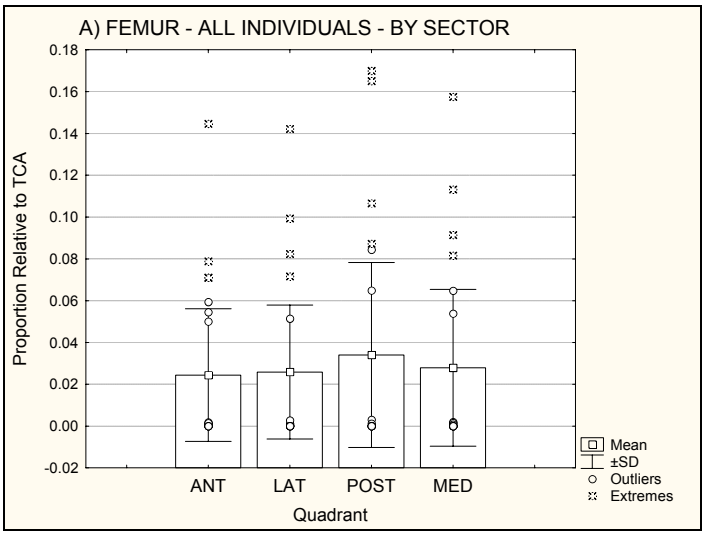


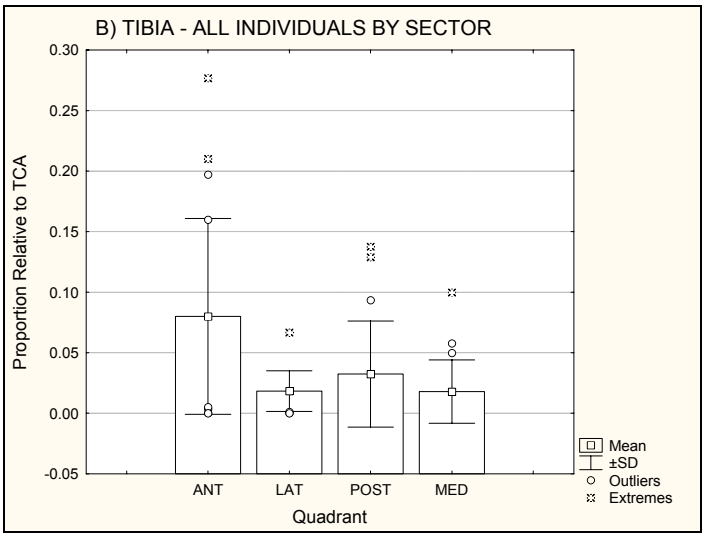


**Figure 5.7: Femoral and tibial proportions (relative to TCA) of intracortically remodeled bone for individual quadrants.**

A) Femur. B) Tibia. See text for description.
Upper outliers > upper value of the box + outlier coefficient x (upper value of the box – lower value of the box). The inverse is true for the lower outliers. Upper extremes > upper value of the box + 2x outlier coefficient x (upper value of the box – lower value of the box). The inverse is true for the lower extremes. *Outlier coefficient = 1.5.

*5.6.3 Factors accounting for variation in primary tissue types across the entire sample*

Multiple regression analyses confirm that the independent variables TCA, PB and PHYLO, chosen based on their purported relationship with intracortical remodeling (with the exception of PHYLO), do account for a significant proportion of the variation observed in this sample. The models yielding the highest adjusted $R^2$ may include all three predictor variables, only two of the three, or in some cases just a single variable (Table 5.1). Dependent upon the element, the relationship between remodeling and the independent variables differs, both in the magnitude of the total variance explained, as well as in the independent variables accounting for the variation. Overall, significant $R^2$ values range between 0.35 and 0.74 with p-values of <.05 to <.0001.

| MULTIPLE REGRESSION RESULTS | | |
|---|---|---|
| Element | Adjusted $R^2$ | Model |
| Femur | 0.66*** | TCA, PB, PHYLO |
| Humerus | 0.74*** | TCA, PB, PHYLO |
| Tibia | 0.35* | TCA, PB |
| Radius | 0.67** | TCA, PB, PHYLO |
| Ulna | 0.72*** | TCA |

**Table 5.1: Multiple regression results for LAM+HYB bone for the entire sample.**
For each element, the model with the highest adjusted $R^2$ was selected. The number of independent variables included in the model differs depending on the element. * indicates p<.05; ** indicates p<.01; ***indicates p<.001.

In all elements without exception, TCA is the strongest predictor of the degree to which the midshaft cortex is remodeled (Table 5.2). The relationship is positively allometric: the greater the cortical area, the greater the proportion of it that is composed of secondary osteons. The relationship between TCA and remodeling in the humerus is clearly visualized in Figure 5.8A. Bivariate plots for all other elements are similar, with a

high proportion of the variation explained by TCA ($r^2$ = .39-.74 depending on the variable; see Figure 5.8).

The multiple regression analyses also indicate that PB is a significant predictor factor for all elements except the ulna (although betas for the tibia are insignificant). In addition, when the bivariate plots of remodeled bone against TCA are categorized by positional behavior category, r and $r^2$ are higher for at least one PB category than for the uncategorized correlation. However, for other PB categories, correlations weaken or are insignificant. Kruskall-Wallis tests identify significant differences among PB categories only in the femur and humerus. In the femur the suspensory atelids display significantly more remodeling than all other PB types (Mann Whitney U tests), and the slow climbers are more highly remodeled than vertical clingers and leapers. In the humerus, differences between all PB categories are significant except for the comparison between vertical clingers and leapers and arboreal quadrupeds. Although there are statistical differences between positional behavior categories, bivariate scatterplots (Figure 5.8B) and boxplots (Figure 5.9) show poor separation between PB categories with the exception of the suspension in the femur and humerus.

PHYLO appears as a predictor variable in the most powerful multiple regression models for the femur, humerus and radius. However in no cases does it yield a significant beta. In addition, graphical methods identify no clear differences among PHYLO categories (e.g., Figure 5.10). Therefore, the effect of phylogeny (and, by association, growth rate) is considered to be marginal.

| MULTIPLE REGRESSION BETAS | | |
|---|---|---|
| Element | Predictor Variable | Beta |
| Femur | TCA | 0.47** |
| | PB | 0.35* |
| | PHYLO | Not significant |
| Humerus | TCA | 0.61*** |
| | PB | 0.39** |
| | PHYLO | Not significant |
| Tibia | TCA | 0.63** |
| | PB | Not significant |
| Radius | TCA | 0.73*** |
| | PB | 0.51* |
| | PHYLO | Not significant |
| Ulna | TCA | 0.86*** |

**Table 5.2: Multiple regression betas.**
For each element, the independent variables for which there are significant betas are listed. Because the variables PHYLO and PB are dummy-coded, each includes more than one vector. Individual vectors may or may not have significant betas. Indicated significances are based on the highest p value for that variable. * Indicates p<.05; ** indicates p<.01; *** indicates p<.001.

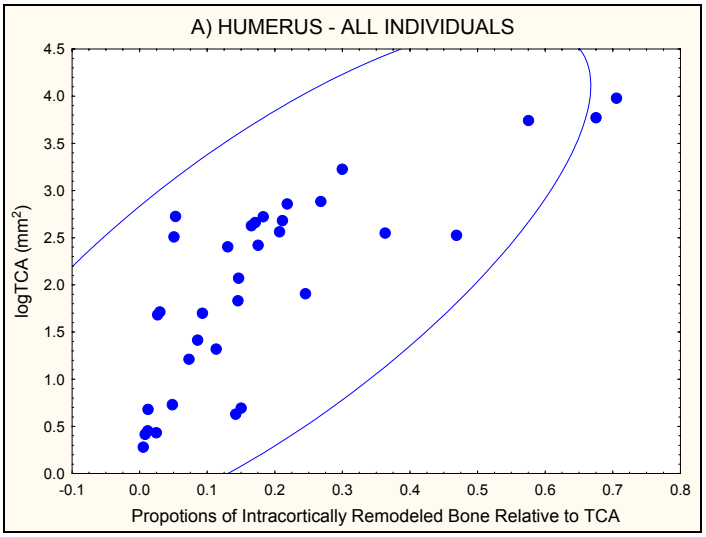


**Figure 5.8: Humeral proportions of remodeled bone relative to TCA, as a function of TCA.**

A) There is a positively allometric relationship between the proportion of remodeled bone and TCA ($r^2$=.59, r=.77, p<.0001). Statistics for other elements: Femur ($r^2$=.45, r=.67, p<.0001); Tibia ($r^2$=.39, r=.62, p<.01); Radius ($r^2$=.62, r=.79, p<.001); Ulna ($r^2$=.74, r=.86, p<.0001).
B) This relationship is strengthened in some cases when the data are categorized by PB (AQ $r^2$=.64, r=.80, p<.01) but weakened in other cases (VCL $r^2$=.47, r=.68, p<..01; SC $r^2$=.39, r=.63, p>.05; SUS $r^2$=1.00, r=1.00, p>.05).

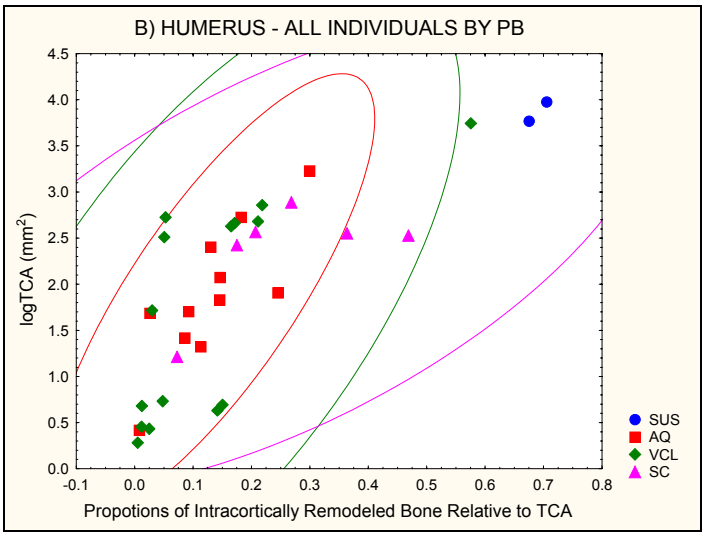


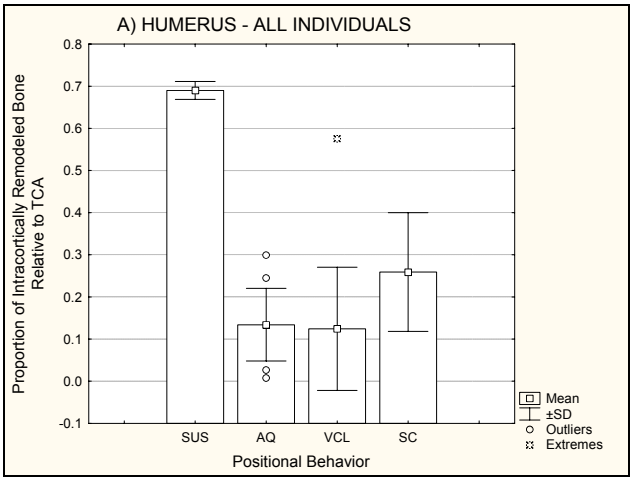


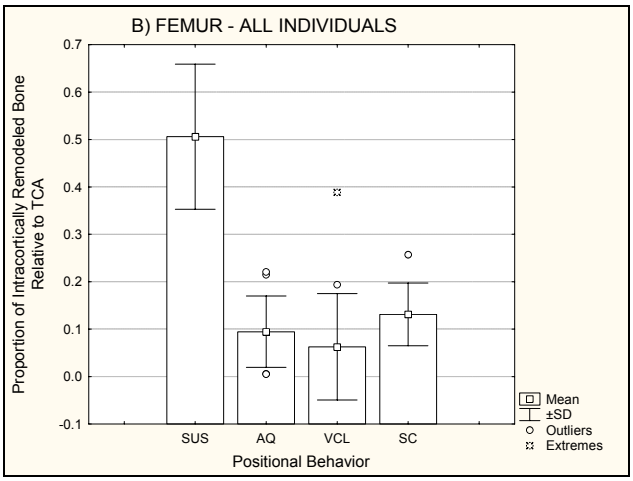


**Figure 5.9: Humeral (A) and femoral (B) proportions of remodeled bone, categorized by PB.**
See text for discussion.

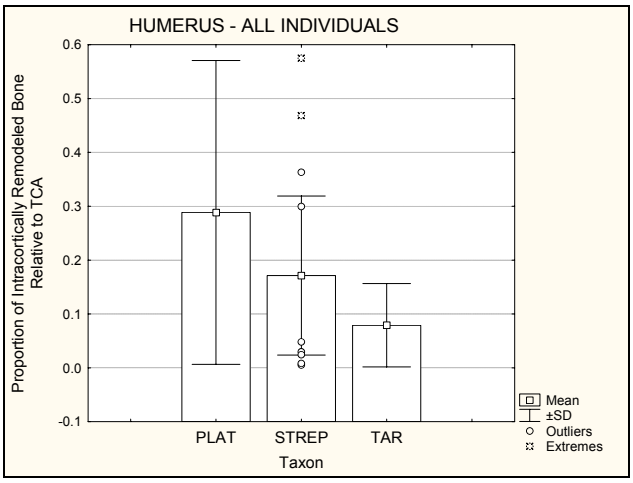


**Figure 5.10: Humeral proportions of remodeled bone, categorized by PHYLO.**

See text for discussion.

*5.6.4 Variation in quadrant patterns of remodeling: comparison within and among positional behavior groups*

When comparisons of values for individual section quadrants are made within and between positional behavior categories, very few clear and significant patterns emerge. The distribution among sectors is generally variable within PB groups, with no significant differences among quadrants.

Three exceptions to this pattern exist. First, in the humeri of vertical-clingers and leapers, the anterior quadrant displays significantly more remodeling than the lateral and posterior quadrants (Kruskall-Wallis test; $p<.05$) (Figure 5.11A). Second, in the radii of arboreal quadrupeds, the anterior quadrant displays significantly less remodeling than the lateral and medial quadrants ($p<.05$) (Figure 5.11B). Finally, in the tibiae of arboreal quadrupeds, the anterior quadrant displays significantly more remodeling than the lateral and medial quadrants ($p<.05$) (Figure 5.11C). These three patterns are comparable to ones seen when the mean for all individuals in the sample is examined.

Although statistically insignificant, another pattern is observable in the femora of vertical-clinger leapers when individual line plots are examined (Figure 5.12A). For the individuals in this group that display more than a trivial amount of remodeling (i.e., more than 1% of the TCA) the posterior cortex is most heavily remodeled.

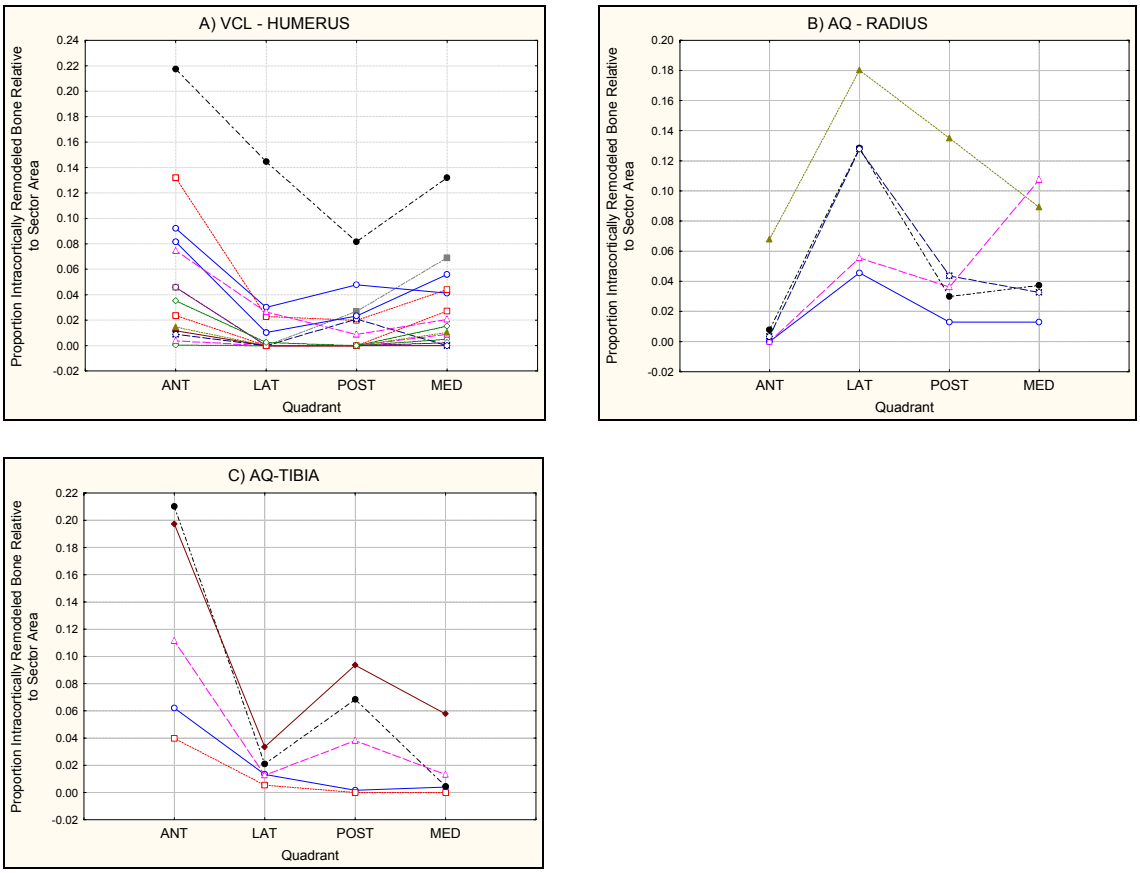


**Figure 5.11: Quadrant patterns of remodeling within PB categories.**
Each line represents a single section/individual. A) Humeral midshafts of vertical-clinger leapers. B) Radial midshafts of arboreal quadrupeds. C) Tibial midshafts of arboreal quadrupeds.

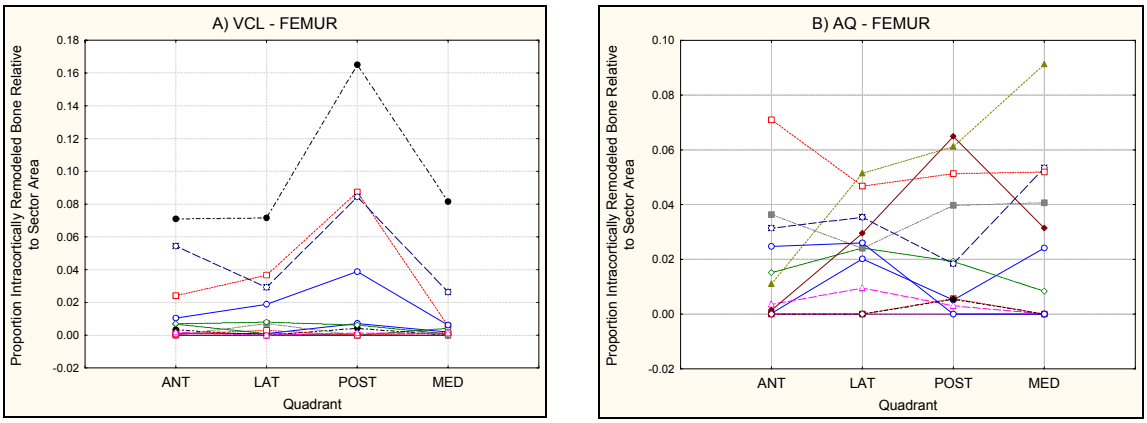


**Figure 5.12: Quadrant patterns of remodeling within PB categories.**
Each line represents a single section/individual. A) Femoral midshafts of vertical-clinger leapers. The posterior cortex displays more remodeling than other quadrants. B) Femoral midshafts of arboreal quadrupeds. No consistent pattern emerges in the femur for this positional behavior category.

Just as there is, in most cases, a lack of statistically significant patterning within positional behavior groups, pronounced differences between groups in the distribution of remodeling around the cortex are generally not present, with a few exceptions. In the humerus, where a strong pattern is present among vertical clingers and leapers, this same concentration of remodeling in the anterior and medial cortices is repeated in arboreal quadrupeds and slow climbers, albeit to a lesser degree (i.e., absent statistical significance), and with more variation among individuals.

When the pattern found among radii in arboreal quadrupeds is compared to the distribution of secondary osteons in vertical-clinger leapers and slow climbers (there are no atelid specimens for radius, ulna or tibia), the only difference is the strength of the pattern in the AQ group. Similarly, the tibial concentration of remodeling in arboreal quadrupeds is present in vertical clinger leapers as well, and present, but much less extreme, among slow climbers. Only in the femur do there appear to be differences in the sectoral distribution among PB categories, with vertical-clinger leapers the only group

displaying a strong pattern of larger percent remodeled area in the posterior cortex. Within other PB categories, sectoral patterns are variable or non-existent (Figure 5.12B).

*5.6.5 Comparison between elements: PB or PHYLO patterns*

When the values for two different elements in individual specimens are compared for the entire sample, there is no taxonomic or functional patterning to the resultant bivariate plots, with two exceptions. The relationship between the proportion of the humerus and the femur that is intracortically remodeled does not vary by positional behavior, or with phylogenetic status. Nor are there any differences for a comparison of the femur and tibia, or radius and ulna. However, for both humerus/radius and humerus/ulna comparisons, proportions of remodeling in the slow climbing lorisid distal elements are generally lower relative to the humerus than what is seen in other taxa (Figure 5.13A). The disparity increases with section size. This peculiarity is also present when absolute, rather than proportional, values are examined (Figure 5.13B).

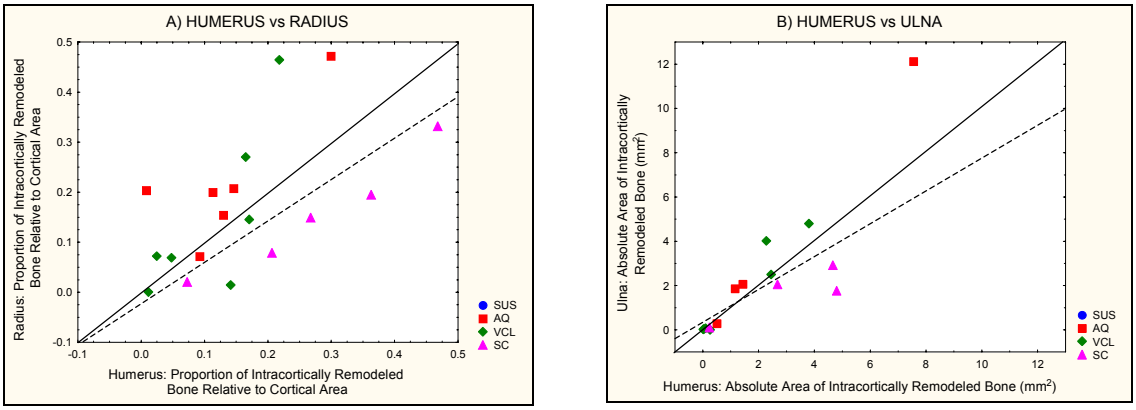


**Figure 5.13: Proportions of remodeled bone in all sample individuals, categorized by PB.** A) In this bivariate plot of percent remodeled bone, the solid diagonal line indicates where the values would fall should the proportion of be equivalent in the humerus and radius within an individual. In almost all cases, the proportion of remodeled bone in the humerus of slow climbers is greater, relative to radius, than in comparably sized individuals from other PB categories. The dashed diagonal line is an arbitrarily drawn separation between slow climbers (below the line) and taxa with all other positional behaviors (above the line). B) A comparison of absolute values (in $mm^2$) for the humerus and ulna.

*5.6.6 Characterization of individual taxa*

5.6.6.1 Intra- and intertaxonomic diversity

Investigations of variation within the sample as a whole highlight some patterned relationships between intracortical remodeling and body size as well as positional behavior. However, within the broad patterns described above, there is evidence of both intra- and intertaxonomic diversity (see for example Figure 5.11). Following is an exploration of this variability. Because within-taxon sample sizes are small, particularly for the tibia, radius and ulna, analyses remain descriptive.

| | Femur | Humerus | Tibia | Radius | Ulna |
|---|---|---|---|---|---|
| Atelidae | 50.6% | 69.0% | | | |
| Calltrichidae | 2.8% | 5.9% | | 7.1% | 11.3% |
| Cheirogaleidae | 5.7% | 8.8% | 6.3% | 20.1% | |
| Lesser Galago | 0.5% | 2.7% | 1.0% | 7.0% | 5.9% |
| Indriidae | 18.5% | 33.5% | 47.1% | 46.4% | 66.9% |
| Lemuridae | 9.5% | 24.1% | 38.2% | 47.2% | 70.4% |
| Lorisidae | 12.6% | 25.7% | 16.7% | 15.4% | 32.2% |
| Greater Galago | 7.4% | 11.0% | 11.4% | 20.8% | 36.9% |
| Cebidae | 16.5% | 17.4% | 20.9% | 18.0% | 35.3% |
| Tarsiidae | 0.4% | 7.9% | 3.8% | 0.7% | 0.4% |

**Table 5.3: Summary of percent intracortically remodeled bone for individual elements and taxa.** Each value represents a mean for the element within a taxon.

5.6.6.2 Consistency[1] within taxa: intrataxonomic variation for individual elements

Consistency in the proportion of the cortex that is composed of intracortically remodeled bone varies between elements and among taxa. In many cases[2], values within a taxon are

[1] Patterns are considered to be *consistent* when all individuals within a taxon have approximately the same proportion of intracortically remodeled tissue.

[2] Each "case" represents a comparison of values among individuals for a single element of a single taxon. Where only one specimen is available (e.g., for the distal elements in some taxa), ranges are necessarily not considered.

similar[3]. In 20 out of 37 cases, however, the range of values for a given element within a taxon exceeds 10% of the TCA. In seven cases, the range exceeds 25% of the total cortical area. This is most extreme when individuals within a taxon vary greatly in size (*Loris tardigradus* vs. *Nycticebus coucang* or *Perodicticus potto*, and *Propithecus* sp. vs. *Indri indri*), with the larger individuals displaying far more remodeling. However, such variability is also present on occasion within taxa where individuals are of approximately equivalent size (among the greater galagos, and among *N. coucang* and *P. potto* individuals). These larger variations in range (exceeding 25% of TCA) occur for all elements, but are restricted to the indriids, lorisids, and greater galagos. Figure 5.14 provides examples of cases with small, moderate and large ranges of variation in intracortical remodeling.

[3] Mean values are considered to be *similar* when the difference between them is <10% of the total periosteal area.

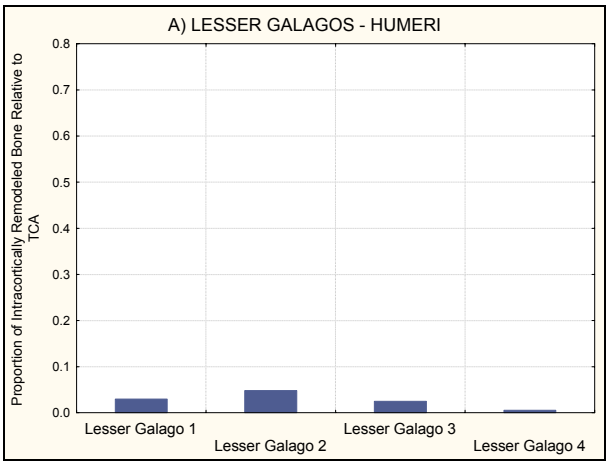


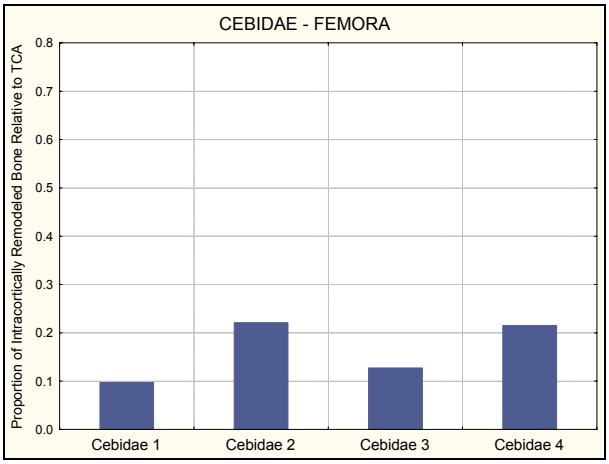


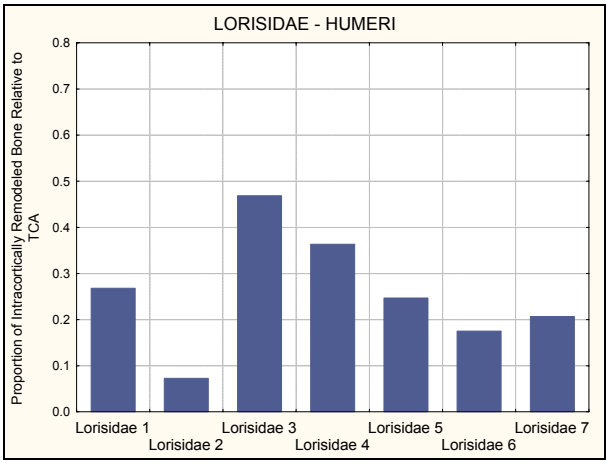


**Figure 5.14: Individual values for proportions of intracortical remodeling.**

A) The humerus of the lesser galagos is an example of a case where proportions of intracortical remodeling are similar.
B) Among the femora of cebids, the range is greater, exceeding 10% of TCA.
C) The lorisid humeri vary greatly in the proportion of remodeling, with the single small *L. tardigradus* individual displaying the least and the single *P. potto* the most. All *N. coucang* values fall between the two extremes.

5.6.6.3 Characterization of patterns of primary tissue type distributions for individual taxa

In the following discussions, I discuss muscle origin and insertion sites. These are not derived from dissections of the study individuals, but rather are based on previous studies of soft tissue anatomy (Stevens et al., 1972; Jouffroy, 1975; Youlatos, 2000). Figure 5.15 depicts the muscular origins and insertions at the midshaft, as compiled from the cited sources. Not every midshaft section necessarily is subject to all of the attachments listed in Figure 5.15. Variation will depend upon the species. Therefore, Figure 5.15 serves only as a summary of possible muscle origins and insertions.

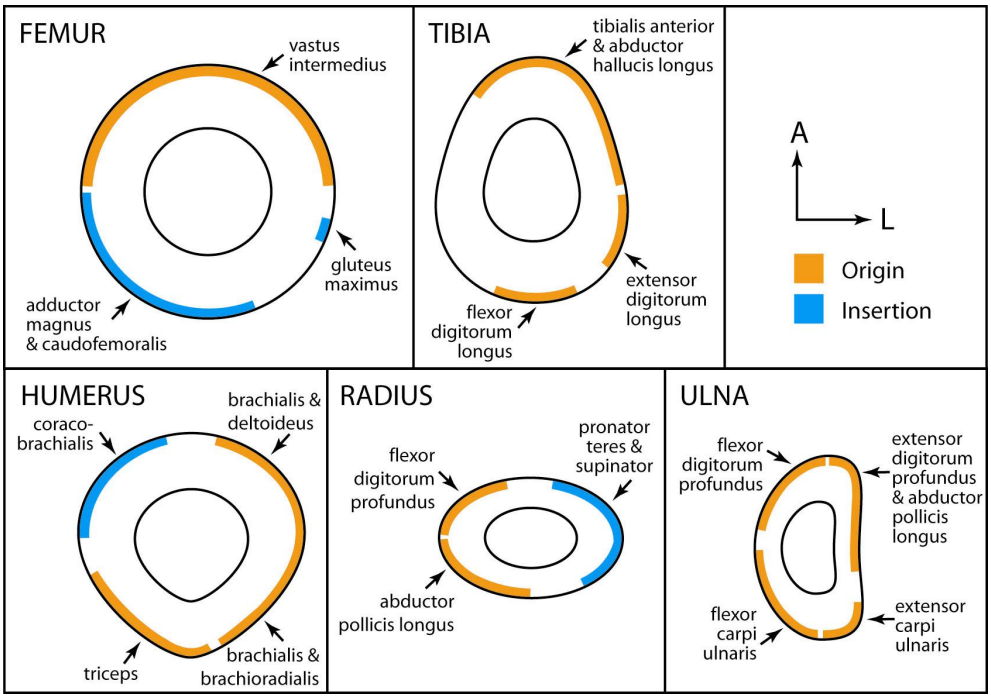


**Figure 5.15: Muscular origins and insertions at the midshaft.**
Abductor hallucis longus: abducts and extends hallux. Abductor pollicis longus: abducts and extends pollex. Adductor magnus: adducts and extends thigh. Adductor pollicis longus: adducts and medially rotates pollex. Brachialis: flexes forearm. Brachioradialis: flexes forearm. Caudofemoralis: extends thigh. Coracobrachialis: flexes and adducts arm. Deltoideus: flexes, medially rotates, abducts, extends and laterally rotates arm. Extensor carpi ulnaris: extends and adducts hand. Extensor digitorum longus: extends hand and digits 2-5. Extensor digitorum profundus (=extensor pollicis longus): extends pollex. Flexor carpi ulnaris: flexes and adducts hand. Flexor digitorum longus: flexes digits 2-5 and plantarflexes foot. Flexor digitorum profundus: flexes digits 2-5 and hand. Gluteus maximus: extends and laterally rotates thigh. Pronator teres: pronates and flexes forearm. Tibialis anterior: dorsiflexes ankle and inverts foot. Triceps brachii: extends forearm. Supinator: supinates forearm. Vastus intermedius of the quadriceps: extends the leg.

*5.6.3.3.1 Lesser galagos.* The cortex in the femora of these three small individuals is almost void of intracortical remodeling, with only a few secondary osteons within the compacted coarse cancellous (CCC) bone areas in two of the three individuals. These are not preferentially present in any one sector of the cortex. Nor is intrataxon variation in cortex size tracked by the intensity of remodeling. Both the largest and smallest of the three individuals display secondary osteons, while the cortex of intermediate size does not. There is sparse remodeling in the four humeral midshafts, located anteriorly and anteromedially in three of the four individuals, as well as posteriorly at the site of extensor muscle attachment (likely the triceps) on the largest individual. With the exception of this last instance, most of the remodeling events are found in endosteal tissue, predominantly within areas of CCC bone. In contrast to the femur, there appears to be a relationship between size and intracortical remodeling, with the smallest cortex displaying the least.

In the two radial midshaft sections, small areas of dense intracortical remodeling are found laterally – likely at the attachment site of the pronator teres muscle – as well as anteriorly in one individual. The secondary osteons are found predominantly surrounded by periosteal bone. In contrast, in the ulna, intracortical remodeling occurs primarily in endosteal areas, including CCC bone. Secondary osteons are also found laterally in concentrated areas (at the site of extensor carpi ulnaris, the extensor digitorum profundus, or the abductor pollicis longus) and anterolaterally. The two tibiae in this sample display few secondary osteons, located anteriorly in periosteal bone at the site of tibialis anterior and abductor hallucis longus attachment, and in one case laterally in endosteal bone.

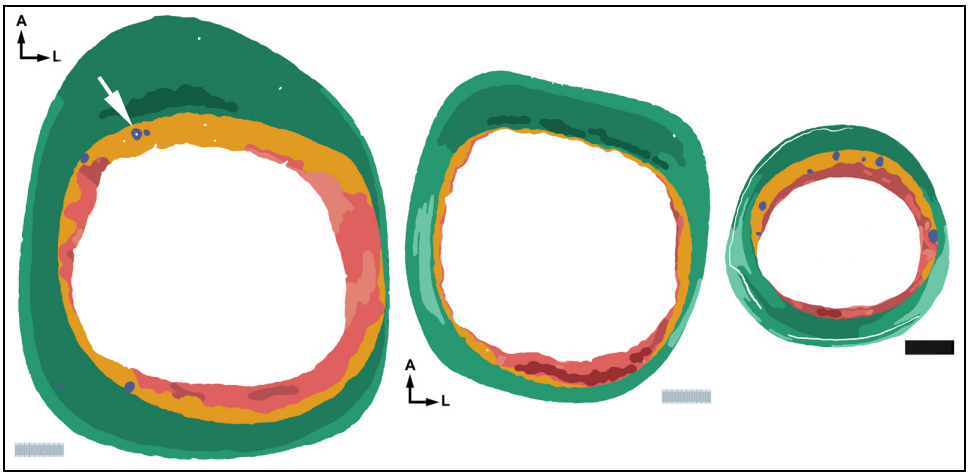


**Figure 5.16: Lesser galago femora.**
*Galago senegalensis* (MNHU 60601), *Galago moholi* (DUPC 2062), *Galago demidovii* (HC 25). See text for description. Purple indicates secondary osteons. For grayscale reproductions, the arrow points to an example of a secondary osteon. Scale bar indicates .5 mm.

*5.6.3.3.2 Greater galagos.* There is some heterogeneity in this taxon in the femur, with one individual displaying a moderate amount of intracortical remodeling (c. 20% of the cortex). In this individual, the remodeling is concentrated in the posterior quadrant and, to a somewhat lesser degree, the anterior quadrant, distributed through the depth of the cortex among a range of primary tissue types. The remaining three individuals display only a few scattered secondary osteons each, concentrated in the CCC bone as well as at a posterolateral site of muscle attachment (likely the gluteus maximus). In the humerus, the amount of remodeling is more consistent among the four sample cortices (c. 5%-17% of the cortex). In two of the four individuals, the secondary osteons are predominantly clustered in the anterior and medial quadrants, with a single secondary osteon laterally in one of the two. In the remaining two individuals, the osteons can be found in all four quadrants, although clustered most notably in the anterior quadrant. In almost all instances, the intracortical remodeling is restricted to endosteal tissue, predominantly surrounded by bone of the CCC type.

In the two sample radii, 14-27% of the cortex is intracortically remodeled, with secondary osteons clustered medially and laterally in one of the two, but distributed in all quadrants in the other. In both individuals the remodeling is within endosteal areas (particularly in CCC bone) or at the boundary between endosteal and periosteal bone, as well as periosteally in areas of the cortex where there is evidence of soft tissue attachment (likely the pronator teres muscle laterally, and the abductor pollicis longus muscle medially). Remodeling at the ulnar midshaft is more widespread than what is found in the radius, or the femur and humerus; c. 31-42% of the cortex is composed of secondary osteons. They are found in all quadrants of the two sample cortices and, like the radius, are predominantly located in endosteal areas (most often surrounded by CCC bone) or at the endosteal/periosteal boundary. They are also found in the periosteal cortex at posterior and anterolateral soft tissue attachment sites (flexor carpi ulnaris or extensor carpi ulnaris posteriorly, and extensor digitorum profundus or abductor pollicis longus anteromedially). Mirroring the situation in the femur, there is substantial variation in the amount of intracortical remodeling at the midshaft tibia: from 1.5-27% in the four sample specimens. In three of the four individuals the remodeling is tightly clustered in the anterior cortex, with sparser distribution laterally, medially or posteriorly. In these individuals the remodeling is found almost exclusively in periosteal bone (tibial endosteal bone areas are generally small, see Chapter 4) and is distributed throughout the radial extent of the cortex. In the fourth individual (containing the least remodeled area) the few secondary osteons are scattered in the anterior and posterior cortices, close to or within the endosteal portion of the bone. The predominance of intracortical remodeling

in the anterior quadrant of the tibia, as is the case in the lesser galagos, coincides with the attachment of the tibialis anterior and abductor hallucis longus muscles.

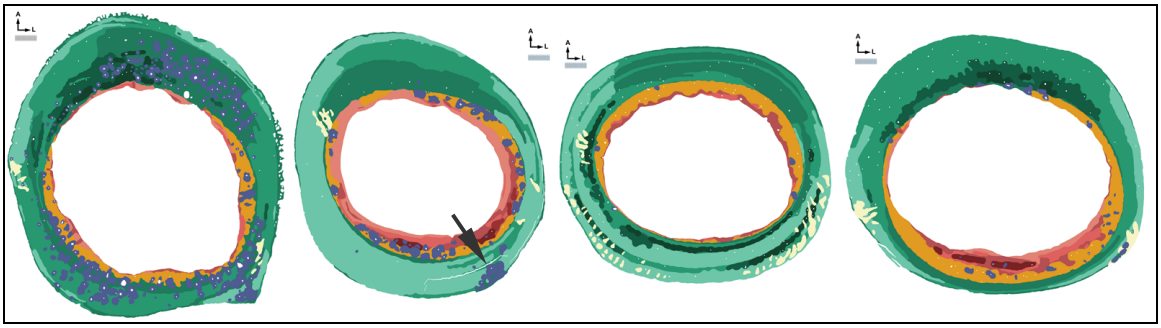

**Figure 5.17: Greater galago femora.**
*Otolemur crassicaudatus* (DUPC 725), *Otolemur crassicaudatus* (HC 31), *Otolemur crassicaudatus* (USNM 365721), *Otolemur crassicaudatus* (CT OA). See text for description. Purple indicates secondary osteons. For grayscale reproductions, the arrow points to an example of a secondary osteon. Scale bar indicates .5 mm.

*5.6.3.3.3 Lorisidae.* In the six lorisid femora there is a moderate but variable amount of intracortical remodeling (6-26% of the cortex), distributed evenly among all four sectors, but concentrated in CCC areas in all but a single individual. In this last individual, remodeling is also found in regions primarily composed of fibrolamellar (FBL) bone as well as, to a lesser degree, in areas with lamellar (LAM), hybrid (HYB) or parallel-fibered (PF) tissue. The six lorisid humeri display more remodeling than the femora, but also intra-individual variation (7-47% of the cortex), with the smallest individual displaying the least remodeling. Secondary osteons are found in all four quadrants of the cortex, with areas of increased density that are not consistent among individuals. Most of the remodeling is concentrated in the endosteal cortex, primarily surrounded by CCC bone. However, there are also secondary osteons found in the periosteal cortex associated with a range of primary tissue types.

In the five sample radii, the amount of intracortical remodeling varies between 2% and 33% of the cortex. The smallest proportion of remodeling is found in the

smallest individual, with only two secondary osteons, located in the posterolateral cortex. In the remaining four individuals, remodeling events are distributed in all quadrants except medially in a single individual. The distribution is even in some individuals, and has a preferred quadrant in others (although this quadrant varies among individuals). The secondary osteonal tissue is largely associated with CCC tissue, but in two individuals it is also found in the periosteal cortex. Variation is also high in the five sample ulnae (remodeled area ranges between 6% and 59% of the cortex), with the smallest individual showing the smallest proportion of intracortically remodeled bone. In all but the latter, secondary osteons are distributed among all quadrants with posterior concentrations in all four, and anteromedial concentrations in three of the four. These coincide with the presence of attachment sites for the flexor and extensor carpi ulnaris posteriorly, and the flexor and/or extensor digitorum profundus anteriorly. Remodeling in all ulnae is primarily clustered in CCC tissue areas, but also at the endosteal/periosteal boundary, in the more endosteal portions of the periosteal bone, and more peripherally in the posterior and anteromedial cortex in some cases, even reaching the periosteum. In the smallest individual, the intracortical remodeling is restricted to a few isolated events in the medial and lateral quadrants of the endosteal cortex.

Unlike the case for other taxa, the tibia does not display a concentration of intracortical remodeling in the anterior cortex. Rather, remodeling is distributed among all quadrants, although with little or none medially in three of the four sections. Remodeling is low (6-16% of the cortex) in three of the four individuals; 37% of the cortex is remodeled in the fourth. The degree to which a cortex is remodeled does not relate to total cortical area. Secondary osteons are found in the endosteal cortex (again

most often surrounded by CCC tissue), at the periosteal/endosteal boundary, or close to endosteal bone in most cases. Exceptions are found in two bones where there is remodeling in the posterior and posteromedial quadrants among various periosteal primary tissue types.

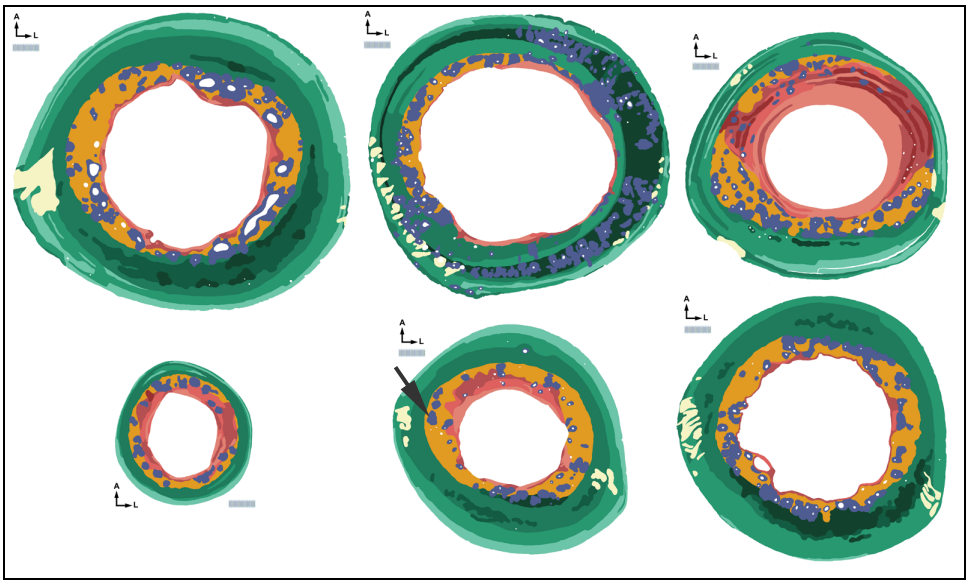

**Figure 5.18: Lorisid femora.**
*Nycticebus coucang* (DUPC 1972), *Perodicticus potto* (DUPC 930), *Nycticebus coucang* (HC 27), *Loris tardigradus* (DUPC 1964), *Nycticebus coucang* (MCZ 36116), *Nycticebus coucang* (MCZ 422). See text for description. Purple indicates secondary osteons. For grayscale reproductions, the arrow points to an example of a secondary osteon. Scale bar indicates .5 mm.

*5.6.6.3.4 Cheirogaleidae*. As with the lorisids, the intracortical remodeling in the femora of this taxon is found exclusively in the CCC parts of the section, but with no preferential sectoral distribution. Two of the four individuals display only a few isolated secondary osteons, while remodeling in the remaining two is more extensive (up to 14% of the cortex). This variation is not size related; while the smallest cortex displays the least remodeling, one of the largest has comparably few osteons. Remodeling in the humeri is also found almost exclusively in the CCC areas of the section, with a few exceptions where the secondary osteons are surrounded by other endosteal tissues, or are in the

periosteal cortex. Unlike the femur, variation is size related; the individual with the smallest cortical area also displays the least remodeling (<1% of the cortex, with larger cortices displaying up to 14%). Intracortical remodeling is preferentially distributed in the medial and lateral cortices, where CCC tissue is also found.

In the two sample radii, secondary remodeling is found in all quadrants except anteriorly and comprises 20% of the cortex in both cases, despite the large difference in total cortical area. Secondary osteons are found predominantly in CCC areas, but also medially in the periosteal cortex at the likely sites of the attachment of the flexor digitorum profundus and/or the abductor pollicis longus muscles. In contrast to the radii, the two sample tibiae contain only 4.5% and 8% secondarily remodeled bone respectively, with the smaller individual displaying less. In both individuals the secondary osteons are clustered in the anterior cortex (with a few isolated osteons posteriorly in the larger cortex). They are surrounded by periosteal parallel-fibered or fibrolamellar bone, although close to the border with the thin endosteal layer. There are no sample ulnae for this taxon.

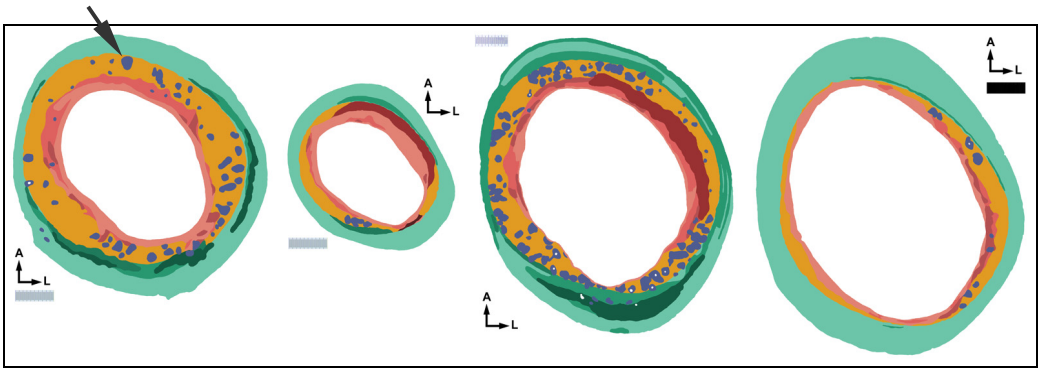


**Figure 5.19: Cheirogaleid femora.**
*Cheirogaleus major* (DUPC 2612), *Microcebus murinus* (DUPC 825), *Cheirogaleus major* (MCZ 44850), *Mirza coquereli* (DUPC 359). See text for description. Purple indicates secondary osteons. For grayscale reproductions, the arrow points to an example of a secondary osteon. Scale bar indicates .5 mm.

*5.6.6.3.5 Indriidae*. Here as well there is heterogeneity in the degree to which the femoral sections are intracortically remodeled. While two of the three femoral sections display large areas of densely congregated secondary osteons (15-39% of the cortex), the third section is almost osteon free (c. 1% of the cortex). In two of the three individuals, osteons are concentrated in the anterior and/or posterior sectors of the anteroposteriorly elongated cortices. In the third individual, the heaviest remodeling is found in the anterolateral and posteromedial sectors. However, the orientation of this section is rotated slightly clockwise relative to the other two (perhaps an artifact of specimen preparation). In all three specimens, the remodeling is found primarily at the extremes of the long axis of the cortex. Remodeling is found mostly, although not exclusively, in regions where the interstitial tissue is of the fibrolamellar type.

The two small indriid humeral midshaft sections (*Propithecus* sp. individuals) display intracortical remodeling comprising 21-22% of the cortex, while the value is 57% for the much larger *Indri indri* individual. In the two sifakas, the remodeling is concentrated anteriorly where there is CCC bone, and also within other endosteal tissues in the anterior cortex. Secondary osteon clusters are also found posterolaterally throughout the thickness of the periosteal tissue at the likely site of brachialis and/or brachioradialis muscle attachment, surrounded mostly by LAM tissue. In one of the two there is a small periosteal medial cluster of osteons, probably at the attachment site of the coracobrachialis muscle. In the large *I. indri*, remodeling again is found largely where there is CCC bone. However, in this case, CCC is found in all quadrants rather than just anteriorly, as is the dense remodeling. Both CCC bone and the incidence of remodeling are greatest in the anterior cortex, where remodeling also crosses over into periosteal

tissue. As with the other two humeri, there is a periosteal cluster of secondary osteons posterolaterally, surrounded by a range of primary tissues, and a medial cluster matching the location in one of the two sifakas.

There is only one each of the radius, ulna and tibia midshafts for this taxon, belonging to a single sifaka. In the radius, secondary osteons (composing 46% of the cortex) are found in all four quadrants, mostly clustered in CCC areas, but also among other endosteal tissues and bridging the boundary between endosteal and periosteal bone. There are also two clusters of periosteal osteons: one anterolaterally where the pronator teres muscle likely inserts, and the other posteromedially where the abductor pollicis longus probably originates. In the ulna, secondary osteons (composing 67% of the cortex) are also found in all four quadrants, with the highest concentrations medially and laterally, and throughout both endosteal and periosteal portions of the cortex, surrounded by a range of primary tissue types. In the tibia, secondary osteons (composing 47% of the cortex) are found in all four quadrants, most predominantly in the anterior quadrant, and least densely laterally and medially. All tibial intracortical remodeling is found within periosteal bone. Anteriorly and posteriorly the distribution spans the entire thickness of the periosteal cortex, while medially and laterally the osteons are preferentially located closer to the periosteal/endosteal boundary. While the remodeling is found surrounded by all primary tissue types, it is often clustered in fibrolamellar areas.

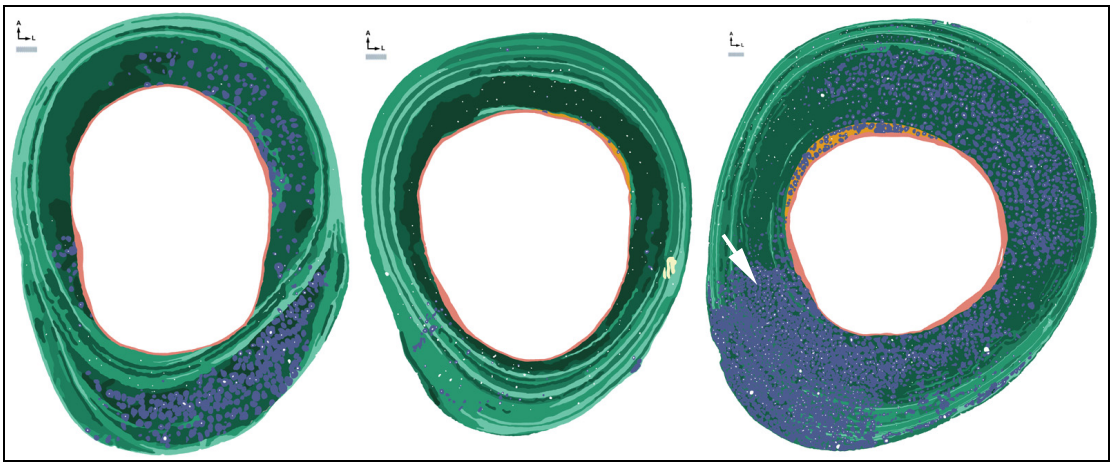

**Figure 5.20: Indriid femora.**
*Propithecus* sp. (MNHU 44684), *Propithecus* sp. (MNHU 44685), *Indri indri* (HC 19). See text for description. Purple indicates secondary osteons. For grayscale reproductions, the arrow points to an example of an intracortically remodeled area. Scale bar indicates .5 mm.

*5.6.6.3.6 Lemuridae.* In the two lemurid femoral specimens examined here, intracortical remodeling varies but remains light: 5% in one individual and 14% in the other. In this case, as would be predicted, it is the larger individual that displays the greater proportion of remodeled bone. Secondary osteons are mostly concentrated in the CCC bone but also may be found elsewhere in the cortex, in areas of fibrolamellar tissue. In one individual the remodeling is found anterolaterally only, while in the other it is distributed around the cortex, but with the highest proportion medially. In the humerus, 18% of the cortex in the smaller of the two specimens is composed of intracortically remodeled bone, while 30% is remodeled in the larger. In both, the remodeling is found in all four quadrants, although with a minimal presence posteriorly. The secondary osteons are generally clustered in CCC bone areas, with some occurrence in other endosteal tissues or in the periosteal portions of the cortex. Most notable within periosteal bone is the presence of medial and posterolateral clusters in the larger individual at the likely sites of

coracobrachialis muscle for the former, and the brachialis and/or brachioradialis muscles for the latter.

There is only one radius, ulna and tibia midshaft section for this taxon. 47% of the radius is intracortically remodeled, with secondary osteons found in all quadrants and most often within CCC bone areas or at the periosteal/endosteal boundary, although also crossing into periosteal bone in the lateral and posterior quadrants. 70% of the ulna is composed of intracortically remodeled bone, found in all four quadrants and throughout the thickness of the cortex, with the least remodeling in non-CCC endosteal tissues and the periosteal portions of the medial and lateral quadrants. The thicker anterior and posterior quadrants contain the largest proportions of remodeling. 38% of the tibia is remodeled, with remodeling found in all four quadrants but most prominently anteriorly, and least prominently in the medial and lateral quadrants. All tibial intracortical remodeling is found within periosteal bone (there is no CCC tissue in this section), distributed throughout the thickness of the cortex anteriorly, but clustered at the periosteal/endosteal border elsewhere. The exceptions to this pattern are two bunches at the periosteal edge, one posterolaterally, and one posteromedially. These may indicate the origin of the flexor tibialis.

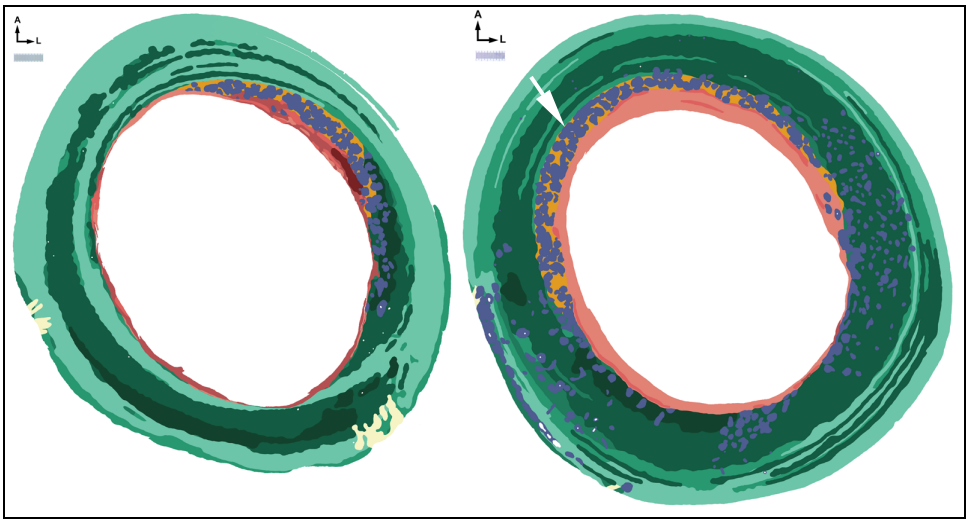

**Figure 5.21: Lemurid femora.**
*Lemur* sp. (HC30), *Varecia variegata* (MCZ 18740). See text for description. Purple indicates secondary osteons. For grayscale reproductions, the arrow points to an example of an intracortically remodeled area. Scale bar indicates .5 mm.

*5.6.6.3.7 Tarsiidae.* Tarsiid femora are characterized by a near absence of intracortical remodeling. Two of the four individuals each have two secondary osteons each, while the other two have none. Two of the four sample humeri display somewhat more remodeling (about 15% of the cortex), concentrated at the endosteal/periosteal boundary anteromedially, and surrounding a large vascular space posteriorly. Each of the remaining two humeri display only a few isolated secondary osteons, in the anterior and medial quadrants, within the endosteal bone or at the boundary between endosteal and periosteal bone.

One of the two sample radii contains no secondary osteons. In the second, two remodeling events are found periosteally in the lateral quadrant, likely at the origin of the pronator teres muscle and/or the insertion of the supinator muscle. One of the two sample ulnae contains no intracortical remodeling. In the other, a single secondary osteon is located within CCC bone anterolaterally. In the two tibiofibulae, the only

intracortical remodeling is found in the region of the fusion between the two bones and within the fibular portion of the cortex in one individual. In all cases the secondary osteons are found within periosteal bone of various primary types (excluding fibrolamellar, of which there is none in these sections).

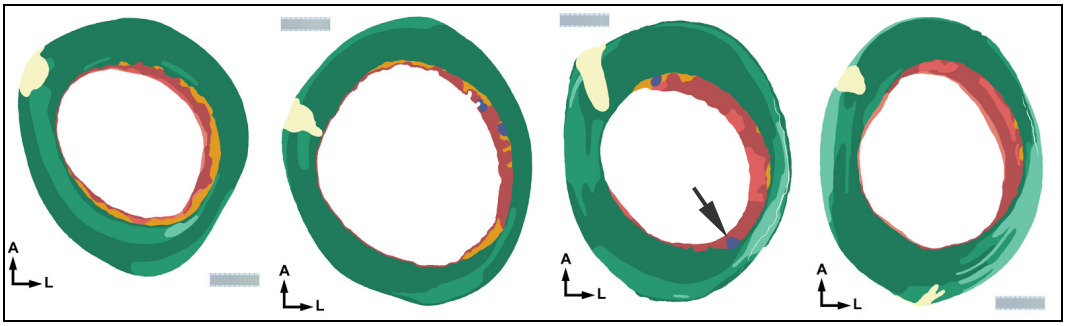


**Figure 7.22: Tarsiid femora.**
*Tarsius spectrum* (MNHU An11318), *Tarsius syrichta* (DUPC 81), *Tarsius spectrum* (HC 16), *Tarsius* sp. (HC 23). See text for description. Purple indicates secondary osteons. For grayscale reproductions, the arrow points to an example of a secondary osteon. Scale bar indicates .5 mm.

*5.6.6.3.8 Callitrichidae*. The two *Callithrix* individuals examined here display very little intracortical remodeling in the femur: 5% in one individual (concentrated in the CCC bone of the medial and lateral sectors), and only two remodeling events in the other, clustered together in the most endosteal portion of the posteromedial periosteal cortex. In this individual there is no CCC bone. Remodeling in the humerus is also light, but is present in larger proportions than in the femur: 3% in one cortex, and 9% in the other. The remodeling in both individuals is found anteromedially and laterally, in regions of the cortex that are mostly composed of CCC bone, but also other endosteal tissues. In one individual there is a remodeling event surrounding a large vascular space in the posterior periosteal cortex.

In the single sample radius, remodeling accounts for 7% of the total cortical area. The secondary osteons are found medially, laterally and posteriorly within the periosteal cortex, but abutting the endosteal tissue (there is no CCC bone in this section). Where the periosteal cortex is thin (laterally and posteriorly) the osteons span its complete width. In the single sample ulna, remodeling accounts for 11% of the cortex. Secondary osteons are found anteriorly, posteriorly and posterolaterally. They are clustered at the periosteal/endosteal boundary. There are no sample tibiae for this taxon.

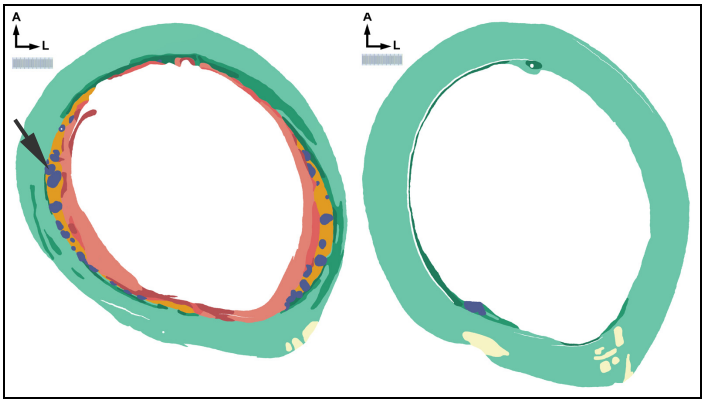


**Figure 5.23: Callitrichid femora.**
*Callithrix geoffroyi* (MNHU 34381), *Callithrix* sp. (HC 28). See text for description. Purple indicates secondary osteons. For grayscale reproductions, the arrow points to an example of a secondary osteon. Scale bar indicates .5 mm.

*2.6.6.3.9 Cebidae.* In the four *Saimiri* femora, intracortical remodeling occurs almost exclusively in the CCC parts of the bone, amounting to between 10% and 22% of the cortex. In two individuals, isolated osteons are also found posteromedially at the probable insertion of the adductor magnus muscle. The sectoral distribution of the remodeling varies from one individual to the next. In the three humeri, remodeling accounts for 13-24% of the cortex, found predominantly in the medial, anterior and lateral quadrants (where CCC bone is found), with small amounts posteriorly. In most cases the intracortical remodeling is concentrated in CCC tissue areas, but also may be

found among other endosteal tissues, and at the periosteal/endosteal boundary. In two of the three individuals a single secondary osteon surrounds a large vascular space in the periosteal posterior cortex.

In the two radii, secondary osteons comprise 15-20% of the total cortical area. Although in both individuals intracortical remodeling is concentrated in CCC areas, among other endosteal tissues, and at the endosteal/periosteal boundary, the quadrant distribution in the two differs. In both, however there is a medial cluster of osteons within the periosteal cortex, likely where the pronator teres and/or the supinator muscles insert. In the two ulnae, secondary osteons account for 31-39% of the cortex. The remodeling is found in CCC areas where they exist, but otherwise are distributed throughout most of the thickness of the periosteal bone (not reaching the periosteum). In both individuals, there is an absence of remodeling events medially. Otherwise the distribution is not equivalent in the two sections, with one displaying the most posteriorly and almost none laterally, and the other showing the least posteriorly. In the three tibiae, remodeling accounts for 15-30% of the cortex, with the largest individual showing the lowest proportion of remodeling. In all three, most of the secondary osteons are clustered in the anterior quadrant, within periosteal bone, and spanning almost the full thickness of the cortex (but not reaching the periosteum). In the smaller two of the three specimens, sparser distributions are also found posteriorly and laterally, mostly close to the endosteal boundary but still within the periosteal cortex.

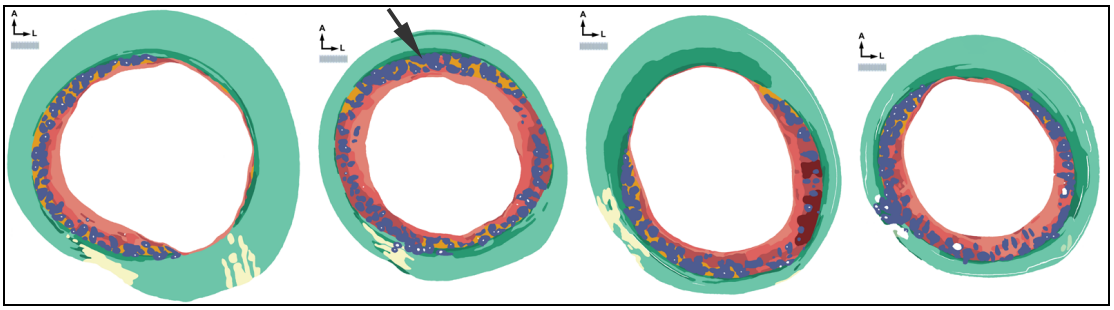

**Figure 5.24: Cebid femora.**
*Saimiri* sp. (MNHU 85197), *Saimiri sciureus* (HC 12), *Saimiri* sp. (HC 13), *Saimiri* sp. (HC14). See text for description. Purple indicates secondary osteons. For grayscale reproductions, the arrow points to an example of an intracortically remodeled area. Scale bar indicates .5 mm.

*2.6.6.3.10 Atelidae.* The two *Ateles* individuals display the largest proportion of femoral intracortical remodeling of all individuals in the sample: 40% of the cortex in one individual, and 61% in the other. The individual with the most remodeling is the larger of the two. In both individuals, the remodeling is distributed around the cortex, with no strong preferential sectoral clustering. In addition, the secondary osteons are located over a range of primary interstitial tissue types, including CCC as well as LAM, HYB and PF bone. In the two humeri, intracortical remodeling covers 67-70% of the cortex, again the largest proportion for all individuals in the study sample. The remodeling is distributed almost evenly among quadrants, and spans the full width of the cortex in most regions, covering endosteal and periosteal primary tissues of various types (including CCC bone), but excluding an endosteal ring of mostly LAM bone. In both individuals there is an absence of remodeling posteriorly in the outer half of the periosteal portions of the cortex. There are no distal skeletal elements for this taxon.

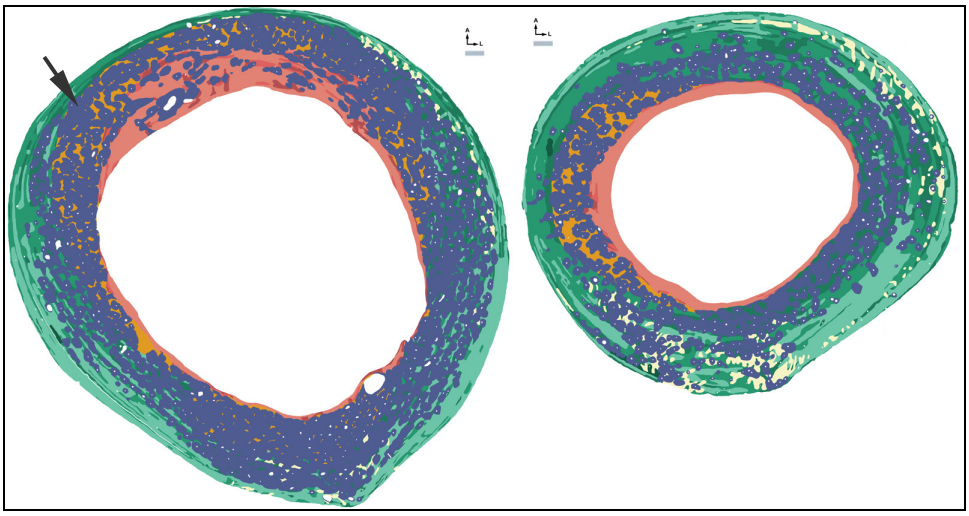

**Figure 5.25: Atelid *femora*.**
*Ateles fusciceps* (FMNH 68811), *Ateles* sp. (MNHU 44079). See text for description. Purple indicates secondary osteons. For grayscale reproductions, the arrow points to an example of an intracortically remodeled area. Scale bar indicates .5 mm.

## 5.7 Discussion

### *5.7.1 Intracortical remodeling and developmental patterns*

In this sample, intracortical remodeling is frequently found in regions that were deposited earlier in development (e.g., portions of the periosteal cortex closest to the endosteal boundary). This finding is consistent with observations of previous researchers, and is in accord with the suggestion that older bone – more likely to have accumulated microdamage and/or necrotic tissue – is more apt to have required repair via replacement of damaged tissue with new bone (a developmental argument that is inseparable from mechanical ones) (Bouvier & Hylander, 1981; Curry, 1984; Burr, 1993; Skedros et al., 1991, 2001; Pfeiffer et al, 1995). The proposition that remodeling will occur in regions where there are existent vascular canals is also supported[4] (de Ricqlès, 1980; Smith,

[4] In contrast to this observation, Enlow (1962a) finds that secondary remodeling is less frequent in more densely vascularized tissues such as plexiform bone relative to less vascularized lamellar areas.

1960b) (e.g., CCC areas[5], or fibrolamellar areas), although it is impossible to know if capillary buds have tunneled into previous avascular bone, for example in lamellar periosteal tissue.[6] These tendencies likely account for some sectoral patterns and element-specific patterns identified in the results section. For example, the concentration of remodeling in the anterior (and sometimes medial and/or lateral) quadrants of sample humeri – and the relative absence posteriorly – coincides with the prevalence of CCC bone in the former (a feature associated with posteriorward drift during development). Enlow has previously commented upon this relationship between the complex CCC bone type and secondary remodeling (e.g., 1962a, 1976). Interestingly, the relative absence of intracortical remodeling posteriorly is evident in all taxa except the lorisids, where the drift pattern is also absent (resulting in a humeral pattern more similar to that found in the femur)[7].

A distinct feature of this sample is the greater relative amount of intracortical remodeling in the elements of the forelimb as compared to the femur (as well as the tibia, although differences between the tibia and forelimb bones are not statistically significant). Because the femur comprises a larger TCA than the humerus, radius or ulna, this pattern cannot be size related (see below). Although the humerus contains more CCC bone than the femur, and the tibia comprises the least CCC bone, the femur displays

---

[5] In CCC bone, the spaces between medullary trabeculae are filled in with bone tissue when formerly medullary regions are incorporated into the compacted cortex during growth remodeling and the enlargement and shaping of the whole bone. Bone is deposited within the cancellous spaces until only the lumen of a vascular canal remains (Enlow, 1963, 1982). Thus CCC bone comprises numerous vascular channels.

[6] Secondary osteons can form in previously avascular bone through osteoclastic resorption by an invading capillary bud (Enlow, 1982).

[7] As was described in Chapter 4, this pattern coincides with the unique positional behavior among the lorisids, where humeri and femora function in a more equivalent fashion than is seen in other primates (e.g., Ishida et al., 1990; Jouffroy & Stern, 1990), and where other features of humeral morphology also point to the distinctiveness of this group (Szalay & Dagosto, 1980).

a larger proportion of CCC bone than both the radius and ulna (see Chapter 4). Therefore, the higher proportions of remodeling in forelimb bones cannot be explained by the presence of CCC bone alone. There is on occasion more remodeling in non-CCC endosteally formed bone than in periosteal bone. It *is* the case that all elements of the forelimb include more endosteal bone (i.e., CCC + other endosteal tissues) than do the femur and tibia. Therefore, the relative abundance of intracortical remodeling in the forelimb may be related to this particular development pattern (although a visual inspection of the radius and ulna sections shows that most remodeling in these is found in CCC tissue). The reason for an increase of remodeling in endosteal PF or LAM tissues, also observed by other researchers (see Enlow, 1963; Burr, 1980; Burr et al., 2001; Jerome & Peterson, 2001; but see Smith, 1960b, and Bromage & Boyde, n.d. for contrary observations), remains obscure, as they are neither necessarily highly vascularized nor older than other regions of the cortex. In addition, mechanical explanations (see below) would predict more intracortical remodeling at the periphery of the bone where strains are highest.

Several possible explanations for this pattern – and the general concentration of remodeling away from the periosteal edges – exist. First, if the function of the intracortical remodeling is to liberate calcium, and if the bone in more peripheral regions of the cortex is not in need of repair to maintain the mechanical properties of the bone, it could conceivably be preferable to remodel where strains are lowest (i.e., endosteally), rather than risk increasing the porosity of bone where strains are high at the periphery of the cortex. In support of this, Burr et al. (2001) found that the mechanical properties (ultimate force, stiffness and work to fracture) of the humerus of *Macaca cynomulgus*

were not reduced due to increase in remodeling and porosity after treatment with parathyroid hormone, because the induced remodeling was concentrated near the endosteal surface. Robling & Stout (1999) found that the drifting osteons preferentially drift towards the endosteum. They interpret this as evidence against a metabolic function because, within endosteally deposition regions of the cortex, endosteal-ward drift means drift towards younger, and less mineralized bone (resulting in liberation of less mineral into the system). However, if there were a need to limit porosity due to remodeling where strains are highest, endosteal-ward drift would be adaptively sensible. Skedros et al. (2001) also posit a metabolically influenced pattern, suggesting that the nearby presence of the marrow might account for the predominance of endosteal remodeling in some quadrants of the cortex in their study of *Odocoileus hemionus hemionus* (mule deer) calcanei.

Another explanation, relevant to all endosteal tissues (including CCC bone) is found in the argument put forth by Otter et al., (1999), where strenuous activity loads bones such that blood flow into the medullary cavity and therefore the internal two thirds of the cortex is reduced, subsequently triggering intracortical remodeling (perhaps through reduction in oxygen or nutrient supply and/or waste removal). This argument is meant to explain the predominance of stress fractures, not in areas of maximum cyclic strain where microdamage accumulates, but rather in other parts of the bone where intracortical porosity has been observed to increase in response to experimental axial loading: in the inner two thirds of the cortex, and near the neutral axis. It is debatable whether this argument, generated to explain patterns of stress fracture resulting from extreme levels of activity in army recruits, is relevant to the normal activity patterns of

primates in their natural habitat. However, the possibility that a difference in the source of arterial flow between the outer and inner parts of the cortex may relate, in some way, to differences in patterns of intracortical remodeling is intriguing.

Having said all this, it is also clear that remodeling is not *restricted* to older regions of bone, or to regions where the interstitial tissue is vascular, or to the endosteal portions of the cortex. Rather, it can be found distributed throughout the thickness of the cortex in some specimens (see, for example, Figures 5.20, 5.25 above). Secondary osteons are often also found clustered at the periphery of the cortex in locations of soft tissue insertion, surrounded by avascular or lightly vascularized periosteally deposited bone. This will be discussed below in reference to localized strain adaptations.

*5.7.2 Intracortical remodeling and body size*

In accord with results for primates described by other authors (principally Paine & Godfrey, 1997; but see also Schaffler & Burr, 1984), I have found that body size (as measured using the proxy TCA) does account for the greatest explained proportion of the variation in intracortical remodeling among individuals. The larger the cortex for a given element, the greater the proportion of that cortex that is likely to be composed of secondary osteons. So, for example, the femur of a lemurid will display more remodeling than the femur of a galagid. This is consistent with findings of Paine & Godfrey (1997) where, in a sample of cercopithecids and galagids, percent secondary osteonal area (including intact and fragmentary osteons) increases with body size in the femur and humerus. In contrast, my results do not support the findings of Schaffler & Burr (1984). These authors suggest that secondary osteonal area does not principally track body size;

rather, they contend that positional behavior is the main factor contributing to variation in percent intracortically remodeled area in a wide range of primates (see below). Although they do acknowledge a body size effect, they argue that exceptions to the size related pattern temper its importance. The small sample sizes (one individual for all taxa except humans) and different methodologies (the authors use a point counting method and only consider intact secondary osteons) may in part account for the different conclusion reached by Shaffler & Burr as compared to Paine & Godfrey or the current study.

The reason for the relationship between body size and remodeling is not entirely evident. It has previously been shown that normal peak strains in bone are not greater in larger mammals, and safety factors have been found to be remarkably consistent among terrestrial mammals (Rubin & Lanyon, 1985; Biewener, 1989a, 1989b, 1990, 1991, 2002, 2005, Blob & Biewener, 1999). Therefore, arguments for greater microdamage (and repair) in larger animals are not well supported by the evidence. In addition, although larger animals live longer, there is no indication that intracortically remodeled area in the primate adult cortex – as a proportion of total cortical area – increases with aging in the adult (Schaffler & Burr, 1984; Burr, 1992; Paine & Godfrey, 1997; Jerome & Peterson, 2001).

There is some evidence that intracortical remodeling may increase with faster growth rates, often present in larger animals (Paine & Godfrey, 1997). However, as described in Chapter 3 and discussed in Chapter 4, faster growth rates are not always associated with larger body size. A phylogenetic pattern reflecting differences in growth rate, such as the one I have identified for FAST bone (another microstructural feature that appears to track body size), is not evident for secondary osteonal area in the current

sample. Previous primate studies support this conclusion. Paine & Godfrey find no evidence within their cercopithecid sample that taxa with faster growth rates remodel larger proportions of the femoral or humeral midshaft cortex. Shaffler & Burr (1984) also find no phylogenetically influenced pattern in their sample. Thus, the relationship between body size and intracortical remodeling, although intuitively sensible, remains somewhat of an explanatory conundrum.

This size dependent pattern is not repeated within individuals; that is, the femur of a given individual will not display more intracortical remodeling proportionately than other, smaller elements for that individual. Within individuals, therefore, the relationship between cross-sectional cortical area and remodeled area is not as would be predicted if cortical area alone was the explanatory factor. Both developmental (see above) and mechanical (see below) explanations must be explored to better understand this pattern.

*5.7.3 Intracortical remodeling and mechanical adaptation*

Although both multiple regression and simpler non-parametric analyses indicate that body size is the principal predictor of the amount of intracortical remodeling in a cortex, positional behavior also clearly accounts for some of the variation observed in this sample.

First, as has been previously observed by other researchers, secondary osteons are often clustered at sites of soft tissues attachment. The suggestion is that tensile stress due to muscular loading in these areas is more likely to result in intracortical remodeling (Portigliatti-Barbos et al., 1983; Skedros et al., 1994; Goldman et al., 2003) and/or that secondary osteons at sites of soft tissue attachment serve to anchor soft tissue deep within

the cortex during remodeling (e.g., Enlow, 1962a; 1966). This clustering accounts for at least one of the element specific patterns identified in the sample: the increase in intracortical remodeling in the lateral quadrant of the radius, relative to other quadrants, is likely due to those secondary osteons grouped at the periosteal margin, coinciding with the attachment there of the pronator teres muscle, a flexor and pronator of the forearm (Figure 5.26). This pattern is apparent in the majority of specimens, the exceptions being two lorisids, and the single indriid radius in the sample (where periosteal clustering occurs in the anterior, rather than lateral, cortex). Other instances of secondary osteon concentrations at muscle attachment sites exist, but the radial example is the only one that is present in the majority of individuals.

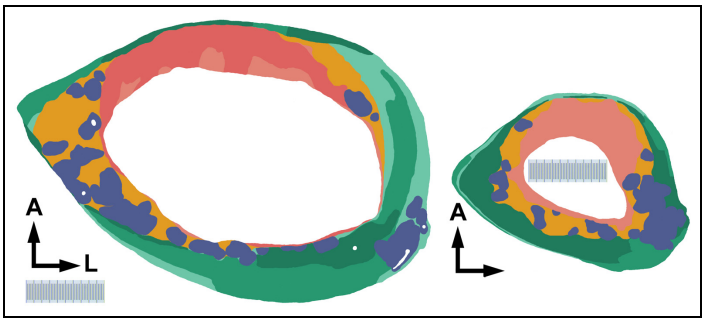


**Figure 5.26: Cheirogaleid radii.**

Mirza coquereli *(DUPC 359),* Microcebus murinus *(DUPC 825).* In both sample cheirogaleid radii, a cluster of secondary osteons is found in the lateral cortex, close to the periosteal margin. Notice also the intracortical remodeling within the CCC (yellow) bone. Scale bar indicates .5 mm.

The pattern of intracortical remodeling in the tibia, where secondary osteons are strongly concentrated in the anterior cortex (Figure 5.27), may also be influenced by the attachments of the tibialis anterior (dorsiflexor and inverter of the foot) and abductor hallucis longus muscles there. This anterior concentration is present in all taxa for which there are tibial specimens, with the exception of the lorisids and the tarsiids. In the former, remodeling is evenly distributed around the cortex while in the latter, the few osteons that are present are located principally at the fusion site of the tibia and fibula.

Unlike the secondary osteonal concentration in the lateral radius, tibial anterior quadrant remodeling events do not necessarily hug the periphery of the bone, but rather are distributed throughout the thickness of the cortex, or may even be concentrated close to the periosteal/endosteal boundary, as in the cheirogaleid specimens. It may be that muscular loads have incurred fatigue microdamage in parts of the cortex that are deep to the surface earlier during the development, or that the muscle induced loads in the adult cortex are great enough to effect microdamage deep into the bone tissue. Alternatively, non-muscular loads due to weight bearing during locomotion may result in the sectoral pattern observed in the tibia. However, even in this case, if the tibia were loaded in bending (as is most often suggested to be the case for mammalian long bones) the stresses would be greatest at the most peripheral reaches of the cortex (Burr, 1993). This should still, theoretically, produce a pattern where intracortical remodeling is concentrated at the outer margins, rather than towards the middle or endosteal parts of the cortical thickness. Only a consideration of bone tissue age and metabolic factors (see above, and as argued by Currey, 1984) provides a reasonable explanation for the distribution of the remodeling within the anterior quadrant.

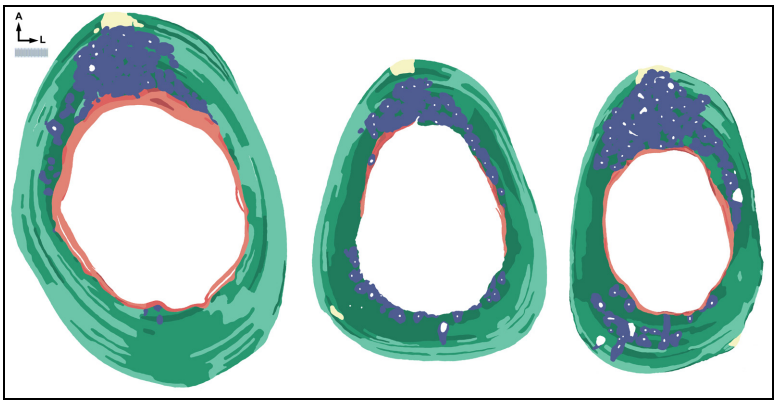


**Figure 5.27: Cebid tibiae.**

*Saimiri* sp. (MNHU 85197), *Saimiri* sp. (HC 13), *Saimiri* sp. (HC14). See text for description.

The tibial anterior quadrant pattern leads to consideration of another potential relationship between mechanical adaptation and intracortical remodeling: the increase in intracortical remodeling activity in regions of tensile load that has previously been reported in the literature. For example, Skedros et al. (2001) find 14.2% less remodeled area in the compression cortex of mature mule deer calcanei than in the tensile cortex.[8] A potential explanation for this lies in the observation that bone tissue is weaker in tension, presumably leading to more microdamage and thus stimulating more repair in the form of intracortical remodeling (Skedros et al., 1994; Burr et al., 1998). Tensile strains lead to interlamellar debonding, as well as crack accumulation, at a faster rate than under compressive loads. The latter may not apply to primary tissues, however, as it is the arresting of cracks by the osteonal boundaries under tensile load that contributes to their accumulation. Under compression, cracks are believed to cut across osteons, resulting in longer, but fewer cracks. It is apparently the accumulation, rather than the length, of the cracks that shortens tensile fatigue life (Burr et al., 1998).

Might the pattern of anterior quadrant intracortical remodeling in tibia correspond with tensile strain in that quadrant? There are no strain gauge data for the study taxa to support this proposition. However, a single strain-gauge study of the *Macaca mulatta* tibial midshaft indicated that this element is subjected to bending loads, superimposed by axial compression, and that the anterior cortex is in tension (Demes et al., 2001). It is possible, therefore, to speculate that the pattern of secondary osteons in the taxa in this study might reflect anterior tension due to an anterior-posterior bending regime.

---

[8] In a separate study of equine third metacarpals, Skedros et al. (1996) find an opposite result. In this case, the compression cortex displays a greater fractional area of secondary osteonal bone than the tension cortex. Given the absence of strain gauge data for the bones and taxa studies here, the possibility must be considered that a quadrant displaying the most remodeling may lie on the compressive, rather than tensile, side of the neutral axis in a bending regime.

Interestingly, the two taxa in which this pattern does not occur provide either structural or behavioral exceptions relative to the others in the study. First, there is no intracortical remodeling anteriorly in the tibiae of the two tarsiids in the sample. In these individuals, the intracortical remodeling occurs only along the site of fusion of the tibia and fibula. Since these two bones are fused, the cross section of the element is altered, and it is likely that the loads are distributed differently than what they would be in species with separate tibiae and fibulae. Therefore, it is not surprising that the same anterior clustering does not occur. Secondly, the four lorisid tibiae display a pattern of roughly equivalent remodeling in all quadrants. Given the deliberate, acrobatic behavior of the members of this family, together with the relative roundness of cross-sections, it has been suggested that bending might not occur preferentially in a single plane in the long bones, and/or that there might be a principal regime of axial loading, at least in the femur and humerus (Demes & Jungers, 1989; Ruff & Runestad, 1992; Terranova, 1995b[9]; Runestad, 1997). Either of these arguments would support a mechanically determined pattern of remodeling that does not favor any one quadrant.

In summary, strong patterns of intracortical remodeling among quadrants in the midshaft tibia potentially reflect a mechanical adaptation, with remodeling preferentially occurring in a quadrant habitually loaded in tension. Are there similar sectoral patterns in other elements in the sample? As noted above, the pattern in the radius is likely related to muscle attachment in the lateral quadrant. There are no significant differences among quadrants in the ulna, despite the likelihood, or at least the possibility that this bone is subjected to bending in some taxa. For example, Demes et al. (1998b) identify

[9] Terranova's (1995) study of midshaft cross-sectional geometry also identifies equivalent anteroposterior and mediolateral bending strengths among cheirogaleids, while in the current sample there is an anterior clustering of secondary remodeling in this family, unlike the distribution in the lorisids.

mediolateral bending in the ulna of *Macaca mulatta*, with the lateral cortex in tension and the medial cortex in compression, albeit with peak strain magnitudes that are lower than those typically reported in the literature for long bone strains in non-primate taxa. They offer, as an explanation for lower strain magnitudes, that the radius might be transmitting a larger portion of the load. Although lower strain magnitudes could be used as an explanation for the lack of a sectoral pattern in intracortical remodeling in the sample ulnae for the current study, a compensatory pattern is not present in the radius. In the latter, only the clustering related to muscle attachment, as described above, is present.

Midshaft loads in the femur of a range of primates have been studied by a number of researchers, although all interpretations of stress and strain rely on cross-sectional geometric parameters, ground reaction forces, kinematic and kinesiological approaches, and investigations of muscular volumes, morphologies and attachments; there have, to date, been no strain gauge data for the midshaft non-human primate femur. Mostly with reference to cross-sectional geometric parameters, it has been argued that, depending upon habitual positional behavior, there are differences in the loads to which a midshaft femur is adapted, although most primates (in particular arboreal primates) are believed to support a greater proportion of their weight in the hindlimbs than the forelimbs (Reynolds, 1985; Kimura, 2002, 2003). For example, it has been found that most leapers display greater anteroposterior (AP = sagittal) bending rigidity than mediolateral (ML = coronal) bending[10], as well as greater resistance to axial compression and torsion than less frequent leapers (Burr et al., 1982, 1989a; Demes & Jungers, 1989, 1993; Terranova, 1995a, 1995b; Runestad Connour et al., 2000). This is in theory due to some

[10] This pattern of AP bending rigidity is de-accentuated in larger leapers. That is, relative to AP, larger leapers have greater ML dimensions at the femoral midshaft, than smaller leapers.

combination of higher peak forces because of larger accelerations of the center of gravity, larger ground reaction forces, and strong muscular contractions of the extensors of the knee and hip (quadriceps and hamstrings respectively) during rapid acceleration at the launching and landing of a leap on flexed limbs[11] (Burr et al., 1982; Terranova, 1995b; Aerts, 1998). In support of this, Aerts (1998) has shown that, in *Galago senegalensis*, the large and powerful quadriceps muscle comprises 53% of all leg muscle mass, and is composed of 87% fast muscle fibers.

Given the potential prevalence of AP bending loads at the midshaft femur of vertical-clinger leapers, the expectation would be for a larger proportion of intracortical remodeling in either the anterior or posterior quadrant with the assumption that one of these would habitually be sustaining tensile strains. The data from the current study are in accord with this prediction. Although not statistically significant, among larger vertical-clinger leapers (i.e., those with a large enough proportion of the cortex remodeled to discern sectoral patterns; three indriids and one greater galago), the posterior quadrant is the most highly remodeled (see Figure 5.12). This remodeling is found throughout the thickness of the periosteal cortex, with concentration neither close to the endosteal boundary, nor close to the periosteal edge. Absent strain gauge data, there is no way to know if the posterior cortex is indeed habitually subjected to tensile or compressive loads (with the anterior cortex under the opposite loading regime). However, given the particularly large mass of the quadriceps muscle, it seems not unlikely that it's contraction could function to compress the anterior cortex while incurring tensile strains in the posterior quadrant.

[11] Terranova (1995b) points out that AP bending rigidity, relative to ML, is higher in leapers that land hindlimbs first.

In contrast, among arboreal quadrupeds in the sample, there is no consistent sectoral pattern of intracortical remodeling (Figure 5.12). This is consistent with suggestions, again based mostly on cross-sectional geometric parameters, that femoral midshafts in more generalized quadrupedal primates are less adapted to substantial bending loads in any preferred plane than those of specialized leapers. Cortical dimensions are rounder, with more even ML and AP bending rigidities (Demes & Jungers, 1993; Terranova, 1995b; Runestad Connour et al., 2000). Likewise, among lorisids there are no differences among quadrant means for percent remodeling, and no consistent patterning among individuals except that in four of six individuals, values for quadrants are very close (less than 1% difference – relative to TCA – among quadrants). Again, this is in accord with the observation that lorisid femoral midshafts are round, and that cross-sectional properties suggest no single axis of preferential habitual loading and greater axial rigidity than torsional or bending rigidity (Demes & Jungers, 1989, 1993; Ruff & Runestad, 1992; Runestad, 1997). The large femoral joints in lorisids are highly mobile, indicative of a wide range of limb orientations and movements, which could load the femoral cortices along multiple planes (Demes & Jungers, 1989; Runestad, 1997). In addition, or in concert with this, it has been suggested that lorisid limb bones are subjected to "strong isometric contraction of muscles… subjecting them to high axial ('balanced') loads" (Ruff & Runestad, 1992, p. 421).

Finally, in the two suspensory atelids in this sample, there is a slight increase in intracortical remodeling in the posterior and medial quadrants of the femur relative to the anterior and lateral quadrants. This pattern is more extreme in the individual with more overall remodeling, but the differences among quadrants are not statistically significant.

These data are in agreement with a previous study suggesting that the femur in atelids, as in generalist quadruped primates, is not as buttressed in the AP plane as leapers (i.e., ML and AP dimensions are more even), indicating a lesser significance of bending loads (Runestad Connour et al., 2000).

In summary then, while femoral sectoral patterns of intracortical remodeling are not as striking as those seen in the tibia, and while differences among sectors are statistically insignificant in all cases, there is some indication that remodeling may vary among positional behavior categories in accord with predicted, but untested, loads. The data described here do not coincide with the findings of Paine & Godfrey (1997), where non-leapers in the sample displayed more remodeling in the posterior quadrant of the femur, *G. senegalensis* remodeled in the posterior and lateral quadrants, and O. *crassicaudatus* showed no quadrant differences in remodeling. This disparity may be in part due to sample composition differences. The non-leapers in Paine & Godfrey's study were all Old World monkeys, some of them habitually terrestrial. In addition, the lesser galagos in my sample had very little intracortical remodeling overall, making it impossible to identify sectoral variation. However, in the greater galagos that displayed substantial intracortical remodeling, this was most heavily concentrated in the posterior cortex.

The humerus does not – in the sample as a whole or within taxa or positional behavior categories – display any sectoral patterning that is independent of the developmental pattern discussed above. That is, most remodeling occurs where there is endosteal bone (principally CCC) and, since this bone preferentially appears in the anterior, medial and lateral quadrants, this is where remodeling events are generally

found (Figure 5.28). Studies of cross-sectional geometry, as well as well as a single strain gauge study on *Hylobates* (potentially comparable to the atelids in this sample) suggest that many primate humeri are not loaded principally in bending (Swartz et al., 1989 for *Hylobates*; Demes & Jungers, 1989 for lorisids, 1993 for a wide range of prosimians; Demes et al., 1991 for indriids; Ruff & Runestad, 1992 for lorisids; Terranova, 1996 for a range of strepsirhines; Runestad, 1997 for lorisids). There may be exceptions to this general observation, for example evident in the increased humeral AP bending rigidity in *Euoticus elegantulus*, a species not included in the current study (Terranova, 1996). Given the apparent lack of habitual bending in any one plane and a predominance of axial loading (either tensile or compressive) for most taxa – as most of the cross-sectional data and the strain gauge study suggest – the lack of mechanically adaptive sectoral patterning in the humerus is not surprising.

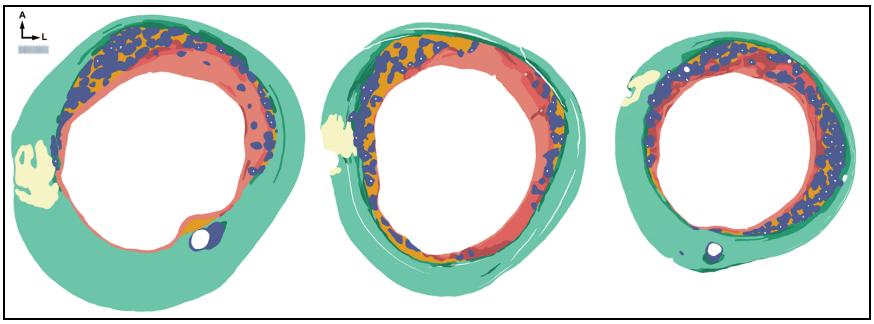

**Figure 5.28: Cebid humeri.**
*Saimiri* sp. (MNHU 85197), *Saimiri* sp. (HC 13), *Saimiri* sp. (HC14). See text for description.

To summarize, with respect to sectoral variation in intracortical remodeling, only the tibia and femur display distinct patterns that are explicable via an examination of limb mechanics and the loads hypothesized to be present across the midshaft cortex. While the absence of a pattern in the humerus may also accurately reflect the mechanical

adaptation of this bone, this explanation must remain more tenuous. The lack of distinctive patterns in the forelimb bones, relative to those of the hindlimb, is interesting in light of the proposition that primates, in particular arboreal species, carry more of their weight in the hindlimb (Reynolds, 1985; Kimura, 2002, 2003). It is tempting to surmise that mechanically adaptive patterns of intracortical remodeling appear in the femur and tibia because these elements are habitually subjected to greater loads than the humerus, radius or ulna. However, an examination of percent remodeling across whole cortices complicates this argument. As described above, the elements of the forelimb comprise larger percent areas of intracortical remodeling than the elements of the hindlimb. Although some of this may be due to developmental patterns (e.g., a preponderance of remodeling in areas of CCC bone), such explanations are incomplete. Unfortunately, mechanical explanations for this hindlimb/forelimb pattern remain, for the time being, elusive.

More fruitful is an examination of the percent intracortically remodeled bone in the proximal vs. distal skeletal elements of a given limb. It has been shown by previous authors that, at least in cursorial non-primate mammals, distal elements tend to intracortically remodel more than proximal elements (Lierberman & Pearson, 2001; Skedros, et al., 2003). Limbs are typically tapered, with distal skeletal elements (e.g., the radius) comprising smaller cross-sections than more proximal elements (e.g., the humerus), resulting in minimized kinetic energy expenditure during locomotory acceleration and deceleration of the distal parts of the limb "through a greater range of velocity than that required by the more proximal parts" (Skedros, et al., 2003, p. 837). Because of reduced cross-sectional area however, distal elements are subjected to higher

strain and may have lower safety factors. The expectation is thus that distal elements will sustain more microdamage and will replace that damaged bone with secondary osteons, rather than strengthen the shaft via apposition at the surfaces.[12]

For example, Lieberman & Pearson (2001) find higher secondary osteon density in the distal elements of the *Ovis aries* (ram) hindlimb, with this discrepancy increasing in exercised individuals. Skedros et al. (2003) identify a similar (although statistically insignificant) pattern in the forelimb of *Odocoileus hemionus* (Rocky Mountain mule deer). In this case, however, while secondary osteon population densities are highest in the most distal element – the phalanx – values for the radius are higher than those for the metacarpal. The authors suggest that some developmental or unidentified mechanical factors may account for this.

In the current study I have found that percent intracortically remodeled bone is higher in distal elements for both limbs. Specifically, in almost all individual cases, values for tibiae and ulnae are greater than femoral and humeral values respectively. This is in accord with predictions of the studies described above. Interestingly, remodeling in the radius does not typically exceed what is seen in the humerus, while remodeling in the ulna exceeds what is found in the radius in most individuals. The low values in the radius, and the discrepancy between the radius and ulna can perhaps be explained via a consideration of their different roles in weight bearing and supination/pronation, although the specifics of loading patterns on these two bones are unknown. Demes et al. (1998b) suggest that, at least in the macaque, the radius might

[12] An alternative prediction, put forth by Currey (1984) is that remodeling will preferentially avoid elements subjected to high strains because secondary osteonal bone is weaker than primary tissue. In this scenario, remodeling occurs primarily to fulfill metabolic demands.

transmit a greater proportion of the load. This is inconsistent with the observations of more remodeling in the ulna.

Another intriguing exception to the proximal/distal skeletal element pattern is yet again found in the lorisid group. In these individuals, there is less distal element intracortical remodeling relative to proximal element remodeling in the forelimb as compared to other PB groups. This pattern is strengthened as body size increases. Unfortunately, no distal atelid bones are available; it would be interesting to determine whether this pattern is characteristic of species that engage in frequent forelimb suspension.

A relationship between kinematic adaptation and intracortical remodeling can further be observed in values of percent remodeling in whole cortices as they vary among positional behavior categories. These are most clearly evident for the femur and humerus. In both of these bones, the suspensory atelids display the most remodeling. Although it could be argued that this pattern is due to body size, the proportion far surpasses that found in comparably sized vertical clinging and leaping species (the indriids). Furthermore, the slow-climbing lorisids display more remodeling than comparably sized vertical-clinger leapers and arboreal quadrupeds. No significant differences are evident among arboreal quadrupeds and vertical-clinger leapers.

Previous comparative investigations of limb mechanical properties among positional behavior categories can partly provide support for the relationships I have described. For example, it has been found by some researchers (but not all; see Demes & Jungers, 1989, 1992), that lorisids display humeri and femora with greater axial strength than other prosimians (Ruff & Runestad, 1992; Runestad, 1997). It is argued that this

may relate to the sustained muscular contraction during gripping both above and in suspension below branch, rather than gravitational forces produced during lorisid locomotion (Ruff & Runestad, 1992; Runestad, 1997). Support for this is found in several lorisid anatomical features: specialized vascular bundles that maintain circulatory flow during sustained compression, a high proportion of slow muscles fibers, and large flexor digitorum longus and soleus muscles for gripping and resistance to fatigue during gripping (Suckling et al., 1969; Hall-Craggs, 1974; Runestad, 1997). With respect to the atelids, Runestad Connour et al. (2000) have found that resistance to femoral torsional loads are slightly lower than in leapers, but that resistance to axial loads in the two groups are similar. Torsional and bending strength in atelid humeri are greater than in large leapers, whereas compressive strength in the atelid humeri are similar to those in small leapers and most generalists, but greater than in large leapers and lemurids. In other words, there is apparently no clear indication, at least based on cross-sectional geometry, that the atelid femora and humeri are adapted to resist greater axial loads than those of other primates. Therefore, while the relatively high percent remodeled areas found in the lorisids are partly supported by the literature, the same finding in atelids is not. However, cross-sectional geometric parameters do not identify the specific loading regime, for example whether axial strains might be compressive or tensile. The presence of more remodeling in lorisids and atelids is intriguing in light of the possibility that both these groups engage in frequent suspension by both hindlimb and forelimb. Although it has been argued that any tensile loads incurred during suspension might be countered by strong muscular contraction (Runestad, 1997), Swartz et al. (1989) have found that, at least in brachiating gibbons, the forelimb bones are loaded in substantial tension. Given

that this conclusion is derived from strain gauge data, it seems not unreasonable to suggest that both atelid and lorisid bones might also be more frequently subjected to tensile loads than those of other, less suspensory, primates.

My findings regarding the difference in percent intracortically remodeled bone for whole cortices are not in accord with the work of Paine & Godfrey (1997).[13] Specifically, these authors find that, although most variation is accounted for by body size, the leaping galagos have relatively more remodeling in the femur than do the less specialized cercopithecids in their sample. In contrast, I find no differences between vertical-clinger leapers and generalized quadrupeds. Schaffler & Burr (1984) include a sample more comparable to the current study, with five overlapping genera, but only femora, and only a single specimen for each genus (with the exception of *Ateles*, for which they have two). These authors identify similar, although not identical, results to those in my study. First, they find that the single vertical-clinger and leaper and all generalized arboreal quadrupeds display similar proportions of intracortical remodeling in the femur. Second, their suspensory group (including both atelids and *Pan troglodytes*) displays more remodeling than the arboreal quadrupeds and vertical-clinger leapers. Both of these observations are consistent with results from the current study. The authors do not, however, identify a difference between their slow-climbing *Nycticebus coucang* individual and arboreal quadrupeds. Both the similarities within, and difference between, their study and the present work must be considered in light of the very small sample sizes in the former.

As a final consideration of the relationship between mechanics and intracortical remodeling, I note the preponderance of remodeling in CCC bone (as discussed in the

[13] The authors' sample is not comparable to mine; the only overlapping taxon is the galagids.

section on developmental patterns), as well as the frequent tendency for secondary osteons to cluster at the reversal between endosteal and periosteal tissues (also observed by Enlow, 1962a). The relationship between CCC bone and remodeling can in part be explained by the relatively vascular nature of this tissue type. However, both phenomena should also be considered in light of the possibility that discontinuities in bone – cement lines at the edges of bone convolutions in CCC tissue as well as the interface between the endosteally and periosteally deposited tissue – might serve to weaken the bone, just as the cement lines around secondary osteons are purported to do (Evans & Vincentelli, 1969; Martin, 1993). If increased microdamage were a consequence of this reduced strength, intracortical remodeling might be required to maintain the integrity of the tissue under habitual loading.

*5.7.4 Intracortical remodeling, phylogeny, growth rate and metabolism*

Unlike the case for primary tissue types, there appears to be no phylogenetic pattern in the distribution of intracortical remodeling within the midshaft cortex, other than that which is already explained by taxon body size and positional behavior patterns. It can reasonably be inferred, therefore, that there are likely no differences in remodeling due to disparities in growth rate. This is in agreement with the findings of both Schaffler & Burr (1984) and Paine & Godfrey (1997), as well as previous observations by Enlow & Brown (1958) on a vertebrate sample with a much broader phylogenetic spread. I have also found that there is no correlation between resting metabolic rate (RMR) and percent intracortical remodeling ($r^2$=.0066, r=.0814, p>.05).

**5.8 Summary and conclusions**

Returning to questions laid out in the Objectives section of this chapter, I offer the following conclusions. First, there is a substantial range in the proportion of intracortically remodeled bone among elements, individuals and primate taxa. Aside from a general preponderance of secondary osteons in areas composed of CCC bone tissue, no single pattern, either with respect to proportions or sectoral distributions, is characteristic of the sample as a whole. Second – as demonstrated by the multiple regression analysis as well as simpler non-parametric and graphical methods – variation in percent remodeling in whole cortices is most fully accounted for by body size, with larger individuals displaying more remodeling. A less substantial portion of this variation can be attributed to diversity in positional behavior. Third, sectoral variation within elements is, in the humerus, best explained through an examination of underlying tissue types and developmentally determined distributions. In other skeletal elements, mechanical factors appear to be significant contributors to differences in percent remodeling among quadrants; either the very local tensile loads applied by soft tissue at muscle attachment sites (in the radius), or more global regimes of stress and strain across whole cortices (in the tibia and femur). Mechanical factors may also account for the increase in remodeled area in the radius and tibia relative to the humerus and femur respectively. In summary, it can be stated with some certainty that both body size and positional behavior are significant factors contributing to the distribution of remodeling among primates, and that both interact with growth and development to produce the patterns observable in this sample. The lorisids are a particularly interesting group in this

respect, as their unique positional behavior is consistently reflected in distinctive intracortical remodeling regimes.

Several tendencies I have identified remain to be properly explained. The preponderance of remodeling in endosteal tissues may or may not conform to expectations based on mechanical loads, depending upon the explanation invoked to account for it. In addition, while body size and percent remodeling are clearly correlated, there are no satisfying justifications for this relationship. Furthermore, some elements display patterns that are consistent with predictions based on mechanics, yet others do not. Finally, there is substantial intrataxon variation, unexplained by both body size and positional behavior. Both the multiple regression analyses and simpler qualitative and quantitative exploration of the data make evident that some of the observed variation remains to be explained. Clearly, then, other factors must be at play: individual or taxon-specific metabolic differences, variation in activity levels and individual lifetime loading on the bones, dietary differences, sex or age. The literature suggests that all of these may have the potential to impact upon intracortical remodeling. What I have shown, however, is that several factors commonly referred to in the literature – body size, and positional behavior – do indeed impact upon the replacement of bone tissue via intracortical remodeling. I have also demonstrated that a consideration of developmental and primary tissue type patterns is critical to the interpretation of intracortical remodeling distribution within a cortex.

# Chapter 6

# Collagen Fiber Orientation

## 6.1 Introduction

Both primary and secondary bone tissues are composed of a mineralized collagen matrix, punctuated by cell lacunae and vascular channels. As described in Chapter 4, the patterning of the collagen matrix is one of the features that assists in the identification of primary tissue types, and is likely of life history and potentially of mechanical significance. However, beyond the general characterization of the collagen matrix (i.e., woven, parallel-fibered or lamellar) is the question of the orientation of collagen fibers within the matrix. Do they lie parallel to the long axis of a bone, perpendicular to it, or somewhere in between (i.e., oblique to the axis of the bone)? It has been suggested that the orientation – which may vary within and between bones – is of mechanical significance, just as are the orientations of beams within an engineered structure. While the relationship between mechanics and collagen fiber orientation (CFO) in secondary osteons (or in cortices including both primary and intracortically remodeled bone) has been explored by a number of researchers, there has been little concern to date with potential variation within and among primary tissues types. Therefore, a comprehensive investigation of collagen fiber orientation in primary tissues, such as this study provides, is much needed. Furthermore, a comparative study of collagen fiber orientation among a range of primates, or in any other mammalian order, has yet to be undertaken.

**6.2 Background on collagen fiber orientation**

Type I collagen comprises the majority of the organic phase of bone matrix (c. 90%, Cowles et al. 1998), synthesized and extruded by osteoblasts. The orientation of collagen fibers in bone tissues is believed to be determined by the osteoblasts that are secreting the collagen molecules (Boyde, 1972; Boyde & Jones, 1998; Jones & Boyde, 1976; Ascenzi & Benvenuti, 1986; Ziv et al., 1996). The osteoblasts are generally elongated in the same direction as the long axis of the collagen they deposit, and each is responsible for its secretory territory within a surface sheet of bone (Jones & Boyde, 1976).

Type I collagen is a fibrous structural protein, composed of molecules that assemble into triple-helical microfibrils. Each microfibril contains two $\alpha_1$ polypeptide chains and one $\alpha_2$ polypeptide chain, and is 300 nm long and 1.23 nm wide. These microfibrils are connected by intermolecular crosslinks, forming collagen fibrils composed of groups of microfibrils. The linking occurs with the microfibrils aligned in parallel arrays, regularly staggered with 40 nm gaps between the end of one and the beginning of the next, resulting in a periodic 67nm banding pattern. The gaps between microfibrils are aligned such that hole zones, or empty channels, are present within the fibril.

Groups of similarly aligned fibrils (approximately .5 μm wide) form collagen fibers (Weiner & Traub, 1992; Rho et al., 1998). Collagen fibers can then aggregate into larger scale collagen fiber bundles (Currey, 1984; Francillon-Vieillot et al. 1990; de Ricqlès et al., 1991; van der Rest, 1991; Volpi & Katz, 1991). Adjacent bundles are connected to each other by some fibers, and may have slightly differing collagen orientations. It is suggested that it is the presence of osteoblastic canaliculi coursing

through a sheet of collagen fibers that results in the bundling (Jones & Boyde, 1976). Within a sheet of bone, there are also areas of similar collagen fiber orientation that are referred to as domains, patches, or zones (Pannarale et al., 1994; Boyde & Jones, 1998: Ascenzi & Lomovstev, 2006).

Other organic compounds present in small quantities in the interfibrillary ground substance include a range of non-collagenous proteins (such as osteopontin, sialoprotein, osteonectin, osteocalcin) and lipids. These likely have varied functions in the mineralization and remodeling of bone (Bonucci, 1984; Francillon-Vieillot et al. 1990; Cowles et al. 1998; Martin et al, 1998; Rho et al., 1998). Water, serving both structural and metabolic functions, constitutes 5-10% of the weight of bone (Boyde & Jones, 1998; Martin et al., 1998).

After deposition by osteoblasts, the matrix collagen (at this unmineralized point referred to as osteoid) becomes mineralized. The mineral phase involves deposition of a form of calcium phosphate, an impure apatite, containing small amounts of $HPO_4$, Na, Mg, citrate, carbonate, K and other impurities (Rho et al., 1998). There is some debate as to whether this is an hydroxyapatite or a carbonated apatite (Currey, 1984; Francillon-Vieillot et al. 1990; Martin et al., 1998; Rho et al., 1998; Wenk & Heidelbach, 1999). The apatite is structured as tiny crystals (also referred to as crystallites) of variable dimensions with average proportions of about 30-50 x 20-25 x 2-3 nm (Weiner & Traub, 1992; Rho et al., 1998; Wenk & Heidelbach, 1999). Deposition of the crystals is thought to begin in the regular channels that exist in between collagen microfibrils, and to proceed from there, eventually filling the interfibrillar ground substance spaces with hydoxyapatite crystals (Boyde, 1980; Martin & Burr, 1989; Francillon-Vieillot et al.

1990; Volpi & Katz, 1991; Weiner & Traub, 1992; Martin et al., 1998). The alignment of the collagen largely determines that of mineral crystals, and therefore the patterning of the latter mimics the former (as determined by x-ray diffraction) with the crystal plates following the long axis of the collagen (Frasca et al., 1978; Ascenzi et al., 1983; Bonucci, 1984; Weiner & Traub, 1992; Wenk & Heidelbach, 1999). Therefore, even after the removal of organics from bone, the mineral provides a record of their positioning. As bone types with closely packed collagen age, they become more mineralized (Bonucci, 1984; Parfitt, 1993; Kingsmill & Boyde, 1998; Osaki et al., 2002).

Collagen fibers in woven-fibered bone form a random matrix. In parallel-fibered bone, successive sheets of fibers have similar orientations (Boyde & Jones, 1998). However, in some forms of lamellar bone (those with successive lamellae of contrasting brightness when imaged in polarized light), there are apparent differences in fiber organization between adjacent lamellae. There has been much debate in the literature as to the underlying collagen organization that result in dark lamellae, bright lamellae, and the alternation between the two. One camp posits that dark lamellae are composed of longitudinal or longitudinally spiraling collagen fibers, bright lamellae of transverse or transversely spiraling fibers, and that regions of lamellar bone composed of alternating lamellae form an orthogonal plywood structure of successive lamellar sheets with collagen fibers at 90º to each other (Gebhardt, 1905; Ascenzi & Bonucci 1967, 1968, 1972). Elaborations on this basic theme include the recognition of some variation in fiber orientation within lamellae, and the presence of connecting fibers between lamellae (Ascenzi & Benvenuti 1986; Pannarale et al., 1994). The most compelling version of this model is that described by Giraud-Guille (1988) – the twisted plywood model – which

has been supported in subsequent studies (Weiner & Traub, 1992; Weiner et al., 1997; Ziv et al., 1996; Ascenzi et al., 2003; Ascenzi & Lomovstev, 2006). In this model, collagen fibers in the core of dark lamellae are oriented longitudinally, fibers in the core of bright lamellae are oriented transversely, and fibers in between these cores arc through a continuous (or possibly graded) range of angles to bridge the difference between the two orthogonal orientations in successive contrasting lamellae. Ascenzi et al. (2003) and Ascenzi & Lomovstev (2006) elegantly and persuasively describe in detail the structures involved in this "twisted plywood" design. Using CPL, confocal microscopy and x-ray diffraction, they show that dark lamellae are composed primarily of longitudinal collagen (c. 70% of all fibers), with a small component of oblique and transverse fibers. In contrast, the transverse component of bright lamellae is no more than c. 45%, with an equally large (or larger) component of oblique fibers, and a very small proportion of longitudinal fibers. The cores of both dark and bright lamellae contain a peak of longitudinal and transverse fibers respectively, with more peripheral sheets of bone within a lamella comprising more oblique fibers. The core of a bright lamella is thinner than that of a dark lamella. These authors also show that, within a sheet of deposited bone, despite an overall preponderance of a particular orientation, there are different domains with different orientations.

A contrasting, and less well-substantiated model proposes that bright and dark lamellae do not contain collagen fibers of different orientations, but rather have different collagen densities (Marotti & Muglia 1988; Marotti, 1993; Ardizzoni, 2001). Bright lamellae are considered to be thinner, collagen-rich (denser), and lacking in osteocyte lacunae, while dark lamellae are thicker, collagen-poor (looser) and contain osteocytes.

Given the preponderance of support for the twisted-plywood model, I proceed under the assumption that this is a more accurate account of lamellar structure, although the complexity of bone leaves open the possibility that refinements or other models may yet emerge.

### 6.3 Hypotheses regarding the factors determining variation in collagen fiber orientation

Beginning with Gebhardt (1905; see also Ascenzi, 1988), it has been suggested that collagen fibers are aligned preferentially within bone to resist different kinds of load. Specifically, tension is best thought to be resisted by fibers that are aligned longitudinally relative to the load, while compression is most effectively resisted by fibers that are aligned transversely (Ascenzi & Bonucci, 1967, 1968; Vincentelli & Evans, 1971). In particular, testing of this hypothesis has been conducted on the fibers found within the lamellae of secondary osteons (Ascenzi & Bonucci, 1967, 1968, 1972; Vincentelli & Evans, 1971), but studies exist for other tissue types as well (e.g., Simkin & Robin, 1974; Riggs et al., 1993a; Mason et al., 1995; McMahon et al., 1995; Lee, 2004; Bromage & Boyde, n.d.). Previous studies will be reviewed at greater length in the discussion section of this chapter.

Whole sections and multiple sections within bones have also been examined to determine the relationship between loading regimes and distribution of varied collagen orientations, incorporating data acquired from areas of both osteonal and non-osteonal bone (e.g., Portigliatti-Barbos et al., 1983; Ascenzi et al., 1987; Boyde & Riggs, 1990; Carando et al., 1989, 1991; Riggs et al. 1993a; Goldman et al., 2003; Lee, 2004; Skedros et al., 2004; Bromage & Boyde, n.d.). Some authors have found that patterns of collagen

fibers across whole bone cross-sections are in accordance with predictions based on inferred and measured strains (e.g., Boyde & Riggs, 1990; Carando et al., 1989, 1991; Kalmey, 2000; Portigliatti-Barbos et al, 1983; Riggs et al., 1993a; but see McMahon et al., 1995). For example in a classic study of the horse radius (Riggs et al., 1993a, 1993b) – a bone regularly subjected to bending – the posterior cortex, incurring compressive strains, displays a preponderance of transverse collagen fibers. Conversely the anterior cortex, which is under tension, has more longitudinal fibers. While these patterns particularly hold true for areas of secondary osteonal bone, results for primary bone are limited and more equivocal (e.g., Simkin & Robin, 1974; Riggs et al., 1993a; Mason et al., 1995; McMahon et al., 1995; Lee, 2004; Bromage & Boyde, n.d.), suggesting that other factors may influence preferred orientation in non-Haversian bone (and perhaps in secondary osteonal bone too; see Bromage & Boyde, n.d.). One implication has been that, with the exception of secondary osteons, collagen fiber orientation is at least in part determined by tissue type (e.g., Riggs et al., 1993a; McMahon et al., 1995; Bromage & Boyde, n.d.). However, results remain largely inconclusive and variation in collagen fiber orientation within primary bone tissues has never been systematically explored.

Two studies that have examined a number of histocompositional variables (extent of intracortical remodeling, collagen fiber orientation, mineralization, porosity, wet and dry density [mineralization + porosity]) have shown that collagen fiber orientation best correlates with selected mechanical properties of bone (Martin & Ishida, 1989; Riggs et al., 1993b). This supports the hypotheses set forth through observation of collagen fiber orientation alone, together providing a persuasive argument for the functional relationship between collagen fiber orientation and mechanical adaptation of bone.

### 6.4 Objectives of the current study

Taking into account the research outlined above, the objectives of the current study are to explore the following questions. As in previous chapters, it is important to note that the questions are not discrete and are not designed to furnish answers that are mutually exclusive.

1) Are there patterns of preferred collagen fiber that are characteristic of the primates in this sample as a whole?
2) Within the primate order, is there significant variation in patterns of collagen fiber orientation among primary tissue types, or intracortically remodeled bone, in long bone midshaft cortices?
3) If so, is this variation non-randomly distributed?
4) If so, are the patterns explained in part or in whole by mechanical and/or developmental factors, as outlined above?
    a. Do preferred collagen orientations vary among primary tissue types?
    b. Does preferred collagen fiber orientation in both primary and secondary bone vary among taxa that are different in their positional behavior and/or adult body size, in accordance with the hypothesis that collagen orientation is determined by principal loads?
5) Do individual taxon patterns reflect variation in the factors outlined above?
6) Are there identifiable phylogenetic patterns that are independent of taxon-specific adaptations?

## 6.5 Methods

### *6.5.1 Polarized light and circularly polarized light imaging*

In this study the orientation of collagen fibers within a cortex is visualized using circularly polarized light (CPL), where a compound light microscope is fitted with a set of polarizing and quarter wave filters.[1] Polarized light imaging identifies patterns of material birefringence, that is, anisotropy of the refractive index based on differences in orientation, expressed as variation in brightness (Bromage et al., 2003). Under polarization, collagen fibers (plus mineral) that are aligned transversely to the plane of section appear maximally bright or white (gray-level value approaching 255), while fibers that run longitudinally appear extinguished or black (gray-level value approaching 0). Fibers with intermediate orientations appear in the continuous range of gray along a 0-255 scale.

Following Boyde et al. (1984), CPL, rather than linearly polarized light (LPL), is used to allow for acquisition of quantitative collagen fiber orientation data for an entire section without rotating the section relative to the filters (see Bromage et al., 2003 for a detailed discussion of LPL and CPL). Two filters are used to obtain LPL images: a polarizer between the specimen and the light source, and an analyzer between the specimen and the oculars (or camera), set with its vibration plane at 90º to the polarizer. The light waves emitted from the polarizer are restricted to a single vibration plane or direction. As they pass through the bone specimen, where collagen fibers are transverse or oblique to the section, there is refraction of the light and the vibration direction changes by 90º, rendering light transmitted by the analyzer, reaching the eye or camera

[1] Recently, some researchers have also employed transmitted microwaves and acoustic velocity methods to assess collagen fiber orientation (Osaki et al., 2002; Skedros et al., 2006).

lens. In contrast, where fibers run longitudinally (perpendicular to the section), the light waves pass through with no refraction and no alteration in wave orientation, and are therefore blocked by the analyzer. The problem with the quantitation of LPL imaging is that a Maltese Cross effect is produced, where there is an extinguishing of light at each position ± 45º or ± 135º to the transmission axis of the analyzer. These areas will appear artifactually dark, regardless of the orientation of the collagen, making it impossible to accurately quantify gray-levels across a section of bone.

In contrast, in CPL imaging, the Maltese Cross effect is eliminated by the addition of two quarter wave filters (Boyde & Riggs, 1990; Bromage et al., 2003). In this case, a retarding quarter wave plate is placed between the polarizer and the specimen at 45º to the polarizer, and a second retarding quarter wave plate is placed between the specimen and the analyzer, at 90º to the first quarter wave plate and 45º to the analyzer. The effect of the below-specimen, two-filter set is to achieve helical vibration planes: circularly polarized light. The helical vibration planes pass through the specimen without changing the birefringent effect achieved though LPL, but with maximal brightness possible at all 360º. After passing though the second, above-specimen filter-set, the circular vibrations are returned to an LPL signal, reaching the eye or camera as a polarized image with no Maltese Cross error.

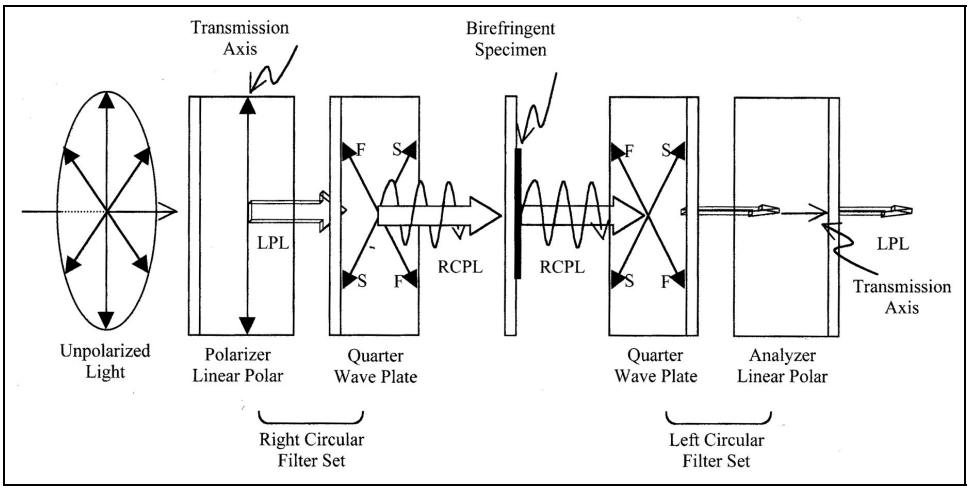


**Figure 6.1: CPL filter configuration.**
From Bromage et al., 2003.

Quantification of collagen fiber orientation is typically performed on monochrome CPL images, most easily captured with a monochrome camera. However, when only a three-chip color CCD camera is available, as was the case for this study, it is still possible to achieve a monochrome image by eliminating two of the three RGB color bands (see Bromage et al., 2003). Imaging with the majority of monochrome cameras most closely resembles the green portion of the visible light spectrum in RGB. Therefore a narrow band-pass green filter was used to eliminate the red and blue bands in this study.

*6.5.2 Standardization of light parameters for quantitative CPL imaging*

The goal of CPL imaging is to able to quantify gray levels, representing variation in the orientation of collagen fibers within the bone. Therefore, it becomes critical that the brightness of light passing through the section be standardized. This is difficult, however, if all section are not imaged during the same session, in the same lab, under identical lighting conditions. It is absolutely necessary to arrive at a means to

consistently achieve the same illuminating system conditions at every imaging session. For this reason, various authors have proposed methods of standardization (e.g., neutral density filter; see Goldman, 2001).

At the Hard Tissue Research Unit (HTRU) we have devised a mineralized turkey tendon standard that allows for standardization within and among laboratories (Bromage et al., 2003). Unlike previously employed standards, it has the added advantage of providing a non-arbitrary brightness baseline. With previous methods, although comparability between specimens is possible, there is no way to know whether the overall brightness level is appropriate. Precision may be high, but without an assessment of accuracy relative to the real orientation of collagen in the bone. That is, peak brightness may not indicate transverse fibers if the illumination is set too high. An overly low illumination level might similarly indicate more longitudinal fibers than are actually present.

Tendons in the gastrocnemius of the turkey (*Meleagris gallopavo*) calcify during development, and can be extracted from the leg of a supermarket turkey. Tendon comprises Type I collagen, as is the case for bone (Rossert & de Crombrugghe, 1996). Unlike bone, however, the collagen in tendons is principally aligned parallel to the long axis of the tendon (Traub et al., 1992). Therefore, a long section of mineralized turkey tendon can reliably be inferred to contain transverse collagen fibers, or fibers that should be maximally bright in CPL. A 100 ±5 μm thick longitudinal section of ossified turkey tendon – cleaned, embedded and sectioned according to the same methods as the bone samples (Chapter 2) – can thus be used for adjustment of illumination parameters before every imaging session.

Image brightness will also be affected by the thickness of a section (brightness increases with increased section thickness), as thickness in part determines the optical path of the light (Boyde & Riggs, 1990). Therefore, for quantification of gray levels, it is of critical importance that section thickness be uniform. A section thickness of 100 ±5 μm was selected, as this is a common standard in previous studies of collagen fiber orientation (e.g., Vincentelli & Evans, 1971; Vincentelli, 1978; Boyde & Riggs, 1990; Bromage, 1992; Riggs et al., 1993a, b; Goldman, 2001; Goldman et al., 2003). Chapter 2 contains a discussion of section preparation techniques, including section thickness measurement.

At the beginning of each imaging session, a prepared turkey tendon section was placed on the stage, coverslipped with ethylene glycol, and the CPL filters were aligned. The lighting parameters and software image setup controls were then adjusted until the lowest gray-level reading (or lowest green band reading when a three-chip RGB color camera is used) was 5. Parameters were then further adjusted so that the highest gray-level reading (or green band reading) was 250. 5 and 250, rather than 0 and 255, were used as the lower and upper limits to avoid the possibility that the parameters were being stretched beyond maximum darkness or brightness. The turkey tendon section was then removed and I proceeded with the imaging of the bone specimens.

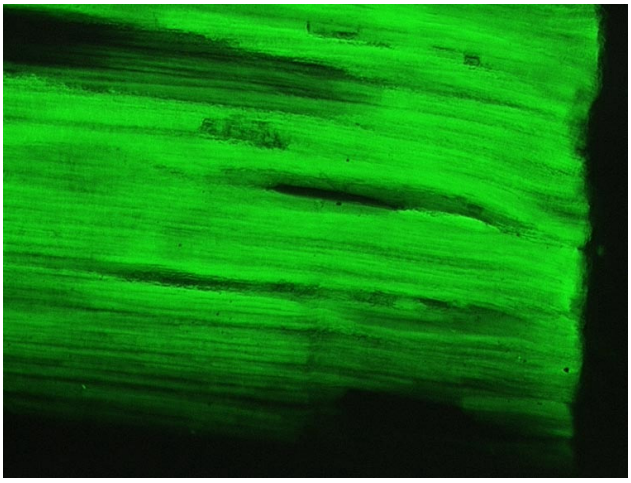

**Figure 6.2: Image of turkey tendon standard, with high-band green filter.**

Maximum green band level is 250, and minimum green band level is 5. (When this image is viewed in a grayscale reproduction, lighter areas represent brighter greens, and darker areas represent darker greens.)

*6.5.3 Image processing*

All CPL images acquired under standard illumination (appearing green due to the use of the green filter) were transferred into Adobe Photoshop and converted to a grayscale image. After this conversion, the maximum grayscale level in the turkey tendon was 215, rather than 250 as it appeared in the green band. In contrast, the lowest pixel values in the green band remained low in grayscale. Therefore, the turkey tendon standard (and all bone images) was stretched by 35 gray level values at the high end to maintain the 5-250 range. To accomplish this, in the 'Levels' function under 'Adjustments' in the 'Image' drop-down menu, the '255' input level was changed to '215'. Note that in the 'Levels' pop-up box, the input levels display a range of 0-255, regardless of the actual range in the image. With careful examination of maximum and minimum gray levels in the image, it was determined that reducing the input value of '255' to '215' resulted in an image with maximum values of 250.

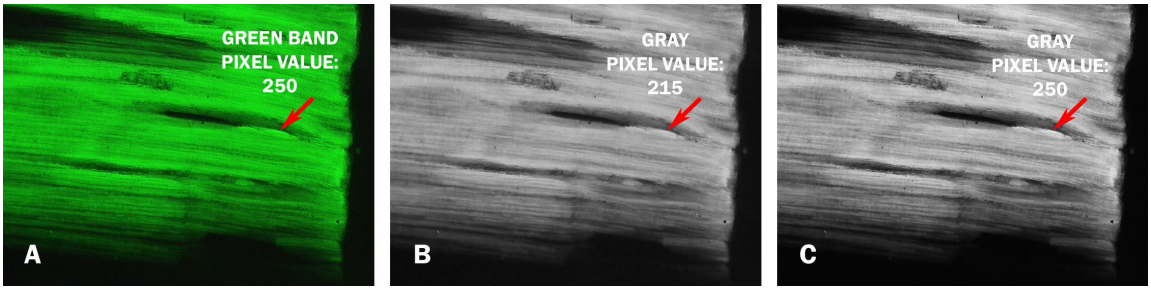


**Figure 6.3: Stretching of turkey tendon standard.**
A) Original image with arrow indicating a region containing pixels with a green band level of 250. (For grayscale reproductions of this image, interpret as per Image 6.2.) B) The original image converted to grayscale. C) The grayscale image after stretching.

After the images were converted in Adobe Photoshop to grayscale and stretched, all non-bone areas were masked in white (grayscale value of 255) using the same masks created for the images in Chapter 4. In addition, by overlaying the tissue type maps on the images, endosteal, periosteal, or intracortically remodeled bone could be masked out in black (grayscale value of 0) in order to isolate different sectors and tissue areas for analysis. Finally, within the periosteal area, individual primary tissue types were also isolated via masking of all other types with black.

Masked images were then converted to indexed color mode in Adobe Photoshop, and a look-up table (LUT) was applied, effectively categorizing all gray values from 5 to 250 into eight color bins, each with an even number of grayscale pixel values, as adapted from a standard in the literature (Riggs et al., 1993b; Goldman, 2001; Goldman et al., 2003). With LUT application, each pixel is assigned to a color bin dependent upon its gray value. This categorization assists mostly with visualization, but also with quantification, of patterns of grayscale pixel value variability. In this LUT scheme, cool colors indicate dark areas, or collagen fibers that course longitudinally in the shaft of the bone, perpendicular to the cross-section. Warm colors indicate bright areas, transverse to

the plane of the section and to the long axis of the bone. White is reserved for non-bone areas, and black for masked bone areas. (See Appendix for LUT color values.)

**Figure 6.4: LUT color-coding scheme.**
(Numbers are for coding of grayscale reproductions of this image: 1=dark blue, 2=medium blue, 3=green, 4=yellow, 5=orange, 6=red, 7=pink, 8=gray.)

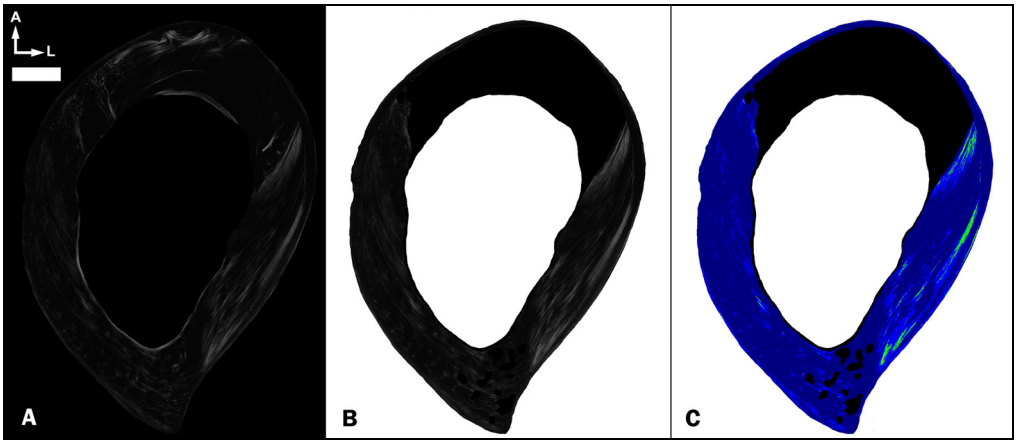


**Figure 6.5: *Galago senegalensis (MNHU 60601)* humerus with masking and application of LUT.**
A) Image after conversion from color (with green filter) to grayscale. B) Image after levels stretching, and masking of non bone (white), as well as intracortical remodeling events and endosteally deposited tissue (black). C) Image after conversion to LUT. (Most of the bone is composed of colors #1 and #2, as per Figure 6.4.)

### *6.5.4 Quantification of collagen fiber orientation*

An Optimas macro (the same one used for quantification of primary tissue types in Chapter 4) was used to quantify the proportions of various LUT bins for periosteal bone within whole cortices. In order to render the LUT image appropriate for use in Optimas, it was converted to grayscale and then inverted (Figure 6.5C). The masked grayscale

image (Figure 6.5B) was also used to obtain mean gray values for the periosteal portion of the whole bone, for individual sectors (following the quadrant scheme described in Chapter 5), and individual periosteal tissue types as well as intracortically remodeled bone. In Adobe Photoshop, means are obtained by selecting the desired area (after masking of undesired areas) and using the expanded 'Histogram' function. These mean gray values were used for the majority of the following analyses.

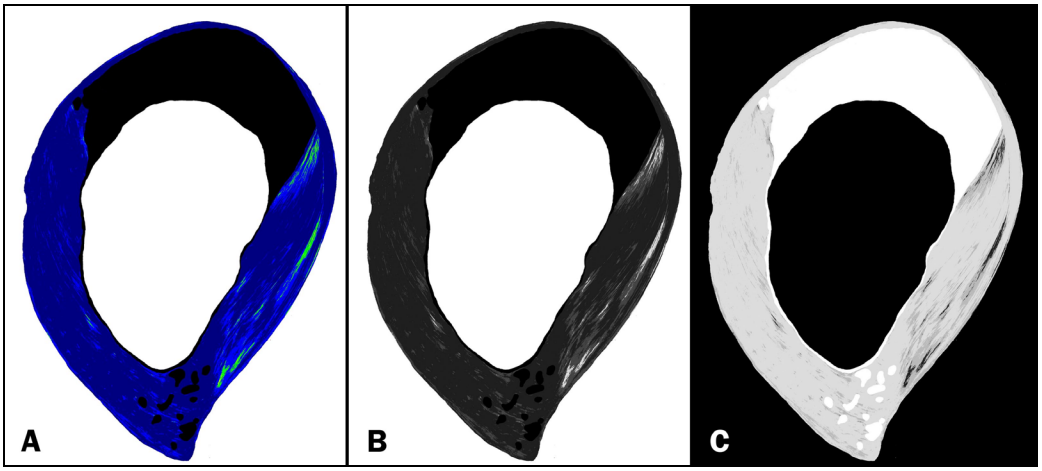


**Figure 6.6:** ***Galago senegalensis (MNHU 60601)*** **humerus with conversion of LUT to Optimas-appropriate format.**
A) LUT image, as per Image 6.5C. B) LUT image after conversion to grayscale. C) Grayscale image after inversion.

### *6.5.5 Statistical and descriptive analyses*

Samples are the same as those in Chapter 4, and the equivalent problems exist with respect to sample composition and distribution. Therefore, as before, I employ nonparametric statistical tests and seek a confluence of significant results as well as the examination of patterns identified via graphical methods to arrive at conclusions. Where sample sizes are too small to allow for meaningful statistical analysis, I employ descriptive methods alone.

First, proportions of LUT bins for periosteal tissue only, relative to total periosteal area, are described for the entire sample, and element means are compared. Non-parametric Sign Tests and Wilcoxon Matched Pairs tests are used to identify differences in the proportion of LUT bins in the sample as a whole, examining each skeletal element independently. Subsequently, mean gray values are examined for whole bones and elements are compared, using Mann Whitney U tests, to isolate significant differences among element means. Next mean gray quadrant values are compared within elements for all individuals as a means to identify differences that may be mechanically determined, and significance is assessed using Sign tests and Wilcoxon Matched Pairs tests. Values for each quadrant are calculated as a proportion of the total periosteal area. Mean gray values are also examined for intracortically remodeled bone, again for whole cortices as well as quadrants. Finally, mean gray values for periosteal primary and secondary osteonal tissues are compared, for both whole bones and sectors (again, Sign tests and Wilcoxen Matched Pairs tests are used to identify significant differences).

Multiple regression analyses are then employed to determine the importance of three independent variables in accounting for the observed variation in collagen fiber orientation. The variables – total cortical area (TCA), positional behavior (PB) and phylogenetic status (PHYLO) – were chosen as best able address the questions raised by a review of the literature, and outlined in the objectives section. These variables are described in Chapter 4. TCA is included as a proxy for body size, and PB as a means to identify variation related to kinematic adaptation. The variable PHYLO is also included as a control for the possibility that there is a phylogenetic effect on patterns of collagen fiber orientation, independent of functional and life history adaptations, although there

are no studies to suggest that this is the case. Multivariate models are examined including all three variables, as well as combinations of two, and are compared to simple regressions for each variable, as described in Chapter 4. Data are further explored via Kruskall-Wallis and Mann Whitney U tests.

Subsequent to this, mean gray values are examined for individual periosteal tissue types, with the goal of identifying patterns that may be developmentally constrained, with statistical differences in brightness among tissue types identified with Sign tests and Wilcoxen Matched Pairs tests. Next, comparisons between skeletal elements (for both periosteal primary and secondary osteonal bone) are examined relative to positional behavior characters. Descriptive analysis is then provided for intra-taxonomic variation in preferred collagen fiber orientation within and between skeletal elements. Finally, patterns characteristic of each taxon are described.

## 6.6 Results

### *6.6.1 Collagen fiber orientation in endosteal tissues*

Endosteal tissues in this sample (including lamellar circumferential=LAM, hybrid=HYB, parallel-fibered=PF, and fibrolamellar and woven bone=FAST, as well as compacted-coarse cancellous bone=CCC) are frequently bright, more so than periosteal and intracortically remodeled tissues. This pattern of endosteal brightness has been observed by other researchers (Carando et al., 1989; McMahon et al., 1995; Bromage & Boyde, n.d.) but has not satisfactorily been explained in terms of either mechanical adaptation or mechanisms of growth and development. Nor can I offer here a persuasive explanation for my, and others', observations. Therefore, I have elected to omit endosteal tissues

from the following analysis, with the understanding that, at some future time, this distinctive pattern should be further explored.

### *6.6.2 Sample-wide patterns of collagen fiber orientation in periosteal primary tissues: whole cortices*

In all elements, without exception, mean values for LUT bins indicating longitudinally oriented fibers are substantially and significantly higher than all other bins (Sign tests; $p<.01$ in all cases). Values at the transverse fiber end of the LUT spectrum are very low (even zero in many cases). Overall then, the periosteal primary tissue types in this sample are characterized by a preponderance of longitudinal fibers.

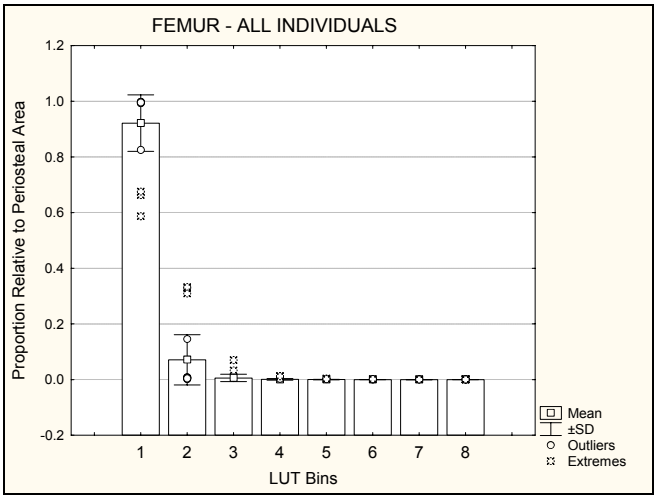


**Figure 6.7: LUT bin values for all sample femora.**

Upper outliers > upper value of the box + outlier coefficient x (upper value of the box – lower value of the box). The inverse is true for the lower outliers.
Upper extremes > upper value of the box + 2x outlier coefficient x (upper value of the box – lower value of the box). The inverse is true for the lower extremes.
*Outlier coefficient = 1.5.
LUT bin numbers as per Figure 6.4.

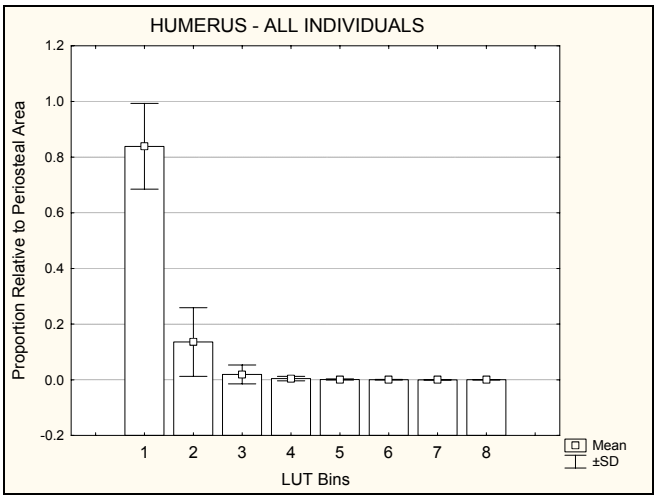


**Figure 6.8: LUT bin values for all sample humeri.**

Legend as per Figure 6.7

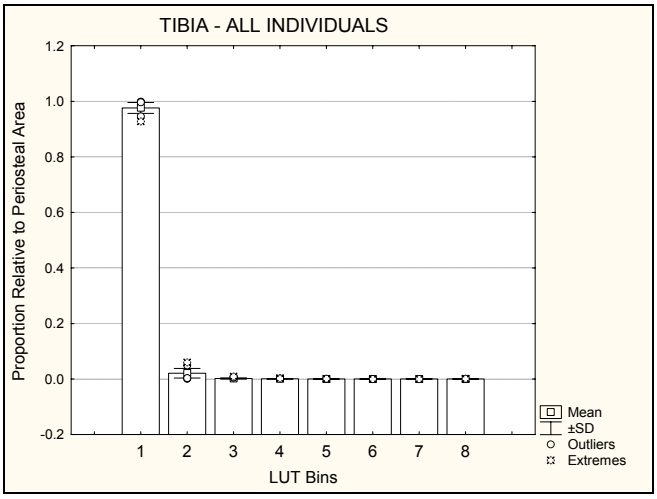


**Figure 6.9: LUT bin values for all sample tibiae.**

Legend as per Figure 6.7.

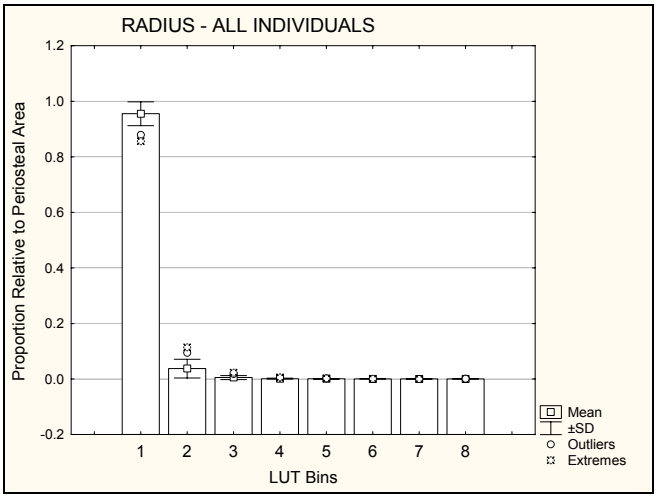


**Figure 6.10: LUT bin values for all sample radii.**

Legend as per Figure 6.7.

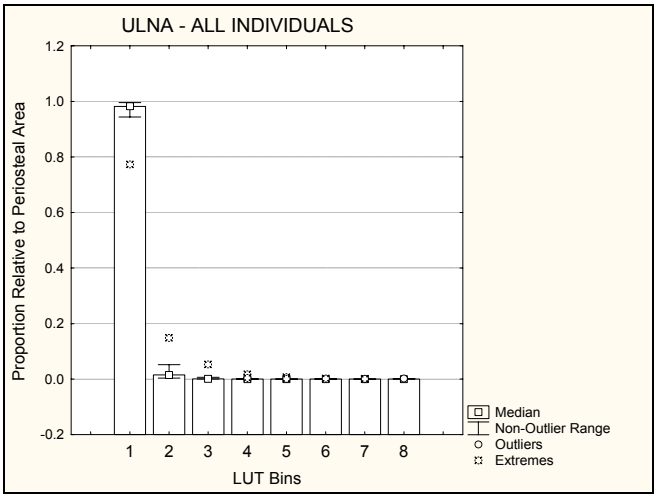


**Figure 6.11: LUT bin values for all sample ulnae.**

Legend as per Figure 6.7.

Small differences exist between element means. For example, the mean for humeri is smaller for bin1 and greater for bin2 than all other elements, indicating a larger proportion of oblique fibers in the humerus (although these are still closer to longitudinal than transverse).

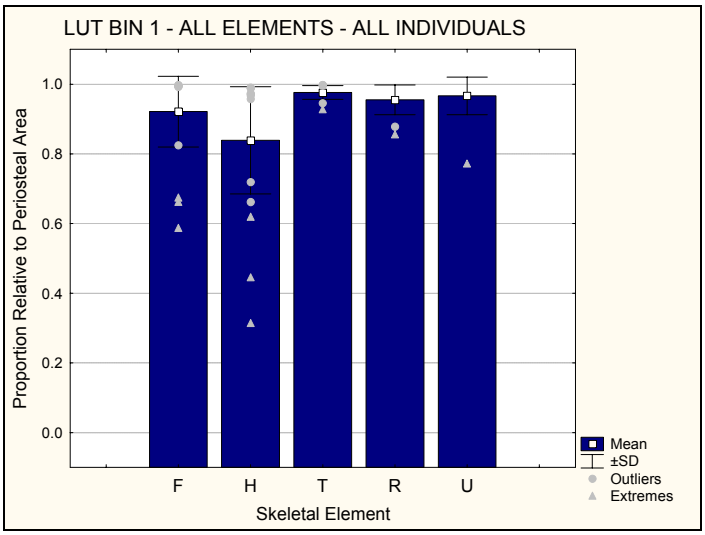


**Figure 6.12: LUT bin1 means for all sample elements.**

F=femur; H=humerus; T=tibia; R=radius, U=ulna.

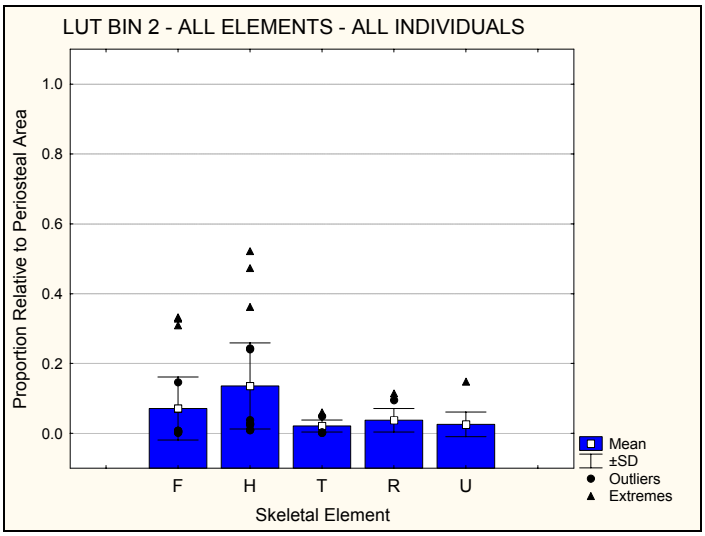


**Figure 6.13: LUT bin2 means for all sample elements.**

Legend as per Figure 6.12.

When mean gray values for all periosteal primary tissue, rather than LUT bin categories, are considered, it is further evident that all fall towards the dark end of the 5-250 grayscale spectrum, indicating a preponderance of longitudinal fibers. In a single humeral section the mean is approximately 46, while all other sections means are below 40, with combined element means below 25. As was the case for the LUT bin results, the combined mean for humeri is higher than for all other elements, indicating more transverse (or oblique) fibers in this element relative to other elements (Mann Whitney U test $p<.001$ for comparisons between the mean for humeri and the mean for all other elements) (Figure 6.14).

This contrast between means for the humerus and other elements extends to individual specimen comparisons. In the majority of instances, the periosteal primary tissues in the humerus are brighter than those of the femur, radius, ulna or tibia of the same individual (e.g., Figure 6.15).

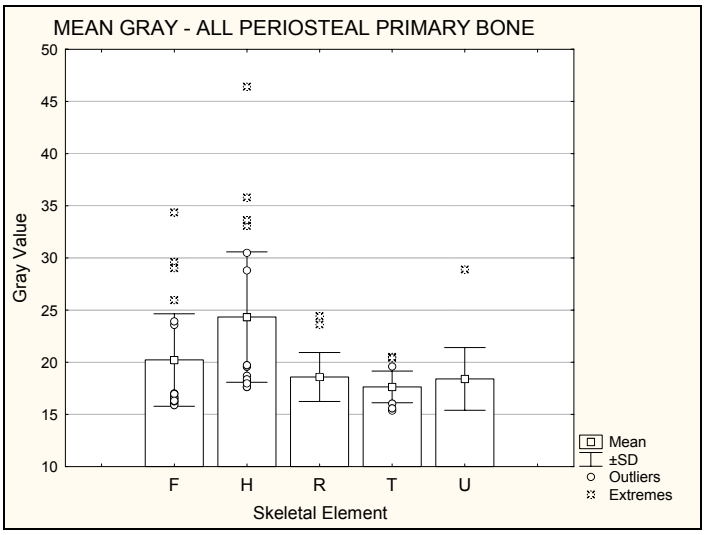


**Figure 6.14: Mean gray values for all elements.**

See text for description. Legend as per Figure 6.12.

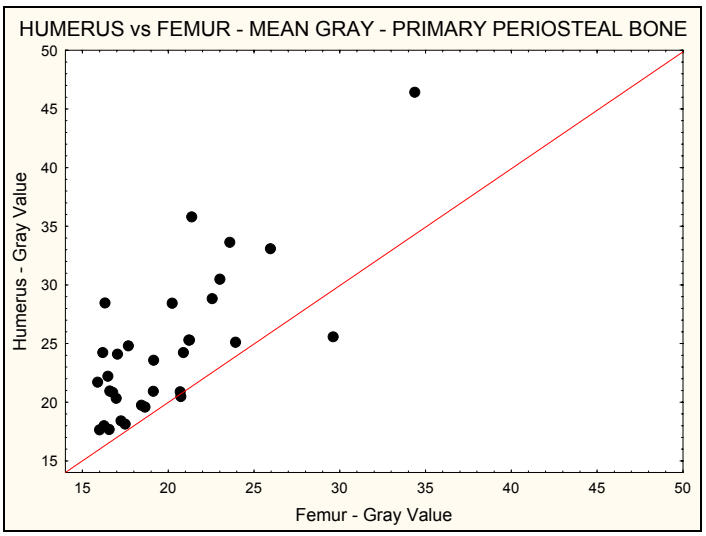


**Figure 6.15: Mean gray value of humeri relative to femora.**

The diagonal red line indicates where all data points would fall if gray values were equivalent in both elements. Each data point indicates a single animal. In the majority of individual cases, the humerus displays higher gray values than the femur.

### *6.6.3 Sample-wide patterns of collagen fiber orientation in periosteal primary tissues: sectoral patterns*

When means for cortical quadrants are compared, including all individuals in the sample, in most cases there are no significant differences among them. Mean values indicate similar brightness in all four quadrants for each skeletal element. Likewise, comparisons among quadrants for individuals identify few patterns of increased brightness or darkness in CPL among periosteal primary tissues.

There are a few exceptions to this trend. First, in the femur, the medial quadrant mean for all individuals together is significantly lower (i.e., darker, indicating more longitudinal collagen fibers) than the lateral and posterior quadrant means, with the difference between lateral and medial quadrants more significant (Sign Test: $p<.01$) than the difference between posterior and medial quadrants ($p<.05$). However, while in scatterplots comparing individual quadrant values the majority of medial quadrant values are lower than posterior and lateral quadrant values, an opposite pattern is evident in a number of individuals, and in several cases values are almost equivalent (e.g., Figure 6.16).

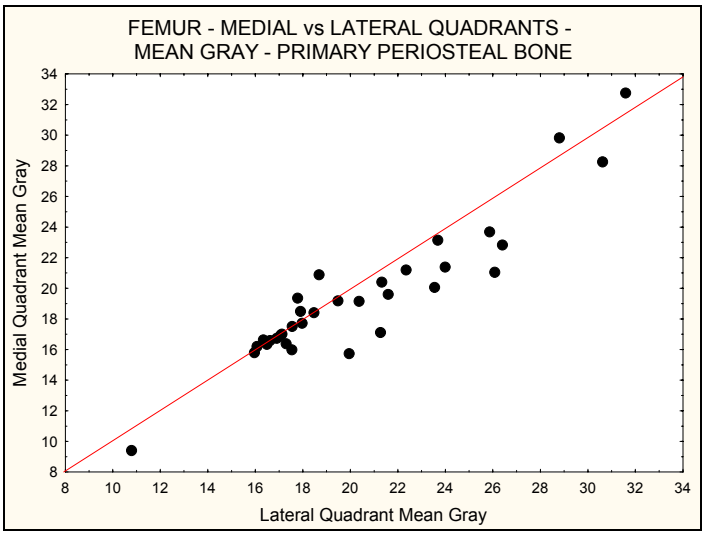


**Figure 6.16: Mean gray value of medial vs. lateral quadrants in the femur.**

The red diagonal line indicates where all data points would fall if gray values were equivalent in both quadrants. Each data point indicates a single animal. See text for description.

Second, in the humerus, a pattern similar to the one seen in the femur exists: the medial quadrant is significantly darker than the posterior or lateral quadrants ($p<.01$-$.05$), with a number of individuals diverging from this pattern (Figure 6.17).

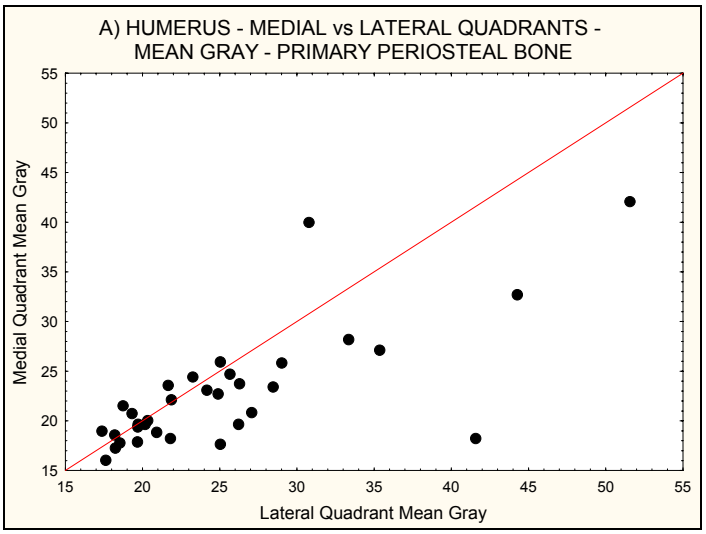


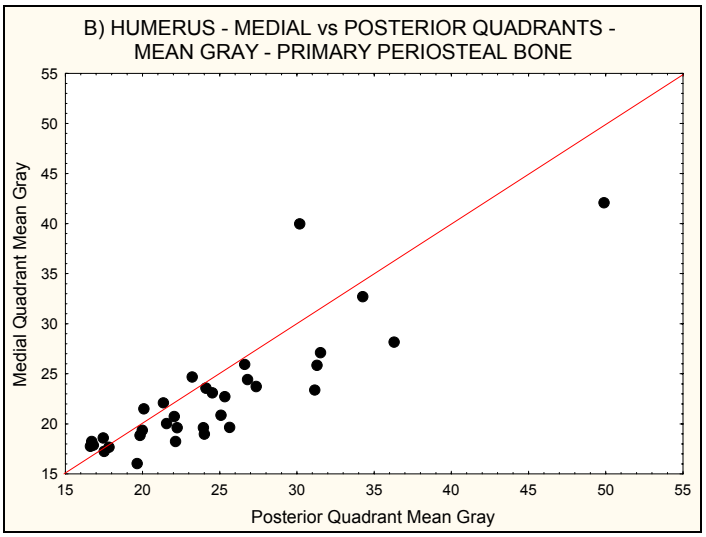


**Figure 6.17: Mean gray value of medial vs. lateral (A) and medial vs. posterior (B) quadrants in the humerus.**

The diagonal red line indicates where all data points would fall if gray values were equivalent in both quadrants. Each data point indicates a single animal. See text for description.

Third, in the radius, the medial quadrant is significantly brighter than the posterior quadrant ($p<.05$). This pattern for the mean of all individuals combined holds true for 13 of 16 individuals (Figure 6.18). Finally, in the ulna, the anterior quadrant is significantly brighter than the posterior quadrant ($p<.05$), with the pattern holding true for 13 out of 16 individuals (Figure 6.19).

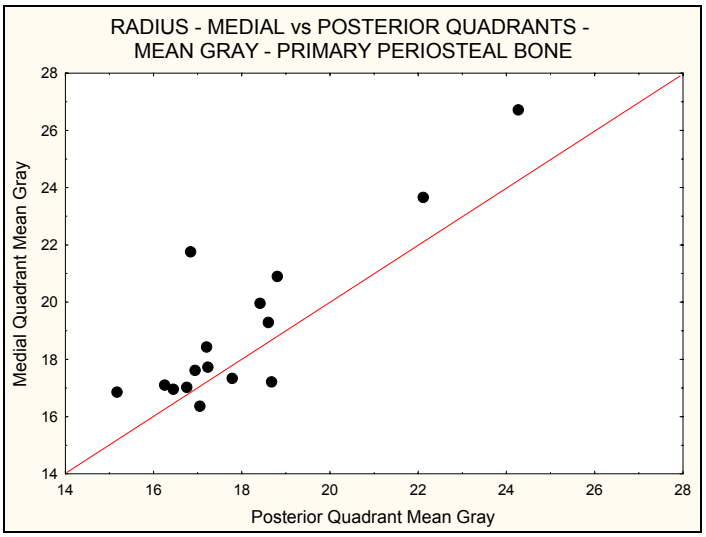


**Figure 6.18: Mean gray value of medial vs. posterior quadrants in the radius.**

The diagonal red line indicates where all data points would fall if gray values were equivalent in both quadrants. Each data point indicates a single animal. See text for description.

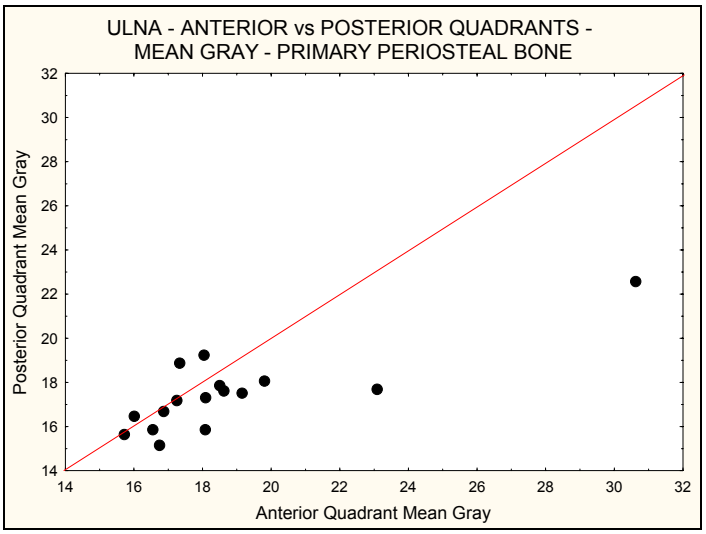


**Figure 6.19: Mean gray value of anterior vs. posterior quadrants in the ulna.**

The diagonal red line indicates where all data points would fall if gray values were equivalent in both quadrants. Each data point indicates a single animal. See text for description.

### *6.6.4 Sample-wide patterns of collagen fiber orientation in intracortically remodeled tissue: whole cortices*

As is the case for periosteal primary tissues, collagen fiber orientations in intracortically remodeled bone are predominantly more longitudinally than transversely oriented. In a single femoral section, the mean gray value for all secondarily remodeled bone is close to 41. In all other individuals, for all elements, mean gray values are below 35 (Figure

6.20). The tibiofibula midshaft section for a single tarsiid individual was omitted from the analyses since a single large osteon at the region of fusion between the tibia and fibula was unusually bright relative to all other sample specimens. Given the very low overall proportion of intracortical remodeling in this individual (and in tarsiids as a whole), this bright osteon resulted in an outlying data point.

Although all secondarily remodeled bone is primarily dark, there are differences among elements in the preferred orientation of collagen fibers (Figure 6.20). Mean values are significantly higher (indicating a larger proportion of more transverse fibers) in the femur and humerus than in the three distal elements (Mann-Whitney U tests: $p<.05$-$.001$), and significantly higher in the tibia than in the ulna ($p<.01$). These patterns are also evident when scatterplots for individual values are examined, except comparisons between the tibia and the femur and humerus. So, for example, in 11 out of 12 individuals, the value for the femur is higher than the value for the ulna (Figure 6.21), and higher than the radius in 10 of 13 individuals. In 13 out of 15 individuals, the humerus is brighter than the radius, and brighter than the ulna in 13 out of 14 individuals. In 10 out 12 cases, the tibia is brighter than the ulna. But in only 10 of 15 cases is the femur brighter than the tibia, and only 11 of 17 cases in the humerus brighter than the tibia (Figure 6.22).

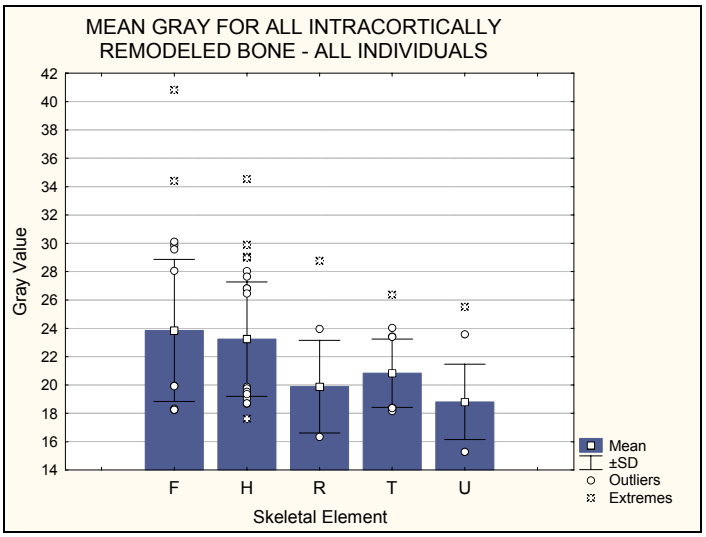


**Figure 6.20: Mean gray value for intracortically remodeled bone comparing skeletal elements.**

See text for description. Legend as per Figure 6.12.

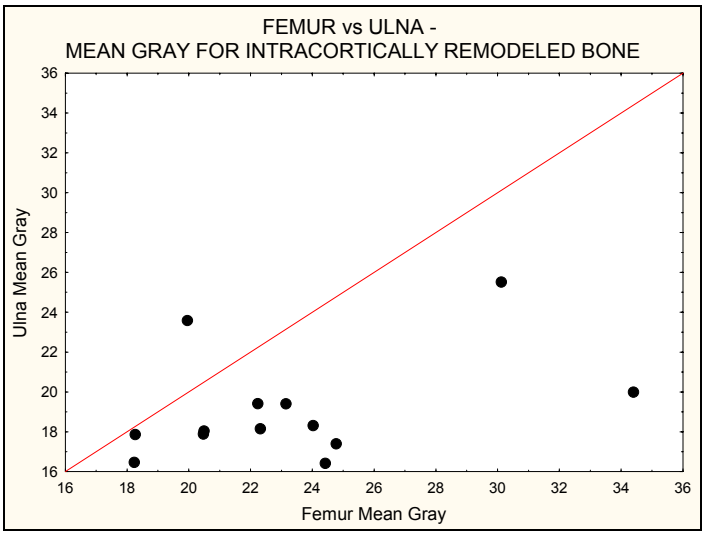


**Figure 6.21: Mean gray value for intracortically remodeled bone in the femur vs. the ulna.**

The diagonal red line indicates where all data points would fall if gray values were equivalent in both skeletal elements. Each data point indicates a single animal. See text for description.

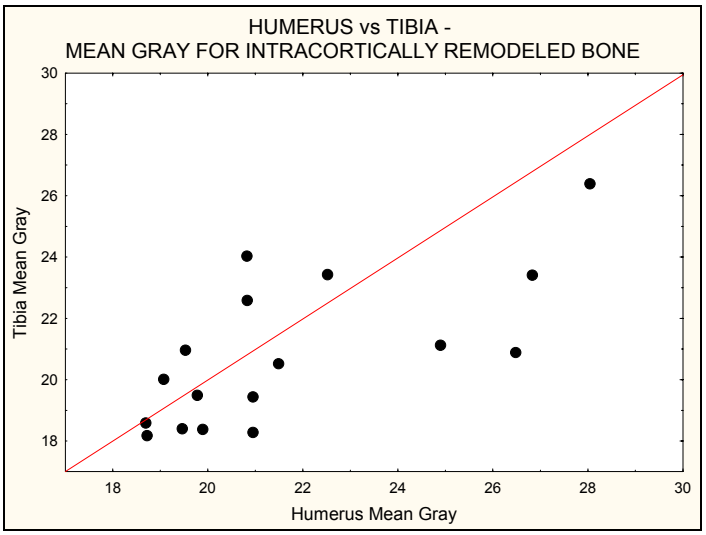


**Figure 6.22: Mean gray value for intracortically remodeled bone in the humerus vs. the tibia.**

The diagonal red line indicates where all data points would fall if gray values were equivalent in both skeletal elements. Each data point indicates a single animal. See text for description.

### *6.6.5 Sample-wide patterns of collagen fiber orientation in intracortically remodeled tissue: sectoral patterns*

With two exceptions, there are no significant differences in brightness among quadrants for intracortically remodeled bone. The first exception is found in the humerus, where the posterior quadrant is significantly brighter than the anterior quadrant (Sign test: $p<.05$). When a scatterplot of individual cases is examined, the relative brightness of the posterior quadrant holds true for 17 of 22 individuals (Figure 6.23). A similar exception is found in the tibia where, again, the posterior quadrant is significantly brighter than the anterior quadrant ($p<.05$), and where the pattern in 11 out of 13 individuals is consistent with the one observed for the mean of all sample tibiae. There are no significant differences among quadrants in the femur, radius or ulna for the mean of all sample individuals combined. It should be noted, however, that scatterplots identify several other instances where one quadrant is generally brighter than another. For example, among radii, nine of 11 medial quadrants are brighter than lateral quadrants. In addition, among tibiae, ten of 13 medial quadrants are brighter than anterior quadrants.

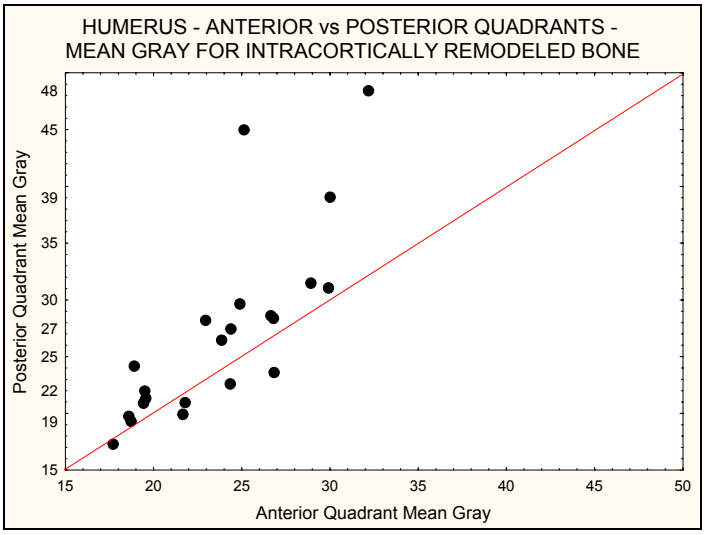


**Figure 6.23: Mean gray value for intracortically remodeled bone in the anterior vs. posterior quadrants of the humerus.**

The diagonal red line indicates where all data points would fall if gray values were equivalent in both quadrants. Each data point indicates a single animal. See text for description.

*6.6.6 Comparing periosteal primary and intracortically remodeled tissue: whole cortices*

When means of all individuals for each skeletal element for periosteal primary tissues and intracortically remodeled tissue are compared, there are robust statistically significant differences between the two for the femur and tibia (Sign test: $p<.001$) and marginally significant differences for the radius ($p<.05$). In all three cases, the values for intracortically remodeled bone are higher, indicating brighter bone, and more transversely oriented collagen fibers (although these are still closer to longitudinal than transverse in most cases). There are no statistically significant differences between intracortically remodeled bone and periosteal primary tissues in the humerus or ulna (Figure 6.24).

A comparison of mean gray values for individuals corroborates the results for the entire sample for the hindlimb bones, but not the radius. For the femur, in 26 of 31 individuals, the mean gray for all intracortically remodeled bone is greater than for periosteal primary bone (Figure 6.25). The same is true for 17 out of 17 tibiae (Figure 6.26), but only 9 out of 15 radii. In the humerus and ulna, a roughly equivalent number

of individuals show brighter periosteal primary tissue as intracortically remodeled tissue (Figure 6.27). In summary, secondarily remodeled bone is brighter than periosteal primary bone in both elements of the hindlimb. While there is a statistically significant difference between means for the radius for these two tissue categories, an examination of the scatterplot of individual values belies this relationship. Therefore, all three forelimb bones can be best described as not displaying differences in collagen fiber orientation between the periosteal primary and secondarily remodeled tissue.

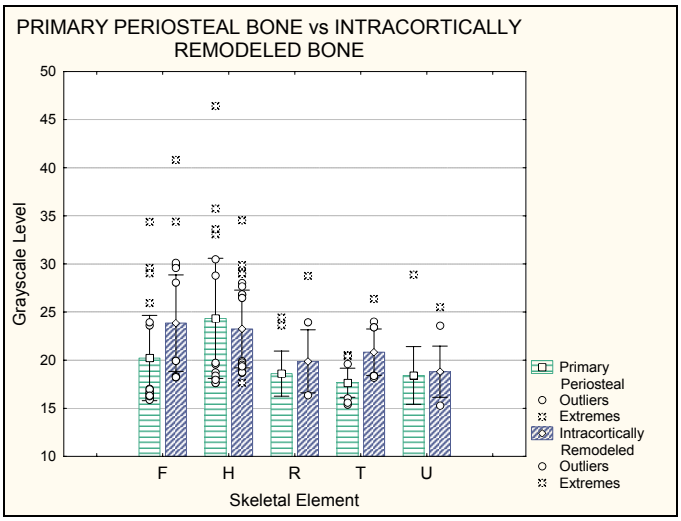


**Image 6.24: Mean gray value for periosteal primary vs. intracortically remodeled bone for all skeletal elements.**

See text for description. Legend as per Figure 6.12.

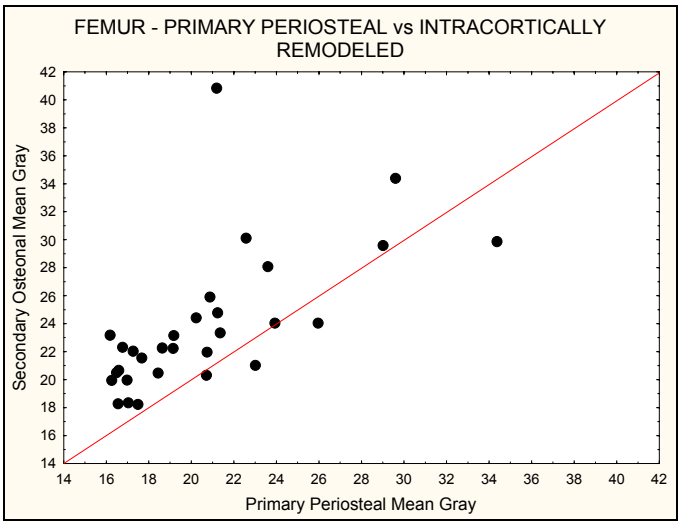


**Image 6.25: Mean gray value for periosteal primary vs. intracortically remodeled bone in the femur.**

The red line indicates where all data points would fall if gray values were equivalent in both tissue areas. Each data point indicates a single animal. See text for description.

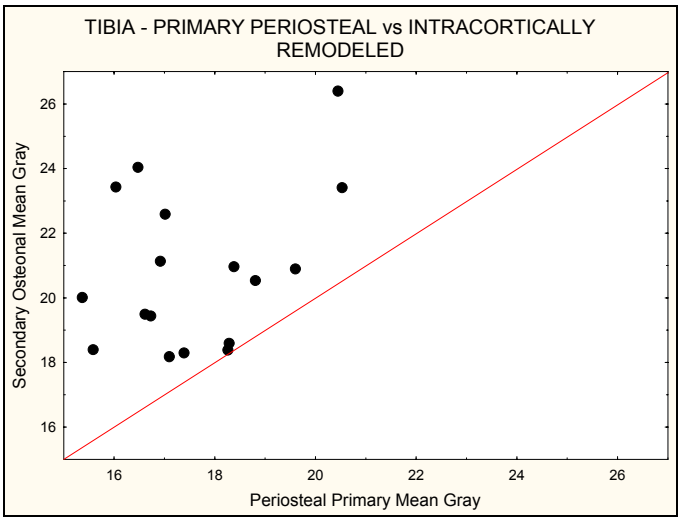


**Figure 6.26: Mean gray value for periosteal primary vs. intracortically remodeled bone for the tibia.**

The diagonal red line indicates where all data points would fall if gray values were equivalent in both tissue areas. Each data point indicates a single animal. See text for description.

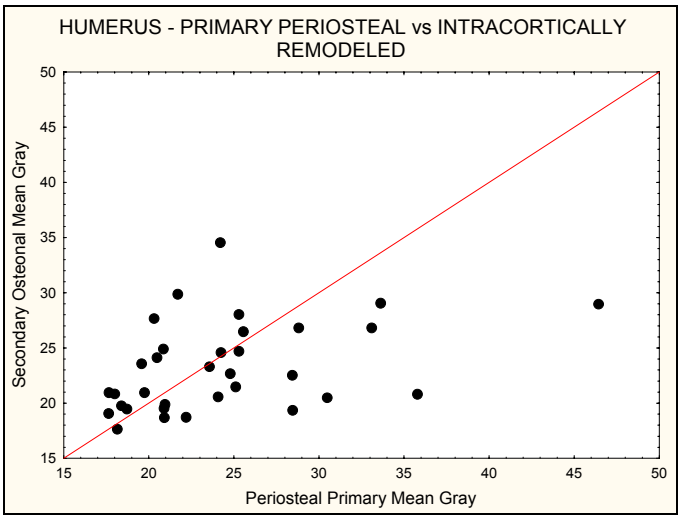


**Figure 6.27: Mean gray value for periosteal primary vs. intracortically remodeled bone for the humerus.**

The diagonal red line indicates where all data points would fall if gray values were equivalent in both tissue areas. Each data point indicates a single animal. See text for description

### *6.6.7 Comparing periosteal primary and intracortically remodeled tissue: sectoral patterns*

When mean grays for individual quadrants are compared, only the femur and tibia display statistically significant differences between periosteal primary tissue and intracortically remodeled tissue. In these two skeletal elements, values for the secondary osteonal bone are brighter than those for the primary tissue in all four quadrants (Sign test: $p<.01$-$<.0001$). This relationship holds true for the majority of individuals, as seen in bivariate scatterplots (e.g., Figures 6.28, 6.29). In contrast, there are no statistically significant

differences between primary and secondary tissue types within quadrants for all three bones of the forelimb, although bivariate scatterplots for the radius indicate brighter intracortically remodeled bone in the majority of individuals for the anterior and posterior quadrants.

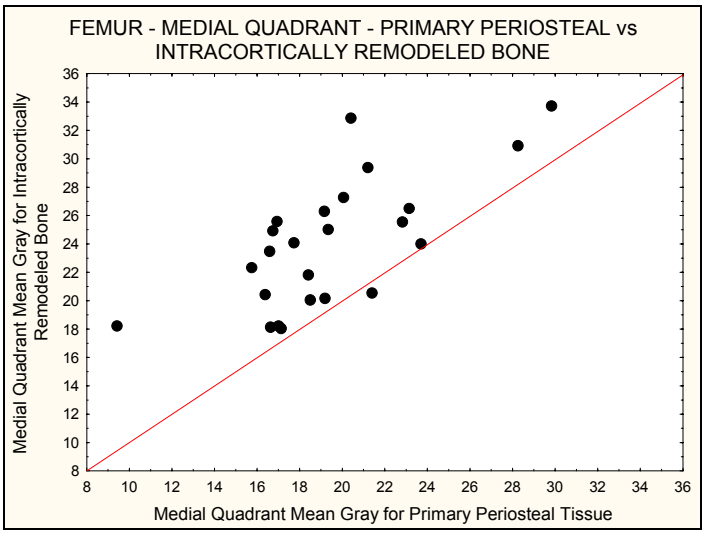


**Figure 6.28: Periosteal primary vs. intracortically remodeled bone for the medial quadrant in the femur.**

The diagonal red line indicates where all data points would fall if gray values were equivalent in both tissue areas. Each data point indicates a single animal. See text for description.

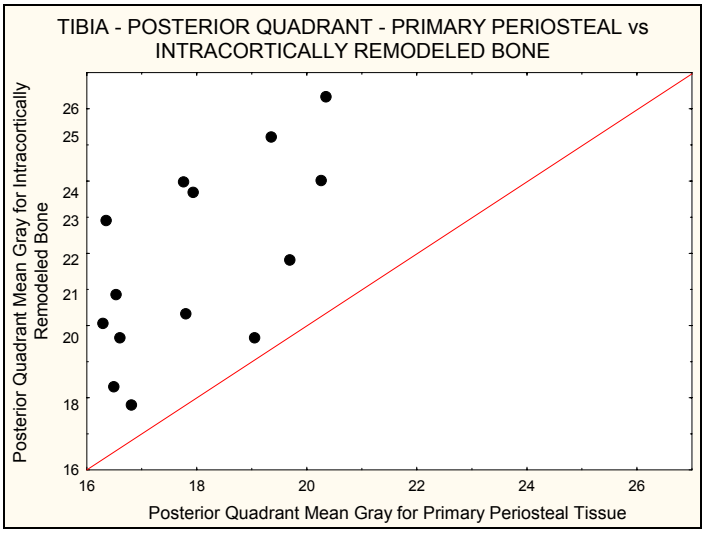


**Figure 6.29: Periosteal primary vs. intracortically remodeled bone for the medial quadrant in the tibia.**

The diagonal red line indicates where all data points would fall if gray values were equivalent in both tissue areas. Each data point indicates a single animal. See text for description.

*6.6.8 Factors accounting for variation in collagen fiber orientation across the entire sample*

Multiple regression analyses indicate that, with respect to primary periosteally deposited bone tissue, the independent variables PB, PHYLO and TCA do account for a significant proportion of the variation observed in this sample. The models yielding the highest adjusted $R^2$ may include all three predictor variables, only two, or in two cases a single variable only. Dependent upon the element, the relationship between collagen fiber orientation (expressed as a mean gray) across entire midshaft cortices and the independent variables differs, both in the magnitude of the total variance explained, as well as the independent variables accounting for the variation. Overall, significant $R^2$ values range between 0.34 and 0.51 with p-values of <.01 to <.0001 (Tables 6.1, 6.2).

With respect to secondary osteonal tissue, the results are more equivocal. Results for only two the five skeletal elements – the tibia and the ulna – indicate any significant relationship between the collagen fiber orientation and the independent predictor variables. For the tibia, the model with the highest adjusted $R^2$ (0.47; $p<.05$) includes the variables PB and PHYLO. For the ulna, all three variables are included in the best model ($R^2 = 0.84$; $p<.01$) (Figures 6.1, 6.3).

| MULTIPLE REGRESSION RESULTS | | | |
|---|---|---|---|
| Tissue Type | Element | Adjusted $R^2$ | Model |
| Periosteal Primary | Femur | 0.50*** | TCA, PB |
| | Humerus | 0.34** | TCA, PB, PHYLO |
| | Tibia | 0.57** | TCA, PB, PHYLO |
| | Radius | 0.44** | TCA |
| | Ulna | 0.91*** | TCA, PB, PHYLO |
| | Ulna[1] | 0.51** | TCA |
| Secondary Osteonal | Femur | none significant | |
| | Humerus | none significant | |
| | Tibia | 0.47* | PB, PHYLO |
| | Radius | none significant | |
| | Ulna | 0.84** | TCA, PB, PHYLO |

**Table 6.1: Multiple regression results for collagen fiber orientation in periosteal primary and intracortically remodeled bone for the entire sample.**
For each element, the model with the highest adjusted $R^2$ was selected. The number of independent variables included in the model differs depending on the element and tissue type. * indicates p<.05; ** indicates p<.01; ***indicates p<.001.
[1] This row provides results for the ulna when outlier specimen Z1 was removed from the sample. Without Z1, the sample size was too small to include all three predictor variables in a multiple regression. The adjusted $R^2$ is provided for the best model that was testable. Therefore, it is possible that the most powerful model, even in the absence of the outlier, may include all three variables.

| MULTIPLE REGRESSION BETAS – PERIOSTEAL PRIMARY TISSUE | | |
|---|---|---|
| **Element** | **Predictor Variable** | **Beta** |
| Femur | TCA | 0.35* |
| | PB | 0.56** |
| Humerus | TCA | Not significant |
| | PB | 0.88** |
| | PHYLO | -0.82* |
| Tibia | TCA | 0.74** |
| | PB | -0.64* |
| | PHYLO | -0.71* |
| Radius | TCA | 0.69** |
| Ulna | TCA | 0.30* |
| | PB | 1.39*** |
| | PHYLO | -1.32*** |
| Ulna[1] | TCA | 0.74** |

**Table 6.2: Multiple regression betas for collagen fiber orientation in periosteal primary bone for the entire sample.**

For each element, the independent variables for which there are significant betas are listed. Because the variables PHYLO and PB are dummy-coded, each includes more than one vector. Individual vectors may or may not have significant betas. Indicated significances are based on the highest p value for that variable. * Indicates p<.05; ** indicates p<.01; *** indicates p<.001.

| MULTIPLE REGRESSION BETAS – SECONDARY OSTEONAL TISSUE | | |
|---|---|---|
| **Element** | **Predictor Variable** | **Beta** |
| Femur | None significant | |
| Humerus | None significant | |
| Tibia | PB | Not significant |
| | PHYLO | -1.06* |
| Radius | None significant | |
| Ulna | TCA | Not significant |
| | PB | 1.22** |
| | PHYLO | -2.0 to –1.2** |

**Table 6.3: Multiple regression betas for collagen fiber orientation in intracortically remodeled bone for the entire sample.**

For each element, the independent variables for which there are significant betas are listed. Because the variables PHYLO and PB are dummy-coded, each includes more than one vector. Individual vectors may or may not have significant betas. Indicated significances are based on the highest p value for that variable. * Indicates $p<.05$; ** indicates $p<.01$; *** indicates $p<.001$.

For periosteal primary tissues, TCA appears as predictor variable in the models with the highest $R^2$ for all five elements although the beta for TCA in the humerus is statistically insignificant. Scatterplots for three of the five elements (the three distal elements) confirm a statistically significant relationship between TCA and collagen fiber orientation, with larger individuals displaying higher mean gray values (brighter cross sections in CPL) indicating a larger proportion of fibers that are oriented more transversely relative to smaller cortices (e.g., Figure 6.30). A weak positively allometric relationship is also observable in a scatterplot for the femur, but with a non-statistically significant $r^2$. Given both the multiple regression and simple correlation results, I conclude that a relationship does exist between collagen fiber orientation in periosteal primary bone and body size, as determined by the proxy measurement TCA.

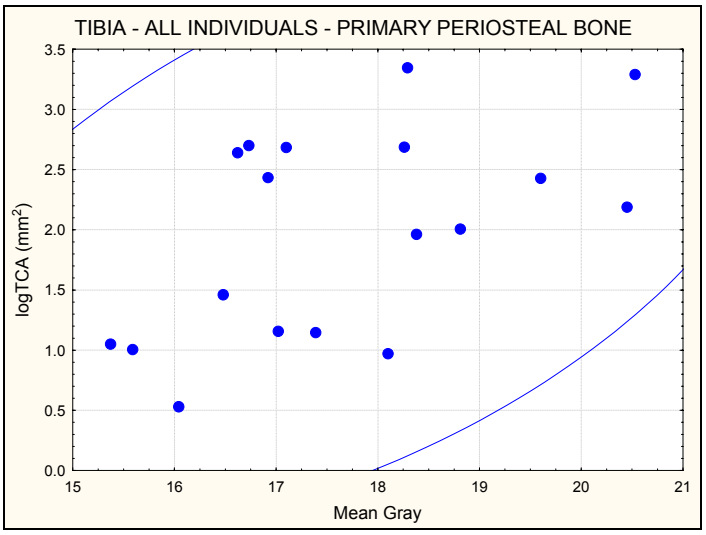


**Figure 6.30: Tibial mean gray values for periosteal primary tissue, as a function of TCA.**

There is a positively allometric relationship between mean gray level and TCA ($r^2$=.28, r=.53, p<.05). Femur: $r^2$=.09, r=.31, p>.05. Radius: $r^2$=.48, r=.69, p<.01. Ulna[1]: $r^2$=.55, r=.74, p<.01.

This does not appear to be the case for intracortically remodeled tissue. Only in the ulna does this factor contribute to the most powerfully explanatory multiple regression model, and even in this case the beta for TCA is insignificant. Furthermore, regressions of TCA on brightness in secondary osteons yield insignificant results for all elements. It therefore is evident that body size is not a significant factor in determining the orientation of collagen fibers within the concentric lamellae of secondary osteons.

The multiple regression analyses indicate that PB is also a factor significantly determinative of collagen fiber orientation in periosteal primary bone in three, and possibly four of five skeletal elements, the radius being the exception. In the ulna, it is unclear whether this variable is of importance. Before the removal of an outlier, PB contributes to the model with the highest adjusted $R^2$. After removal of the outlying data point, the *n* was too small to run a multiple regression analysis with all three predictor variables included. A model including PB and TCA provided a statistically significant adjusted $R^2$ that was only slightly lower than the highest $r^2$ when only TCA was included in the analysis (0.42 vs. 0.51). Therefore, it seems reasonable to conclude that PB

accounts for some of the variation in collagen fiber orientation in the ulna, as well as the femur, humerus and tibia.

Basic non-parametric statistics and graphical depictions of the data support the multiple regression results in some cases, but not in others. For the femur, Mann Whitney U tests identify significant differences among PB categories: values for vertical-clinger leapers are statistically significantly lower (indicating more longitudinal collagen fibers on average) than in arboreal quadrupeds ($p<.001$) and slow-climbers ($p<.05$), and values for slow climbers are lower than in arboreal quadrupeds ($p<.05$) (Figure 6.31). In addition, a PB categorization of a correlation scatterplot for femoral TCA against gray value yields a statistically significant positively allometric relationship for vertical-clinger leapers ($r^2=0.42$, $p<.05$) (Figure 6.32). (The relationship with TCA is not statistically significant when the sample is examined without categorization.) Although the correlation for arboreal quadrupeds is not statistically significant, an examination of the scatterplot suggests that brightness increases to a greater extent with body size in this group than in vertical-clinger leapers. Among humeri, values are again significantly lower in vertical-clinger leapers than in arboreal quadrupeds ($p<.05$). In this case, however, no PB categories yield significant correlations between TCA and gray value.

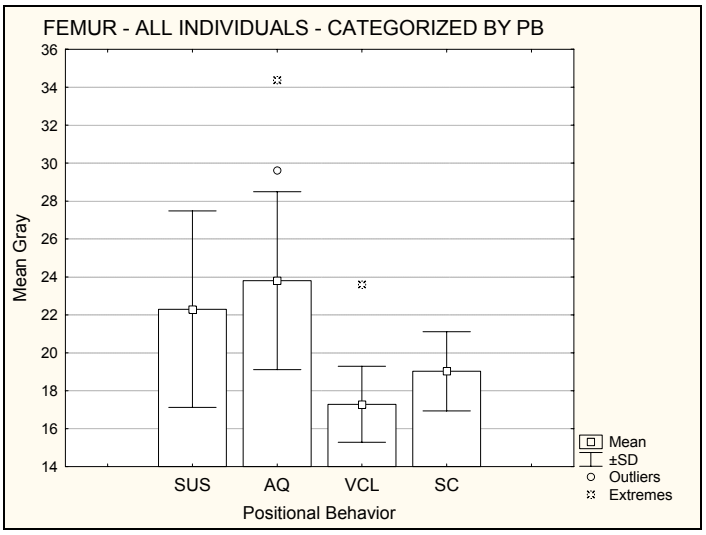


**Figure 6.31: Femoral mean gray values for periosteal primary tissue, categorized by PB.**

See text for description.

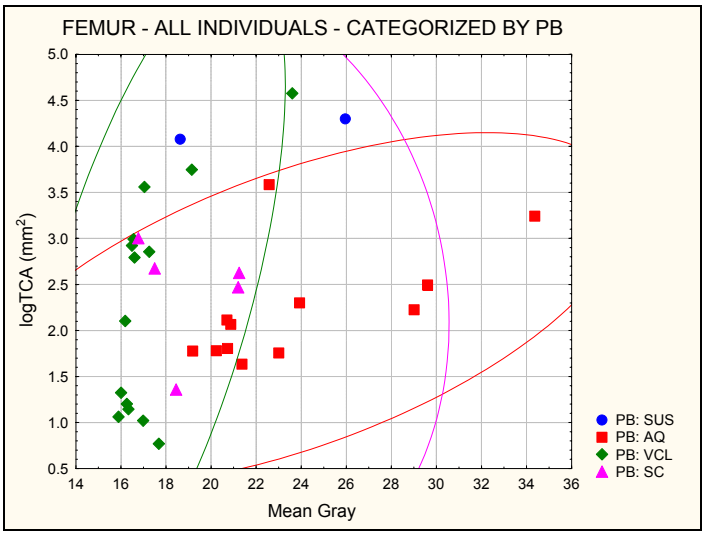


**Figure 6.32: Femoral mean gray values for periosteal primary tissue, as a function of TCA, categorized by PB.**

There is a positively allometric relationship between mean gray and TCA for vertical-clinger leapers. ($r^2$=0.42., r=.65, p<.05).

No statistically significant differences are found among PB categories for other skeletal elements, although means for vertical-clinger leapers are lowest in all cases. However, for both the tibia and radius, categorized scatterplots indicate statistically significant positively allometric relationships for some PB categories. In the tibia, it is the arboreal quadrupeds that show an increase in brightness with body size, with higher $r^2$ than for all PB categories combined ($r^2$ = 0.91; p<.01). In the radius, both arboreal

quadrupeds and vertical clinger-leapers show positively allometric relationships with TCA, with higher $r^2$ in both cases than in the sample as a whole ($r^2 = 0.87$ and 0.94 respectively). In the former, as with the femur, brightness increases faster with body size than in the latter. In summary, the totality of evidence suggests a weak and inconsistent relationship between collagen fiber orientation in periosteal primary tissue and positional behavior.

With respect to secondary osteonal bone, the multiple regression analyses suggest that PB is not a significant factor in determining the brightness (and by proxy the collagen fiber orientation) of the tissue. In only two of five elements (the tibia and ulna) does PB contribute to the model with the higher $R^2$, and only the analysis for the ulna yields a significant beta value. Nor do simple non-parametric statistics or graphical approaches consistently indicate that there is a relationship between the PB and collagen fiber orientation in secondary osteonal bone. Although there are statistically significant differences between PB categories in a couple of instances (between the vertical-clinger leapers and arboreal quadrupeds for the femur and tibia), these are not repeated in other elements.[2]

[2] It should be noted, however, that for all skeletal elements, the mean gray for all sample individuals is lower for the vertical-clinger leaper group than for the arboreal quadruped group.

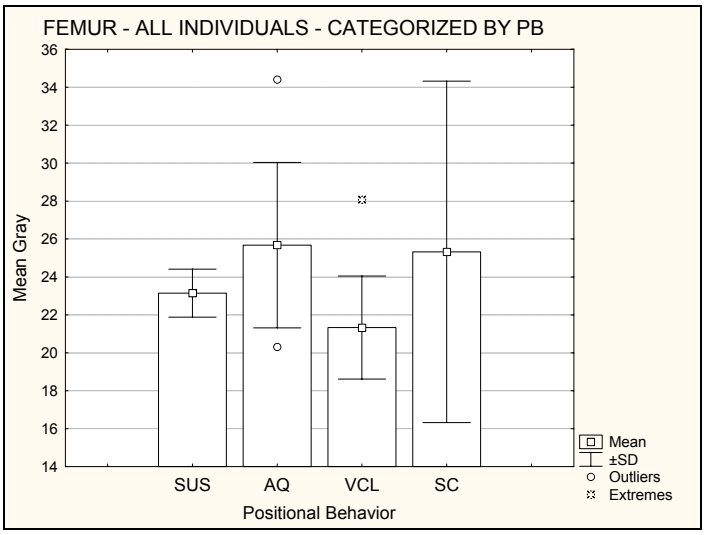


**Figure 6.33: Femoral mean gray values for intracortically remodeled bone, categorized by PB.**

See text for description.

Multiple regression analysis results indicate that PHYLO is a significant predictor for collagen fiber orientation in periosteal primary bone in two out of five skeletal elements (when the ulna is considered without the outlier data point). In these two – the humerus and tibia – betas are also significant for PHYLO. However, the absence of an identified effect for the other skeletal elements, as well as a general lack of detectable repeated pattern or significant differences among PHYLO groups when simple non-parametric and graphical methods are used, suggests that PHYLO is not an important predictor of collagen fiber orientation in periosteal primary tissue.[3]

Likewise, PHYLO appears as a predictor factor for collagen fiber orientation in secondary osteonal bone in the multiple regression models with the highest $R^2$ in only two skeletal elements: the tibia and the ulna, both times with significant betas. However, only in the femur are there any significant differences among PHYLO groups (between the platyrrhines and tarsiids: $p<.05$). Therefore, is appears unlikely that PHYLO is a significant predictor for orientation of collagen fiber in intracortically remodeled bone.

[3] Statistically significant differences do exist among PHYLO groups for periosteal primary tissue in the femur, but these are not repeated in other skeletal elements.

*6.6.9 Collagen fiber orientation and tissue type*

Examination of the multiple regression results leads to the conclusion that, although the three independent variables do account for some significant proportion of variation in collagen fiber orientation, much of the diversity remains unexplained. While there has been little previous discussion of this in the literature (see Smith, 1960a; Riggs et al, 1993a; McMahon et al., 1995; Goldman et al., 2003; Lee, 2004; Skedros & Hunt, 2004; Bromage & Boyde, n.d.), a preliminary inspection of the CPL images relative to tissue type maps (see Chapter 4) suggests a relationship between tissue type and collagen fiber orientation, where more transverse fibers are associated with slower depositing tissues. The following analysis explores this possibility in greater depth.

Mean gray values for individual tissue types (LAM, LAM+HYB, HYB, PF, FAST) across entire cortices, combined for all individuals for each skeletal element, were examined relative to each other (Table 6.4). For all skeletal elements there are statistically different differences among primary tissue types. LAM bone is brighter than all other tissue types in all elements except the radius, where it is brighter than all tissue types except FAST. These differences are statistically significant for the comparisons between LAM and LAM+HYB bone, LAM and HYB bone, as well as LAM and PF bone in all elements (Sign test: $p<.01$ to $p<.0001$). LAM bone is statistically significantly brighter than FAST bone only in the humerus. For all other elements there are no statistically meaningful differences between these two tissue types. In all elements, LAM+HYB bone is statistically brighter than HYB bone ($p<.05$ to $p<.0001$), and brighter than PF bone in the femur, humerus and ulna. There are no statistically meaningful differences between brightness values for HYB and PF tissue in any of the skeletal

elements. The combined picture is one where LAM and FAST tissues, in particular the former, contain the highest proportion of more transverse collagen fibers (although, as noted previously, these are still closer to longitudinal than transverse), whereas HYB and PF tissues comprise the largest proportion of more longitudinal collagen fibers (e.g., Figure 6.34).

| SIGN TEST RESULTS | | | | | |
|---|---|---|---|---|---|
| | Femur | Humerus | Tibia | Radius | Ulna |
| LHxPF | **0.0027** | **0.0000** | 0.2386 | 0.0801 | **0.0244** |
| LHxFAST | 0.0990 | **0.0000** | 0.2278 | 1.0000 | 1.0000 |
| LHxLAM | **0.0000** | **0.0000** | **0.0012** | **0.0002** | **0.0055** |
| LHxHYB | **0.0000** | **0.0000** | **0.0060** | **0.0012** | **0.0265** |
| PFxFAST | **0.0001** | 0.0725 | **0.0026** | 0.0736 | **0.0233** |
| PFxLAM | **0.0000** | **0.0000** | **0.0019** | **0.0002** | **0.0055** |
| PFxHYB | 0.1116 | 0.4862 | 0.4795 | 0.4533 | 0.0801 |
| FASTxLAM | 1.0000 | **0.0000** | 0.7518 | 1.0000 | 0.6831 |
| FASTxHYB | **0.0001** | 0.0817 | **0.0159** | 1.0000 | 0.4497 |
| LAMxHYB | **0.0000** | **0.0000** | **0.0012** | **0.0002** | **0.0055** |

**Table 6.4: Sign test results for comparison among periosteal primary tissue type mean gray values for all skeletal elements.**
Bolded values are statistically significant.

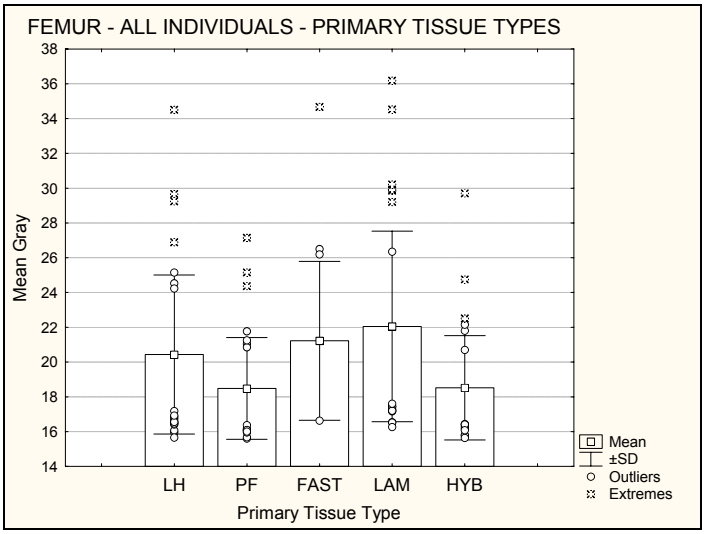


**Figure 6.34: Femoral mean gray values for individual periosteal primary tissue types.**

See text for description. LH=lamellar+hybrid; PF=parallel-fibered; FAST=woven+fast fibrolamellar+slow fibrolamellar; LAM=lamellar; HYB=hybrid.

The pattern seen for sample means is repeated when values for individual specimens are compared. For example, in the vast majority of specimens, the mean gray value for LAM tissue throughout the periosteal cortex is higher than the value for PF tissue. There is a generally correlated relationship between an increase in brightness for the two tissue types (i.e., if one individual has a high mean gray value for LAM tissue relative to other individuals, the value for PF tissue is also likely to be high[4]), but the increase is faster for LAM bone than PF bone ($r^2$=.79, r=.63, p<.0001) (Figure 6.35). Some relationships become clearest when individual values are compared. For example, although there are no significant differences between LAM and FAST bone in the radius or humerus, bivariate scatterplots for these show that FAST bone is brighter than LAM bone for the majority of individuals.

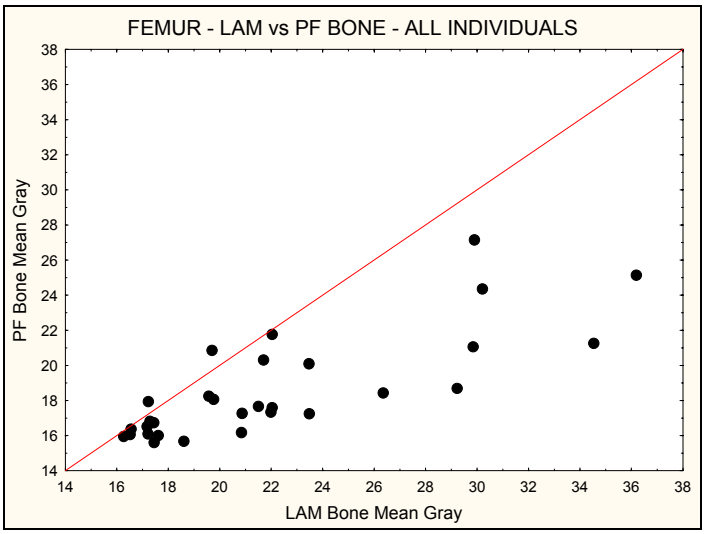


**Figure 6.35: Mean gray values for LAM vs. PF bone in the femur.**
The diagonal red line indicates where all data points would fall if gray values were equivalent in both tissue types. Each data point indicates a single animal. See text for description.

[4] This raises the possibility that differences between individuals may in part be due to illumination error, despite stringent adherence to methods designed to eliminate, or at least substantially reduce, such error.

A comparison between secondary osteonal bone (OST) and primary tissue types in the periosteal portions of the cortex shows that the former, composed of concentric lamellae, is on average similar in brightness to primary lamellar tissue (Figure 6.36). In all skeletal elements, there are no statistically significant differences in mean gray between LAM and OST tissues. In addition, bivariate plots show no consistent pattern of elevated brightness in either of these two tissue types relative to the other (Figure 6.37).

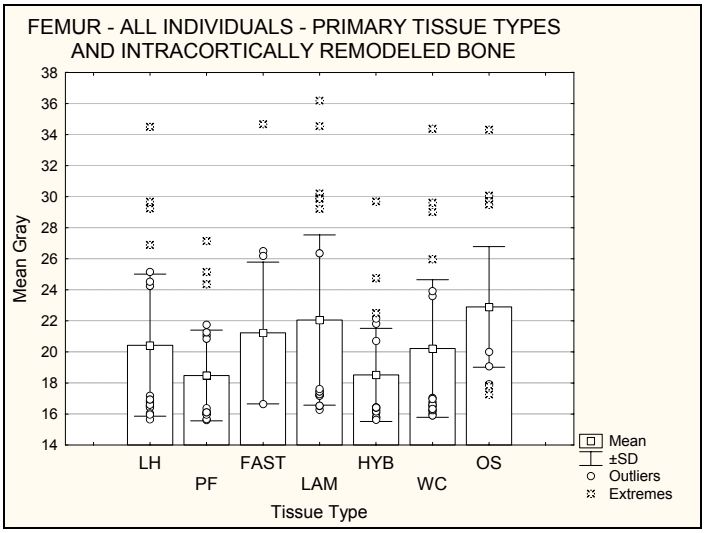


**Figure 6.36: Femoral mean gray values for individual periosteal primary tissue types and intracortically remodeled bone.**

See text for description. LH=lamellar+hybrid; PF=parallel-fibered; FAST=woven+fast fibrolamellar+slow fibrolamellar; LAM=lamellar; HYB=hybrid; WC=whole cortex; OS=intracortically remodeled bone.

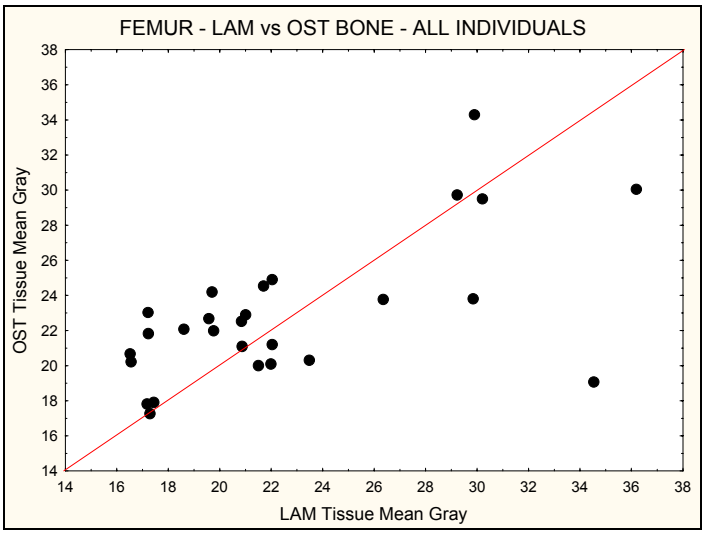


**Figure 6.37: Mean gray values for LAM vs. intracortically remodeled bone in the femur.**

The diagonal red line indicates where all data points would fall if gray values were equivalent in both tissue types. Each data point indicates a single animal. See text for description.

Similarly, differences between secondary osteonal and FAST tissue are insignificant in all elements except the tibia ($p<.05$). In the latter, for 10 of 11 individuals, the mean gray value for intracortically remodeled tissue is higher than for FAST tissue. However, for the ulna, while a small *n* precludes statistical significance, five of six individuals show brighter FAST tissue than secondary osteonal tissue. Bivariate scatterplots for the other three elements show no pattern of elevated brightness for either tissue. I therefore conclude that there is no consistent difference in preferred collagen fiber orientation between FAST and intracortically remodeled tissues.

In contrast, mean grays for intracortically remodeled tissue are higher than those for PF or HYB tissue in all skeletal elements (with all individuals combined). These differences are statistically significant for the comparison between secondary osteons and PF for all elements except the ulna ($p<.05$ to $p<.0001$), and for the comparison between secondary osteons and HYB for the femur, humerus and tibia ($p<.001$ to $p<.0001$). In summary, secondary osteonal tissues have mean collagen fiber orientations comparable to those found in periosteal primary LAM and FAST bone.

*6.6.10 Comparison between elements: PB patterns in periosteal primary tissue*

When the periosteal primary tissue mean gray-values for two different elements are compared for the entire sample (looking at individuals rather than sample means), there is a functional patterning to the resultant bivariate plots in several cases. First, when femoral and tibial values are compared in a bivariate scatterplot, it is evident not only that arboreal quadrupeds have brighter cortices than vertical-clinger leapers and slow climbers, but also that femoral brightness increases at a greater rate relative to tibial

brightness in the arboreal quadrupeds (Figure 6.38). In other words, for an individual with a given tibial mean gray, the femur is likely to have a higher mean grey in an arboreal quadruped than a vertical clinger leaper or slow climber. This pattern is repeated when the radius is compared to the femur and, to a lesser degree, when the ulna is compared to the femur.

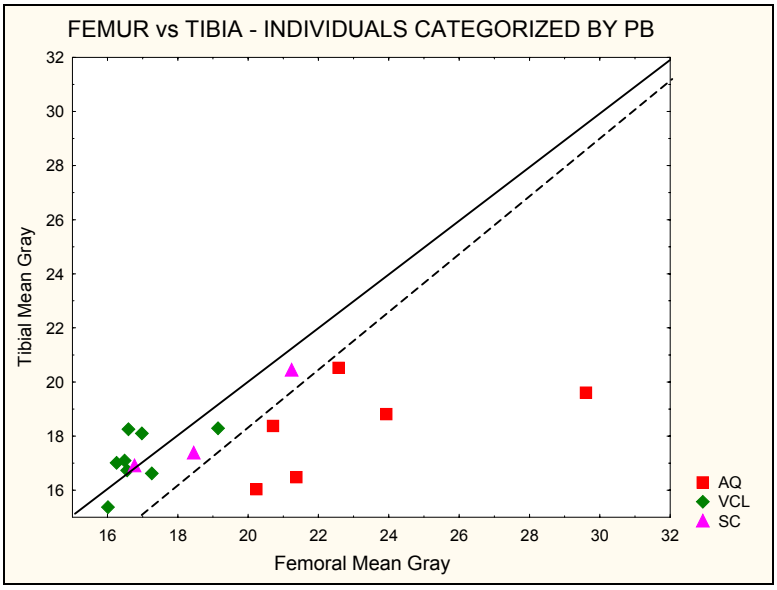


**Figure 7.38: Mean gray values for all sample individuals in the femur vs. the tibia, categorized by PB.** In this bivariate plot of periosteal primary tissue tibial and femoral mean gray, the solid diagonal line indicates where the values would fall should the values be equivalent in the tibia and femur for an individual. In almost all cases, the mean gray values in the femur of arboreal quadrupeds are greater, relative to tibia, than in comparably sized individuals from other PB categories. The dashed diagonal line is an arbitrarily drawn separation between arboreal quadrupeds (below the line) and taxa with all other positional behaviors (above the line). AQ=arboreal quadruped; VCL=vertical clinger and leaper; SC=slow climber.

Second, comparisons of the humerus and tibia or humerus and ulna show that, while in some individuals the humerus may be brighter than others, the mean gray range for the tibia and radius remains within a small, and low, gray level range (e.g., values for the humerus range between 17.6 and 46.4, whereas the range for the tibia is 15.4-20.5;

see Table 6.5). In addition, humeral values for the arboreal quadrupeds are usually greater than those for the vertical clingers leapers and most slow climbers, while the range of values for the tibia and radius are similar among PB groups (Figure 6.39). These observations also apply to the comparison of humerus and ulna, with the exception of a single outlying AQ ulnar data point.

| Element | Range |
|---|---|
| Femur | 15.9-34.4 |
| Humerus | 17.6-46.4 |
| Tibia | 15.4-20.5 |
| Radius | 16.3-24.4 |
| Ulna | 15.9-28.9 |

**Table 6.5: Element ranges for mean gray values for all sample individuals.**

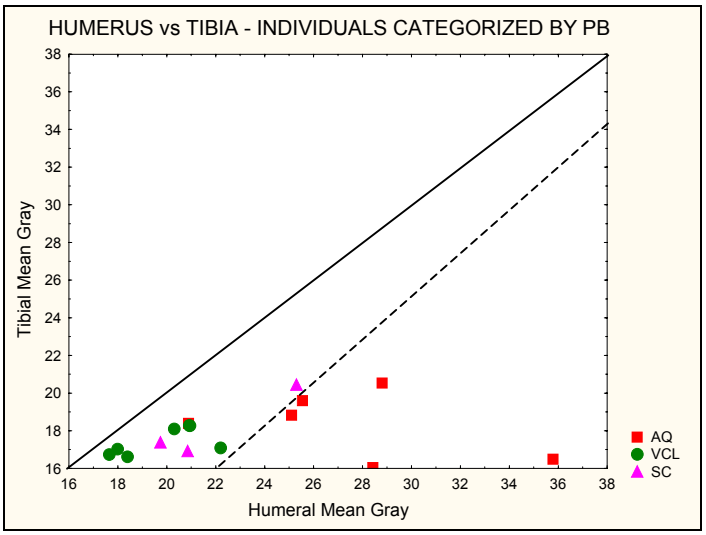


**Figure 6.39: Mean gray values for all sample individuals in the humerus vs. the tibia, categorized by PB.**

In this bivariate plot of periosteal primary tibial and humeral mean gray, the solid diagonal line indicates where the values would fall should the values be equivalent in the humerus and tibia for an individual. In almost all cases, the mean gray values in the humerus of arboreal quadrupeds are greater, relative to tibia, than in comparably sized individuals from other PB categories. The dashed diagonal line is an arbitrarily drawn separation between arboreal quadrupeds (below the line) and taxa with all other positional behaviors (above the line).

Comparisons between the femur and humerus, as well as between all pairs of distal elements, yield no differences among positional behavior groups.

*6.6.11 Comparison between elements: PB patterns in secondary osteonal tissue*

When the secondary osteonal tissue mean gray-values for two different elements are compared for the entire sample (looking at individuals rather than sample means), there are no functional patterns to the resultant bivariate plots, with one exception. While in most individual cases the brightness values are higher for the femur than the radius, in arboreal quadruped individuals this contrast is more pronounced, with secondary osteons in the femur brighter relative to the radius than in vertical-clinger leapers and slow climbers (Figure 6.40).

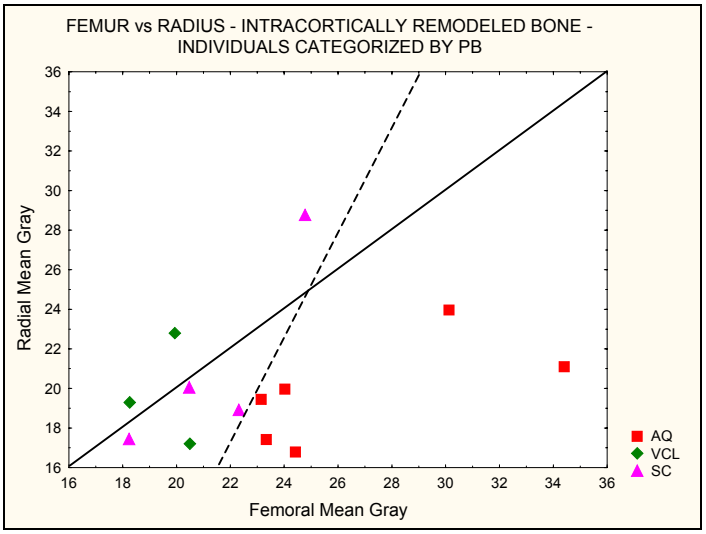


**Figure 6.40: Mean gray values for all sample individuals in the femur vs. the radius, categorized by PB.**

In this bivariate plot of secondary osteonal femoral and radial mean gray, the solid diagonal line indicates where the values would fall should they be equivalent in the femur and radius for an individual. In almost all cases, mean gray values in the femur of arboreal quadrupeds are greater, relative to radius, than in comparably sized individuals from other PB categories. The dashed diagonal line is an arbitrarily drawn separation between arboreal quadrupeds (right of the line) and taxa with all other positional behaviors (left of the line).

*6.6.12 Comparison between sectors: PB patterns in periosteal primary tissue*

When bivariate plots of different cortical quadrants are categorized by PB, no patterns of sectoral brightness characteristic of different PB groups emerge for any of the five skeletal elements, with two exceptions.

First, in the humerus, there is a greater disparity in brightness between the lateral and anterior quadrants in arboreal quadrupeds relative to vertical clinger leapers, slow climbers and suspensory individuals (Figure 6.41). In the majority of AQ, the lateral quadrant is brighter than the anterior quadrant, while in the majority of individuals from the other three PB groups, values are similar, or the lateral quadrant is only slightly brighter. They same pattern in the humerus is seen when the posterior and anterior quadrants are compared, with the posterior quadrant more likely to be bright relative to the anterior quadrant in arboreal quadrupeds as compared to other PB groups.

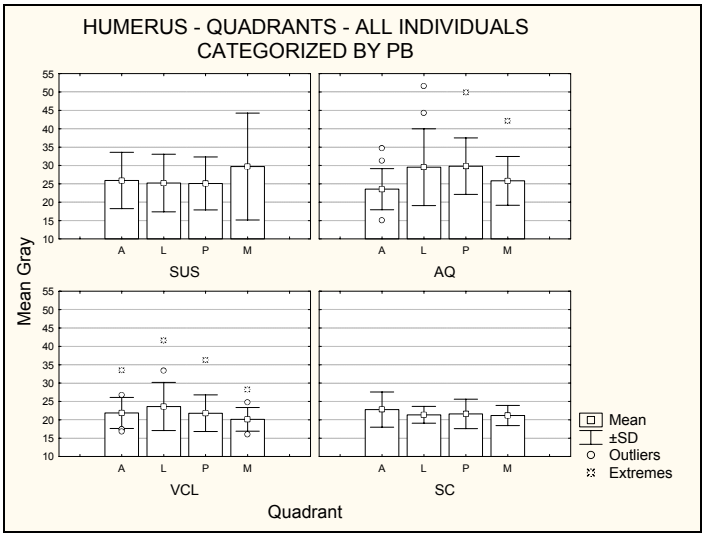


**Figure 6.41: Humeral periosteal primary bone mean gray values for individual quadrants, categorized by PB.**

See text for description.
A=anterior; L=lateral; P=posterior; M=medial. SUS=suspensory; AQ=arboreal quadruped; VCL=vertical clinger and leaper; SC=slow climber.

Second, in the radius, the medial quadrant is more likely to be brighter relative to the lateral and posterior quadrants in arboreal quadrupeds as compared to vertical-clinger leapers and slow climbers (there are no suspensory specimens for the radius) (Figure 6.42).

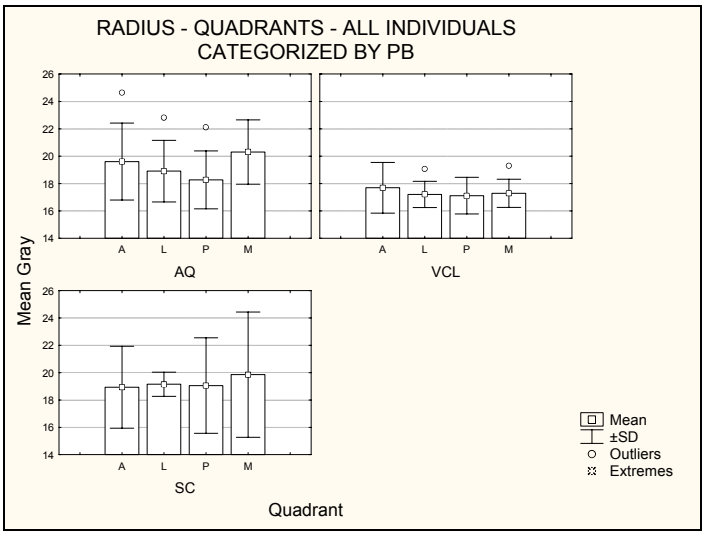


**Figure 6.42: Radial periosteal primary bone mean gray values for individual quadrants, categorized by PB.**

See text for description. Legend as per Figure 6.41.

*6.6.13 Comparison between sectors: PB patterns in secondary osteonal tissue*

When bivariate plots of different cortical quadrants are categorized by PB, no patterns of sectoral brightness characteristic of different PB groups emerge for any of the five skeletal elements.

*6.6.14 Characterization of individual taxa*

6.6.14.1 Intra- and intertaxonomic diversity

Investigations of variation within the sample as a whole highlight some patterned relationships between collagen fiber orientation and body size as well as positional

behavior. However, within the broad patterns described above, there is evidence of both intra- and intertaxonomic diversity. Following is an exploration of this variability. Because within-taxon sample sizes are small – particularly for the tibia, radius and ulna – analyses remain descriptive.

| | | Femur | Humerus | Tibia | Radius | Ulna |
|---|---|---|---|---|---|---|
| Atelidae | PP | 22.3 | 26.34 | - | - | - |
| | OST | 23.15 | 25.19 | - | - | - |
| Calltrichidae | PP | 19.97 | 22.02 | - | 16.71 | 17.95 |
| | OST | 22.56 | 23.72 | - | 19.43 | 19.41 |
| Cheirogaleidae | PP | 21.37 | 29.73 | 16.26 | 18.30 | 16.82 |
| | OST | 23.67 | 24.60 | 23.73 | 17.10 | 16.42 |
| Lesser Galago | PP | 16.63 | 21.35 | 15.48 | 16.58 | 16.15 |
| | OST | 22.37 | 21.45 | 19.21 | 17.54 | 16.79 |
| Indriidae | PP | 19.93 | 26.21 | 18.29 | - | 19.90 |
| | OST | 22.88 | 22.77 | 18.59 | - | 19.42 |
| Lemuridae | PP | 28.48 | 37.62 | 20.53 | 23.63 | 28.91 |
| | OST | 30.00 | 27.91 | 23.41 | 23.97 | 25.52 |
| Lorisidae | PP | 19.03 | 21.86 | 18.25 | 19.37 | 18.12 |
| | OST | 25.32 | 23.25 | 21.94 | 21.30 | 17.48 |
| Greater Galago | PP | 16.73 | 19.80 | 17.18 | 18.76 | 17.85 |
| | OST | 20.36 | 19.84 | 18.87 | 18.25 | 17.95 |
| Cebidae | PP | 25.82 | 23.85 | 18.93 | 19.40 | 18.40 |
| | OST | 27.09 | 22.50 | 20.79 | 20.52 | 19.15 |
| Tarsiidae | PP | 16.37 | 22.11 | 17.56 | 16.84 | 16.89 |
| | OST | 19.94 | 24.44 | 35.72<br>22.59 | 22.80 | 23.59 |

**Table 6.6: Summary of whole cortex mean grays for individual elements and taxa, for both periosteal primary and secondary osteonal tissue.**
Each value represents a mean for the element within a taxon. The two values for intracortically remodeled bone in the tarsiid tibiae represent means with and without the inclusion of a single tibiofibula containing one very bright secondary osteon. PP=periosteal primary tissue; OST=intracortically remodeled.

6.6.14.2 Consistency[5] within taxa: intrataxonomic variation for individual elements

Consistency in the mean gray values and patterns of mean gray among quadrants varies between elements and among taxa. In 10 cases[6] for periosteal primary tissue, both magnitude and patterns of brightness are similar[7] (e.g., Figure 6.43). In six cases, two or more individuals are similar in magnitude and pattern of brightness, with a single outlier (e.g., Figure 6.44). In six cases, magnitude of brightness may be close among individuals, but with different quadrant patterns (e.g., Figure 6.45). The reverse is true in three cases, with similar patterns of brightness among quadrants, but with overall gray values divergent (e.g., Figure 6.46). Finally, in 11 cases, there is no consistency at all among individuals (e.g., Figure 6.47). There is no taxon or element regularity with respect to consistency among individuals or lack thereof. That is to say, no one taxon or skeletal element is more or less likely to display uniformity among individuals.

[5] Collagen fiber orientation is considered to be *consistent* when all individuals within a taxon have approximately the same magnitude and patterns of brightness across the cortex for a given skeletal element. Consistency is assessed through visual inspection of graphically depicted data.

[6] Each "case" represents a comparison of values for individuals for a single element of a single taxon. Where only one specimen is available (e.g., for the distal elements in some taxa), ranges are necessarily not considered.

[7] Patterns are considered similar when the difference between gray values among individuals for a given quadrant do not exceed five gray scale values, and when the relationships among quadrant values are generally the same for all individuals (e.g., if the value for the anterior quadrant is greater than that for all other values in one individual, that is also the case for all other individuals).

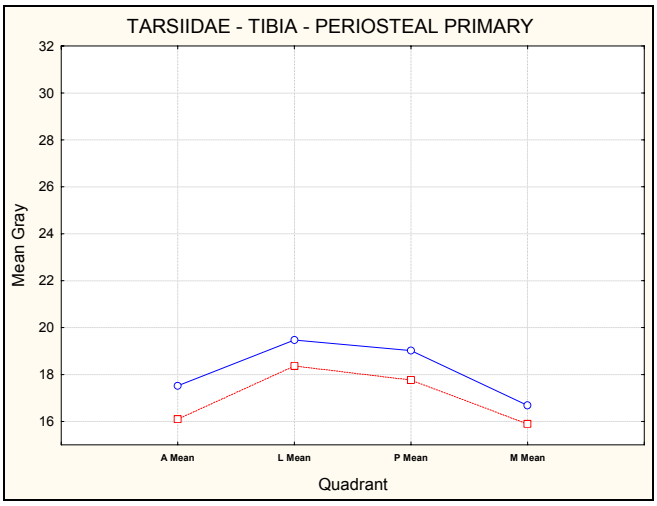


**Figure 6.43: Example of similar magnitude and pattern of brightness.**

A Mean=anterior quadrant; L Mean= lateral quadrant; P Mean=posterior quadrant; M Mean=medial quadrant.

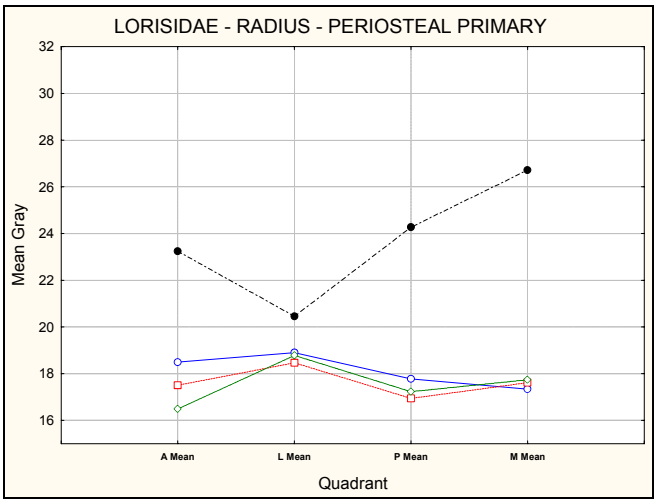


**Figure 6.44: Example of similar magnitude and pattern of brightness with a single outlier.**

Legend as per Figure 6.43.

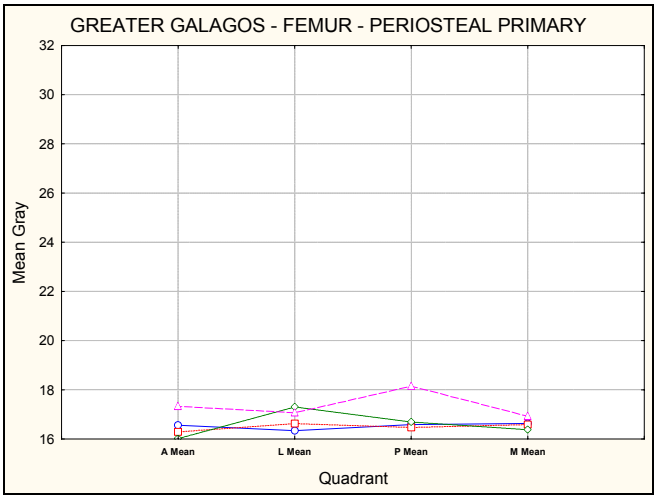


**Figure 6.45: Example of similar magnitude of brightness, but variable pattern.**

Legend as per Figure 6.43.

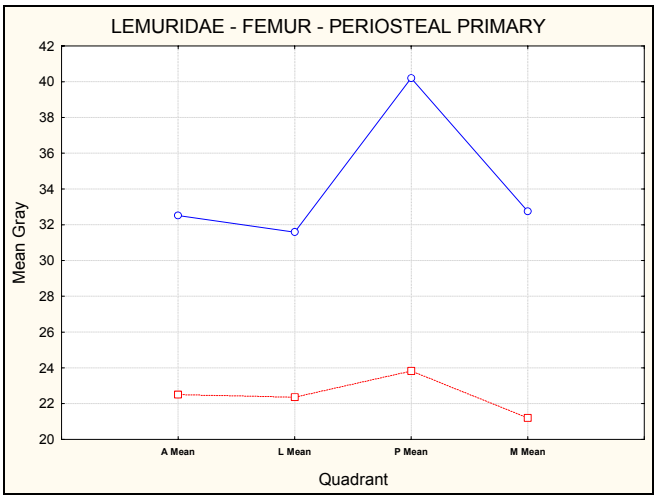


**Figure 6.46: Example of similar pattern of brightness, but variable magnitude.**

Legend as per Figure 6.43.

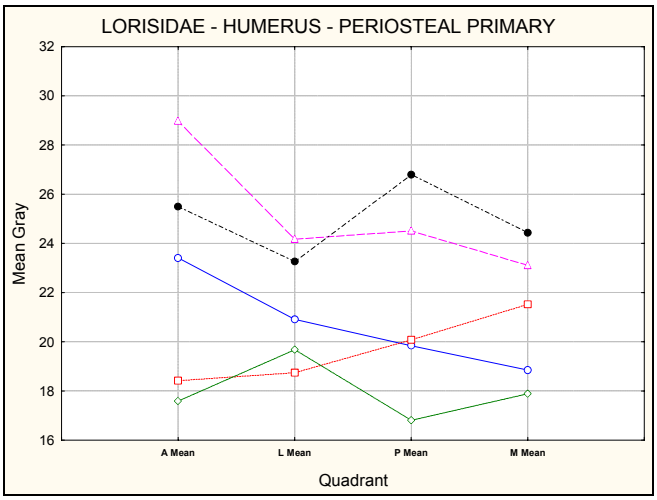


**Figure 6.47: Example of variable magnitude and brightness.**

Legend as per Figure 6.43.

Results are similar for secondary osteonal bone. In only less than 25% of cases (5 of 23) do individuals show similar magnitude and quadrant patterning of mean gray brightness[8].

[8] In 22 cases there is either only one individual, or there are data gaps for some quadrants (where there is no intracortical remodeling) yielding no data for comparison between individuals.

6.6.14.3 Characterization of patterns of collagen fiber orientation for individual taxa

*6.6.14.3.1 Lesser galagos.* The range in periosteal primary tissue gray values for all quadrants in all elements for lesser galagos is c.15-28, and 10-28 for secondary osteonal tissue. (Each number represents the mean of pixel gray values, on a scale of 0-255, for a single quadrant in an individual specimen section.) Two out of three femoral sections show a similar pattern in both magnitude and quadrant brightness for periosteal primary tissue, with a peak brightness in periosteal primary tissue in the lateral quadrant, displaying grey values 3.5-4.5 units higher than in all other quadrants (each unit indicating a pixel gray scale value on a scale of 0-255). Likewise, both sample ulna sections are consistent in their pattern of collagen fiber orientation in periosteal primary tissue. The posterior quadrant is darker than all other quadrants, although the range in mean gray values among quadrants does not exceed 1.5 units. Finally, for the tibia, both individuals show a similar pattern and magnitude, with all quadrants in both individuals displaying gray level values between 15 and 16. For the humerus and radius, there is no consistency among elements for periosteal primary tissue in the pattern of brightness between quadrants. In the radius, however, the brightness magnitude is similar among individuals and quadrants.

Intracortical remodeling is limited for lesser galagos (see Chapter 5) and therefore no comparisons can be made for individual elements within taxa.

*6.6.14.3.2 Greater galagos.* The range in periosteal primary tissue gray values for all quadrants in all elements for lesser galagos is c.16-25, and 15-26 for secondary osteonal tissue. In the tibia, three of four individuals show a similar quadrant pattern for periosteal

primary tissue with a similar mean gray magnitude. In these individuals, the lateral and medial quadrants are brighter than the anterior and posterior quadrants, although differences between quadrants do not exceed 1.5 gray scale units. The pattern for the two ulna sections is also similar, with the lateral quadrant displaying higher values than the posterior and medial quadrants. Again, however, the range among quadrants and individuals does not exceed 2.5 gray value units. For all other elements, there is no consistency among individuals in the quadrant pattern, although brightness magnitudes are similar among individuals for the femur and radius.

The two ulna specimens show similar quadrant patterns and magnitudes of brightness for secondary osteonal tissue. In both individuals, the lateral quadrant is brighter than the anterior and posterior quadrants, and the medial quadrant is brighter than the posterior quadrant. Differences between quadrants remain below 1.5 gray value units. For all other elements, either there is no consistency among individuals (although brightness is consistent for the humerus and radius), or too few data points to compare.

*6.6.14.3.3 Lorisidae.* The range in periosteal primary tissue gray values for all quadrants in all elements for lorisids is c. 9-29, and 16-47 for secondary osteonal tissue. In the radius, three of four individuals show similar patterns and magnitudes of brightness. In these three, the lateral quadrant is brighter than all other quadrants, while in the fourth individual the lateral quadrant is the darkest. In this last individual, values for all quadrants are higher than in the other three. For all other skeletal elements, there is no consistency among individuals in quadrant patterns, although magnitudes of brightness are similar for the tibia and ulna.

Patterns and magnitudes of brightness among individuals for secondary osteonal bone are variable for all skeletal elements.

*6.6.14.3.4 Cheirogaleidae*. The range in periosteal primary tissue gray values for all quadrants in all elements for cheirogaleids is c. 15-44, and 16-48 for secondary osteonal tissue. There are two instances where a single quadrant in a single individual provides a very high value relative to other data for the cheirogaleids, as well as for the sample as a whole. These are the lateral quadrant in one sample humerus (periosteal primary tissue), and the posterior quadrant in a different humeral specimen (intracortically remodeled tissue.) With the exception of the tibia, there are no consistent quadrant patterns of collagen fiber orientation (only a single specimen is available for the ulna). In the tibia, the anterior quadrant is brightest in both individuals, although the total range between quadrants and individuals does not exceed approximately one gray scale unit. In other words, values for all quadrants in both individuals are nearly equivalent. In the radius, although quadrant patterns are dissimilar, overall magnitude of brightness is the same. In the humerus, in three out of four individuals, the lateral quadrant is brighter than all other quadrants (although very close to the value for the posterior quadrant in one of the three).

Patterns and magnitudes of brightness among individuals for secondary osteonal bone are variable for all skeletal elements except the radius, where both sample individuals have very similar values for the lateral, posterior and medial quadrants (with the posterior quadrant brightest in both cases). In one of the two individuals there is no remodeling in the anterior quadrant.

*6.6.14.3.5 Indriidae*. The range in periosteal primary tissue gray values for all quadrants in all elements for indriids is c. 15-36, and 18-32 for secondary osteonal tissue. There are no sample radii for this taxon, and only a single tibia and ulna. Neither the femur nor humerus display any regularity among individuals in quadrant patterns or magnitude of brightness for periosteal primary tissues.

Although magnitudes of brightness vary among individuals, quadrant patterns are generally consistent among individuals for intracortically remodeled tissue in the femur. In all three sample individuals, the anterior quadrant is brighter than both lateral and posterior quadrants, as well as the medial quadrant in two of the three (in the third, the medial quadrant is brightest). In two out of three humeral sections, the pattern of brightness in intracortically remodeled bone is similar, although magnitudes are different. In these two, the posterior quadrant is brighter than all other quadrants. In the third humeral specimen the lateral quadrant is brightest.

*6.6.14.3.6 Lemuridae*. The range in periosteal primary tissue gray values for all quadrants in all elements for lemurids is c. 19-52, and 22-36 for secondary osteonal tissue. For periosteal primary tissue, in both the humerus and femur, quadrant patterns are similar for the two sample individuals, with a large disparity in magnitude of brightness (one individual has particularly high gray scale values relative to most other specimens in the sample as a whole). In the femur, both individuals show a peak in brightness in the posterior quadrant. In the humerus, both individuals have anterior and medial quadrants that are darker than the lateral and posterior quadrants. There is only a single specimen each for the radius, ulna and tibia.

With respect to secondary osteonal tissue, only the humerus provides comparative data for all four quadrants. In this case, the two sample individuals are similar in quadrant pattern, but not magnitude of brightness: both show a brightness peak in the posterior quadrant.

*6.6.14.3.7 Tarsiidae*. The range in periosteal primary tissue gray values for all quadrants in all elements for tarsiids is c. 15-42, and 17-55 for secondary osteonal tissue. There are a few instances where a single quadrant or an adjacent pair of quadrants, in a single individual, provides a very high value relative to other data for the tarsiids, as well as for the sample as a whole. These are the lateral quadrant in one humerus (periosteal primary tissue), the lateral and posterior quadrants in one tibia (secondary remodeled tissue), and the medial quadrant for one sample humerus (secondary remodeled tissue).

In both the radius and tibia, the two sample individuals display very similar quadrant patterns and magnitudes of brightness for periosteal primary tissue. In the former, all quadrants have values within one gray level unit of each other (i.e., all quadrants are equally bright). In the tibia, the lateral quadrant is brightest, followed closely by the posterior quadrant, with lower values for both the anterior and medial quadrants. In the femur and ulna, while magnitudes of brightness are similar among individuals, quadrant patterns are not. In the humerus, neither pattern nor brightness is consistent.

Intracortical remodeling is sparse in the tarsiids, barring comparison of collagen fiber orientation among individuals across whole cortices.

*6.6.14.3.8 Callitrichidae*. The range in periosteal primary tissue gray values for all quadrants in all elements for callitrichids is c. 15-24, and 17-28 for secondary osteonal tissue. There are no tibia specimens for this taxon, and only one individual each for the radius and ulna. In the femur, both sample specimens display similar quadrant patterns and similar magnitudes of brightness in periosteal primary tissue. In both individuals, the lateral quadrant is darker than the medial, anterior and posterior quadrants. In the humerus, neither pattern nor magnitudes of brightness are similar.

Because remodeling is sparse in this taxon, no pattern assessment is possible for secondary osteonal tissue in any of the skeletal elements.

*6.6.14.3.9 Cebidae*. The range in periosteal primary tissue gray values for all quadrants in all elements for cebids is c. 17-31, and 18-45 for secondary osteonal tissue. The posterior quadrant in the humerus (secondary osteonal tissue) in a single individual provides a very high value relative to other data for the cebids, as well as for the sample as a whole. In both the radius and ulna, the two sample individuals show similar quadrant patterns and magnitudes of brightness for periosteal primary tissue. In the radius, the medial quadrant is brighter than all other quadrants, and the posterior quadrant is darker than the lateral quadrant. In the ulna, the posterior quadrant is darker than the anterior and lateral quadrants. For both elements, the range between quadrants within individuals does not exceed 2.5 gray scale units. Among the three specimens for the humerus, two display a similar pattern and magnitude of brightness, while the third is an outlier. In the former two, the posterior quadrant is brighter, and the anterior is darkest.

In the tibia, magnitudes are similar, but patterns are variable, while in the femur neither pattern nor magnitudes show a consistent pattern among the four individuals.

As is the case with periosteal primary tissue, patterns of collagen fiber orientation in intracortically remodeled tissue in the ulna are consistent between individuals. In both sample specimens, the lateral quadrant is the darkest, and the anterior quadrant is the brightest, followed by the posterior quadrant. In the humerus, two of three individuals show a peak in the posterior quadrant (relative to roughly equal values among all other quadrants), with this peak being extreme in one individual (see above). Neither the femur, tibia nor radius show any consistent patterns, although magnitudes are similar among individuals in the tibia.

*6.6.14.3.10 Atelidae*. The range in periosteal primary tissue gray values for all quadrants in all elements for atelids is c. 18-40, and 21-28 for secondary osteonal tissue. In the femur, both atelid individuals show a similar quadrant pattern for periosteal primary bone – the posterior quadrant is brighter than the medial or lateral quadrants – although values are higher for one individual. Neither pattern nor magnitude is similar in the humerus. There are no radius, ulna or tibia specimens for this taxon.

With respect to secondary osteonal tissue, the two femoral sections again show a similar quadrant pattern as well as similar brightness magnitudes. In both individuals, the posterior quadrant is the brightest (comparable to the periosteal primary tissue). In the humerus, magnitudes, but not patterns, are similar.

6.6.14.4 Summary of patterns of collagen fiber orientation for individual taxa

The preceding qualitative descriptions demonstrate that, while there are occasional apparent patterns of collagen fiber orientation around a cortex within taxa, these are the exception rather than the rule. More typically, both fiber orientations in whole cortices and the relationship between fiber orientations among quadrants vary within taxa. This most parsimoniously leads to the conclusion that there are no distinctive patterns that characterize individual taxa or skeletal elements within taxa. Within this context, any instance of consistency can be seen as a chance, and insignificant, occurrence. Alternatively, it could be suggested that there are biological imperatives driving the patterns in some elements and taxa more than in others. The latter seems implausible, but all options will be considered in the following discussion.

## 6.7 Discussion

### *6.7.1 Range of variation in collagen fiber orientation in the study sample*

In contrast to previous collagen fiber orientation (CFO) studies (e.g., Portigliatti Barbos et al., 1983; Ascenzi et al., 1987; Carando et al., 1989; Carando et al., 1991; Riggs et al., 1993a; Skedros et al., 1996, 2003, 2004), where variation apparently ranges widely within periosteal portions of the cortex, data from this study indicate that CFO is predominantly longitudinal in the selected primate sample, with few exceptions. For example, Table 6.6 demonstrates that, with only two exceptions, mean whole cortex grayscale values (for all specimens of a single element within a taxon combined) are 30 or below. This is the case for both primary periosteally deposited tissue, as well as

secondary osteonal bone. Possible explanations for this discrepancy between past and present results are as follows.

Most previous CFO studies do not employ a standard by which to assess illumination parameters and/or the relative brightness and darkness of bone in circularly polarized light (CPL). In early papers (e.g., Evans & Vincentelli, 1969, 1974; Vincentelli & Evans, 1971; Vincentelli, 1978; Portigliatti Barbos et al., 1983; Ascenzi et al., 1987) authors describe "light" or "bright" lamellae and/or osteons and "dark" lamellae and/or osteons, but there is no discussion of the process by which an illumination level is chosen. It is therefore possible that maximally bright lamellae, as identified in these papers, do not in effect represent transverse collagen, but rather are composed of oblique fibers that have artificially been brightened when viewing and capturing polarized light images.

Beginning with Boyde et al. (1984), and Portigliatti-Barbos et al. (1984), and as refined by Boyde & Riggs (1990) a number of researchers have employed methods to quantify CFO. Boyde & Riggs (1990) allocate image pixels into 16 color-coded bins according to individual pixel grayscale value. The relative sizes of these bins are then quantifiable, allowing for comparisons of CFO patterns across and among bone sections. This method is repeated, sometimes with modification, in other papers (e.g., Carando et al., 1990; Goldman et al., 2003) including in the current research, although it is often used solely for visualization, rather than quantification, purposes. In 1992, Bromage describes a division between tissue comprising 0-50% bright lamellae vs. 51-100% bright lamellae. Yet another approach (again used in the current research) employs mean gray

values or an index of mean gray values to compare within and among sample sections (e.g., Goldman, 2001; Goldman et al., 2003).

However, while such methods allow for the determination of the proportion of transverse and longitudinal lamellae, or the relative brightness of regions of cross-sections or whole cross-sections, these approaches still do not provide a means to set biologically appropriate lighting parameters. Most researchers have taken care to assure that illumination is consistent within their study sample (either by imaging all sections in a single session, recording illumination parameters so that they can be replicated in subsequent sessions, or employing an illumination standard such as a neutral density filter). However, a fundamental problem remains: could the illumination parameters, somewhat arbitrarily determined, be artificially brightening or, less likely[9], darkening the image?

In the present study, I have used ossified turkey tendon (described above) as a biologically appropriate standard for setting illumination parameters. It is under these conditions that all sample sections were imaged, and therefore the overall "darkness" (i.e., preponderance of longitudinally oriented collagen fibers) is considered to be real, rather than an artifact of arbitrary illumination. This is further corroborated by the occasional presence of maximally bright bone, even within this sample. For example, circumferential lamellar bone around the periosteal margin in some sections displays maximally bright areas. More frequently, the endosteal circumferential lamellae typically lining the medullary cavity, as well as parts of the CCC bone, may be maximally bright. This suggests that the sections have not been imaged under artificially dark conditions.

[9] The artificial darkening of an image is deemed less likely because it is increasing the illumination that allows one to more clearly see structures and variation in brightness across a section.

In addition, a *Vespertilio* (particolored bat) midshaft femur imaged while investigating the utility of the turkey tendon standard has provided more evidence that some bones do appear maximally bright under these conditions.

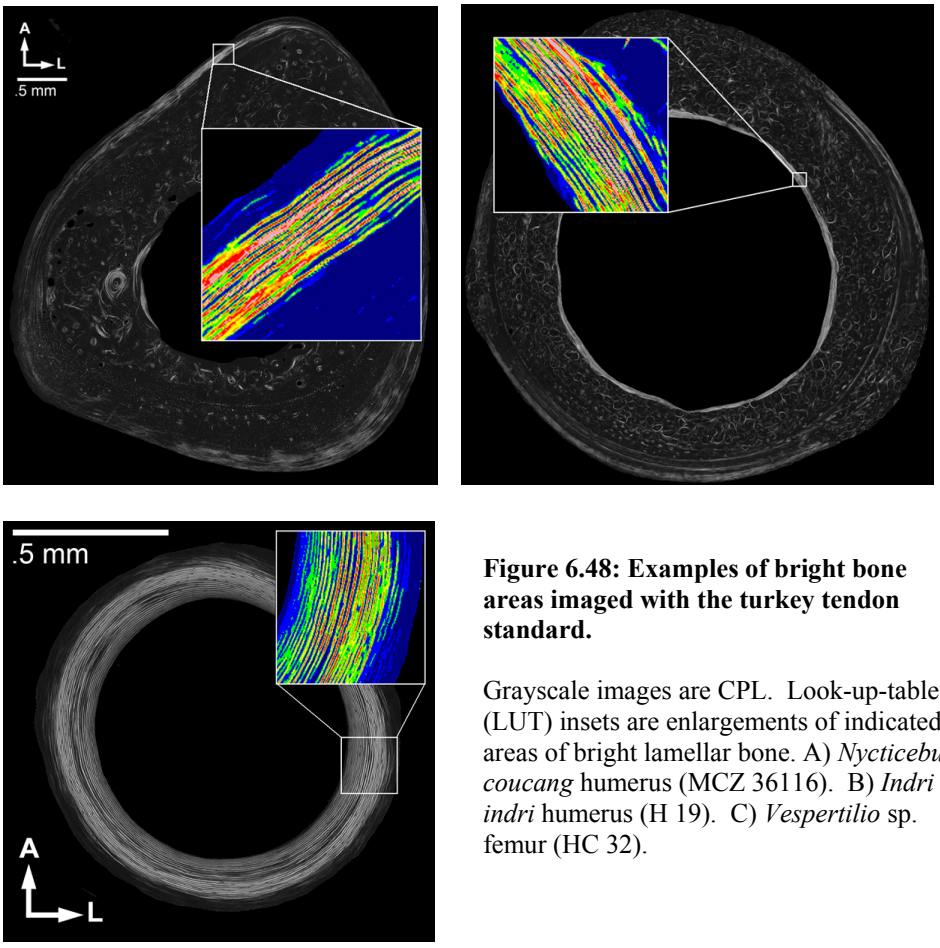


**Figure 6.48: Examples of bright bone areas imaged with the turkey tendon standard.**

Grayscale images are CPL. Look-up-table (LUT) insets are enlargements of indicated areas of bright lamellar bone. A) *Nycticebus coucang* humerus (MCZ 36116). B) *Indri indri* humerus (H 19). C) *Vespertilio* sp. femur (HC 32).

This is not to suggest that the turkey tendon standard eliminates all illumination error. It is evident from the current data that, despite the rigorous use of this standard, there are global differences in brightness between sections that are likely not attributable to differences in CFO. For example, although brightness appears to vary among tissue types (see below), in some sections *all* tissue types are darker than those same tissue

types in other sections. In other words, if LAM bone is brighter in section A than in section B, the same will be the case for PF, HYB and FAST bone. This suggests that the same illumination parameters are nevertheless resulting in variable image brightness among specimens. This does not detract from the observation that most sections are globally dark in periosteally deposited areas. Rather, it suggests that small variations in brightness may be present among images, perhaps due to diversity in section properties (e.g., mineral density, specimen preservation), undetected fluctuations in lighting, unidentified section thickness measurement error, or some other factor.

*6.7.2 Collagen fiber orientation and primary tissue type*

Within the overall darkness that prevails among the sample sections, a noticeable source of variation in brightness – and therefore in presumed CFO – is tissue type. The data indicate that LAM bone is generally brightest (comprising the largest proportion of transverse collagen fibers) followed closely by, and in some cases equivalent in brightness to FAST bone (fibrolamellar and woven tissues). Both of these types are brighter than HYB or PF types, which presumably contain higher proportions of longitudinal collagen fibers. This is not to suggest that all LAM bone is bright. On the contrary, there are many individual instances of dark LAM bone within the sample sections[10] (Figure 6.49). Rather, it is on average that LAM bone comprises more transverse fibers than other tissue types (with the frequent exception of FAST bone). Similarly, while most PF bone is dark, it is possible to find fields of this tissue where fibers are aligned transversely to the plane of the section.

[10] Variation in circumferential lamellar bone brightness is also described in Bromage & Boyde (n.d.), and Lee (2004).

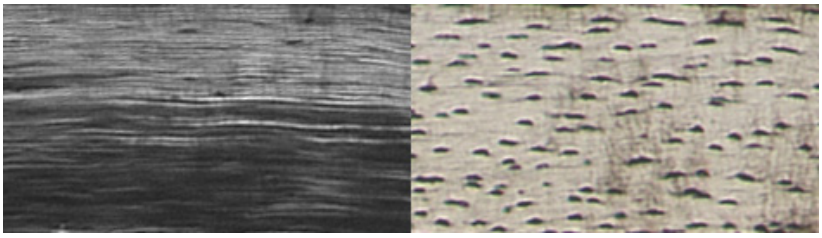

**Figure 6.49: Example of an area with both bright and dark lamellar bone.**
*Lemur* sp. humerus (H 30). Left image: non standardized CPL. Right image: conventional transmitted light.

These results lead to the speculation that slower depositing tissue (i.e., LAM bone) may comprise more transverse fibers, or may at least have an enhanced capacity to deposit concentrated domains of transverse collagen. The question that then needs to be asked is: why do rapid deposition FAST tissues display brightness approaching, equivalent to, or even on occasion surpassing the brightness of lamellar bone? The answer to this question must lie in the composition of fibro-lamellar bone. As described in Chapter 4, this complex tissue comprises a network of woven and lamellar fibrillar structures. While the rapidly depositing woven matrix may be dark, infilling via lamellar bone around vascular canals may produce concentrations of transverse collagen. Indeed, the lamellae around vascular canals in fibro-lamellar bone often appear bright. (Bright lamellae are also often seen around the primary osteons within expanses of dark PF, HYB or LAM bone). The combined effect, therefore, is to produce a tissue with an average brightness that is similar to the average for lamellar tissue alone.

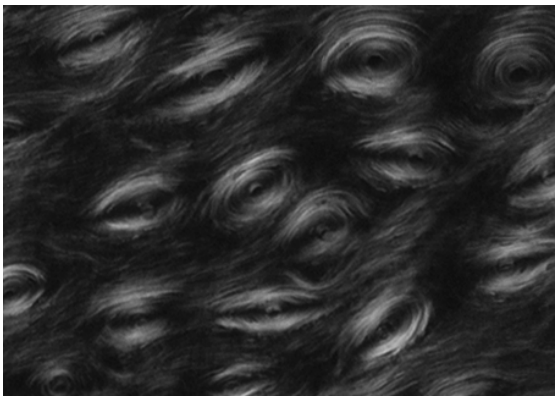

**Figure 6.50: Example of fibrolamellar bone with bright primary osteons.**

*Lemur* sp. femur (HC 30). This CPL image has been adjusted in Adobe Photoshop to enhance contrast.

Variation in collagen fiber orientation associated with tissue type has been commented upon in a few earlier studies, although it has not previously been quantified (Smith, 1960a; Bromage, 1992; Bromage & Boyde, n.d.; Riggs et al, 1993a; McMahon et al., 1995; Goldman et al., 2003; Lee, 2004; Skedros & Hunt, 2004). For the most part, the observations of previous researchers have been in accord with those described here. Smith (1960a) notes that woven fibered bone, while displaying a disorganized fibrillar matrix, is mostly composed of longitudinally oriented collagen fibers. Goldman et al. (2003), in a study of human midshaft femora, find the collagen in periosteal circumferential lamellar bone to be principally transverse in orientation. In a growth series study of alligator femora, Lee (2004) finds a predominantly longitudinal orientation for most of the collagen but does find regions comprising more transverse collagen. As is the case with the present study, these are most frequently coincident with LAM bone although – also in accord with the present study – Lee finds that PF bone may also appear bright. Skedros et al. (2006) also mention "highly birefringent circumferential lamellar bone" (p. 146).

In an investigation of CFO and vascular canal patterning in fibrolamellar bone, Skedros & Hunt (2004) find that laminar tissues (those with vascular canals running

circumferentially in the transverse plane) contain larger proportions of oblique-to-transverse collagen. Although it has can be argued that both features may be a mechanical adaptation to compressive load, the authors also speculate that more laminar canal patterning may result in more transverse collagen, where "the primary bone matrix is deposited on the primary vascular network, which exhibits a preferred orientation" (p. 132). This is not inconsistent with the results for fibrolamellar bone found in the present study.

Finally, McMahon et al. (1995), following Bromage & Boyde (n.d.), suggest a possible relationship between tissue type and CFO. For example, they posit that brightness in the medial cortex of the *Ovis aries* (sheep) midshaft calcaneus may be due to the preponderance of CCC bone there. Bromage & Boyde (n.d.) previously identify this relationship in their investigation of CFO in the *Macaca fascicularis* (long-tailed macaque) mandible, although with some instances of dark CCC bone. While this observation cannot directly be compared to those in the current study (I have not examined CFO in endosteally deposited bone), it serves as yet another example of the potential relationship between tissue type and CFO.

Bromage & Boyde (n.d.) offer perhaps the most thorough theoretical discussion of this issue to date. There the authors consider the impact of developmental constraints (and associated variation in tissue type) on CFO. For example, they consider how "construction rules", potentially developmentally constrained, might govern the orientation at which osteoblasts lay down collagen (see also Bromage, 1992). Although the authors do not explicitly mention tissue type as a determinate factor (i.e., a source of "constructional rules"), it is not unreasonable to consider that the different fibrillar matrix

patterns found in different tissue types might provide variable opportunities for orientation of collagen fibers.

Only in a single paper do the observations regarding tissue type and CFO contrast with the results of the current study. Riggs et al. (1993a), in an ontogenetic series of horse radii, do find areas of bright circumferential lamellar bone, as have I. However, in contrast to my findings, the authors determine that woven bone is more likely to be composed of transverse fibers. They find that fibrolamellar tissues are generally dark, and that the component of these tissues that may be bright is the woven bone, whereas PF and LAM regions of the fibrolamellar complex are dark. As Figure 6.50 demonstrates, this is clearly not the case in fibro-lamellar tissues examined in the current study. The reason for this discrepancy between studies is unclear. It is possible that the differences may be due to imaging methodologies or, alternatively, real variation among fibrolamellar tissues.

Given the observation of more transverse collagen in LAM bone, the question that ultimately must be asked is: why? Is there an enhanced capacity among osteoblasts to position collagen transversely when deposition is slow? Interestingly, the brightest periosteal lamellae are often at the periosteum where, presumably, deposition was at its slowest as the animal neared mature body proportions.

Regardless of the answer to the question, it is clear that the relationship between CFO and tissue type must change the manner in which many CFO studies are performed. Consideration of tissue type has not, to date, been the norm (e.g., Kalmey, 2000; Kalmey & Lovejoy, 2002; Skedros et al., 2004; Ramasamy & Akkus, 2007). Yet, as Goldman et al. (2003) conclude, “if various bone tissue types influence global patterning of collagen

fiber orientation differently, the ability to distinguish them in future studies would help elucidate the relationship between collagen fiber patterning and the mechanical properties of bone" (p. 443). Clearly, in the absence of consideration of tissue type, explanations of mechanical adaptation and the functional significance of variation in CFO remain incomplete.

For example, in the present sample, the mean gray value for periosteal primary bone is greater (i.e., comprising more transverse or oblique fibers) in the humerus than in all other bones. However, humeri also contain a larger proportion of lamellar tissue in the periosteal cortex (see Chapter 4). In contrast, the mean gray value for all tibiae is lower (i.e., comprising fewer transverse or oblique fibers) than in all other bones (although it is not significantly different from values for the femur, ulna and radius). This, however, is not surprising when one considers that tibiae typically contain a large proportion of PF bone at midshaft and the smallest average proportion of lamellar bone among all skeletal elements. Therefore, any assumption, based on CFO, that the humerus incurs more compressive loading than all other bones, or that the tibia is subjected to more tension, must be tempered by consideration of tissue type. (The possibility that tissue type variation, itself, may in part represent a response to mechanical load was considered in Chapter 4).

### 6.7.3 *Collagen fiber orientation and intracortical remodeling*

As is the case for CFO in periosteal primary tissue types, and within cortices as a whole, secondary osteons comprise an overwhelming proportion of longitudinally oriented fibers. In all specimen cross-sections except two, mean gray values for CFO are less than

35. Of the remaining two individuals, one has a mean gray value of 41, and the other is considered to be an outlier[11].

This is in contrast to observations in some other studies, where secondary osteons often appear bright. In papers such as those by Ascenzi & Bonucci (1968), Vincentelli & Evans (1971) and Vincentelli (1978) the authors examine individual remodeling events and find that some are "light" or "bright" indicating a preponderance of transverse lamellae[12].

Other studies, looking at CFO distributions across whole cortices – which are partly and often largely composed of secondary osteonal tissue (the latter for example in the adult human long bone midshaft) – also describe bright regions of the cortex where bright osteons explicitly or likely contribute (e.g., Ascenzi et al., 1987 in pathologically bowed human femora; Boyde & Riggs, 1990; Riggs et al., 1993a, 1993b in horse radii[13]; Carando et al., 1991 in human humeri, ulnae and radii; Bromage, 1992 in the macaque circumorbital region; McMahon et al., 1995 in sheep calcanei[14]; Skedros et al., 1996 in horse third metacarpals; Kalmey & Lovejoy, 2002 in human and *Pan troglodytes*

---

[11] In this single tarsiid tibiofibula (DUPC 81), there is a single unusually bright osteon at the site of the fusion between tibia and fibula. While this in itself may constitute and interesting exception – perhaps with mechanically adaptive significance – it deviates so markedly from all other specimens (including another tarsiid tibiofibula) that it was removed from the sample for analysis of secondary osteon CFO.

[12] Ascenzi & Bonucci (1968) classify secondary osteons into three types, according to brightness and presumed CFO. Type I is bright and considered to be composed primarily of transverse fibers, Type II displays alternating orientations in successive lamellae, and Type III is composed primarily of longitudinal fibers. Evans & Vincentelli (1969, 1974) and Vincentelli & Evan's (1971) classification scheme also involves three brightness categories, again with one comprising the most transverse lamellae. These authors note, however, that they find very few osteons matching the Type I category of Ascenzi & Bonucci, (i.e., appearing homogenously bright in polarized light). Vincentelli (1978) employs five categories to classify osteon brightness, where Type 1 osteons correspond most closely to the Type I of Ascenzi & Bonucci. Ascenzi and colleagues eventually appear to abandon the "Type" nomenclature, and begin to use the terms "bright", "alternating", and "dark" to describe the three typical osteon forms previously identified (Ascenzi et al., 1982 and subsequent papers).

[13] Boyde & Riggs (1990) do not specify the tissue types found in the horse radius. However, later studies by this group (Riggs et al., 1993a) do differentiate among tissue types in the horse radius, and specifically discuss the presence of secondary osteons with transverse or oblique lamellae in some regions of the cortex.

[14] McMahon et al. (1995) differentiate between tissue types, and specifically mention bright osteons in some regions of the cortex.

[chimpanzee] femoral necks[15]; Goldman et al., 2003 in human midshaft femora[16]; Skedros et al., 2004, 2006 in mule deer calcanei).

While some of these studies standardize lighting parameters to maintain within-study consistency, none use an objective standard. Therefore, as is discussed above with reference to primary tissue types, there may be differences in brightness among studies, and relative to the current results, that are due to variation in underlying imaging parameters. This may go some way in explaining the disparity in results between my study and these others. However, it can be probably be assumed (although there is no way to be sure) that the experienced researchers in this group make educated decisions regarding lighting parameters, and that they do not increase brightness in extreme. The question then remains: why the near absence of bright secondary osteons in my sample when these clearly are apparent in other studies? This is best considered in the section on mechanical adaptation below.

It should be noted that others have observed a *preponderance* of dark secondary osteons in their samples, although not to the exclusion of brighter ones (e.g., Evans & Vincentelli, 1974 in human cortical bone; Portigliatti Barbos et al., 1983 in a human midshaft femur; Carando et al., 1989 in human tibiae and fibulae; Goldman et al., 2003 in human midshaft femora; Bromage & Boyde, n.d. in macaque mandibles). In addition, recent work by Ascenzi and colleagues has elegantly demonstrated that, even within the bright lamellae of secondary osteons of the "alternating" type, the majority of collagen fibers are oriented oblique to the plane of a cross-section (Ascenzi et al., 2003; Ascenzi &

[15] Kalmey & Lovejoy (2002) do not differentiate among tissue types, but images in the publication clearly show bright secondary osteons (p. 330).
[16] Goldman et al. (2003) comment that much of the brightness found in midshaft human femora might be due to remnants of primary circumferential lamellar bone, but do not rule out the possibility that secondary osteons may contribute to brightness in some cases.

Lomovstev, 2006). Therefore, there is reason to believe that even osteons with bright lamellae will not typically appear maximally birefringent in CPL when the lighting parameters are set appropriately.[17] Indeed, in Figures 6.51 and 6.52 – demonstrating occasional bright osteons in the current sample – maximal brightness (pink and gray in the LUT images) is rarely observed.

Although secondary osteonal bone in my study is dark, there is variation within the sample. First, there are occasional osteons within the sample that are bright, or at least brighter than the majority of other osteons, and brighter than surrounding tissue. In most cases these are not maximally bright (i.e., do not appear to be composed primarily of transverse lamellae). These for the most part are isolated remodeling elements and are more typically found in the larger individuals in the sample[18]. In only two sections (both *Saimiri* femora) are groupings of brighter osteons found. These are clustered within CCC bone, and are more frequent in one of the two sections. In two other sample *Saimiri* femora, this pattern is not observed. It therefore seems imprudent to assume that it is adaptively meaningful.

Second, even among dark osteons, a typical pattern is one where the outermost lamella or two (adjacent to the cement line) are bright, and sometimes the innermost lamella or two as well. The bright outer-ring pattern has been observed by other authors (e.g., Riggs et al., 1993a; McMahon et al., 1995), although I am aware of no proposed explanations for this pattern. Given the conclusion here that slower depositing tissues are

[17] Although Ascenzi and colleagues have not examined collagen orientation in primary tissues, it is tempting to speculate that the same pattern they have identified in osteonic lamellae applies. That is, even the brightest regions are generally composed of domains where collagen fibers run oblique to the plane of the section, rather than parallel. This hypothesis, of course, requires verification.

[18] Larger animals may display more brighter osteons simply because they have more remodeling events overall, and are therefore more likely to include the random bright osteon.

often brighter, is seems possible that this pattern is indicative of a slower lamella deposition at the onset and termination of osteonal infilling. The observation that, aside from their bright outer rings, the majority of secondary osteons are dark reinforces the conclusion that lamellar bone has an enhanced *capacity* to deposit transverse collagen, but will not *necessarily* do so.

Finally, both the femur and humerus display significantly brighter secondary osteonal bone than all three distal elements. Likewise, intracortically remodeled bone is brighter in the tibia than in the ulna. This contrasts with the pattern for periosteal primary tissue, where only the humerus is significantly brighter than other skeletal elements. In addition, in both the femur and tibia, intracortically remodeled bone is brighter than periosteal primary tissue. Explanations for variation among skeletal elements in the brightness of secondary osteonal bone can be considered in light of mechanical imperatives. This will be discussed in a following section. However, it again is necessary to take into account the potential relationships between tissue type and CFO, as they may interact with brightness variation due to mechanical load variability. For example, the brightness of secondary osteons relative to primary bone tissue in the sample tibia could be contributed to by the relative darkness of primary tissue in the tibia, likely explained at least in part by a preponderance of PF bone (c. 50% of the periosteal primary cortex on average). In contrast, mean brightness values in the humerus may not differ between periosteal primary and secondary remodeled bone (despite the brightness of humeral intracortically remodeled bone as compared to the tibia) because of the preponderance of LAM+HYB tissue in the former (over 80% of the cortex on average).

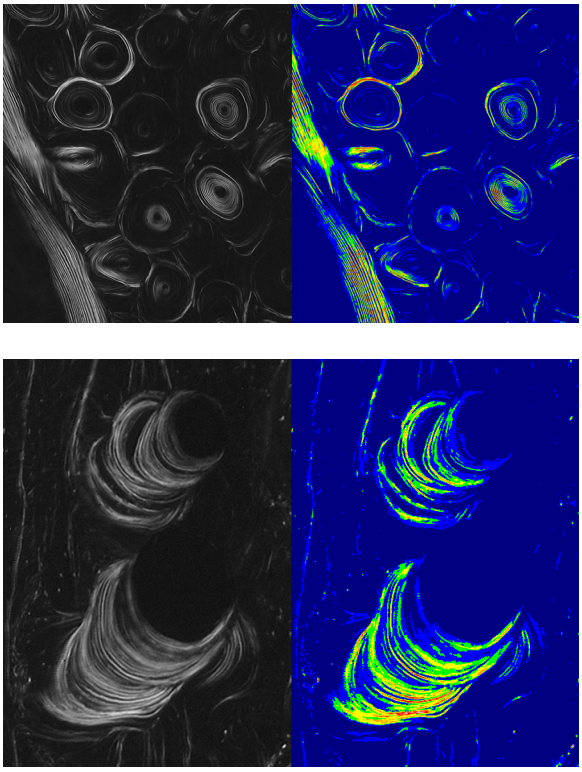

**Figure 6.51: Examples of bright secondary osteons.**

In both cases, the images on the left are standardized CPL. The images on the right are LUT versions of the CPL. A) A single brighter osteon amid typically dark osteons. Notice also the characteristic bright rings at the outer periphery of several osteons (*Ateles fusciceps* femur, FMNH 68811). B) Two bright drifting osteons (*Ateles* sp. humerus, MNHU 44079).

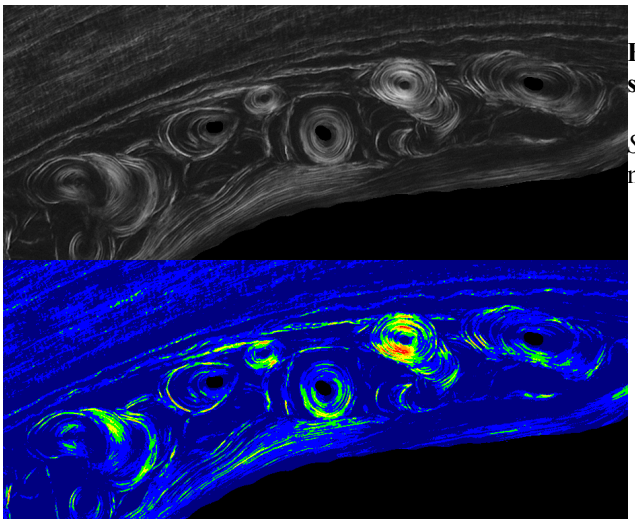

**Figure 6.52: Example of a grouping of bright secondary osteons.**

*Saimiri sciureus* femur (MNHU 85197). Image modes as for Figure 6.51

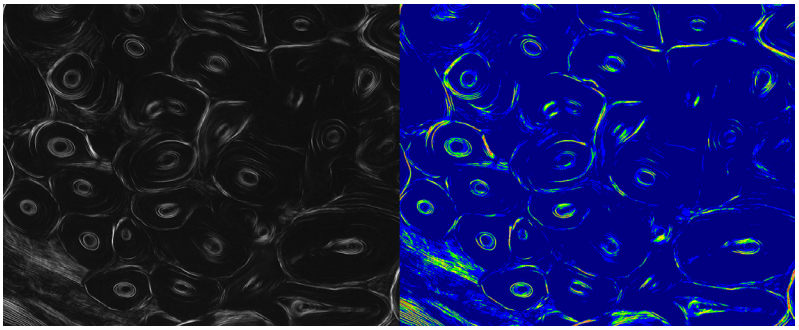

**Figure 6.53: Example of ringed secondary osteons.**

*Ateles fusciceps* femur (FMNH 68811). Notice the bright inner and outer rings. Image modes as for Figure 6.51.

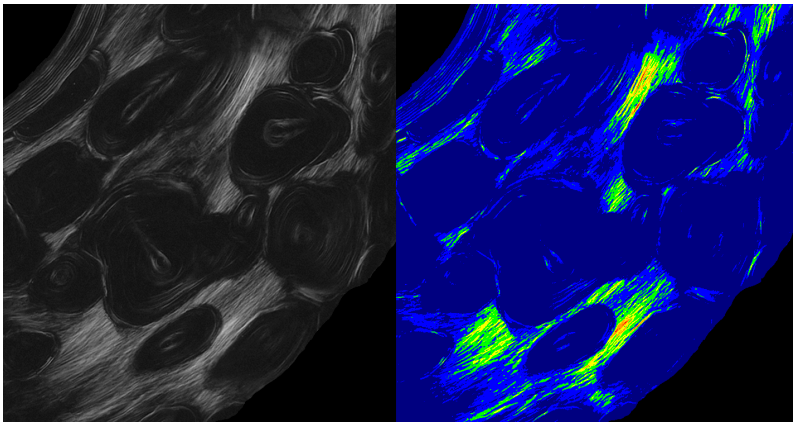

**Figure 6.54: Example of dark secondary osteons replacing bright primary tissue.**

*Propithecus* sp. humerus (MNHU 44685).

*6.7.4 Collagen fiber orientation and body size*

With respect to periosteal primary tissues, the data suggest a relationship between body size (as assessed using the proxy variable TCA) and CFO. This is particularly evident in the tibia, ulna and radius, and less so in the femur and humerus. This finding should, as before, be interpreted in light of the observed relationship between CFO and primary tissue type. While there is no apparent relationship between TCA and PF bone or LAM+HYB (or LAM) bone in the three distal elements, a positively allometric relationship between FAST bone and TCA exists for all elements except the ulna (see Chapter 4). Therefore, higher average grayscale values in the midshaft tibiae, radii and ulnae of larger individuals can partly be explained by the presence of more FAST tissue which, as noted above, is on average brighter than PF bone and is often as bright, or even

brighter than LAM bone. However, this relationship between TCA and FAST bone does not explain why larger femora and humeri are *not* typically brighter, or why larger ulnae *are* (given the absence of correlation between TCA and FAST bone for this skeletal element).

It has previously been shown that normal peak strains in bone are not greater in larger mammals, and safety factors have been found to be remarkably consistent among terrestrial mammals (Rubin & Lanyon, 1985; Biewener, 1989a, 1989b, 1990, 1991, 2002, 2005, Blob & Biewener, 1999). A relationship between body size and CFO in periosteal primary tissues (or any bone tissues) has not, to my knowledge, previously been observed. In addition, the data identify no relationship between TCA and CFO for secondary osteonal bone. Given the available evidence, it therefore seems most prudent to conclude (until further examination of this issue) that the relationship between body size and collagen fiber orientation is not evidence of kinematic adaptation. Rather, either a developmental explanation may apply, or the relationship described by the data is non-significant.

*6.7.5 Collagen fiber orientation and positional behavior*

The data presented here suggest that, while there are tentative indications that CFO may be reflective of differences in positional behavior – and concomitant loads on bones – there is no easily identified mechanically adaptive patterning to the orientation of collagen fibers among the sample primate taxa. While some consistencies between skeletal elements and within positional behavior categories hint at a pattern to be gleaned, these are limited in number and scope. More typically, an apparently random variation

reigns both within and between taxa. The one consistent feature across the sample is that, as mentioned above, these bones are dark (i.e., are composed primarily of longitudinally oriented collagen fibers). This in itself may constitute a mechanically adaptive response to load, perhaps the most compelling one offered by this sample. This possibility, along with others, will be discussed below.

The results reported here are in contrast to a number of previous studies in the literature, particularly with respect to intracortically remodeled bone. Beginning with the work of Gebhardt (1905), it has been suggested that collagen fibers of different orientations are variably adapted to different kinds of load: tension, compression, torsion and shearing. This proposal has since been supported in numerous studies, experimental and otherwise, beginning with examinations of solitary secondary osteon units, and leading to the investigations of whole cross sections and serial sections through whole bones. Since the 1970s, and in particular in recent papers, the mechanical properties of single osteonic lamellae have also been examined (e.g., Ascenzi et al., 1973, 1982; Rho et al., 1999; Ascenzi et al., 2003; Ascenzi & Lomovstev, 2006; Xu et al., 2003; Hofmann et al., 2006) although I am aware of only one paper which specifically addresses the relative tensile and compressive strengths in dark and light lamellae. In this publication (Ascenzi et al., 2003) the authors contend that their findings on lamellar structure support previous hypotheses regarding optimal resistance to varied loads. Specifically, they find that dark osteonic lamellae contain more longitudinally oriented collagen fibers and are therefore likely more resistant to axial tension and bending, while bright osteonic lamellae, with a higher proportion of transverse collagen fibers, are better designed to resist axial compression and torsion.

In a triad of papers in the late1960s and early 1970s, Ascenzi and Bonucci (1967, 1968, 1972) demonstrated that secondary osteons composed primarily of longitudinal fibers (Type III osteons) were best adapted to axial tensile loads (1967), while those composed primarily of transverse fibers (Type I osteons) were better resistant to axial compressive loads (1968). They also determined that osteons with longitudinal fibers were least resistant to shearing strain, while those with transverse lamellae or alternating lamellae (Type II osteons) were equally resistant to shear (1972). Subsequent research on adult human leg bones by Evans & Vincentelli (1969, 1974), and Vincentelli & Evans (1971), partly corroborates these findings. The 1969 study finds no correlation between percentage dark osteons in a break area and tensile stress and strain, but a high positive correlation with shearing strength. Positive correlations are also found between shearing strength and intermediate osteons, with a negative correlation between bright osteons and shearing strength. These results are contrary to those of Ascenzi & Bonucci. However, the 1971 paper demonstrates that dark osteons have more tensile strength than brighter osteons (presumably those with fewer longitudinal collagen fibers), while the 1974 paper finds a correlation between compressive strength and both bright and intermediate osteons. These results are consistent with those of Ascenzi & Bonucci.

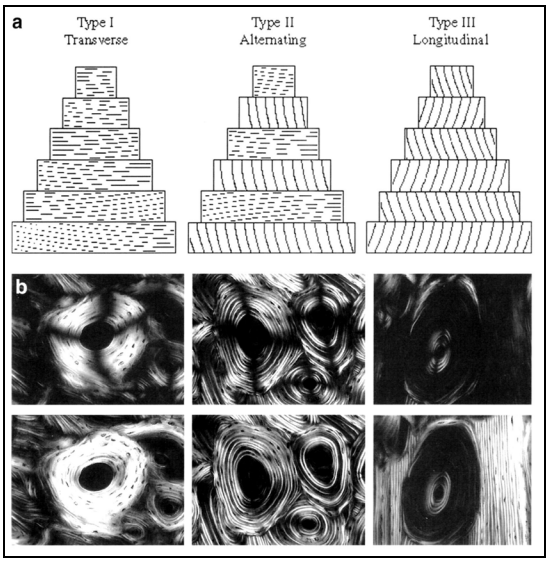


**Figure 6.55: Examples of three classically categorized secondary osteon types.**

From Bromage et al., 2003. The upper three polarized light images were acquired with *linearly* polarized light, and the Maltese Cross effect is visible. The bottom three images were acquired with *circularly* polarized light, and the Maltese Cross error is eliminated.

In the period of time since these seminal papers, interpretation of patterns of brightness has been, and continues to be, applied to whole cortices in a variety of vertebrate species, with most researchers finding variation within cortices, and many able to correlate this to hypothesized or experimentally determined loads. In some cases, the bones that are examined are highly remodeled, while others consist wholly or in part of primary tissues. The first of these papers is Vincentelli (1978), where secondary osteons in the anterior cortex in human tibiae are darker than those found posteriorly. Although the authors do not speculate on the mechanical correlates of this pattern, comparable anteroposterior disparities are found in subsequent studies. For example, in 1983, Portigliatti Barbos et al. see a similar pattern in the primary and intracortically remodeled bone of a single midshaft human femur. Here, an increase in brightness medially and posteriorly relative to anteriorly and laterally is attributed to a stress-strain pattern due to bending, where the medial and posterior cortices experience compression, and the lateral and anterior ones undergo tension. Likewise, Boyde & Riggs (1990), and Riggs et al. (1993a, b) identify a bending pattern in horse radii, again with the posterior quadrant

displaying the highest proportion of transverse fibers, presumably in response to demonstrated (via *in vivo* strain gauge studies) compression in that region of the cortex. Skedros et al. (1996), in a study of the equine third metacarpal, provide data that support the association between strain mode (but not magnitude) and CFO, where regions of the cortex demonstrated to undergo compression during bending displayed more transverse fibers than those undergoing tension. Skedros et al. (2003) and Skedros & Hunt (2004) in a study of subadult and adult domestic turkey ulnae find a similar pattern of more oblique-to-transverse collagen fibers in the region of the cortex undergoing compression (dorsally), relative to the region subjected to tension (ventrally). However, in adults this pattern was diminished, where ventrally there was a proportion of oblique-to-transverse fibers comparable to that found dorsally. The authors interpret this as a potential adaptation to shear strains due to torsional loading superimposed upon bending during the more complex adult wing-flapping behavior.[19]

In a study of Rocky Mountain mule dear calcanei, Skedros et al., (2004) again find differences in CFO between tension and compression cortices, although this characteristic pattern is absent in the youngest individuals, and only appears in subadult and older specimens. The relationship they note between this age related pattern and the distribution of intracortical remodeling will be discussed below. Finally, Kalmey & Lovejoy (2002) find evidence of cantilevered beam loading in the *Pan troglodytes* femoral neck, with the superior cortex dark (resisting tension) and the inferior cortex bright (resisting compression). It should be noted, however, that these authors do not

[19] These authors note that variable primary tissue type among cortical regions may also be influencing relative brightness measurements.

control for tissue types, which appear to vary considerably among the sample images they provide.

Another typical pattern is one where opposing quadrants of a cortex display similar brightness, contrasting with adjacent quadrants (Ascenzi et al., 1987; Carando et al., 1989, 1991). This has also been attributed to resistance to bending, although with no discussion of preferred adaptation to tension and compression on apposing sides of the bending plane.

A number of studies, although still identifying regional differences in brightness under polarized light, are more equivocal about the mechanical significance of this variation in CFO. Bromage (1992) overall finds a correlation between CFO and masticatory-related strains in the circumorbital region of a female *Macaca fascicularis*. Similarly, Bromage & Boyde (n.d.) find repeated patterns of CFO in two *M. fascicularis* mandibles but cannot consistently relate these to in vivo strain patterns. These two papers discuss the potential of developmentally constrained construction rules and tissue type to govern patterns of CFO. McMahon et al. (1995) find increased brightness in the medial and lateral quadrants of sheep calcanei. These authors warn that there is complex, compound loading in the sheep calcaneus, and potentially different loading regimes depending upon locomotor behavior. Therefore, they conclude that "to assess the correspondence properly between strain distribution and pattern of collagen fiber orientation, a complete history of the total strain regimen influencing collagen alignment must be attained. Incomplete strain information could lead to inaccurate assessments" (p. 154). Goldman et al., (2003) in a study of midshaft adult human femora, find intra-sample diversity in the pattern of collagen fiber orientation across the cortex, with

individual variation tending to "overwhelm any trend at the population sample level" (p. 441) (the latter being a correspondence with expected mechanical bending loads, with the posteromedial cortex optimized to resist compression, and the anterolateral cortex optimized to resist tension). Finally, Lee (2004), in an ontogenetic study of *Alligator mississippiensis* mid-diaphysis femora finds that a loading regime of bending is reflected in all age groups (even prehatching individuals), with the dorsal compression cortex brighter than the ventral tension cortex. (It should be noted that these tissues are not significantly remodeled.) The author does point out, however, that the high magnitude of shear strain is not reflected in the bones: transverse fibers, hypothesized to be more resistant to shear, do not predominate in the sample. Lee suggests that bone growth dynamics, specifically the "longitudinal shifting of subperiosteal osteoid during femoral elongation" (p. 206) is responsible for the predominant longitudinal CFO pattern throughout the cortex.

Where authors specifically differentiate between primary and secondary remodeled bone, there has been some suggestion that remodeled bone may be more mechanically adaptive than primary tissues, with the latter likely more developmentally constrained. For example, Riggs et al. (1993a, b) find that, among horse radii, primary bone tissues were largely dark, whereas CFO distributions across the cortex in intracortically remodeled conformed to a bending pattern, with the caudal cortex displaying more transverse and oblique fibers in response to compressive loads. Similarly, Skedros et al. (2004) find that it is the presence of secondary osteons in mule deer calcanei that produces the characteristic CFO pattern of adaptation to bending. This pattern is absent in younger individuals where the cortices are composed principally of

primary bone tissues. This finding is in accord with the proposition that remodeling in part functions to realign collagen fibers in response to habitual loads (Lanyon et al., 1982; Burr et al., 1989b; Riggs et al., 1993a). In contrast, while McMahon et al. (1995) do find variation in secondary osteonal CFO across sheep calcaneus cross-sections, these do not conform to expectations based on observed in vivo lading regimes. Similarly Bromage & Boyde (1998, n.d.) determine that both primary and secondary tissue collagen fiber alignments are dependent upon other factors apart from mechanical ones.

In the present sample, very few consistent and mechanically significant patterns of CFO can be discerned. First, there is the observation that the humerus has brighter periosteal primary bone than all other skeletal elements. This is followed by the femur, with the three distal elements the darkest[20]. The brightness of the humerus can easily be explained by consideration of tissue type. This skeletal element comprises the most LAM tissue, which is usually brighter than either PF or HYB bone. The femur contains the second largest proportion of PF bone relative to slower deposition tissues, while the three distal elements contain the most. Therefore, the relative brightness of periosteal primary tissue in all five skeletal elements is most simply explained by variation in primary tissue types. An argument could be made that, in addition to developmentally determined patterning, the femur and, in particular the humerus, may be brighter due to greater compressive loads on these bones. However, in the absence of appropriate strain gauge data, this cannot be substantiated.

Second, vertical-clinger leapers tend to have darker bones relative to other positional behavior categories, with respect to both primary and secondary tissues. This

[20] Evans & Vincentelli (1969) also identify a difference between the human femur and tibia, with the femur displaying a higher proportion of "light" secondary osteons, and the tibia a higher proportion of "dark" secondary osteons.

difference is statistically significant only for the contrast between vertical-clinger leapers and arboreal quadrupeds for primary tissues in the humerus and femur, and between vertical-clinger leapers and slow climbers for primary tissues in the femur. Given previous research, an explanation of this pattern would predict that axial tensile loads (in all examined skeletal elements) are greater among vertical clinger leapers and/or that compressive or torsional/shear loads are lesser. However, as discussed in Chapter 5, cross-sectional geometric studies of the femur, combined with anatomical and kinematic observations, suggest greater resistance to axial compression and torsion (as well as antero-posterior bending, discussed below) in leaper specialists relative to less frequent leapers (Burr et al., 1982, 1989a; Demes & Jungers, 1989,1993; Terranova, 1995a, 1995b; Aerts, 1998; Runestad Connour et al., 2000). The CFO data tell the opposite story. Greater cortical thickness in leapers (associated in previous papers with compressive strength (e.g., Terranova, 1995a; Demes & Jungers, 1993) could be related to resistance to axial tension rather than compression (for example, in response to muscular contractions during rapid acceleration at the launching and landing of a leap), but absent in vivo strain data, this must remain in the realm of speculation.

A third observation is that, among sample radii, the medial quadrant is brightest, and the lateral and/or posterior quadrants are darkest, in both periosteal primary and secondary osteonal bone. This pattern is particularly strong among arboreal quadrupeds. Again, it is possible to speculate that radii, and especially those of arboreal quadrupeds, are subjected to mediolateral bending loads. I am familiar with no observational or experimental data to support this supposition, but the possibility exists that this is the case. Interestingly, as discussed in Chapter 5, secondary remodeling clusters at the

posterolateral cortex in radii, likely in response to the presence of a pronator teres muscle attachment there. It is possible that tension applied to the bones at this location during flexion and rotation of the forearm may lead to deposition of more tension-resistant collagen fibers than elsewhere in the cortex. This could be particularly emphasized among arboreal quadrupeds due the habitual pronation of the forearm during locomotion. A clustering of remodeling events in the anterior cortex of the tibia (see Chapter 5), however, is not associated with a greater proportion of longitudinally oriented collagen fibers. Nor does the lack of sectoral variation in the CFO in the tibia correspond with the observation (based solely on strain gauge data from the *Macaca mulatta*; Demes et al., 2001) that this bone is subjected to bending loads. Likewise, there are no significant differences among quadrants in the ulna, despite the likelihood, or at least the possibility that this bone is subjected to bending in some taxa. For example, Demes et al. (1998) identify mediolateral bending in the ulna of *Macaca mulatta*, with the lateral cortex in tension and the medial cortex in compression.

A fourth pattern is one where, in the humerus, the posterior cortex is brightest relative to all other quadrants, in both primary and secondary osteonal bone, again especially among arboreal quadrupeds. Cross-sectional geometric studies suggest that in many primate species humeri are not loaded principally in bending (Swartz et al., 1989 for *Hylobates*, including strain gauge data; Demes & Jungers, 1989 for lorisids, 1993 for a wide range of prosimians; Demes et al., 1991 for indriids; Ruff & Runestad, 1992 for lorisids; Terranova, 1996 for a range of strepsirhines; Runestad, 1997 for lorisids) with exceptions evident for example in the increased humeral anteroposterior bending rigidity in *Euoticus elegantulus* (Terranova, 1996). Runestad Connour et al., (2000)

demonstrated that generalist quadrupedal primates display greater resistance to bending in the coronal plane than do leapers, a finding that does not coincide with greater brightness in the posterior cortex for that positional behavior group.[21] Again, absent knowledge of the *in vivo* loads on the bones, a satisfactory explanation of this pattern remains elusive.

There are no comparable sectoral patterns in the femur, ulna or tibia, despite the predictions, based on cross-sectional geometry and/or strain gauge data, that these bones are subjected to bending loads, at least in some primate taxa (Burr et al., 1982, 1989; Demes et al., 1998, 2001; Demes & Jungers, 1989, 1993; Terranova, 1995a, 1995b; Runestad Connour et al., 2000).

In the fifth observed pattern, mean values for secondary osteonal bone are brighter than for periosteal primary tissue in both the femur and tibia, but not in the forelimb bones. The discrepancy between hindlimb elements and the humerus is partly explicable via an appreciation of the brightness of primary tissue in the latter. It is not surprising that secondary osteons are no brighter than the predominantly bright lamellar tissue they have replaced. However, neither the ulna nor radius periosteal primary tissue is significantly brighter than either the femur or tibia. The increased brightness of secondary remodeled bone in the femur and tibia ideally would be explained as an adaptation to compressive loads in these bones, where the remodeled tissue optimizes a mechanical adaptation not fully realized in developmentally constrained primary tissue. Indeed, most primates (in particular arboreal primates) are believed to support a greater proportion of their weight in the hindlimbs than the forelimbs (Reynolds, 1985; Kimura,

[21] Confounding the comparison to the current study is the authors' finding that lemurids group with leapers in this respect, whereas I have included them among generalist arboreal quadrupeds.

2002, 2003). This may go some way in explaining the presence of this pattern in the femur and tibia, and its absence in the three forelimb bones.

The last and most interesting observation is one mentioned earlier in this discussion: with only a few weak exceptions, all cortices in this sample (both periosteal primary tissue and intracortically remodeled bone) are dark. That is, the vast majority of periosteal and secondary osteonal bone in the sample is composed of tissue with a predominant longitudinal collagen fiber orientation. This observation (to a greater or lesser extent) has been made by several other researchers with respect to a range of vertebrate samples (Riggs et al., 1993a [with respect to primary bone tissues]; McMahon et al., 1995; Skedros et al., 1996; Goldman et al., 2003; Lee, 2004; Bromage & Boyde, n.d.). The potential mechanical significance of this finding is as follows. It has been previously determined that bone is stronger in compression than tension (Burr et al., 1998; Skedros et al., 1994). Given some component of tensile loading along a bone shaft and consequent stresses across a cross sectional area – *even if this is not the principal load in that region* – osteocytes may respond by depositing collagen longitudinally in order to resist that tensile load. McMahon et al. have dubbed this the "tension-resistance priority" hypothesis. They find support for this in the observed preponderance of longitudinally oriented collagen in the sheep calcaneus, even in regions determined to be subjected primarily to compression. Bromage & Boyde (n.d.) describe a similar mismatch between load and CFO in the mandibular corpus of *Macaca fascicularis*. Skedros et al., (1996) show that, in the equine third metacarpal, regions that are subjected to tension only at higher gait speeds display longitudinal fibers, despite peak compressive loads during other locomotor behaviors. Finally, Goldman et al. (2003) find a mean

brightness index of 89.94 (indicating a preponderance of longitudinal collagen) for their sample of midshaft human femora. Intriguingly, Ascenzi et al. (2006) have recently shown that in the dark lamellae of alternate osteons, the proportion of collagen fibers that are aligned longitudinally is c. 70%. In contrast, in bright lamellae, the proportion of fibers aligned transversely is only c. 45%. This again points to the importance of a mechanical design to resist tensile loading.

It should be noted that a predominance of longitudinally oriented collagen fibers does not suggest that compression is not effectively resisted. As Bromage & Boyde (n.d.) suggest, it is simply that these fibers resist tension more effectively than compression. Support for this proposal is provided by Ramasamy & Akkus (2007). In their study of Swiss-Webster mouse femora, they find that the anterior quadrant, containing more longitudinal fibers, is more resistant to tension than the posterior quadrant. However, interestingly, both quadrants are equally resistant to compression, despite the greater proportion of oblique or transverse fibers in the posterior quadrant. This very persuasively suggests that longitudinal fibers are appropriate for the job in many complex loading situations.[22]

This begs the question: why, in so many other studies, are there cortical regions with a predominant oblique/transverse collagen fiber orientation. What makes the current sample different from these others? First, it is important to consider that, with the exception of the work of Kalmey (Kalmey, 2000; Kalmey & Lovejoy, 2002), there have been no previous examinations of collagen fiber orientation in non-human primate bone. Furthermore, in that project, only the femoral neck, and not the midshaft of the femur,

[22] Lee (2004) provides an alternate explanation for the predominance of longitudinal collagen in his sample of *Alligator mississippiensis*. He suggests that the "longitudinal growth dynamics" (p. 205) of the sample femora are responsible for this pattern.

was examined. Therefore, there are no comparable primate studies to which to compare the current one.

One possible explanation for the discrepancy between my study and others is found in the consideration of tissue type and development. As discussed by Bromage & Boyde (n.d.) and McMahon et al. (1995), developmental constraints may preclude certain microstructural arrangements, or encourage others, leading to taxon specific patterns of brightness and darkness in CPL that are not necessarily mechanically adaptive in the sense of proximate causality. Another possibility to consider is that, relative to artiodactyl long bones for example, primate long bones are subjected to a greater range of loading patterns during the individuals' varied and less specialized positional behavior. Certainly primate limb joints have greater degrees of freedom (even among the specialized vertical-clinger leapers) than what is seen among cursorial quadrupeds where movement is largely constrained to the sagittal plane. In the case of greater diversity in loads across the cortex, even some instance of tension, despite a peak compressive strain, could be sufficient to produce a matrix with longitudinal fiber orientation.[23] In addition, it is possible that strain magnitudes are smaller in primates relative to taxa examined in other studies. The limited strain gauge data that exist suggest that this may indeed be the case. Demes et al. (1998, 2001) find that in both the *Macaca mulatta* tibia and ulna, strain magnitudes were lower than what has been recorded for a range of other animals. Similar results were obtained for the three forelimb bones of the brachiating *Hylobates* (Swartz et al., 1989). One could therefore speculate that compressive loads, where they

[23] In the *Macaca mulatta* ulna and tibia, Demes et al. (1998, 2001) find that patterns of loading (e.g., the axis of bending) do not change within individuals, even when gait is varied (from walking to galloping). However, it should be noted that the rhesus macaque is more cursorial and terrestrial than any of the taxa examined in the current study. In addition, Demes et al. do find variation in the direction of bending in the femur for one individual when it engaged in climbing behavior, as apposed to walking or galloping.

do occur among primates, are not sufficient enough to overcome the "tension-resistance priority".

The argument could be made that bright regions of the cortex are largely absent in this sample because of the paucity of secondary remodeling, where adaptation to load is more likely to occur. However, even in the individuals with considerable intracortical remodeling (the larger lemurs and the atelids) the secondary osteonal tissue is dark and displays very little variation throughout the cortex. Finally, there is always the possibility that methodological differences may result in divergent results among studies. As noted above, this is the first study to employ a biologically appropriate illumination standard. (But, as also noted above, it does not seem likely that all previous studies were inappropriately illuminated to the extent that results would be wholly invalid.) In addition, in this study endosteal tissue (including the frequently bright CCC bone) was excluded from analyses. This may lead to a lack of comparability between results. However, at least in some of the previous studies (e.g., Riggs et al., 1993a) is it evident that areas of transverse collagen fiber orientation extend throughout the depth of the cortex. In summary, while there is no doubt that differences in methodological approach should be considered, it is also clear that, beyond methodology, the results of the current study contrast markedly with those of many previous researchers.

Overall, then, I conclude that with the exception of a few weak and largely inexplicable patterns, there is very little distinct evidence of mechanical adaptation in the distribution of preferred collagen fiber orientation among the primates of this sample. Variation is substantial within taxa[24], with almost no distinction among positional

[24] Goldman et al. (2003) also found significant individual variation in patterns of CFO in their sample of midshaft human femora. In addition, Demes et al. (1998, 2001) report individual variation in axes of

behavior groups. Specialized primates such as the lorisids or atelids are not differentiated from the more generalized arboreal quadrupeds. The single strong exception to this absence of evident mechanical adaptation perhaps lies in the overall darkness of the bones, as discussed above.

*6.7.6 Collagen fiber orientation and phylogeny*

Phylogeny does not appear to be a significant factor in determining relative brightness of collagen fiber orientation across whole cortices for either periosteal primary tissue or secondarily remodeled bone.

**6.8 Summary and conclusions**

Returning to questions laid out in the Objectives section of this chapter, I offer the following conclusions. First, an overall preponderance of longitudinally oriented collagen is characteristic of both the periosteal primary and intracortically remodeled bone in the primates of this sample. While there is some variation within this predominantly "dark" realm, the variation does not for the most part break down along taxon or positional behavior lines. Where variation does occur among groups, it is not usually simply understood via interpretations of mechanical loads on the bones, as would be predicted given previous research on the factors affecting collagen fiber orientation. A potential exception to this lack of relationship between mechanical adaptation and CFO is the possibility that longitudinal fibers predominate as a means to strengthen bone in tension.

---

bending in the ulna of *Macaca mulatta*, perhaps providing some indication that behavioral differences among animals may underlay differences in microstructural morphology.

It is apparent that one of the principle factors accounting for the small range of variation that does exist is primary tissue type, where slower depositing bone is more likely to comprise a larger proportion of oblique to transverse collagen fibers. While there is some suggestion that CFO may also correlate with body size (with larger individuals displaying more oblique to transverse fibers) this relationship is neither consistent nor easily explicable through consideration of size-related changes in mechanical load or developmental. The data indicate that, in this sample, there is no relationship between CFO and phylogeny.

# Chapter 7

# Summary, Conclusions and Future Research

## 7.1 Introduction

Bone tissue can both respond to and record the processes and behaviors that characterize individual life histories. It therefore offers a unique opportunity for expanding on insights derived from macro-morphological studies of the skeleton. However, the extent and significance of variation in bone microstructure in primates, as well as other mammals, is largely unknown. The goals of this project were therefore to explore and gain an understanding of the relationship between life history and mechanical adaptation on the one hand, and variation in three bone microstructural features on the other. The microstructural variables are: 1) primary tissue type, 2) intracortical remodeling, and 3) collagen fiber orientation. These were examined via conventional transmitted and circularly polarized light microscopy in midshaft sections from the adult humerus, radius, ulna, femur and tibia in a comparative sample of extant primates including both strepsirhines and haplorhines. The 10 sample taxa were chosen to provide a range of body sizes, growth and metabolic patterns, positional behaviors, and evolutionary relationships.

This study has shown that variation in the three microstructural variables exists among primates, that this variation is often non-randomly distributed, and that it is sometimes explicable via a consideration of developmental patterns, growth rate, body size, positional behavior and phylogeny. However, the study also clearly demonstrates that much of the diversity in the sample is not explained by these variables. This

suggests that more work must to be done to illuminate the factors that impact upon bones as they grow. It also serves as a warning that, at present, micro-morphological features must be employed only with a full understanding of their current limitations – in addition their exciting potential – as tools in the study of fossil taxa.

## 7.2 Summary of findings

### *7.2.1 Primary tissue types*

Regarding the distribution of primary tissue types in the sample long bone midshaft sections, the following observations were discussed in Chapter 4: 1) There is a preponderance of slow-forming primary tissue types among the sample primates, in accord with the general "slow" life-history of primates relative to members of other mammalian orders. 2) Within this general scheme, substantial variation in tissue types is present among taxa and between skeletal elements. 3) This variation is partly explained through an understanding of the development of the bone at the level of the cross-section. For example, posteriorward drift in the midshaft humerus, present in almost all taxa, results in a typical pattern of compacted coarse cancellous deposition in the anterior quadrant of the cortex. 4) Variation in the periosteal portions of the cortex is also partly correlated with body size. Specifically, the proportion of rapidly depositing tissues is increased in larger cortices (from larger individuals). 5) Organismal growth rate is another factor that accounts for some of the variation observed in the sample. In particular, a difference is seen between strepsirhines and platyrrhines, with the latter displaying lower proportions of fast depositing tissues, in accord with their slower growth rates. However, this pattern is not evident when taxa within suborders are compared, and

both the cheirogaleids and tarsiids provide exceptions to the pattern found within their respective suborders. 6) Positional behavior accounts for some proportion of the variation in primary tissue types seen in the sample, although the significance of the observed patterns is not readily evident. 7) Phylogenetic differentiation among taxa (again, specifically between the sample strepsirhines and platyrrhines) largely tracks associated variation in growth rates. Therefore, it is not considered to be a factor with relevance independent of its correlation with adaptive features. A possible exception is found in the unique tarsiid pattern.

*7.2.2 Intracortical remodeling*

Regarding the patterns of intracortical remodeling in the sample long bone midshaft sections, the following observations were discussed in Chapter 5: 1) There is substantial variation within and between taxa, and among skeletal elements, in the proportion of a cortex that is intracortically remodeled. 2) There are no patterns, with respect to either proportion or location of intracortical remodeling, that are characteristic of the sample as a whole. 3) Some of the observed distributions are best explained as a correlate of underlying primary tissue type and developmental patterns. For example, there is a frequent concentration of secondary osteons in areas where the interstitial bone is of the highly vascular compacted coarse cancellous type. 4) Most of the variation in the proportion of a cortex that will be composed of intracortically remodeled bone can be explained by differences in body size, with larger individuals displaying more remodeling. However, current understanding of the relationship between mechanical strains and body mass provide no satisfying justification for this observed pattern. 5)

Some distribution or proportion patterns seem to be accounted for, at least in part, by mechanical adaptation. For example, clusters of secondary osteons are frequently found at the site of muscle insertion in the radius. In addition, there is evidence of a response to a bending regime at the midshafts of femora and tibiae, with differences in the prevalence of intracortical remodeling between tension and compression cortices. Finally, in accord with the suggestion that intracortical remodeling, as apposed to growth remodeling, is more like to occur in the distal elements of a limb, more of the cortex in humerus and femur is composed of secondary osteons than in the radius and tibia respectively. 6) There are no phylogenetically distributed patterns of intracortical remodeling. 7) Significant intrataxon variation in patterns of intracortical remodeling exists, as well as intertaxon variation, much of which remains unexplained by the independent variables considered in this study.

*7.2.3 Collagen fiber orientation*

Regarding patterns of preferred collagen fiber orientation in the sample long bone midshaft sections, the following observations were discussed in Chapter 6: 1) There is a preponderance of longitudinally oriented collagen in the periosteal primary and secondary osteonal tissues of the sample primate taxa. 2) Although some instances of a significantly greater proportion of oblique to transverse collagen do exist, these are not typically correlated with taxon or positional behavior category. 3) Where variation does occur among taxa, this does not correspond with positional behavior and inferred patterns of mechanical load. Therefore, the hypothesis that preferred collagen fiber orientation responds differentially to tensile and compressive strain is not strongly supported in this

study, either for primary periosteal or secondary remodeled bone. An interesting exception might relate to the "tension-resistance priority" hypothesis, where, in the presence of both tensile and compressive loads on bone, the collagen aligns to resist the tension, compensating for the elevated weakness of bone under tension, relative to compression. 4) Body size appears to account for some proportion of the variation in collagen fiber orientation in the sample, with larger individuals displaying more transverse to oblique collagen. A persuasive explanation for this observation is not currently available. 5) There is a strong relationship between primary tissue type and collagen fiber orientation, where slower deposition tissues are more likely to display higher proportions of oblique or transverse collagen fibers. 6) There are no phylogenetically distributed patterns of preferred collagen fiber orientation.

### 7.3 Conclusions

With respect to the objectives set out in the Introduction chapter I conclude that, in some cases, the previously proposed hypotheses regarding variability in bone microstructural features are supported by the results of this project. Specifically, primary tissue types are in part reflective of life history features, and secondary remodeling is principally related to body size with some correlation to mechanical adaptation (although with substantial unexplained variation). Regarding preferred collagen fiber orientation, previous observations of a correlation with principal strains are not definitively repeated here. However, the suggestion by several earlier researchers that collagen fibers might be variably aligned in different tissue types is well substantiated by the current data. Indeed, I believe this finding to be one of the most compelling contributions of this thesis. Never

before has this association been systematically explored or quantified. Another particularly interesting result is the discovery of differences between the proximal and distal elements of both forelimbs and hindlimbs; proximal elements display greater proportions of slow depositing primary periosteal bone tissue, less intracortical remodeling, and more oblique to transverse collagen fibers. This is intriguing in light of potential differences in pattern formation and constraints among limb segments (Lovejoy et al., 1999; Hamrick, 2001, 2002).

## 7.4 Contributions

### *7.4.1 To anthropology*

First and foremost, this project has generated previously unavailable data regarding bone microstructural variation in primates. Two of the three variables that I examine (primary tissue types and collagen fiber orientation) have never before been described or quantified in a broad range of primates. Only with the accessibility of such a body of information can the usefulness of future bone microstructural studies be assessed.

Second, in determining that variation does exist among primate species, and that it is highly patterned in some instances, it becomes clear that there is the potential to explain this variation in terms of taxon-specific life histories and behaviors. A question asked at the outset was the following: given a cross section of bone, what can we learn of the mechanical adaptation and life history of an individual? While results of this study indicate that the creation of a new database of microstructural features cannot resolve intractable debates within the anthropological community or definitively answer many questions, there is the potential of identifying previously obscure aspects of primate

paleo-behavior, biology, and ecology. Relationships between bone microstructure and mechanical adaptation may allow for more refined determination of life history and positional behavior in fossil individuals, as a means to reconstruct their life-ways. For example, the lorisids in this study consistently display unique patterns of primary tissue type distribution and intracortical remodeling, coincident with their unique positional behavior mode. Identification of this pattern in fossil specimens would serve to strengthen an association with the lorisid clade, or at least the lorisid locomotory model.

The results have further potential value in the study of primate evolutionary history. As outlined in Chapter 3, many controversial questions endure in this field, for example: who are the specific ancestors to living strepsirhines and haplorhines? On the one hand, it has been suggested that omomyids are ancestral to both anthropoids and tarsiids, while adapids are ancestral to, or are the sister group of the living strepsirhines. A competing view proposes that omomyids are ancestral to tarsiids only, and that adapids are ancestral to anthropoids. Yet a third scenario suggests that the ancestor group to anthropoids is neither adapid nor omomyid, and as yet unidentified. Other variations on these themes exist (e.g., Krishtalka & Schwartz, 1978; Rosenberger & Szalay, 1980; Szalay et al., 1987; Szalay & Dagosto, 1988; Dagosto, 1988, 1993; Rasmussen, 1994; Simons et al., 1995; Simons, 1997; Shoshani et al., 1996). Because results from this study indicate that there is a recognizable difference in primary tissue type patterns between strepsirhines, platyrrhines and tarsiids (likely linked at least in part to disparate life histories), this suggests that microstructural tools could be employed in addressing this question with respect to fossil material. For example, the three platyrrhine taxa examined here display a greater proportion of slow-depositing lamellar bone, in accord

with their extended growth period, while the larger bodied strepsirhines display a greater proportion of fast-depositing fibrolamellar bone. Thus, where unresolved issues regarding the evolutionary history of the primate order abound, these tools may prove invaluable.

Equally important is the observation that, although there are associations between the microstructural variables examined here and aspects of the life history and mechanical adaptation of primates, these variables cannot and should not be used to interpret fossil specimens without a consideration of all the factors that may impact upon them. For example, use of collagen fiber orientation to determine patterns of strain across a cortex would likely be invalid in the absence of a consideration of developmental regimes and tissue type, given the observation here that tissue type and collagen fiber orientation are correlated.

*7.4.2 Beyond anthropology*

Beyond the contributions that this project has made to the study of primate microstructure, it also adds to the field of comparative bone microstructure in general. This research constitutes one of several ongoing projects in the Hard Tissue Research Unit (HTRU) formerly of Hunter College, City University of New York, and now located at the New York University College of Dentistry (e.g., Goldman, 2001; McFarlin, 2006). As a whole, the laboratory is generating a database of information with applications to anthropology, to mammalogy and to the study of vertebrate skeletons in general. As noted previously, this area of study has yielded a wealth of information regarding many vertebrates, with results applicable, for example, to the reconstruction of dinosaur

physiological adaptations (Curry, 1998; Botha & Chinsamy, 2000; Erickson & Tumanova, 2000; Erickson et al., 2001; Horner et al., 2000; Horner & Padian, 2004; de Ricqlès et al., 2000; Padian et al., 2001). Conversely, accounts of variation in mammalian bone microstructure – and particularly how it may occur within a single order of mammals – have been limited. By enlarging the database of vertebrate bone microstructural studies, this research enriches the context within which patterns of variability in all vertebrates are interpreted.

This work is also relevant to clinical bone research. Those who study bone for the purpose of understanding healthy human patterns and pathologies often limit their exploration to the small number of species used in experimental contexts. Similarly such research is restricted to the particular bone patterns typically found in adult humans, and judged to be "normal" mature bone. The range of variation within and among living taxa, especially in the order that includes humans, provides a backdrop for understanding the variation that can be present in human bone, even among adults. In this way, observed pathologies can be explored within the context of understanding the microstructural variation that is normally possible in the primate order.

New methods (all devised in cooperation with faculty and fellow students at the HTRU) were developed during this project that will be available to the world of bone biologists and micro-anatomists at large. Our imaging, in high-resolution, of whole bone cortices using the Syncroscopy Montage Explorer software (Synoptics Inc.) obviates the laborious and/or inaccurate montaging of numerous individual frames. The illumination standard we have implemented for CPL image acquisition (see Chapter 6) is particularly important, as it is the relative brightness of the image that is the quantifiable variable of

interest. Only with an illumination standard applicable across laboratories can diverse samples be compared with any confidence. In conjunction with this, the development of a method of monochrome CPL image acquisition using a color camera would allow those without monochrome cameras to undertake quantitative CPL work. Our system, using Adobe Photoshop and Optimas Image Analysis software (Media Cybernetics), to identify and mask primary tissue types and intracortical remodeling events facilitates the visualization and quantification of said types. In addition, the close scrutiny of variation in tissue types among closely related taxa has led to the refinement of existing tissue typology schemes. Changes that we suggest have been discussed with colleagues at laboratories with similar research interests, and it is possible that a formally updated description of tissue types, in the form of a joint publication, may be required.

Other methodological advances include the development of a bone reconstruction method, as described in the Materials and Methods chapter, as well as the design and construction, in cooperation with Paleo-Tech Concepts, Inc., of a osteometric board fitted with a laser diode attachment, to facilitate length measurements other than maximum length. These are tools that would allow any bone biologist or micro-anatomist to pursue the collection of museum specimens.

**7.5 Future research**

First, the methods employed in this project will be applied to a small selection of fossil primates – plesiadapiforms, omomyids, and adapids – that are currently available for analysis. All the microstructural features examined here are potentially preserved in

fossilized bone material (Enlow, 1966). This will provide the first attempt at application of the results to interpretation of paleobiological features among extinct primates.

The specimen preparation for this project was designed in part to facilitate the future investigation of other micro- and ultra-structural features of bone. It is my intent to examine – via backscattered electron microscopy – variation in mineral density within and between sections. This is yet another variable hypothesized, and demonstrated, to impact upon the material properties of a bone, therefore with potential relevance to the interpretation of strain milieu (Vincentelli & Evans, 1971; Martin & Ishida, 1989; Martin, 1993; Parfitt, 1993; Goldman et al., 2003). In addition, the sample will be used to investigate the relationships among osteocyte lacunar form and density, osteocyte canalicular networks, tissue type, tissue deposition rates, and organismal physiological and growth adaptations. This work will be part of a larger endeavor, centered at the HTRU, to address questions regarding chronobiological rhythms and life history adaptations among vertebrates as a whole.

The project reported on here was undertaken with a number of specific questions in mind. Some of these have been answered, and some have not. In several instances the results have led to new questions, which should be addressed in future research, either at HTRU, or in cooperation with colleagues at other laboratories with complementary facilities. For example, the data have shown that there is an association between primary tissue type and positional behavior. Yet neither the differences in mechanical properties among primary tissue types, nor the specific strains across the midshaft in almost all the long bones of extant primate taxa, are known. A coordinated investigation in this area might serve to further explain the distribution of primary tissue types across a cortex.

Another intriguing area to explore would be the association between collagen fiber orientation and primary tissue type. I have found that slower-deposition tissues are more likely to contain oblique or transverse collagen fibers, but the mechanism by which this occurs, and the reason for this correlation, are unknown.

Additionally, collagen fiber orientation and primary tissue type distribution in endosteally deposited bone tissue has largely been excluded from the analyses in this project. It is clear, however, that different patterns are found endosteally than I have described for periosteally deposited bone. Therefore, endosteal bone, potentially responding differentially to similar stimuli (or similarly to different stimuli), or providing a record of differences in developmental paradigms between endosteal and periosteal bone, should be further examined.

The apparent differences between distal and proximal segments of both hindlimbs and forelimbs – in all three microstructural variables examined here – also warrant further inquiry. Such an investigation ideally would involve an ontogenetic sample from a single taxon, including all five long bones, in combination with experimentally acquired strain data (or finite element modeling data).

Finally, in the course of this project, it has become evident that the development of software to facilitate the automated identification of tissue types and quantification of percent tissue types, as a function of cortical area, should be initiated (ideally in concert with a bioinfomatics laboratory). New methods would then become available to the community of bone biologists and comparative bone histologists at large.

# Appendix A

# A Note On Cross-Sectional Geometry

## A.1 Introduction

One of the ways in which the mechanical adaptation of long bones is manifested macroscopically is in their cross-sectional geometry along the shaft. Geometric parameters are useful to combine with microstructure, as datasets for both levels of inquiry can be acquired from the same cross-sections. While cross-sectional geometry was not pursued in depth in this study, the data are readily available for future investigation. It should be noted however, that cross-sectional geometric parameters have previously been well explored among many of the taxa included in the current study. In addition, the study sample sizes, while appropriate for an investigation of microstructure (given the labor-intensive nature of specimen preparation and data acquisition), are smaller than is ideal and typically found in studies of cross-sectional geometry, where alternative and more expedient methods of data acquisition are possible. Finally, although in some cases microstructural patterns were such that comparison to cross-sectional geometric parameters of the individual specimens could be useful (e.g., when remodeling was more densely distributed on one side of the neutral axis, see the Discussion sections of Chapters 5 and 6), such instances were the exception.

## A.2 Background on cross-sectional geometry

Following the principles of engineering regarding the mechanical properties of beams, cross sections should be shaped to best resist the forces of axial compression, axial

tension, bending and torsion (see Burr, 1980; Turner & Burr, 1993; Tencer & Johnson, 1994; Thomason, 1995). However, unlike some artificially engineered materials, bone tissue is not isotropic, and strength throughout the cortex is not only dependent on geometry but also on variable material properties (Thomason, 1995). The closest match to engineering models is found at midshaft, away from the complicated forces incurred at joint surfaces (Lanyon & Rubin, 1985). Consequently, cross-sectional geometry studies are most often performed at midshaft, and even those that include sections from other regions of the bone should avoid the largely trabecular metaphyseal and epiphyseal regions (Ruff, 1983). Given this restriction, and even with the anisotropy of bone, a good concordance between predicted loads based on cross-sectional geometry, and those found in strain-gauge and other experimental analyses has generally been found (Ruff, 1989; although see Demes et al., 1998, 2001).

A series of parameters can be calculated which provide quantitative assessment of the rigidity of bones resisting forces at the level of the cross-section (Burr et al., 1982; Ruff & Hayes, 1983a; Ruff, 1989; Turner & Burr, 1993). 1) Cortical cross-sectional area provides a measure of strength of a long bone in axial compression or tension. 2) Cross-sectional moments of inertia (I) are measures of material around an axis (incorporating information on both total area and distance from the neutral axis), and when maximum (Imax = highest value for I) and minimum (Imin = lowest value for I) are identified, these can indicate the direction of the beam's greatest and least stiffness in bending (Imax and Imin respectively), and the position of the neutral axis. The latter is the plane through the bone where no stresses are incurred during bending. In bending, the bone on one side of this axis is usually subject to tension, while on the other side it is subject to compression.

In theory, a bone that is built to resist bending in one plane will be elliptical in cross-section, while one that resists bending in all planes (or torsion) will be circular. 3) Bending rigidity can also be tracked using the section modulus (Z) which also takes into consideration the amount of bone located away from the neutral axis (Terranova, 1995a). 4) Strength in torsion (in circular or near-circular sections only) can be estimated by calculating the polar moment of inertia (J), which is equal to the sum of Imax and Imin. However, J can only reliably be used to estimate the effects of torsion in cylindrical sections (i.e., those where the Imax/Imin ratios do not exceed 1.5) (Daegling, 2002).

Cross-sectional geometry studies can be categorized as one of three general kinds. First there are those studies, limited in number, that examine cross-sectional geometric parameters relative to known loads on the bone, as determined by *in vivo* via strain-gauge protocols (e.g., Demes et al., 1998, 2001). Second are studies that attempt to broadly correlate the shape of cross sections with the habitual loads on the bone. These have been performed on both living and fossil taxa, and may or may not be correlated with the results of strain-gauge data, but the association with some prior estimation of load patterns (e.g., through behavioral observation and morphological analysis) is critical; the results of cross-sectional geometry alone ideally should not be used to determine mechanical loads. It should be noted that, although strain-gauge studies often support the load patterns predicted by examination of cross-sectional geometry, this is not always the case, and therefore results must be interpreted with caution (Lanyon & Rubin, 1985; Demes et al, 1991, 1998; Thomason, 1995). A number of such studies exist for living primates, including humans. Although comparisons between them may yield some contradictory results and differing interpretations, in general they provide support for the

association between mechanics and cross-sectional geometry, with body size, phylogeny, sex and age as additional factors to consider (e.g., Jungers & Minns, 1979; Burr, 1980; Burr et al., 1982, 1989a; Ruff & Hayes, 1983b; Ruff, 1989; Ruff & Runestad, 1992; Schaffler et al., 1985; Demes & Jungers, 1989; Demes et al., 1991; Terranova, 1995a, 1995b; Feik et al., 1997; Runestad, 1997).

A third approach attempts to track remodeling alterations in shape in response to changes in applied forces. These studies provide support for the hypothesis that bones accommodate changes in habitual loading regimes: cross-sectional geometric measurements will be altered through deposition and/or resorption at the endosteal and periosteal surfaces. While the mechanisms of mechanosensation (the means by which the bone senses change in mechanical loads) are not fully understood, it is generally assumed that alterations in bone shape (growth remodeling), both during and after the attainment of adult body size, are largely determined by mechanical stimuli activating the bone cells. It appears that the number of strain cycles, peak strain magnitude, rate of strain change, strain duration, and strain distribution can all effect change in cross-sectional geometry (Lanyon, 1984). It is suggested that the system's assessment of "appropriateness" regarding local responses to stimulus is likely genetically determined, that is selected for (Lanyon & Rubin, 1985; Rubin & Lanyon, 1985; Biewener et al., 1986) and may vary among groups of animals (Kodama et al., 1999). The relationship between adaptive remodeling and mechanics has been widely accepted, although not unanimously (e.g., see Bertram & Swartz, 1991). Many surgical experiments have been performed with results that appear to support the causal relationship between mechanical stimuli and bone cross-sectional shape modifications (e.g., Chamay & Tschantz, 1972; Lanyon et al., 1982;

Rubin & Lanyon, 1985; Burr et al., 1989b). This is corroborated in non-surgical, load manipulation studies (e.g., Ruff et al., 1991; Biewener & Bertram, 1994; Lieberman, 1996; Lieberman & Crompton, 1998).

**A.3 Some preliminary data**

Following is an example of cross-sectional geometric acquired from the current sample. I offer this both as a means to indicate the potential of future investigations in this vein, as well as to point out the general concordance with studies already published.

Figure A.1 describes the relationship between total cortical area (TCA = an indication of strength when subjected to axial compressive or tensile loads) at the midshaft femur relative to the midshaft humerus, where values greater than 1.0 indicate stronger femora and values less than 1.0 indicate stronger humeri. As is evident from this graph, humeri and femora of slow climbers and suspensory primates are apparently designed to be equally resistant to these loading regimes (i.e., values close to 1.0). In contrast, femora of vertical clingers and leapers are more likely to display greater axial load strength than humeri, whereas results vary among arboreal quadrupeds. Only the difference between slow climbers and vertical clingers and leapers is statistically significant (Mann Whitney U test; $p<.01$). Given a larger sample, the difference between suspensory primates and vertical clingers and leapers might also prove statistically significant. However, the current sample size for the former is restricted to two individuals.

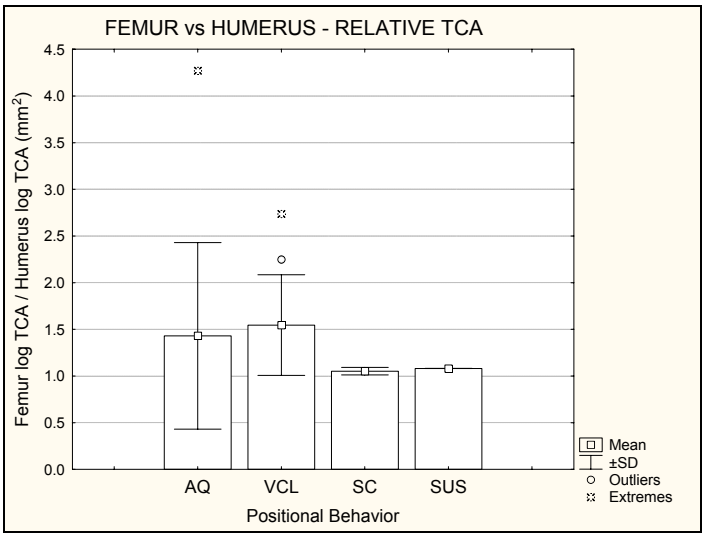


**Figure A.1: Relative strength of the femur and humerus in axial compression or tension.**

See text for description.
AQ=arboreal quadrupedalism;
VCL=vertical clinging and leaping;
SC=slow climbing;
SUS=suspension.

These results are consistent with findings by previous researchers, in particular with respect to the slow climbers and vertical-clinger leapers. For example, Demes & Jungers (1989, 1993) find equivalent compressive strengths in the humerus and femur among lorisids, whereas most other prosimians in their sample display femora that are stronger than humeri in compression. Terranova (1995a, 1995b) describes femoral compressive strengths in galagid leapers that are greater than those of humeri (e.g., the compressive strength in the *Galago moholi* midshaft femur is almost 50% greater than that of the humerus, while the femur of the less specialized *Otolemur crassicaudatus* is about 25% stronger in compression than the humerus, a difference that is not statistically significant). This is in contrast to the similar humeral and femoral TCA for a number of strepsirhine taxa that are not specialized leapers. Finally, Runestad (1997) also determines that, in lorisids (as well as among generalist quadrupedal primate taxa) the humerus and femur are equivalent in their resistance to axial loading and torsion.

### A.4 Conclusions

The potential remains, using the current sample, to further examine cross-sectional geometric parameters. Such an approach, in combination with the microstructural data, may serve to refine the interpretation of the mechanical environment to which a bone is subjected during life, within the context of its developmental trajectory. However, it is not expected that the cross-sectional data for this sample will diverge significantly from the results already reported in the literature. Nor is it likely that such data will radically change the interpretation of the microstructure results, as discussed in Chapters 4, 5, and 6, and reviewed in Chapter 7.

# Appendix B

# Color Mapped Specimen Images

## B.1 Introduction

All scales indicate 0.5mm. Within taxon groups images are to scale. However, differences in scale are present between taxon groups. Look-up-table (LUT) transformed circularly polarized light images are not provided as the majority are almost uniformly dark (i.e., collagen fibers run longitudinally and LUT scale color is dark blue) and, at the scale possible here, do not show detail allowing for qualitative interpretation.

## B.2 Lesser galagos

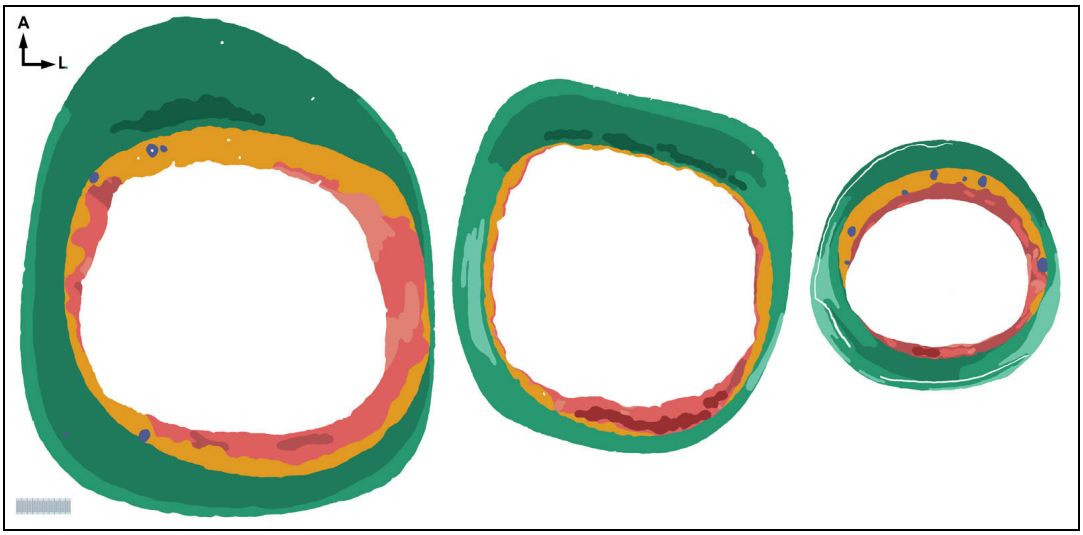


**Figure B.1: Lesser galago femora.**
*Galago senegalensis* (MNHU 60601), *Galago moholi* (DUPC 2062), *Galagoides demidovii* (H 25).

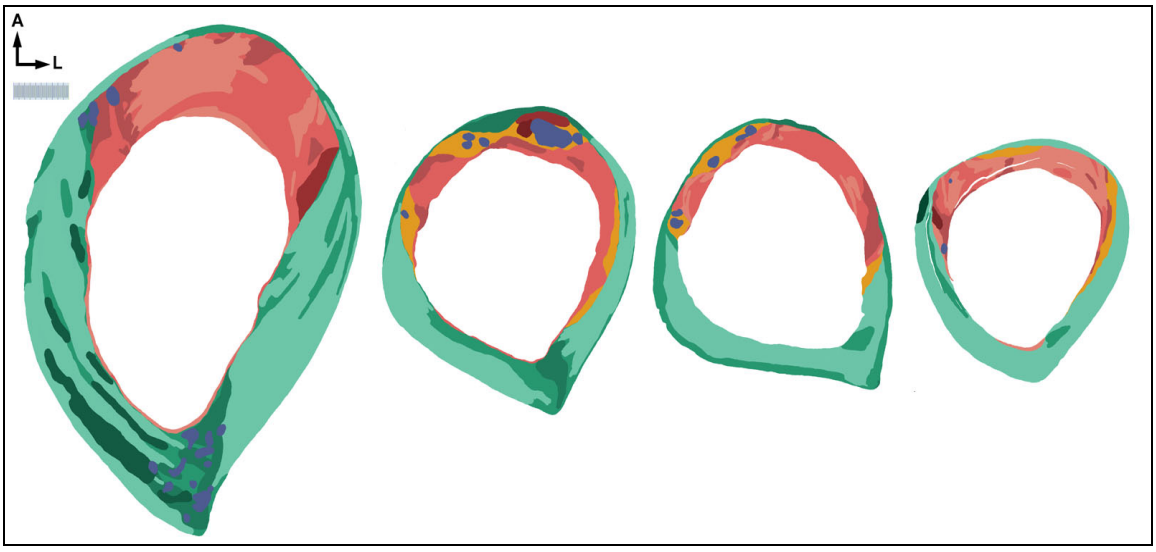


**Figure B.2: Lesser galago humeri.**
*Galago senegalensis* (MNHU 60601), *Galago moholi* (DUPC 2062), *Galago moholi* (DUPC 3173), *Galagoides demidovii* (H 25).

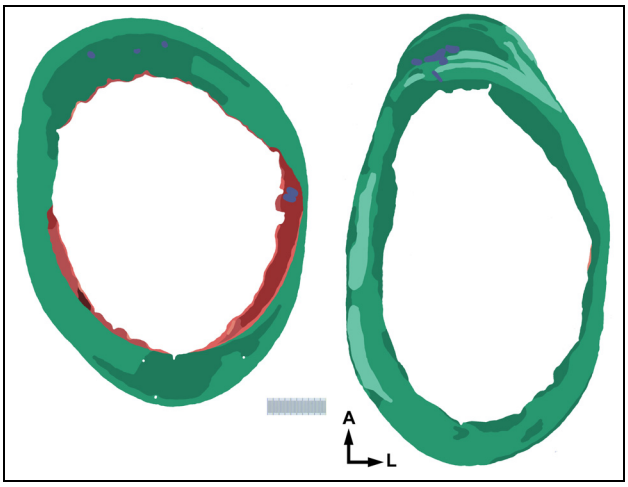


**Figure B.3: Lesser galago tibiae.**
*Galago moholi* (DUPC 2062), *Galago moholi* (DUPC 3173).

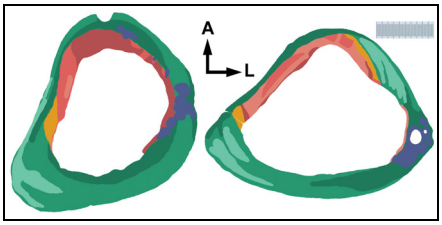


**Figure B.4: Lesser galago radii.**
*Galago moholi* (DUPC 2062), *Galago moholi* (DUPC 3173).

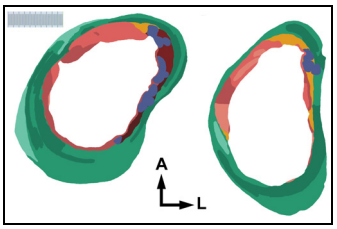


**Figure B.5: Lesser galago ulnae.**
*Galago moholi* (DUPC 2062), *Galago moholi* (DUPC 3173).

## B.3 Greater galagos

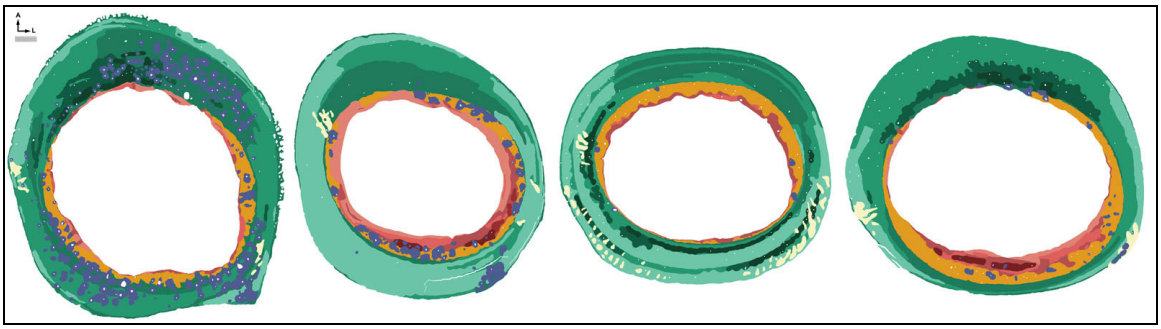

**Figure B.6: Greater galago femora.**
*Otolemur crassicaudatus* **(**DUPC 725), *Otolemur crassicaudatus* (HC 31), *Otolemur crassicaudatus* (USNM 365721), *Otolemur crassicaudatus* (CT OA).

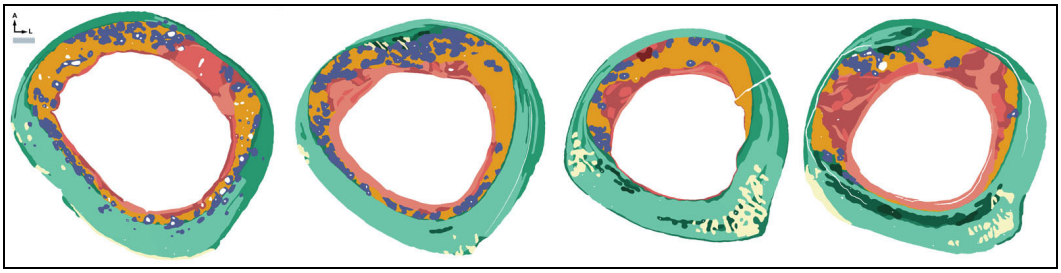

**Figure B.7: Greater galago humeri.**
*Otolemur crassicaudatus* **(**DUPC 725), *Otolemur crassicaudatus* (HC 31), *Otolemur crassicaudatus* (USNM 365721), *Otolemur crassicaudatus* (CT OA).

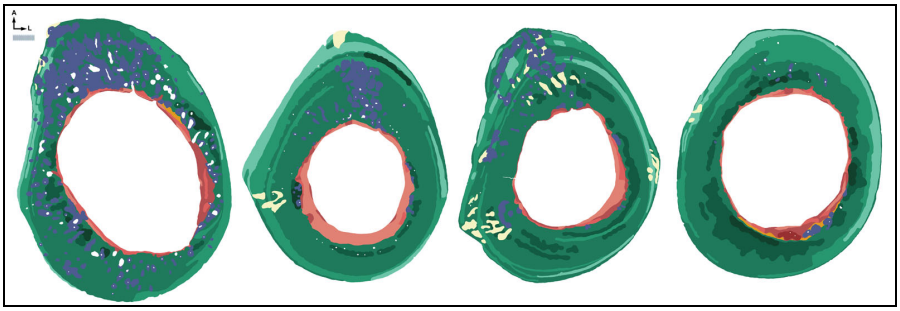

**Figure B.8: Greater galago tibiae.**
*Otolemur crassicaudatus* **(**DUPC 725), *Otolemur crassicaudatus* (HC 31), *Otolemur crassicaudatus* (USNM 365721), *Otolemur crassicaudatus* (CT OA).

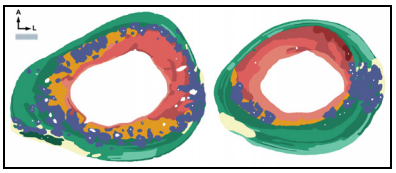

**Figure B.9: Greater galago radii.**
*Otolemur crassicaudatus* **(**DUPC 725), *Otolemur crassicaudatus* (HC 31).

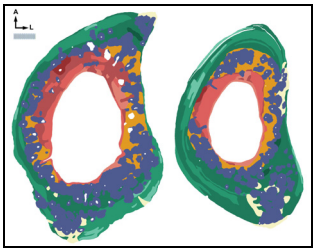

**Figure B.10: Greater galago ulnae.**
*Otolemur crassicaudatus* **(**DUPC 725), *Otolemur crassicaudatus* (HC 31).

## B.4 Lorisidae

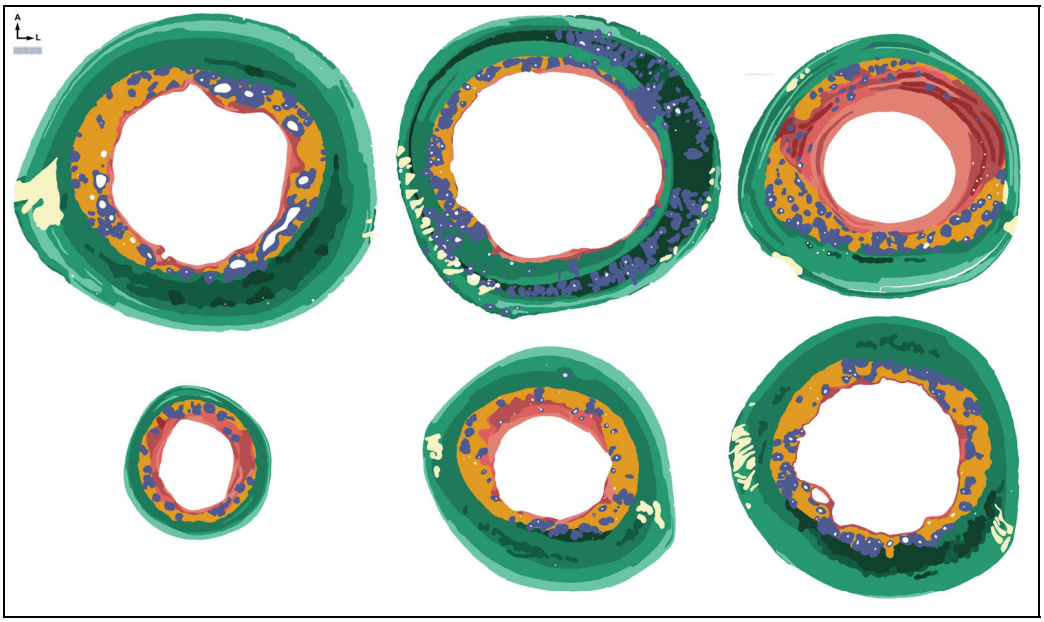

**Figure B.11: Lorisid femora.**
*Nycticebus coucang* (DUPC 1972), *Perodicticus potto* (DUPC 930), *Nycticebus coucang* (HC 27), *Loris tardigradus* (DUPC 1964), *Nycticebus coucang* (MCZ 36116), *Nycticebus coucang* (MCZ 422).

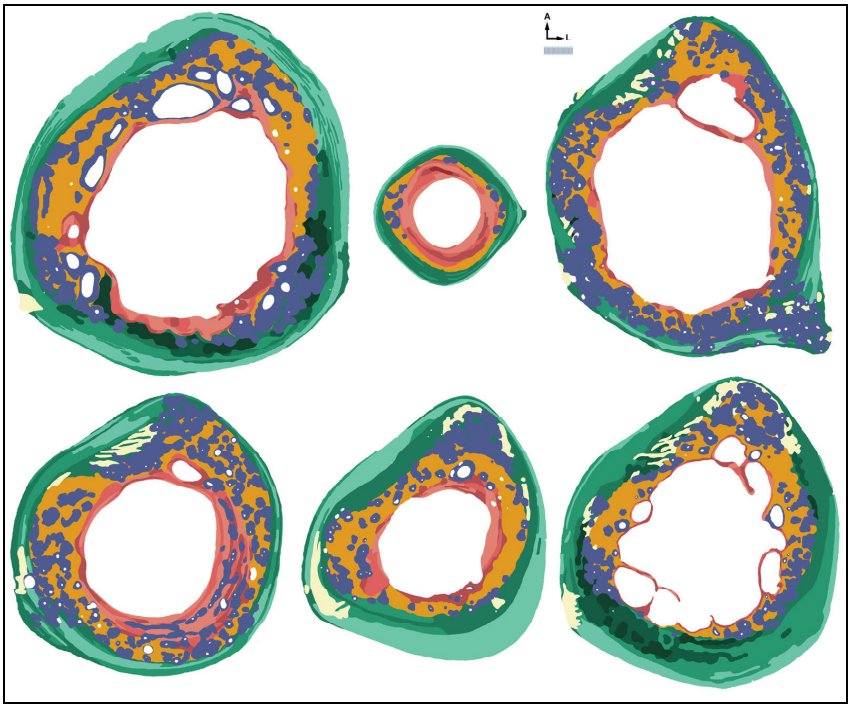

**Figure B.12: Lorisid humeri.**
*Nycticebus coucang* (DUPC 1972), *Loris tardigradus* (DUPC 1964), *Perodicticus potto* (DUPC 930), *Nycticebus coucang* (HC 27), *Nycticebus coucang* (MCZ 36116), *Nycticebus coucang* (MCZ 422).

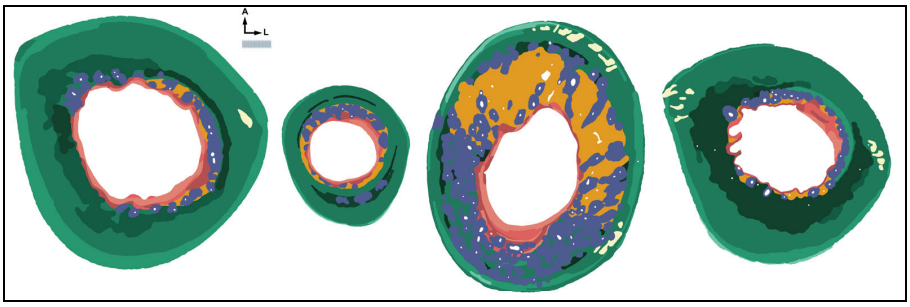

**Figure B.13: Lorisid tibiae.**
*Nycticebus coucang* (DUPC 1972), *Loris tardigradus* (DUPC 1964), *Nycticebus coucang* (HC 27), *Nycticebus coucang* (MCZ 422).

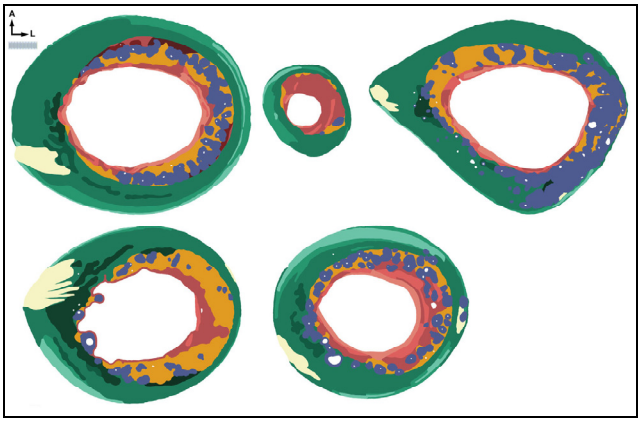

**Figure B.14: Lorisid radii**.
*Nycticebus coucang* (DUPC 1972), *Loris tardigradus* (DUPC 1964), *Perodicticus potto* (DUPC 930), *Nycticebus coucang* (MCZ 422), *Nycticebus coucang* (HC 27).

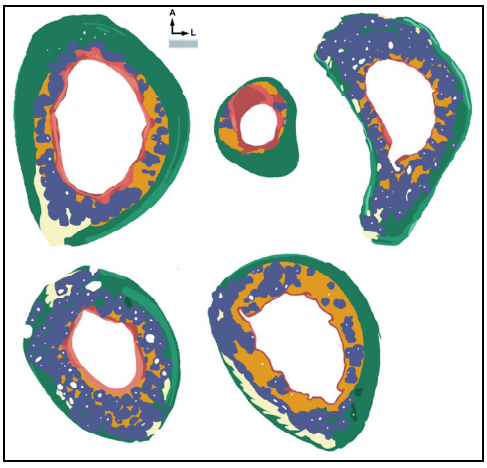

**Figure B.15: Lorisid ulnae**
*Nycticebus coucang* (DUPC 1972), *Loris tardigradus* (DUPC 1964), *Perodicticus potto* (DUPC 930), *Nycticebus coucang* (HC 27), *Nycticebus coucang* (MCZ 422).

## B.5 Lemuridae

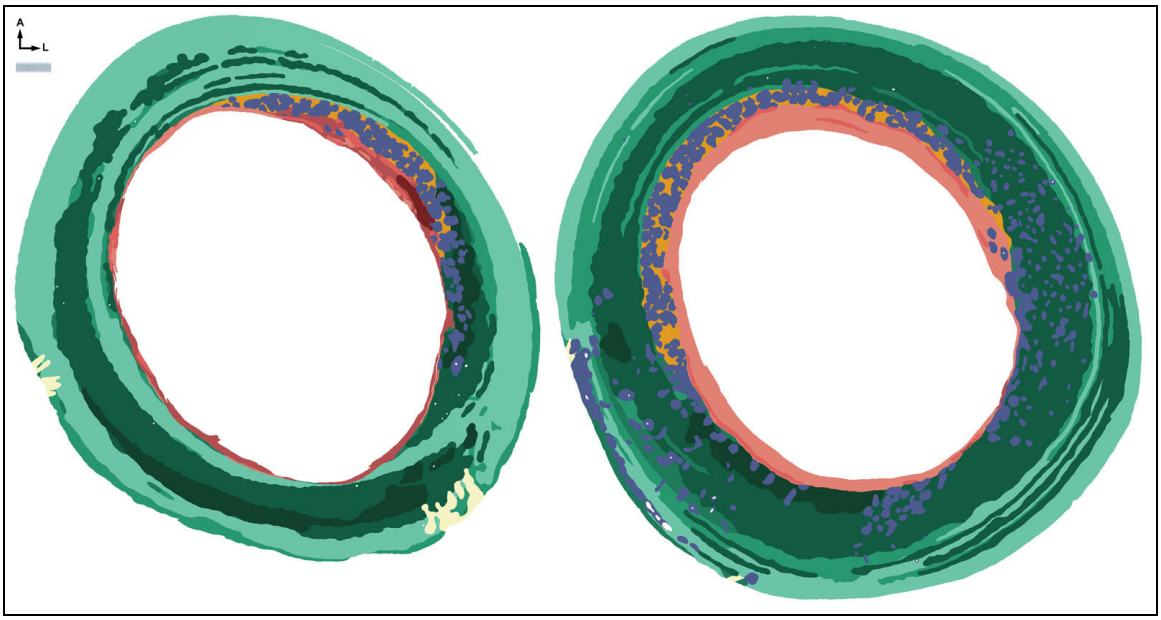

**Figure B.16: Lemurid femora.**
*Lemur* sp. (HC 30), *Varecia variegata* (MCZ 18740).

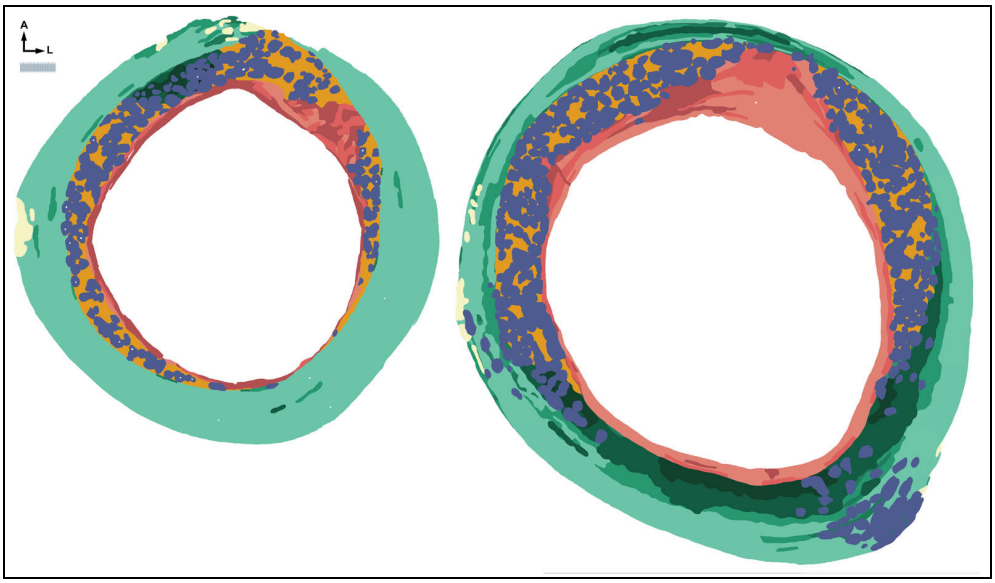

**Figure B.17: Lemurid humeri**.
*Lemur* sp. (HC 30), *Varecia variegata* (MCZ 18740).

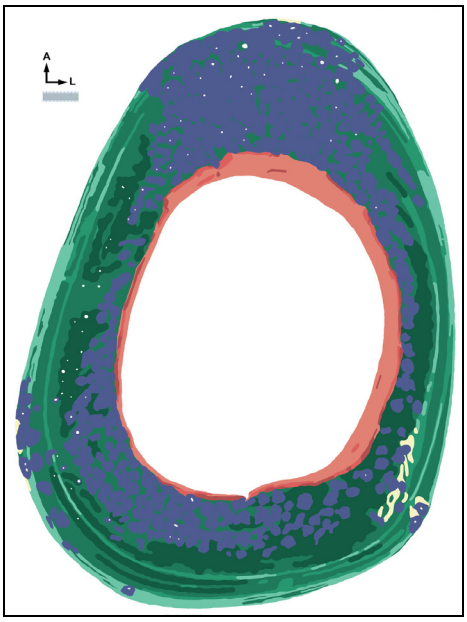


**Figure B.18: Lemurid tibia**.
*Varecia variegata* (MCZ 18740).

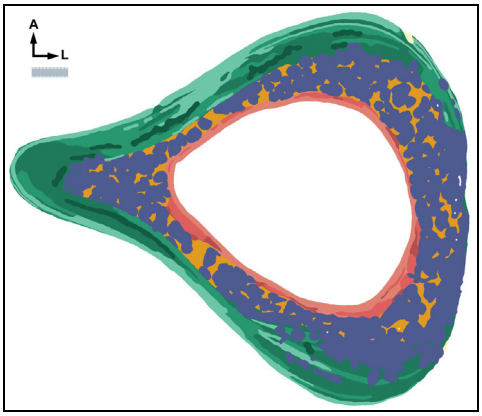


**Figure B.19: Lemurid radius.**
*Varecia variegata* (MCZ 18740).

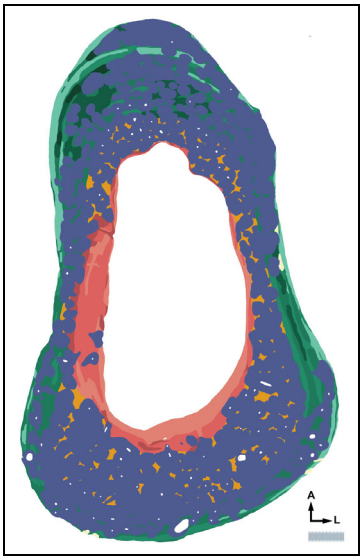


**Figure B.20: Lemurid ulna**.
*Varecia variegata* (MCZ 18740).

## B.6 Indriidae

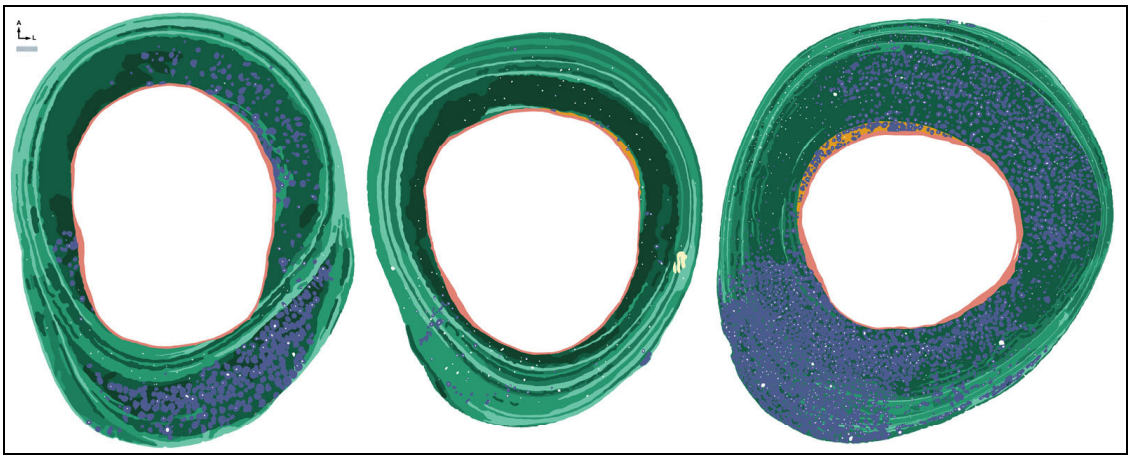

**Figure B.21: Indriid femora.**
*Propithecus* sp. (MNHU 44684), *Propithecus* sp. (MNHU 44685), *Indri indri* (HC 19).

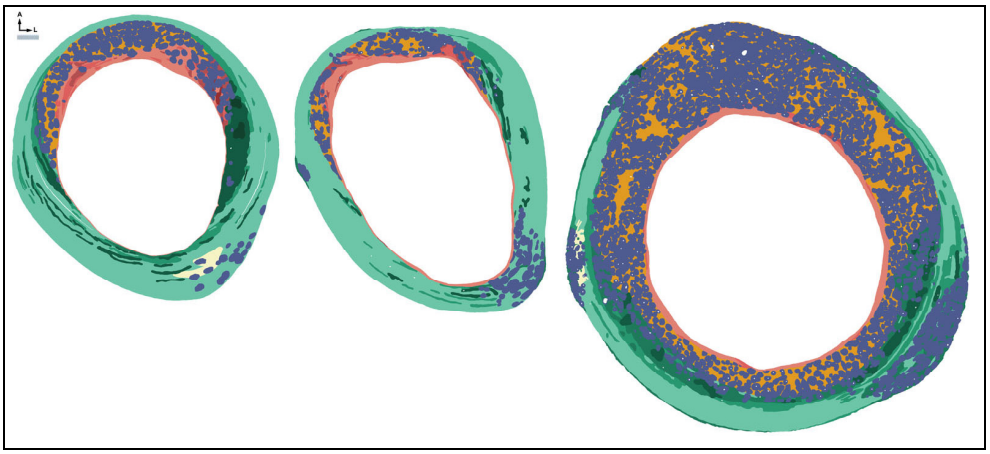

**Figure B.22: Indriid humeri**.
*Propithecus* sp. (MNHU 44684), *Propithecus* sp. (MNHU 44685), *Indri indri* (HC 19).

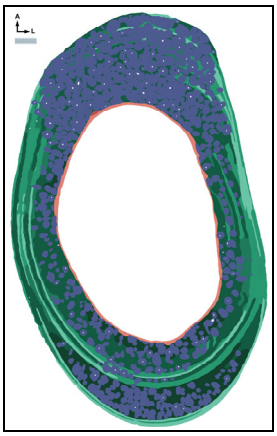

**Figure B.23: Indriid tibia.**
*Propithecus* sp. (MNHU 44684).

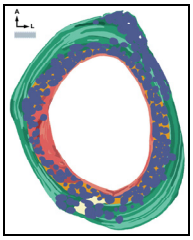

**Figure B.24: Indriid radius.**
*Propithecus* sp. (MNHU 44684).

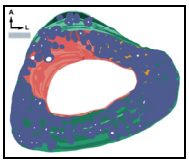

**Figure B.25: Indriid ulna.**
*Propithecus* sp. (MNHU 44684).

## B.7 Cheirogaleidae

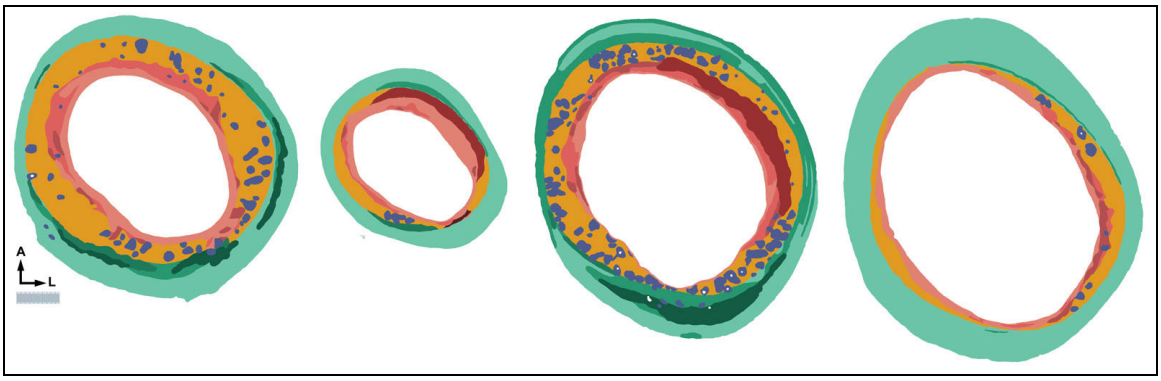


**Figure B.26: Cheirogaleid femora.**
*Cheirogaleus major* (DUPC 2612), *Microcebus murinus* (DUPC 825), *Cheirogaleus major* (MCZ 44850), *Mirza coquereli* (DUPC 359).

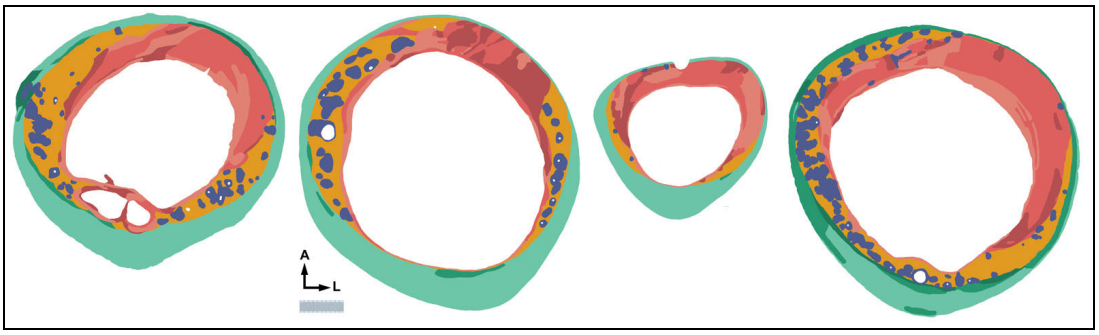


**Figure B.27: Cheirogaleid humeri**.
*Cheirogaleus major* (DUPC 2612), *Mirza coquereli* (DUPC 359), *Microcebus murinus* (DUPC 825), *Cheirogaleus major* (MCZ 44850).

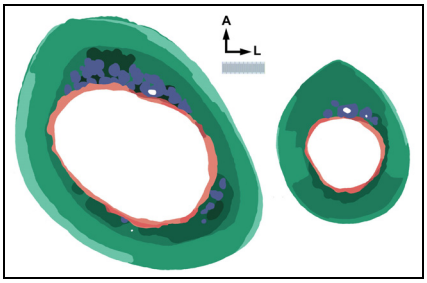


**Figure B.28: Cheirogaleid tibiae.**
*Mirza coquereli* (DUPC 359), *Microcebus murinus* (DUPC 825).

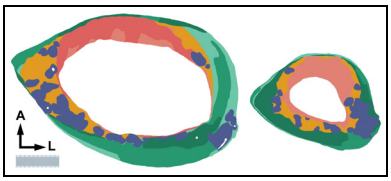


**Figure B.29: Cheirogaleid radii.**
*Mirza coquereli* (DUPC 359), *Microcebus murinus* (DUPC 825).

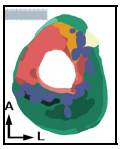


**Figure B.30: Cheirogaleid ulna.**
*Microcebus murinus* (DUPC 825).

## B.8 Tarsiidae

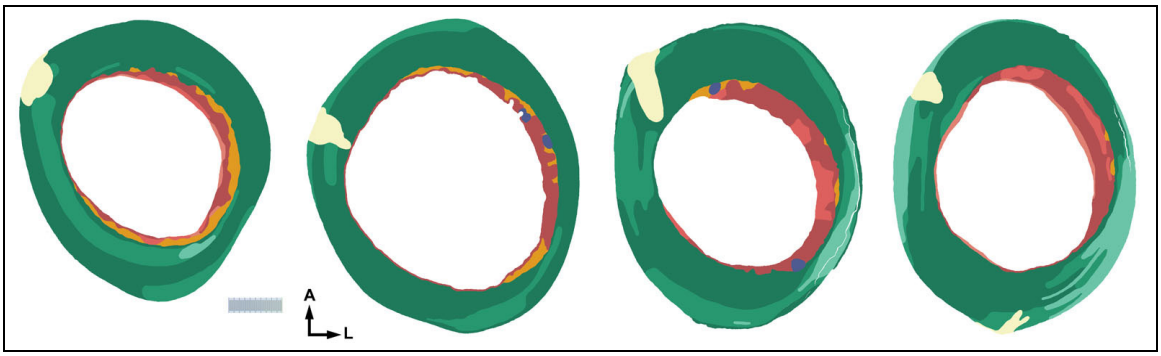


**Figure B.31: Tarsiid femora.**
*Tarsius spectrum* (MNHU An11318), *Tarsius syrichta* (DUPC 81), *Tarsius spectrum* (HC 16), *Tarsius* sp. (HC 23).

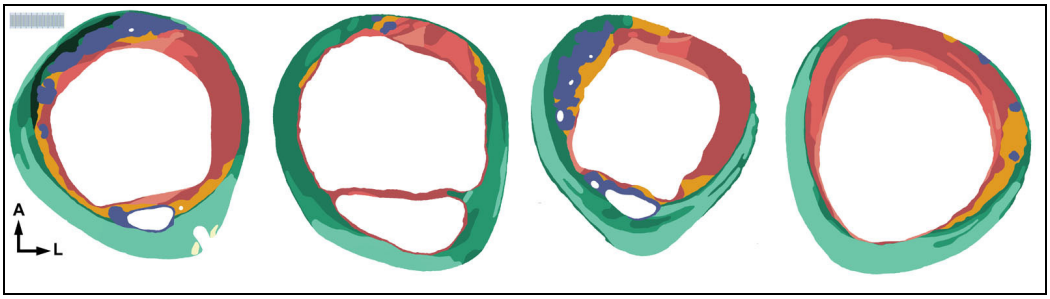


**Figure B.32: Tarsiid humeri.**
*Tarsius spectrum* (MNHU An11318), *Tarsius syrichta* (DUPC 81), *Tarsius spectrum* (HC 16), *Tarsius* sp. (HC 23).

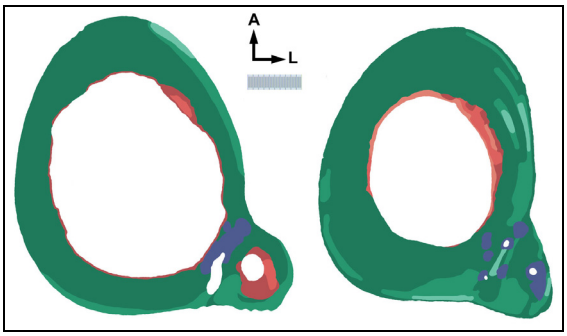


**Figure B.33: Tarsiid tibiae.**
*Tarsius syrichta* (DUPC 81), *Tarsius spectrum* (HC 16).

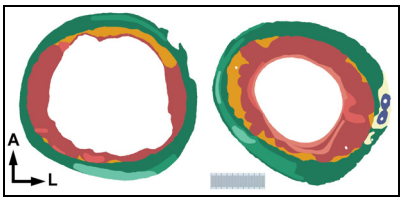


**Figure B.34: Tarsiid radii**
*Tarsius syrichta* (DUPC 81), *Tarsius spectrum* (HC 16).

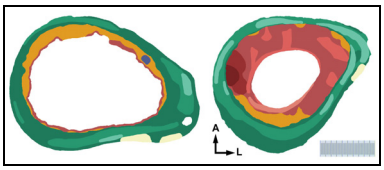


**Figure B.35: Tarsiid ulnae**.
*Tarsius syrichta* (DUPC 81), *Tarsius spectrum* (HC 16).

## B.9 Callitrichidae

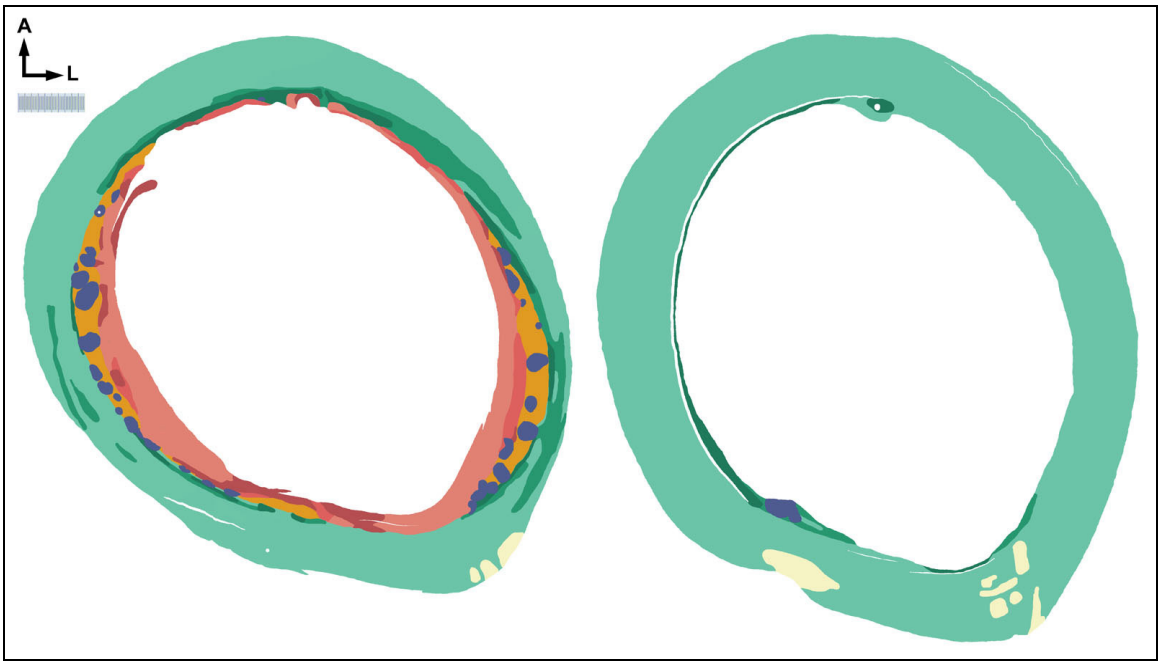


**Figure B.36: Callitrichid femora**.
*Callithrix geoffroyi* (MNHU 34381), *Callithrix* sp. (HC 28).

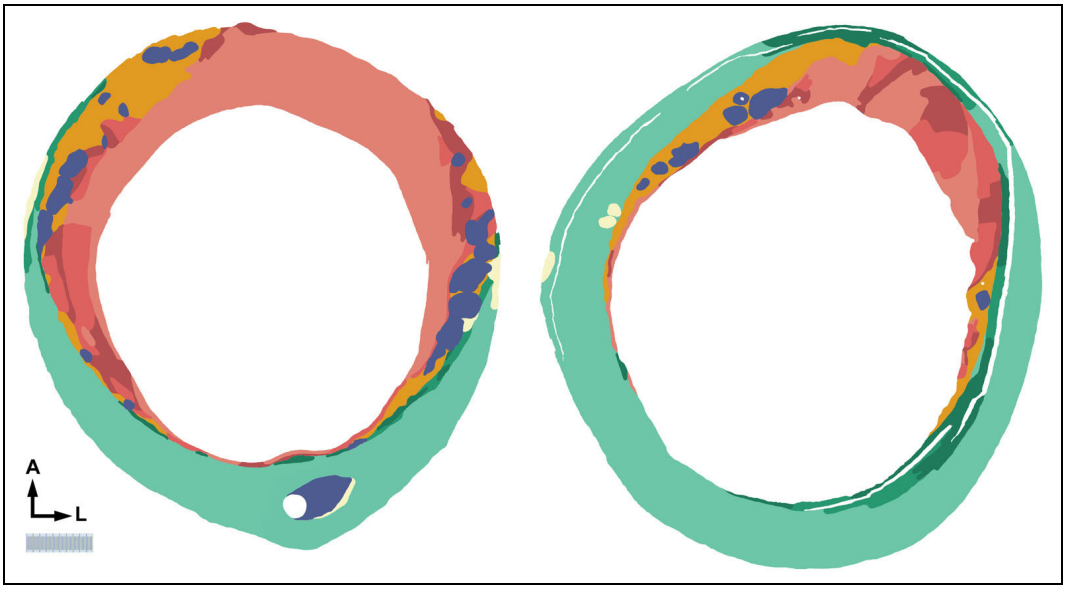


**Figure B.37: Callitrichid humeri**.
*Callithrix geoffroyi* (MNHU 34381), *Callithrix* sp. (HC 28).

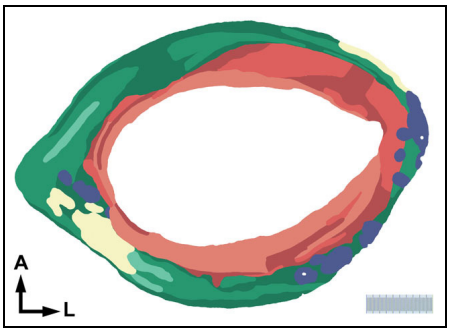


**Figure B.38: Callitrichid radius.**
*Callithrix geoffroyi* (MNHU 34381).

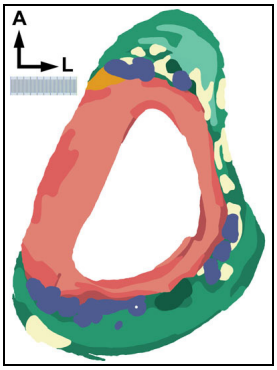


**Figure B.39: Callitrichid ulna.**
*Callithrix geoffroyi* (MNHU 34381).

## B.10 Cebidae

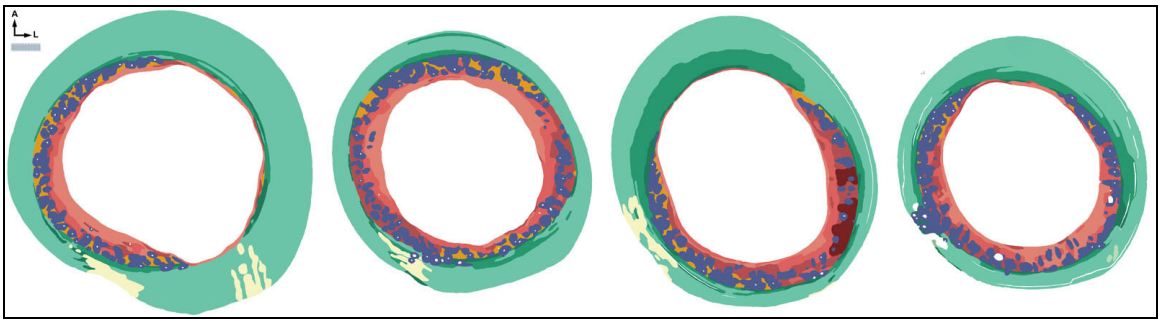

**Figure B.40: Cebid femora.**
*Saimiri* sp. (MNHU 85197), *Saimiri sciureus* (HC 12), *Saimiri* sp. (HC 13), *Saimiri* sp. (HC 14).

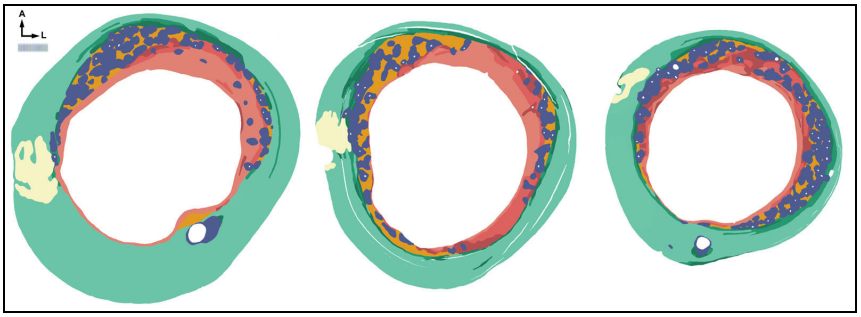

**Figure B.41: Cebid humeri**.
*Saimiri* sp. (MNHU 85197), *Saimiri* sp. (HC 13), *Saimiri* sp. (HC 14).

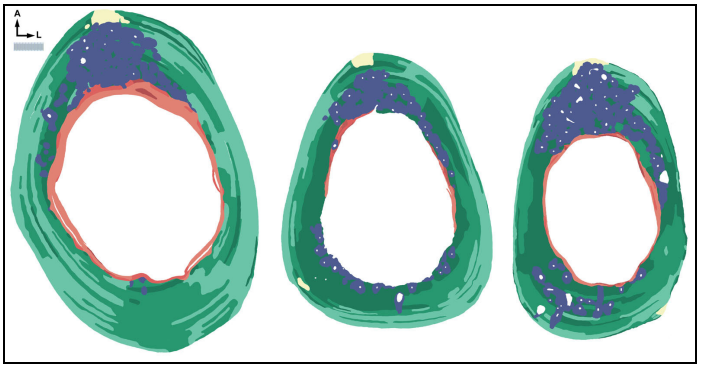

**Figure B.42: Cebid tibiae**.
*Saimiri* sp. (MNHU 85197), *Saimiri* sp. (HC 13), *Saimiri* sp. (HC 14).

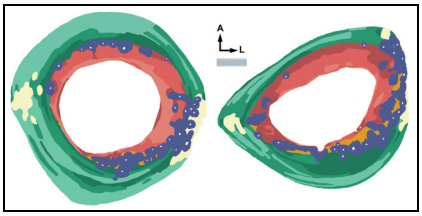

**Figure B.43: Cebid radii.**
*Saimiri* sp. (MNHU 85197), *Saimiri* sp. (HC 13).

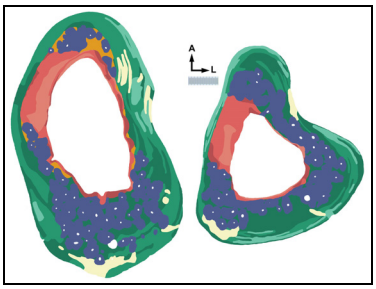

**Figure B.44: Cebid ulnae**.
*Saimiri* sp. (MNHU 85197), *Saimiri* sp. (HC 13).

## B.11 Atelidae

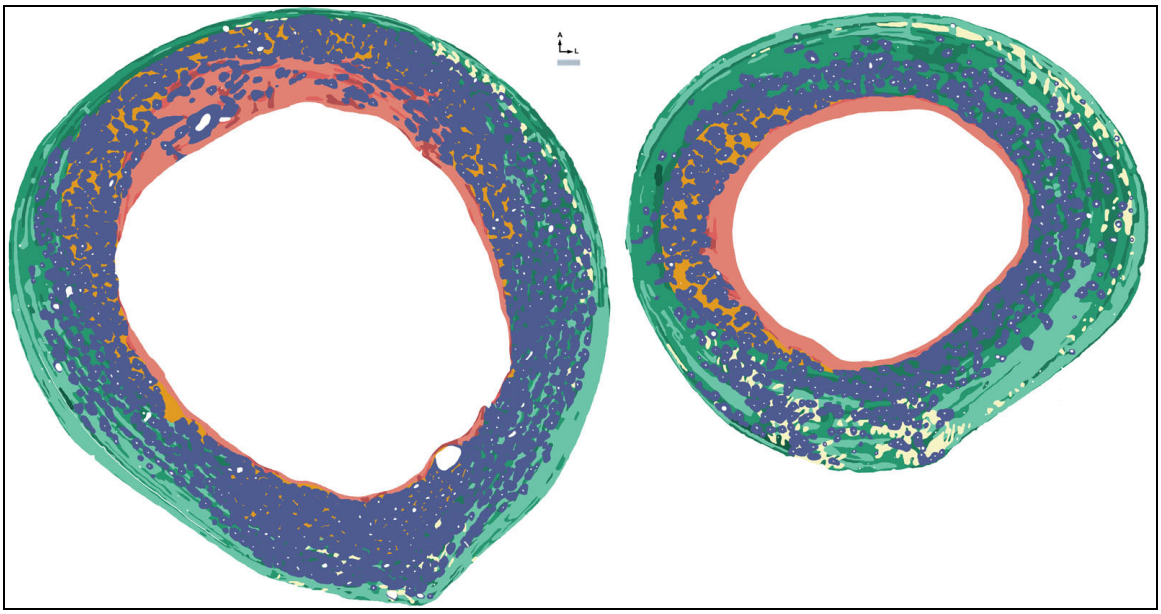

**Figure B.45: Atelid femora.**
*Ateles fusciceps* (FMNH 68811), *Ateles* sp. (MNHU 44079).

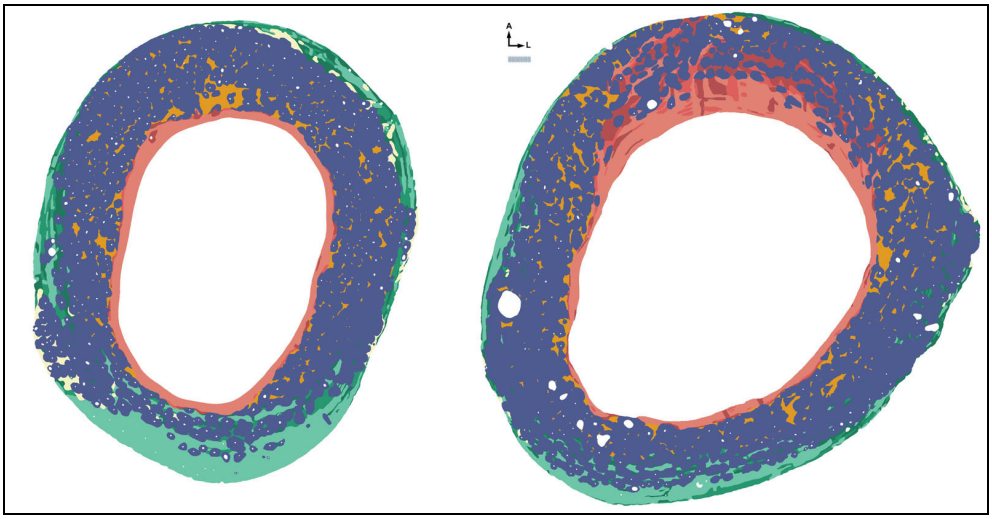

**Figure B.46: Atelid humeri**.
*Ateles fusciceps* (FMNH 68811), *Ateles* sp. (MNHU 44079).

# Appendix C

## Data Tables

| Taxon | Genus | Species | Spec. # | PHYLO | PB | TCA ($mm^2$) | %OST | %CCC | %SF | %P |
|---|---|---|---|---|---|---|---|---|---|---|
| Atelidae | Ateles | sp. | MNHU 44079 | PLAT | SUS | 59.1 | 39.8% | 2.2% | 4.7% | 45.5% |
| Atelidae | Ateles | fusciceps | FMNH 68811 | PLAT | SUS | 73.6 | 61.4% | 2.6% | 1.0% | 26.3% |
| Callitrichidae | Callithrix | sp. | MNHU 34381 | PLAT | AQ | 5.9 | 5.0% | 5.5% | 0.2% | 68.9% |
| Callitrichidae | Callithrix | geoffroyi | HC 28 | PLAT | AQ | 6.1 | 0.6% | 0.0% | 3.0% | 96.4% |
| Cheirogaleidae | Cheirogaleus | major | DUPC 2612 | STREP | AQ | 5.8 | 6.7% | 31.3% | 0.0% | 44.0% |
| Cheirogaleidae | Mirza | coquereli | DUPC 359 | STREP | AQ | 5.1 | 1.6% | 14.0% | 0.0% | 69.4% |
| Cheirogaleidae | Microcebus | murinus | DUPC 825 | STREP | AQ | 5.9 | 0.5% | 4.6% | 0.0% | 19.6% |
| Cheirogaleidae | Cheirogaleus | major | MCZ 44850 | STREP | AQ | 7.9 | 14.1% | 19.7% | 0.0% | 46.2% |
| Lesser Galago | Galago | senegalensis | MNHU 60601 | STREP | VCL | 8.2 | 0.4% | 17.4% | 0.0% | 65.5% |
| Lesser Galago | Galago | moholi | DUPC 2062 | STREP | VCL | 3.8 | 0.0% | 10.4% | 0.0% | 76.4% |
| Lesser Galago | Galago | moholi | DUPC 3173 | STREP | VCL | | | | | |
| Lesser Galago | Galagoides | demidovii | HC 25 | STREP | VCL | 2.2 | 1.2% | 14.6% | 0.0% | 65.2% |
| Indriidae | Propithecus | sp. | MNHU 44684 | STREP | VCL | 42.4 | 15.4% | 0.0% | 0.0% | 79.1% |
| Indriidae | Propithecus | sp. | MNHU 44685 | STREP | VCL | 35.1 | 1.1% | 0.5% | 0.3% | 94.9% |
| Indriidae | Indri | indri | HC 19 | STREP | VCL | 97.0 | 38.9% | 0.7% | 0.0% | 57.7% |
| Lemuridae | Lemur | sp. | HC 30 | STREP | AQ | 25.6 | 5.1% | 0.9% | 1.5% | 87.0% |
| Lemuridae | Varecia | variegata | MCZ 18740 | STREP | AQ | 36.0 | 13.9% | 1.6% | 0.1% | 76.7% |
| Lorisidae | Nycticebus | coucang | DUPC 1972 | STREP | SC | 20.1 | 10.3% | 11.7% | 3.1% | 69.9% |
| Lorisidae | Loris | tardigradus | DUPC 1964 | STREP | SC | 3.9 | 12.8% | 11.8% | 0.0% | 51.1% |
| Lorisidae | Perodicticus | potto | DUPC 930 | STREP | SC | 14.5 | 25.7% | 3.8% | 2.9% | 62.9% |
| Lorisidae | Nycticebus | coucang | HC 27 | STREP | SC | 14.2 | 11.5% | 11.3% | 1.4% | 43.0% |
| Lorisidae | Nycticebus | coucang | USNM 317187 | STREP | SC | 9.9 | 9.2% | 15.8% | 1.9% | 70.3% |
| Lorisidae | Nycticebus | coucang | MCZ 36116 | STREP | SC | 11.8 | 6.2% | 15.3% | 2.0% | 67.3% |
| Lorisidae | Nycticebus | coucang | MCZ 422 | STREP | SC | 13.8 | 12.0% | 14.5% | 3.1% | 67.0% |
| Greater Galago | Otolemur | crassicaudatus | DUPC 725 | STREP | VCL | 19.9 | 19.4% | 6.6% | 0.9% | 69.0% |
| Greater Galago | Otolemur | crassicaudatus | HC 31 | STREP | VCL | 18.6 | 7.4% | 5.6% | 1.0% | 71.3% |
| Greater Galago | Otolemur | crassicaudatus | USNM 365721 | STREP | VCL | 16.3 | 0.5% | 11.2% | 4.7% | 78.4% |
| Greater Galago | Otolemur | crassicaudatus | CT OA | STREP | VCL | 17.4 | 2.2% | 14.7% | 1.7% | 71.0% |
| Cebidae | Saimiri | sp. | MNHU 85197 | PLAT | AQ | 12.1 | 9.7% | 1.9% | 4.3% | 73.4% |
| Cebidae | Saimiri | sciureus | HC 12 | PLAT | AQ | 9.3 | 22.1% | 2.8% | 1.9% | 48.6% |
| Cebidae | Saimiri | sp. | HC 13 | PLAT | AQ | 10.0 | 12.7% | 1.6% | 2.9% | 64.7% |
| Cebidae | Saimiri | sp. | HC 14 | PLAT | AQ | 8.3 | 21.5% | 0.5% | 0.5% | 59.7% |
| Tarsiidae | Tarsius | spectrum | MNHU An11318 | TAR | VCL | 2.9 | 0.0% | 4.7% | 3.0% | 83.0% |
| Tarsiidae | Tarsius | syrichta | DUPC 81 | TAR | VCL | 2.8 | 0.7% | 2.4% | 3.1% | 84.9% |
| Tarsiidae | Tarsius | spectrum | HC 16 | TAR | VCL | 3.3 | 0.8% | 0.9% | 4.4% | 80.3% |
| Tarsiidae | Tarsius | sp. | HC 23 | TAR | VCL | 3.1 | 0.0% | 0.2% | 3.1% | 81.9% |

**Table C.1: Femur primary tissue type and intracortical remodeling data Part I**
PHYLO=phylogenetic status; PB=positional behavior; TCA=total cortical area; %OST=proportion of cortex that is composed of secondary osteons, relative to TCA; %CCC=proportion of cortex that is composed of compacted coarse cancellous tissue, relative to TCA; %SF= proportion of cortex that is Sharpey fibers, relative to TCA; %P= proportion of cortex that is composed of primary periosteal tissue, relative to TCA.

| %E | %P WOV | %P FFBL | %P SFBL | %P PF | %P HYB | %P LAM | %P FAST | %P LAM+HYB |
|---|---|---|---|---|---|---|---|---|
| 7.8% | 0.0% | 0.0% | 0.6% | 20.6% | 43.8% | 35.0% | 0.6% | 78.8% |
| 8.6% | 0.0% | 0.0% | 0.2% | 16.5% | 31.2% | 52.0% | 0.2% | 83.3% |
| 20.4% | 0.0% | 0.0% | 0.0% | 6.5% | 13.3% | 80.2% | 0.0% | 93.5% |
| 0.0% | 0.0% | 0.0% | 0.0% | 2.4% | 1.0% | 96.5% | 0.0% | 97.6% |
| 18.0% | 0.0% | 0.0% | 10.6% | 6.9% | 6.5% | 76.0% | 10.6% | 82.5% |
| 15.1% | 0.0% | 0.0% | 0.0% | 0.0% | 2.6% | 97.4% | 0.0% | 100.0% |
| 11.4% | 0.0% | 0.0% | 0.0% | 4.7% | 7.5% | 87.8% | 0.0% | 95.3% |
| 20.0% | 0.0% | 0.0% | 14.6% | 2.0% | 47.3% | 36.1% | 14.6% | 83.4% |
| 16.6% | 0.0% | 0.0% | 4.2% | 79.4% | 16.4% | 0.0% | 4.2% | 16.4% |
| 13.2% | 0.0% | 0.0% | 5.4% | 29.0% | 58.1% | 7.5% | 5.4% | 65.6% |
| | | | | | | | | |
| 19.0% | 0.0% | 0.0% | 0.0% | 43.3% | 30.8% | 25.9% | 0.0% | 56.7% |
| 5.5% | 0.0% | 9.5% | 45.2% | 1.5% | 25.7% | 18.1% | 54.7% | 43.8% |
| 3.2% | 0.0% | 23.4% | 14.6% | 20.2% | 24.5% | 17.3% | 38.0% | 41.8% |
| 2.7% | 0.0% | 0.0% | 59.0% | 16.5% | 17.0% | 7.4% | 59.0% | 24.5% |
| 5.5% | 0.0% | 8.5% | 29.9% | 1.8% | 8.2% | 51.5% | 38.4% | 59.8% |
| 7.7% | 0.0% | 3.4% | 52.6% | 3.3% | 18.8% | 21.9% | 56.0% | 40.7% |
| 5.0% | 0.0% | 0.0% | 17.9% | 35.5% | 29.3% | 17.4% | 17.9% | 46.7% |
| 24.3% | 0.0% | 0.0% | 0.0% | 61.8% | 14.1% | 24.1% | 0.0% | 38.2% |
| 4.7% | 1.1% | 23.9% | 0.9% | 25.7% | 39.7% | 8.6% | 26.0% | 48.3% |
| 32.7% | 0.0% | 1.3% | 1.0% | 21.6% | 56.3% | 19.8% | 2.2% | 76.1% |
| 2.9% | 0.0% | 0.6% | 0.0% | 72.1% | 8.3% | 18.9% | 0.6% | 27.2% |
| 9.2% | 0.0% | 1.6% | 4.8% | 41.5% | 30.9% | 21.3% | 6.4% | 52.1% |
| 3.4% | 0.0% | 12.1% | 8.0% | 38.7% | 40.4% | 0.8% | 20.0% | 41.3% |
| 4.1% | 0.0% | 3.4% | 7.6% | 33.6% | 41.5% | 14.0% | 11.0% | 55.5% |
| 14.7% | 0.0% | 0.0% | 0.0% | 23.9% | 18.6% | 57.5% | 0.0% | 76.1% |
| 5.2% | 0.0% | 8.7% | 4.1% | 22.9% | 25.8% | 38.5% | 12.8% | 64.3% |
| 10.5% | 0.0% | 2.3% | 13.9% | 12.9% | 56.1% | 14.9% | 16.2% | 71.0% |
| 10.6% | 0.0% | 0.0% | 0.0% | 2.6% | 6.8% | 90.6% | 0.0% | 97.4% |
| 24.6% | 0.0% | 0.0% | 0.0% | 4.6% | 12.6% | 82.8% | 0.0% | 95.4% |
| 18.1% | 0.0% | 0.0% | 0.0% | 6.0% | 28.0% | 66.0% | 0.0% | 94.0% |
| 17.8% | 0.0% | 0.0% | 0.0% | 4.3% | 18.2% | 77.5% | 0.0% | 95.7% |
| 9.3% | 0.0% | 0.0% | 0.0% | 73.6% | 25.1% | 1.3% | 0.0% | 26.4% |
| 8.8% | 0.0% | 0.0% | 0.0% | 84.4% | 15.6% | 0.0% | 0.0% | 15.6% |
| 13.7% | 0.0% | 0.0% | 0.0% | 65.5% | 28.7% | 5.8% | 0.0% | 34.5% |
| 14.8% | 0.0% | 0.0% | 0.0% | 66.5% | 14.7% | 18.8% | 0.0% | 33.5% |

**Table C.2: Femur primary tissue type and intracortical remodeling data Part II**
%E= proportion of cortex that is composed of primary endosteal tissue, relative to TCA. All the following values are for periosteal tissue type relative to periosteal primary bone area. %P WOV= woven-fibered; %P FFBL= fast fibrolamellar; %P SFBL=slow fibrolamellar; %P PF=parallel-fibered; %P HYB=hybrid; %P LAM=lamellar; %P FAST=woven-fibered+fast fibrolamellar+slow fibrolamellar; %P LAM+HYB=lamellar+hybrid.

| %E WOV | %E FFBL | %E SFBL | %E PF | %E HYB | %E LAM | %E FAST | %E LAM+HYB |
|---|---|---|---|---|---|---|---|
| 0.0% | 0.0% | 0.0% | 2.3% | 7.8% | 89.9% | 0.0% | 97.7% |
| 0.0% | 0.0% | 0.0% | 14.6% | 0.0% | 85.4% | 0.0% | 85.4% |
| 0.0% | 0.0% | 0.0% | 17.7% | 15.3% | 67.0% | 0.0% | 82.3% |
| 0.0% | 0.0% | 0.0% | 0.0% | 0.0% | 0.0% | 0.0% | 0.0% |
| 0.0% | 0.0% | 0.0% | 10.1% | 31.6% | 58.3% | 0.0% | 89.9% |
| 0.0% | 0.0% | 0.0% | 18.5% | 15.7% | 65.8% | 0.0% | 81.5% |
| 1.4% | 0.0% | 25.9% | 2.4% | 13.3% | 57.1% | 27.2% | 70.4% |
| 0.0% | 0.0% | 40.2% | 13.9% | 25.7% | 20.2% | 40.2% | 45.9% |
| 0.0% | 0.0% | 0.0% | 9.1% | 69.7% | 21.1% | 0.0% | 90.9% |
| 0.0% | 0.0% | 30.9% | 9.0% | 54.2% | 6.0% | 30.9% | 60.1% |
| | | | | | | | |
| 0.0% | 0.0% | 4.7% | 64.1% | 23.3% | 8.0% | 4.7% | 31.2% |
| 0.0% | 0.0% | 0.0% | 45.5% | 0.0% | 54.4% | 0.0% | 54.5% |
| 0.0% | 0.0% | 0.0% | 0.2% | 0.0% | 99.8% | 0.0% | 99.8% |
| 0.0% | 0.0% | 0.0% | 0.0% | 0.0% | 99.9% | 0.0% | 99.9% |
| 0.0% | 8.2% | 0.0% | 55.9% | 19.2% | 16.7% | 8.2% | 35.9% |
| 0.0% | 0.0% | 0.0% | 0.8% | 0.0% | 99.2% | 0.0% | 99.2% |
| 0.0% | 0.0% | 0.0% | 45.4% | 23.2% | 31.4% | 0.0% | 54.6% |
| 0.0% | 0.0% | 2.7% | 41.4% | 34.2% | 21.6% | 2.7% | 55.8% |
| 0.0% | 0.0% | 0.0% | 23.0% | 15.5% | 61.5% | 0.0% | 77.0% |
| 0.0% | 0.0% | 18.0% | 23.9% | 16.5% | 41.7% | 18.0% | 58.1% |
| 0.0% | 0.0% | 0.0% | 100.0% | 0.0% | 0.0% | 0.0% | 0.0% |
| 0.0% | 0.0% | 0.0% | 33.6% | 33.8% | 32.6% | 0.0% | 66.4% |
| 0.0% | 0.0% | 0.0% | 77.4% | 22.6% | 0.0% | 0.0% | 22.6% |
| 0.0% | 0.0% | 0.0% | 39.2% | 23.0% | 37.7% | 0.0% | 60.8% |
| 0.0% | 5.6% | 4.2% | 21.6% | 14.9% | 53.7% | 9.8% | 68.6% |
| 0.0% | 0.0% | 0.0% | 80.0% | 16.2% | 3.8% | 0.0% | 20.0% |
| 0.0% | 16.0% | 0.0% | 34.1% | 25.6% | 24.3% | 16.0% | 49.9% |
| 0.0% | 0.0% | 0.0% | 16.0% | 24.9% | 59.1% | 0.0% | 84.0% |
| 0.0% | 0.0% | 0.0% | 24.9% | 37.7% | 37.4% | 0.0% | 75.1% |
| 0.0% | 17.5% | 0.0% | 32.8% | 34.3% | 15.5% | 17.5% | 49.7% |
| 0.0% | 0.0% | 0.0% | 19.2% | 34.2% | 46.6% | 0.0% | 80.8% |
| 0.0% | 0.0% | 0.0% | 73.2% | 17.5% | 9.3% | 0.0% | 26.8% |
| 0.0% | 0.0% | 0.0% | 100.0% | 0.0% | 0.0% | 0.0% | 0.0% |
| 0.0% | 0.0% | 0.0% | 72.7% | 27.3% | 0.0% | 0.0% | 27.3% |
| 0.0% | 0.0% | 0.0% | 61.8% | 21.1% | 17.1% | 0.0% | 38.2% |

**Table C.3: Femur primary tissue type and intracortical remodeling data Part III**
All values are for endosteal tissue type relative to endosteal primary bone area. %E WOV= woven-fibered; %E FFBL= fast fibrolamellar; %E SFBL=slow fibrolamellar; %E PF=parallel-fibered; %E HYB=hybrid; %E LAM=lamellar; %E FAST=woven-fibered+fast fibrolamellar+slow fibrolamellar; %E LAM+HYB=lamellar+hybrid.

| Spec. # | P A Mean | P L Mean | P P Mean | P M Mean | TPA Mean | O A Mean | O L Mean | O P Mean | O M Mean | TOA Mean |
|---|---|---|---|---|---|---|---|---|---|---|
| MNHU 44079 | 18.4 | 18.5 | 19.9 | 18.4 | 18.6 | 21.3 | 22.0 | 23.7 | 21.8 | 22.3 |
| FMNH 68811 | 28.2 | 25.9 | 27.8 | 23.7 | 26.0 | 24.1 | 23.3 | 24.8 | 24.0 | 24.0 |
| MNHU 34381 | 19.0 | 17.8 | 20.2 | 19.3 | 19.2 | na | 21.4 | 20.9 | 25.0 | 23.1 |
| HC 28 | 22.2 | 18.7 | 20.9 | 20.9 | 20.7 | na | na | 22.0 | na | 22.0 |
| DUPC 2612 | 24.3 | 24.0 | 21.9 | 21.4 | 23.0 | 20.6 | 21.7 | 20.5 | 20.6 | 21.0 |
| DUPC 359 | 17.9 | 26.1 | 22.9 | 21.1 | 21.4 | 22.9 | 21.1 | 28.6 | na | 23.3 |
| DUPC 825 | 19.2 | 21.6 | 20.0 | 19.6 | 20.2 | na | na | 24.4 | na | 24.4 |
| MCZ 44850 | 21.4 | 20.4 | 21.0 | 19.2 | 20.9 | 25.4 | 25.1 | 26.2 | 26.3 | 25.9 |
| MNHU 60601 | 16.2 | 20.0 | 16.1 | 15.7 | 16.2 | 23.2 | na | 21.2 | 22.3 | 23.2 |
| DUPC 2062 | 15.7 | 16.1 | 16.1 | 16.2 | 16.0 | na | na | na | na | na |
| DUPC 3173 | | | | | | | | | | |
| HC 25 | 16.3 | 21.3 | 17.1 | 17.1 | 17.7 | 23.3 | 27.0 | 18.3 | 18.0 | 21.6 |
| MNHU 44684 | 20.2 | 18.0 | 18.4 | 17.7 | 19.1 | 23.4 | 22.8 | 21.6 | 24.1 | 22.2 |
| MNHU 44685 | 17.1 | 17.1 | 16.9 | 17.0 | 17.0 | 19.6 | 18.6 | 18.1 | 18.2 | 18.3 |
| HC 19 | 24.2 | 23.7 | 22.6 | 23.1 | 23.6 | 29.5 | 29.0 | 28.0 | 26.5 | 28.1 |
| HC 30 | 32.5 | 31.6 | 40.2 | 32.8 | 34.4 | 27.8 | 31.8 | na | na | 29.9 |
| MCZ 18740 | 22.5 | 22.4 | 23.8 | 21.2 | 22.6 | 28.3 | 30.1 | 35.4 | 29.4 | 30.1 |
| DUPC 1972 | 16.6 | 16.9 | 16.7 | 16.7 | 16.8 | 21.1 | 21.2 | 22.9 | 24.9 | 22.3 |
| DUPC 1964 | 17.1 | 17.9 | 19.6 | 18.5 | 18.5 | 20.2 | 21.3 | 20.7 | 20.1 | 20.5 |
| DUPC 930 | 9.4 | 10.8 | 9.4 | 9.4 | 17.5 | 17.8 | 18.7 | 18.1 | 18.2 | 18.2 |
| HC 27 | | | | | | | | | | |
| USNM 317187 | | | | | | | | | | |
| MCZ 36116 | 20.6 | 21.3 | 21.1 | 20.4 | 21.2 | 34.9 | 47.3 | 44.6 | 32.9 | 40.8 |
| MCZ 422 | 19.9 | 23.6 | 20.8 | 20.1 | 21.2 | 22.1 | 23.4 | 26.5 | 27.3 | 24.8 |
| DUPC 725 | 16.6 | 16.3 | 16.6 | 16.6 | 16.6 | 17.8 | 19.1 | 18.3 | 18.2 | 18.3 |
| HC 31 | 16.3 | 16.6 | 16.5 | 16.6 | 16.5 | 20.7 | 18.2 | 20.9 | 23.5 | 20.5 |
| USNM 365721 | 16.0 | 17.3 | 16.7 | 16.4 | 16.6 | 18.1 | 21.0 | na | 20.5 | 20.6 |
| CT OA | 17.3 | 17.1 | 18.1 | 16.9 | 17.3 | 20.0 | 24.2 | 20.9 | 25.6 | 22.0 |
| MNHU 85197 | 30.2 | 28.8 | 29.6 | 29.8 | 29.6 | 37.4 | na | 33.6 | 33.7 | 34.4 |
| HC 12 | 27.2 | 30.6 | 29.4 | 28.3 | 29.0 | 29.7 | 31.0 | 26.7 | 30.9 | 29.6 |
| HC 13 | 22.8 | 26.4 | 25.6 | 22.8 | 23.9 | 27.8 | 23.7 | 23.4 | 25.6 | 24.0 |
| HC 14 | 21.8 | 19.5 | 21.0 | 19.2 | 20.7 | 20.1 | 20.0 | 20.9 | 20.2 | 20.3 |
| MNHU An11318 | 15.7 | 16.0 | 16.0 | 15.8 | 15.9 | na | na | na | na | na |
| DUPC 81 | 16.2 | 17.6 | 17.0 | 17.5 | 17.0 | na | 20.0 | na | na | 20.0 |
| HC 16 | 15.8 | 16.5 | 16.5 | 16.3 | 16.3 | 18.6 | na | 19.8 | na | 19.9 |
| HC 23 | 15.8 | 17.5 | 16.4 | 16.0 | 16.3 | na | na | na | na | na |

**Table C.4: Femur collagen fiber orientation data Part I**

P A Mean=mean gray value for periosteal primary tissue in the anterior quadrant of the cortex; P L Mean=same as previous, for lateral quadrant; P P Mean= same as previous, for posterior quadrant; P M Mean= same as previous, for medial quadrant; TPA Mean=mean gray value for periosteal primary tissue for all quadrants combined. O A Mean=mean gray value for secondary remodeled tissue in the anterior quadrant of the cortex; O L Mean=same as previous, for lateral quadrant; O P Mean= same as previous, for posterior quadrant; O M Mean= same as previous, for medial quadrant; TOA Mean=mean gray value for secondary osteonal tissue for all quadrants combined.

| FAST Mean | PF Mean | HYB Mean | LAM Mean | LAM+HYB Mean |
|---|---|---|---|---|
| 20.0 | 18.1 | 18.1 | 19.8 | 18.8 |
| 26.5 | 21.1 | 21.8 | 29.9 | 26.9 |
| 0.0 | 18.3 | 16.8 | 19.6 | 19.2 |
| 0.0 | 17.3 | 18.0 | 20.9 | 20.8 |
| 21.0 | 17.3 | 19.2 | 23.5 | 23.1 |
| 0.0 | 0.0 | 18.5 | 21.0 | 21.0 |
| 0.0 | 20.9 | 18.6 | 19.7 | 19.6 |
| 22.2 | 21.8 | 19.5 | 22.0 | 20.7 |
| 17.1 | 16.1 | 16.6 | 0.0 | 16.6 |
| 16.6 | 15.6 | 15.8 | 17.5 | 16.0 |
| | | | | |
| 0.0 | 16.2 | 17.0 | 20.8 | 18.5 |
| 18.7 | 17.6 | 18.1 | 22.0 | 19.8 |
| 17.5 | 16.8 | 16.4 | 17.3 | 16.8 |
| 23.7 | 21.3 | 22.2 | 34.5 | 25.2 |
| 34.7 | 25.2 | 24.8 | 36.2 | 34.5 |
| 21.4 | 18.7 | 18.9 | 29.2 | 24.5 |
| 17.6 | 15.7 | 16.3 | 18.6 | 17.2 |
| 0.0 | 17.4 | 16.6 | 22.0 | 19.7 |
| 20.5 | 16.8 | 15.8 | 17.4 | 16.1 |
| | | | | |
| | | | | |
| 26.2 | 20.1 | 20.1 | 23.5 | 21.5 |
| 24.3 | 20.3 | 20.7 | 21.7 | 20.7 |
| 17.4 | 16.5 | 16.2 | 17.2 | 16.4 |
| 0.0 | 16.4 | 16.4 | 16.6 | 16.5 |
| 18.3 | 16.1 | 16.4 | 16.5 | 16.5 |
| 18.5 | 17.9 | 16.8 | 17.2 | 16.9 |
| 0.0 | 27.2 | 29.7 | 29.9 | 29.7 |
| 0.0 | 24.4 | 22.5 | 30.2 | 29.3 |
| 0.0 | 18.4 | 19.1 | 26.4 | 24.3 |
| 0.0 | 17.7 | 18.3 | 21.5 | 20.9 |
| 0.0 | 16.0 | 15.6 | 16.3 | 15.7 |
| 0.0 | 16.8 | 17.9 | 0.0 | 17.9 |
| 0.0 | 16.1 | 16.5 | 17.2 | 16.6 |
| 0.0 | 16.0 | 16.1 | 17.6 | 16.9 |

**Table C.5: Femur collagen fiber orientation data Part II**
FAST Mean=mean gray value for periosteal FAST tissue in all quadrants combined; PF Mean=same as previous for periosteal PF tissue; HYB Mean=same as previous for periosteal HYB tissue; LAM=same as previous for periosteal LAM tissue; LAM+HYB Mean=same as previous for periosteal LAM+HYB tissue.

| Taxon | Genus | Species | Spec. | PHYLO | PB | TCA ($mm^2$) | %HAV | %CCC | %SF | %P |
|---|---|---|---|---|---|---|---|---|---|---|
| Atelidae | Ateles | sp. | MNHU 44079 | PLAT | SUS | 43.4 | 67.5% | 3.3% | 1.8% | 19.1% |
| Atelidae | Ateles | fusciceps | FMNH 68811 | PLAT | SUS | 53.5 | 70.5% | 3.9% | 0.3% | 9.7% |
| Callitrichidae | Callithrix | sp. | MNHU 34381 | PLAT | AQ | 5.5 | 9.3% | 8.7% | 1.2% | 35.1% |
| Callitrichidae | Callithrix | geoffroyi | HC 28 | PLAT | AQ | 5.4 | 2.6% | 7.3% | 0.6% | 69.6% |
| Cheirogaleidae | Cheirogaleus | major | DUPC 2612 | STREP | AQ | 4.1 | 8.6% | 19.3% | 0.0% | 36.6% |
| Cheirogaleidae | Mirza | coquereli | DUPC 359 | STREP | AQ | 3.7 | 11.3% | 17.8% | 0.0% | 42.5% |
| Cheirogaleidae | Microcebus | murinus | DUPC 825 | STREP | AQ | 1.5 | 0.8% | 7.8% | 0.0% | 42.2% |
| Cheirogaleidae | Cheirogaleus | major | MCZ 44850 | STREP | AQ | 6.2 | 14.5% | 14.8% | 0.0% | 28.0% |
| Lesser Galago | Galago | senegalensis | MNHU 60601 | STREP | VCL | 5.6 | 3.0% | 0.0% | 0.0% | 65.4% |
| Lesser Galago | Galago | moholi | DUPC 2062 | STREP | VCL | 2.1 | 4.8% | 10.0% | 0.0% | 59.5% |
| Lesser Galago | Galago | moholi | DUPC 3173 | STREP | VCL | 1.5 | 2.5% | 6.1% | 0.0% | 62.3% |
| Lesser Galago | Galagoides | demidovii | HC 25 | STREP | VCL | 1.3 | 0.5% | 6.4% | 0.0% | 59.9% |
| Indriidae | Propithecus | sp. | MNHU 44684 | STREP | VCL | 17.4 | 21.8% | 2.4% | 1.4% | 66.3% |
| Indriidae | Propithecus | sp. | MNHU 44685 | STREP | VCL | 14.6 | 21.1% | 2.5% | 0.0% | 66.3% |
| Indriidae | Indri | indri | HC 19 | STREP | VCL | 42.2 | 57.5% | 9.5% | 0.3% | 28.0% |
| Lemuridae | Lemur | sp. | HC 30 | STREP | AQ | 15.3 | 18.3% | 7.7% | 1.6% | 61.9% |
| Lemuridae | Varecia | variegata | MCZ 18740 | STREP | AQ | 25.2 | 30.0% | 4.8% | 0.7% | 47.1% |
| Lorisidae | Nycticebus | coucang | DUPC 1972 | STREP | SC | 17.9 | 26.8% | 15.7% | 0.5% | 45.6% |
| Lorisidae | Loris | tardigradus | DUPC 1964 | STREP | SC | 3.4 | 7.3% | 12.5% | 0.0% | 30.2% |
| Lorisidae | Perodicticus | potto | DUPC 930 | STREP | SC | 12.5 | 46.9% | 16.5% | 3.0% | 24.6% |
| Lorisidae | Nycticebus | coucang | HC 27 | STREP | SC | 12.8 | 36.3% | 15.9% | 2.8% | 28.5% |
| Lorisidae | Nycticebus | coucang | USNM 317187 | STREP | SC | 8.9 | 24.7% | 27.8% | 8.4% | 37.7% |
| Lorisidae | Nycticebus | coucang | MCZ 36116 | STREP | SC | 11.3 | 17.5% | 17.6% | 5.1% | 49.7% |
| Lorisidae | Nycticebus | coucang | MCZ 422 | STREP | SC | 13.0 | 20.7% | 13.7% | 5.3% | 55.8% |
| Greater Galago | Otolemur | crassicaudatus | DUPC 725 | STREP | VCL | 13.8 | 16.5% | 18.5% | 2.1% | 46.3% |
| Greater Galago | Otolemur | crassicaudatus | HC 31 | STREP | VCL | 14.3 | 17.1% | 17.2% | 1.4% | 47.2% |
| Greater Galago | Otolemur | crassicaudatus | USNM 365721 | STREP | VCL | 12.3 | 5.1% | 15.5% | 8.4% | 60.4% |
| Greater Galago | Otolemur | crassicaudatus | CT OA | STREP | VCL | 15.3 | 5.3% | 11.5% | 4.3% | 50.4% |
| Cebidae | Saimiri | sp. | MNHU 85197 | PLAT | AQ | 11.1 | 13.0% | 2.5% | 5.0% | 63.9% |
| Cebidae | Saimiri | sciureus | HC 12 | PLAT | AQ | | | | | |
| Cebidae | Saimiri | sp. | HC 13 | PLAT | AQ | 8.0 | 14.6% | 8.3% | 3.8% | 52.5% |
| Cebidae | Saimiri | sp. | HC 14 | PLAT | AQ | 6.7 | 24.5% | 2.8% | 2.1% | 53.9% |
| Tarsiidae | Tarsius | spectrum | MNHU An11318 | TAR | VCL | 2.0 | 15.0% | 7.3% | 0.6% | 46.6% |
| Tarsiidae | Tarsius | syrichta | DUPC 81 | TAR | VCL | 1.6 | 1.2% | 2.2% | 0.0% | 71.7% |
| Tarsiidae | Tarsius | spectrum | HC 16 | TAR | VCL | 1.9 | 14.2% | 7.0% | 0.0% | 49.1% |
| Tarsiidae | Tarsius | sp. | HC 23 | TAR | VCL | 2.0 | 1.2% | 7.5% | 0.0% | 46.2% |

**Table C.6: Humerus primary tissue type and intracortical remodeling data Part I**
As per Table C.1.

| %E | %P WOV | %P FFBL | %P SFBL | %P PF | %P HYB | %P LAM | %P FAST | %P LAM+HYB |
|---|---|---|---|---|---|---|---|---|
| 8.4% | 0.0% | 0.0% | 0.0% | 14.3% | 18.1% | 67.6% | 0.0% | 85.7% |
| 15.6% | 0.0% | 0.0% | 0.0% | 23.3% | 15.9% | 60.8% | 0.0% | 76.7% |
| 45.7% | 0.0% | 0.0% | 0.0% | 4.4% | 6.0% | 89.6% | 0.0% | 95.6% |
| 19.9% | 0.0% | 0.0% | 0.0% | 11.6% | 6.1% | 82.3% | 0.0% | 88.4% |
| 35.5% | 0.0% | 0.0% | 0.0% | 4.7% | 5.8% | 89.4% | 0.0% | 95.3% |
| 28.4% | 0.0% | 0.0% | 0.0% | 0.0% | 5.3% | 94.7% | 0.0% | 100.0% |
| 49.3% | 0.0% | 0.0% | 0.0% | 0.0% | 0.8% | 99.2% | 0.0% | 100.0% |
| 42.6% | 0.0% | 0.0% | 0.0% | 10.7% | 47.3% | 42.1% | 0.0% | 89.3% |
| 31.6% | 0.0% | 0.0% | 11.4% | 6.7% | 14.9% | 67.0% | 11.4% | 81.9% |
| 25.7% | 0.0% | 0.0% | 0.0% | 14.8% | 19.6% | 65.7% | 0.0% | 85.2% |
| 29.1% | 0.0% | 0.0% | 0.0% | 2.8% | 36.4% | 60.7% | 0.0% | 97.2% |
| 33.1% | 2.2% | 0.0% | 0.0% | 0.0% | 8.3% | 89.5% | 2.2% | 97.8% |
| 8.0% | 0.0% | 1.2% | 16.9% | 1.5% | 11.2% | 69.1% | 18.1% | 80.3% |
| 10.1% | 0.0% | 0.0% | 5.7% | 1.7% | 6.6% | 86.1% | 5.7% | 92.6% |
| 4.6% | 0.0% | 0.0% | 7.9% | 20.9% | 22.5% | 48.7% | 7.9% | 71.2% |
| 10.6% | 0.1% | 1.1% | 0.9% | 1.0% | 3.7% | 93.2% | 2.1% | 96.9% |
| 17.4% | 0.0% | 5.9% | 20.1% | 2.6% | 17.2% | 54.2% | 26.0% | 71.4% |
| 11.4% | 0.3% | 8.9% | 5.7% | 16.1% | 34.0% | 35.1% | 14.9% | 69.1% |
| 50.0% | 0.0% | 0.0% | 0.0% | 0.0% | 71.0% | 29.0% | 0.0% | 100.0% |
| 9.1% | 0.4% | 0.0% | 0.0% | 40.8% | 33.5% | 25.3% | 0.4% | 58.8% |
| 16.4% | 0.0% | 0.0% | 0.0% | 37.8% | 34.9% | 27.2% | 0.0% | 62.2% |
| 1.4% | 0.0% | 0.0% | 0.4% | 14.7% | 17.9% | 67.0% | 0.4% | 84.9% |
| 10.0% | 0.0% | 0.0% | 0.0% | 38.1% | 12.0% | 49.8% | 0.0% | 61.9% |
| 4.5% | 0.0% | 7.8% | 15.2% | 20.4% | 39.6% | 16.9% | 23.0% | 56.6% |
| 16.6% | 0.0% | 0.0% | 0.0% | 6.3% | 30.4% | 63.4% | 0.0% | 93.7% |
| 17.1% | 0.0% | 1.2% | 1.0% | 7.7% | 12.7% | 77.4% | 2.2% | 90.1% |
| 10.6% | 0.0% | 0.7% | 4.4% | 8.1% | 17.5% | 69.2% | 5.1% | 86.8% |
| 28.5% | 0.0% | 3.7% | 12.2% | 7.5% | 13.6% | 63.0% | 15.9% | 76.6% |
| 15.6% | 0.0% | 0.0% | 0.0% | 3.7% | 3.3% | 92.9% | 0.0% | 96.3% |
| | | | | | | | | |
| 20.8% | 0.0% | 0.0% | 0.0% | 11.3% | 7.2% | 81.5% | 0.0% | 88.7% |
| 16.7% | -0.0% | 0.0% | 0.0% | 4.3% | 13.3% | 82.3% | 0.0% | 95.7% |
| 30.5% | 9.3% | 0.0% | 0.0% | 17.5% | 11.5% | 61.7% | 9.3% | 73.3% |
| 25.0% | 0.0% | 0.0% | 0.0% | 45.2% | 33.9% | 20.9% | 0.0% | 54.8% |
| 29.8% | 0.0% | 0.0% | 0.0% | 32.6% | 14.1% | 53.3% | 0.0% | 67.4% |
| 45.0% | 0.0% | 0.0% | 0.0% | 12.3% | 11.8% | 75.9% | 0.0% | 87.7% |

**Table C.7: Humerus primary tissue type and intracortical remodeling data Part II**
As per Table C.2.

| %E WOV | %E FFBL | %E SFBL | %E PF | %E HYB | %E LAM | %E FAST | %E LAM+HYB |
|---|---|---|---|---|---|---|---|
| 0.0% | 0.0% | 0.0% | 6.8% | 7.9% | 85.3% | 0.0% | 93.2% |
| 0.0% | 0.0% | 0.0% | 24.3% | 14.7% | 61.0% | 0.0% | 75.7% |
| 0.0% | 0.0% | 0.0% | 12.2% | 15.4% | 72.3% | 0.0% | 87.8% |
| 0.0% | 0.0% | 0.0% | 24.2% | 30.1% | 45.6% | 0.0% | 75.8% |
| 0.0% | 0.0% | 0.0% | 13.5% | 47.2% | 39.4% | 0.0% | 86.5% |
| 0.0% | 0.0% | 0.0% | 43.4% | 30.8% | 25.8% | 0.0% | 56.6% |
| 0.0% | 0.0% | 0.0% | 22.4% | 40.4% | 37.2% | 0.0% | 77.6% |
| 0.0% | 0.0% | 0.0% | 12.1% | 58.4% | 29.5% | 0.0% | 87.9% |
| 0.0% | 0.0% | 4.5% | 13.5% | 43.2% | 38.9% | 4.5% | 82.0% |
| 0.0% | 3.0% | 6.0% | 19.2% | 71.8% | 0.0% | 9.0% | 71.8% |
| 0.0% | 0.0% | 0.0% | 17.7% | 61.6% | 20.7% | 0.0% | 82.3% |
| 2.8% | 0.0% | 0.0% | 15.1% | 25.5% | 56.6% | 2.8% | 82.1% |
| 0.0% | 0.0% | 2.5% | 15.5% | 21.0% | 61.0% | 2.5% | 82.0% |
| 0.0% | 0.0% | 0.0% | 13.7% | 11.0% | 75.3% | 0.0% | 86.2% |
| 0.0% | 0.0% | 0.0% | 2.3% | 9.1% | 88.7% | 0.0% | 97.7% |
| 0.0% | 0.0% | 0.0% | 59.6% | 24.9% | 15.4% | 0.0% | 40.4% |
| 0.0% | 0.0% | 0.0% | 12.7% | 28.8% | 58.6% | 0.0% | 87.3% |
| 0.0% | 0.0% | 0.0% | 34.4% | 19.9% | 45.7% | 0.0% | 65.6% |
| 0.0% | 0.0% | 1.7% | 61.4% | 0.0% | 36.9% | 1.7% | 36.9% |
| 0.0% | 0.0% | 0.0% | 31.9% | 23.1% | 45.0% | 0.0% | 68.1% |
| 0.0% | 0.0% | 0.0% | 23.2% | 34.7% | 42.2% | 0.0% | 76.8% |
| 0.0% | 0.0% | 0.0% | 100.0% | 0.0% | 0.0% | 0.0% | 0.0% |
| 0.0% | 0.0% | 0.0% | 41.5% | 27.7% | 30.8% | 0.0% | 58.5% |
| 0.0% | 0.0% | 0.0% | 61.4% | 14.7% | 23.9% | 0.0% | 38.6% |
| 0.0% | 0.0% | 0.0% | 36.1% | 40.4% | 23.5% | 0.0% | 63.9% |
| 0.0% | 0.0% | 0.0% | 20.8% | 12.0% | 67.2% | 0.0% | 79.2% |
| 0.0% | 5.6% | 0.0% | 49.9% | 30.9% | 13.6% | 5.6% | 44.5% |
| 0.0% | 0.0% | 0.0% | 39.9% | 15.2% | 44.9% | 0.0% | 60.1% |
| 0.0% | 0.0% | 0.0% | 5.5% | 14.0% | 80.5% | 0.0% | 94.5% |
| | | | | | | | |
| 0.0% | 0.0% | 0.0% | 16.1% | 33.1% | 50.8% | 0.0% | 83.9% |
| 0.0% | 0.0% | 0.0% | 34.0% | 31.9% | 34.1% | 0.0% | 66.0% |
| 0.0% | 0.0% | 0.0% | 73.0% | 16.2% | 10.8% | 0.0% | 27.0% |
| 0.0% | 0.0% | 0.0% | 58.0% | 34.0% | 8.1% | 0.0% | 42.0% |
| 0.0% | 0.0% | 0.0% | 78.0% | 7.5% | 14.5% | 0.0% | 22.0% |
| 0.0% | 0.0% | 0.0% | 54.0% | 34.2% | 11.8% | 0.0% | 46.0% |

**Table C.8: Humerus primary tissue type and intracortical remodeling data Part III**
As per Table C.3.

| Spec. # | P A Mean | P L Mean | P P Mean | P M Mean | TPA Mean | O A Mean | O L Mean | O P Mean | O M Mean | TOA Mean |
|---|---|---|---|---|---|---|---|---|---|---|
| MNHU 44079 | 20.5 | 19.7 | 20.0 | 19.4 | 19.6 | 24.4 | 23.8 | 22.6 | 23.0 | 23.4 |
| FMNH 68811 | 31.3 | 30.8 | 30.2 | 40.0 | 33.1 | 26.8 | 25.3 | 28.4 | 27.1 | 26.7 |
| MNHU 34381 | 15.0 | 21.7 | 24.1 | 23.6 | 23.6 | 23.0 | 20.1 | 28.2 | 25.5 | 23.2 |
| HC 28 | 18.8 | 17.4 | 24.0 | 19.0 | 20.5 | 24.1 | 26.3 | na | 21.1 | 23.9 |
| DUPC 2612 | 24.5 | 35.4 | 31.5 | 27.1 | 30.5 | 19.5 | 20.8 | 22.0 | 20.0 | 19.8 |
| DUPC 359 | 31.2 | 44.3 | 34.3 | 32.7 | 35.8 | 26.1 | 32.7 | na | 19.7 | 27.7 |
| DUPC 825 | 24.1 | 28.5 | 31.2 | 23.4 | 28.4 | 19.4 | na | na | 24.3 | 27.4 |
| MCZ 44850 | 23.9 | 26.2 | 25.6 | 19.7 | 24.2 | 32.2 | 32.4 | 48.4 | 30.4 | 34.5 |
| MNHU 60601 | 22.6 | 27.1 | 25.1 | 20.9 | 24.2 | 26.8 | na | 23.6 | na | 24.3 |
| DUPC 2062 | 18.4 | 18.5 | 16.6 | 17.8 | 17.6 | 18.7 | na | na | 24.7 | 18.1 |
| DUPC 3173 | 22.4 | 21.8 | 16.7 | 18.2 | 18.7 | 19.5 | na | na | 18.7 | 18.7 |
| HC 25 | 26.8 | 24.9 | 25.3 | 22.7 | 24.8 | 11.3 | na | na | 23.6 | 34.3 |
| MNHU 44684 | 22.6 | 20.3 | 21.6 | 20.0 | 20.9 | 18.7 | 18.6 | 19.3 | 18.3 | 18.7 |
| MNHU 44685 | 21.3 | 25.7 | 23.2 | 24.7 | 24.1 | 19.6 | 22.8 | 21.3 | 19.9 | 20.3 |
| HC 19 | 33.4 | 33.4 | 36.3 | 28.2 | 33.6 | 28.9 | 29.0 | 31.5 | 27.8 | 28.8 |
| HC 30 | 34.7 | 51.6 | 49.9 | 42.1 | 46.4 | 29.9 | 28.7 | 31.1 | 27.5 | 28.9 |
| MCZ 18740 | 25.4 | 29.0 | 31.3 | 25.9 | 28.8 | 24.9 | 25.3 | 29.7 | 28.8 | 22.7 |
| DUPC 1972 | 23.4 | 20.9 | 19.8 | 18.9 | 20.9 | 24.4 | 25.3 | 27.5 | 23.7 | 24.7 |
| DUPC 1964 | 18.4 | 18.7 | 20.1 | 21.5 | 19.7 | 20.0 | 20.5 | na | 21.4 | 20.5 |
| DUPC 930 | 17.6 | 19.7 | 16.8 | 17.9 | 18.1 | 17.7 | 18.1 | 17.3 | 17.8 | 17.3 |
| HC 27 | | | | | | | | | | |
| USNM 317187 | | | | | | | | | | |
| MCZ 36116 | 29.0 | 24.2 | 24.5 | 23.1 | 25.3 | 23.9 | 23.2 | 26.5 | 26.4 | 24.5 |
| MCZ 422 | 25.5 | 23.3 | 26.8 | 24.4 | 25.3 | 26.6 | 29.1 | 28.6 | 29.1 | 27.8 |
| DUPC 725 | 17.4 | 18.2 | 17.5 | 17.3 | 17.7 | 21.7 | 20.7 | 19.9 | 20.6 | 20.5 |
| HC 31 | 24.7 | 21.9 | 21.4 | 22.1 | 22.2 | 18.6 | 19.3 | 19.8 | 18.4 | 18.5 |
| USNM 365721 | 21.7 | 20.2 | 22.2 | 19.6 | 20.9 | 20.3 | na | na | 19.6 | 19.6 |
| CT OA | 20.4 | 18.2 | 17.5 | 18.6 | 18.4 | 19.4 | 19.8 | na | 20.8 | 19.5 |
| MNHU 85197 | 21.7 | 25.0 | 26.6 | 25.9 | 25.6 | 25.1 | 23.9 | 45.0 | 25.4 | 26.3 |
| HC 12 | | | | | | | | | | |
| HC 13 | 20.1 | 26.3 | 27.4 | 23.7 | 25.1 | 21.8 | 21.8 | 21.0 | 21.1 | 21.2 |
| HC 14 | 19.7 | 19.3 | 22.1 | 20.8 | 20.9 | 18.9 | 19.0 | 24.2 | 18.8 | 19.2 |
| MNHU An11318 | 21.7 | 19.7 | 23.9 | 19.6 | 21.7 | 30.0 | na | 39.1 | 21.5 | 30.0 |
| DUPC 81 | 20.2 | 25.1 | 17.8 | 17.7 | 20.3 | 27.7 | na | na | na | 32.0 |
| HC 16 | 17.4 | 17.6 | 19.6 | 16.1 | 18.0 | 19.4 | na | 20.9 | 21.7 | 20.8 |
| HC 23 | 16.9 | 41.6 | 22.2 | 18.2 | 28.5 | 17.4 | na | na | 19.6 | 20.0 |

**Table C.9: Humerus collagen fiber orientation data part I**
As per Table C.4.

| FAST Mean | PF Mean | HYB Mean | LAM Mean | LAM+HYB Mean |
|---|---|---|---|---|
| 0.0 | 18.6 | 19.1 | 19.6 | 19.5 |
| 0.0 | 28.2 | 31.0 | 35.3 | 34.4 |
| 0.0 | 18.8 | 19.7 | 24.0 | 23.7 |
| 0.0 | 18.8 | 19.5 | 20.7 | 20.7 |
| 0.0 | 20.5 | 19.5 | 31.4 | 30.6 |
| 0.0 | 0.0 | 24.8 | 35.6 | 35.0 |
| 0.0 | 0.0 | 23.0 | 27.3 | 27.3 |
| 0.0 | 22.9 | 22.2 | 26.6 | 24.3 |
| 19.6 | 20.3 | 20.1 | 26.4 | 25.2 |
| 0.0 | 17.4 | 16.2 | 17.7 | 17.3 |
| 0.0 | 16.5 | 16.5 | 18.1 | 17.5 |
| 22.9 | 0.0 | 18.5 | 24.8 | 24.3 |
| 18.2 | 21.9 | 17.3 | 21.5 | 20.8 |
| 21.6 | 19.1 | 17.8 | 24.6 | 24.2 |
| 28.7 | 26.8 | 24.9 | 41.3 | 36.3 |
| 34.1 | 27.1 | 24.9 | 47.8 | 46.9 |
| 25.5 | 23.0 | 21.8 | 33.2 | 30.2 |
| 20.4 | 18.0 | 17.6 | 25.0 | 21.6 |
| 0.0 | 18.2 | 19.5 | 24.1 | 21.5 |
| 0.0 | 17.4 | 17.7 | 20.1 | 18.6 |
| | | | | |
| | | | | |
| 0.0 | 20.0 | 20.4 | 30.8 | 28.7 |
| 27.5 | 23.0 | 21.7 | 34.1 | 25.3 |
| 0.0 | 17.7 | 17.3 | 17.6 | 17.5 |
| 20.1 | 18.4 | 20.1 | 23.1 | 22.6 |
| 23.2 | 19.4 | 19.1 | 21.5 | 21.0 |
| 18.8 | 21.1 | 17.7 | 18.1 | 18.0 |
| 0.0 | 20.8 | 20.5 | 25.9 | 25.7 |
| | | | | |
| 0.0 | 18.6 | 19.1 | 26.4 | 25.8 |
| 0.0 | 19.3 | 17.9 | 21.5 | 21.0 |
| 26.0 | 20.1 | 18.1 | 22.3 | 21.6 |
| 0.0 | 18.1 | 22.5 | 21.8 | 22.2 |
| 0.0 | 16.5 | 15.8 | 19.7 | 18.8 |
| 0.0 | 19.6 | 18.2 | 31.7 | 29.8 |

**Table C.10: Humerus collagen fiber orientation data part II**
As per Table C.5.

| Taxon | Genus | Species | Spec. | PHYLO | PB | TCA ($mm^2$) | %HAV | %CCC | %SF | %P |
|---|---|---|---|---|---|---|---|---|---|---|
| Atelidae | Ateles | sp. | MNHU 44079 | PLAT | SUS | | | | | |
| Atelidae | Ateles | fusciceps | FMNH 68811 | PLAT | SUS | | | | | |
| Callitrichidae | Callithrix | sp. | MNHU 34381 | PLAT | AQ | 2.9 | 7.1% | 0.0% | 6.1% | 43.7% |
| Callitrichidae | Callithrix | geoffroyi | HC 28 | PLAT | AQ | | | | | |
| Cheirogaleidae | Cheirogaleus | major | DUPC 2612 | STREP | AQ | | | | | |
| Cheirogaleidae | Mirza | coquereli | DUPC 359 | STREP | AQ | 1.9 | 19.9% | 12.3% | 0.0% | 46.1% |
| Cheirogaleidae | Microcebus | murinus | DUPC 825 | STREP | AQ | 0.9 | 20.3% | 13.3% | 0.0% | 39.2% |
| Cheirogaleidae | Cheirogaleus | major | MCZ 44850 | STREP | AQ | | | | | |
| Lesser Galago | Galago | senegalensis | MNHU 60601 | STREP | VCL | | | | | |
| Lesser Galago | Galago | moholi | DUPC 2062 | STREP | VCL | 1.1 | 6.9% | 2.0% | 0.0% | 73.1% |
| Lesser Galago | Galago | moholi | DUPC 3173 | STREP | VCL | 0.9 | 7.2% | 3.0% | 0.0% | 71.5% |
| Lesser Galago | Galagoides | demidovii | HC 25 | STREP | VCL | | | | | |
| Indriidae | Propithecus | sp. | MNHU 44684 | STREP | VCL | 9.7 | 46.4% | 2.2% | 0.9% | 40.2% |
| Indriidae | Propithecus | sp. | MNHU 44685 | STREP | VCL | | | | | |
| Indriidae | Indri | indri | HC 19 | STREP | VCL | | | | | |
| Lemuridae | Lemur | sp. | HC 30 | STREP | AQ | | | | | |
| Lemuridae | Varecia | variegata | MCZ 18740 | STREP | AQ | 13.9 | 47.2% | 5.2% | 0.1% | 38.8% |
| Lorisidae | Nycticebus | coucang | DUPC 1972 | STREP | SC | 8.4 | 14.9% | 7.8% | 3.7% | 61.2% |
| Lorisidae | Loris | tardigradus | DUPC 1964 | STREP | SC | 1.7 | 2.0% | 4.0% | 0.0% | 58.5% |
| Lorisidae | Perodicticus | potto | DUPC 930 | STREP | SC | 7.0 | 33.1% | 10.4% | 1.6% | 46.1% |
| Lorisidae | Nycticebus | coucang | HC 27 | STREP | SC | 6.3 | 19.4% | 5.6% | 3.1% | 53.1% |
| Lorisidae | Nycticebus | coucang | USNM 317187 | STREP | SC | | | | | |
| Lorisidae | Nycticebus | coucang | MCZ 36116 | STREP | SC | | | | | |
| Lorisidae | Nycticebus | coucang | MCZ 422 | STREP | SC | 6.5 | 7.8% | 20.2% | 7.5% | 54.5% |
| Greater Galago | Otolemur | crassicaudatus | DUPC 725 | STREP | VCL | 8.1 | 27.0% | 11.3% | 3.5% | 35.8% |
| Greater Galago | Otolemur | crassicaudatus | HC 31 | STREP | VCL | 7.0 | 14.5% | 2.9% | 4.2% | 45.7% |
| Greater Galago | Otolemur | crassicaudatus | USNM 365721 | STREP | VCL | | | | | |
| Greater Galago | Otolemur | crassicaudatus | CT OA | STREP | VCL | | | | | |
| Cebidae | Saimiri | sp. | MNHU 85197 | PLAT | AQ | 5.6 | 15.4% | 0.3% | 5.3% | 58.6% |
| Cebidae | Saimiri | sciureus | HC 12 | PLAT | AQ | | | | | |
| Cebidae | Saimiri | sp. | HC 13 | PLAT | AQ | 4.4 | 20.7% | 2.5% | 3.3% | 45.7% |
| Cebidae | Saimiri | sp. | HC 14 | PLAT | AQ | | | | | |
| Tarsiidae | Tarsius | spectrum | MNHU An11318 | TAR | VCL | | | | | |
| Tarsiidae | Tarsius | syrichta | DUPC 81 | TAR | VCL | 0.9 | 0.0% | 7.2% | 0.0% | 54.2% |
| Tarsiidae | Tarsius | spectrum | HC 16 | TAR | VCL | 1.3 | 1.4% | 7.7% | 2.4% | 43.4% |
| Tarsiidae | Tarsius | sp. | HC 23 | TAR | VCL | | | | | |

**Table C.11: Radius primary tissue type and intracortical remodeling data Part I**
As per Table C.1.

| %E | %P WOV | %P FFBL | %P SFBL | %P PF | %P HYB | %P LAM | %P FAST | %P LAM+HYB |
|---|---|---|---|---|---|---|---|---|
| | | | | | | | | |
| | | | | | | | | |
| 43.1% | 0.0% | 0.0% | 0.0% | 40.3% | 53.4% | 6.4% | 0.0% | 59.7% |
| | | | | | | | | |
| | | | | | | | | |
| 21.7% | 0.0% | 0.0% | 0.0% | 23.8% | 53.9% | 22.3% | 0.0% | 76.2% |
| 27.2% | 0.0% | 0.0% | 0.0% | 71.0% | 23.1% | 5.9% | 0.0% | 29.0% |
| | | | | | | | | |
| | | | | | | | | |
| 18.0% | 0.0% | 0.0% | 0.0% | 31.4% | 56.5% | 12.2% | 0.0% | 68.6% |
| 18.3% | 0.0% | 0.0% | 0.0% | 37.6% | 39.8% | 22.6% | 0.0% | 62.4% |
| | | | | | | | | |
| 10.3% | 0.0% | 0.0% | 1.1% | 21.6% | 39.6% | 37.8% | 1.1% | 77.4% |
| | | | | | | | | |
| | | | | | | | | |
| | | | | | | | | |
| 8.6% | 0.0% | 0.0% | 8.4% | 37.7% | 26.4% | 27.5% | 8.4% | 53.9% |
| 12.5% | 0.0% | 2.2% | 6.3% | 68.4% | 17.0% | 6.2% | 8.5% | 23.2% |
| 35.5% | 0.0% | 0.0% | 0.0% | 68.7% | 25.0% | 6.3% | 0.0% | 31.3% |
| 8.7% | 0.4% | 2.6% | 2.5% | 87.9% | 3.8% | 2.7% | 5.5% | 6.6% |
| 18.9% | 0.0% | 0.0% | 6.0% | 62.4% | 14.5% | 17.0% | 6.0% | 31.6% |
| | | | | | | | | |
| | | | | | | | | |
| 10.1% | 1.8% | 22.7% | 2.9% | 60.3% | 5.0% | 7.4% | 27.3% | 12.4% |
| 22.4% | 0.0% | 0.0% | 4.0% | 31.2% | 58.1% | 6.8% | 4.0% | 64.9% |
| 32.6% | 0.0% | 0.0% | 0.0% | 35.1% | 41.9% | 22.9% | 0.0% | 64.9% |
| | | | | | | | | |
| | | | | | | | | |
| 20.3% | 0.0% | 0.0% | 0.0% | 19.2% | 29.4% | 51.4% | 0.0% | 80.8% |
| | | | | | | | | |
| 27.8% | 0.0% | 0.0% | 0.0% | 26.4% | 43.0% | 30.7% | 0.0% | 73.6% |
| | | | | | | | | |
| | | | | | | | | |
| 38.5% | 0.0% | 0.0% | 0.0% | 78.5% | 10.6% | 10.9% | 0.0% | 21.5% |
| 45.1% | 0.0% | 0.0% | 0.0% | 73.7% | 21.6% | 4.7% | 0.0% | 26.3% |
| | | | | | | | | |

**Table C.12: Radius primary tissue type and intracortical remodeling data Part II**
As per Table C.2.

| %E WOV | %E FFBL | %E SFBL | %E PF | %E HYB | %E LAM | %E FAST | %E LAM+HYB |
|---|---|---|---|---|---|---|---|
| | | | | | | | |
| | | | | | | | |
| 0.0% | 0.0% | 0.0% | 25.7% | 31.8% | 42.5% | 0.0% | 74.3% |
| | | | | | | | |
| | | | | | | | |
| 0.0% | 0.0% | 0.0% | 0.0% | 83.6% | 16.4% | 0.0% | 100.0% |
| 0.0% | 0.0% | 0.0% | 0.0% | 0.0% | 100.0% | 0.0% | 100.0% |
| | | | | | | | |
| | | | | | | | |
| 0.0% | 0.0% | 0.0% | 63.3% | 30.9% | 5.8% | 0.0% | 36.7% |
| 0.0% | 0.0% | 0.0% | 15.7% | 30.1% | 54.2% | 0.0% | 84.3% |
| | | | | | | | |
| 0.0% | 0.0% | 2.0% | 18.1% | 48.0% | 31.9% | 2.0% | 79.9% |
| | | | | | | | |
| | | | | | | | |
| | | | | | | | |
| 0.0% | 0.0% | 0.0% | 9.4% | 32.8% | 57.8% | 0.0% | 90.6% |
| 9.5% | 6.4% | 0.0% | 43.2% | 13.9% | 27.0% | 15.9% | 40.9% |
| 0.0% | 0.0% | 0.0% | 87.3% | 10.0% | 2.7% | 0.0% | 12.7% |
| 0.0% | 0.0% | 0.0% | 29.4% | 32.1% | 38.5% | 0.0% | 70.6% |
| 0.0% | 0.0% | 0.0% | 44.1% | 32.4% | 23.6% | 0.0% | 55.9% |
| | | | | | | | |
| | | | | | | | |
| 0.0% | 0.0% | 0.0% | 91.7% | 8.3% | 0.0% | 0.0% | 8.3% |
| 0.0% | 0.0% | 0.0% | 22.4% | 61.3% | 16.3% | 0.0% | 77.6% |
| 0.0% | 2.0% | 5.6% | 30.1% | 24.0% | 38.2% | 7.7% | 62.2% |
| | | | | | | | |
| | | | | | | | |
| 0.0% | 0.0% | 0.0% | 12.8% | 53.1% | 34.2% | 0.0% | 87.2% |
| | | | | | | | |
| 0.0% | 0.0% | 0.0% | 46.2% | 45.4% | 8.4% | 0.0% | 53.8% |
| | | | | | | | |
| | | | | | | | |
| 0.0% | 0.0% | 0.0% | 92.0% | 8.0% | 0.0% | 0.0% | 8.0% |
| 0.0% | 0.0% | 0.0% | 75.4% | 7.3% | 17.3% | 0.0% | 24.6% |

**Table C.13: Radius primary tissue type and intracortical remodeling data Part III**
As per Table C.3.

| Spec. # | P A Mean | P L Mean | P P Mean | P M Mean | TPA Mean | O A Mean | O L Mean | O P Mean | O M Mean | TOA Mean |
|---|---|---|---|---|---|---|---|---|---|---|
| MNHU 44079 | | | | | | | | | | |
| FMNH 68811 | | | | | | | | | | |
| MNHU 34381 | 16.4 | 16.6 | 16.3 | 17.1 | 16.7 | na | 18.7 | 21.7 | 20.5 | 19.4 |
| HC 28 | | | | | | | | | | |
| DUPC 2612 | | | | | | | | | | |
| DUPC 359 | 19.4 | 18.3 | 16.8 | 21.8 | 18.6 | na | 16.7 | 18.0 | 17.6 | 17.4 |
| DUPC 825 | 19.9 | 17.0 | 17.2 | 18.4 | 18.0 | 18.1 | 16.4 | 17.5 | 17.4 | 16.8 |
| MCZ 44850 | | | | | | | | | | |
| MNHU 60601 | | | | | | | | | | |
| DUPC 2062 | 16.9 | 16.5 | 16.8 | 17.0 | 16.9 | 21.9 | 18.0 | na | na | 18.7 |
| DUPC 3173 | 16.0 | 16.7 | 15.2 | 16.9 | 16.3 | na | 16.3 | na | na | 16.3 |
| HC 25 | | | | | | | | | | |
| MNHU 44684 | | | | | | | | | | |
| MNHU 44685 | | | | | | | | | | |
| HC 19 | | | | | | | | | | |
| HC 30 | | | | | | | | | | |
| MCZ 18740 | 24.7 | 22.8 | 22.1 | 23.7 | 23.6 | 26.2 | 23.3 | 23.9 | 24.0 | 24.0 |
| DUPC 1972 | 18.5 | 18.9 | 17.8 | 17.3 | 18.0 | 19.2 | 18.7 | 19.3 | 18.1 | 18.9 |
| DUPC 1964 | 17.5 | 18.5 | 16.9 | 17.6 | 17.6 | na | 20.1 | 18.2 | na | 20.1 |
| DUPC 930 | 16.5 | 18.8 | 17.2 | 17.7 | 17.4 | 17.1 | 17.6 | 16.9 | 19.3 | 17.5 |
| HC 27 | | | | | | | | | | |
| USNM 317187 | | | | | | | | | | |
| MCZ 36116 | | | | | | | | | | |
| MCZ 422 | 23.3 | 20.5 | 24.3 | 26.7 | 24.4 | 25.5 | 32.0 | 24.1 | 38.7 | 28.8 |
| DUPC 725 | 19.6 | 19.1 | 18.6 | 19.3 | 19.3 | 18.8 | 19.2 | 19.6 | 19.5 | 19.3 |
| HC 31 | 20.5 | 17.3 | 18.7 | 17.2 | 18.3 | na | 17.2 | 16.7 | 17.3 | 17.2 |
| USNM 365721 | | | | | | | | | | |
| CT OA | | | | | | | | | | |
| MNHU 85197 | 19.7 | 19.7 | 18.8 | 20.9 | 19.9 | 20.2 | 20.0 | 22.1 | 26.4 | 21.1 |
| HC 12 | | | | | | | | | | |
| HC 13 | 17.7 | 19.0 | 18.4 | 20.0 | 19.0 | 21.5 | 20.2 | 19.4 | 18.9 | 20.0 |
| HC 14 | | | | | | | | | | |
| MNHU An11318 | | | | | | | | | | |
| DUPC 81 | 16.5 | 16.7 | 17.1 | 16.4 | 16.8 | na | na | na | na | na |
| HC 16 | 16.7 | 16.9 | 16.5 | 17.0 | 16.9 | na | 22.8 | na | na | 22.8 |
| HC 23 | | | | | | | | | | |

**Table C.14: Radius collagen fiber orientation data Part I**
As per Table C.4.

| FAST Mean | PF Mean | HYB Mean | LAM Mean | LAM+HYB Mean |
|---|---|---|---|---|
| | | | | |
| | | | | |
| 0.0 | 16.6 | 16.7 | 17.4 | 16.8 |
| | | | | |
| | | | | |
| 0.0 | 17.6 | 16.9 | 19.6 | 17.7 |
| 0.0 | 17.4 | 16.2 | 17.6 | 16.5 |
| | | | | |
| | | | | |
| 0.0 | 16.4 | 16.6 | 18.1 | 16.8 |
| 0.0 | 15.6 | 15.6 | 17.0 | 16.0 |
| | | | | |
| | | | | |
| | | | | |
| | | | | |
| | | | | |
| 21.2 | 20.5 | 21.8 | 29.2 | 25.3 |
| 18.1 | 17.1 | 18.5 | 26.3 | 20.3 |
| 0.0 | 17.5 | 16.9 | 19.5 | 17.4 |
| 18.4 | 16.9 | 20.5 | 24.7 | 22.1 |
| | | | | |
| | | | | |
| | | | | |
| 27.1 | 21.8 | 20.7 | 22.1 | 21.3 |
| 29.3 | 18.0 | 18.8 | 23.4 | 19.3 |
| 0.0 | 17.1 | 17.6 | 21.7 | 19.0 |
| | | | | |
| | | | | |
| 0.0 | 19.2 | 19.6 | 20.2 | 20.0 |
| | | | | |
| 0.0 | 17.8 | 18.8 | 20.4 | 19.4 |
| | | | | |
| | | | | |
| 0.0 | 16.8 | 16.0 | 17.2 | 16.6 |
| 0.0 | 16.8 | 17.1 | 17.3 | 17.0 |
| | | | | |

**Table C.15: Radius collagen fiber orientation data Part II**
As per Table C.5.

| Taxon | Genus | Species | Spec. | PHYLO | PB | TCA ($mm^2$) | %HAV | %CCC | %SF | %P |
|---|---|---|---|---|---|---|---|---|---|---|
| Atelidae | Ateles | sp. | MNHU 44079 | PLAT | SUS | | | | | |
| Atelidae | Ateles | fusciceps | FMNH 68811 | PLAT | SUS | | | | | |
| Callitrichidae | Callithrix | sp. | MNHU 34381 | PLAT | AQ | 2.6 | 11.3% | 0.9% | 7.2% | 36.2% |
| Callitrichidae | Callithrix | geoffroyi | HC 28 | PLAT | AQ | | | | | |
| Cheirogaleidae | Cheirogaleus | major | DUPC 2612 | STREP | AQ | | | | | |
| Cheirogaleidae | Mirza | coquereli | DUPC 359 | STREP | AQ | | | | | |
| Cheirogaleidae | Microcebus | murinus | DUPC 825 | STREP | AQ | | | | | |
| Cheirogaleidae | Cheirogaleus | major | MCZ 44850 | STREP | AQ | | | | | |
| Lesser Galago | Galago | senegalensis | MNHU 60601 | STREP | VCL | | | | | |
| Lesser Galago | Galago | moholi | DUPC 2062 | STREP | VCL | 1.0 | 7.7% | 0.8% | 0.0% | 69.1% |
| Lesser Galago | Galago | moholi | DUPC 3173 | STREP | VCL | 0.7 | 4.1% | 5.4% | 0.0% | 70.1% |
| Lesser Galago | Galagoides | demidovii | HC 25 | STREP | VCL | | | | | |
| Indriidae | Propithecus | sp. | MNHU 44684 | STREP | VCL | 7.2 | 66.9% | 0.4% | 0.0% | 18.6% |
| Indriidae | Propithecus | sp. | MNHU 44685 | STREP | VCL | | | | | |
| Indriidae | Indri | indri | HC 19 | STREP | VCL | | | | | |
| Lemuridae | Lemur | sp. | HC 30 | STREP | AQ | | | | | |
| Lemuridae | Varecia | variegata | MCZ 18740 | STREP | AQ | 17.2 | 70.4% | 2.0% | 0.2% | 16.1% |
| Lorisidae | Nycticebus | coucang | DUPC 1972 | STREP | SC | 6.8 | 26.2% | 8.4% | 5.2% | 49.4% |
| Lorisidae | Loris | tardigradus | DUPC 1964 | STREP | SC | 1.7 | 6.2% | 10.2% | 0.0% | 53.0% |
| Lorisidae | Perodicticus | potto | DUPC 930 | STREP | SC | | | | | |
| Lorisidae | Nycticebus | coucang | HC 27 | STREP | SC | 5.0 | 58.7% | 5.6% | 3.6% | 23.7% |
| Lorisidae | Nycticebus | coucang | USNM 317187 | STREP | SC | | | | | |
| Lorisidae | Nycticebus | coucang | MCZ 36116 | STREP | SC | | | | | |
| Lorisidae | Nycticebus | coucang | MCZ 422 | STREP | SC | 5.4 | 37.6% | 24.5% | 6.1% | 27.9% |
| Greater Galago | Otolemur | crassicaudatus | DUPC 725 | STREP | VCL | 9.4 | 42.4% | 6.8% | 1.9% | 31.2% |
| Greater Galago | Otolemur | crassicaudatus | HC 31 | STREP | VCL | 7.9 | 31.4% | 7.2% | 3.6% | 45.9% |
| Greater Galago | Otolemur | crassicaudatus | USNM 365721 | STREP | VCL | | | | | |
| Greater Galago | Otolemur | crassicaudatus | CT OA | STREP | VCL | | | | | |
| Cebidae | Saimiri | sp. | MNHU 85197 | PLAT | AQ | 6.7 | 31.1% | 2.1% | 5.9% | 47.0% |
| Cebidae | Saimiri | sciureus | HC 12 | PLAT | AQ | | | | | |
| Cebidae | Saimiri | sp. | HC 13 | PLAT | AQ | 4.7 | 39.5% | 0.0% | 3.3% | 44.2% |
| Cebidae | Saimiri | sp. | HC 14 | PLAT | AQ | | | | | |
| Tarsiidae | Tarsius | spectrum | MNHU An11318 | TAR | VCL | | | | | |
| Tarsiidae | Tarsius | syrichta | DUPC 81 | TAR | VCL | 0.8 | 0.8% | 15.5% | 3.5% | 73.0% |
| Tarsiidae | Tarsius | spectrum | HC 16 | TAR | VCL | 1.0 | 0.0% | 6.4% | 0.9% | 48.7% |
| Tarsiidae | Tarsius | sp. | HC 23 | TAR | VCL | | | | | |

**Table C.16: Ulna primary tissue type and intracortical remodeling data Part I**
As per Table C.1.

| %E | %P WOV | %P FFBL | %P SFBL | %P PF | %P HYB | %P LAM | %P FAST | %P LAM+HYB |
|---|---|---|---|---|---|---|---|---|
| | | | | | | | | |
| | | | | | | | | |
| 44.3% | 0.0% | 0.0% | 5.9% | 21.3% | 58.9% | 13.9% | 5.9% | 72.8% |
| | | | | | | | | |
| | | | | | | | | |
| | | | | | | | | |
| | | | | | | | | |
| | | | | | | | | |
| | | | | | | | | |
| 22.5% | 0.0% | 0.0% | 0.0% | 39.4% | 50.2% | 10.3% | 0.0% | 60.6% |
| 20.5% | 0.0% | 0.0% | 0.0% | 44.0% | 52.1% | 3.9% | 0.0% | 56.0% |
| | | | | | | | | |
| 14.2% | 0.0% | 3.8% | 2.6% | 54.6% | 26.3% | 12.7% | 6.3% | 39.1% |
| | | | | | | | | |
| | | | | | | | | |
| | | | | | | | | |
| 11.3% | 0.0% | 2.6% | 15.0% | 34.7% | 23.9% | 23.8% | 17.6% | 47.7% |
| 10.9% | 0.0% | 0.0% | 0.0% | 87.1% | 12.9% | 0.0% | 0.0% | 12.9% |
| 30.6% | 0.0% | 0.0% | 0.0% | 99.5% | 0.5% | 0.0% | 0.0% | 0.5% |
| | | | | | | | | |
| 8.4% | 0.0% | 0.0% | 1.5% | 68.8% | 29.6% | 0.0% | 1.5% | 29.6% |
| | | | | | | | | |
| | | | | | | | | |
| 3.8% | 0.0% | 0.0% | 2.9% | 93.1% | 4.0% | 0.0% | 2.9% | 4.0% |
| 17.6% | 0.0% | 0.0% | 1.5% | 40.9% | 50.6% | 7.0% | 1.5% | 57.6% |
| 11.8% | 0.0% | 0.0% | 0.9% | 63.8% | 28.4% | 6.9% | 0.9% | 35.3% |
| | | | | | | | | |
| | | | | | | | | |
| 13.9% | 0.0% | 0.0% | 0.0% | 35.0% | 55.4% | 9.6% | 0.0% | 65.0% |
| | | | | | | | | |
| 13.0% | 0.0% | 0.0% | 0.0% | 52.3% | 26.8% | 20.9% | 0.0% | 47.7% |
| | | | | | | | | |
| | | | | | | | | |
| 7.2% | 0.0% | 0.0% | 0.0% | 63.2% | 32.7% | 4.1% | 0.0% | 36.8% |
| 44.0% | 0.0% | 0.0% | 0.0% | 37.4% | 39.5% | 23.1% | 0.0% | 62.6% |
| | | | | | | | | |

**Table C.17: Ulna primary tissue type and intracortical remodeling data Part II**
As per Table C.2.

| %E WOV | %E FFBL | %E SFBL | %E PF | %E HYB | %E LAM | %E FAST | %E LAM+HYB |
|---|---|---|---|---|---|---|---|
| | | | | | | | |
| | | | | | | | |
| 0.0% | 0.0% | 0.0% | 5.8% | 28.5% | 65.8% | 0.0% | 94.2% |
| | | | | | | | |
| | | | | | | | |
| | | | | | | | |
| | | | | | | | |
| | | | | | | | |
| | | | | | | | |
| 7.3% | 12.1% | 0.0% | 35.2% | 43.0% | 2.4% | 19.4% | 45.4% |
| 0.0% | 0.0% | 0.0% | 29.4% | 35.5% | 35.1% | 0.0% | 70.6% |
| | | | | | | | |
| 0.0% | 0.0% | 0.0% | 7.0% | 53.4% | 39.6% | 0.0% | 93.0% |
| | | | | | | | |
| | | | | | | | |
| | | | | | | | |
| 0.0% | 0.0% | 0.0% | 10.8% | 50.3% | 38.9% | 0.0% | 89.2% |
| 0.0% | 0.0% | 0.0% | 31.6% | 42.5% | 25.9% | 0.0% | 68.4% |
| 0.0% | 0.0% | 0.0% | 73.4% | 23.0% | 3.6% | 0.0% | 26.6% |
| | | | | | | | |
| 0.0% | 0.0% | 0.0% | 28.8% | 11.6% | 59.6% | 0.0% | 71.2% |
| | | | | | | | |
| | | | | | | | |
| 0.0% | 0.0% | 0.0% | 94.5% | 5.5% | 0.0% | 0.0% | 5.5% |
| 0.0% | 0.0% | 4.8% | 50.4% | 32.9% | 11.9% | 4.8% | 44.8% |
| 0.0% | 0.0% | 3.3% | 14.3% | 61.2% | 21.3% | 3.3% | 82.4% |
| | | | | | | | |
| | | | | | | | |
| 0.0% | 0.0% | 0.0% | 19.1% | 51.1% | 29.8% | 0.0% | 80.9% |
| | | | | | | | |
| 0.0% | 0.0% | 0.0% | 14.0% | 62.7% | 23.3% | 0.0% | 86.0% |
| | | | | | | | |
| | | | | | | | |
| 0.0% | 0.0% | 0.0% | 100.0% | 0.0% | 0.0% | 0.0% | 0.0% |
| 0.0% | 4.0% | 8.4% | 59.2% | 22.8% | 5.6% | 12.4% | 28.4% |

**Table C.18: Ulna primary tissue type and intracortical remodeling data Part III**
As per Table C.3.

| Spec. # | P A Mean | P L Mean | P P Mean | P M Mean | TPA Mean | O A Mean | O L Mean | O P Mean | O M Mean | TOA Mean |
|---|---|---|---|---|---|---|---|---|---|---|
| MNHU 44079 | | | | | | | | | | |
| FMNH 68811 | | | | | | | | | | |
| MNHU 34381 | 18.6 | 17.4 | 17.6 | 16.2 | 18.0 | 18.8 | 19.6 | 19.8 | 17.6 | 19.4 |
| HC 28 | | | | | | | | | | |
| DUPC 2612 | | | | | | | | | | |
| DUPC 359 | | | | | | | | | | |
| DUPC 825 | 18.1 | 17.1 | 15.9 | 18.0 | 16.8 | 16.2 | 16.5 | 15.9 | 16.7 | 16.4 |
| MCZ 44850 | | | | | | | | | | |
| MNHU 60601 | | | | | | | | | | |
| DUPC 2062 | 16.6 | 16.2 | 15.9 | 16.7 | 16.4 | 17.2 | 18.4 | 15.9 | na | 18.3 |
| DUPC 3173 | 16.7 | 15.8 | 15.2 | 16.4 | 15.9 | 15.4 | 12.8 | na | na | 15.3 |
| HC 25 | | | | | | | | | | |
| MNHU 44684 | 23.1 | 19.3 | 17.7 | 19.7 | 19.9 | 19.3 | 19.4 | 19.3 | 19.6 | 19.4 |
| MNHU 44685 | | | | | | | | | | |
| HC 19 | | | | | | | | | | |
| HC 30 | | | | | | | | | | |
| MCZ 18740 | 30.6 | 21.7 | 22.6 | 41.6 | 28.9 | 26.9 | 24.4 | 23.2 | 31.4 | 25.5 |
| DUPC 1972 | 17.3 | 17.6 | 18.9 | 18.3 | 17.9 | 17.9 | 18.1 | 18.4 | 17.9 | 18.2 |
| DUPC 1964 | 16.9 | 17.7 | 16.7 | 18.7 | 17.4 | 17.1 | 19.0 | 23.8 | 17.3 | 17.9 |
| DUPC 930 | 18.5 | 17.1 | 17.9 | 19.2 | 18.1 | 16.4 | 16.5 | 16.6 | 16.6 | 16.5 |
| HC 27 | | | | | | | | | | |
| USNM 317187 | | | | | | | | | | |
| MCZ 36116 | | | | | | | | | | |
| MCZ 422 | 18.0 | 19.1 | 19.3 | 20.2 | 19.1 | 16.6 | 16.6 | 18.0 | 17.9 | 17.4 |
| DUPC 725 | 17.3 | 17.7 | 17.2 | 16.7 | 17.3 | 18.2 | 18.5 | 17.3 | 18.0 | 17.9 |
| HC 31 | 19.2 | 19.0 | 17.5 | 18.2 | 18.4 | 17.9 | 18.3 | 18.0 | 18.2 | 18.0 |
| USNM 365721 | | | | | | | | | | |
| CT OA | | | | | | | | | | |
| MNHU 85197 | 19.8 | 18.9 | 18.1 | 19.0 | 19.0 | 21.2 | 18.6 | 20.1 | 19.3 | 20.0 |
| HC 12 | | | | | | | | | | |
| HC 13 | 18.1 | 18.1 | 17.3 | 17.2 | 17.8 | 18.7 | 17.7 | 18.4 | 18.3 | 18.3 |
| HC 14 | | | | | | | | | | |
| MNHU An11318 | | | | | | | | | | |
| DUPC 81 | 16.0 | 19.2 | 16.5 | 16.1 | 17.6 | na | 23.6 | na | na | 23.6 |
| HC 16 | 15.7 | 16.2 | 15.6 | 16.5 | 16.2 | na | na | na | na | na |
| HC 23 | | | | | | | | | | |

**Table C.19: Ulna collagen fiber orientation data Part I**
As per Table C.4.

| FAST Mean | PF Mean | HYB Mean | LAM Mean | LAM+HYB Mean |
|---|---|---|---|---|
| | | | | |
| | | | | |
| 21.6 | 17.6 | 17.4 | 19.0 | 17.7 |
| | | | | |
| | | | | |
| | | | | |
| 15.9 | 15.7 | 17.3 | 16.6 | 17.2 |
| | | | | |
| | | | | |
| 0.0 | 15.2 | 17.8 | 20.2 | 16.5 |
| 0.0 | 15.6 | 15.7 | 17.8 | 15.8 |
| | | | | |
| 21.3 | 17.9 | 18.4 | 26.0 | 21.3 |
| | | | | |
| | | | | |
| | | | | |
| 26.5 | 22.7 | 23.6 | 47.5 | 35.1 |
| 0.0 | 17.6 | 19.1 | 0.0 | 19.1 |
| 0.0 | 17.2 | 21.2 | 0.0 | 21.2 |
| 0.0 | 16.4 | 18.6 | 27.3 | 20.3 |
| | | | | |
| | | | | |
| | | | | |
| 21.5 | 19.2 | 18.5 | 0.0 | 18.5 |
| 20.7 | 16.6 | 17.4 | 20.1 | 17.7 |
| 18.3 | 17.9 | 18.6 | 20.9 | 19.0 |
| | | | | |
| | | | | |
| 0.0 | 18.5 | 18.8 | 22.6 | 19.4 |
| | | | | |
| 0.0 | 17.3 | 17.7 | 19.3 | 18.4 |
| | | | | |
| | | | | |
| 0.0 | 18.3 | 16.2 | 17.1 | 16.3 |
| 0.0 | 16.3 | 16.0 | 16.3 | 16.1 |
| | | | | |

**Table C.20: Ulna collagen fiber orientation data Part II**
As per Table C.5.

| Taxon | Genus | Species | Spec. | PHYLO | PB | TCA ( $mm^2$) | %HAV | %CCC | %SF | %P |
|---|---|---|---|---|---|---|---|---|---|---|
| Atelidae | Ateles | sp. | MNHU 44079 | PLAT | SUS | | | | | |
| Atelidae | Ateles | fusciceps | FMNH 68811 | PLAT | SUS | | | | | |
| Callitrichidae | Callithrix | sp. | MNHU 34381 | PLAT | AQ | | | | | |
| Callitrichidae | Callithrix | geoffroyi | HC 28 | PLAT | AQ | | | | | |
| Cheirogaleidae | Cheirogaleus | major | DUPC 2612 | STREP | AQ | | | | | |
| Cheirogaleidae | Mirza | coquereli | DUPC 359 | STREP | AQ | 4.3 | 8.1% | 0.0% | 0.0% | 84.5% |
| Cheirogaleidae | Microcebus | murinus | DUPC 825 | STREP | AQ | 1.7 | 4.5% | 0.0% | 0.0% | 88.9% |
| Cheirogaleidae | Cheirogaleus | major | MCZ 44850 | STREP | AQ | | | | | |
| Lesser Galago | Galago | senegalensis | MNHU 60601 | STREP | VCL | | | | | |
| Lesser Galago | Galago | moholi | DUPC 2062 | STREP | VCL | 2.9 | 0.8% | 0.0% | 0.0% | 86.5% |
| Lesser Galago | Galago | moholi | DUPC 3173 | STREP | VCL | 2.7 | 1.3% | 0.0% | 0.0% | 98.6% |
| Lesser Galago | Galagoides | demidovii | HC 25 | STREP | VCL | | | | | |
| Indriidae | Propithecus | sp. | MNHU 44684 | STREP | VCL | 28.4 | 47.1% | 0.0% | 0.0% | 50.2% |
| Indriidae | Propithecus | sp. | MNHU 44685 | STREP | VCL | | | | | |
| Indriidae | Indri | indri | HC 19 | STREP | VCL | | | | | |
| Lemuridae | Lemur | sp. | HC 30 | STREP | AQ | | | | | |
| Lemuridae | Varecia | variegata | MCZ 18740 | STREP | AQ | 26.9 | 38.2% | 0.0% | 0.7% | 51.6% |
| Lorisidae | Nycticebus | coucang | DUPC 1972 | STREP | SC | 11.4 | 7.6% | 1.1% | 0.3% | 83.8% |
| Lorisidae | Loris | tardigradus | DUPC 1964 | STREP | SC | 3.2 | 15.9% | 4.5% | 0.0% | 70.7% |
| Lorisidae | Perodicticus | potto | DUPC 930 | STREP | SC | | | | | |
| Lorisidae | Nycticebus | coucang | HC 27 | STREP | SC | 11.4 | 36.9% | 20.8% | 1.8% | 32.9% |
| Lorisidae | Nycticebus | coucang | USNM 317187 | STREP | SC | | | | | |
| Lorisidae | Nycticebus | coucang | MCZ 36116 | STREP | SC | | | | | |
| Lorisidae | Nycticebus | coucang | MCZ 422 | STREP | SC | 8.9 | 6.4% | 1.3% | 1.5% | 85.8% |
| Greater Galago | Otolemur | crassicaudatus | DUPC 725 | STREP | VCL | 14.9 | 27.4% | 0.3% | 0.3% | 64.7% |
| Greater Galago | Otolemur | crassicaudatus | HC 31 | STREP | VCL | 14.7 | 7.5% | 0.0% | 1.6% | 81.2% |
| Greater Galago | Otolemur | crassicaudatus | USNM 365721 | STREP | VCL | 14.7 | 9.1% | 0.0% | 4.1% | 81.3% |
| Greater Galago | Otolemur | crassicaudatus | CT OA | STREP | VCL | 14.1 | 1.5% | 0.6% | 0.3% | 90.9% |
| Cebidae | Saimiri | sp. | MNHU 85197 | PLAT | AQ | 11.3 | 14.8% | 0.0% | 1.0% | 73.9% |
| Cebidae | Saimiri | sciureus | HC 12 | PLAT | AQ | | | | | |
| Cebidae | Saimiri | sp. | HC 13 | PLAT | AQ | 7.4 | 17.5% | 0.0% | 1.2% | 79.1% |
| Cebidae | Saimiri | sp. | HC 14 | PLAT | AQ | 7.1 | 30.4% | 0.0% | 0.9% | 63.5% |
| Tarsiidae | Tarsius | spectrum | MNHU An11318 | TAR | VCL | | | | | |
| Tarsiidae | Tarsius | syrichta | DUPC 81 | TAR | VCL | 2.6 | 3.8% | 0.0% | 0.0% | 88.8% |
| Tarsiidae | Tarsius | spectrum | HC 16 | TAR | VCL | 3.2 | 3.8% | 0.0% | 0.0% | 91.1% |
| Tarsiidae | Tarsius | sp. | HC 23 | TAR | VCL | | | | | |

**Table C.21: Tibia primary tissue type and intracortical remodeling data Part I**
As per Table C.1.

| %E | %P WOV | %P FFBL | %P SFBL | %P PF | %P HYB | %P LAM | %P FAST | %P LAM+HYB |
|---|---|---|---|---|---|---|---|---|
| | | | | | | | | |
| | | | | | | | | |
| | | | | | | | | |
| | | | | | | | | |
| | | | | | | | | |
| 7.4% | 0.5% | 3.4% | 8.8% | 18.4% | 53.8% | 15.1% | 12.7% | 68.9% |
| 6.6% | 0.0% | 0.0% | 10.1% | 55.3% | 32.9% | 1.7% | 10.1% | 34.6% |
| | | | | | | | | |
| | | | | | | | | |
| 12.7% | 0.0% | 0.0% | 0.0% | 36.6% | 63.4% | 0.0% | 0.0% | 63.4% |
| 0.1% | 0.0% | 0.0% | 0.0% | 36.4% | 49.5% | 14.1% | 0.0% | 63.6% |
| | | | | | | | | |
| 2.7% | 0.0% | 12.6% | 43.1% | 8.2% | 21.6% | 14.6% | 55.6% | 36.2% |
| | | | | | | | | |
| | | | | | | | | |
| | | | | | | | | |
| 9.5% | 0.0% | 0.0% | 33.1% | 42.1% | 11.0% | 13.8% | 33.1% | 24.8% |
| 7.2% | 0.0% | 5.8% | 18.5% | 52.3% | 23.4% | 0.0% | 24.3% | 23.4% |
| 8.9% | 4.7% | 6.5% | 0.0% | 79.3% | 8.0% | 1.6% | 11.2% | 9.5% |
| | | | | | | | | |
| 7.6% | 4.6% | 3.1% | 0.4% | 63.7% | 23.0% | 5.2% | 8.1% | 28.2% |
| | | | | | | | | |
| | | | | | | | | |
| 4.9% | 0.1% | 31.1% | 4.0% | 52.0% | 11.7% | 1.1% | 35.2% | 12.8% |
| 7.3% | 0.0% | 2.1% | 5.5% | 64.2% | 23.3% | 4.9% | 7.5% | 28.3% |
| 9.6% | 0.0% | 2.0% | 3.0% | 60.4% | 22.5% | 12.1% | 5.0% | 34.6% |
| 5.5% | 0.0% | 0.0% | 11.5% | 62.1% | 18.9% | 7.5% | 11.5% | 26.4% |
| 6.7% | 0.0% | 3.4% | 16.4% | 46.2% | 23.3% | 10.8% | 19.8% | 34.0% |
| 10.4% | 0.0% | 0.0% | 0.0% | 10.2% | 44.5% | 45.3% | 0.0% | 89.8% |
| | | | | | | | | |
| 2.1% | 0.0% | 0.0% | 0.0% | 35.9% | 29.9% | 34.2% | 0.0% | 64.1% |
| 5.2% | 0.0% | 0.0% | 0.0% | 36.6% | 41.8% | 21.6% | 0.0% | 63.4% |
| | | | | | | | | |
| 7.4% | 0.0% | 0.0% | 0.0% | 84.7% | 14.0% | 1.3% | 0.0% | 15.3% |
| 5.1% | 0.0% | 0.0% | 0.0% | 80.0% | 17.0% | 3.0% | 0.0% | 20.0% |
| | | | | | | | | |

**Table C.22: Tibia primary tissue type and intracortical remodeling data Part II**
As per Table C.2.

| %E WOV | %E FFBL | %E SFBL | %E PF | %E HYB | %E LAM | %E FAST | %E LAM+HYB |
|---|---|---|---|---|---|---|---|
| | | | | | | | |
| | | | | | | | |
| | | | | | | | |
| | | | | | | | |
| | | | | | | | |
| 0.0% | 0.0% | 0.0% | 8.4% | 18.6% | 72.9% | 0.0% | 91.5% |
| 0.0% | 0.0% | 0.0% | 14.2% | 45.8% | 40.0% | 0.0% | 85.8% |
| | | | | | | | |
| | | | | | | | |
| 2.1% | 0.0% | 47.8% | 27.8% | 19.7% | 2.6% | 49.9% | 22.3% |
| 0.0% | 0.0% | 0.0% | 9.8% | 2.3% | 87.9% | 0.0% | 90.2% |
| | | | | | | | |
| 0.0% | 0.0% | 0.1% | 2.3% | 0.0% | 97.5% | 0.1% | 97.5% |
| | | | | | | | |
| | | | | | | | |
| | | | | | | | |
| 0.0% | 0.0% | 0.0% | 11.2% | 14.0% | 74.9% | 0.0% | 88.8% |
| 0.0% | 0.0% | 0.0% | 35.3% | 16.9% | 47.9% | 0.0% | 64.7% |
| 0.0% | 0.0% | 0.0% | 31.6% | 24.2% | 44.2% | 0.0% | 68.4% |
| | | | | | | | |
| 0.0% | 0.0% | 0.0% | 42.1% | 21.6% | 36.3% | 0.0% | 57.9% |
| | | | | | | | |
| | | | | | | | |
| 0.0% | 0.0% | 0.0% | 42.6% | 38.0% | 19.4% | 0.0% | 57.4% |
| 0.0% | 0.0% | 0.0% | 48.8% | 34.8% | 16.4% | 0.0% | 51.2% |
| 0.0% | 0.0% | 0.0% | 12.2% | 6.3% | 81.5% | 0.0% | 87.8% |
| 0.0% | 0.0% | 0.0% | 28.8% | 24.8% | 46.4% | 0.0% | 71.2% |
| 0.0% | 0.0% | 8.9% | 41.1% | 20.8% | 29.3% | 8.9% | 50.0% |
| 0.0% | 0.0% | 0.0% | 3.9% | 20.2% | 75.9% | 0.0% | 96.1% |
| | | | | | | | |
| 0.0% | 0.0% | 0.0% | 31.0% | 30.8% | 38.2% | 0.0% | 69.0% |
| 0.0% | 0.0% | 0.0% | 11.8% | 16.3% | 71.9% | 0.0% | 88.2% |
| | | | | | | | |
| 0.0% | 0.0% | 0.0% | 79.9% | 20.1% | 0.0% | 0.0% | 20.1% |
| 0.0% | 0.0% | 0.0% | 25.5% | 37.7% | 36.8% | 0.0% | 74.5% |
| | | | | | | | |

**Table C.23: Tibia primary tissue type and intracortical remodeling data Part III**
As per Table C.3.

| Spec. # | P A Mean | P L Mean | P P Mean | P M Mean | TPA Mean | O A Mean | O L Mean | O P Mean | O M Mean | TOA Mean |
|---|---|---|---|---|---|---|---|---|---|---|
| MNHU 44079 | | | | | | | | | | |
| FMNH 68811 | | | | | | | | | | |
| MNHU 34381 | | | | | | | | | | |
| HC 28 | | | | | | | | | | |
| DUPC 2612 | | | | | | | | | | |
| DUPC 359 | 16.6 | 16.4 | 16.4 | 16.4 | 16.5 | 23.3 | 25.7 | 22.9 | 28.2 | 24.0 |
| DUPC 825 | 16.6 | 16.0 | 15.7 | 15.6 | 16.0 | 23.8 | 20.3 | na | na | 23.4 |
| MCZ 44850 | | | | | | | | | | |
| MNHU 60601 | | | | | | | | | | |
| DUPC 2062 | 15.4 | 15.8 | 15.1 | 15.3 | 15.4 | 17.7 | 20.8 | na | na | 20.0 |
| DUPC 3173 | 15.7 | 15.8 | 15.5 | 15.2 | 15.6 | 18.4 | na | na | na | 18.4 |
| HC 25 | | | | | | | | | | |
| MNHU 44684 | 18.1 | 17.9 | 19.1 | 17.2 | 18.3 | 18.0 | 18.3 | 19.7 | 19.3 | 18.6 |
| MNHU 44685 | | | | | | | | | | |
| HC 19 | | | | | | | | | | |
| HC 30 | | | | | | | | | | |
| MCZ 18740 | 21.6 | 19.2 | 20.3 | 21.1 | 20.5 | 22.3 | 23.2 | 24.0 | 26.5 | 23.4 |
| DUPC 1972 | 16.6 | 17.0 | 16.5 | 17.4 | 16.9 | 20.7 | 21.8 | 20.9 | 20.4 | 21.1 |
| DUPC 1964 | 17.1 | 18.0 | 17.8 | 16.2 | 17.4 | 17.4 | 18.4 | 20.3 | 17.7 | 18.3 |
| DUPC 930 | | | | | | | | | | |
| HC 27 | | | | | | | | | | |
| USNM 317187 | | | | | | | | | | |
| MCZ 36116 | | | | | | | | | | |
| MCZ 422 | 19.9 | 19.5 | 20.4 | 21.7 | 20.5 | 25.6 | 24.6 | 26.3 | 33.9 | 26.4 |
| DUPC 725 | 16.8 | 16.9 | 16.3 | 17.1 | 16.7 | 19.0 | 20.3 | 20.1 | 20.0 | 19.4 |
| HC 31 | 17.1 | 17.5 | 16.5 | 17.3 | 17.1 | 17.7 | 20.4 | 18.3 | 21.0 | 18.2 |
| USNM 365721 | 19.7 | 17.4 | 16.8 | 19.0 | 18.3 | 19.4 | 18.3 | 17.8 | 18.9 | 18.4 |
| CT OA | 15.9 | 17.2 | 16.6 | 17.0 | 16.6 | 19.2 | 19.2 | 19.7 | 15.0 | 19.5 |
| MNHU 85197 | 18.5 | 19.0 | 19.4 | 21.6 | 19.6 | 20.7 | na | 25.2 | 22.3 | 20.9 |
| HC 12 | | | | | | | | | | |
| HC 13 | 18.3 | 18.2 | 19.7 | 18.5 | 18.8 | 19.9 | 20.9 | 21.8 | 21.1 | 20.5 |
| HC 14 | 20.3 | 18.1 | 17.9 | 17.6 | 18.4 | 19.9 | 20.8 | 23.7 | 25.3 | 21.0 |
| MNHU An11318 | | | | | | | | | | |
| DUPC 81 | 17.5 | 19.5 | 19.0 | 16.7 | 18.1 | na | 54.6 | 42.3 | na | 48.8 |
| HC 16 | 16.1 | 18.4 | 17.8 | 15.9 | 17.0 | na | 20.4 | 24.0 | na | 22.6 |
| HC 23 | | | | | | | | | | |

**Table C.24: Tibia collagen fiber orientation data Part I**
As per Table C.4.

| FAST Mean | PF Mean | HYB Mean | LAM Mean | LAM+HYB Mean |
|---|---|---|---|---|
| | | | | |
| | | | | |
| | | | | |
| | | | | |
| | | | | |
| 18.1 | 16.2 | 15.9 | 16.9 | 16.1 |
| 17.2 | 16.0 | 15.7 | 17.5 | 15.8 |
| | | | | |
| | | | | |
| 0.0 | 15.0 | 15.3 | 0.0 | 15.3 |
| 0.0 | 15.6 | 15.5 | 15.6 | 15.5 |
| | | | | |
| 18.3 | 16.5 | 17.2 | 21.4 | 18.8 |
| | | | | |
| | | | | |
| | | | | |
| 19.4 | 18.7 | 19.3 | 30.9 | 25.7 |
| 18.2 | 16.2 | 17.0 | 0.0 | 17.0 |
| 22.3 | 16.6 | 17.5 | 19.1 | 17.8 |
| | | | | |
| | | | | |
| | | | | |
| | | | | |
| 23.3 | 19.1 | 18.0 | 19.5 | 18.1 |
| 17.5 | 16.5 | 16.9 | 17.6 | 17.0 |
| 17.6 | 17.1 | 16.4 | 17.9 | 17.1 |
| 18.2 | 17.2 | 19.2 | 20.3 | 19.5 |
| 17.3 | 16.6 | 16.1 | 16.6 | 16.2 |
| 0.0 | 18.0 | 18.8 | 20.6 | 19.8 |
| | | | | |
| 0.0 | 17.2 | 17.9 | 21.6 | 19.8 |
| 0.0 | 17.7 | 17.6 | 21.3 | 18.8 |
| | | | | |
| 0.0 | 18.0 | 18.8 | 17.9 | 18.7 |
| 0.0 | 16.8 | 17.2 | 22.8 | 18.0 |
| | | | | |

**Table C.25: Tibia collagen fiber orientation data Part II**
As per Table C.5.

# Appendix D

# Imaging and Image Processing Functions

## D.1 Introduction

All images were acquired with the Leica-Leitz DMRX/E Universal Microscope, configured with a Marzhauser motorized stage and CPL filters and utilizing Syncroscopy Montage Explorer (Synoptics, Ltd.) image acquisition software according to the following protocols. These protocols may be adapted to any microscope and software setup with the requisite features.

## D.2 LM imaging

1. The desired specimen is placed on the stage (coverslipped with a drop of ethylene glycol).
2. Illumination is set to maximize visualization of bone features, with care taken not to over-illuminate (i.e., no white areas should appear within the bone).
3. The specimen is moved to a non-bone area and the "white balance" is set using Syncroscopy controls.
4. Shade correction may then be applied if there is visible error (e.g., a difference in color temperature from one side of the image to the other).
5. The entire specimen is then imaged. Subsequent specimens may be imaged within the same session without changing the "white balance" or applying a shade correction.

### D.3 Quantitative CPL imaging

1. A polarizer, analyzer, and two quarter-wave plates are aligned in the light path of the microscope as per Chapter 6.
2. A narrow band-pass green filter is placed in the light path positioned below all four CPL filters.
3. A 100 micron (±5 microns) turkey tendon slide is placed on the stage (coverslipped with a drop of ethylene glycol).
4. The slide is scanned to find a field of view where both brightest (indicating transverse collagen fibers) and darkest regions are represented, and lighting is then adjusted until the green band reading in Syncroscopy software shows a range of 5-250. This may require adjustment of other setup functions (e.g., "gain"). This image is then captured and saved for future imaging sessions.
5. The turkey tendon section is removed, and the desired specimen is placed on the stage (coverslipped with a drop of ethylene glycol).
6. The complete specimen is then imaged, *without adjustment of lighting or setup parameters*. Only the focus can be modified.
7. Additional specimens may subsequently be imaged.
8. For each new imaging session (i.e., when returning after the microscope has been turned off, or after an extended period without imaging), the previously captured turkey tendon image is loaded for viewing. The turkey tendon specimen is placed on the specimen stage and the field of view is matched to that of the saved image. Lighting is then adjusted as before.

9. CPL images to be used for visualization purposes only can be acquired without the green filter, and can be illuminated to best provide qualitative information regarding collagen fiber orientation.

**D.4 LM image processing**

1. Captured images are rotated to position the orientation dot (see Chapter 2) at the anterior midline (i.e., with equal maximum medial and lateral measurements from an anterior midline passing through the orientation dot). The rotation degrees are recorded to facilitate a matched rotation of CPL images.
2. Images are masked in Adobe Photoshop (8.0) by changing all non-bone areas to white, including vascular canals equal to or greater than a threshold Brush Tool diameter of nine pixels (for a 72 dpi image at 796 pixels/mm). A combination of the Eraser Tool, Brush Tool and Magic Wand Tool are used for the masking. In most cases, the periosteal and endosteal perimeters of the bone, as well as the vascular canals, must be masked with the Eraser Tool or Brush Tool.
3. An orientation guide (indicating 'anterior' and 'lateral') and .5mm scale is pasted into the corner of each masked image.

**D.5 CPL image processing**

1. CPL images (those acquired either with or without the green filter) are pasted in Photoshop over the rotated and masked LM images, on a separate layer.
2. The opacity of the CPL layer is reduced so that landmark features in the two images can be aligned (osteocyte lacunae, vascular canals, bone edges).

3. To achieve alignment, the CPL layer only is rotated (Edit>Transform>Rotate) to match the orientation of the LM images.
4. The white, non-bone mask of the LM image layer is selected (Select>Color Range>Fuzziness set to include all non-bone and exclude all bone).
5. This mask is copied and pasted onto a separate layer. This mask can remain white, or can be filled with black depending upon the intended use of the image (see Chapter 6). The LM layer is deleted, and the CPL and mask layers are flattened into a single layer.
6. An orientation guide and .5mm scale is pasted into the corner of each CPL image.

### D.6 Quantitative CPL look-up-table

1. Look-up-table (LUT) set-up:

| Pixel # | Color | R | G | B |
|---|---|---|---|---|
| 1 | Black | 0 | 0 | 0 |
| 2-32 | Dark Blue | 0 | 0 | 128 |
| 33-64 | Light Blue | 0 | 0 | 255 |
| 65-96 | Green | 0 | 255 | 0 |
| 97-128 | Yellow | 255 | 255 | 0 |
| 129-160 | Orange | 255 | 160 | 0 |
| 161-192 | Red | 255 | 0 | 0 |
| 193-224 | Pink | 255 | 160 | 160 |
| 225-255 | Gray | 200 | 200 | 200 |
| 256 | White | 255 | 255 | 255 |

**Table D.1: Look-up-table (LUT) set-up.**

2. See Chapter 6 for further details.

## References Cited

Abbott S, Trinkaus E, and Burr DB (1996) Dynamic bone remodeling in later Pleistocene fossil hominids. American Journal of Physical Anthropology *99:*585-601.

Acharjyo LN, and Misra R (1973) Notes on the birth and growth of a slow loris (*Nycticebus coucang*) in captivity. Journal of the Bombay Natural History Society *70:*193-195.

Aerts P (1998) Vertical jumping in *Galago senegalensis*: the quest for an obligate mechanical power amplifier. Philosophical Transactions of the Royal Society of London B *353:*1607-1620.

Amprino R (1946) La structure du tissue osseux envisagee comme expression de differences dans la vitesse de l'accroissement. Archives de Biologie *LVII:*315-330.

Amprino R (1948) A contribution to the functional meaning of the substitution of primary by secondary bone tissue. Acta Anatomica *5:*291-300.

Amprino R, and Godina G (1947) La struttura delle ossa nei vertebrati: ricerche comparative negli anfibi e negli amnioti. Commentationes Pontificia Accademia Delle Scienze *11(9)*:329-465.

Anemone RL (1990) The VCL hypothesis revisited: patterns of femoral morphology among quadrupedal and saltatorial prosimian primates. American Journal of Physical Anthropology *83(3)*:373-393.

Anemone RL (1993) The functional anatomy of the hip and thigh in primates. In DL Gebo (ed.): Postcranial Adaptation in Nonhuman Primates. DeKalb: Northern Illinois University Press, pp. 150-174.

Ardizzoni A (2001) Osteocyte lacunar size-lamellar thickness relationships in human secondary osteons. Bone *28*.

Ascenzi A (1988) The micromechanics versus the macromechanics of cortical bone – a comprehensive presentation. Journal of Biomechanical Engineering *110*:357-363.

Ascenzi A, and Benvenuti A (1986) Orientation of collagen fibers at the boundary betwen two successive osteonic lamellae and its mechanical interpretation. Journal of Biomechanics *19:*455-463.

Ascenzi A, and Bonucci E (1967) The tensile properties of single osteons. Anatomical Record *158:*375-386.

Ascenzi A, and Bonucci E (1968) The compressive properties of single osteons. Anatomical Record *161:*377-392.

Ascenzi A, and Bonucci E (1972) The shearing properties of single osteons. Anatomical Record *172:*499-510.

Ascenzi A, Bonucci E, and Simkin A (1973) An approach to the mechanical properties of single osteonic lamellae. Journal of Biomechanics *6:*227-235.

Ascenzi A, Benvenuti A, and Bonucci E (1982) The tensile properties of single osteonic lamellae: technical problems and preliminary results. Journal of Biomechanics *15*.

Ascenzi A, Bigi A, Ripamonti A, and Roveri N (1983) X-ray diffraction analysis of transversal osteonic lamellae. Calcified Tissue International *35:*279-283.

Ascenzi A, Boyde A, Portigliatti Barbos M, and Carando S (1987) Micro-biomechanics vs. macro-biomechanics in cortical bone. A micromechanical investigation of femurs deformed by bending. Journal of Biomechanics *20:*1045-1053.

Ascenzi M-G, Ascenzi A, Benvenuti A, Burghammer M, Panzavolta S, and Bigi A (2003) Structural differences between "dark" and "bright" isolated human osteonic lamellae. Journal of Structural Biology *141:*22-33.

Ascenzi M-G, and Lomovstev A (2006) Collagen orientation patterns in human secondary osteons, quantified in the radial direction by confocal microscopy. Journal of Structural Biology *153(1)*:14-30.

Aubin J (1998) Advances in the oseoblast lineage. Biochemistry and Cell Biology *76:*899-910

Bateman N (1954) Bone growth: a study of the grey-lethal and microphthalmic mutants of the mouse. Journal of Anatomy *88(2)*:212-62.

Beard C (1993) Origin and evolution of gliding in early Cenozoic Dermoptera (Mammalia, Primatomorpha). In RDE MacPhee (ed.): Primates and Their Relatives in Phylogenetic Perspective. New York: Plenum Press, pp.63-90.

Beard KC, Krishtalka L, and Stucky RK (1991) First skulls of the early Eocene primate Shoshonius cooperi and the anthropoid-tarsier dichotomy. Nature *349(6304)*:64-67.

Bertram JEA, and Swartz SM (1991) The 'law of bone transformation': a case of crying Wolff? Biological Review *66:*245-273.

Biewener A (1989a) Mammalian terrestrial locomotion and size. BioScience *39:*776-790.

Biewener AA (1989b) Scaling body support in mammals: limb posture and muscle mechanics. Science *245:*45-48.

Biewener AA (1990) Biomechanics of mammalian terrestrial locomotion. Science *250:*1097-1103.

Biewener A (1991) Musculoskeletal design in relation to body size. Journal of Biomechanics *24:*19-29.

Biewener A (1992) Overview of structural mechanics. In A Biewener (ed.): Biomechanics -- Structures and Systems: A Practical Approach. Oxford: Oxford University Press, pp. 1-20.

Biewener AA (2002) Future directions for the analysis of musculoskeletal design and locomotor performance. Journal of Morphology *252*:38-51.

Biewener AA (2005) Biomechanical consequences of scaling. Journal of Experimental Biology *208(Pt 9)*:1665-76. Review.

Biewener AA, and Bertram JEA (1994) Structural response of growing bone to exercise and disuse. Journal of Applied Physiology *76:*946-55.

Biewener AA, Swartz SM, and Bertram JEA (1986) Bone modeling during growth: dynamic strain equilibrium in the chick tibiotarsus. Calcified Tissue International *39:*390-395.

Blob R, and Biewener A (1999) *In vivo* locomotor strain in the hindlimb bones of *Alligator mississippiensis* and *Iguana iguana*: implications for the evolution of limb bone safety factor and non-sprawling limb posture. Journal of Experimental Biology *202:*1023-1046.

Bock WJ (1977) Adaptation and the comparative method. In M Hecht and e al. (eds.): Major Patterns in Vertebrate Evolution. New York: Plenum, pp. 57-82.

Bock WJ (1991) Explanations in konstruktionsmorphologie and evolutionary morphology. In N Schmidt-Kittler and K Vogel (eds.): Constructional Morphology and Evolution. Berlin: Springer-Verlag, pp. 9-29.

Boinski S (1989) The positional behavior and substrate use of squirrel monkeys: ecological implications. Journal of Human Evolution *18*:659-677.

Bonis Ld, Lebeau M, and Ricqles Ad (1972) Etude de la repartition des types de tissues osseux chez les vertebres tetrapodes au moyen de l'analyse factorielle des correspondences. Comptes Rendus de L'Academie des Sciences, Serie D *274:*3084-3087.

Bonucci E (1984) The structural basis of calcification. In A Ruggeri and PM Motta (eds.): Ultrastructure Of the Connective Tissue Matrix. Boston: Martinus Nijhoff Publishers, pp.165-191.

Botha J, and Chinsamy A (2000) Growth patterns deduced from the bone histology of the cynodonts *Daidemodon* and *Cynognathus*. Journal of Vertebrate Paleontology *20(4)*:705-711.

Bouvier M, and Hylander WL (1981) Effect of bone strain on cortical bone structure in macaques (*Macaca mulatta*). Journal of Morphology *167:*1-12.

Boyde A (1972) Scanning electron microscope studies of bone. In GH Bourne (ed.): The Biochemistry and Physiology of Bone. New York: Academic Press, pp. 259-310.

Boyde A (1980) Electron microscopy of the mineralizing front. Metabolic Bone Disease and Related Research *2S:*69-78.

Boyde A, and Jones S (1998) Aspects of anatomy and devlopment of bone. In M Zaidi (ed.): Advances in Organ Biology, Volume 5A. Stamford: JAI Press Inc., pp. 3-44.

Boyde A, and Riggs CM (1990) The quantitative study of the orientation of collagen in compact bone slices. Bone *11:*35-39.

Boyde A, Bianco P, Portigliatti-Barbos M, and Ascenzi A (1984) Collagen orientation in compact bone. I. A new method for the determination of the proportion of collagen parallel to the plane of compact bone sections. Metabolic Bone Disease and Related Research *5*:299-307.

Bromage TG (1986) A comparative scanning electron microscope study of facial growth and remodeling in early hominids. PhD diss., University of Toronto.

Bromage TG (1992) Microstructural organization and biomechancs of the macaque circumorbital region. In P Smith P and E Tchernov (eds.): Structure, Function and Evolution of Teeth. London: Freund Publishing House, p 257–272.

Bromage TG, and Boyde A (n.d.) Preferential intracortical remodeling and growth of the macaque mandible: developmental constraints on growth and adaptation of bone.

Bromage TG, Goldman HM, McFarlin SC, Warshaw JW, Boyde A, and Riggs CM (2003) Circularly polarized light standards for investigations of collagen fiber orientation in bone. The Anatomical Record (Part B: New Anatomist) *274B*:157-168.

Buffrénil Vde, and Pascal M (1984) Croissance et morphogenèse postnatales de la mandibule du Vison (Mustela vison Schreibner): donnes sur la dynamique et l'interprétation fonctionelle des depots osseux mandibulaires. Canadian Journal of Zoology *62*:2026-2037.

Burr DB (1979) Patterns of variability in mineralization of the primate femoral diaphysis. American Journal of Physical Anthropology *51:*219-32.

Burr D (1980) The relationships among physical, geometrical and mechanical properties of bone, with a note on the properties of nonhuman primate bone. Yearbook of Physical Anthropology *23:*109-146.

Burr DB (1992) Estimated intracortical bone turnover in the femur of growing macaques: implications for their use as models in skeletal pathology. Anatomical Record *232:*180-9.

Burr DB (1993) Remodeling and the repair of fatigue damage. Calcified Tissue International *53:*S75-S81.

Burr DB, Piotrowski G, Martin RB, and Cook PN (1982) Femoral mechanics in the lesser bushbaby (*Galago senegalensis*): structural adaptations to leaping in primates. Anatomical Record *202*:419-29.

Burr DB, Martin RB, Schaffler MB, and Radin EL (1985) Bone remodeling in response to *in vivo* fatigue microdamage. Journal of Biomechanics *18:*189-200.

Burr DB, Ruff CB, and Johnson C (1989a) Structural adaptations of the femur and humerus to arboreal and terrestrial environments in three species of macaque [published erratum appears in American Journal of Physical Anthropology 1989 Dec;80(4):501]. American Journal of Physical Anthropology *79:*357-67.

Burr DB, Schaffler MB, Yang KH, Wu DD, Lukoschek M, Kandzari D, Sivaneri N, Blaha JD, and Radin EL (1989b) The effects of altered strain environments on bone tissue kinetics. Bone *10:*215-21.

Burr DB, Schaffler MB, Yang KH, Lukoschek M, Sivaneri N, Blaha JD, and Radin EL (1989c) Skeletal change in response to altered strain environments: is woven bone a response to elevated strain? Bone *10:*223-33.

Burr DB, Turner CH, Naick P, Forwood MR, Ambrosius W, Hasan MS, and Pidaparti R (1998) Does microdamage accumulation affect the mechanical properties of bone? Journal of Biomechanics *31(4)*:337-45.

Burr DB, Hirano T, Turner CH, Hotchkiss C, Brommage R, and Hock JM (2001) Intermittently administered human parathyroid hormone(1-34) treatment increases intracortical bone turnover and porosity without reducing bone strength in the humerus of ovariectomized cynomolgus monkeys. Journal of Bone and Mineral Research *16(1)*:157-65.

Cant JGH, Youlatos D, and Rose MD (2001) Locomotor behavior if Lagothrix lagothricha and Ateles Belzebuth in Yasuni National Park, Ecuador: general patterns and nonsuspensory modes. Journal of Human Evolution *41*:141-166.

Carando S, Portigliatti Barbos M, Ascenzi A, and Boyde A (1989) Orientation of collagen in human tibial and fibular shaft and possible correlation with mechanical properties. Bone *10:*139-142.

Carando S, Portigliatti-Barbos M, Ascenzi A, Riggs CM, and Boyde A (1991) Macroscopic shape of, and lamellar distribution within, the upper limb shafts, allowing inferences about mechanical properties. Bone *12:*265-269.

Carter DR (1987) Mechanical loading history and skeletal biology. Journal of Biomechanics *20:*1095-1109.

Carter DR, Wong M, and Orr TE (1991) Musculoskeletal ontogeny, phylogeny, and functional adaptation. Journal of Biomechanics *24:*3-16.

Carter DR, van der Meulen MCH, and Beaupré GS (1996) Mechanical factors in bone growth and development. Bone *18:*5S-10S.

Castanet J, and Ricqles Ad (1986-87) Sur la relativite de la notion d'osteones primaires et secondaires et de tissus osseux primaire et secondaire en general. Annales des Sciences Naturelles, Zoologie, Paris 13e Serie *8:*103-109.

Castanet J, Grandin A, Abourachid A, and Ricqles Ad (1996) Expression of growth dynamic in the structure of the periosteal bone in the mallard *Anas platyrhynchos*. Comptes Rendus de l'Academie des Sciences de la Vie *319:*301-8.

Castanet J, Rogers KC, Cubo J, and Boisard JJ (2000) Periosteal bone growth rates in extant ratites (ostriche and emu). Implications for assessing growth in dinosaurs. Comptes Rendus de l'Academie des Sciences III *323(6)*:543-50.

Castanet J, Cubo J, and de Margerie E (2001) Significantion de l'histodiversité osseuse: le message de l'os. Biosystema – Systématique et Paléontologie *19*:133-147.

Castanet J, Croci S, Aujard F, Perret M, Cubo J, and Margerie Ed (2004) Lines of arrested growth in bone and age estimation in a small primate: *Microcebus murinus*. Journal of Zoology *263(1)*:31-39.

Chamay A, and Tschantz P (1972) Mechanical influences in bone remodeling, experimental research on Wolff's Law. Journal of Biomechanics *5:*173-180.

Charles-Dominique P (1971a) Eco-ethologie des prosimiens du Gabon. Revue Biologia Gabonica *7:*121-228.

Charles-Dominique P (1971b) Eco-ethologie et vie sociale des prosimiens du Gabon. Bull. Soc. Ecol. *II:*318-326.

Chiu C-H, and Hamrick MW (2002) Evolution and development of the primate limb skeleton. Evolutionary Anthropology *11:*94-107.

Cooper RR, Milgram JW, and Robinson RA (1966) Morphology of the osteon. Journal of Bone and Joint Surgery *48A:*1239-1271.

Covert HH, and Williams BA (1994) Recently recovered specimens of North American Eocene omomyids and adapids and their bearing on debates about Anthropoid origins. In JG Fleagle and RF Kay (eds.): Anthropoid Origins. New York: Plenum Press, pp. 29-54.

Cowles EA, DeRome ME, Pastizzo G, Brailley LL, and Gronowicz GA (1998) Mineralization and the expression of matrix proteins during *in vivo* bone development. Calcified Tissue International *62:*74-82.

Crawford GNC (1940) The evolution of the Haversian pattern. Journal of Anatomy 74:284-299.

Cubo J, Berge C, Quilhac A, Margerie Ed, and Castanet J (2002) Heterochronic patterns in primate evolution: evidence from endochondral ossification. European Journal of Morphology *40(2)*:81-8.

Currey JD (1960) Differences in the blood supply of bone of different histological types. Quarterly Journal of Microscopical Science *101:*351-370.

Currey JD (1964) Some effects of ageing on human Haversian systems. Journal of Anatomy (London) *98:*69-75.

Currey J (1968) The adaptation of bones to stress. Journal of Theoretical Biology *20:*91-106.

Currey J (1984) The Mechanical Adaptation of Bones. Princeton: Princeton University Press.

Currey JD (1999) The design of mineralized hard tissues for their mechanical functions. Journal of Experimental Biology *202:*3285-3294.

Curry K (1998) Histological quantification of growth rates in Apatosaurus. Journal of Vertebrate Paleontology *18(3)*:36A-37A.

Daegling DJ (2002) Estimation of torsional rigidity in primate long bones. Journal of Human Evolution *43:*229-239.

Dagosto M (1988) Implications of postcranial evidence for the origin of euprimates. Journal of Human Evolution *17:*35-56.

Dagosto M (1993) Postcranial anatomy and locomotor behavior in Eocene primates. In DL Gebo (ed.): Postcranial Adaptation in Nonhuman Primates. DeKalb: Northern Illinois University Press, pp. 199-219.

Dagosto M (1994) Testing positional behavior of Malagasy lemurs: a randomized approach. American Journal of Physical Anthropology *94:*189-202.

Dagosto M, and Gebo DL (1998) Methodological issues in studying positional behavior: meeting Ripley's challenge. In E Strasser, J Fleagle, A Rosenberger and H McHenry (eds.): Primate Locomotion: Recent Advances. New York: Plenum Press, pp. 5-29.

Delson E, and Rosenberger AL (1980) Phyletic perspectives on platyrrhine origins and anthropoid relationships. In RL Ciochon and AB Chiarelli (eds.): Evolutionary Biology of the New World Monkeys and Continental Drift. Plenum Publishing Corporation, pp. 445-458.

Delson E, Terranova CJ, Jungers WL, Sargis EL, Jablonski NG, and Dechow PC (2000) Body mass in Cercopithecidae (Primates, Mammalia): estimation and scaling in extinct and extant taxa. Anthropological Papers of the American Museum of Natural History *83*:1-159.

Demes B, and Gunther MM (1989) Biomechanics and allometric scaling in primate locomotion and morphology. Folia Primatologica *53:*125-141.

Demes B, and Jungers WL (1989) Functional differentiation of long bones in lorises. Folia Primatologica *52:*58-69.

Demes B, and Jungers WL (1993) Long bone cross-sectional dimensions, locomotor adaptations and body size in prosimian primates. Journal of Human Evolution *25(19)*:57-74.

Demes B, Jungers W, and Nieschalk U (1990) Size-and speed-related aspects of quadrupedal walking in slender and slow lorises. In F Jouffroy, M Stack and C Niemitz (eds.): Gravity, Posture and Locomotion in Primates. Firenze: Il Sedicesimo, pp. 175-197.

Demes B, Jungers WL, and Selpien K (1991) Body size, locomotion, and long bone cross-sectional geometry in indriid primates. American Journal of Physical Anthropology *86*:537-47.

Demes B, Jungers WL, Fleagle JG, Wunderlich RE, Richmond BG, and Lemelin P (1996) Body size and kinematics in Malagasy vertical clingers and leapers. Journal of Human Evolution *31(4)*:367-388.

Demes B, Fleagle JG, and Lemelin P (1998a) Myological correlates of prosimian leaping. Journal of Human Evolution *34(4)*:385-399.

Demes B, Stern JTJ, Hausman MR, Larson SG, McLeod KJ, and Rubin CT (1998b) Patterns of strain in the macaque ulna during functional activity. American Journal of Physical Anthropology *106*:87-100.

Demes B, Fleagle JG, and Jungers WL (1999) Takeoff and landing forces of leaping strepsirhine primates. Journal of Human Evolution *37:*279-292.

Demes B, Qin Y-X, Stern JTJ, Larson SG, and Rubin CT (2001) Patterns of strain in the macaque tibia during functional activity. American Journal of Physical Anthropology *116:*257-265.

Demeter G, and Mátyás J (1928) Mikroskopisch verleichend-anatomische Studien an Röhrenknochen mit besonderer Rucksicht auf die Unterscheidung menschlicher und tierischer Knochen. Zeitschrift fur Anatomie und Entwicklungsgeschichte *87:*45-99.

Doty SB (1981) Morphological evidence of gap junctions between bone cells. Calcified Tissue International *33(5)*:509-12.

Ducy P, Schinke T, and Karsenty G (2000) The osteoblast: a sophisticated fibroblast under central surveillance. Science *289:*1501-1504.

Dunbar DC (1988) Aerial maneuvers of leaping lemurs: the physics of whole-body rotations while airborne. American Journal of Physical Anthropology *16:*291-303.

Dykyj D (1980) Locomotion of the slow loris in a designed substrate context. American Journal of Physical Anthropology *52:*577-586.

Enlow DH (1962a) Functions of the Haversian system. American Journal of Anatomy *110*:269-305.

Enlow DH (1962b) A study of the postnatal growth and remodeling of bone. American Journal of Anatomy *110*:79-101.

Enlow DH (1963) Principles of Bone Remodeling. Springfield: Charles C. Thomas.

Enlow DH (1966) An evaluation of the use of bone histology in forensic medicine and anthropology. In FG Evans (ed.): Studies on the Anatomy and Function of Bone and Joints. New York: Springer-Verlag, pp. 93-112.

Enlow DH (1968) Wolff's law and the factor of architectonic circumstance. American Journal of Orthodontics *54:*803-822.

Enlow DH (1976) The remodeling of bone. Yearbook of Physical Anthropology *20*:19-34.

Enlow DH (1982) Handbook of Facial Growth. Philadelphia: W.B. Saunders Company.

Enlow DH, and Brown SO (1956) A comparative histological study of fossil and recent bone tissues. Part I. Texas Journal of Science *VIII:*405-443.

Enlow HM, and Brown SO (1957) A comparative histological study of fossil and recent bone tissues. Part II. Texas Journal of Science *IX:*186-214.

Enlow DH, and Brown SO (1958) A comparative histological study of fossil and recent bone tissues. Part III. Texas Journal of Science *X:*187-230.

Enlow DH, and Hans MG (1996) Essentials of Facial Growth. Philadelphia: W.B. Saunders Company.

Epker B, N., and Frost HM (1965) A histological study of remodeling at the periosteal, haversial canal, cortical endosteal, and trabecular endosteal surfaces in human rib. Anatomical Record *152:*129-136.

Ericksen MF (1991) Histologic estimation of age at death using the anterior cortex of the femur. American Journal of Physical Anthropology *84(2)*:171-9.

Erickson GM, and Tumanova TA (2000) Growth curve of *Psittacosaurus mongoliensis* Osborn (Ceratopsia: Psittacosauridae) inferred from long bone histology. Zoological Journal of the Linnean Society *130*:551-566.

Erickson GM, Rogers KC, and Yerby SA (2001) Dinosaurian growth patterns and rapid avian growth rates. Nature *412(6845)*:429-33.

Evans G, and Bang S (1967) Differences and relationships between the physical properties and the microscopic structure of human femoral, tibial and fibular cortical bone. American Journal of Anatomy *120:*79-88.

Evans FG, and Riolo ML (1970)Relations between the fatigue life and histology of adult human cortical bone. Journal of Bone and Joint Surgery – American Volume *52(8)*:1579-86.

Evans FG, and Vincentelli R (1969) Relation of collagen fiber orientation to some mechanical properties of human cortical bone. Journal of Biomechanics *2*:63-71.

Evans FG, and Vincentelli R (1974) Relations of the compressive properties of human cortical bone to histological structure and calcification. Journal of Biomechanics *7*:1-10.

Falsetti AB, and Cole TMI (1992) Relative growth of the postcranial skeleton in callitrichines. Journal of Human Evolution *23:*79-92.

Feik SA, Thomas CDL, and Clement JG (1997) Age-related changes in cortical porosity of the midshaft of the human femur. Journal of Anatomy *191:*407-416.

Fleagle JG (1985) Size and adaptation in primates. In WL Jungers (ed.): Size and Scaling in Primate Biology. New York: Plenum Press.

Fleagle JG (1998) Primate Adaptation and Evolution, Second Edition. San Diego, Academic Press.

Fleagle JG, and Mittermeier RA (1980) Locomotor behavior, body size, and comparative ecology of seven Surinam monkeys. American Journal of Physical Anthropology *52:*301-314.

Fleagle JG, Kay RF, and Anthony MRL (1997) Fossil New World monkeys. In RF Kay, RH Madden, RL Cifelli and JJ Flynn (eds.): Vertebrate Paleontology in the Neotropics: The Miocene Fauna of La Venta, Colombia. Washington, DC: Smithsonian Institution Press, pp. 473-495.

Fontaine R (1990) Positional behavior in *Saimiri boliviensis* and *Ateles geoffroyi*. American Journal of Physical Anthropology *82:*485-508.

Foote J (1913) The comparative histology of the femur. Smithsonian Miscellaneous Collections *61*:1-9.

Foote J (1916) A contribution to the comparative histology of the femur. Smithsonian Contributions to Knowledge *35*(3).

Ford SM (1988) Postcranial adaptations of the earliest platyrrhine. Journal of Human Evolution *17:*155-192.

Francillion-Vieillot H, de Buffrenil V, Castanet J, Geraudie J, Meunier FJ, Sire JY, Zylberberg L, and de Ricqles A (1990) Microstructure and mineralization of vertebrate skeletal tissues. In JG Carter (ed.): Skeletal Biomineralization: Patterns, Processes and Evolutionary Trends. New York: Van Nostrand Reinhold, pp. 471-530.

Frasca P, Harper RA, and Katz JL (1978) Mineral and collagen fiber orientation in human secondary osteons. Journal of Dental Research *57:*526-533.

Frost HM (1963) Bone Remodeling Dynamics. Springfield: Thomas.

Frost HM (1986) Intermediary Organization of the Skeleton, Volume 1. Boca Raton: CRC Press, Inc.

Galliari CA (1988) A study of postnatal appendicular maturation in captive-born squirrel monkeys (*Saimiri boliviensis*). American Journal of Primatology *16*:51-61.

Garber PA, and Leigh SR (1997) Ontogenetic variation in small-bodied New World Primates: Implications for patterns of reproduction and infant care. Folia Primatologica *68:*1-22.

Gebhardt W (1905) Über funktionell wichtige Anordnungsweisen der feineren und gröberen Bauelemente des Wirbeltierknochens. Arch. Entwickl. Org. *20*:187-322.

Gebo DL (1987) Locomotor diversity in prosimian primates. American Journal of Primatology *13:*271-281.

Gebo DL, and Dagosto M (1988) Foot anatomy, climbing, and the origin of the Indriidae. Journal of Human Evolution *17:*135-154.

Genoud M, Martin RD, and Glaser D (1997) Rate of metabolism in the smallest simian primate, the pygmy marmoset (*Cebuella pygmaea*). American Journal of Primatology *41(3)*:229-245.

Giraud-Guille MM (1988) Twisted plywood architecture of collagen fibrils in human compact bone osteons. Calcified Tissue International *42:*167-180.

Glassman D, and Wells J (1984) Positional and activity behavior in a captive slow loris: a quantitative assessment. American Journal of Primatology *7:*121-132.

Godfrey LR (1988) Adaptive diversification of Malagasy strepsirrhines. Journal of Human Evolution *17:*93-134.

Godfrey LR, Samonds KE, Jungers WL, and Sutherland MR (2001) Teeth, brains, and primate life histories. American Journal of Physical Anthropology *114:*192-214.

Godfrey LR, Samonds KE, Jungers WL, Sutherland MR, and Irwin MT (2004) Ontogenetic correlates of diet in Malagasy lemurs. American Journal of Physical Anthropology *123*:250-276.

Godinot M (1990) An introduction to the history of primate locomotion. In FK Jouffroy, MH Stack and C Niemitz (eds.): Gravity, Posture and Locomotion in Primates. Firenze: Il Sedicesimo, pp. 45-60.

Goldman HM (2001) Histocomposition and Geometry at the Human Mid-shaft Femur. PhD diss., The City University of New York.

Goldman H, Kindsvater J, and Bromage T (1998) Correlative light and backscattered electron microscopy of bone--Part I: Specimen preparation methods. Scanning *21:*40-43.

Goldman HM, Blayvas A, Boyde A, Howell PGT, Clement JG, and Bromage TG (2000) Correlative light and backscattered electron microscopy of bone -- Part II: Automated image analysis. Scanning *22:*337-344.

Goldman HM, Bromage TG, Thomas CD, Clement JG (2003) Preferred collagen fiber orientation in the human mid-shaft femur. Anatomical Record Part A *272(1*):434-45.

Greenberg GL, and Boyde A (1997) Convenient and controllable direct-view 3D imaging in conventional light microscopes: approaches via illumination and inspection. Proceedings of the Royal Microscopical Society *32(2)*:87-101.

Hall-Craggs ECB (1974) Physiological and histochemical parameters in comparative locomotor studies. In RD Martin, GA Doyle and AC Walker (eds.): Prosimian Biology. London: Duckworth, pp. 829-845.

Hamrick M (1999a) Development of epiphyseal structure and function in *Didelphis virginiana* (Marsupiala, Didelphidae). Journal of Morphology *239:*283-296.

Hamrick MW (1999b) A chondral modeling theory revisited. Journal of Theoretical Biology *201:*201-208.

Hamrick MW (2001) Primate origins: evolutionary change in digital ray patterning and segmentation. Journal of Human Evolution *40*:339-351.

Hamrick MW (2002) Developmental mechanisms of digit reduction. Evolution & Development *4:*247-248.

Hamrick MW, McPherron AC, Lovejoy CO, and Hudson J (2000) Femoral morphology and cross-sectional geometry of adult myostatin-deficient mice. Bone *27:*343-349.

Han Z-H, Palnitkar S, Sudhaker Rao D, Nelson D, and Parfitt AM (1997) Effects of ethnicity and age or menopause on the remodeling and turnover of iliac bone: implications for mechanisms of bone loss. Journal of Bone and Mineral Research *12:*498-508.

Haring DM, and Wright PC (1989) Hand-raising a Philippine tarsier, *Tarsius syrichta*. Zoo Biology *8*:265-274.

Hartwig WC (1994) Patterns, puzzles and perspectives on platyrrhine origins. In RS Corruccini and RL Ciochon (eds.): Integrative Paths to the Past: Paleoanthropological Advances in Honor of F. Clark Howell. Englewood Cliffs: Prentice Hall, pp. 69-93.

Hartwig WC (1996) Perinatal life history traits in New World monkeys. American Journal of Primatology *40:*99-130.

Harvey PH, and Clutton-Brock TH (1985) Life history variation in primates. Evolution *39:*559-581.

Harvey PH, Martin RD, and Clutton-Brock TH (1987) Life histories in comparative perspective. In BB Smuts, DL Cheney, RM Seyfarth, RW Wrangham and TT Struhsaker (eds.): Primate Societies. Chicago and London: The University of Chicago Press.

Hofmann T, Heyroth F, Meinhard H, Fränzel W, and Raum K (2006) Assessment of composition and anisotropic elastic properties of secondary osteon lamellae. Journal of Biomechanics *39(12)*:2282-2294.

Horner JR, and Padian K (2004) Age and growth dynamics of *Tyrannosaurus rex*. Proceedings of the Royal Society of London Series B-Biological Sciences *271(1551)*:1875-80.

Horner JR, de Ricqles A, and Padian K (2000) Long bone histology of the hadrosaurid dinosaur *Maiasaura peeblesorum*: growth dynamics and physiology based on an ontogenetic series of skeletal elements. Journal of Vertebrate Paleontology *20*:115-129.

Ishida H, Hirasaki E, and Matano S (1992) Locomotion of the slow loris betwen discontinuous substrates. In S Matano, R Tuttle, H Ishida and M Goodman (eds.): Topics in Primatology, Volume 3: Evolutionary Biology, Reproductive Endocrinology, and Virology. Tokyo: University of Tokyo Press, pp. 139-152.

Ishida H, Jouffroy F, and Nakano Y (1990) Comparative dynamics of pronograde upside down horizontal quadrupedalism in the slow loris (*Nycticebus coucang*). In F Jouffroy, M Stack and C Niemitz (eds.): Gravity, Posture and Locomotion in Primates. Firenze: Il Sedicesimo, pp. 209-220.

Jenkins FA Jr, Dombrowski PJ, and Gordon EP (1978) Analysis of the shoulder in brachiating spider monkeys. American Journal of Physical Anthropology *48*:65-76.

Jerome CP, and Peterson PE (2001) Nonhuman primate models in skeletal research. Bone *29(1)*:1-6.

Joffe TH (1997) Social pressures have selected for an extended juvenile period in primates. Journal of Human Evolution *32:*593-605.

Johnson SE, and Shapiro LJ (1998) Positional behavior and vertebral morphology in atelines and cebines. American Journal of Physical Anthropology *105:*333-354.

Jolly CJ, and Gorton AT (1974) Proportions of the extrinsic foot muscles in some lorisid prosimians. In RD Martin, GA Doyle and AC Walker (eds.): Prosimian Biology. London: Duckworth, pp. 801-815.

Jones S, and Boyde A (1976) Is there a relationship between osteoblasts and collagen orientation in bone? Israel Journal of Medical Sciences *12:*98-107.

Jouffroy FK (1975) Osteology and myology of the lemuriform postcranial skeleton. In I Tattersal and RW Sussman (eds.): Lemur Biology. New York: Plenum Press, pp. 149-192.

Jouffroy FK, and Lessertisseur J (1979) Relationships between limb morphology and locomotor adaptations among prosimians: an osteometric study. In ME Morbeck, H Preuschoft and N Gomberg (eds.): Environment, Behavior, and Morphology: Dynamic Interactions in Primates. New York: Gustav Fischer, pp. 143-181.

Jouffroy F, and Petter A (1990) Gravity-related kinematic changes in lorisine horizontal locomotion in relation to position of the body. In F Jouffroy, M Stack and C Niemitz (eds.): Gravity, Posture and Locomotion in Primates. Firenze: Il Sedicesimo, pp. 199-208.

Jouffroy FK, and Stern JTJ (1990) Telemetered EMG study of the antigravity versus propulsive actions of knee and elbow muscles in the slow loris. In FK Jouffroy, MH Stack and C Neimitz (eds.): Gravity, Posture and Locomotion in Primates. Firenze: Il Sedicesimo, pp. 221-236.

Jouffroy FK, Gasc JP, Decombas M, and Oblin S (1974) Biomechanics of vertical leaping from the ground in Galago alleni: a cineradiographic analysis. In RD Martin, GA Doyle and AC Walker (eds.): Prosimian Biology. London: Duckworth, pp. 817-827.

Jouffroy F, Renous S, and Gasc J (1983) Etude cineradiographique des deplacements du membre anterieur du potto de Bosman (*Perodicticus potto*, P.L.S. Muller, 1766) au cours de la marche quadrupede sur une branche horizontale. Annales des Sciences Naturelles, Zoologie, Paris *5*:75-87.

Jouffroy FK, Berge C, and Niemitz C (1984) Comparative study of the lower extremity in the genus *Tarsius*. In C Niemitz (ed.): Biology of the Tarsiers. New York: Gustav Fischer Verlag, pp. 167-190.

Jowsey J (1966) Studies of Haversian systems in man and some animals. Journal of Anatomy *100:*857-864.

Jowsey J (1968) Age and species differences in bone. Cornell Veterinarian *58:*74-94.

Jungers WL (1985) Body size and scaling of limb proportions in primates. In WL Jungers (ed.): Size and Scaling in Primate Biology. New York: Plenum Press, pp. 345-381.

Jungers WL, and Minns RJ (1979) Computed tomography and biomechanical analysis of fossil long bones. American Journal of Physical Anthropology *50:*285-290.

Kaack B, Walker L, and Brizzee KR (1979) The growth and development of the squirrel monkey (*Saimiri sciureus*). Growth *43*:116-135.

Kalmey JK (2000) Collagen Fiber Orientation and Locomotor Loading in Primates, Kent State University.

Kalmey JK, and Lovejoy CO (2002) Collagen fiber orientation in the femoral necks of apes and humans: do their histological structures reflect differences in locomotor loading? Bone *31(2)*:327-332.

Kappeler PM (1996) Causes and consequences of life-history variation among strepsirhine primates. American Naturalist *148:*868-891.

Kappeler PM (1998) Nests, tree holes, and the evolution of primate life histories. American Journal of Primatology *46:*7-33.

Kappeler PM (2000) Lemur origins: rafting by groups of hibernators? Folia Primatologica *71*:422-425.

Kay RF, Thorington RWJ, and Houde P (1990) Eocene plesiadapiform shows affinities with flying lemurs not primates. Nature *345:*342-344.

Kay RF, Thewissen JGM, and Yoder AD (1992) Cranial anatomy of *Ignacius graybullianus* and the affinities of the Plesiadapiformes. American Journal of Physical Anthropology *89(4)*:477-498.

Kerley ER (1965) The microscopic determination of age in human bone. American Journal of Physical Anthropology *23(2)*:149-63.

Kimura T (2002) Primate limb bones and locomotor types in arboreal or terrestrial environments. Zeitschrift für Morphologie und Anthropologie *83:*201-219.

Kimura T (2003) Differentiation between fore- and hindlimb boes and locomotor behavior in primates. Folia Primatologica *74:*17-32.

King SJ (2003) An evolutionary perspective on differential craniodental and postcranial growth and development in primates. PhD diss., University of Massachusetts.

King SJ, Godfrey LR, and Simons EL (2001) Adaptive and phylogenetic significance of ontogenetic sequences in *Archaeolemur*, subfossil lemur from Madagascar. Journal of Human Evolution *41:*545-576.

Kingsmill VJ, and Boyde A (1998) Variation in the apparent density of human mandibular bone with age and dental status. Journal of Anatomy *192(Pt 2)*:233-244.

Kirkwood JK (1985) Patterns of growth in primates. Journal of Zoology, London (A) *205:*123-136.

Klevezal GA (1996) Recording structures of mammals. Determination of age and reconstruction of life history. Rotterdam:A.A. Balkema.

Kodama Y, Dimai HP, Wergedal J, Sheng M, Malpe R, Kutilek S, Beamer W, Donahue LR, Rosen C, Baylink DJ, and Farley J (1999) Cortical tibial bone volume in two strains of mice: effects of sciatic neurectomy and genetic regulation of bone reponse to mechanical loading. Bone *25:*183-190.

Kohn LAP, Olson P, and Cheverud JM (1997) Age of epiphyseal closure in tamarins and marmosets. American Journal of Primatology *41:*129-139.

Kozlowski J, and Weiner J (1997) Interspecific allmometries are by-products of body size optimization. American Naturalist *149:*352-380.

Krause DW (1991) Were paromomyids gliders? Maybe, maybe not. Journal of Human Evolution *21*:177-188.

Krishtalka L (1978) Paleontology and geology of the Badwater Creek area, central Wyoming. Part 15. Review of the late Eocene primates from Wyoming and Utah, and the Plesitarsiiformes. Annals of the Carnegie Museum *47(15)*:335-360.

Krishtalka L, and Schwartz JH (1978) Phylogenetic relationships of plesiadapiform-tarsiiform primates. Annals of the Carnegie Museum *47*:515-540.

Lanyon LE (1984) Functional strain as a determinant for bone remodeling. Calcified Tissue International *36:*S56-S61.

Lanyon LE (1986) Biomechanical factors in adaptation of bone structure to function. In? (ed.): Current Concepts of Bone Fragility. Berlin: Springer-Verlag, pp. 19-33.

Lanyon LE (1987) Functional strain in bone tissue as an objective, and controlling stimulus for adaptive bone remodelling. Journal of Biomechanics *20:*1083-1093.

Lanyon LE (1993) Osteocytes, strain detection, bone modeling and remodeling. Calcified Tissue International *53:*S102-S107.

Lanyon LE, and Rubin CT (1985) Functional adaptation in skeletal structures. In M Hildebrand, DM Bramble, KF Liem and DB Wake (eds.): Functional Vertebrate Morphology. Cambridge: Harvard University Press, pp. 1-25.

Lanyon LE, Goodship AE, Pye CJ, and MacFie JH (1982) Mechanically adaptive bone remodelling. Journal of Biomechanics *15:*141-154.

Lee AH (2004) Histological organization and its relationship to function in the femur of *Alligator mississippiensis.* Journal of Anatomy *204*:197–207

Leigh SR (1992) Patterns of variation in the ontogeny of primate body size dimorphism. Journal of Human Evolution *23:*27-50.

Leigh SR, and Terranova CJ (1998) Comparative perspectives on bimaturism, ontogeny, and dimorphism in lemurid primates. International Journal of Primatology *19:*723-749.

Leonard WR, Robertson ML, Snodgrass JJ, and Kuzawa CW (2003) Metabolic correlates of hominid brain evolution. Comparative Biochemistry and Physiology Part A *136:*5-15.

Lieberman DE (1996) How and why humans grow thin skulls: experimental evidence for systemic robusticity. American Journal of Physical Anthropology *101:*217-236.

Lieberman DE, and Crompton AW (1998) Responses of bone to stress: constraints on symmorphosis. In ER Weibel, CR Taylor and L Bolis (eds.): Principles of Animal

Design: The Optimization and Symmorphosis Debate. Cambridge: Cambridge University Press, pp. 78-86.

Lieberman DE, and Pearson OM (2001) Trade-off between modeling and remodeling responses to loading in the mammalian limb. Bulletin of the Museum of Comparative Zoology. *156*:269-282.

Long JO, and Cooper RW (1968) Physical growth and dental eruption in captive-bred squirrel monkeys, *Saimiri sciureus* (Leticia, Columbia). In LA Rosenblum and RW Cooper (eds.): The Squirrel Monkey. New York: Academic Press, pp. 193-205.

Lovejoy CO, Cohn MJ, and White TD (1999) Morphological analysis of the mammalian postcranium: a developmental perspective. Proceedings of the National Academy of Sciences USA *96:*13247-13252.

Manocha SL (1979) Physical growth and brain development of captive-bred male and female squirrel monkeys, *Saimiri sciureus*. Experientia *35*:96-98.

Margerie Ed (2002) Laminar bone as an adaptation to torsional loads in flapping flight. Journal of Anatomy *201(6)*:521-526.

Margerie Ed, Cubo J, and Castanet J (2002) Bone typology and growth rate: testing and quantifying 'Amprino's rule' in the mallard (*Anas platyrhynchos*). Comptes Rendus Biologies *325*:221–230

Margerie Ed, Robin JP, Vernier D, Cubo J, Groscolas, R, and Castanet J (2004) Assessing a relationship between bone microstructure and growth rate: a fluorescent labelling study in the king penguin chick (*Aptenodytes patagonicus*). Journal of Experimental Biology *207(Pt 5)*:869-79.S

Margerie Ed, Sanchez S, Cubo J, and Castanet J (2005) Torsional resistance as a principal component of the structural design of long bones: comparative multivariate evidence in birds. The Anatomical Record Part A *282A:*49-66.

Marotti G (1993) A new theory of bone lamellation. Calcified Tissue International *53:*S47-S56.

Marotti G, and Muglia M (1988) A scanning electron microscope study of human bony lamellae. Proposal for a new model of collagen lamellar organization. Archivio Italiano di Anatomia e di Embriologia *93:*163-173.

Marotti G, Ferretti M, Muglia MA, Palumbo C, and Palazzini S (1992) A quantitative evaluation of osteoblast-oteocyte relationships on growing endosteal surface of rabbit tibiae. Bone *13:*363-368.

Martin RB (1991) Determinants of the mechanical properties of bones [published erratum appears in J Biomech 1992 Oct;25(10):1251]. Journal of Biomechanics *24 Suppl 1:*79-88.

Martin RD (1992) Goeldi and the dwarfs: the evolutionary biology of the small New World monkeys. Journal of Human Evolution *22:*367-393.

Martin B (1993) Aging and strength of bone as a structural material. Calcified Tissue International *53:*S34-S40.

Martin RD (1995) Prosimians: from obscurity to extinction? In L Alterman, GA Doyle and MK Izard (eds.): Creatures of the Dark: The Nocturnal Primates. New York: Plenum Press, pp. 535-563.

Martin RB (2000a) Does osteocyte formation cause the nonlinear refilling of osteons? Bone *26:*71-78.

Martin RB (2000b) Toward a unifying theory of bone remodeling. Bone *26:*1-6.

Martin RB, and Burr DB (1989) Structure, Function, and Adaptation of Compact Bone. New York: Raven Press.

Martin RB, and Ishida J (1989) The relative effects of collagen fiber orientation, porosity, density, and mineralization on bone strength. Journal of Biomechanics *22:*419-26.

Martin RB, Burr DB, and Sharkey NA (1998) Skeletal Tissue Mechanics. New York, Springer.

Mason MW, Skedros JG, and Bloebaum RD (1995) Evidence of strain-mode-related cortical adaptation in the diaphysis of the horse radius. Bone *17(3)*:229-37.

Masters JC, Anthony NM, de Wit MJ, and Mitchell A (2005) Reconstructing the evolutionary history of the Lorisidae using morphological, molecular, and geological data. American Journal of Physical Anthropology *127(4)*:465-480.

McFarlin, SC (2006) Ontogenetic variation in long bone microstructure in catarrhines and its significance for life history research. PhD diss., The City University of New York.

McMahon JM, Boyde A, and Bromage TG (1995) Pattern of collagen fiber orientation in the ovine calcaneal shaft and its relation to locomotor-induced strain. Anatomical Record *242:*147-158.

McNab BK, and Wright PC (1987) Temperature regulation and oxygen consumption in the Philippine tarsier *Tarsius syrichta*. Physiological Zoology *60*:596-600.

Meldrum DJ, Dagosto M, and White J (1997) Hindlimb suspension and hind foot reversal in Varecia variegata and other arboreal mammals. American Journal of Physical Anthropology *103(1)*:85-102.

Mittermeier RA (1978) Locomotion and posture in *Ateles geoffroyi* and *Ateles paniscus*. Folia Primatologica *30*:161-193.

Moss ML (1964) The phylogeny of mineralized tissues. International Review of General and Experimental Zoology *1:*297-331.

Moss ML, and Cowin SC (1997) Mechanosensory mechanisms in bone. In R Lanza, R Langer and W Chick (eds.): Principles of Tissue Engineering. R. G. Landes Company, pp. 645-659.

Müller EF (1982) Heart rate in slow loris (*Nycticebus coucang*). Folia Primatologica *38:*250-258.

Nakatsukasa M, Takai M, and Setoguchi T (1997) Functional morphology of the postcranium and locomotor behavior of *Neosaimiri fieldsi*, a Saimiri-like middle Miocene platyrrhine. American Journal of Physical Anthropology *102(4)*:515-544.

Napier JR, and Napier PH (1967) A Handbook of Living Primates. London: Academic Press.

Napier JR, and Walker AC (1967) Vertical clinging and leaping -- a newly recognized category of locomotor behavior of primates. Folia Primatologica *6:*204-219.

Newell-Morris L, and Sirianni JE (1982) Parameters of bone growth in the fetal and infant macaque (*Macaca nemestrina*) humerus as documented by trichromatic bone labels. In AD Dixon and BG Sarnat (eds.): Factors and Mechanisms Influencing Bone Growth. New York: Alan R. Liss, Inc., pp. 243-258.

Niemitz C (1983) New results on the locomotion of *Tarsius bancanus*, Horsfield, 1821. Annales des Sciences Naturelles, Zoologie, Paris Series *13*:89-100.

Ortmann S, Heldmaier G, Schmid J, and Ganzhorn JU (1997) Spontaneous daily torpor in Malagasy mouse lemurs. Naturwissenschaften *84:*28-32.

Osaki S, Tohno S, Tohno Y, Ohuchi K, Takakura Y (2002) Determination of the orientation of collagen fibers in human bone. Anatomical Record *266(2)*:103-107.

Otter MW, Qin YX, Rubin CT, and McLeod KJ (1999) Does bone perfusion/reperfusion intiate bone remodeling and the stress fracture syndrome? Medical Hypotheses *53(5)*:363-368.

Owen M (1978) Histogenesis of bone cells. Calcified Tissue Research *25(3)*:205-7.

Oxnard CE (1973) Some locomotor adaptations among lower primates: implications for primate evolution. Symposia of the Zoological Society of London *33:*255-299.

Oxnard C, German R, and McArdle J (1981a) The functional morphometrics of the hip and thigh in leaping prosimians. American Journal of Physical Anthropology *54:*481-498.

Oxnard CE, German R, Jouffroy FK, and Lessertisseur J (1981b) A morphometric study of limb proportions in leaping prosimians. American Journal of Physical Anthropology *54:*421-430.

Padian K, Ricqles AJd, and Horner JR (2001) Dinosaurian growth rates and bird origins. Nature *412(6845):*405-8.

Paine RR, and Godfrey LR (1997) The scaling of skeletal microanatomy in non-human primates. Journal of Zoology, London *241:*803-821.

Palumbo C, Palazzini S, and Marotti G (1990) Morphological study of intercellular junctions during osteocyte differentiation. Bone *11:*401-406.

Pannarale L, Braidotti P, Alba Ld, and Gaudio E (1994) Scanning electron microscopy of collagen fiber orientation in the bone lamellar system in non-decalcified human samples. Acta Anatomica *151:*36-42.

Parfitt AM (1993) Bone age, mineral density, and fatigue damage. Calcified Tissue International *53:*S82-S86.

Parker ST (1999) The life history and development of great apes in comparative perspective. In ST Parker, RW Mitchell and HL Miles (eds.): The Mentalities of Gorillas and Orangutans: Comparative Perspectives. Cambridge: Cambridge University Press, pp. 43-69.

Partridge L, and Harvey PH (1988) The ecological context of life history evolution. Science *241:*1449-1455.

Peabody FE (1961) Annual growth zones in vertebrates (living and fossil). Journal of Morphology *108*:11-62.

Perret M, Aujard F, and Vannier G (1998) Influence of daylength on metabolic rate and daily water loss in the male prosimian primate *Microcebus murinus*. Comparative Biochemistry and Physiology Part A *119*:981-989.

Petter JJ, and Hladik CM (1970) Observations sure le domaine vital et la densité de population de Loris tardigradus dans les forêts de Ceylan. Mammalia *34:*394-409.

Pfeiffer S, Lazenby R, and Chiang J (1995) Brief communication: cortical remodeling data are affected by sampling location. American Journal of Physical Anthropology *96:*89-92.

Porter CA, Page SL, Czelusniak J, Schneider H, Schneider MPC, Sampaio I, and Goodman M (1997) Phylogeny and evolution of selected primates as determined by sequences of the e-globin locus and 5' flanking regions. International Journal of Primatology *18(2)*:261-295.

Portigliatti-Barbos M, Bianco P, and Ascenzi A (1983) Distribution of osteonic and interstitial components in the human femoral shaft with reference to structure, calcification and mechanical properties. Acta Anatomica *115:*178-186.

Portigliatti-Barbos M, Bianco P, Ascenzi A, and Boyde A (1984) Collagen orientation in compact bone. II. Distribution of lamellae in the whole of the human femoral shaft with reference to its mechanical properties. Metabolic Bone Disease & Related Research *5*:309-315.

Poux C, and Douzery EJP (2004) Primate phylogeny, evolutionary rate variations, and divergence times: a contribution from the nuclear gene IRBP. American Journal of Physical Anthropology *124(1)*:1-16.

Preuschoft H (1990) Gravity in primates and its relation to body shape and locomotion. In FK Jouffroy, MH Stack and C Niemitz (eds.): Gravity, Posture and Locomotion in Primates. Firenze: Il Sedicesimo.

Preuschoft H, Witte H, and Fischer M (1995) Locomotion in nocturnal primates. In L Alterman, G Doyle and M Izard (eds.): Creatrures of the Dark: The Nocturnal Prosimians. New York: Plenum Press, pp. 453-472.

Preuschoft H, Günther MM, and Christian A (1998) Size dependence in prosimian locomotion and its inplications for the distribution of body mass. Folia Primatologica *69:*60-81.

Pucciarelli HM, Mune MC, Oyhenart EE, Orden AB, Villanueva ME, Rodriguez RR, and Pons ER (2000) Growth of skeletal components in the young suirrel monkey (*Saimiri sciureus boliviensis*): a longitudinal experiment. American Journal of Physical Anthropology *112*:57-68.

Quekett J (1849) On the intimate structure on bone, as composing the skeleton in the four great classes of animals, viz., mammals, birds, reptiles, and fishes, with some remarks on the great value of the knowledge of such structure in determining the affinities of minute fragments of organic remains. Transactions of the Microscopical Society of London *2*:46-58.

Quekett J (1855) Descriptive and Illustrated Catalogue of the Histological Series Contained in the Museum of the Royal College of Surgeons of England. Prepared for the Microscope. London: Royal College of Surgeons.

Ramasamy JG, and Akkus O (2007) Local variations in the micromechanical properties of mouse femur: the involvement of collagen fiber orientation and mineralization. Journal of Biomechanics *40(4)*:910-918.

Rasmussen DT (1994) The different meanings of a tarsiois-anthropoid clade and a new model of anthropoid origin. In JF Fleagle and RF Kay (eds.): Anthropoid Origins. New York: Plenum Press, pp. 335-360.

Rasmussen DT, and Izard MK (1988) Scaling of growth and life history traits relative to body size, brain size, and metabolic rate in lorises and galagos (Lorisidae, Primates). American Journal of Physical Anthropology *75:*357-367.

Rasmussen DT, and Nekaris KA (1998) Evolutionary history of lorisiform primates. Folia Primatologica *69:*250-285.

Rasmussen DT, Conroy GC, and Simons EL (1998) Tarsier-like locomotor specializations in the Oligocene primate *Afrotarsius*. Proceedings of the National Academy of Sciences USA *95*:14848-14850.

Ravosa MJ, Meyers DM, and Glander KE (1993) Relative growth of the limbs and trunk in sifakas: heterochronic, ecological, and functional considerations. American Journal of Physical Anthropology *92*:499-520.

Reynolds TR (1985) Stresses on the limbs of quadrupedal primates. American Journal of Physical Anthropology *67:*351-62.

Rho J-Y, Kuhn-Spearing L, and Zioupos P (1998) Mechanical properties and the hierarchical structure of bone. Medical Engineering & Physics *20:*92-102.

Rho J-Y, Zioupos P, Currey JD, and Pharr GM (1999) Variations in the individual thick lamellar properties within osteons by nanoindentation. Bone *25:*295-300.

Richard AF, Dewar R, E., Schwartz M, and Ratsirarson J (2000) Mass change, environmental variability and female fetility in wild *Propithecus verreauxi*. Journal of Human Evolution *39*:381-391.

Ricqles Ad (1968) Recherches paleohistologiques sur les os longs des tetrapodes. I - Origine du tissue osseux plexiforme des dinosauriens sauropodes. Annales de Paleontologie (Vertebres) *54:*131-145.

Ricqles Ad (1969) Recherches paleohistologiques sur les os longs des tetrapodes. II - Quelques observations sur la structure des os longs des theriodontes. Annales de Paleontologie (Vertebres) *55:*1-52.

Ricqles Ad (1975) Recherches paleohistologiqus sur es os longs des tetrapodes. VII - Sur la classification, la signification fonctionelle et l'histoire des tissues osseux des tetrapodes (premiere partie). Annales de Paleontologie (Vertebres) *61:*51-129 (plus plates).

Ricqles Ad (1976) Recherches paleohistologiqus sur es os longs des tetrapodes. VII - Sur la classification, la signification fonctionelle et l'histoire des tissues osseux des tetrapodes (deuxieme partie). Annales de Paleontologie (Vertebres) *62:*71-126.

Ricqles Ad (1977a) Recherches paleohistologiqus sur es os longs des tetrapodes. VII - Sur la classification, la signification fonctionelle et l'histoire des tissues osseux des tetrapodes (deuxieme partie, fin). Annales de Paleontologie (Vertebres) *63:*133-160.

Ricqles Ad (1977b) Recherches paleohistologiqus sur es os longs des tetrapodes. VII - Sur la classification, la signification fonctionelle et l'histoire des tissues osseux des tetrapodes (deuxieme partie, suite). Annales de Paleontologie (Vertebres) *63:*33-56.

Ricqles Ad (1978a) Recherches paleohistologiqus sur es os longs des tetrapodes. VII - Sur la classification, la signification fonctionelle et l'histoire des tissues osseux des tetrapodes (troisieme partie). Annales de Paleontologie (Vertebres) *64:*85-111.

Ricqles Ad (1978b) Recherches paleohistologiqus sur es os longs des tetrapodes. VII - Sur la classification, la signification fonctionelle et l'histoire des tissues osseux des tetrapodes (troisieme partie, fin). Annales de Paleontologie (Vertebres) *64:*153-184.

Ricqles Ad (1980) Tissue structures of dinosaur bone: functional significance and possible relation to dinosaur physiology. In Thomas and Olson (eds.): A Cold Look at the Warm-Blooded Dinosaurs. Boulder: Westview Press.

Ricqles Ad (1992) Some remarks on palaeohistology from a comparative evolutionary point of view. In G Grupe and AN Garland (eds.): Histology of Ancient Human Bone: Methods and Diagnosis. Berlin: Springer-Verlag, pp. 37-77.

Ricqles Ad, Meunier F, Castanet J, and Francillon-Vieillot H (1991) Comparative microstructure of bone. In B Hall (ed.): Bone--Volume 3: Bone Matrix and Bone Specific Products. Boca Raton: CRC Press, pp. 1-78.

Ricqlès Ad, Padian K, Horner JR, and francillion-Vieillot H (2000) Palaeohistology of the bones of pterosaurs (Reptilia: Archosauria): anatomy, ontogeny, and biomechanical implications. Zoological Journal of the Linnean Society *129*:349-385.

Riggs CM, Lanyon LE, and Boyde A (1993a) Functional associations between collagen fiber orientation and locomotor strain direction in cortical bone of the equine radius. Anatomy and Embryology *187:*231-238.

Riggs CM, Vaughan LC, Evans GP, Lanyon LE, and Boyde A (1993b) Mechanical implications of collagen fibre orientation in cortical bone of the equine radius. Anatomy and Embrology *187:*239-248.

Rizzoli R, and Bonjour J-P (1999) Physiology of calcium and phosphate homeostasis. In MJ Seibel, SP Robins and JP Bilzekian (eds.): Dynamics of Bone and Cartilage Metabolism. San Diego: Academic Press, pp. 247-259.

Roberts M (1994) Growth, development, and parental care in the western tarsier (*Tarsius bancanus*) in capitivity: evidence for a "slow" life-history and nonmonogamous mating system. International Journal of Primatology *15*:1-28.

Robling AG, and Stout SD (1999) Morphology of the drifting osteon. Cells Tissues Organs *164:*192-204.

Roos C, Schmitz J, and Zischler H (2004) Primate jumping genes elucidate strepsirrhine phylogeny. Proceedings of the National Academy of Sciences USA *101(29)*: 10650–10654.

Rose MD (1993) Functional anatomy of the elbow and the forearm in primates. In DL Gebo (ed.): Postcranial Adaptation in Nonhuman Primates. Dekalb: Northern Illinois University Press, pp. 70-95.

Rosenberger A, L. (1992) Evolution of feeding niches in New World monkeys. American Journal of Physical Anthropology *88:*525-562.

Rosenberger AL (2002) Platyrrhine paleontology and systematics: the paradigm shifts. In WC Hartwig (ed.): The Primate Fossil Record. Cambridge: Cambridge University Press, pp. 151-159.

Rosenberger AL, and Szalay FS (1980) On the tarsiiform origins of Anthropoidea. In RL Ciochon and AB Chiarelli (eds.): Evolutionary Biology of the New World Monkeys and Continental Drift. New York: Plenum Press, pp. 139-157.

Ross C (1991) Life history patterns of New World monkeys. International Journal of Primatology *12:*481-502.

Ross C (1998) Primate life histories. Evolutionary Anthropology *6(2):*54-63.

Rossert J, and de Crombrugghe B (1996) Type I collagen: structure, synthesis, and regulation. In JP Bilzikian, LG Raisz and GA Rodan (eds.): Principles of Bone Biology. San Diego: Academic Press, pp. 127-142.

Rowe N (1995) The Pictorial Guide to the Living Primates. East Hampton: Pogonias Press.

Rubin CT, and Lanyon LE (1985) Regulation of bone mass by mechanical strain magnitude. Calcified Tissue International *37:*411-417.

Ruff CB (1983) The contribution of cancellous bone to long bone strength and rigidity. American Journal of Physical Anthropology *61:*141-3.

Ruff CB (1989) New approaches to structural evolution of limb bones in primates. Folia Primatologica (Basel) *53:*142-59.

Ruff CB (2003) Long bone articular and diaphyseal structure in Old World monkeys and apes II: estimation of body mass. American Journal of Physical Anthropology *120(1)*:16-37.

Ruff CB, and Hayes WC (1983a) Cross-sectional geometry of Pecos Pueblo femora and tibiae--a biomechanical investigation: II. Sex, age, side differences. American Journal of Physical Anthropology *60:*383-400.

Ruff CB, and Hayes WC (1983b) Cross-sectional geometry of Pecos Pueblo femora and tibiae--a biomechanical investigation: I. Method and general patterns of variation. American Journal of Physical Anthropology *60:*359-81.

Ruff C, and Runestad J (1992) Primate limb bone structural adaptations. Annual Review of Anthropology *21:*407-33.

Ruff C, Scott W, and Liu A (1991) Articular and diaphyseal remodeling of the proximal femur with changes in body mass in adults. American Journal of Physical Anthropology *86:*397-413.

Runestad JA (1997) Postcranial adaptations for climbing in Loridae (Primates). Journal of Zoology, London *242:*261-290.

Runestad Connour J, Glander K, and Vincent F (2000) Postcranial adaptations for leaping in primates. Journal of Zoology, London *251:*79-103.

Sacher GA, and Staffeldt EF (1974) Relation of gestation time to brain weight for placental mammals: Implications for the theoty of vertebrate growth. American Naturalist *108(963)*:593-615.

Sander PM (2000) Long bone histology of the Tendaguru sauropods: Implications for growth and biology. Paleobiology *26(3)*:466-488.

Schaffler MB, and Burr DB (1984) Primate cortical bone microstructure: relationship to locomotion. American Journal of Physical Anthropology *65:*191-197.

Schaffler MD, and Burr DB (1988) Stiffness of compact bone: effects of porosity and density. Journal of Biomechanics *21(1)*:13-6.

Schaffler MB, Burr DB, Jungers WL, and Ruff CB (1985) Structural and mechanical indicators of limb specialization in primates. Folia Primatologica (Basel) *45:*61-75.

Schaffler MB, Radin EL, and Burr DB (1989) Mechanical and morphological effects of strain rate on fatigue of compact bone. Bone *10:*207-14.

Schaffler MB, Radin EL, and Burr DB (1990) Long-term fatigue behavior of compact bone at low strain magnitude and rate. Bone *11:*321-326.

Schilling A, Richard J-P, and Servière J (2001) Effect of aging on circadian activity in gray mouse lemurs. International Journal of Primatology *22*:25-41.

Schmid J (1998) Daily torpor in mouse lemurs, *Microcebus* spp.: metabolic rate and body temperature (abstract). Folia Primatologica *69:*403.

Schmid J (2000) Daily torpor in the gray mouse lemur (*Microcebus murinus*) in Madagascar: energetic consequences and biological significance. Oecologia *123*:175-183.

Schmid J (2001) Daily torpor in free-ranging gray mouse lemurs (*Microcebus murinus*) in Madagascar. International Journal of Primatology *22:*1021-1031.

Schmid J, and Kappeler PM (1998) Fluctuating sexual dimorphism and differential hibernation by sex in a primate, the gray mouse lemur (*Microcebus murinus*). Behavioral Ecology and Sociobiology *43*:125-132.

Schmid J, and Speakman JR (2000) Daily energy expenditure of the grey mouse lemur (*Microcebus murinus*): a small primate that uses torpor. Journal of Comparative Physiology B *170*:633-641.

Schmidt-Nielsen K (1984) Scaling: Why is Animal Size So Important. Cambridge: Cambridge University Press.

Schmitz J, Roos C, and Zischler H (2005) Primate phylogeny: molecular evidence from retroposons. Cytogenetic and Genome Research *108(1-3)*:26-37.

Schneider I, Schneider H, Schneider MP, and Silva A (2004) The prion protein and New World primate phylogeny. Genetics and Molecular Biology *27(4)*:505-510.

Schulze H, and Meier B (1995) Behavior of captive *Loris tardigradus nordicus*: a qualitative description, including some information about morphological bases of behavior. In L Alterman, G Doyle and M Izard (eds.): Creatures of the Dark: The Nocturnal Primates. New York: Plenum Press, pp. 221-249.

Schwartz GT, Samonds KE, Godfrey LR, Jungers WL, and Simons EL (2002) Dental microstructure and life history in subfossil Malagasy lemurs. Proceedings of the National Academy of Sciences USA *99:*6124-6129.

Seeman E (1997) From density to structure: growing up and growing old on the surfaces of bone. Journal of Bone and Mineral Research *12:*509-521.

Shoshani J, Groves CP, Simons EL, and Gunnell GF (1996) Primate phylogeny: morphological vs molecular results. Molecular Phylogenetics and Evolution *5(1)*:102-154.

Silcox M (2002) The phylogeny and taxonomy of plesiadapiforms. American Journal of Physical Anthropology *Suppl. 34*:141-142.

Simkin A, and Robin G (1974) Fracture formation in differing collagen fiber pattern of compact bone. Journal of Biomechanics *7:*183-188.

Simmons NB (1993) The importance of methods: archontan phylogeny and cladistic analysis of morphological data. In RDE MacPhee (ed.): Primates and Their Relatives in Phylogenetic Perspectives. New York: Plenum Press, pp. 1-61.

Simons EL (1997) Discovery of the smallest Fayum Egyptian primates (Anchomomyini, Adapidae). Proceedings of the National Academy of Sciences USA *94*:180-184.

Simons EL, Rasmussen DT, and Gingerich PD (1995) New cercomoniine adapid from Fayum, Egypt. Journal of Human Evolution *29*:577-589.

Singer SS, Schmitz J, Schwiegk C, and Zischler H (2003) Molecular cladistic markers in New World monkey phylogeny (Platyrrhini, Primates). Molecular Phylogenetics and Evolution *26*:490–501.

Singh IJ, and Gunberg DL (1970) Estimation of age at death in human males from quantitative histology of bone fragments. American Journal of Physical Anthropology *33(3)*:373-81.

Singh IJ, Tonna EA, and Gandel CP (1974) A comparative histological study of mammalian bone. Journal of Morphology *144:*421-438.

Singh I, Sandhu H, and Herskovits M (1991) Bone vascularity. In B Hall (ed.): Bone--Volume 3: Bone Matrix and Bone Specific Products. Boca Raton: CRC Press, pp. 141-164.

Skedros JG, and Hunt KJ (2004) Does the degree of laminarity correlate with site-specific differences in collagen fibre orientation in primary bone? An evaluation in the turkey ulna diaphysis. Journal of Anatomy *205(2)*:121-34.

Skedros JG, Mason MW, and Bloebaum RD (1994) Differences in osteonal micromorphology between tensile and compressive cortices of a bending skeletal system: indications of potential strain-specific differences in bone microstructure. Anatomical Record *239:*405-413.

Skedros JG, Mason MW, Nelson MC, and Bloebaum RD (1996) Evidence of structural and material adaptation to specific strain features in cortical bone. Anatomical Record *246:*47-63.

Skedros JG, Mason MW, and Bloebaum RD (2001) Modeling and remodeling in a developing artiodactyl calcaneus: a model for evaluating Frost's Mechanostat hypothesis and its corollaries. Anatomical Record *263(2)*:167-85.

Skedros JG, Synrowsky CL, Parry TR, and Bloebaum RD (2003) Regional differences in cortical bone organization and microdamage prevalence in Rocky Mountain mule deer. Anatomical Record *274A(1)*:837-50.

Skedros JG, Hunt KJ, and Bloebaum RD (2004) Relationships of loading history and structural and material characteristics of bone: development of the mule deer calcaneus. Journal of Morphology *259*: 281-307.

Skedros JG, Sorenson SM, Takano Y, and Turner CH (2006) Dissociation of mineral and collagen orientations may differentially adapt compact bone for regional loading environments: Results from acoustic velocity measurements in deer calcanei. Bone *39(1):*143-151.

Smith JW (1960a) The arrangement of collagen fibres in human secondary osteons. Journal of Bone and Joint Surgery *42B:*588-605.

Smith JW (1960b) Collagen fibre patterns in mammalian bone. Journal of Anatomy (London) *94:*329-344.

Smith BH (1989) Dental development as a measure of life history in primates. Evolution *43:*683-688.

Smith BH (1992) Life history and the evolution of human maturation. Evolutionary Anthropology *1:*134-142.

Smith RJ, and Jungers WL (1997) Body mass in comparative primatology. Journal of Human Evolution *32:*523-559.

Starck JM, and Chinsamy A (2002) Bone microstructure and developmental plasticity in birds and other dinosaurs. Journal of Morphology *254(3)*:232-46.

Steiper ME, Ruvolo M (2003) New World monkey phylogeny based on X-linked G6PD DNA sequences. Molecular Phylogenetics and Evolution *27*:121–130.

Stevens J, Edgerton V, and Mitton S (1971) Gross anatomy of hindlimb skeletal system of the *Galago senegalensis*. Primates *12*:313-321.

Stevens J, Mitton S, and Edgerton V (1972) Gross anatomy of hindlimb skeletal muscles of the *Galago senegalensis*. Primates *13:*83-101.

Stout SD, and Paine RR (1994) Brief communication: bone remodeling rates: a test of an algorithm for estimating osteons. American Journal of Physical Anthropology *93:*123-129.

Suckling JA, Suckling EE, and Walker AC (1969) Suggested function of the vascular bundles in the limbs of *Perodicticus potto*. Nature *221:*379-380.

Sussman RW (2002) Adaptive array of lemurs of Madagascar revisited. Evolutionary Anthropology *Supplement 1:*75-78.

Sussman RW, and Kinzey WG (1984) The ecological role of the Callitrichidae: a review. American Journal of Physical Anthropology *64:*419-449.

Swartz SM, Bertram JEA, and Biewener AA (1989) Telemetered in vivo strain analysis of locomotor mechanics of brachiating gibbons. Nature *342(6247)*:270-272.

Swartz SM, Parker A, and Huo C (1998) Theoretical and empirical scaling patterns and topological homology in bone trabeculae. The Journal of Experimental Biology *210:*573-590.

Szalay FS (1981) Phylogeny and the problem of adaptive significance: the case of the earliest primates. Folia Primatologica *36*:157-182.

Szalay FS (2000) Function and adaptation in paleontology and phylogenetics: why do we omit darwin? Palaeontologia Electronica *3(2)*: http://palaeo-electronica.org/2000_2/darwin/issue2_00.htm

Szalay FS, and Dagosto M (1980) Locomotor adaptations as reflected on the humerus of paleogene primates. Folia Primatologica *34:*1-45.

Szalay FS, and Dagosto M (1988) Evolution of hallucial grasping in the primates. Journal of Human Evolution *17:*1-33.

Szalay FS, and Decker RL (1974) Origins, evolution, and function of the tarsus in late Cretaceous Eutheria and Paleocene primates. In FA Jenkins (ed.): Primate Locomotion. New York: Academic Press, pp. 239-259.

Szalay FS, and Delson E (1979) Evolutionary History of the Primates. New York, Academic Press.

Szalay FS, and Katz CC (1973) Phylogeny of lemurs, galagos and lorises. Folia Primatologica *19*:88-103.

Szalay FS, and Lucas SG (1993) Craniskeletal morphology of archontans, and diagnoses of chiroptera, volitantia and archonta. In RDE MacPhee (ed.): Primates and Their Relatives in Phylogenetic Perspective. New York: Plenum Press.

Szalay FS, and Lucas SG (1996) The postcranial morphology of Paleocene *Chriacus* and *Mixodectes* and the phylogenetic relationships of archontan mammals. New Mexico Museum of Natural History and Science Bulletin *7*.

Szalay FS, Tattersal I, and Decker RL (1975) Phylogenetic relationships of *Plesiadapis*– postcranial evidence. Contributions to Primatology *5*:136-166.

Szalay FS, Rosenberger AL, and Dagosto M (1987) Diagnosis and differentiation of the Order Primates. Yearbook of Physical Anthropology *30:*75-105.

Szalay FS, and Sargis EJ (2001) Model-based analysis of postcranial osteology of marsupials from the Palaeocene of Itaboraí (Brazil) and the phylogenetics and biogeography of Metatheria. Geodiversitas *23*:139-302.

Tardif SD, and Bales KL (2004) Relations among birth condition, maternal condition, and postnatal growth in captive common marmoset monkeys (*Callithrix jacchus*). American Journal of Primatology *62:*83-94.

Teitelbaum SL (2000) Bone resorption by osteoclasts. Science *289:*1504-1508.

Tencer AF, and Johnson KD (1994a) Basic concepts in biomechanics of fractures and fixation: Biomechanics in Orthopedic Trauma: Bone Fracture and Fixation. UK: Martin Dunitz, pp. 1-17.

Tencer AF, and Johnson KD (1994b) Factors affecting the strength of bone: Biomechanics in Orthopedic Trauma: Bone Fracture and Fixation. UK: Martin Dunitz, pp. 18-33.

Terranova C (1995a) Functional morphology of leaping behaviors in galagids: associations between landing limb use and diaphyseal geometry. In L Alterman, GA Doyle and MK Izard (eds.): Creatures of the Dark: The Nocturnal Prosimians. New York: Plenum Press, pp. 473-493.

Terranova CJ (1995b) Leaping behaviors and the functional morphology of strepsirhine primate long bones. Folia Primatologica *61*:181-201.

Terranova CJ (1996) Variation in the leaping of lemurs. American Journal of Primatology *40:*145-165.

Terranova CJ, and Coffman BS (1997) Body weights of wild and captive lemurs. Zoo Biology *16*:17-30.

Thomas CD, Stein MS, Feik SA, Wark JD, and Clement JG (2000) Determination of age at death using combined morphology and histology of the femur. Journal of Anatomy *196( Pt 3)*:463-71.

Thomason JJ (1995) To what extent can the mechanical environment of a bone be inferred from its internal architecture? In JJ Thomason (ed.): Functional Morphology in Vertebrate Paleontology, pp. 249-263.

Traub W, Arad T, and Weiner S (1992) Growth of mineral crystals in turkey tendon collagen fibers. Connective Tissue Research *28*:99-111.

Turner CH, and Burr DB (1993) Basic biomechanical measurements of bone: a tutorial. Bone *14:*595-608.

Turnquist JE, Schmitt D, Rose MD, and Cant JGH (1999) Pendular motion in the brachiation of captive *Lagothrix* and *Ateles*. American Journal of Physical Anthropology *48(4)*:263-281.

van der Rest M, Aubert-Foucher E, Dublet B, Eichenberger D, Font B, and Goldschmidt D (1991) Structure and function of the fibril-associated collagens. Biochemical Society Transactions *19(4)*:820-4.

Verborgt O, Gibson GJ, and Schaffler MB (2000) Loss of osteocyte integrity in association with microdamage and bone remodeling after fatigue in vivo. Journal of Bone and Mineral Research *15(1)*:60-7.

Vincentelli R (1978) Relation between collagen fiber orientation and age of osteon formation in human tibial compact bone. Acta Anatomica *100:*120-128.

Vincentelli R, and Evans FG (1971) Relations among mechanical properties, collagen fibers, and calcification in adult human cortical bone. Journal of Biomechanics *4:*193-201.

Vincentelli R, and Grigorov M (1985) The effects of Haversian remodeling on the tensile properties of human cortical bone. Journal of Biomechanics *18:*201-207.

Volpi M, and Katz EP (1991) On the adaptive structures of the collagen fibrils of bone and cartilage. Journal of Biomechanics *24:*67-77.

Walker A (1969) The locomotion of lorises, with special reference to the potto. East African Wildlife Journal *7*:1-5.

Walker A (1974) Locomotor adaptations in past and present prosimian primates. In FA Jenkins Jr. (ed.): Primate Locomotion. New York: Academic Press, pp. 349-381.

Walker A (1979) Prosimian locomotor behavior. In GA Doyle and RD Martin (eds.): The Study of Prosimian Behavior. Academic Press, Inc., pp. 543-565.

Wang L, Fritton SP, Cowin SC, and Weinbaum S (1999) Fluid pressure relaxation depends upon osteonal microstructure: modeling an oscillatory bending experiment. Journal of Biomechanics *32*:663-672.

Warren RD, and Crompton RH (1998) Diet, body size, and the energy costs of locomotion in saltatory primates. Folia Primatologica *69 (Supplement 1):*86-100.

Warshaw J, McFarlin SC, Bromage TG, and Szalay FS (2000) Some bone microstructural variables in extant therians, and their relationship to life history, locomotion, and phylogeny. Journal of Vertebrate Paleontology *20(Supplement 3)*:76A-77A.

Watts ES (1990) Evolutionary trends in primate growth and development. In Rousseau C. J. de (ed.): Primate Life History and Evolution. New York: Wiley-Liss, pp. 89-104.

Weiner S, and Traub W (1992) Bone structure: from angstroms to microns. The FASEB Journal *6*.

Weiner S, Arad T, Sabanay I, and Traub W (1997) Rotated plywood structure of primary lamellar bone in the rat: orientations of the collagen fibril arrays. Bone *20:*509-514.

Weisenseel KA, Izard MK, Nash LT, Ange RL, and Poorman-Allen P (1998) A comparison of reproduction in two species of *Nycticebus*. Folia Primatologica *69:*321-324.

Wenk HR, and Heidelbach F (1999) Crystal alignment of carbonated apatite in bone and calcified tendon: results from quantitative texture analysis. Bone *24(4)*:361-9.

Wickelski M, and Ricklefs RE (2001) The physiology of life histories. Trends in Ecology and Evolution *19:*479-481.

Wolfe, A and Sleeper B (1997) Primates: The Amazing World of Lemurs, Monkeys, and Apes. San Francisco: Chronicle Books.

Wright PC (1999) Lemur traits and Madagascar ecology: coping with an island environment. Yearbook of Physical Anthropology *42*:31-72.

Xu J, Rho JY, Mishra SR, and Fan1 Z (2003) Atomic force microscopy and nanoindentation characterization of human lamellar bone prepared by microtome sectioning and mechanical polishing technique. Journal of Biomedical Materials Research *67A:*719-726.

Yeni YN, Brown CU, Wang Z, and Norman TL (1997) The influence of bone morphology on fracture toughness of the human femur and tibia. Bone *21:*453-459.

Yoder AD, Cartmill M, Ruvolo M, Smith K, and Vilgalys R (1996) Ancient single origin for Malagasy primates. Proceedings of the National Academy of Sciences USA *93*:5122-5126.

Yoder AD, Irwin JA, and Payseur BA (2001) Failure of the ILD to determine data combinability for slow loris phylogeny. Systematic Biology *50(3)*:408-424.

Youlatos D (2000) Functional anatomy of the forelimb muscles in Guianan atelines (Platyrrhini: Primates). Annales des Sciences Naturelles *21:*137-151.

Zioupos P, Currey JD, and Casinos A (2001) Tensile fatigue in bone: are cycles-, or time to failure, or both, important? Journal of Theoretical Biology *210(3)*:389-99.

Ziv V, Sabanay I, Arad T, Traub W, and Weiner S (1996) Transitional structures in lamellar bone. Microscopy Research and Technique *33(2)*:203-213.